

Springer Series on Polymer and Composite Materials

Vijay Kumar Thakur
Manju Kumari Thakur *Editors*

Functional Biopolymers

 Springer

Springer Series on Polymer and Composite Materials

Series editor

Susheel Kalia, Dehradun, India

More information about this series at <http://www.springer.com/series/13173>

Vijay Kumar Thakur · Manju Kumari Thakur
Editors

Functional Biopolymers

 Springer

Editors

Vijay Kumar Thakur
Faculty in Manufacturing, Enhanced
Composites and Structures Centre, School
of Aerospace, Transport and
Manufacturing
Cranfield University
Cranfield, Bedfordshire
UK

Manju Kumari Thakur
Division of Chemistry
Himachal Pradesh University
Shimla, Himachal Pradesh
India

ISSN 2364-1878 ISSN 2364-1886 (electronic)
Springer Series on Polymer and Composite Materials
ISBN 978-3-319-66416-3 ISBN 978-3-319-66417-0 (eBook)
<https://doi.org/10.1007/978-3-319-66417-0>

Library of Congress Control Number: 2017950024

© Springer International Publishing AG 2018

This work is subject to copyright. All rights are reserved by the Publisher, whether the whole or part of the material is concerned, specifically the rights of translation, reprinting, reuse of illustrations, recitation, broadcasting, reproduction on microfilms or in any other physical way, and transmission or information storage and retrieval, electronic adaptation, computer software, or by similar or dissimilar methodology now known or hereafter developed.

The use of general descriptive names, registered names, trademarks, service marks, etc. in this publication does not imply, even in the absence of a specific statement, that such names are exempt from the relevant protective laws and regulations and therefore free for general use.

The publisher, the authors and the editors are safe to assume that the advice and information in this book are believed to be true and accurate at the date of publication. Neither the publisher nor the authors or the editors give a warranty, express or implied, with respect to the material contained herein or for any errors or omissions that may have been made. The publisher remains neutral with regard to jurisdictional claims in published maps and institutional affiliations.

Printed on acid-free paper

This Springer imprint is published by Springer Nature
The registered company is Springer International Publishing AG
The registered company address is: Gewerbestrasse 11, 6330 Cham, Switzerland

Preface

During the last few decades, there has been an escalating demand for clean, pollution-free environment and high urgency for minimising fossil fuel. It has led to an increasing demand for the development of high-performance cultured products from biological and renewable resources. Functional biopolymers and their respective composites as well as various other materials are one of the most suitable alternates to fulfil such alarming urgency. Biopolymers refer to the class of polymers having biological origin. These may be linear or cross-linked combinations of their respective monomer units. Biopolymers are generally classified into several categories depending on several factors such as (a) degradability (b) polymer backbone (c) monomers, etc. Biodegradable polymers are typical type of polymers which degrade or break down after their intended purpose and form by-products like environmental gases (CO_2 , N_2), water, biomass and inorganic and organic salts. Non-biodegradable polymers are the substances that do not break down to a natural, environmental safe condition over time by biological processes. Depending on monomer, units like monosaccharide, amino acids, nucleotides, natural biopolymer are commonly classified into polysaccharides, proteins and nucleic acids. Biopolymers are currently being used as substitute to traditional synthetic materials because they are more sustainable, renewable and more importantly eco-friendly in nature. Furthermore, the functional materials prepared using biopolymers exhibit suitable properties such as high mechanical resistance, thermogravimetric, oxygen barrier, biodegradation and chemical resistance to name a few. In reality, there is not a single material which can achieve wide range of properties for which design of composites, in particular with biopolymers, is an attempt for substantial improvement of properties. The biopolymers can also be functionalised for better compatibility during preparation of composites and other materials.

In this book, different types of biopolymers and their functional materials are presented along with some critical issues, advantages and disadvantages. The prime aim and focus of this book is to present recent advances in the synthesis, processing and applications of *Functional Biopolymers* as new innovative sustainable materials. It reflects the recent theoretical advances and experimental results and open new avenues for researchers as well as readers working in the field of polymers and

sustainable materials. Different topics covered in this book include but are not limited to: Structural Analysis of Functional Biopolymers Based Materials; Nano-optical Biosensors; Functionalization of Tamarind Gum For Drug Delivery; Biopolymer Composite Materials With Antimicrobial Effects; Functional Biocomposites of Calcium Phosphate-Chitosan And Its Derivatives; Surface Properties Of Thermoplastic Starch Materials Reinforced With Natural Fillers; Functional Biopolymer Composites; Cellulose-Enabled Polylactic Acid (PLA) Nanocomposites; Epoxidized Vegetable Oils For Thermosetting Resins; Philosophical Study on Composites; Smart Materials For Biomedical Applications and Emulgels for Drug Delivery.

We express our sincere thanks to all the authors, who have contributed their extensive experience through their work for the success of this book. We would also like to thank Dr. Susheel Kalia (Series Editor) along with publisher for invaluable help in the organisation of the editing process.

Vijay Kumar Thakur, Ph.D.
Cranfield University, Cranfield, UK

Manju Kumari Thakur, M.Sc., M.Phil., Ph.D.
Himachal Pradesh University, Shimla, India

Contents

1	Nano-optical Biosensors for Assessment of Food Contaminants	1
	M.S. Attia, Ahmed E.M. Mekky, Ziya Ahmed Khan and M.S.A. Abdel-Mottaleb	
2	Functionalization of Tamarind Gum for Drug Delivery	25
	Amit Kumar Nayak and Dilipkumar Pal	
3	Biopolymer Composite Materials with Antimicrobial Effects Applied to the Food Industry	57
	Kelvia Álvarez, Vera A. Alvarez and Tomy J. Gutiérrez	
4	Functional Biocomposites of Calcium Phosphate–Chitosan and Its Derivatives for Hard Tissue Regeneration Short Review	97
	L. Pighinelli, D. Wawro, M.F. Guimarães, R.L. Paz, G. Zanin, M. Kmiec, M.F. Tedesco, M. Silva and O.V. Reis	
5	Surface Properties of Thermoplastic Starch Materials Reinforced with Natural Fillers	131
	Tomy J. Gutiérrez, Romina Ollier and Vera A. Alvarez	
6	Functional Biopolymer Composites	159
	Sarat K. Swain, Adrushya J. Pattanayak and Amrita P. Sahoo	
7	Cellulose-Enabled Polylactic Acid (PLA) Nanocomposites: Recent Developments and Emerging Trends	183
	Wei Dan Ding, Muhammad Pervaiz and Mohini Sain	
8	Epoxidized Vegetable Oils for Thermosetting Resins and Their Potential Applications	217
	Carmen-Alice Teacă, Dan Roșu, Fulga Tanasă, Mădălina Zănoagă and Fănică Mustață	

9 Philosophical Study on Composites and Their Drilling Techniques 239
Sikiru Oluwarotimi Ismail and Hom Nath Dhakal

10 Multicomponent, Semi-interpenetrating-Polymer-Network and Interpenetrating- Polymer-Network Hydrogels: Smart Materials for Biomedical Applications 281
Nazire Deniz Yilmaz

11 Emulgels: Application Potential in Drug Delivery 343
Amit Verma, Ankit Jain, Ankita Tiwari and Sanjay K. Jain

About the Editors



Vijay Kumar Thakur Ph.D. Faculty in Manufacturing Enhanced Composites and Structures Centre School of Aerospace, Transport and Manufacturing Cranfield University, Cranfield, Bedfordshire MK43 0AL

Email: Vijay.Kumar@cranfield.ac.uk

T: +44 (0) 1234 750111 x2344

Prior to commencing in the School of Aerospace, Transport and Manufacturing at Cranfield University, Dr. Vijay Kumar Thakur was working as a Staff Scientist in the School of Mechanical and Materials Engineering at Washington State University, USA (2013–2016). Some of his other prior significant appointments include being a Research Scientist in Temasek Laboratories at Nanyang Technological University, Singapore (2009–2012) and a Visiting Research Fellow in the Department of Chemical and Materials Engineering at LHM–Taiwan. He did his post-doctoral study in Materials Science & Engineering at Iowa State University and received Ph.D. in Polymer Chemistry (2009).

In his academic career, he has published more than 100 SCI journal research articles in the field of chemical sciences/materials science and holds one United States patent. He has also published 33 books and 35 book chapters on the advanced state of the art of polymer science/materials science/nanotechnology with numerous publishers. His research interests include the synthesis and processing of biobased polymers, composites; nanostructured materials, hydrogels, polymer micro-/nanocomposites, nanoelectronic materials,

novel high dielectric constant materials, engineering nanomaterials, electrochromic materials, green synthesis of nanomaterials and surface functionalization of polymers/nanomaterials. Application aspects range from automotive to aerospace, energy storage, water purification and biomedical fields.

Vijay is an editorial board member of several international journals, as well as a member of scientific bodies around the globe. Some of his significant appointments include Associate Editor for Materials Express (SCI); Advisory Editor for SpringerPlus (SCI); Editor for Energies (SCI); Editor for Cogent Chemistry (SCI); Associate Editor for Current Smart Materials; Associate Editor for Current Applied Polymer Science; Regional Editor for Recent Patents on Materials Science (Scopus); and Regional Editor for Current Biochemical Engineering (CAS). He also serves on the Editorial Advisory Board of Polymers for Advanced Technologies (SCI) and is on the Editorial Board of Journal of Macromolecular Science, Part A: Pure and Applied Chemistry (SCI), International Journal of Industrial Chemistry (SCI), Biointerface Research in Applied Chemistry (SCI) and Advances in Natural Sciences: Nanoscience and Nanotechnology (SCI).



Manju Kumari Thakur M.Sc., M.Phil., Ph.D.
Assistant Professor

Division of Chemistry, Government Degree
College Bhoranj

Himachal Pradesh University, Shimla, India
Email: shandilyamn@gmail.com

She has been working as an Assistant Professor of Chemistry at the Division of Chemistry, Government Degree College Sarkaghat Himachal Pradesh University—Shimla, India since June 2010. She received her B.Sc. in Chemistry, Botany and Zoology; M.Sc., M.Phil. in Organic Chemistry and Ph.D. in Polymer Chemistry

from the Chemistry Department at Himachal Pradesh University—Shimla, India. She has rich experience in the field of organic chemistry, biopolymers, composites/nanocomposites, hydrogels, applications of hydrogels in the removal of toxic heavy metal ions, drug delivery, etc. She has published more than 30 research papers in several international journals, co-authored five books and has also published 25 book chapters in the field of polymeric materials.

Chapter 1

Nano-optical Biosensors for Assessment of Food Contaminants

M.S. Attia, Ahmed E.M. Mekky, Ziya Ahmed Khan
and M.S.A. Abdel-Mottaleb

Abstract In the last decades, the optical biosensors have great attention, especially, when the biosensor is inserted into a good host such as tetraethoxyorthosilicate (TEOS) polymer and molecular imprinted polymer with no interference. This method gives a transparent nano-optical biosensor with new optical properties to increase the impact of the proposed analytical method which has wide linear range and very low detection limit. In this chapter, the transparent nano-optical sensor is inserted into TEOS polymer and imprinted template in molecular imprinted nanopolymer for the determination of different food contaminants such as different bacteria (*Salmonella*, *Staphylococcus aureus* and *Campylobacter*), Aflatoxin produced by different *Aspergillus flavus* and *Aspergillus parasiticus* species of fungi and *E. coli* bacteria. The nano-optical biosensors were used for the determination of food contaminants in different food samples with a high-performance analytical method.

1 Introduction

The biosensor has many advantages over other types of sensor and is exploited profitably mainly by the medical and pharmaceutical sector. The biosensors are used for sensing the main important targets such as glucose in diabetics patients, toxicity of some foods, and food-borne pathogens including *E. coli*, *Salmonella*, and aflatoxin (Thusu 2014a, b). Two types of biosensors include (1) sophisticated, rapid,

M.S. Attia (✉) · M.S.A. Abdel-Mottaleb
Department of Chemistry, Faculty of Science,
Ain Shams University, Abbassia, Cairo 11566, Egypt
e-mail: Mohamed_sam@yahoo.com; Mohd_mostafa@sci.asu.edu.eg

A.E.M. Mekky · Z.A. Khan
Chemistry Department, Faculty of Science,
University of Jeddah, P.O. Box 80327, Jeddah 21589, Saudi Arabia

A.E.M. Mekky
Chemistry Department, Faculty of Science,
Cairo University, Giza 12613, Egypt

very sensitive with a high accurate measurement machines in the laboratory for the complex biological interactions and components and (2) new prototype devices for use by nonspecialists for in situ or home monitoring. A new approach in which the molecular imprinted polymer (MIP) with nanotechnology is introduced in the last decades (Turiel and Martin-Esteban 2010). This approach depends on the selection of functional monomers to self-assemble around a target analyte. This chapter, concerns by the determination of different food contaminants such as different bacteria (*Salmonella*, *Staphylococcus aureus* and *Campylobacter*), Aflatoxin produced by different *Aspergillus flavus* and *Aspergillus parasiticus* species of fungi and *E. coli* bacteria by using dopped nano-optical sensors in tetraethylorthosilicate (TEOS) polymer prepared by the sol-gel method and molecular imprinted nanopolymer.

1.1 Characteristics of Optical Biosensor

Selectivity: The biosensor must have a high selectivity for the analyte and have little interference with moieties that have a chemical structure similar to that of the analyte.

Sensitivity: The biosensor should be able to measure the analyte many times by the same accuracy in small time intervals.

Linearity of response: It should have a wide linear range similar to the concentration range over which the target analysis is to be measured.

Reproducibility of signal response: Repeating the sample concentration measurements gives the same results.

Quick response time and recovery time: The time required for the biosensor to respond to the selected analyte. This time should be quick enough so that real-time monitoring can take place in an efficient manner. The recovery time of the sensor should be as small as possible for reusability of the biosensor system.

Stability and operating life: The biosensors should be stable in different media such as biochemical and environmental conditions (Thakur and Ragavan 2010).

1.2 Biosensor Components

A biosensor is a molecular device that converts a biological response into a detectable measurable signal. A biosensor is formed from three components: **the sensor material** such as; metal, glass, polymer, or even paper, onto which a bioreceptor is coupled. **The bioreceptor, such as** antibodies, enzymes, nucleic acid aptamers or single-stranded DNA, cellular structures/cells, biomimetic, and bacteriophage (phage) (Velusamy et al. 2010), is coupled with the sensor through different immobilizing techniques which may be physical or chemical.

1.3 *Sensor Materials*

The nanostructure biomaterials are used in the last decades in the development of many devices, including sensor technology with unique capabilities for data collection, processing, and recognition with minimal false positive counts. Carbon nanotubes (CNT's) are conducting, act as electrodes, and generate electrochemiluminescence (ECL) in aqueous solutions (Vaseashta and Dimova-Malinovska 2005). Therefore, the sensor surface is formed from metal, polymer, glass-doped nanomaterial which has a similar dimension to biomolecules like proteins and DNA.

1.4 *Sensor Designs*

The technique used for the physical or chemical fixation of bioreceptor which can be cells, organelles, enzymes, or other proteins (e.g., monoclonal antibodies) onto a solid support, or into a solid matrix or retained by a membrane, is used in order to increase their stability. The methods used can be physical retention or chemical binding.

1.4.1 *Physical Adsorption Method*

This method depends on the adsorption of the enzyme or other biological materials on solid support, for example, alumina, charcoal, clay, cellulose, kaolin, silica gel, glass, collagen, carbon pellets, and advanced material such as carbon nanotubes (CNTs). A simple procedure is when microbial cells are immobilized by simple absorption by placing the cells on a porous cellulose membrane, generating pastes when enzymes or tissue are mixed with graphite powder and liquid paraffin.

1.4.2 *Physical Entrapment Method*

The biomaterial and transducer are contacted by inert membranes. These membranes include cellulose acetate (dialysis membrane); polycarbonate (Nucleopore), synthetic non-permselective material; Collagen, a natural protein; PTFE: polytetrafluoroethylene (trade name Teflon) and is a synthetic polymer selectively permeable to gases. Nafion, (a Dupont material), is biocompatible and shown to be stable in cell culture and the human body. Polymeric gels can be used and prepared in a solution containing the biomaterial.

1.5 *Transducing Element*

The transducing element gives a measurable signal that is proportional to the concentration of the analyte/bioreceptor. Three types of the transducers are available, they are optical, electrochemical, and mass based.

1.5.1 **Optical Transducers**

Optical transducers can be subdivided into light absorption, fluorescence/phosphorescence, reflectance, refractive index, and bio/chemiluminescence. In fluorescence, the method of determination depends on the preparation of transparent host doped with the biosensor for sensing the metabolites produced from the different food contaminants such as; *Salmonella*, *E. coli* and aflatoxin. In reflectance, three methods are used such as surface plasmon resonance (SPR) (Biacore 2014), total internal reflection fluorescence (TIFR), and attenuated total reflectance (ATR).

1.5.2 **Fiber Optic Biosensors**

Fiber optic biosensors FOBS (Leung et al. 2007) have many applications in food quality and safety (Narsaiah et al. 2012) such as detection of *Salmonella*, *E. coli* and *Listeria* in food. FOBS based on the type of interactions with an analyte, can be divided into two groups: affinity and catalytic. According to their mode of action, optical biosensors have been subdivided into five subgroups: (a) plain fluorometric sensors; (b) direct and indirect indicator-mediated chemical sensors; (c) direct enzymatic biosensors; (d) indicator-mediated enzymatic biosensors; and (e) affinity biosensors.

1.5.3 **Electrochemical Transduction Methods**

It is subdivided as the measurement of amperometric (current), impedimetric (impedance), potentiometric (potential) and conductometric for the determination of food contaminants. The amperometric sensors are better than potentiometric devices in which it has a wide linear range. Most of the work has been done on amperometric and potentiometric biosensors with little work being devoted to conductometric biosensors (Adley and Ryan 2014). Modern electrochemical techniques have low detection limits (10^{-7} – 10^{-9} mol/L or 30 ppb) for gaseous compounds (Yang et al. 2012). A range of detector components (antibody, DNA) has been used in the detection of *Campylobacter* spp. using both amperometric and impedimetric transducers (Yang et al. 2013). Electrochemical enzyme-based biosensors have dominated the market in the food (Zhai et al. 2013).

1.5.4 Mass-Based Transducers

In which the change in the mass is used to detect the food contaminants. The two main types of mass-based sensors are (1) bulk wave (BW) or quartz crystal microbalance (QCM) and (2) surface acoustic wave (SAW).

A QCM is a real mass sensor belonging to a wider class of inertial mass sensors (Mecea 2006).

Acoustic wave sensors (AWS) monitor the change in oscillation frequency when the device responds to the input stimulus. AWS is divided into: (1) flexural plate wave resonators (FPW); (2) bulk acoustic wave resonators (BAW); (3) shear-horizontal acoustic plate mode resonators (SAW); and (4) surface acoustic wave resonators (SAW). The important application of SAW is used for monitoring humidity in food packaging system (Reyes et al. 2013).

2 Methods of Preparations

2.1 Sol–Gel Process

The sol–gel is a wet chemical technique used for the synthesis of new porous nanomaterials with well-defined structures and complex shapes. It is well known that this technique is relatively simple and through a pre-orientation of the network, the distribution of the components in molecules can be easily controlled.

For a long time, sol–gel techniques have been used for the fabrication of both glassy and ceramic materials (Dislich 1971a; Yan and Row 2006; Chiodini et al. 1999; Marzolin et al. 1998). The polycondensation reactions of the obtained gel material undergo a two-phase system containing both liquid phase and solid phase. These two phases have morphologies range from discrete particles (colloid) to continuous polymer networks. With the evaporation of some amount of solvents, a gel-like property of the colloid solution was obtained (Klein and Garvey 1980; Brinker et al. 1982). Generally, two types of reactions are used to obtain the material by sol–gel technique; (i) acid-catalyzed sol formation, in which there is a formation of an open continuous network of low-density polymers that exhibit certain advantages with regard to physical properties in the formation of high-performance glass and glass/ceramic components in two and three dimensions (Allman III 1983), (ii) base-catalyzed sol formation, in which the particles are allowed to grow till sufficient size to become colloids (Allman III and Onoda Jr 1984; Sakka and Kamiya 1982) (Fig. 1).

In both the types of reactions, the inorganic network containing a liquid phase (gel) was formed. The gel is obtained due to the formation of metal oxide by connecting the metal center with oxo (M-O-M) or hydroxo (M-OH-M) bridges, which undergoes transition to give metal-oxo or metal-hydroxo polymer in solution.

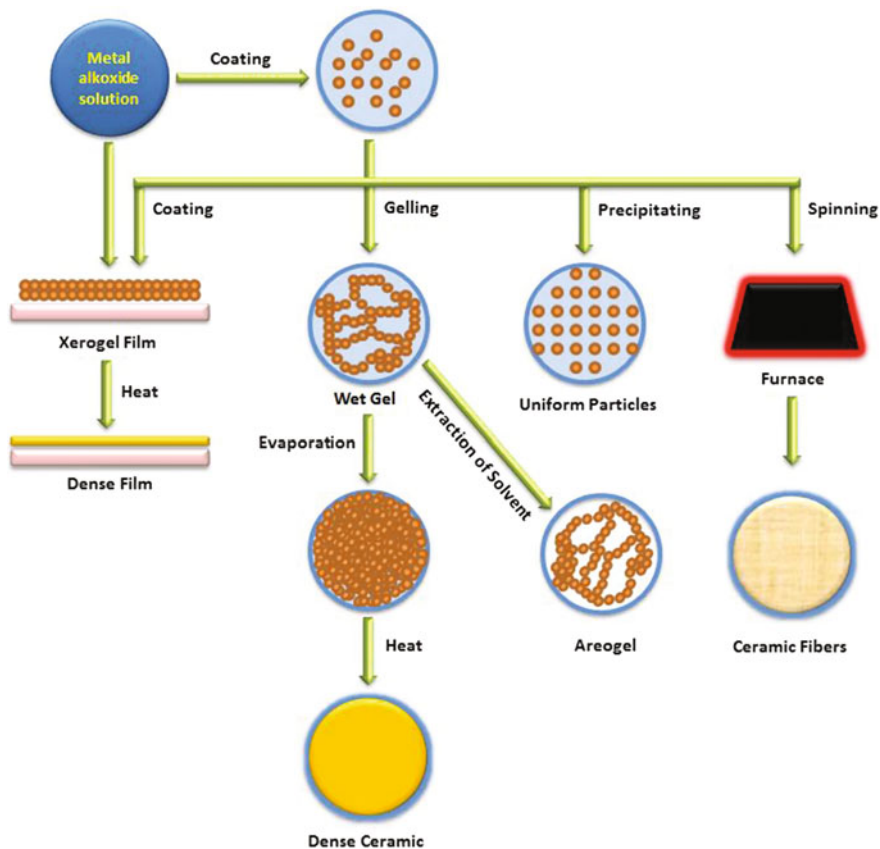
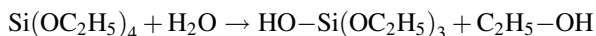


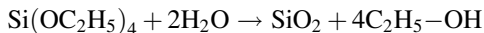
Fig. 1 Schematic diagram for different stages and pathways in sol-gel technology

2.1.1 Mechanism of Sol-Gel Formation

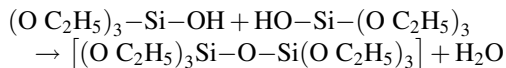
The well-known precursors are the alkoxides ($\text{Si}(\text{OR})_4$), e.g., tetramethylorthosilicate (TMOS), $\text{Si}(\text{OCH}_3)_4$ or tetraethyl orthosilicate (TEOS) $\text{Si}(\text{OC}_2\text{H}_5)_4$ in the sol-gel formation. The alkoxides are used as ideal chemical precursors for sol-gel synthesis due to its reaction with water easily. Si atoms undergo hydrolysis to form a hydroxytriethylorthosilicate or a hydroxytrimethylorthosilicate. The reaction is called hydrolysis because a hydroxyl ion becomes attached to the silicon atom as follows:



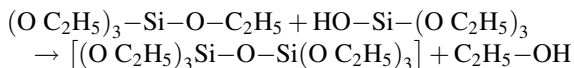
An excess of water or hydrolysis catalyst, such as acetic acid or hydrochloric acid, is used for the complete hydrolysis of the reaction.



On partial hydrolysis reaction, the intermediate species such as, $[(\text{O C}_2\text{H}_5)_2\text{-Si-(OH)}_2]$ or $[(\text{O C}_2\text{H}_5)_3\text{-Si-(OH)}]$ or siloxane $[\text{Si-O-Si}]$ may obtain.



or



Thus, polymerization is associated with the formation of a one-, two-, or three-dimensional network of siloxane $[\text{Si-O-Si}]$ bonds accompanied by the production of H_2O and $\text{C}_2\text{H}_5\text{-OH}$ species (Fig. 2).

In the presence of a catalyst, water or ethyl alcohol may be obtained. A branched polymer was obtained because a completed hydrolyzed monomer $\text{Si}(\text{OH})_4$ is tetrafunctional (can branch or bond in four different directions). However, under certain conditions, e.g., low water concentration or incomplete hydrolysis, partial branching will occur because less than four groups of the OC_2H_5 or OH groups (ligands) will be capable of condensation. The mechanisms of hydrolysis and condensation and the factors that control the structure toward linear or branched structures are the most critical issues of sol-gel science and technology (Dislich

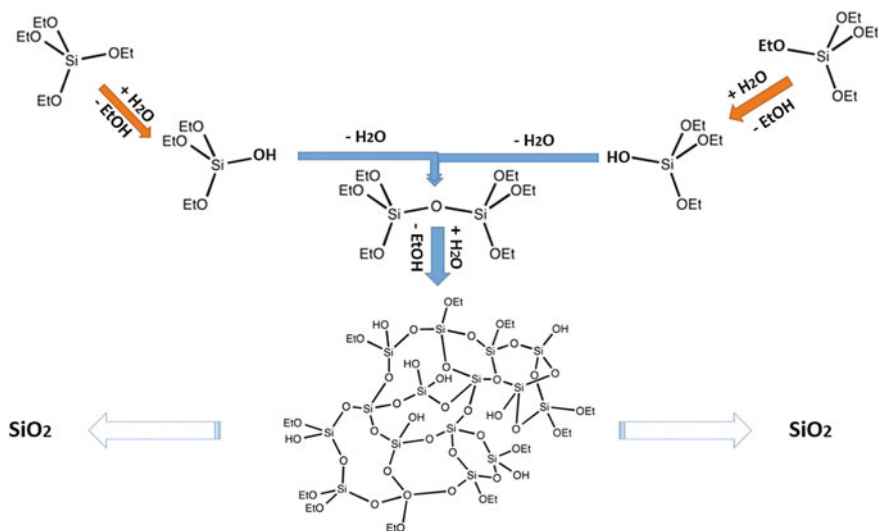


Fig. 2 Mechanism of the condensation of TEOS in sol gel process

1971b; Matijevic 1986; Brinker and Mukherjee 1981; Sakka and Kamiya 1980; Yoldas 1979; Prochazka and Klug 1983; Ikesue et al. 1995; Ikesue 2002).

2.1.2 Preparation of Nano-optical Sensor Doped in TEOS

In the preparation of the nano-optical sensor doped in sol-gel, the following three steps were carried out:

- (i) The optical sensor was dissolved in ethanol in 25 mL flask.
- (ii) The sol matrix was prepared as follows: a mixture consisting of tetraethoxysilane (TEOS), ethanol and water in 1:5:1 molar ratio was refluxed for 1 h to give the precursor sol solution in the presence of a few drops of diluted HCl solution as catalyst.
- (iii) Finally, an appropriate amount of the sensor and the precursor solution were mixed and stirred together for 15 min until the mixture become homogeneous. The developed complex-dispersed sol solution was cast into a polystyrene cup with diameters (3, 0.2, 0.8 cm) and kept at 25 °C in the air for 2 weeks. The produced cast was heated at 100–500 °C for 24 h to give solidified and transparent composite sample (Attia et al. 2010, 2012a, b; Attia and Aboaly 2010; Attia 2010) (Fig. 3).

The above-reported method suffers from some disadvantage in which the cracking has taken place for the product and cast optical sensor, which is converted into small species. Some modification was introduced to the method in which the sol after reflux was transferred into the deep freezer at zero temperature to expel the

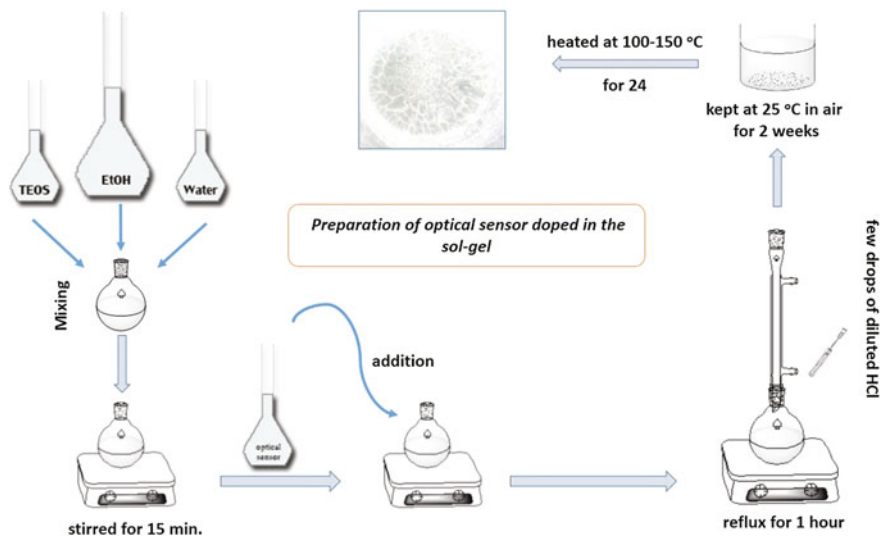


Fig. 3 Synthesis of the nano-optical sensor doped in sol gel matrix

trapped gases and decreasing the cracking process of the optical sensor (Fig. 4) (Attia et al. 2014a, b).

2.1.3 Hybrid Nanomaterials

Hybrid materials, which have unique properties, are obtained by combining with the rigidity and high thermal stability of the inorganic material and the flexibility, ductility, and process ability of the organic polymers. The optical transparency, mechanical properties, thermal and weathering resistance of the polymer materials are used as a host for biosensor applications (Zou et al. 2008). The high mechanical strength, permeability, thermal and chemical stability, a relatively low refractive index and a high surface area of the silica nanoparticles (SiNPs) leading to improved properties of the incorporated optical sensor in SiNPs polymer films enhance the mechanical properties and also reduce its thermal degradation at high temperature. Its insulation properties also improve and protect the sensor from the surrounding chemical interaction as well as preventing the quenching of the emission intensity of the sensor occurred by the surrounding environment such as hydroxyl solvents (Ray and Okamoto 2003).

The synthesis of transparent SiNPs as a hybrid polymer is carried out by sol-gel method either by basic or acidic catalysis (Shang et al. 2002; Zhang et al. 2013). Silica-polymer hybrid thin film materials can be obtained by simply mixing organic and inorganic components; however, it is usually difficult to obtain a homogeneous polymer mixture of silica and organic material due to the formation of SiNP aggregates that strongly affect the properties of the hybrid material.

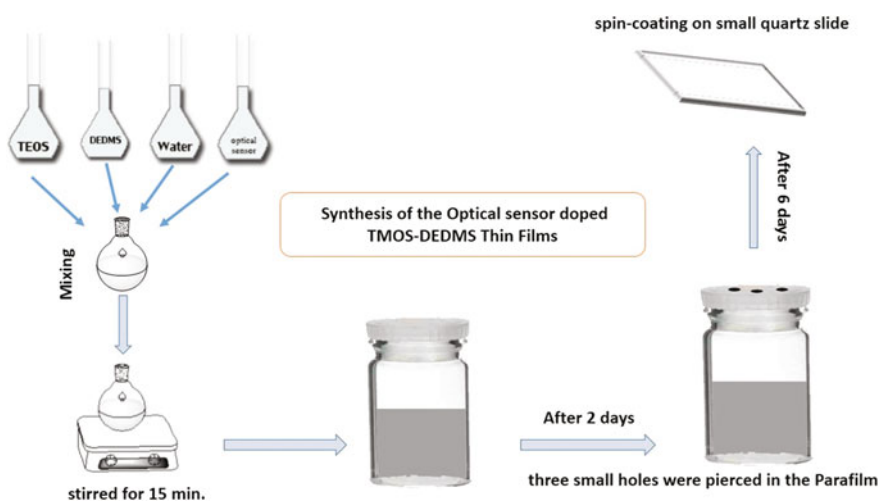


Fig. 4 Synthesis of the thin film nano-optical sensor doped in sol-gel matrix

2.1.4 Preparation of Poly Aniline–Ag–Cu Nanocomposite Thin Film by Sol–Gel Method

The nanocomposite of polyaniline (PANI) and metals were prepared by the oxidative polymerization of aniline and the reduction process of metal compound in the presence of nitric acid and PVA. 2.5 g of PVA was completely dissolved in 40 mL deionized water and stirred on the hot plate at 80–90 °C. 0.5 g of silver nitrate and copper acetate was dissolved in deionized water and was added drop by drop into PVA solution by using a pipette. Magnetic stirring continued until the solution becomes a brownish yellow viscous liquid. 1.25 mL of aniline was added to the solution followed by 1.0 mol/L nitric acid (HNO₃) (Huda et al. 2014).

2.1.5 Preparation of Optical Sensor ZnO Nano-rods for Assessment of *Salmonella*

A preliminary processed by ultrasound in acetone and dried in a nitrogen flow of ZnO nano-rods was performed before the grown nano-rods of a powder-like structure. The ZnO nano-rods formed a layer on the substrate, which was further annealed at 300 °C in the air for 1 h (Roman et al. 2014).

2.2 *Molecular Imprinting Nanomaterial Polymer*

Molecular imprinted polymers (MIPs) are biomimetic nanomaterials. The MIP offers unique opportunities. In this technique, polymer network is formed which acts as synthetic receptors. The imprinted polymers then can selectively bind to the organic molecules for desired application (Yan and Row 2006). The molecular imprinted materials have high mechanical and chemical stability. It is easy to prepare with low manufacturing cost and can be reused (He et al. 2007; Menaker et al. 2009; Mayes and Whitcombe 2005; Cai et al. 2010; Yongqin et al. 2013). The MIP materials have specific interaction sites and cavities within the polymer structure. These cavities can be fabricated in both charged and neutral states for analytes/templates.

The combination of nanotechnology with the molecularly imprinted technique gives molecularly imprinted nanomaterials that exhibit enhanced sensitivity and selectivity, which may eventually lead to the development of more suitable matrices for desired applications (Malitesta et al. 2012). The imprinted materials with nanoscale dimensions have a greater impact on nanoscience and technology. A wide range of imprinted nanomaterial morphologies, including nanocapsules, nanospheres, nanoshells, nanocrystals, nanoclusters, nanofibers, nano-rods, and nanoparticles has been developed (Abhilash 2010; Gültekin et al. 2012; Wang et al. 2012). The shape and size of the imprinted nanomaterial depend on the conditions and methodology for synthesis. A large number of imprinted nanomaterials have

already been developed, such as imprinted nanoparticles (Imp-NPs) (Poma et al. 2013), imprinted nanocomposites (Imp-NCs) (Matsui et al. 2009) and imprinted hybrid materials (Lakshmi et al. 2009) for a number of applications such as separation science (Cheong et al. 2013a; Li et al. 2012a), molecular recognition (Guan et al. 2008), chemical sensing of different analytes (Li et al. 2012b) clinical diagnostics (Cai et al. 2010; Piletsky et al. 2006), drug delivery (Cunliffe et al. 2005), solid-phase extraction (Fuchs et al. 2012), synthesis and catalysis (Alexander et al. 2003), environmental analysis (Pichon and Chapuis-Hugon 2008), enantioselective recognition (Cheong et al. 2013b), and, most importantly, chemical sensing (Mujahid et al. 2010). The ease of preparing imprinted nanomaterials and straight forward compliance also plays a decisive role in achieving greater success as compared to other receptors (Tokonami et al. 2009). The interactions and the compatibility between the template and monomers in a typical polymer matrix play an important role (Esfandiyari-Manesh et al. 2011). A number of methods are used to prepare the imprinted nanomaterials, including bulk, suspension, multistep swelling, mini-emulsion, and core-shell and precipitation polymerizations (Kryscio and Peppas 2012).

2.2.1 Approach of Molecular Imprinted Polymer Formation

For the synthesis of molecular imprinting polymer, generally, two approaches have been proposed on the basis of covalent and non-covalent interactions between the templates (Fig. 5) and functional monomers (Fig. 6). In all the cases, the functional monomers have been chosen to interact with the functional groups of the imprinted molecule. The special binding sites are formed by covalent or, more commonly, non-covalent interaction between the functional group of imprint template, initiator (Fig. 7) and the monomer, followed by a cross-linked copolymerization in the presence of a cross-linker (Fig. 8) (Yan and Row 2006). The non-covalent approach has been used more extensively due to the following reasons: (1) non-covalent protocol is easily conducted, avoiding the tedious synthesis of pre-polymerization complex, (2) removal of the template is generally much easier, usually accomplished by continuous extraction, and (3) a greater variety of functionality can be introduced into the MIP binding site using non-covalent methods.

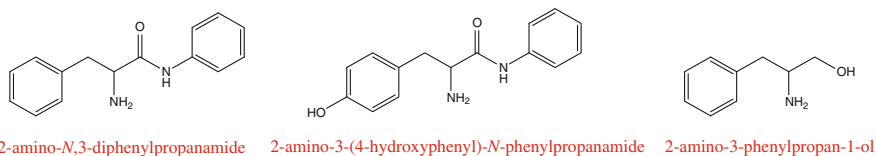


Fig. 5 Some examples on the used template in MIP technology

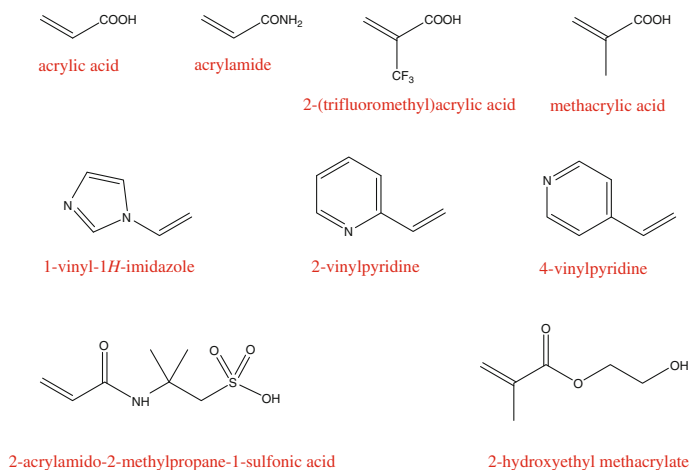


Fig. 6 Some examples on the used monomers in MIP technology

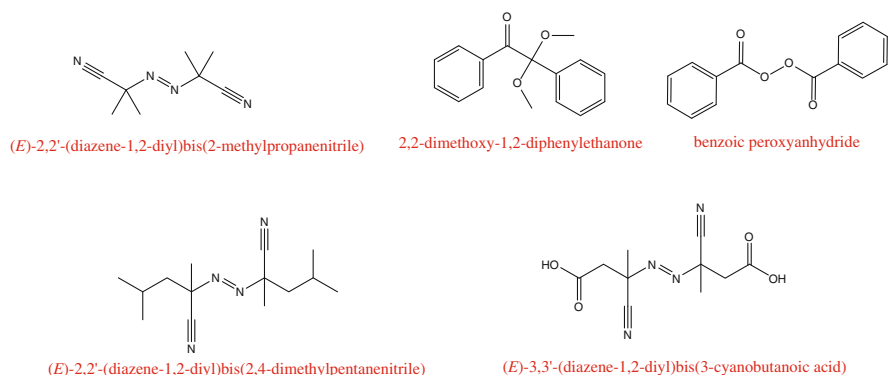


Fig. 7 Some examples on the used initiators in MIP technology

Covalent Approach

In the covalent approach, a polymerizable molecule is covalently coupled with the imprinted molecule. After the copolymerization with a cross-linker, a chemical method is used to separate the imprint molecule from the highly cross-linked polymer. The first MIP was obtained by using specific sugar or amino acid derivatives, which contained a polymerizable function such as vinylphenylboronate by covalent imprinting method (Malitesta et al. 2012; Poma et al. 2013). The selectivity of MIP for analyte depends on the ratios of cross-linker, the functional monomer, and template. The releasing of the template from MIP is carried out by the reversible covalent interactions in which the acid hydrolysis procedure is used to cleave the covalent bonds between the template and the functional monomer.

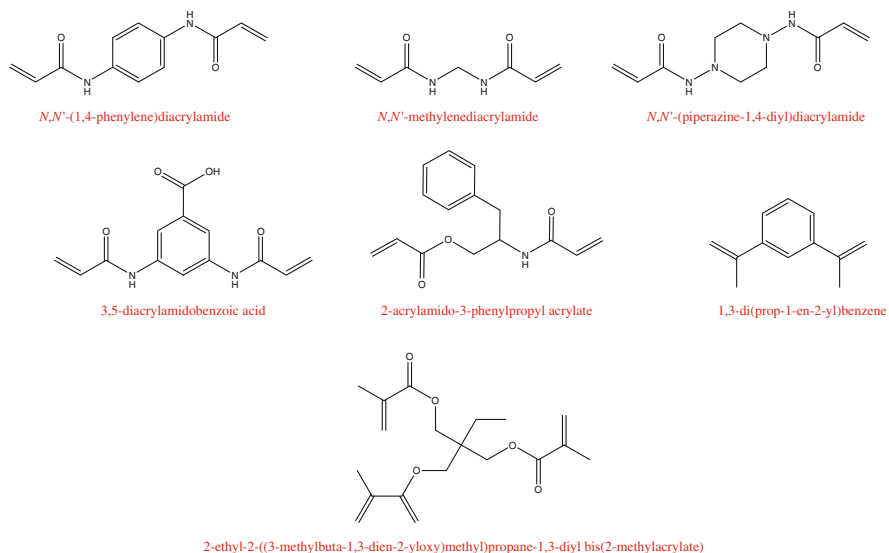


Fig. 8 Some examples on the used cross-linkers in MIP technology

Non-covalent Approach

The frequently used method to prepare MIP is the non-covalent approach due to its simplicity. In this approach, the template and functional monomer form a complex through non-covalent intermolecular interactions. The special binding sites are formed by the self-assembly between the template and monomer, followed by a cross-linked copolymerization (Matsui et al. 2009; Lakshmi et al. 2009). The imprint molecules interact, during both the imprinting procedure and the rebinding, with the polymer via non-covalent interactions, e.g., ionic, hydrophobic and hydrogen bonding (Fig. 9). The drawback of the non-covalent approach is set by the peculiar molecular recognition conditions. Due to the random nature of complex formation which may lead to different orientations of the two species and therefore different types of imprinted cavities. The formation of interactions between monomers and the template is more stabilized in hydrophobic environment over polar environment. Some restrictions in the covalent binding between the monomer and the polymer, such as some molecules characterized by a single interacting group such as an isolated carboxyl, generally give imprinted polymers with very limited molecular recognition properties. The non-covalent methods are important for two reasons: the methodology is far easier than covalent methods, and it produces higher affinity binding sites versus covalent methods. The increased number of binding interactions with the polymer binding site may account for greater accuracy of the site, and thus impart greater affinity and selectivity to the site. The trends in binding and selectivity in non-covalently imprinted polymers are

explained best by incorporating multiple functional monomers for the highest affinity binding sites.

2.3 Molecular Imprinted Nanomaterials

2.3.1 Imprinted Nanoparticles (Imp-NPs)

Imp-NPs are prepared by various methods such as precipitation, mini- and micro-emulsion, core-shell, and free radical polymerization (Cheong et al. 2013a). The precipitation in which the monomer, template, and initiator are completely soluble in the presence of the cross-linker upon the reaction begins, the polymer is formed as precipitated material.

2.3.2 Imprinted Nanospheres

The imprinted nanosphere is prepared by precipitation polymerization which is used for the recognition of desired species (Li et al. 2012c). Imp-NPs were prepared by dilution of pre-polymerization mixtures, during optimizing a number of parameters, such as the template to monomer ratio, the functional monomer to cross-linker ratios, the type, and amount of the cross-linking monomer, the concentration of salts for buffers and the pH (He et al. 2007; Piletsky et al. 2006; Tokonami et al. 2009).

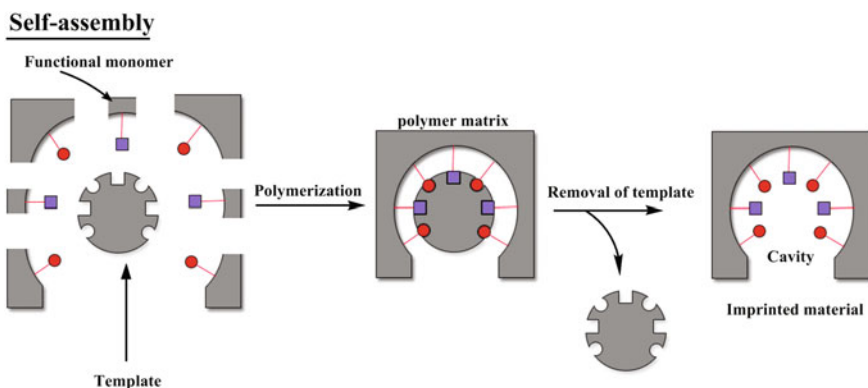


Fig. 9 Schematic diagram for non-covalent approach for synthesis of MIP

2.3.3 Imprinted Nanoshells

Emulsion/suspension polymerization has also been used for the preparation of Imp-NPs in which the mechanical agitation is used to mix a monomer, initiator, cross-linker, and template in more than one liquid phase by using the free radical polymerization mechanism (Alexander et al. 2003; Pichon and Chapuis-Hugon 2008; Mujahid et al. 2010). In some studies, the imprinted cavities were formed in an ethylene glycol dimethacrylate (EDGMA) shell for the recognition of cholesterol. Ma and co-authors synthesized a more selective core-shell Imp-NPs for β -estradiol on silica (Abhilash 2010). The fabrication of bovine hemoglobin protein Imp-NPs with a magnetic polystyrene core is performed by multistep core-shell polymerization mechanism with 3-aminophenylboronic acid as the monomer and sol-gel process (Gültekin et al. 2012; Wang et al. 2012; Esfandyari-Manesh et al. 2011; Takeda and Kobayashi 2005).

2.3.4 Imprinted Nanofibers

Nanofibers are nanostructures with diameters in the nanometer range. They have been resourcefully used in sensing applications. Piperno and co-authors (Michael et al. 1995) immobilized polymer nanofibers in Imp-NPs for an amino acid derivative and used them in a fluorescence-based sensor for dansyl-L-phenylalanine detection. An Imp-nanofiber membrane was synthesized using *N*- α -benzyloxycarbonyl-D-glutamic acid (Z-D-Glu) or *N*- α -benzyloxycarbonyl-L-glutamic acid (Z-L-Glu) as imprint molecules for sensing amino acid derivatives. Cellulose acetate was also used to synthesize Imp-nanofiber membranes by the electrospay method for the same analytes.

3 Application of Nano-optical Biosensor for Determination of Food Contaminants

3.1 Plasmonic Nano-biosensors for Detection of *E. coli* Bacteria

Biosensors work on the principle of refractive index changes induced by chemicals applied on the nanopatterned surface and measurement of LSPR wavelength shifts caused by this difference in refractive index change. Fabrications are done with E-Beam Lithography (EBL) which allows more precise control in fabrication in terms of shape, size, and periodicity compared to the other nanopatterning techniques. The first step of fabrication is the preparation of sapphire samples for EBL lithography. Preparation starts with spin coating the sensor with E-line resist at 4000 rpm for 40 s, baking the surface at 110 °C for 2 min, and then coating the

surface with aqua-save since the sample is to be introduced into E-line device (<http://www.nanotechnology.bilkent.edu.tr/eng/photonic>).

3.2 PANI–Ag–Cu Nanocomposite Thin Films Based Impedimetric Microbial Sensor for Detection of E. coli Bacteria

PANI–Ag–Cu nanocomposite thin films were prepared by sol–gel method and deposited on the glass substrate using the spin coating technique. Polyaniline was synthesized by chemical oxidative polymerization of aniline monomer in the presence of nitric acid. The films were characterized using XRD, FTIR, and UV–visible spectroscopy. The performance of the sensor was conducted using electrochemical impedance spectroscopy to obtain the change in impedance of the sensor film before and after incubation with *E. coli* bacteria in water. The peaks in the XRD pattern confirm the presence of Ag and Cu nanoparticles in face-centered cubic structure.

Impedance analysis indicates that the change in impedance of the films decreases with the presence of *E. coli*. The sensitivity on *E. coli* increases for the sample with high concentration of Cu (Huda et al. 2014).

3.3 A Nanoporous Membrane-Based Impedimetric Immunosensor for Label-Free Detection of Pathogenic Bacteria in Whole Milk

A nanoporous membrane-based impedimetric immunosensor was used for the label-free detection of bacterial pathogens in whole milk. A simple and rapid method to modify a commercially available alumina nanoporous membrane with hyaluronic acid (HA) effectively reduced the non-specific binding of biomolecules and other cells, and permitted successful immobilization of antibodies. *Escherichia coli* O157:H7, one of the most harmful food-borne pathogenic bacteria, was tested as a model pathogen in this study (Joung et al. 2013).

3.4 A Micro-fluidic Nano-biosensor for the Detection of Pathogenic Salmonella

Quantum dot nanoparticles were used to detect *Salmonella* cells. For selective detection of *Salmonella*, *anti-Salmonella* polyclonal antibodies were covalently immobilized onto the quantum dot surface. To separate and concentrate the cells

from the sample, super paramagnetic particles and a microfluidic chip were used. A portable fluorometer was developed to measure the fluorescence signal from the quantum dot nanoparticles attached to *Salmonella* in the samples. The sensitivity for detection of pathogenic *Salmonella* was evaluated using serially diluted *Salmonella*. The detection limit of the sensor was 103 CFU/mL *Salmonella* in both borate buffer and food extract (Giyoungh et al. 2015).

3.5 DNA Functionalized Direct Electrodeposited Gold Nano-aggregates for Efficient Detection of *Salmonella typhi*

The electrochemical DNA biosensor for the detection of *Salmonella typhi* in urine and blood samples was fabricated by direct electrodeposition of gold nano-aggregates (GNAs). *Salmonella typhi* (*S. typhi*) specific 5'-amine modified single-stranded DNA (ssDNA, NH₂-(C6)-5'-CGTGCGCGACGCCCGCCGCC3') was covalently immobilized on to GNAs-ITO (indium tin oxide) electrode. The detection of *S. typhi* from urine and blood samples using fabricated ssDNA-GNA-ITO bio-electrode showed promising results and have the potential to be used as a sensor for real patient samples (Anu et al. 2015).

3.6 Nano-gold Sensor for Detection of *Salmonella* spp. in Foods

A polymerase chain reaction and a novel method using DNA-gold nanoparticles conjugates for specificity and high sensitivity detection of *Salmonella* spp. was reported.

The technology utilizes gold nanoparticles derivatized with thiol modified oligonucleotides that are designed to bind complementary DNA targets. The hybridization between the target (*inv A* of *Salmonella*) and nanoparticle probes creates links between the nanoparticles resulting in the formation of nanoparticle aggregates and color shift that can be used for *Salmonella* detection in foods. Probes and primers for target DNA (*inv A* gene of *Salmonella*) were designed and ordered (Patel et al. 2006).

3.7 Carbon Nanotube Immunosensor for *Salmonella*

Rapid and easy detection of food-borne bacteria such as *Salmonella* would be a useful tool for protecting public health. An ideal sensor technology would be small

and cheap enough to enable automated detection of food-borne disease at multiple locations along the product chain, from harvest and transportation to point-of-use in the kitchen. Biosensors that combine biological elements for target recognition with an all-electronic, nano-enabled readout element are promising candidates for use as very large sensor arrays that could assist medical diagnosis or other analysis through the simultaneous quantification of hundreds of biological and/or biomolecular targets using a single small-volume sample. Therefore, the investigation of the carbon nanotube-based immunosensor to detect *Salmonella* was applied (Khamis et al. 2011).

3.8 Application of Room Temperature Photoluminescence from ZnO Nano-rods for Salmonella Detection

ZnO nano-rods grown by gaseous disperse synthesis were used to determine the *Salmonella*. This is performed by the two emission bands emitted from ZnO nano-rods at 376 and 520 nm. A bio-sensitive layer is prepared by immobilization of *Anti-Salmonella* antibodies (Ab) from liquid solutions on the ZnO surface. After further reaction with *Salmonella* antigens (Ag), the PL intensity is found to decrease proportional to antigen concentrations in the range of 1000–1,000,000 cell/mL (Roman et al. 2014).

3.9 Real-Time and Sensitive Detection of Salmonella typhimurium Using an Automated Quartz Crystal Micro Balance (QCM) Instrument with Nanoparticles Amplification

A rapid and real-time detection of *Salmonella typhimurium* was performed by quartz crystal microbalance (QCM) instrument with a microfluidic system. The QCMA-1.0 bare gold sensor chip which contains two sensing array was modified by covalently immobilizing the monoclonal capture antibody on the active spot and a mouse IgG antibody on the control spot using a conventional amine coupling chemistry (EDC-NHS). The binding of the *Salmonella* cells onto the immobilized *anti-Salmonella* antibody alters the sensor frequency which was correlated to cells concentration in the buffer samples. *Salmonella* cells were detected using direct, sandwich, and sandwich assay with antibody conjugated gold nanoparticles (Faridah et al. 2013).

3.10 Universal Biomolecular Signal Transduction-Based Nano-electronic Bio-detection System

The development of rapid and ultrasensitive detection technologies are a long-standing goal for researchers in the bio-detection fields. Nanowire field-effect transistor (nano-FET) devices have shown great promise in label-free and ultrasensitive detection of biological agents. However, critical application problems in using this technology have not been addressed, particularly the difficulties of FET sensing surface modification for various targets and lower detection specificity in real biological samples. A novel molecular signal transduction system reported herein overcomes such problems. With this system, various complicated biomolecular interactions are “translated” into simple signal molecules with universal sequences (Wusi et al. 2008).

3.11 Highly Sensitive SERS-Based Immunoassay of Aflatoxin B1 Using Silica-Encapsulated Hollow Gold Nanoparticles

Aflatoxin B1 (AFB1) is carcinogenic contaminant in foods. Because of its potential toxicity, it is considered as an extremely hazardous compound to the human nervous system. AFB1 is used as a biochemical marker to evaluate the degree of food spoilage. In this study, a novel surface-enhanced Raman scattering (SERS) based immunoassay platform using silica-encapsulated hollow gold nanoparticles (SEHGNs) and magnetic beads was developed for highly sensitive detection of AFB1. Quantitative analysis of AFB1 was performed by monitoring the intensity change of the characteristic peaks of Raman reporter molecules. The limit of detection (LOD) of AFB1, determined by this SERS-based immunoassay, was determined to be 0.1 ng/mL (Juhui et al. 2015).

3.12 A Simple and Rapid Optical Biosensor for Detection of Aflatoxin B1 Based on Competitive Dispersion of Gold Nano-rods

A one-step and label-free gold nano-rods optical biosensor is used for the assessment of aflatoxin B1 (AFB1). In this research, gold nano-rods (GNRs) were employed as a sensing platform, which showed high stability under high ionic strength conditions without the addition of any stabilizing agent. The developed method could effectively reduce false results caused by undesirable aggregation, which is a big problem for spherical gold nanoparticles. The absorption intensity of

UV-vis spectra served as the sensing indicator, with dynamic light scattering (DLS) measurement as another sensing tool with a linear range from 0.5 to 20 ng/mL. And the limit of detection (LOD) was 0.16 ng/mL, indicating an excellent sensitivity with absorbance result (Xia et al. 2013).

References

- Abhilash M (2010) Potential applications of nanoparticles. *Int J Pharma Bio Sci* 1:1–12
- Adley C, Ryan MP (2014) Conductometric biosensor for high throughput screening of pathogens in food. In: Bhunia AK, Kim MS, Taitt CR (eds) High throughput screening for food safety assessment: biosensor technologies, hyperspectral imaging and practical applications. Elsevier, Cambridge, pp 315–326
- Alexander C, Davidson L, Hayes W (2003) Imprinted polymers: artificial molecular recognition materials with applications in synthesis and catalysis. *Tetrahedron* 59:2025–2057
- Allman III RM (1983) Structural variations in colloidal crystals, M.S. thesis, UCLA
- Allman III RM, Onoda Jr GY (1984) Unpublished work, IBM T.J. Watson Research Center
- Anu S, Meenakshi C, Singh MP, Verma HN, Surinder PS, Kavita A (2015) DNA functionalized direct electro-deposited gold nanoaggregates for efficient Detection of *Salmonella typhi*. *Bioelectrochemistry* 105:7–15
- Attia MS (2010) Spectrofluorimetric assessment of ramipril using optical sensor samarium ion–doxycycline complex doped in sol–gel matrix. *J Pharm Biomed Anal* 51:7–11
- Attia MS, Aboaly MM (2010) Highly sensitive and selective spectrofluorimetric determination of metoclopramide hydrochloride in pharmaceutical tablets and serum samples using Eu 3⁺ ion doped in sol–gel matrix. *Talanta* 82:78–84
- Attia MS, Othman AM, Aboaly MM, Abdel-Mottaleb MSA (2010) Novel spectrofluorimetric method for measuring the activity of the enzyme α -l-fucosidase using the nano composite optical sensor samarium(iii)–doxycycline complex doped in sol–gel matrix. *Anal Chem* 82:6230–6236
- Attia MS, Youssef AO, Essawy AA, Abdel-Mottaleb MSA (2012a) A highly luminescent complexes of Eu(III) and Tb(III) with norfloxacin and gatifloxacin doped in sol–gel matrix: a comparable approach of using silica doped Tb(III) and Eu(III) as optical sensor. *J Lumin* 132:2741–2746
- Attia MS, Ramsis MN, Khalil LH, Hashem SG (2012b) Spectrofluorimetric assessment of chlorzoxazone and Ibuprofen in pharmaceutical formulations by using Eu-tetracycline HCl optical sensor doped in sol–gel matrix. *J Fluoresc* 22:779–788
- Attia MS, Youssef AO, El-Sherif RH (2014a) Durable diagnosis of seminal vesicle and sexual gland diseases using the nano optical sensor thin film Sm-doxycycline complex. *Anal Chim Acta* 835:56–64
- Attia MS, Zoulghena H, Abdel-Mottaleb MSA (2014b) A new nano-optical sensor thin film cadmium sulfide doped in sol–gel matrix for assessment of α -amylase activity in human saliva. *Analyst* 139:793–800
- Biacore. <https://www.biacore.com/lifesciences/index.html>. Accessed 14 Jan 2014
- Brinker CJ, Mukherjee SP (1981) Conversion of monolithic gels to glasses in a multicomponent silicate glass system. *J Mater Sci* 16:1980–1988
- Brinker CJ, Keefer KD, Schaefer DW, Ashley CS (1982) Sol–gel transition in simple silicates. *J Non Cryst Solids* 48:47–64
- Cai D, Ren L, Zhao H, Xu C, Zhang L, Yu Y, Wang H, Lan Y, Roberts MF, Chuang JH, Naughton MJ, Ren Z, Thomas C (2010) A molecular-imprint nanosensor for ultrasensitive detection of proteins. *Nat Nanotechnol* 5:597–601

- Cheong WJ, Yang SH, Ali F (2013a) Molecular imprinted polymers for separation science: a review of reviews. *J Sep Sci* 36:609–628
- Cheong WJ, Ali F, Choi JH, Lee JO, Sung KY (2013b) Recent applications of molecular imprinted polymers for enantio-selective recognition. *Talanta* 106:45–59
- Chiodini N, Morazzoni F et al (1999) Sol–gel synthesis of monolithic tin-doped silica glass. *J Mater Chem* 9:2653–2658
- Cunliffe D, Kirby A, Alexander C (2005) Molecularly imprinted drug delivery systems. *Adv Drug Deliv Rev* 57:1836–1853
- Dislich H (1971a) New routes to multicomponent oxide glasses. *Angew Chem Int Ed* 10:363–370
- Dislich H (1971b) New routes to multicomponent oxide glasses. *Angew Chem Int Ed Eng* 10: 363–372
- Esfandyari-Manesh M, Javanbakht M, Atyabi F, Mohammadi A, Mohammadi S, Akbari-Adergani B, Dinarvand R (2011) Dipyrindamole recognition and controlled release by uniformly sized molecularly imprinted nanospheres. *Mater Sci Eng, C* 31:1692–1699
- Faridah S, Yildiz U, Ibtisam ET (2013) Real-time and sensitive detection of *Salmonella typhimurium* using an automated quartz crystal microbalance(QCM) instrument with nanoparticles amplification. *Talanta* 115:761–767
- Fuchs Y, Soppera O, Haupt K (2012) Photopolymerization and photostructuring of molecularly imprinted polymers for sensor applications—a review. *Anal Chim Acta* 717:7–20
- Giyoung K, Moon J-H, Moh C-Y, Lim J (2015) A microfluidic nano-biosensor for the detection of pathogenic *Salmonella*. *Biosen Bioelectron* 67:243–247
- Guan G, Liu B, Wang Z, Zhang Z (2008) Imprinting of molecular recognition sites on nanostructures and its applications in chemosensors. *Sensors* 8:8291–8320
- Gültekin A, Ersöz A, Denizli A, Say R (2012) Gold–silver-nanoclusters having cholic acid imprinted nanoshell. *Talanta* 93:364–370
- He C, Long Y, Pan J, Li K, Liu F (2007) Application of molecularly imprinted polymers to solid-phase extraction of analytes from real samples. *J Biochem Biophys Methods* 70:133–150
- Huda A, Norshafadzila MN, Noor ANA, Aidil AH (2014) PANI–Ag–Cu nanocomposite thin films based impedimetric microbial sensor for detection of *E. coli* bacteria. *J Nanomater*, ID 951640
- Ikesue A (2002) Polycrystalline Nd: YAG ceramics lasers. *Opt Mater* 19:183–187
- Ikesue A, Kinoshita T, Kamata K, Yoshida K (1995) Fabrication and optical properties of high-performance polycrystalline Nd: YAG ceramics for solid-state lasers. *J Am Ceram Soc* 78:1033–1040
- Joung C-K, Kim H-N, Lim M-C, Jeon T-J, Kim H-Y, Kim Y-R (2013) Ananoporous membrane-based impedimetric immunosensor for label-free detection of pathogenic bacteria in whole milk. *Biosen. Bioelectronics* 44:210–215
- Juhui K, Chankil L, Jaebum C (2015) Highly sensitive SERS-based immunoassay of aflatoxin B1 using silica-encapsulated hollow gold nanoparticles. *J Hazard Mater* 285:11–17
- Khamis SM, Jones RA, Johnson ATC (2011) Carbon nanotube immunosensor for *Salmonella*. *AIP Adv* 1:22106
- Klein LC, Garvey GJ (1980) Kinetics of the sol–gel transition. *J Non Cryst Solids* 38:45–50
- Kryscio DR, Peppas NA (2012) Critical review and perspective of macromolecularly imprinted polymers. *Acta Biomater* 8:461–473
- Lakshmi D, Bossi A, Whitcombe MJ, Chianella I, Fowler SA, Subrahmanyam S, Piletska EV, Piletsky SA (2009) Electrochemical sensor for catechol and dopamine based on a catalytic molecularly imprinted polymer-conducting polymer hybrid recognition element. *Anal Chem* 81:3576–3584
- Leung A, Shankar PM, Mutharasan R (2007) A review of fiber-optic biosensors. *Sens Actuators B Chem* 125:688–703
- Li H, Xu W, Wang N, Ma X, Niu D, Jiang B, Liu L, Huang W, Yang W, Zhou Z (2012a) Synthesis of magnetic molecularly imprinted polymer particles for selective adsorption and separation of dibenzothiophene. *Microchim Acta* 179:123–130
- Li J, Wei G, Zhang Y (2012b) Molecularly imprinted polymers as recognition elements in sensors. In: *Molecularly imprinted sensors*. Elsevier, Amsterdam, pp 35–55

- Li J, Wei G, Zhang Y (2012c) Molecularly imprinted polymers as recognition elements in sensors. Molecularly imprinted sensors. Elsevier, Amsterdam, pp 35–55
- Malitesta C, Mazzotta E, Picca RA, Poma A, Chianella I, Piletsky SA (2012) MIP sensors—the electrochemical approach. *Anal Bioanal Chem* 402:1827–1846
- Marzolin C, Smith SP et al (1998) Fabrication of glass microstructures by micro-molding of sol-gel precursors. *Adv Mater* 10(8):571–574
- Matićević E (1986) Monodispersed colloids: art and science. *Langmuir* 2:12–20
- Matsui J, Takayose M, Akamatsu K, Nawafune H, Tamaki K, Sugimoto N (2009) Molecularly imprinted nanocomposites for highly sensitive SPR detection of a non-aqueous atrazine sample. *Analyst* 134:80–86
- Mayes AG, Whitcombe MJ (2005) *Adv Drug Del Rev* 57:1742–1778
- Mecea VM (2006) Is quartz crystal microbalance really a mass sensor? *Sens Actuators A Phys* 128:270–277
- Menaker A, Syritski V, Reut J, Öpik A, Horváth V, Gyurcsányi RE (2009) Electrosynthesized surface-imprinted conducting polymer microrods for selective protein recognition. *Adv Mater* 21:2271–2275
- Michael J, Whitecome M, Rodrigue E, Villar P (1995) A new method for the introduction of recognition site functionality into polymers prepared by molecular imprinting: synthesis and characterization of polymeric receptors for cholesterol. *J Am Chem Soc* 117:7105–7111
- Mujahid A, Lieberzeit PA, Dickert FL (2010) Chemical sensors based on molecularly imprinted sol-gel materials. *Materials* 3:2196–2217
- Narsaiah K, Jha SN, Bhardwaj R, Sharma R, Kumar R (2012) Optical biosensors for food quality and safety assurance—a review. *J Food Sci Technol* 49:383–406
- Ohk SH, Bhunia AK (2013) Multiplex fiber optic biosensor for detection of *Listeria monocytogenes*, *Escherichia coli* O157:H7 and *Salmonella enterica* from ready-to-eat meat samples. *Food Microbiol* 33:166–171
- Patel JR, Bhagwat AA, Sanglay GC, Solomon MB (2006) Rapid detection of *Salmonella* from hydrodynamic pressure-treated poultry using molecular beacon real-time PCR. *Food Microbiol* 23:39–46
- Pichon V, Chapuis-Hugon F (2008) Role of molecularly imprinted polymers for selective determination of environmental pollutants—a review. *Anal Chim Acta* 622:48–61
- Piletsky SA, Turner NW, Laitenberger P (2006) Molecularly imprinted polymers in clinical diagnostics—future potential and existing problems. *Med Eng Phys* 28:971–977
- Poma A, Guerreiro A, Whitcombe MJ, Piletska EV, Turner APF, Piletsky SA (2013) Solid-phase synthesis of molecularly imprinted polymer nanoparticles with a reusable template—“plastic antibodies”. *Adv Funct Mater* 23:2821–2827
- Prochazka S, Klug FJ (1983) Infrared-transparent mullite ceramic. *J Am Ceram Soc* 66:874–880
- Ray SS, Okamoto M (2003) Polymer/layered silicate nanocomposites: a review from preparation to processing. *Prog Polym Sci* 28:1539–1641
- Reyes PI, Li J, Duan Z, Yang X, Cai Y, Huang Q, Lu Y (2013) ZnO surface acoustic wave sensors built on zein-coated flexible food packages. *Sens. Lett* 11:539–544
- Roman V, Volodymyr K, Nikolay S, Yulia O, Sergey G, Zanda G, Nicolay P, Rositsa Y, Donats E, Valentyn S, Arnolds U (2014) Application of room temperature photoluminescence from ZnO nanorods for *Salmonella* detection. *IEEE Sens J* 14(6):2028–2034
- Sakka S, Kamiya K (1980) Glasses from metal alcoholates. *J Non Cryst Solids* 42:403–421
- Sakka S, Kamiya K (1982) The sol-gel transition in the hydrolysis of metal alkoxides in relation to the formation of glass fibers and films. *J Non Cryst Solids* 48:31–46
- Shang XY, Zhu ZK, Yin J, Ma XD (2002) Compatibility of soluble polyimide/silica hybrids induced by a coupling agent. *Chem Mater* 14:71–77
- Takeda K, Kobayashi T (2005) Bisphenol A imprinted polymer adsorbents with selective recognition and binding characteristics. *Sci Technol Adv Mater* 6:165–171
- Thakur MS, Ragavan KV (2010) Biosensors in food processing. *J Food Sci Technol* 50:625–641
- Thusu R (2014a) Strong growth predicted for biosensor market. <http://www.sensorsmag.com/specialty-markets/medical/strong-growth-predicted-biosensors-market-7640>

- Thusu R (2014b) Sensors facilitating health monitoring. <http://www.sensorsmag.com/specialty-markets/medical/sensors-facilitate-health-monitoring-8365>
- Tokonami S, Shiigi H, Nagaoka T (2009) Review: micro-and nanosized molecularly imprinted polymers for high-throughput analytical applications. *Anal Chim Acta* 641:7–13
- Turiel E, Martin-Esteban A (2010) Molecularly imprinted polymers for sample preparation: a review. *Anal Chim Acta* 668:87–99
- Vaseashta A, Dimova-Malinovska D (2005) Nanostructured and nanoscale devices, sensors and detectors. *Sci Technol Adv Mater* 6:312–318
- Velusamy V, Arshak K, Korostynska O, Oliwa K, Adley C (2010) An overview of food borne pathogen detection: in the perspective of biosensors. *Biotechnol Adv* 28:232–254
- Wang HT, Wu X, Zhao H, Quan X (2012) Enhanced photocatalytic degradation of tetracycline hydrochloride by molecular imprinted film modified TiO₂ nanotubes. *Chin Sci Bull* 57: 601–605
- Wusi CM, Nirankar NM, Shiva KR, Eric C, Brian F, Paul W, Gary KM (2008) Universal bio-molecular signal transduction-based nano-electronic bio-detection system. *Sens Actuators B* 133:547–554
- Xia X, Xiangjiang L, Yanbin L, Yibin Y (2013) A simple and rapid optical biosensor for detection of aflatoxin B1 based on competitive dispersion of gold nano rods. *Biosen Bioelectronics* 47:361–367
- Yan H, Row KH (2006) Characteristic and synthetic approach of molecularly imprinted polymer. *Int J Mol Sci* 7:155–178
- Yang X, Zitova A, Kirsch J, Fergus JW, Overfelt RA, Simonian AL (2012) Portable and remote electrochemical sensing system for detection of tricresyl phosphate in gas phase. *Sens Actuators B Chem* 161:564–569
- Yang X, Kirsch J, Simonian A (2013) *Campylobacter* spp. detection in the 21st century: a review of the recent achievements in biosensor development. *J Microbiol Methods* 95:48–56
- Yoldas BE (1979) Monolithic glass formation by chemical polymerization. *J Mater Sci* 14:1843–1849
- Yongqin L, Tianwei T, Frantisek S (2013) Molecular imprinting of proteins in polymers attached to the surface of nanomaterials for selective recognition of biomacromolecules. *Biotechnol Adv* 31:1172–1186
- Zhai D, Liu B, Shi Y, Pan L, Wang Y, Li W, Zhang R, Yu G (2013) Highly sensitive glucose sensor based on Pt nanoparticle/polyaniline hydrogel heterostructures. *ACS Nano* 7:3540–3546
- Zhang S, Yu A, Song X, Liu X (2013) Synthesis and characterization of waterborne UV-curable polyurethane nanocomposites based on the macromonomer surface modification of colloidal silica. *Prog Org Coat* 76:1032–1039
- Zou H, Wu S, Shen J (2008) Polymer/silica nanocomposites: preparation, characterization, properties, and applications. *Chem Rev* 108:3893–3957

Chapter 2

Functionalization of Tamarind Gum for Drug Delivery

Amit Kumar Nayak and Dilipkumar Pal

Abstract Tamarind gum is a plant polysaccharide extracted from seed endosperm of the plant, *Tamarindus indica* Linn. (Family: Fabaceae). It is a neutral, nonionic, and branched polysaccharide having water solubility, hydrophilic, gel-forming, and mucoadhesive properties. In addition, tamarind gum is biodegradable, biocompatible, noncarcinogenic, and nonirritant. Tamarind gum is employed as a potential biopolymer in the fields of pharmaceutical, cosmetic, and food applications. In the recent years, it is widely tested and employed in various drug delivery applications as effective pharmaceutical excipients. Tamarind gum is being exploited in the formulation of oral, colon, ocular, buccal, and nasal drug delivery systems. Though tamarind gum is extensively used in various drug delivery formulations, it has some potential drawbacks such as unpleasant odor, dull color, poor solubility in water, tendency of fast degradability in aqueous environment. To overcome these restrictions, tamarind gum has been functionally derivatized through chemical treatment with a variety of functional groups such as carboxymethyl, acetal, hydroxyl alkyl, thiol, polymer grafting, etc. Recently, various functionally derivatized tamarind gums hold a great promise as potential pharmaceutical excipients in different kinds of improved drug delivery systems mainly because of its improved stability (lower degradability). These functionally derivatized tamarind gums hold enhanced mechanical behavior as well as competence in prolonged period-controlling drug releases. The present chapter contends with a broad review of different kinds of functionalizations of tamarind gum for their use in the development of various improved drug delivery systems. The first part includes sources, compositions, properties and uses of tamarind gum. Then, the latter part contains a comprehensive review of different functionalizations of tamarind gum in drug delivery.

A.K. Nayak (✉)

Department of Pharmaceutics, Seemanta Institute
of Pharmaceutical Sciences, Mayurbhanj 757086, Odisha, India
e-mail: amitkrnayak@yahoo.co.in

D. Pal

Department of Pharmaceutical Sciences, Guru Ghasidas
Vishwavidyalaya, Koni, Bilaspur 495009, Chhattisgarh, India

Keywords Tamarind gum · Functionalization · Carboxymethylation
Thiolation · Graft modification · Drug delivery

1 Introduction

Day by day, the medicinal and biomedical uses of various plant-derived materials are gaining significance over synthetic materials because of large availability in nature, eco-friendly renewable, and sustainable extraction facility with lower cost (Nayak et al. 2010, 2012; Pal and Mitra 2010; Pal et al. 2012). Among these materials, plant-derived natural gums have recently established their worth as biopolymers due to their biosafety, biodegradability, and inexpensive sustainable productions from the natural resources (Hasnain et al. 2010; Avachat et al. 2011; Nayak et al. 2015; Nayak and Pal 2012). Plant-derived gums are those natural polysaccharides, which contain manifold sugar units interconnected to compose macromolecular structures with a broad range of physiological characteristics (Nayak and Pal 2012, 2016). Gums are actually pathological byproducts of plants. Gums contain some salts (sodium, potassium, calcium, magnesium, etc.) of complex materials (Nayak and Pal 2016). Almost all natural gums are able to form gels (i.e., three-dimensional molecular networks). Gel strength of gums depends on several issues of the gum characteristics like molecular structure, concentration, ionic strength, pH, temperature, etc. (Jani et al. 2009; Rana et al. 2011). The natural gums exhibit swelling capacity as a result of the trap of larger water volume in-between the branches as well as chains (Nayak and Pal 2016). The majority of natural gums is metabolized by intestinal microflora and finally, is able to degrade the simpler sugar components (Rana et al. 2011; Prajapati et al. 2013). Moreover, intestinal enzymes are able to cleave these gums at the specific sites (Rana et al. 2011).

Recently, various plant-derived natural gums are being investigated and employed in the different kinds of drug delivery systems on account of their diverse characteristics (Jani et al. 2009; Prajapati et al. 2013). Most of these gums are biodegradable, biocompatible, and also safe enough for oral consumption (Prajapati et al. 2013). Unfortunately, there are several potential drawbacks with the use of plant-derived native gums in biomedical as well as pharmaceutical applications. These drawbacks include pH responsive solubility, uncontrolled hydration rate, viscosity decrease after longer storage, chances of microbial contaminations, etc. (Rana et al. 2011). To overcome these above-said drawbacks of plant-derived native gums, various kinds of functionalizations of different plant-derived native gums through chemical modifications like carboxymethylation (Pal et al. 2011; Das et al. 2014), carbamoylethylation (Sharma et al. 2004), cyanoethylation (Goyal et al. 2008), thiolation (Sharma and Ahuja 2011), graft modification (Mishra et al. 2006; Pandey et al. 2014), etc., are being researched by various groups. These functionalized natural gums not only limit various weaknesses of native gums but also make possible the utilization prospects as improved drug delivery excipients.

Amongst a variety of plant-derived polysaccharides, tamarind gum is promising biopolymer (Pal and Nayak 2015; Nayak 2016). It is extracted from tamarind seed endosperm and often, it is also called as tamarind kernel gum. Food and Drug Administration (FDA) has recognized this plant polysaccharide as a generally regarded safe (GRAS) substance in their GRAS Notice (2014). Therefore, it should be considered as safe for oral consumption. It is widely utilized as polymer in various applications such as pharmaceutical, cosmetic, food, chemical engineering, paper, textile, etc. (Pal and Nayak 2015; Nayak 2016). In the recent years, tamarind gum is being researched and exploited as valuable excipients in a variety of dosage systems for improved drug deliveries (Manchanda et al. 2014; Pal and Nayak 2015; Nayak 2016). Currently, the properties of tamarind gum have been improved through functionally modifications by chemical derivatization with different functional groups such as carboxymethyl, acetal, hydroxyl alkyl, thiol, etc. (Goyal et al. 2007, 2008; Kaur et al. 2012a, b). Additionally, grafting modifications of tamarind gum are also helpful to improve various potential polymer properties of tamarind gum (Manchanda et al. 2014). On the basis of the above discussion, the present chapter contends with a broad review of different kinds of functionalizations of tamarind gum for their use in the development of various improved drug delivery systems. The first part includes sources, compositions, properties, and uses of tamarind gum. Then, the latter part contains a comprehensive review of different functionalizations of tamarind gum in drug delivery.

2 Tamarind Gum: Sources, Composition, Properties, and Uses

2.1 Sources

Tamarind gum is a plant polysaccharide extracted from seed endosperm of the plant, *Tamarindus indica* Linn. (commonly known as ‘Indian date’; ‘Imli’, in Hindi; Family: Fabaceae) seeds (Pal and Nayak 2012). The extraction procedure of tamarind gum was first reported by Rao et al. (1946) and they extracted it from tamarind seed kernel powder. Rao and Srivastava (1973) and then Nandi (1975) further modified this extraction procedure to extract tamarind gum on the laboratory scales. In general, chemical and enzymatic procedures of tamarind gum extraction are employed. In chemical extraction procedure, tamarind seed kernel powder is generally soaked in the boiled water and then filtered to separate the extracted mucilage. The collected filtered mucilage material is put into the equal volume of ethanol or acetone to obtain precipitate gum. The extracted precipitate is then dried as tamarind gum (Nayak and Pal 2011). The enzymatic extraction procedure includes mixing up of tamarind seed kernel powder with ethanol and following reaction with the protease (an enzyme). Subsequent to the enzymatic treatment by protease, it is centrifuged. The supernatant is collected and treated with ethanol to

obtain precipitation of tamarind gum. The extracted precipitate is then dried as tamarind gum (Tattiyakul et al. 2010).

2.2 Composition

Tamarind gum is a neutral, non-charged and branch-structured polysaccharide (Nayak 2016). It is composed of (1 → 4)-β-D-glucan backbone-substituted with side chains of α-D-xylopyranose and β-D-galactopyranosyl (1 → 2)-α-D-xylopyranose linked (1 → 6) to glucose residues, where 55.4% of glucose, 28.4% of xylose and 16.2% of galactose units are present corresponding to a molar ratio of 2.8:2.25:1.0 (i.e., glucose:xylose:galactose) (Nayak and Pal 2011; Pal and Nayak 2015). Therefore, it is regarded as galactoxyloglucan (Nayak 2016). In the tamarind gum structure, glucose residues (80%) are substituted by xylose residues (1–6 linked) along with partly substituted by p-1–2 galactose residues (Lang et al. 1992; Manchanda et al. 2014). The molecular structure of tamarind gum is presented in Fig. 1. It is already reported that the molecular weight of tamarind gum is $2.5\text{--}6.5 \times 10^5$ (Zhang et al. 2008; Pal and Nayak 2015).

2.3 Properties and Uses

Tamarind gum is an aqueous soluble and hydrophilic polysaccharide (Nayak 2016). It swells in aqueous solutions to produce mucilaginous gels, which usually confirms characteristic rheological behavior of non-Newtonian and pseudoplastic nature

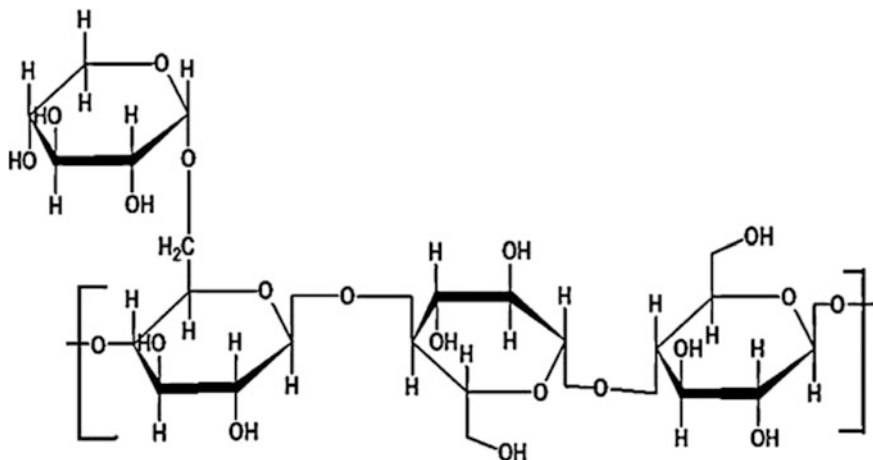


Fig. 1 Chemical structure of tamarind gum

(Joseph et al. 2012; Pal and Nayak 2015). The high degree substitution of glucan chains in the tamarind gum structure generates stiff as well as extended conformation with the aqueous volume occupancy in larger amounts in aqueous solutions. The native form of tamarind gum also demonstrates a tendency of self-aggregation in the aqueous solutions (Pal and Nayak 2015). The tamarind gum self-aggregates comprise lateral assemblies of single polysaccharidic strands, which can be explicated by the so-called Kuhn's model (Gupta et al. 2010; Nayak 2016). Tamarind gum is not soluble in the cold water, in general, and easily soluble in the warm water to produce highly viscous mucilaginous gels with broad pH tolerance along with adhesivity (Rao and Srivastava 1973). Like other natural gums, it is not soluble in methanol, ethanol, acetone, and ether (Joseph et al. 2012). It is stable in acidic pH. Tamarind gum can also forms gels in acidic as well as neutral pH. It possesses the ability to produce highly viscous gels with sugars (Gupta et al. 2010). Tamarind gum has been found as a biodegradable, biocompatible, noncarcinogenic, non-irritant polymer (Khanna et al. 1987; Avachat et al. 2011). It has also been illustrated as bioadhesive as well as mucomimetic biopolymer. Tamarind gum has also revealed anti-inflammatory, hepatoprotective, and antidiabetic nature (Samal and Dangi 2014). It also possesses film forming property with high flexibility and good tensile strength, high drug holding capacity, and high thermal stability (Pal and Nayak 2015). Like other xyloglucans, tamarind gum is not digested by the influence of human digestive enzymes. It may be considered as part of the dietary fiber fraction of the diet. However, it is fermented by means of intestinal microbiota (Hartemink et al. 1996). Even after degradation of the carbohydrate polymeric backbone of tamarind gum, several polysaccharide strains representing numerous species are capable to ferment into oligosaccharides (Nayak 2016).

Tamarind gum has already found its potential applications in the fields of food, pharmaceutical and cosmetic science (Pal and Nayak 2015; Nayak 2016). Recent years, tamarind gum is widely studied and also employed as one of the emerging plant-derived natural polysaccharides as pharmaceutical excipients (such as, thickener, suspending agent, emulsifier, gelling agent, binder, release modifier, etc.) in various drug delivery applications (Deveswaran et al. 2009; Gupta et al. 2010; Pal and Nayak 2015; Nayak 2016). Tamarind gum is employed as useful excipient in the formula of matrix tablets for numerous drugs (Chanda et al. 2008; Chandramouli et al. 2012). It is also exploited in the development of oral (Pal and Nayak 2012; Nayak et al. 2014a; Nayak 2016), buccal (Bangle et al. 2011; Avachat et al. 2013), colon (Mishra and Khandare 2011), nasal (Datta and Bandyopadhyay 2006), and ocular (Mehra et al. 2010) drug deliveries. Furthermore, tamarind gum finds its utilization as mucoadhesive biopolymers in the formulation of different bio-mucoadhesive drug delivery systems (Datta and Bandyopadhyay 2006; Bangle et al. 2011; Avachat et al. 2013; Pal and Nayak 2015; Nayak 2016). Tamarind gum has been exploited for the preparation of various multiple-unit sustained drug releasing carriers, such as spheroids, beads, microparticles, etc., for oral administration (Kulkarni et al. 2005; Nayak and Pal 2011, 2013; Nayak et al. 2013, 2014a, b; Pal and Nayak 2012; Jana et al. 2013; Bera et al. 2015).

3 Rationality of Tamarind Gum Functionalization

Though tamarind gum is extensively used in various biomedical applications including its wide application ranges in pharmaceutical formulations as excipients, it has some potential drawbacks (Manchanda et al. 2014; Pal and Nayak 2015; Nayak 2016). Native tamarind gum possesses unpleasant odor and dull color, (Kaur et al. 2012a; Meenakshi and Ahuja 2015). It also exhibits its poor solubility in water (Kaur et al. 2012a). Additionally, tamarind gum usually displays the presence of water insoluble components and possesses tendency of fast degradability in aqueous environment (Meenakshi and Ahuja 2015). To overcome these restrictions, tamarind gum has been functionalized by chemical modifications through incorporating a variety of functional groups (i.e., modifications of various functional groups of polymer structure) like carboxymethyl, acetal, hydroxyl alkyl, thiol, etc. (Goyal et al. 2008; Kaur et al. 2012a, b). Besides these, tamarind gum is also modified through polymer grafting (Manchanda et al. 2014). The functional derivatization of tamarind gum with functional groups interrupts the native tamarind gum structure organization, and thus, revealing the hydration of carbohydrate networks (Lang et al. 1992; Kaur et al. 2012b). These properties help to achieve high viscosity and low degradability. These functional derivatizations of tamarind gum also improve the self-life of it (Rana et al. 2011). In recent times, various functionally derivatized tamarind gum holds a great promise as potential pharmaceutical excipients in different kinds of improved drug delivery systems mainly because of its improved stability (lower degradability) (Rana et al. 2011; Kaur et al. 2012a; Meenakshi and Ahuja 2015).

4 Carboxymethylated Tamarind Gum in Drug Delivery

4.1 Carboxymethylation

Carboxymethylated gums are those modified gums, which are synthesized from the native gum through functional modification by the chemical means of attaching pendant carboxylic acid groups ($-\text{COOH}$) to the native gum structures (Togru and Arsian 2003; Olusola et al. 2014; Rana et al. 2011). Recently, in the polymer research, carboxymethyl modifications (i.e., carboxymethylation) of gums are an extensively studied conversion because of its technical simplicity low cost of chemical reagents and wide applications (Parvathy et al. 2005). Carboxymethylation of gums leads to add a variety of promising characteristics (Togru and Arsian 2003; Olusola et al. 2014). Generally, carboxymethylated gums exhibit to enhance hydrophilicity in addition to clarity of solutions as compared to that of the native gums (Rana et al. 2011). These potential characteristics improvement of the native gum makes them more soluble in aqueous medium. In general, native gums are made carboxymethylated through the conventional method by Williamson's etherification

reaction using monochloroacetic acid and sodium hydroxide in the aqueous milieu at higher temperature (Khalil et al. 1990). The Williamson's etherification reaction may direct to the nonspecific degradation via β elimination and/or peeling reaction initiated at decreasing sugar units because of highly alkaline pH environment, which sequentially decreases the molecular weight of the derivatized gum (Parvathy et al. 2005). Various natural gums are already carboxymethylated through this method (Maity and Sa 2014a, b).

Carboxymethyl tamarind gum is the carboxylic derivative of tamarind gum. The introduction of carboxymethyl group into the tamarind gum enables an anionic nature to it (Goyal et al. 2007). Carboxymethylation of tamarind gum makes it comparatively microbial as well as enzymatic resistant than the native gum (Manchanda et al. 2015). Carboxymethyl tamarind gum possesses higher viscosity and lower degradability in aqueous environments (Goyal et al. 2007). It also has the capacity to produce higher swelling in aqueous environments (Manchanda et al. 2015; Meenakshi and Ahuja 2015).

4.2 Carboxymethylated Tamarind Gum Matrix Tablets for Sustained Drug Delivery

In an investigation, Manchanda et al. (2015) reported the matrix-forming potential of carboxymethyl tamarind gum to develop and optimize sustained drug releasing matrix tablets. They have chosen glipizide (an effective oral antidiabetic; BCS class-II drug; short biological half-life of about 3.5 h) to assess the sustained drug releasing matrix-forming potential of carboxymethyl tamarind gum. In this study, Manchanda et al. (2015) synthesized carboxymethyl tamarind gum via carboxymethylation technique, where conventional carboxymethylation method using strong sodium hydroxide and monochloroacetic under heterogeneous reaction conditions was followed.

The synthesized product of carboxymethyl tamarind gum was found brownish-white in color. The melting point of it was found as 252–256 °C. The synthesized carboxymethyl tamarind gum was found soluble in water. The pH and viscosity of synthesized carboxymethyl tamarind gum solution (1% w/v) were 6.9 and 1225–1715 cps (at various shear rates), respectively. The carboxymethyl tamarind gum was characterized for its micromeritic characteristics, viz., bulk density, tapped density, angle of repose, Hausner's ratio, and Carr's index. In micromeritic evaluation of the synthesized carboxymethyl tamarind gum, bulk density of 0.60 g/cm³, tapped density of 0.80 g/cm³, angle of repose of 18.6°, Hausner's ratio of 1.15, and Carr's index of 32.0°. 17% of loss on drying were measured.

Utilizing the synthesized carboxymethyl tamarind gum, matrix tablets of glipizide (an oral antidiabetic drug) were formulated via direct compression technique. For the formulation optimization of these matrix tablets of glipizide, a 3² full

factorial optimization design with two independent variables and three dependent variables was employed to optimize drug release profile using response surface methodology. Concentration of carboxymethyl tamarind gum and type of diluent (here lactose, starch and microcrystalline cellulose) were analyzed as independent variables in the 3^2 full factorial design. The dependent variables (responses) selected were percent of glipizide release at 4, 8 h and swelling index. From the results, the response surface plots related with independent variables and dependent variables were developed to select the optimum formulation. To prepare matrix tablets of glipizide using the synthesized carboxymethylated tamarind gum, granules were prepared. The granules were characterized for their micromeritic properties and the angle of repose was found as 23° – 31° , which indicates satisfactory flow behavior of these prepared granules. The drug contents, average weights, weight variations, friabilities, and harnesses of all these glipizide matrix tablets were assessed. The uniform drug content in these matrix tablets was observed as it was within $95 \pm 2\%$. The average weight and weight variation were within the pharmacopoeial limit. The range hardnesses and friabilities were 6.5 – 7.1 kg/cm^2 and 0.24 – 0.65% , respectively. The results of hardness and friability indicated suitable mechanical strength, which are helpful for good handling of these prepared matrix tablets.

The Fourier transform infrared spectroscopy (FTIR) and differential scanning calorimetry (DSC) analyses confirmed the absence of drug (glipizide)-polymer (carboxymethylated tamarind gum) interaction within these matrix tablets. Scanning electron microscopy (SEM) analyses revealed comparatively rougher surface of carboxymethylated tamarind gum than native tamarind gum.

The swelling behavior of these carboxymethylated tamarind gum matrix tablets of glipizide was evaluated in phosphate buffer medium, pH 7.4. Swelling indices were found to be increased with the concentrations of carboxymethylated tamarind gum using microcrystalline cellulose as diluent. These matrix tablets were also assessed for in vitro glipizide-releasing pattern in phosphate buffer medium, pH 7.4. In vitro glipizide-releasing pattern was observed inversely proportional to the carboxymethylated tamarind gum concentrations and depends on type of diluents. The in vitro glipizide-releasing from all these tablets suggested sustained drug releasing pattern over 20 h. The drug release also followed the kinetic model of zero-order and mechanism of non-Fickian drug release (anomalous release).

4.3 Carboxymethylated Tamarind Gum Nanoparticles for Ocular Drug Delivery

Biopolymeric nanoparticles made of carboxymethylated tamarind gum for ocular drug delivery were formulated by Kaur et al. (2012a). They have utilized commercial carboxymethylated tamarind gum to prepare ocular nanoparticles of tropicamide (an anti-muscarinic drug). In this study, interactions between anionic carboxymethylated tamarind gum and divalent Ca^{2+} -ions were employed to prepare

ionotropically gelled nanoparticulate carriers made of carboxymethylated tamarind gum. On the basis of this mechanism, tropicamide loaded carboxymethylated tamarind gum nanoparticles were formulated via ionotropic gelation using Ca^{2+} -ions as ionic cross-linker ion as well as dioctyl sulfosuccinate as stabilizing agent. The formulation of these nanoparticles of tropicamide was optimized through employing three levels and two factors based central composite design. Carboxymethylated tamarind gum concentrations and calcium chloride (as cross-linker) concentrations were chosen as independent factors. Encapsulation efficiency and particle size were analyzed as responses (dependable factors). The preliminary trial study containing 13 experimental run suggested that the concentrations of carboxymethylated tamarind gum and Ca^{2+} -ions influenced the particle sizes of the carboxymethylated tamarind gum nanoparticles loaded with tropicamide. This occurrence can be infer that the anionic carboxymethylated tamarind gum concentration possessed more pronounced effect than the ionotropic cross-linker (calcium chloride) concentration on the particle size of these ionotropically gelled carboxymethylated tamarind gum nanoparticles containing tropicamide. An increment in carboxymethylated tamarind gum concentration was found to increase the particle sizes of these nanoparticles. This occurrence can be explained by insufficient interaction of cross-linker with polymer used. This occurrence can also be explained by the fact that the increased polymer concentrations enhanced the viscosity of the solution. It was also found that the increase in drug encapsulation of these nanoparticles with the declining polymer concentrations and raising concentration of cross-linker can be due to the high cross-linking at the raising concentration of cross-linker. The increasing polymer (here carboxymethylated tamarind gum) concentration resulted in declining of drug encapsulation in these nanoparticles, which was more pronounced at the higher cross-linking concentration of calcium chloride during nanoparticles preparation.

The optimal calculated values of these two investigated factors were estimated as 0.10% w/v of carboxymethylated tamarind gum concentration and 0.11% w/v calcium chloride to formulate optimized carboxymethylated tamarind gum nanoparticles containing tropicamide. The optimized formulation of tropicamide loaded carboxymethylated tamarind gum nanoparticles showed particle size of 339 nm and drug encapsulation efficiency of 15.57%.

The ionotropic interaction between anionic carboxymethylated tamarind gum and divalent Ca^{2+} -ions was demonstrated by FTIR spectroscopy. Optimized tropicamide loaded nanoparticles were characterized via transmission electron microscopy (TEM) analysis. The TEM microphotograph of the optimized nanoparticles revealed the ovoid morphological shape (Fig. 2) and particle sizes were found within the range of 2–40 nm.

Ex vivo corneal permeation of the optimized tropicamide loaded nanoparticles was evaluated using isolated goat cornea by the modified Franz diffusion cell. The result of the corneal permeation of the optimized nanoparticles was compared with the result of corneal permeation of conventional tropicamide aqueous solution. No significant difference between the percentages of corneal tropicamide permeation from these two ocular formulations (optimized tropicamide loaded nanoparticles

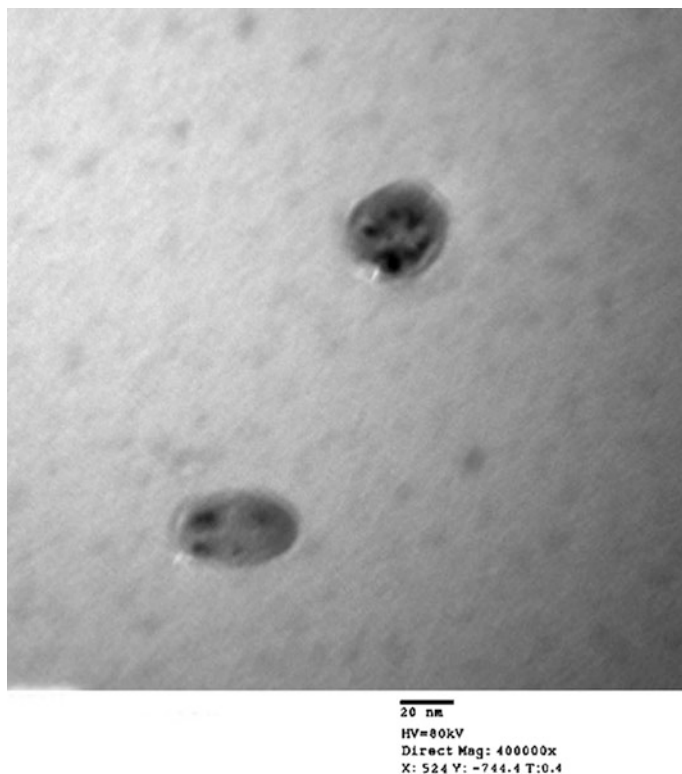


Fig. 2 TEM microphotograph of tropicamide loaded carboxymethylated tamarind gum nanoparticles (Kaur et al. 2012a, b). Copyright ©2011 with permission from Elsevier B.V.

and conventional tropicamide aqueous solution) was observed. Ex vivo mucoadhesivity of these carboxymethylated tamarind gum nanoparticles was judged through measuring the adsorbed mucin amounts by the tested nanoparticles within 24 h. 87.67% of absorbed mucin was estimated by the mucin glycoprotein assay of nanosuspension containing optimized tropicamide loaded carboxymethylated tamarind gum nanoparticles. Being an anionic polymer, carboxymethylated tamarind gum contains $-\text{COOH}$ groups, which could form hydrogen bonds with the oligosaccharide chains of mucin. Mucin adsorption by tropicamide loaded optimized carboxymethylated tamarind gum clearly indicated excellent mucoadhesivity of these nanoparticulate carriers for ocular delivery of tropicamide.

Ex vivo ocular tolerance of these optimized carboxymethylated tamarind gum nanoparticles containing tropicamide was assessed using hen's egg test on the chorioallantoic membrane (CAM) of chicken eggs. The results of this ex vivo ocular tolerance study indicated that these optimized tropicamide loaded nanoparticles were nonirritant and excellent ocular tolerability. The results of ex vivo corneal tropicamide permeations, ex vivo mucoadhesion as well as ex vivo ocular

tolerance studies clearly demonstrated the suitability of these optimized tropicamide loaded carboxymethylated tamarind gum nanoparticles as an effective ocular drug delivery carrier.

4.4 Carboxymethylated Tamarind Gum Spheroids for Controlled Drug Delivery

In a research, Gowda et al. (2014) designed controlled drug releasing spheroids composed of carboxymethylated tamarind gum. They utilized commercial carboxymethylated tamarind gum to formulate these controlled drug releasing spheroids. The commercial carboxymethylated tamarind gum was characterized for pH and viscosity. The pH of 1% w/v solution of carboxymethylated tamarind gum was found as 4.50 ± 0.29 . This value was considered as advantageous to be used to develop drug releasing carriers as this would not cause any chances of gastrointestinal irritation when consumed orally. 38 cps viscosity in distilled water, 40 cps viscosity in pH 1.2 buffer, and 45 cps viscosity in pH 7.2 buffer were measured for 1% w/v solution of carboxymethylated tamarind gum.

Gowda et al. (2014) employed extrusion/spheronization technique for the preparation of these carboxymethylated tamarind gum spheroids to investigate the influence of compression of prepared spheroids into the matrix tablets for controlled drug release. In this work, lornoxicam (a NSAID) was used as model drug. Owing to undersized biological half-life of lornoxicam (approximately 3–5 h) and to restrict the chances of the gastrointestinal disturbances, it should be beneficial to be used through controlled releasing carriers for oral use. In these formulations of carboxymethylated tamarind gum, spheroids containing lornoxicam and microcrystalline cellulose were utilized as spheronization enhancer. For the different formulations, lornoxicam loaded spheroids were prepared through maintaining different ratios of microcrystalline cellulose:carboxymethylated tamarind gum:lornoxicam (drug), such as, 72.5:2.5:2.5% w/w (BD-1), 70:5:25% w/w (BD-2), 67.5:7.5:25% w/w (BD-3), 65:10:25% w/w (BD-4), 62.5:12.5:25% w/w (BD-5), and 60:10:25% w/w (BD-6). From the optimization study, Gowda et al. (2014) identified the optimal formula of process variable settings for optimized spheroids, which were prepared at 6000 rpm for 5–15 min of time durations.

The narrow range of spheroids size distribution was seen, when spheroids were formed using carboxymethylated tamarind gum of 2.5–15.0% w/w concentrations. In case of spheroids made of above 15% w/w of carboxymethylated tamarind gum, the extrusion mass cohesiveness was found to be augmented and this might have resulted due to the fact of greater resistance to stream through the extruder die utilized. An extrusion of the wetted mass through wetted die was noticed with the water level rising. This resulted tacky extrudates for the further processing were attained when carboxymethylated tamarind gum concentration in the preparation of spheroids was less than 15% w/w. From the preliminary trial studies, it was noticed

that the resistance of extrudate amounts at higher concentration of carboxymethylated tamarind gum (more than 15% w/w) to round up by the spheronizer device was found to be comparatively greater. The level of carboxymethylated tamarind gum concentrations was selected less than 15% w/w in the carboxymethylated tamarind gum spheroids containing lornoxicam prepared. From the results of the preliminary trial experimentation, it was observed that spheroids production was sufficient with the maximum percentage yield and acceptable level of sphericity, when spheronization time of 15 min and spheronization speed of 1600 rpm were employed.

Various micromeritic characteristics such as mean particle sizes, angles of repose, trapped densities, granule densities, Carr's indices, and friability values of different batches of lornoxicam loaded carboxymethylated tamarind gum spheroids were measured. The results indicated any significant differences among various batches of carboxymethylated tamarind gum spheroids. Mean particle sizes of these lornoxicam loaded carboxymethylated tamarind gum spheroids were measured as 1125 ± 0.56 to 1345 ± 0.23 μm . The friability values of these spheroids were measured within the range of 0.43 ± 0.08 to $0.53 \pm 0.07\%$, which indicated that the friability values of all the batches were within the compendia limits. The angles of repose of these spheroids were measured within the range of 23.45° – 26.30° , suggesting good quality of flow properties of these lornoxicam loaded carboxymethylated tamarind gum spheroids.

The SEM analyses of these lornoxicam loaded carboxymethylated tamarind gum spheroids demonstrated spherical shaped morphology with smooth surface. The smooth surface morphology of these spheroids might have influenced the results of the friability and angle of response. These spheroids were also subjected to the DSC analyses and the DSC results indicated that the decomposition temperature of the encapsulated drug, lornoxicam (i.e., 218.74 $^\circ\text{C}$) was almost same, even when it was processed with the carboxymethylated tamarind gum and other excipients to prepare these spheroids. This phenomenon may be explained by the fact that there was absence of interactions between lornoxicam and excipients used in the preparation of lornoxicam loaded carboxymethylated tamarind gum spheroids. These results indicated that lornoxicam was in stable form within these formulated carboxymethylated tamarind gum spheroids.

Drug loadings (%) among all these of lornoxicam loaded carboxymethylated tamarind gum spheroids were within the range of 19.59 ± 1.12 – $22.30 \pm 0.39\%$. The highest drug loading was observed for the spheroids of formulation BD-1 ($22.30 \pm 0.39\%$). Drug entrapment efficiencies were measured within the range in-between 91.42 ± 1.12 and $96.04 \pm 0.20\%$. The highest entrapment efficiency was found for the spheroids formulation BD-3 among all the spheroids prepared.

The optimized formulation of lornoxicam loaded carboxymethylated tamarind gum spheroids was compressed with mixing 20% Avicel[®] PH 200 as filler and 10% w/w anhydrous lactose. Actually, prior to the compression, slugs were prepared using prepared spheroids, Avicel[®] PH 200 and anhydrous lactose. Then, slugs of prepared spheroids, Avicel[®] PH 200, and anhydrous lactose were passed through the Multimilli screen (0.5"). The granules were sieved through sieve #40. The

ultimate granules were processed through blending with 1% of magnesium stearate and then compressed for 1 min with various fixed loads of 5–12.5 tons by using a hydraulic press (containing 12.7 mm die with flat faced punches). The weight variations, hardness, and friability of these prepared compressed matrices were assessed. Hardness and friability of these compressed matrixes were found within pharmacopoeial limits. Therefore, it was seen that hardness and friability were found to be increased with the increasing of compression forces.

For the *in vitro* dissolution study, lornoxicam loaded spheroids made of carboxymethylated tamarind gum were capsulated within hard gelatin capsules. The *in vitro* dissolution was performed using freshly prepared dissolution media of phosphate buffer, pH 7.2 at the temperature of 37 ± 1 °C, and paddle-speed of 50 rpm. In *in vitro* dissolution, it was observed that the increasing carboxymethylated tamarind gum concentration level from 2.5 to 15% directed a significant decrease in drug releases from these lornoxicam loaded carboxymethylated tamarind gum spheroids. It was also observed that lornoxicam loaded spheroids BD-1, BD-2, and BD-3 made of carboxymethylated tamarind gum in concentration of 2.5, 5 and 7.5% w/w released 97.20 ± 1.50 , 79.35 ± 1.70 , and $66.89 \pm 1.40\%$, respectively, at the end of 7 h of *in vitro* dissolution study, demonstrating polymer (here carboxymethylated tamarind gum) concentration was insufficient to sustain the drug release. In contrast, lornoxicam release from BD-4 spheroids made of 10% carboxymethylated tamarind gum was found significantly sufficient in comparison with other formulation batches of spheroids. The formulation BD-4 was found to release drug of $98.13 \pm 0.90\%$ at 12 h. The sustained drug release could be because of high concentration of carboxymethylated tamarind gum. This occurrence could be a characteristic sign of slower penetration of dissolution media into the matrix. The formulation BD-5 and BD-6 containing 12.50% w/w and 15% w/w carboxymethylated tamarind gum exhibited insufficient release of drug due to high carboxymethylated tamarind gum concentration. The sustained drug releases from these spheroids were following in order of BD-6 > BD-5 > BD-4 > BD-3 > BD-2 > BD-1. Among all these formulations, spheroids BD-4 composed of 10% w/w carboxymethylated tamarind gum were identified as optimized formulation on the basis of its physicochemical as well as release characteristics. The drug release from spheroids BD-4 showed zero-order kinetic model, which is an indicative of controlled release. In the stability study, it was found that these spheroids were found to be stable enough over 60 days.

4.5 Carboxymethylated Tamarind Gum-Chitosan Interpolymeric Complexation-Based Film Coating for Colon Drug Delivery

Kaur et al. (2010) developed chitosan (deacetylated chitin, cationic natural polymer)-carboxymethylated tamarind gum interpolymer complexation film for the

better delivery of budesonide (a second generation glucocorticoids) in the colon. In designing of such an improved colon drug delivery system, they have planned to coat uncoated budesonide tablets of 25 mg average weight, which contained 3 mg of budesonide. These tablets were formulated through weight granulation procedure using Eudrajit L100-55 or chitosan-carboxymethylated tamarind gum inter polymeric complex as binder.

Average weight of uncoated core tablets was calculated as 24.67 ± 1.10 mg and this result was within the USP tolerance limit. Axial as well as radial diameters of uncoated core tablets were within 1.75–1.80 and 3.98–4.02 mm, respectively. Hardness of these uncoated tablets was measured 4.50 ± 0.50 kg/cm² and friability was measured within the range, 0.36–0.46% w/w. The uncoated budesonide tablets formulated with 10% w/w Eudrajit L100-55 or chitosan-carboxymethylated tamarind gum inter polymeric complex as binders demonstrated to show cracking of the tablet matrix in-between 30 min, when exposed to 0.1 M HCl. 27.20 ± 1.25 mg was measured as average weight of the coated matrix tablets and it was within the official limit. 2.02–2.08 and 4.01–4.15 mm were measured as the axial and radial diameter of these coated tablets. Though, these coated tablets displayed swelling as these showed any cracking following the contact of these matrix tablets to 0.1 M HCl for a period of 2 h.

The formation of interpolymeric complex between cationic chitosan and anionic carboxymethylated tamarind gum was confirmed by FTIR spectroscopy. Actually, carboxymethylated tamarind gum possesses negative ionic charge because of the presence of –COOH groups through the carboxymethylation; while owing to the presence of NH₃⁺ groups, chitosan possesses positive charge. The processing of both the polymers of opposite charges (negative charged carboxymethylated tamarind gum and positive charged chitosan) undergone a spontaneous, which results in a solid mass due to interpolymeric complexation. Kaur et al. (2010) studied viscosity of chitosan-carboxymethylated tamarind gum mixture solution to investigate the stoichiometric complexation between the two oppositely charged polymers. They found to decrease as the proportion of chitosan in the chitosan-carboxymethylated tamarind gum mixture decreased. The minimum viscosity of the supernatant of the chitosan-carboxymethylated tamarind gum was obtained through reacting cationic chitosan with anionic carboxymethylated tamarind gum in the ratio of 2:3, which indicated minimum reaction.

Chitosan-carboxymethylated tamarind gum inter polymeric complex films were evaluated for swelling in acidic buffer (pH 1.2) for 2 h and in alkaline buffer (pH 7.4) for 22 h. Kaur et al. (2010) found considerably low swelling of interpolymeric complex films in the alkaline pH. The swelling of interpolymeric complex films exhibited a decreasing of limiting value, when carboxymethylated tamarind gum concentration was found decreasing in the chitosan-carboxymethylated tamarind gum interpolymeric complex to 60% w/w. In addition, with the increasing concentration of carboxymethylated tamarind gum, swelling index was found to be increased. The interpolymeric complex films composed of 30:70 ratio of chitosan-carboxymethylated tamarind gum exhibited an enhanced swelling pattern

in comparison with those, which were composed with chitosan-carboxymethylated tamarind gum in a ratio of 40:60.

The *in vitro* releasing of drug from formulated tablets was assessed in different pH 1.2 for 2 h, pH 7.4 for 3 h, and pH 6.8 for 19 h. The uncoated budesonide tablets containing Eudragit L100-55 as binding agent exhibited the release of 24% drug (budesonide) in the acidic pH (1.2) within 2 h. The residual amount of budesonide was found to be released speedily from these uncoated tablets in alkaline pH (7.4) within 4 h. The tablets coated with chitosan:carboxymethylated tamarind gum ratio of 60:40 released budesonide of 6% in the acidic pH (1.2) and furthermore, release of 21% budesonide was detected in the alkaline pH (7.4). The uncoated budesonide matrix tablets containing 40:60 or 50:50 ratio of chitosan-carboxymethylated tamarind gum as binder were found to have released 50 and 52% of budesonide, respectively on the acidic pH. Furthermore, these tablets were found to be released 72 and 75% of budesonide, respectively, in the pH 7.4. These results suggested that the chitosan-carboxymethylated tamarind gum, when employed alone as a binding agent, was unable to sustain the release of budesonide in acidic pH (stomach pH). In addition, the matrix tablets containing 50:50 ratio of chitosan:carboxymethylated tamarind gum employing as binding agent and when these matrix tablets were coated using the same solution, it was found to release 9% of budesonide in the alkaline pH of 7.4 (intestinal pH). These chitosan-carboxymethylated tamarind gum interpolymeric complex based matrix tablets were found to release 28% of budesonide in the alkaline pH of 6.8 within 24 h. The total releases of budesonide in pH 6.8 after 24 h, which was found to be released in pH 6.8 after 24 h, were 16%.

In vitro release of budesonide from tablets containing chitosan-carboxymethylated tamarind gum interpolymeric complex or Eudragit L100-55 was used as binding agent on the chronological exposure to the dissolution media containing rat cecal content or chitosanase enzyme of a variety of pH-range (1.2, 7.4 and 6.8). The budesonide release was significantly ($p < 0.05$) amplified in the rat cecal content containing dissolution media in comparison with that of the dissolution media lacking rat cecal content. The releases of budesonide in rat cecal contents after 24 h from these chitosan-carboxymethylated tamarind gum matrix tablets containing Eudragit L100-55 as binding agent were improved to 99, 70 and 59%, from 84, 36 and 25%, respectively, when these uncoated tablets were coated with chitosan-carboxymethylated tamarind gum using 40:60, 50:50 and 60:40 ratio. The ultimate contact of these budesonide matrix tablets containing chitosan:carboxymethylated tamarind gum of 50:50 as binding agent, which were also coated using the same solution released budesonide of 74% to the release medium containing rat cecal contents. However, in the release medium absenting rat cecal content, it was found to release budesonide of 30%. Increment in the *in vitro* release of budesonide in the release medium containing rat cecal contents revealed the susceptibility of interpolymeric complex (composed of chitosan and carboxymethylated tamarind gum) to the polysaccharides present in the colon. The absolute budesonide release was not evidenced even after a period of 24 h from the

coated matrix tablets coated with chitosan:carboxymethylated tamarind gum in a ratio of 40:60 or 50:50. The presence of enzyme, chitosanase improved the budesonide release amount from these coated interpolymeric complex matrix tablets. It was also observed that the ultimate contact of these matrix tablets coated using chitosan and carboxymethylated tamarind gum ratio of 40:60 or 50:50 in the dissolution medium containing chitosanase for a period of 19 h augmented the in vitro budesonide release amount from these coated matrix tablets containing Eudragit L100-55 as binding agent to 92.43 and 83.25%, respectively, in the release medium containing rat cecal contents. However, in the release medium absenting rat cecal content, it was found to release budesonide of 70.50 and 59.80%, respectively. Release kinetic of budesonide was found to be following zero-order kinetic model as well as transport mechanism of super case-II in each release media studied including release media containing chitosanase and rat cecal content. These results suggested resistance of the interpolymeric complex between chitosan and carboxymethylated tamarind gum in the release media of different pH studied. As per the results, the in vitro budesonide release occurred because of slower erosion of the polymeric matrix. The budesonide matrix tablets coated with 40:60 and 50:50 ratio of chitosan:carboxymethylated tamarind gum containing Eudragit L100-55 or chitosan:carboxymethylated tamarind gum as binder were observed to show physical as well as chemical stability on storage at relative humidity of 75% and temperature of 40 °C. Any kinds of color changes as well as weight of these tablets were not observed.

In the pharmacokinetic study in the Sprague-Dawley rats, the uncoated budesonide matrix tablets containing Eudragit L100-55 were found incapable to retard the release of budesonide, in vivo. The in vivo plasma concentration of budesonide was observed to augment rapidly after oral administration of uncoated matrix tablets. 1091.99 ng/ml of t_{\max} was attained within 2 h. The period to attain C_{\max} after oral administration of uncoated matrix tablets was observed to delay to 8 h for the coated tablets. The in vivo results clearly suggested the incapability of the interpolymeric complex films to resist the budesonide release in the gastric pH. Nevertheless, the in vivo plasma concentration in rats orally administered with the coated matrix tablets of 50:50 and 40:60 ratio of chitosan:carboxymethylated tamarind gum augmented progressively after a time period of 4 h and after 8 h, it was found turned down. These results suggested the proneness of the polymers employed (chitosan and carboxymethylated tamarind gum) to degrade the matrix by the polysaccharidases present in the colon. Histopathology of rat colon after oral administration of the chitosan-carboxymethylated tamarind gum interpolymeric complex film coated tablets exhibited a significant decrease ($p < 0.05$) in the TNBS-induced ulcerative colitis in comparison to that after the oral administration of the uncoated matrix tablets. From this study, it was found that the matrix tablets coated with chitosan and carboxymethylated tamarind gum in a ratio of 40:60 can be envisioned to recommend a great deal of guarantee in colonic delivery of drugs.

4.6 Carboxymethylated Tamarind Gum-Poly Vinyl Alcohol Cryogels for Sustained Drug Release

In a research, Meenakshi and Ahuja (2015) prepared and characterized composite cryogels of carboxymethylated tamarind gum-poly vinyl alcohol employing freeze–thaw treatment. Metronidazole (an imidazole derivative and antibacterial agent) widely used in bacterial vaginosis and periodontitis was investigated as model drug in this study. Metronidazole-loaded carboxymethylated tamarind gum-poly vinyl alcohol cryogels were optimized using three factors and three levels central composite design employing the concentration of carboxymethylated tamarind gum, concentration of poly vinyl alcohol and freeze–thaw cycle numbers as the factors (independable variables); whereas in vitro drug release rate was estimated as the response (dependable variable). The optimization analysis by response surface methodology showed the combined influence of concentrations of carboxymethylated tamarind gum as well as poly vinyl alcohol on the in vitro release of metronidazole from these cryogels. At the lower levels of carboxymethylated tamarind gum on increase of poly vinyl alcohol concentration, the percentage metronidazole release was found decreased, which can be explained by the fact of cryogel formation with higher cross-linking density. With the increasing concentration of carboxymethylated tamarind gum, the release of metronidazole was found to be increased. However, the effect of carboxymethylated tamarind gum concentration was found to be comparatively more prominent at the higher levels of poly vinyl alcohol. At the medium as well as lower levels of poly vinyl alcohol, increased concentration of carboxymethylated tamarind gum resulted increment followed by fall in the in vitro drug release rate. The enhancement in carboxymethylated tamarind gum concentration resulted in higher percentage in drug release. In contrast, this increased the contact of these newly synthesized cryogels to freeze–thaw cycles from medium to lower levels, which decreased the drug releasing rate. The optimized calculated parameters were poly vinyl alcohol concentration of 8.45%, carboxymethylated tamarind gum concentration of 6.00 w/v and freeze–thaw cycles of 4 and this showed percent drug release of 75.77% (optimization predicted value was 79.77%; percent prediction error of 4.93%).

In vitro swelling behavior of optimized carboxymethylated tamarind gum-poly vinyl alcohol composite cryogel was carried out in phosphate buffer solution (pH 6.8) for 24 h. Swelling patterns of different prepared cryogels demonstrate deviations of swelling rates. Nevertheless, any significant model explaining link in-between the swelling behaviors, freeze–thaw cycling as well as concentration of polymers employed to prepare cryogels might not be found. The swelling patterns of optimized carboxymethylated tamarind gum-poly vinyl alcohol cryogels also indicated an early rapid drug release rate and slower rate towards an equilibrium swelling.

The optimized carboxymethylated tamarind gum-poly vinyl alcohol cryogels was characterized by means of SEM, FTIR, DSC, and XRD analyses. The SEM photographs revealed that the carboxymethylated tamarind gum particles were of

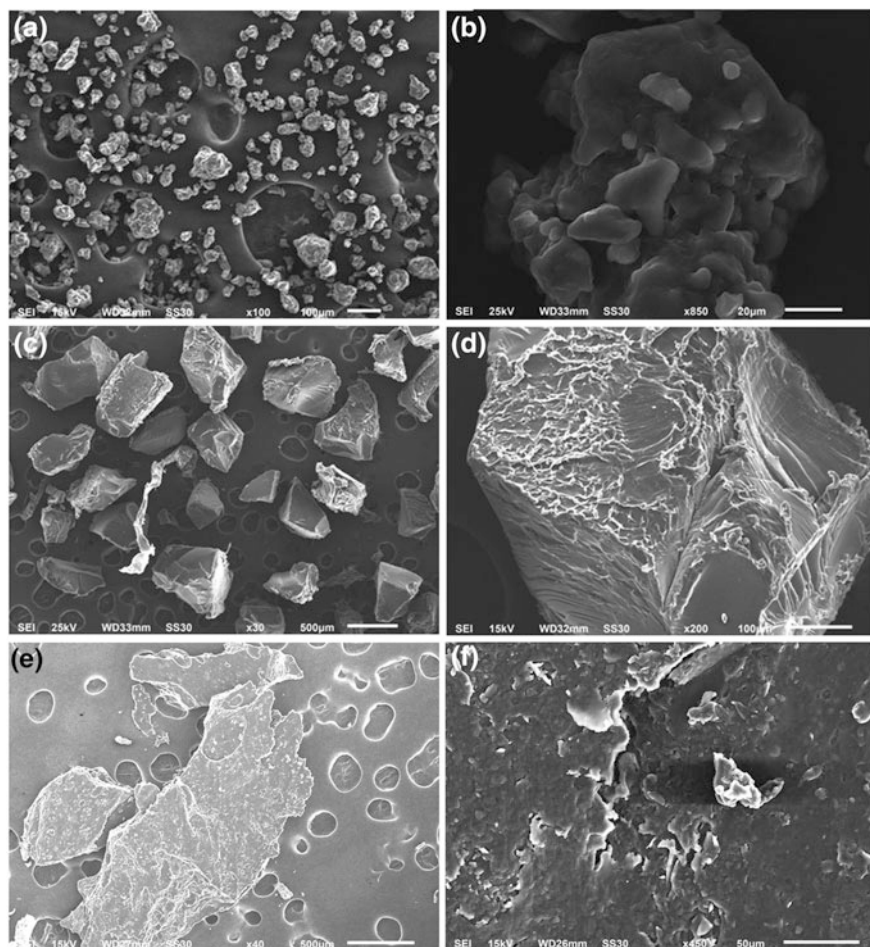


Fig. 3 SEM photograph showing **a** shape and **b** surface of carboxymethylated tamarind gum, **c** shape and **d** surface of poly vinyl alcohol, **e** shape and **f** surface of carboxymethylated tamarind gum-poly vinyl alcohol composite cryogel (Meenakshi and Ahuja 2015). Copyright ©2014 with permission from Elsevier B.V.

polyhedral shaped with striated surface. The newly synthesized composite cryogel particles made of carboxymethylated tamarind gum-poly vinyl alcohol appeared as amorphous flakes with a granular as well as porous surface (Fig. 3). FTIR, XRD, and DSC analyses indicated the chemical interactions between carboxymethylated tamarind gum and poly vinyl alcohol in the synthesized cryogel structure. In addition, DSC analysis revealed higher thermal stability of these carboxymethylated tamarind gum-poly vinyl alcohol cryogels.

5 Thiolated Tamarind Gum in Drug Delivery

5.1 Thiolation

Mucoadhesion of naturally derived polysaccharide through derivatization with thiol functional group containing reagents has been employed to enhance the bio-mucoadhesive as well as cohesive characteristics of various polymers (Sharma and Ahuja 2011). Thiolated polymers (commonly called as thiomers) are considered as latest generation of biomucoadhesive polymers, which mimic the natural mechanism of secreted mucus glycoprotein through covalently fixing on the mucus layer by means of disulfide bonds (Bernkop-Schnürch et al. 2003; Bahulkar et al. 2015). Thiol ($-SH$) side chains of different polymers can interact with the sulfur-rich subdomains of mucus glycoprotein bonding through disulfide bonds in-between the mucus layer and mucoadhesive polymers (Sharma and Ahuja 2011). These thiolated polysaccharides structure stronger covalent bonds ($S-S$ disulfide bonds) via appearing in contact with mucus glycoproteins (Bernkop-Schnürch et al. 2003). This improved mucoadhesion facilitates localization of dosage systems at the drug targeting site (Sharma and Ahuja 2011; Bahulkar et al. 2015). In addition, the disulfide bonds enhance the stability of matrices through delaying disintegration and erosion by increasing swelling behaviors (Bahulkar et al. 2015). Apart from the mucoadhesivity addition, thiolation of polysaccharides imparts enhancement of oral permeation of proteins and peptides (Bernkop-Schnürch et al. 2003), inhibition of efflux proteins, enzymes (Bernkop-Schnürch et al. 2001), and exhibits in situ gelling properties (Kraus et al. 2003). Thiolation or thiol modification of numerous natural polymers such as karaya gum (Bahulkar et al. 2015), alginate (Martinez et al. 2011), pectin (Sharma and Ahuja 2011), xyloglucan (Mahajan et al. 2013; Sonawane et al. 2014), gellan gum, etc., has been profitably researched.

5.2 Thiolated Tamarind Gum in Mucoadhesive Drug Delivery

Kaur et al. (2012a, b) synthesized and characterized thiolated tamarind gum. The thiol functionalized tamarind gum was synthesized through esterification by using thioglycolic acid with hydrochloric acid, where esterification of hydroxyl ($-OH$) groups of galactoxylan moiety of tamarind gum with the carboxylic ($-COOH$) groups of thioglycolic acid occur. Through the repeated washings using methanol, the unreacted acid was removed. The determination of thiol ($-SH$) group substitution on the synthesized thiolated tamarind gum was done through thiol groups quantifications by means of the Ellman's method. Thiolated tamarind gum was estimated 104.50 mM of thiol groups/gram through the Ellman's method.

The thiol functionalized tamarind gum was found as off white colored and also found soluble in water. Thiolated tamarind gum was characterized via infrared (IR) and DSC analyses. Both the instrumental analyses (IR and DSC) confirmed the thiol functionalization on the tamarind gum. The IR spectra of thiolated gum displayed the characteristic peak of thiol ($-SH$) groups (2586.54 cm^{-1}) and hydroxyl ($-OH$) groups (3367.71 cm^{-1}). The DSC thermal curve showed a broad endotherm at $81.87\text{ }^{\circ}\text{C}$ (heat of infusion, 22.85 J/g) followed by a fairly sharp endotherm at $145.38\text{ }^{\circ}\text{C}$ (heat of fusion, 75.88 J/g). Thiolated tamarind gum was also characterized by XRD and the X-ray diffractogram of thiolated tamarind gum showed a typical pattern of diffraction, which was similar to the native tamarind gum with the absence of sharp peaks with greater intensity demonstrating a higher crystallinity degree due to thiolation. SEM analyses of thiolated tamarind gum displayed a polyhedral morphology. The surface morphology of thiolated tamarind gum revealed a rougher surface of thiolated tamarind gum compared to native tamarind gum (Fig. 4).

Compacts (13 mm diameter) of thiolated tamarind gum (200 mg) and native tamarind gum (200 mg) were prepared via direct compression technique. Compacts were assessed for the mucoadhesive potential and compared. The maximum forces of the detachment of thiolated tamarind gum compacts and native tamarind gum compacts from mucin-coated model membrane were measured as 4062.50 ± 845.15 and $592.90 \pm 161.48\text{ mN}$, respectively. These results indicated improved mucoadhesion of thiolated tamarind gum as compared to the native tamarind gum (6.85 fold greater).

On the basis of the mucoadhesive results, mucoadhesive gels of metronidazole (as a model drug) composed native and thiolated tamarind gum. These 1% w/v metronidazole mucoadhesive gels were prepared by employing Carbopol 974 P as a gelling agent. The viscosities of these gels were determined by Brookfield viscometer. Viscosities of these gels were in order of: native tamarind gum > Metrogyl[®] > thiolated tamarind gum (Fig. 5). Biomucoadhesive strengths of these prepared and marketed gels were also compared to marketed gel of metronidazole (Metrogyl[®]). Mucoadhesive strengths of these gels were estimated by modified physical balance using fresh chicken intestinal membrane from the gel surface and maximum mucoadhesivity was measured for the mucoadhesive gels of metronidazole-containing thiolated tamarind gum as mucoadhesive agent. The mucoadhesive strengths of these mucoadhesive gels were in order of: thiolated tamarind gum > native tamarind gum > Metrogyl[®]. The adhesiveness and hardness of these gels were measured in the order of: native tamarind gum > Metrogyl[®] > thiolated tamarind gum. The cohesiveness of these mucoadhesive gels was found in the order of: thiolated tamarind gum > tamarind gum > Metrogyl[®]. Among these, mucoadhesive gels of thiolated tamarind gum exerted highest cohesiveness, least values of hardness and adhesiveness.

In vitro drug releases from these mucoadhesive gels containing metronidazole (made of thiolated tamarind gum and native tamarind gum) were compared with marketed metronidazole gel (Metrogyl[®]). From the in vitro metronidazole releasing

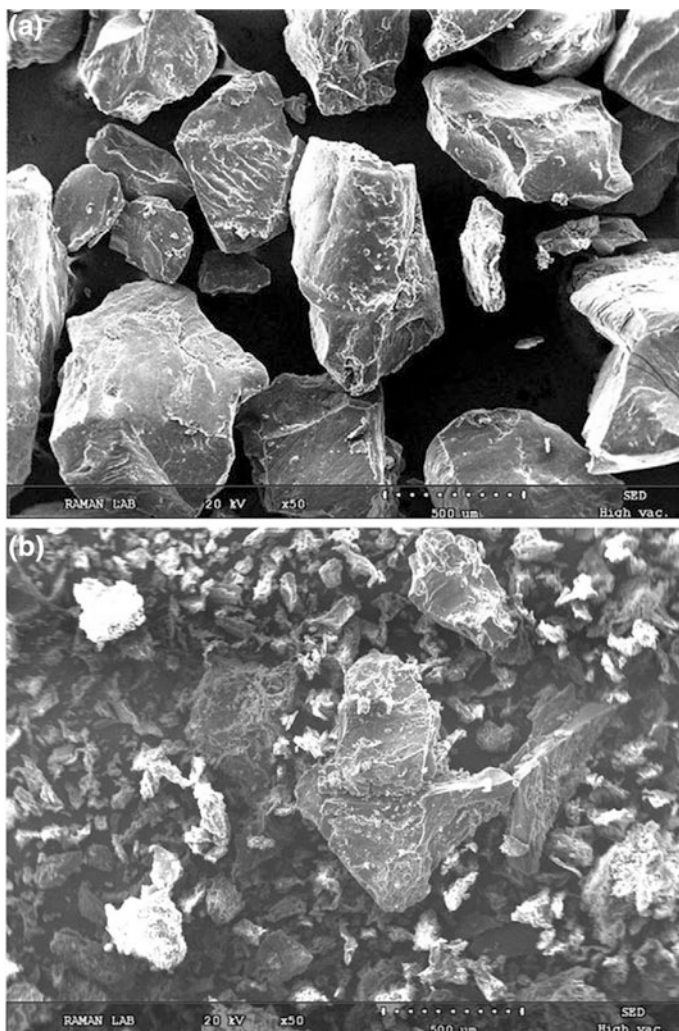


Fig. 4 SEM images of **a** native tamarind gum and **b** thiolated tamarind gum (Kaur et al. 2012a, b). Copyright ©2012 with permission from Elsevier Ltd.

pattern, it was seen that the marketed gel provided the slowest metronidazole release, followed by thiolated tamarind gum; whereas the fastest metronidazole release was measured from the metronidazole gel containing native tamarind gum as mucoadhesive agent (Fig. 6). These gels were found dependent upon the diffusion of metronidazole from the viscous gel matrix. Native tamarind gum and marketed gel formulations of metronidazole followed first-order kinetic model of drug releasing, while thiolated tamarind gum-based mucoadhesive gel formulation of metronidazole followed best fit Higuchi's square root kinetic model. The *in vitro*

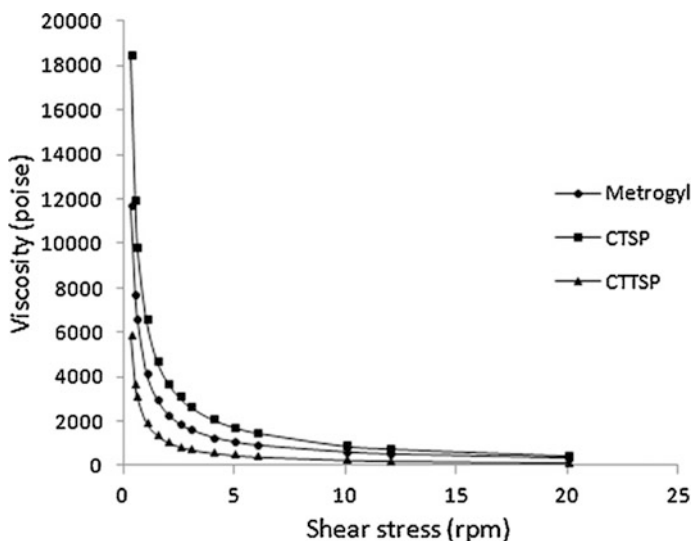


Fig. 5 Rheological profile of various mucoadhesive gels (Kaur et al. 2012a, b). Copyright ©2012 with permission from Elsevier Ltd.

metronidazole release from the thiolated tamarind gum-based mucoadhesive gels of metronidazole was found to follow diffusion-based drug release mechanism.

6 Graft-Modified Tamarind Gum in Drug Delivery

6.1 Graft Modification

Grafting of polymers is an effectual method for the modification of characteristics of various natural polymers as well as synthetic polymers (Singha et al. 2008; Thakur and Thakur 2015; Thakur et al. 2016). The modification of natural polymeric substances through graft copolymerization proffers opportunities to tailor their physical as well as chemical characteristics, to functionalize polymeric structures for imparting advantageous characteristics onto these and also uniting the benefits of both synthetic and natural polymers (Wang and Wang 2013; Thakur et al. 2012, 2013a, b, c, d, 2014a, b; Thakur and Singha 2011). Therefore, grafting copolymerization is currently considered as an effectual procedure for the enhancement of the compatibility in-between natural and synthetic polymers to synthesize new polymeric materials with improved hybrid properties (Bhattacharya and Mishra 2004; Bhattacharya and Ray 2009). Grafting of polymers entails the attachment of polymeric chains, typically a monomer, to the backbone polymeric structure (Thakur et al. 2014a; Thakur and Thakur 2015). Important methods

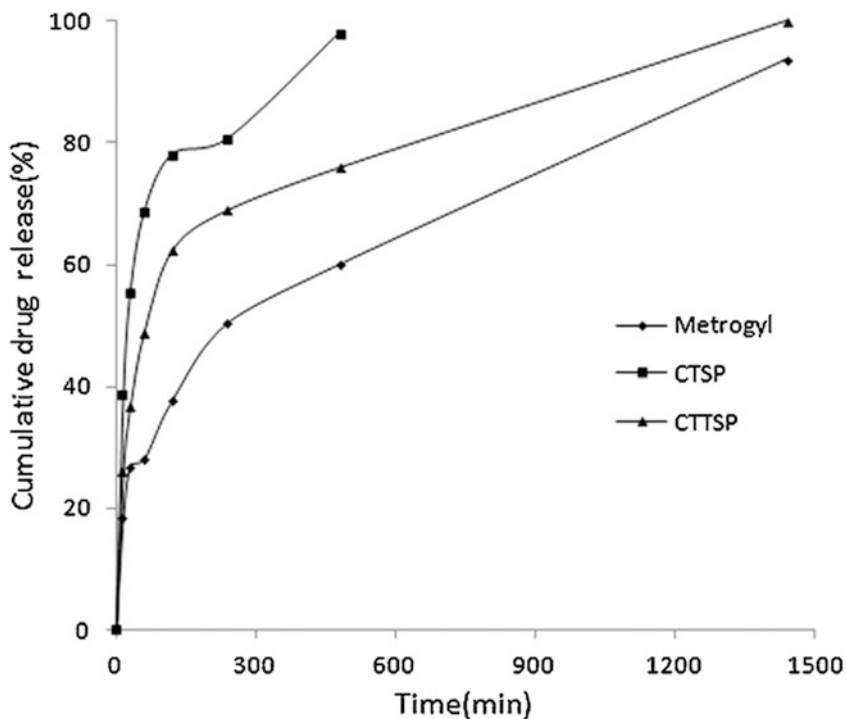


Fig. 6 In vitro release profile of metronidazole from various mucoadhesive gels (Kaur et al. 2012a, b). Copyright ©2012 with permission from Elsevier Ltd.

employed for the polymer grafting are conventional radical grafting, monomer radical grafting, high-energy initiation grafting, microwave-assisted grafting, radiation initiation grafting, electron beam initiated grafting, atom transfer radical grafting, etc. (Bhattacharya and Mishra 2004; Bhattacharya and Ray 2009; Wang and Wang 2013; Thakur and Thakur 2015). Recent years, using graft copolymerization methods, synthetic grafts have been introduced in numerous polysaccharides like cellulose (Thakur et al. 2013a), alginate (Sand et al. 2010), chitosan (Prashanth and Tharanathan 2003), xanthan gum (Pandey et al. 2001), guar gum (Pandey et al. 2014, 2015), amylopectin (Sarkar et al. 2013; Ahuja et al. 2014), gum tragacanth (Masoumi and Ghaemy 2014; Hemmati and Ghaemy 2016; Singh et al. 2016), tamarind gum (Ahuja et al. 2013; Ghosh and Pal 2013; Meenakshi et al. 2014), gum acacia (Tiwari and Singh 2008), gellan gum (Vijan et al. 2012; Nandi et al. 2015), okra gum (Mishra and Pal 2007; Mishra et al. 2008), cashew gum (Guilherme et al. 2005), gum ghatti (Rani et al. 2012; Mittal et al. 2014, 2015), psyllium polysaccharide (Singh et al. 2008), bael gum (Setia and Kumar 2014), etc.

6.2 Tamarind Gum-g-Polyacrylamide as Matrix for Controlled Release of Drug

Ghosh and Pal (2013) investigated pH dependent hydrogels of graft-modified tamarind gum as matrix-forming material for controlling of drug release. The graft-modified tamarind gum was chemically synthesized by means of grafting with polyacrylamide chains on the tamarind gum backbone in the microwave irradiation and presence of a reaction initiator (i.e., ceric ammonium nitrate). The graft copolymerization mechanism is based on the fact, where the microwave energy is being absorbed by the polysaccharidic structure and produces free radicals. Free radicals are usually recombined with each other via the steps of initiation, propagation, and termination to synthesize grafted copolymer of tamarind gum. Different graft copolymers of tamarind gum and polymethacrylamide were synthesized as a result of altering reaction constraints and optimized copolymerization with the respect of percent grafting (%), intrinsic viscosity, and radius of gyration.

The synthesized tamarind gum-g-polyacrylamide was evaluated for the matrix-forming materials for controlled release using aspirin (a NSAID, widely used in various pain relief man agent). To prepare tamarind gum-g-polyacrylamide matrix tablets of aspirin, guar gum was employed as binder in the ratios of 10:1:0.3. The prepared tablet matrix was characterized by FTIR and SEM analyses. FTIR results clearly indicated nonexistence of any kinds of chemical interaction(s) in-between aspirin and the tamarind gum-g-polyacrylamide matrix, recommending aspirin-tamarind gum-g-polyacrylamide matrix compatibility in the matrix tablets. SEM analyses revealed morphological changes, indicating physical (but, not chemical) interaction in-between aspirin and the tablet matrix (Fig. 7).

The swelling behavior of these tamarind gum-g-polyacrylamide matrix tablets of aspirin was measured at 37 °C in buffer solutions of different pH (1.2, 6.8 and 7.4) for 24 h. On contact with the buffer solutions, dry polymeric matrices of the tablets (tamarind gum-g-polyacrylamide) might be hydrated, swelled and then, formed a gel-like barrier layer, which delayed in vitro releasing of drug from the grafted matrices. It was also seen that the swelling pattern of tablet matrices was found

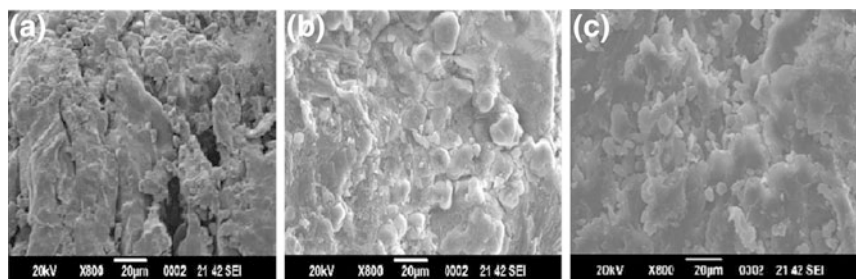


Fig. 7 SEM photographs of **a** tamarind gum-g-polyacrylamide **6**, **b** aspirin, and **c** tablet (Ghosh and Pal 2013). Copyright ©2013 with permission from Elsevier B.V.

higher with the increment in percent grafting. The matrix erosion rate was found lower with the increment in percent grafting. This occurrence can be characterized by the fact that the larger hydrodynamic volume should be occupied by higher molecular weight polymeric chains due to hydration. Since the polymeric chains of the swelled matrices became more hydrated, it experienced simultaneous swelling of tablet matrices, drug dissolution and also, drug diffusion into the bulk swelling medium. After attaining the equilibrium swelling, ionic strengths of the polymeric matrices were amplified. This produces lesser rate of erosion of the polymeric matrices and this phenomenon maintains the delayed drug release or controlled drug release from the drug releasing matrices. In view of the fact that, with the enhancement in the equilibrium swelling of the tablet matrices, the ionic strengths of the matrices raise and this occurs in declining of the rate of erosion similar to the lesser drug releasing rate from the matrices.

In vitro drug release behavior of these synthesized tamarind gum-g-polyacrylamide matrix tablets of aspirin was evaluated using dissolution apparatus USP in 900 ml of the buffer solutions of different pH (1.2, 6.8 and 7.4) maintained at 37 °C and 100 rpm. The drug (here aspirin) was found to be released completely from these matrix tablets after 24 h. In this research, it was detected that the rate of in vitro aspirin release from the newly synthesized tamarind gum-g-polyacrylamide based matrix tablets was low in the acidic pH but found to be released in much higher rate in the neutral as well as alkaline pHs. This was also observed that higher percent grafting lowered the rate of aspirin releases (controlled). It was also seen that with the increasing of percent grafting, swelling of matrices was found to be increased; whereas the erosion of tablet matrices and the release rate of aspirin were found decreased. The aspirin release rate from these tamarind gum-g-polyacrylamide based matrix tablets containing aspirin followed zero-order kinetic model and non-Fickian diffusion mechanism (Fig. 8), recommending the controlled release of aspirin. These types of grated tamarind gum based hydrogel tablets can be useful for the lesser gastrointestinal tract targeted drug delivery through oral administration.

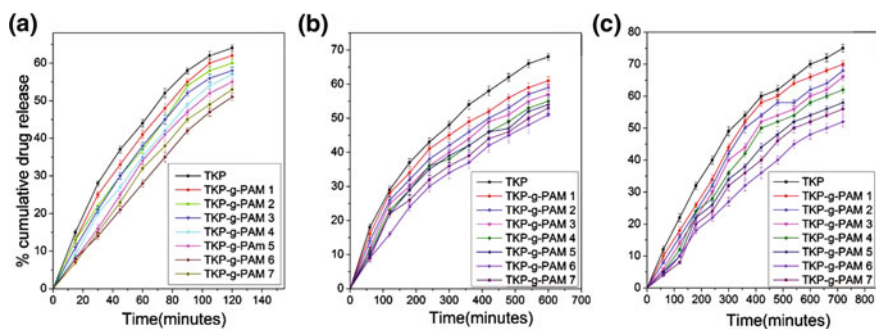


Fig. 8 Cumulative in vitro drug release profiles of tamarind gum-g-polyacrylamide based matrix tablets containing aspirin at **a** pH 1.2, **b** pH 6.8, and **c** pH 7.4. (Ghosh and Pal 2013). Copyright ©2013 with permission from Elsevier B.V.

6.3 *Tamarind Gum-g-Poly(N-Vinyl-2-Pyrrolidone) in Mucoadhesive Drug Delivery*

Ahuja et al. (2013) synthesized graft copolymers of tamarind gum with *N*-vinyl-2-pyrrolidone through microwave assisted graft copolymerization technique using ammonium persulfate as initiator and evaluated the synthesized graft copolymers of tamarind gum for the use as mucoadhesive polymers in the mucoadhesive drug delivery. In this research, the tamarind gum was isolated from tamarind kernel powder. Aqueous solutions containing 10% w/v native tamarind gum, 1% w/v *N*-vinyl-2-pyrrolidone and 10 mM/mL were irradiated using a microwoven at 20–60% microwave power for 60–150 s to prepare different batches of graft copolymers of tamarind gum. The process of graft copolymerization was statistically optimized by means of central composite design (2 factors and 3 levels), where microirradiation exposure time and microwave power were evaluated as independent factors and grafting efficiencies were analyzed as dependent responses. The statistical optimization-based response surface methodology indicated a mutual influence of microwave power and exposure time on percent grafting efficiency. It was also noticed that maximum grafting of *N*-vinyl-2-pyrrolidone on the tamarind gum took place at the lower microwave power for a longer time or at higher microwave power for a smaller period of exposing. At the elevated microwave power exposure for an exposure time of longer period resulted in lesser grafting efficiency, which appeared to be due to hydrolysis or degradation of the polymeric backbone. The optimal parameters were obtained 20% microwave power and 132 s microwave exposure time. The optimized batch of tamarind gum-g-poly (*N*-vinyl-2-pyrrolidone) has a maximum percent of grafting efficiency of 51.60% (where the predicted value was 56.86%).

These graft copolymers of tamarind gum and *N*-vinyl-2-pyrrolidone were also characterized using SEM, FTIR, XRD, and DSC analyses. These characterization analyses confirmed the formation of tamarind gum-g-poly(*N*-vinyl-2-pyrrolidone). The tamarind gum-g-poly(*N*-vinyl-2-pyrrolidone) was also assessed for biomucoadhesive application through the preparation of buccal patches containing metronidazole. Weight variation, thickness, assay, and friability of these metronidazole-containing buccal patches were assessed. The buccal patches were found of uniform weight (average) and uniform drug contents. The thickness of these patches was found within the range, 1.02–1.12 mm. The friability of the buccal patches was of less than 2%. The *in vitro* metronidazole release from these buccal patches composed of tamarind gum-g-poly(*N*-vinyl-2-pyrrolidone) was also tested. Almost similar drug releasing pattern was observed from these patches. These buccal patches exhibited drug release (less than 80%) and good *ex vivo* mucoadhesion time with chicken pouch membrane over a period of 9.3 h.

7 Conclusion

Though tamarind gum offers a great alternative to the other natural polysaccharides, it is imperative to understand the effect of introduction of suitable functional groups on its chemical structure for the better end applications in different areas. Tamarind gum is a plant-derived biocompatible polysaccharide, which is cheap and easily available in the nature. Various functionalized tamarind gum materials like carboxymethylated tamarind gum, thiolated tamarind gum, graft copolymerized tamarind gum, etc., have been explored as improved biomaterial for the formulation of effective drug delivery devices to achieve the desired drug releasing profiles because of their favorable physicochemical, biological, and mechanical properties. Several research works for the different types and patterns drug delivery applications employing various functionalized tamarind gum demonstrate the significant usefulness of the functional modifications of tamarind gum. The current chapter focuses on the different functionalized tamarind gum materials as prospective biopolymers in the formulation of effective drug delivery systems, which should be supportive for the drug delivery researchers.

References

- Ahuja M, Kumar S, Kumar A (2013) Tamarind seed polysaccharide-g-poly(*N*-vinyl-2-pyrrolidone): microwave-assisted synthesis, characterization and evaluation as mucoadhesive polymer. *Int J Polym Mater Polym Biomater* 62:544–549
- Ahuja M, Thakur K, Kumar A (2014) Amylopectin-g-poly(*N*-vinyl-2-pyrrolidone): synthesis, characterization and in vitro release behavior. *Carbohydr Polym* 108:127–134
- Avachat AM, Dash RR, Shrotriya SN (2011) Recent investigations of plant based natural gums, mucilages and resins in novel drug delivery systems. *Indian J Pharm Educ Res* 45:86–99
- Avachat A, Gujar KN, Wagh KV (2013) Development and evaluation of tamarind seed glucan-based mucoadhesive buccal films of rizatriptan benzoate. *Carbohydr Polym* 91: 537–542
- Bahulkar SS, Maunot NM, Surwase SS (2015) Synthesis, characterization of thiolated karaya gum and evaluation of effect of pH on its mucoadhesive and sustained release properties. *Carbohydr Polym* 130:183–190
- Bangle GS, Shinde GV, Umalkar DG, Rajesh KS (2011) Natural mucoadhesive material based buccal tablets of nitrendipine-formulation and in-vitro evaluation. *J Pharm Res* 4:33–38
- Bera H, Boddupalli S, Nandikonda S, Kumar S, Nayak AK (2015) Alginate gel-coated oil-entrapped alginate–tamarind gum–magnesium stearate buoyant beads of risperidone. *Int J Biol Macromol* 78:102–111
- Bernkop-Schnürch A, Walker G, Zasti H (2001) Thiolation of polycarbophil enhances its inhibition of intestinal brush border membrane bound aminopeptidase N. *J Pharm Sci* 90:1907–1914
- Bernkop-Schnürch A, Kast CE, Guggi D (2003) Permeation enhancing polymers in oral delivery of hydrophilic molecules: thioimer/GSH systems. *J Control Release* 93:95–103
- Bhattacharya A, Mishra BN (2004) Grafting: a versatile means to modify polymers-technique, factors and application. *Prog Polym Sci* 29:767–814

- Bhattacharya A, Ray P (2009) Basic features and techniques. In: Bhattacharaya A, Rawlins J, Ray P (eds) *Polymer grafting and crosslinking*. Wiley, Hoboken
- Chanda R, Mahapatro SK, Mitra T, Roy A, Bahadur S (2008) Development of oral mucoadhesive tablets of tarbutalline sulphate using some natural materials extracted from *Albemoschus esculentus* and *Tamarindus indica*. *Res J Pharm Res* 1:46–51
- Chandramouli Y, Firoz S, Vikram A, Padmaja C, Chakravarthi RN (2012) Design and evaluation of controlled release matrix tablets of acyclovir sodium using tamarind seed polysaccharide. *J Pharm Biol* 2:55–62
- Das B, Dutta S, Nayak AK, Nanda U (2014) Zinc alginate-carboxymethyl cashew gum microbeads for prolonged drug release: development and optimization. *Int J Biol Macromol* 70:505–515
- Datta R, Bandyopadhyay AK (2006) A new nasal drug delivery system for diazepam using natural mucoadhesive polysaccharide obtained from tamarind seeds. *Saudi Pharm J* 14:115–119
- Deveswaran R, Abraham S, Bharath S, Basavraj BV, Furtado S, Madhavan V (2009) Design and characterization of diclofenac sodium tablets containing tamarind seed polysaccharide as release retardant. *Int J PharmTech Res* 1:191–195
- Ghosh S, Pal S (2013) Modified tamarind kernel polysaccharide: a novel matrix for control release of aspirin. *Int J Biol Macromol* 58:296–300
- Gowda DV, Mahammad N, Vishnu Datta M (2014) Design and evaluation of carboxymethyl tamarind kernel polysaccharide controlled release spheroids/pellets and investigating the influence of compression. *Int J Pharm Pharmaceut Sci* 7:103–109
- Goyal P, Kumar V, Sharma P (2007) Carboxymethylation of tamarind kernel powder. *Carbohydr Polym* 69:251–255
- Goyal P, Kumar V, Sharma P (2008) Cyanoethylation of tamarind kernel powder. *Starch/Strake* 60:41–47
- GRAS Notice (GRN) (2014) No. 503, Determination of the GRAS status of the addition of tamarind seed polysaccharide to conventional foods as a stabilizer and thickener. <http://www.fda.gov/Food/IngredientsPackagingLabeling/GRAS/NoticeInventory/default.htm>
- Guilherme MR, Reis AV, Takahashi SH, Rubira AF, Feitosa JPA, Muniz EC (2005) Synthesis of a novel superabsorbent hydrogel by copolymerization of acrylamide and cashew gum modified with glycidyl methacrylate. *Carbohydr Polym* 61:464–471
- Gupta V, Puri R, Gupta S, Jain S, Rao GK (2010) Tamarind kernel gum: an upcoming natural polysaccharide. *Syst Rev Pharm* 1:50–54
- Hartemink R, Van Laere KMJ, Mertens AKC, Rombouts FM (1996) Fermentation of xyloglucan by intestinal bacteria. *Anaerobe* 2:223–230
- Hasnain MS, Nayak AK, Singh R, Ahmad F (2010) Emerging trends of natural-based polymeric systems for drug delivery in tissue engineering applications. *Sci J UBU* 1:1–13
- Hemmati K, Ghaemy M (2016) Synthesis of new thermo/pH sensitive drug delivery systems based on tragacanth gum polysaccharide. *Int J Biol Macromol* 87:415–425
- Jana S, Saha A, Nayak AK, Sen KK, Basu SK (2013) Aceclofenac-loaded chitosan-tamarind seed polysaccharide interpenetrating polymeric network microparticles. *Colloids Surf B Biointerfaces* 105:303–309
- Jani GK, Shah DP, Prajapati VD, Jain V (2009) Gums and mucilages: versatile excipients for pharmaceutical formulations. *Asian J Pharm Sci* 4:309–323
- Joseph J, Kanchalochana SN, Rajalakshmi G, Hari V, Durai RD (2012) Tamarind seed polysaccharide: a promising natural excipients for pharmaceuticals. *Int J Green Pharm* 6: 270–278
- Kaur G, Jain S, Tiwary AK (2010) Chitosan-carboxymethyl tamarind kernel powder interpolymer complexation: investigations for colon drug delivery. *Sci Pharm* 78:57–78
- Kaur H, Ahuja M, Kumar S, Dilbaghi N (2012a) Carboxymethyl tamarind kernel polysaccharide nanoparticles for ophthalmic drug delivery. *Int J Biol Macromol* 50:833–839
- Kaur H, Yadav S, Ahuja M, Dilbaghi N (2012b) Synthesis, characterization and evaluation of thiolated tamarind seed polysaccharide as a mucoadhesive polymer. *Carbohydr Polym* 90:1543–1549

- Khalil MI, Hasehem A, Habiesh A (1990) Carboxymethylation of maize starch. *Starch/Starke* 42:60–63
- Khanna M, Nandi RC, Sarin JP (1987) Standardization of tamarind seed polyose for pharmaceutical use. *Indian Drugs* 24:268–269
- Krauand AH, Leitner VM, Bernkop-Schnürch A (2003) Improvement in the in situ gelling properties of deacetylated gellan gum by immobilization of thiol groups. *J Pharm Sci* 92: 1234–1241
- Kulkarni GT, Gowthamarajan K, Dhobe RR, Yohanar F, Suresh B (2005) Development of controlled release spheroids using natural polysaccharide as release modifier. *Drug Deliv* 12:201–206
- Lang P, Masci G, Dentini M, Crescenzi V, Cooke D, Gidley MJ, Fanutti C, Reid JSG (1992) Tamarind seed polysaccharide: preparation, characterization and solution properties of carboxylated, sulphated and alkalaminated derivatives. *Carbohydr Polym* 17:185–198
- Mahajan HS, Tyagi VK, Patil RR, Dusunge SB (2013) Thiolated xyloglucan: synthesis, characterization and evaluation as mucoadhesive in situ gelling agent. *Carbohydr Polym* 91:618–625
- Maity S, Sa B (2014a) Ca-carboxymethyl xanthan gum mini-matrices: swelling, erosion and their impact on drug release mechanism. *Int J Biol Macromol* 68:78–85
- Maity S, Sa B (2014b) Development and evaluation of Ca²⁺ ion crosslinked carboxymethyl xanthan gum tablet prepared by wet granulation technique. *AAPS PharmSciTech* 15:920–927
- Manchanda R, Arora SC, Manchanda R (2014) Tamarind seed polysaccharide and its modification-versatile pharmaceutical excipients—a review. *Int J PharmTech Res* 6:412–420
- Manchanda R, Srivastava B, Arora SC, Manchanda R (2015) Optimization of carboxymethyl tamarind seed polysaccharide based glipizide matrix tablets using 3² full factorial design and response surface methodology. *Der Pharm Lett* 7:297–309
- Martinez A, Iglesias I, Lozano R, Teijon JM, Blanco MD (2011) Synthesis and characterization of thiolated alginate–albumin nanoparticles stabilized by disulfide bonds. Evaluation as drug delivery systems. *Carbohydr Polym* 83:1311–1321
- Masoumi A, Ghaemy M (2014) Removal of metal ions from water using nanohydrogel tragacanth gum-g-polyamidoxime: isotherm and kinetic study. *Carbohydr Polym* 108:206–215
- Meenakshi, Ahuja M (2015) Metronidazole loaded carboxymethyl tamarind kernel polysaccharide-polyvinyl alcohol cryogels: preparation and characterization. *Int J Biol Macromol* 72:931–938
- Meenakshi, Ahuja M, Verma P (2014) MW-assisted synthesis of carboxymethyl tamarind kernel polysaccharide-g-polyacrylonitrile: optimization and characterization. *Carbohydr Polym* 113:532–538
- Mehra GR, Manish M, Rashi S, Neeraj G, Mishra DN (2010) Enhancement of miotic potential of pilocarpine by tamarind gum based in situ gelling ocular dosage form. *Acta Pharm Sci* 52: 145–154
- Mishra MU, Khandare JN (2011) Evaluation of tamarind seed polysaccharide as a biodegradable carrier for colon specific drug delivery. *Int J Pharm Pharmaceut Sci* 3:139–142
- Mishra A, Pal S (2007) Polyacrylonitrile-grafted okra mucilage: a renewable reservoir to polymeric materials. *Carbohydr Polym* 68:95–100
- Mishra A, Yadav A, Pal S, Singh A (2006) Biodegradable graft copolymers of fenugreek mucilage and polyacrylamide: a renewable reservoir to biomaterials. *Carbohydr Polym* 65:58–63
- Mishra A, Clark JH, Pal S (2008) Modification of okra mucilage with acrylamide: synthesis, characterization and swelling behaviour. *Carbohydr Polym* 72:608–615
- Mittal H, Jindal R, Kaith BS, Maity A, Ray SS (2014) Synthesis and flocculation properties of gum ghatti and poly(acrylamide-co-acrylonitrile) based biodegradable hydrogels. *Carbohydr Polym* 114:321–329
- Mittal H, Jindal R, Kaith BS, Maity A, Ray SS (2015) Flocculation and adsorption properties of biodegradable gum-ghatti-grafted poly(acrylamide-co-methacrylic acid) hydrogels. *Carbohydr Polym* 115:617–628

- Nandi RC (1975) A process for preparation of polyose from the seeds of *Tamarindus indica*. Indian Patent 142092
- Nandi G, Patra P, Priyadarshini R, Kaity S, Ghosh LK (2015) Synthesis, characterization and evaluation of methacrylamide grafted gellan as sustained release tablet matrix. *Int J Biol Macromol* 72:965–974
- Nayak AK (2016) Tamarind seed polysaccharide-based multiple-unit systems for sustained drug release. In: Kalia S, Averous L (eds) *Biodegradable and bio-based polymers: environmental and biomedical applications*. WILEY-Scrivener, Hoboken, pp 469–492
- Nayak AK, Pal D (2011) Development of pH-sensitive tamarind seed polysaccharide-alginate composite beads for controlled diclofenac sodium delivery using response surface methodology. *Int J Biol Macromol* 49:784–793
- Nayak AK, Pal D (2012) Natural polysaccharides for drug delivery in tissue engineering. *Everyman's Sci XLVI*:347–352
- Nayak AK, Pal D (2013) Ionotropically-gelled mucoadhesive beads for oral metformin HCl delivery: formulation, optimization and antidiabetic evaluation. *J Sci Ind Res* 72:15–22
- Nayak AK, Pal D (2016) Chitosan-based interpenetrating polymeric network systems for sustained drug release. In: Tiwari A, Patra HK, Choi J-W (eds) *Advanced theranostics materials*. WILEY-Scrivener, Hoboken, pp 183–208
- Nayak AK, Pal D, Pany DR, Mohanty B (2010) Evaluation of *Spinacia oleracea* L. leaves mucilage as innovative suspending agent. *J Adv Pharm Technol Res* 1:338–341
- Nayak AK, Pal D, Pradhan J, Ghorai T (2012) The potential of *Trigonella foenum-graecum* L. seed mucilage as suspending agent. *Indian J Pharm Educ Res* 46:312–317
- Nayak AK, Pal D, Malakar J (2013) Development, optimization and evaluation of emulsion-gelled floating beads using natural polysaccharide-blend for controlled drug release. *Polym Eng Sci* 53:338–350
- Nayak AK, Pal D, Santra K (2014a) Development of calcium pectinate-tamarind seed polysaccharide mucoadhesive beads containing metformin HCl. *Carbohydr Polym* 101:220–230
- Nayak AK, Pal D, Santra K (2014b) Tamarind seed polysaccharide-gellan mucoadhesive beads for controlled release of metformin HCl. *Carbohydr Polym* 103:154–163
- Nayak AK, Pal D, Santra K (2015) Screening of polysaccharides from tamarind, fenugreek and jackfruit seeds as pharmaceutical excipients. *Int J Biol Macromol* 79:756–760
- Olusola A, Toluwalope AG, Olutayo O (2014) Carboxymethylation of *Anacardium occidentale* L. exudate gum: synthesis and characterization. *Sch Acad J Pharm* 3:213–216
- Pal D, Mitra S (2010) A preliminary study on the in vitro antioxidant activity of the stems of *Opuntia vulgaris*. *J Adv Pharm Technol Res* 1:268–272
- Pal D, Nayak AK (2012) Novel tamarind seed polysaccharide-alginate mucoadhesive microspheres for oral gliclazide delivery. *Drug Deliv* 19:123–131
- Pal D, Nayak AK (2015) Alginates, blends and microspheres: controlled drug delivery. In: Mishra M (ed) *Encyclopedia of biomedical polymers and polymeric biomaterials*. Taylor & Francis Group, New York, pp 89–98
- Pal S, Gorain MK, Giri A, Bandyopadhyay A, Panda AB (2011) In-situ silica incorporated carboxymethyl tamarind: development and application of a novel hybride nanocomposite. *Int J Biol Macromol* 49:1152–1159
- Pal D, Banerjee S, Ghosh A (2012) Dietary-induced cancer prevention: an expanding research arena of emerging diet related to healthcare system. *J Adv Pharm Technol Res* 3:16–24
- Pandey BPK, Kumar R, Taunk K (2001) Graft copolymerization of acrylamide onto xanthan gum. *Carbohydr Polym* 46:185–189
- Pandey VS, Verma SK, Yadav M, Behari K (2014) Guar gum-g-*N,N'*-dimethylacrylamide: synthesis, characterization and applications. *Carbohydr Polym* 99:284–290
- Parvathy KS, Susheelamma NS, Tharanathan RN, Goankar AK (2005) A simple non-aqueous method for carboxymethylation of galactomannan. *Carbohydr Polym* 62:137–141
- Prajapati VD, Jani GK, Moradiya NG, Randeria NP (2013) Pharmaceutical applications of various natural gums, mucilages and their modified forms. *Carbohydr Polym* 92:1685–1699

- Prashanth KVH, Tharanathan RN (2003) Studies on graft copolymerization of chitosan with synthetic monomers. *Carbohydr Polym* 54:343–353
- Rana V, Rai P, Tiwari AK, Singh RS, Kenedy JF, Knill CJ (2011) Modified gums: approaches and application in drug delivery. *Carbohydr Polym* 83:1031–1047
- Rani P, Sen G, Mishra S, Jha U (2012) Microwave assisted synthesis of polyacrylamide grafted gum ghatti and its application as flocculant. *Carbohydr Polym* 89:275–281
- Rao PS, Srivastava HC (1973) Tamarind. In: Whistler RL (ed) *Industrial Gums*, 2nd edn. Academic Press, New York, pp 369–411
- Rao PS, Ghosh TP, Krishna S (1946) Extraction and purification of tamarind seed polysaccharide. *J Sci Ind Res* 4:705
- Samal PK, Dangi JS (2014) Isolation, preliminary characterization and hepatoprotective activity of polysaccharides from *Tamarindus indica* L. *Carbohydr Polym* 102:1–7
- Sand A, Yadav M, Mishra DK, Behari K (2010) Modification of alginate by grafting of *N*-vinyl-2-pyrrolidone and studies of physicochemical properties in terms of swelling capacity, metal-ion uptake and flocculation. *Carbohydr Polym* 80:1147–1154
- Sarkar A, Mandre NR, Panda AB, Pal S (2013) Amylopectin grafted with poly(acrylic acid): development and application of a high performance flocculent. *Carbohydr Polym* 95:753–759
- Setia A, Kumar R (2014) Microwave assisted synthesis and optimization of *Aegle marmelos*-*g*-poly(acrylamide): release kinetics studies. *Int J Biol Macromol* 65:462–470
- Sharma R, Ahuja M (2011) Thiolated pectin—synthesis, characterization and evaluation as a mucoadhesive polymer. *Carbohydr Polym* 85:658–663
- Sharma BR, Kumar V, Soni PL (2004) Carbamoylethylation of guar gum. *Carbohydr Polym* 58:449–451
- Singh B, Chauhan N, Kumar S (2008) Radiation crosslinked psyllium and polyacrylic acid based hydrogels for use in colon specific drug delivery. *Carbohydr Polym* 73:446–455
- Singh B, Varshney L, Francis S, Rajneesh (2016) Designing tragacanth gum based sterile hydrogel by radiation method for use in drug delivery and wound dressing applications. *Int J Biol Macromol* 88:586–602
- Singha AS, Shama A, Thakur VK (2008) X-ray diffraction, morphological, and thermal studies on methylmethacrylate graft copolymerized *Saccharum ciliare* fiber. *Int J Polym Anal Charact* 13 (6):447–462
- Sonawane S, Bhalekar M, Shimpi S (2014) Preparation and evaluation of microspheres of xyloglucan and its thiolated xyloglucan derivative. *Int J Biol Macromol* 69:499–505
- Tattiyakul J, Muangnapoh C, Poommarinvarakul S (2010) Isolation and rheological properties of tamarind seed polysaccharide from tamarind kernel powder using protease enzyme and high-intensity ultrasound. *J Food Sci* 75:253–260
- Thakur VK, Singha AS (2011) Rapid synthesis, characterization, and physicochemical analysis of biopolymer-based graft copolymers. *Int J Polym Anal Charact* 16(3):153–164
- Thakur VK, Thakur MK (2015) Recent advances in green hydrogels from lignin: a review. *Int J Biol Macromol* 72:834–847
- Thakur VK, Singha AS, Thakur MK (2012) In-air graft copolymerization of ethyl acrylate onto natural cellulosic polymers. *Int J Polym Anal Charact* 17(1):48–60
- Thakur VK, Thakur MK, Gupta RK (2013a) Graft copolymers from cellulose: synthesis, characterization and evaluation. *Carbohydr Polym* 97:18–25
- Thakur VK, Thakur MK, Gupta RK (2013b) Rapid synthesis of graft copolymers from natural cellulose fibers. *Carbohydr Polym* 98:820–828
- Thakur VK, Singha AS, Thakur MK (2013c) Synthesis of natural cellulose-based graft copolymers using methyl methacrylate as an efficient monomer. *Adv Polym Technol* 32(S1):E741–E748
- Thakur VK, Thakur MK, Gupta RK (2013d) Graft copolymers from natural polymers using free radical polymerization. *Int J Polym Anal Charact* 18(7):495–503
- Thakur VK, Thakur MK, Gupta RK (2014a) Graft copolymers of natural fibers for green composites. *Carbohydr Polym* 104:87–93
- Thakur VK, Thunga M, Madbouly SA, Kessler MR (2014b) PMMA-*g*-SOY as a sustainable novel dielectric material. *RSC Adv* 4(35):18240–18249

- Thakur MK, Thakur VK, Gupta RK, Pappu A (2016) Synthesis and applications of biodegradable soy based graft copolymers: a review. *ACS Sustain Chem Eng* 4(1):1–17
- Tiwari A, Singh V (2008) Microwave induced synthesis of gum acacia-graft-polyaniline. *Carbohydr Polym* 74:427–434
- Togru H, Arslan N (2003) Production of carboxymethyl cellulose from sugar beet pulp cellulose and rheological behaviour of carboxymethylcellulose. *Carbohydr Polym* 54:74–84
- Vijan V, Kaity S, Biswas S, Isaac J, Ghosh A (2012) Microwave assisted synthesis and characterization of acrylamide grafted gellan, application indrug delivery. *Carbohydr Polym* 90:496–506
- Wang A, Wang W (2013) Gum-g-copolymers: synthesis, properties and applications. In: Kalia S, Sabaa MW (eds) *Polysaccharide based graft copolymers*. Springer, Berlin
- Zhang J, Xu S, Zhang S, Du Z (2008) Preparation and characterization of tamarind gum/sodium alginate composite gel beads. *Iran Polym J* 17:899–906

Chapter 3

Biopolymer Composite Materials with Antimicrobial Effects Applied to the Food Industry

Kelvia Álvarez, Vera A. Alvarez and Tomy J. Gutiérrez

Abstract Over the past decade, there has been a marked increase in consumer demand for healthy foods that are convenient, safe, with a longer useful life, and packaged using eco-materials. This has prompted both scientists and the food industry to investigate new strategies for food processing, handling, and packaging. In particular, films and coatings made from biodegradable and edible composite materials with antimicrobial effects, either due to intrinsic characteristics or through the incorporation of traditional or natural antimicrobial composites have been developed. These materials have proved to be a novel alternative to extend the shelf-life of foods, while maintaining their physical, chemical, and sensory properties and, most importantly, ensuring food safety. They also serve as a barrier against moisture loss from foods and the entry of oxygen. In addition, they can convey different bioactive compounds, some of which have an antimicrobial effect on important pathogenic microorganisms, thus ensuring food safety. All of this with an advantageous cost–benefit ratio. In this chapter, we review various biopolymer-based antimicrobial composites incorporated in films and coatings and their effects on different food matrices. Finally, factors that should be considered when developing composite materials with antimicrobial effects, as well as toxicological aspects and the regulatory status of these materials are discussed.

K. Álvarez · T.J. Gutiérrez

Faculty of Sciences, Institute of Food Science and Technology (ICTA), Central University of Venezuela (UCV), PO Box 47097, Caracas 1041-A, Venezuela

V.A. Alvarez (✉) · T.J. Gutiérrez (✉)

Thermoplastic Composite Materials (CoMP) Group, Faculty of Engineering, Institute of Research in Materials Science and Technology (INTEMA), National University of Mar del Plata (UNMDP), National Council of Scientific and Technical Research (CONICET), Colón 10850, Mar del Plata 7600, Buenos Aires, Argentina
e-mail: alvarezvera@fi.mdp.edu.ar; alvarezvera@gmail.com

T.J. Gutiérrez

e-mail: tomy.gutierrez@fi.mdp.edu.ar; tomy_gutierrez@yahoo.es

© Springer International Publishing AG 2018

V.K. Thakur and M.K. Thakur (eds.), *Functional Biopolymers*,
Springer Series on Polymer and Composite Materials,
https://doi.org/10.1007/978-3-319-66417-0_3

Keywords Antimicrobials · Composite materials · Edible coatings
Edible films · Natural fillers · Packaging · Thermoplastic materials

1 Introduction

Lifestyle and diet changes driven by the patterns of modern society have led to a greater acquisition by consumers of ready-to-eat products. These foods should provide adequate nutritional values for the proper functioning of the body and be microbiologically safe. The packaging should also be practical and, when discarded, friendly to the environment (Cagri et al. 2004). Such points have proved to be a challenge for the food and polymer industries, both technologically (development of new strategies for processing, handling, and packaging) and logistically (management, marketing, and appropriate delivery systems). This is largely because ready-to-eat foods require greater manipulation during processing, and are therefore more susceptible to attack by deteriorative and pathogenic microorganisms. This could lead to potential public health problems if they are not adequately processed, handled, and distributed (Beuchat 1996; Díaz-Cinco et al. 2005). Proper treatment, packaging, and storage are thus required to prevent contamination of these products and increase their useful life (Cagri et al. 2004).

The food industry has traditionally implemented several strategies to ensure food safety, namely cooling, dehydration, acidification, packaging in a modified atmosphere, fermentation, and/or the use of antimicrobials. This with the aim to control the growth of microorganisms in foods such as sausages, sliced cheeses, ready-to-cook meat products, and fresh-cut fruit and vegetables (Davidson et al. 2013). New preservation techniques are, however, being studied and successfully applied to these products. One of these is the use of edible coatings and films based on biodegradable polymers with added antimicrobial substances (Wang et al. 2016).

Of course, it must be said that a wide variety of packaging materials of inedible origins, such as polypropylene and polyethylene films, are already available to the food industry. However, although these materials do protect food from environmental pollution, they are non-biodegradable and thus not environmentally friendly (Michalska-Požoga et al. 2016; Thakur et al. 2014c). Because of this, packaging materials made with edible films and coatings derived from proteins, lipids, and polysaccharides are being studied and applied to food products. These biodegradable and environmentally friendly materials have been shown to act as barriers against water vapor, gases, and volatile compounds. They also serve as carriers of antimicrobial substances, antioxidants, flavorings, and vitamins, which can increase the quality, safety, functionality, and useful life of foodstuffs (Gennadios et al. 1997; Cagri et al. 2004; Lin and Zhao 2007; Rojas-Graü et al. 2009).

Two fundamental procedures have been used to control the behavior of microorganisms in food through the application of films: 1—the incorporation of antimicrobial agents into the polymeric matrix and 2—the generation of bioactive polymeric matrices on the surface of foods, which hinder the growth of

microorganisms (Silvera-Almitrán et al. 2012). As regards the first of these, numerous traditional and natural antimicrobials have been incorporated into films, including benzoates, propionates, sorbates, parabens, acidifying agents (acetic acid, lactic acid, etc.), curing salts (sodium chloride and sodium nitrite), natural agents (essential oils, lysozyme, liquid smoke), and bacteriocins (Cagri et al. 2004; Raybaudi-Massilia and Mosqueda-Melgar 2012). For example, amino groups on the C2 of films prepared from chitosan act on the biological capabilities of microorganisms. This affects their metabolic processes, thus restricting their growth (Silvera-Almitrán et al. 2012). In this chapter, we focus on edible films and coatings derived from proteins, lipids, and polysaccharides, either with antimicrobial substances added or with their own intrinsic antimicrobial activity, applied to ready-to-eat foods.

2 Antimicrobial Agents Incorporated into Edible Films and Coatings

Food antimicrobials are chemical compounds or substances that may retard the growth of microbes or cause their death when they are incorporated into a food matrix (Davidson and Zivanovic 2003). The main targets for these antimicrobials are toxin-producing pathogenic microorganisms, microorganisms that cause infections, and deteriorative microorganisms whose metabolic end products produce undesirable odors and flavors, problems with texture and the discoloration of the product (Davidson et al. 2013).

The grouping of antimicrobials into specific types is not easy, since some of those are considered as traditional and/or synthetics can also be found naturally in foods. Nevertheless, they are currently classified by some authors as traditional and naturals (naturally occurring compounds), while taking into account certain considerations (Raybaudi-Massilia et al. 2009; Davidson et al. 2013) as follows.

Antimicrobials are called traditional when they: (1) have been used for many years, (2) have been tested in many countries as food antimicrobials, and (3) have been produced by chemical synthesis. This classification does not imply that a traditional or synthetic preservative is any less effective from a microbiological point of view than one of natural origin, or vice versa.

Nonetheless, natural antimicrobial agents derived from plants, animals, microbial, and inorganic nanoparticles are preferred nowadays by consumers, due to their active promotion as “non-harmful” additives to the organism, and thus “healthier” than nonnatural or synthetic chemical substances. Table 1 shows some traditional and natural antimicrobial agents, which have been added to food packaging materials in order to obtain functional biopolymers with antimicrobial activity.

In addition, the incorporation of antimicrobial agents such as organic acids, bacteriocins, enzymes, plant extracts, and polysaccharides into edible films and coatings, has proven to be a novel alternative to retard or inhibit the growth of

Table 1 Some traditional and natural antimicrobial agents for the development of functional biopolymers

Antimicrobial agent	Biopolymeric material		References	
	Film	Coating		
Traditional	Malic acid	Alginate, milk whey protein	Gadang et al. (2008), Raybaudi-Massilia et al. (2008a, b)	
	Acetic acid	Chitosan	Bégin and Van Calsteren (1999)	
	Formic acid	Chitosan	Bégin and Van Calsteren (1999)	
	Lactic acid	Chitosan	Bégin and Van Calsteren (1999), Ye et al. (2008)	
	Lauric acid	Soy protein	Dawson et al. (2007)	
	Propionic acid	Zein	Janes et al. (2002), Valencia-Chamorro et al. (2009)	
	Potassium sorbate	Chitosan	Pranoto et al. (2005a, b), Ye et al. (2008), Valencia-Chamorro et al. (2009)	
	Sodium benzoate	Chitosan	Ye et al. (2008), Valencia-Chamorro et al. (2009)	
	Natural or new	Chitosan	Chitosan	Bégin and Van Calsteren (1999), Pen and Jiang (2003), Devlieghere et al. (2004), Dong et al. (2004), González-Aguilar et al. (2005, 2009), Pranoto et al. (2005a, b), Sebiti et al. (2005), Chien et al. (2007), Sangsuwan et al. (2008), Ye et al. (2008), Dutta et al. (2009), Vargas et al. (2009)
		Enzymes (lysozyme and ovotransferin)	Chitosan, alginate, carrageenan	Cha et al. (2002), Seol et al. (2009).
Essential oils		Chitosan, alginate, soy protein	Pranoto et al. (2005a, b), Oussalah et al. (2006a, b), Rojas-Graü et al. (2007), Raybaudi-Massilia et al. (2008a, b)	
Bacteriocins (nisin, enterocins and pediocins)		Chitosan, alginate, carrageenan, soy protein, cellulose, zein	Cha et al. (2002), Janes et al. (2002), Franklin et al. (2004), Pranoto et al. (2005a, b), Dawson et al. (2007), Millette et al. (2007), Gadang et al. (2008), Marcos et al. (2008), Santiago-Silva et al. (2009)	
Grapeseed and grapefruit extracts	Alginate, carrageenan, gelatin	Milk whey protein, soy protein	Cha et al. (2002), Theivendran et al. (2006), Gadang et al. (2008), Hong et al. (2009)	

(continued)

Table 1 (continued)

Antimicrobial agent	Biopolymeric material		References
	Film	Coating	
Green tea extract	Gelatin	Soy protein	Theivendran et al. (2006), Hong et al. (2009)
Species powder	Caseinate, milk whey protein		Outtara et al. (2002)
Vanillin		Alginate, cellulose, apple puree, chitosan	Rojas-Graü et al. (2007), Sangsuwan et al. (2008)

Table 2 Effect of functional biopolymers on foods

Matrix type	Antimicrobial added	Food applied	Effect	References
Alginate	Nisin	Ground beef	Reductions of more than 3.0 log CFU/g of the population of <i>Brochothrix thermosphacta</i>	Cutter and Siragusa (1997)
Alginate	Nisin	Chicken	Reductions of more than 4.0 log CFU/g of the population of <i>Salmonella enterica</i> ser. Typhimurium	Natrajan and Sheldon (2000)
Alginate	Nisin	Meat fillets	Reductions of more than 2.5 log CFU/g of the population of <i>Staphylococcus aureus</i>	Millette et al. (2007)
Alginate	Lysozyme/Nisin	Smoked salmon	Reductions in populations of <i>L. monocytogenes</i> and <i>Salmonella enterica</i> serovar Anatum in a range between 2.2 and 2.8 log CFU/g	Datta et al. (2008)
Alginate	Enterotoxin A and B	Baked sliced ham	Bacteriostatic effect on the population of <i>L. monocytogenes</i>	Marcos et al. (2008)
Alginate	Essential oil of oregano, cinnamon and savory	Meat fillets	Reduction of more than 1.0 log CFU/g of the population of <i>S. enterica</i> serovar Typhimurium applying alginate films with essential oils of oregano or cinnamon. Reduction of more than 2.0 log CFU/g of the population of <i>E. coli</i> O157:H7 applying alginate films with oregano essential oil	Oussalah et al. (2006a, b)
Alginate	Essential oil of oregano, cinnamon, and savory	Baked ham and bologna sliced	Reductions of more than 2.0 log CFU/g of populations of <i>Salmonella enterica</i> serovar Typhimurium and <i>L. monocytogenes</i> in bologna and cooked ham slices applying alginate films with cinnamon essential oil	Oussalah et al. (2007)
Carraegenan	Ovotransferin	Fresh chicken	Reductions of 2.0 log CFU/g for the total population of microorganisms and 3 log CFU/g for <i>E. coli</i> when carrageenan films were applied with ovotransferin and EDTA	Seol et al. (2009)

(continued)

Table 2 (continued)

Matrix type	Antimicrobial added	Food applied	Effect	References
Chitosan	Cinnamaldehyde and acetic, propionic, and lauric acids	Cooked ham, bologna, and pastrami	The growth of Enterobacteriaceae and <i>Serratia liquefaciens</i> was delayed or completely inhibited, while the lactic acid bacteria were unaffected	Quattara et al. (2000)
Chitosan	Lysozyme	Mozzarella cheese	Reduction of 1.0 log CFU/g of populations of <i>L. monocytogenes</i> , <i>E. coli</i> , and <i>Pseudomonas fluorescens</i>	Duan et al. (2007)
Chitosan	Natamycin	Cheese	Reductions of 1.1 log CFU/g of yeast and mold populations	Fajardo et al. (2010)
Chitosan	Potassium sorbate, sodium lactate, and diacetate	Smoked salmon	Inactivation of the population of <i>L. monocytogenes</i>	Jiang et al. (2011)
Chitosan	Green tea extract	Pork sausages	Complete inhibition of microbial growth	Siripatrawan and Noipha (2012)
CMC	Potassium sorbate	Fresh pistachio	Inhibition of mold growth	Sayanjali et al. (2011)
Cellulose	Pediocin	Baked sliced ham	Films with pediocin (50%) caused a reduction of 2.0 log CFU/g of the population of <i>L. innocua</i> while films with pediocin to 25 or 50% only caused a reduction of 0.5 log CFU/g of the population of <i>Salmonella</i> sp.	Santiago-Silva et al. (2009)
Cellulose	Nisin	“Frankfurt”-type sausages	Reductions of about 2.0 log CFU/g in the population of <i>L. monocytogenes</i> and 3.3 log CFU/g in the population of total aerobics	Nguyen et al. (2008)
Methylcellulose/hydroxypropyl methylcellulose	Nisin	Sausages	Reductions of more than 2.0 log CFU/g of the population of <i>L. monocytogenes</i>	Franklin et al. (2004)

(continued)

Table 2 (continued)

Matrix type	Antimicrobial added	Food applied	Effect	References
Apple-based films	Cinnamaldehyde and carvacrol	Meat and chicken	Antimicrobial activity of the films turned out to be dependent on the concentration, temperature, and antimicrobial, being the greatest reductions in the populations of <i>Salmonella enterica</i> and <i>E. coli</i> O157:H7 (4.3–6.8 log CFU/g) at a concentration 3% of either antimicrobial (cinnamaldehyde or carvacrol) at 23 °C. While at 4 °C the reductions achieved in these populations were lower and carvacrol was more effective than the cinnamaldehyde	Ravishankar et al. (2009)
Apple-based films	Cinnamaldehyde and carvacrol	Ham	Films containing carvacrol were more effective than those containing cinnamaldehyde to reduce the population of <i>L. monocytogenes</i> inoculated. Besides, greater reductions were found at 23 °C than at 4 °C	Ravishankar et al. (2009)
Apple-based films	Cinnamaldehyde and carvacrol	Chicken	Films containing cinnamaldehyde were more effective than those containing carvacrol to reduce the population of <i>Campylobacter jejuni</i> . Besides, greater reductions of that population were observed at 23 °C compared to 4 °C	Mild et al. (2011)

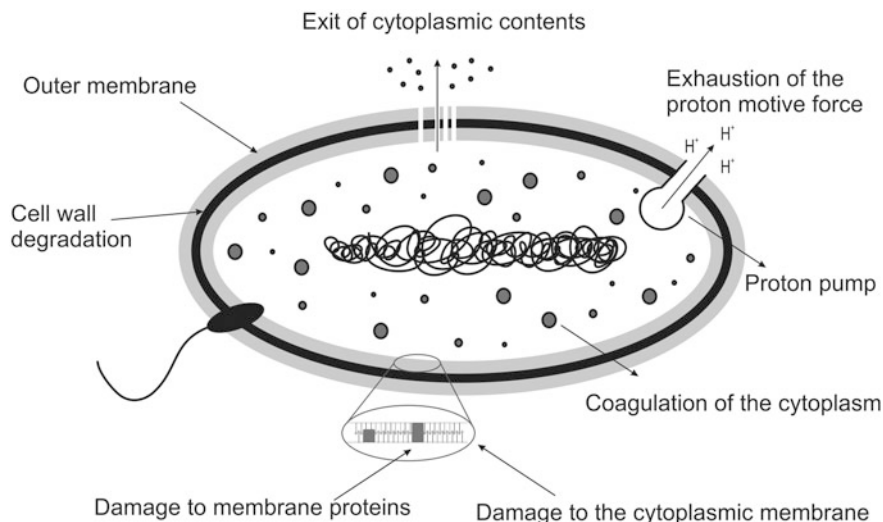


Fig. 1 Mechanisms of action of functional biopolymers from the incorporation of antimicrobial agents

bacteria, yeasts, and molds in a wide range of foods. The resulting improvement in food quality and safety has meant that the application of these agents is becoming ever more common (Table 2). Figure 1 summarizes the possible mechanisms of action of antimicrobial agents used in the development of functional biopolymers.

2.1 Traditional Antimicrobial Agents

Organic acids are the most traditional and commonly used preservation agents in the food industry. Some of these, for example, citric, malic, lauric, propionic, tartaric, benzoic, sorbic and lactic acid, have been incorporated into edible films and coatings, either indirectly or in salt form. Their spectrum of antimicrobial action is very wide, and results from a direct decrease in the pH of the substrate or growth medium due to an increase in the proton concentration. This alters the permeability of the cell membrane due to interactions between the membrane proteins and phospholipids, thus affecting its functioning (Davidson et al. 2013). Furthermore, the non-dissociated forms of weak organic acids can penetrate the lipidic bilayer of the cell membrane of microorganisms more easily. Once inside, the acid molecule is forcibly dissociated into anions and protons due to the near-neutral pH in the cell cytoplasm. This leads to cell inactivation by damage to cell signaling, active transport mechanisms, and genetic material (Stratford and Eklund 2003).

2.2 *Natural Antimicrobial Agents*

Depending on their origin, natural antimicrobials may be classified as vegetable, animal, microbial, or inorganic.

2.2.1 *Agents of Vegetable Origin*

Vegetable antimicrobials are those compounds naturally present in different plant parts, such as stems, bark, roots, flowers, and fruits, which have an inhibitory or bactericidal effect on microorganisms. Among the compounds in this group that have been applied to biopolymer-based edible films and coatings are essential oils, spices, and other extracts.

Essential Oils

Essential oils are aromatic oily liquids derived from plant parts (flowers, seeds, leaves, twigs, grass, wood, fruits, and roots). They consist of a complex mixture of compounds such as terpenes, alcohols, ketones, phenols, acid, aldehydes, and esters (Burt 2004; Ayala-Zavala et al. 2005) that can be obtained by fermentation, extraction, or distillation. Essential oils and their components have been used since ancient times as flavorings in food. However, some of them, for example, those extracted from oregano, cinnamon, clove, lemongrass, palmarosa, thyme, savory, pepper and garlic, and some of their active compounds, such as carvacrol, cinnamaldehydes, eugenol, citral, geraniol, and thymol, have recently been incorporated as antimicrobial agents into biopolymer-based edible films and coatings (Oussalah et al. 2004, 2006a; Pranoto et al. 2005a; Raybaudi-Massilia et al. 2008a, b; Rojas-Graü et al. 2009). There is no one mechanism of action of essential oils on microorganisms, as they consist of multiple chemical compounds that act on different targets on and within microbial cells (Burt 2004). Nychas et al. (2003), Burt (2004) and Oussalah et al. (2006b) indicate that essential oils can cause degradation of the cell wall, damage to the cytoplasmic membrane and membrane proteins, the output of cell content, coagulation of the cytoplasm, and a decrease in the proton motive force. Nychas et al. (2003) suggest that the mode of action of essential oils is dependent on their concentration, such that low concentrations inhibit enzymes associated with energy production, while high concentrations can cause the precipitation of proteins.

Vanillin

Vanillin (4-hydroxy-3-methoxybenzaldehyde) is a phenolic aldehyde present in vanilla beans. It has been used in edible coatings both as a flavoring and an

antimicrobial agent (Rojas-Graü et al. 2007). Vanillin is effective against Gram-positive and Gram-negative microorganisms, yeasts, and molds (Walton et al. 2003), but is most active against this last and non-lactic Gram-positive bacteria (Davidson et al. 2013). According to scientific studies, the inhibitory and bactericidal activity of vanillin lies mainly in its ability to negatively affect the integrity of the microorganism cytoplasmic membrane. This results in the loss of ions, thus unbalancing pH homeostasis and inhibiting respiratory activity (Fitzgerald et al. 2004).

Green Tea, Grapefruit, and Grape Seed Extracts

Green tea (GTE), grape seed (GS), and grapefruit seed (GFS) extracts have also been added to edible coatings in order to obtain composite biopolymers, due to the fact that they contain high concentrations of phenolic compounds. Polyphenols, particularly flavonoids such as catechins, are the most abundant compounds in GTE (Almajano et al. 2008) and many of its antimicrobial and antioxidant properties have been attributed to catechin fractions such as epicatechin (EC), epigallocatechin (EGC), epigallocatechin gallate (EGCg), epicatechin gallate (ECg), catechin gallate (Cg), and galocatechin gallate (GCg) (Frei and Higdon 2003). Taylor et al. (2005) note that studies conducted in the past 20 years have shown that polyphenolic catechins in green tea, particularly EGCg and ECg, can inhibit microbial growth in a wide range of Gram-positive and Gram-negative microorganisms. Shimamura et al. (2007) showed that the antimicrobial activity of these two catechins can be attributed mainly to the galloyl fraction (g), which is absent in EC and EGC. These authors also reported that EGCg can be directly linked to the precipitation of the peptidoglycan layer in microorganisms, thus interfering with their biosynthesis. Gram-positive bacteria are more sensitive to this action than Gram-negative bacteria, due to the presence of an outer membrane in the latter that serves as a barrier to antibacterials. The physiological function of the outer membrane of Gram-negative bacteria, and the low affinity between the polysaccharides contained within it and EGCg limit the linking of EGCg to the peptidoglycan layer, thus protecting them from antimicrobial activity (Shimamura et al. 2007).

GS and GFS are also rich sources of monomeric phenolic compounds such as the catechins EC and ECg, procyanidin dimer, trimer, and tetramer, which can act as antiviral and anti-mutagenic agents (Saito et al. 1998). GS and GFS are effective mainly against Gram-positive bacteria, with gallic acid the main active component (Jayaprakasha et al. 2003). The mechanisms of antimicrobial action proposed for GS and GFS, are that the fractions containing phenolic components and procyanidins may act on cell membrane proteins, producing the loss of K^+ , glutamic acid, and intracellular RNA, among others, as well as altering the fatty acid composition of the membrane (Rozes and Peres 1998; Heggers et al. 2002).

2.2.2 Agents of Animal Origin

Among the antimicrobials incorporated into edible films and coatings originating from animals are enzymes such as lysozyme and ovotransferin, as well as the polysaccharide, chitosan.

Enzymes

Lysozyme (peptidoglycan *N*-acetylmuramoyl hydrolase EC3.2.1.17) is an enzyme found in mammalian milk, tears and other secretions, bird eggs, insects, and fish. This enzyme catalyzes the hydrolysis of the glycosidic α -1, 4 bond between *N*-acetylmuramic acid and *N*-acetylglucosamine found in the peptidoglycan layer of bacterial cell walls (Davidson et al. 2013). Lysozyme is more effective against Gram-positive bacteria than Gram-negative bacteria, probably because in the former the peptidoglycan layer of the cell wall is more exposed. It is currently classified as a traditional antimicrobial and has been approved by several countries for its use in foods (Davidson et al. 2013).

Another enzyme, ovotransferrin (commonly known as “conalbumin”) is the second most important protein in egg white. It is a glycoprotein belonging to the transferrin family, linked to iron, which transports and sequesters iron ions (Fe^{+3}) (Ko et al. 2008). Ovotransferrin inhibits several Gram-positive and Gram-negative bacteria and yeasts including: *Escherichia coli*, *Pseudomonas* spp., *Streptococcus mutans*, *Staphylococcus aureus*, *Bacillus cereus*, *Salmonella enteritidis*, and *Candida*, although it is most effective in Gram-positive bacteria (Ko et al. 2008; Davidson et al. 2013). The mechanism of ovotransferrin antimicrobial action is not yet fully understood, but it was thought to have the ability to bind to Fe^{+3} , since this is the principal mechanism of action of ovotransferrin. More recent studies have, however, shown that its antimicrobial action is through a direct interaction with the bacterial surface. This produces an increase in the permeability of the outer membrane of Gram-negative bacteria, which can subsequently cause damage to the biological functions of the cytoplasmic membrane (Ibrahim et al. 2000).

Chitosan

Another type of antimicrobial of animal origin used in biopolymeric coatings and films is chitosan, a linear binary heteropolysaccharide composed of *N*-acetylglucosamine and glucosamine associated with the β -(1, 4) link (Thakur and Thakur 2014; Thakur and Voicu 2016). Chitosan is obtained commercially by the deacetylation of chitin, an abundant constituent of fungi and the exoskeletons of crustaceans and insects (Pranoto et al. 2005b; Sebti et al. 2005). This compound could potentially be used in a wide range of applications due to its biodegradability, biocompatibility, antimicrobial activity, nontoxicity, and versatile physical and chemical properties (Dutta et al. 2009). The mechanisms of the antimicrobial action

of chitin, chitosan, and their derivatives are still largely unknown. However, studies done by Liu et al. (2004) showed that chitosan increases the permeability of both the outer and inner membranes of bacterial cells to break point, with the subsequent leakage of cytoplasmic content. The authors attributed this damage or bactericidal effect to the electrostatic interaction between the positively charged amino groups (NH_3^+) of the chitosan and the negatively charged phosphoryl groups (PO_3^-) of the phospholipidic components of the cell membrane.

2.2.3 Agents of Microbial Origin

Among the antimicrobial compounds of microbial origin incorporated into biopolymer composites (Thakur et al. 2014a, b) are bacteriocins such as nisin, pediocin, and enterocin.

Bacteriocins are peptides or proteins produced by different microorganisms that have an inhibitory or bactericidal effect on other microorganisms. Bacteriocins produced by lactic acid bacteria are separated into two main groups: lactacins and lactocins (produced by *Lactobacillus* spp.), and lysine (produced by *Lactococcus lactis*) and pediocins (produced by *Pedococcus acidilactici*) (Marugg 1991; Davidson and Zivanovic 2003). Another group of commonly studied bacteriocins are enterocins, which are produced by species in the genus *Enterococcus*. Of these bacteriocins, the most studied and applied has been nisin, a small heat stable 34 amino acid peptide. Nisin shows bactericidal activity against Gram-positive bacteria and their spores, but is ineffective against Gram-negative bacteria (Helander and Mattila-Sandholm 2000). The low antimicrobial effectiveness of nisin against Gram-negative bacteria is due to the fact that they have a protective outer membrane covering both the cytoplasmic membrane and the peptidoglycan layer which is also thinner. The inner surface of this outer membrane contains phosphoglycerides, and the outer surface lipopolysaccharide molecules (LPS). These together create a hydrophilic surface (Nikaido 1996) that acts as a barrier against the penetration of hydrophobic and macromolecular substances. Nisin is a hydrophobic macromolecule and is thus unable to traverse the outer membranes of Gram-negative bacteria, which means it cannot reach its site of action (Helander and Mattila-Sandholm 2000).

On the other hand, the mechanism of action of lysine involves its interaction with precursors of peptidoglycan and the formation of transient pores in the cytoplasmic membrane of the target organism (Abee et al. 1994). This leads to a decrease in proton motive force and a loss of cell ions, amino acids, and ATP (Crandall and Montville 1998). Lysine can also interfere in the biosynthesis of cell walls, however, some researchers have suggested that this may simply be a consequence of energy loss and the depolarization of the membrane resulting from pore formation and the onset of autolysis (Thomas et al. 2000).

Pediocins and enterocins have not been well characterized, and their mode of action on microorganisms is still not at all clear. Their antimicrobial nature has been

demonstrated, however, with strong activity reported against pathogenic microorganisms (Sobrino-López and Martín-Belloso 2008; Santiago-Silva et al. 2009). Bhunia et al. (1991) indicated that pediocin initially causes the loss of viability of sensitive cells when it binds to nonspecific receptors (probably lipoteichoic acids). Once these nonspecific sites are saturated, the pediocin molecules bind to specific receptors, leading to changes in membrane integrity. This causes the cells to lose potassium ions and other small molecules, as well as lowering their ability to multiply. In some strains, the cell membrane may also lose its structural integrity and undergo lysis. In resistant Gram-positive bacteria, the specific receptors are absent or are not available for bonding, and in Gram-negative bacteria both nonspecific and pediocin-specific receptors are absent. As regards enterocins, Krämer and Brandis (1975) indicated that they may inhibit DNA, RNA, and protein synthesis, as well as preventing the accumulation of isoleucine, and causing the exit of already accumulated isoleucine. These effects on biochemical processes may indicate an obstruction of the energy supply and an alteration in membrane permeability.

2.2.4 Agents of Inorganic Origin

Inorganic antimicrobial agents, such as zinc oxide, titanium oxide, and silver, have been frequently incorporated as nanoparticles (NPs) in biopolymer-based matrices with the purpose of inhibiting the microbial growth of different pathogenic and deteriorative microorganisms (Table 3). In addition, NPs have helped to improve the physicochemical and mechanical properties of these matrices, which in recent years has generated the development of functional biopolymers that can be used as food packaging materials. Nevertheless, the migration of these NPs toward food is a key point in determining their antimicrobial efficacy. In addition, NPs have been subject of discussion due to their potentially counterproductive effects on the health of consumers (Llorens et al. 2012). Because of this, the food and polymer industries have been cautious over the use of these types of antimicrobial agents.

3 Factors to Consider in the Choice of Antimicrobials for Obtaining Functional Biopolymers

Antimicrobial effectiveness depends on several factors related to the food itself, storage conditions, handling, and the type of microorganism to be controlled. The preservation of food is best achieved when the following aspects are known and taken into account: microorganisms to be inhibited, type of antimicrobial and its concentration, temperature and time of storage, food pH, buffering capacity, and the presence of other agents that may affect its useful life (Davidson et al. 2013).

Table 3 Functional biopolymers made from inorganic nanocomposites with antimicrobial effects

Inorganic nanocomposites	Microorganisms inhibited	References
Zinc oxide	<i>Escherichia coli</i> O157:H7	Becheri et al. (2008), Liu et al. (2009), Rahman et al. (2013), El Saeed et al. (2015), Shankar et al. (2015)
Titanium oxide	<i>Diaporthe actinidia</i> , <i>Escherichia coli</i> , <i>Listeria monocytogenes</i> , <i>Penicillium expansum</i> , <i>Pseudomonas aeruginosa</i> , <i>Salmonella choleraesuis</i> , <i>Staphylococcus aureus</i> , and <i>Vibrio parahaemolyticus</i>	Wist et al. (2002), Chawengkijwanich and Hayata (2008), Lan et al. (2013), Ammendolia et al. (2014), Othman et al. (2014), Bogdan et al. (2015)
Silver	<i>Bacillus megaterium</i> , <i>Bacillus subtilis</i> , <i>E. coli</i> , <i>Janthinobacterium lividum</i> , <i>Klebsiella pneumonia</i> , <i>M. smegmatis</i> , <i>P. aeruginosa</i> , <i>P. aeruginosa</i> , <i>S. aureus</i> , <i>S. epidermidis</i> , <i>S. flexneri</i> , and <i>S. typhi</i>	Sondi and Salopek-Sondi (2004), Sharma et al. (2009), Valodkar et al. (2010), Yoksan and Chirachanchai (2010), Božanić et al. (2011), Dallas et al. (2011), Mohanty et al. (2012), Raji et al. (2012), Wang et al. (2013), Kahrilas et al. (2014), Salunke et al. (2014), Taheri et al. (2014), Franci et al. (2015), Ibrahim (2015), Latif et al. (2015)

According to Gould (1989), the factors affecting antimicrobial activity may be classified into microbial, intrinsic, extrinsic, and processing. Microbial factors influence inherent resistance (vegetative cells vs. spores, differences between strains), start number and growth rate, interaction with other microorganisms (competition, antagonism), cell composition (Gram reaction), cell status (lesions), and the ability to form films. Intrinsic factors are those associated with the food itself such as nutrients, pH, buffering capacity, oxide-reduction potential, and water activity. Extrinsic factors include storage time, temperature, atmosphere and relative humidity. Finally, processing factors affecting antimicrobial activity are food composition, the replacement of native microflora, changes in microbial populations, and changes in the microstructure of foods.

4 Determination of Antimicrobial Activity

The principal method used to evaluate the antimicrobial activity of films derived from composite biopolymers is the disk diffusion method. This method, one could say, is an adaptation of the method developed by Davidson and Parish (1989) used to determine the antimicrobial activity of chemical agents including antibiotics. The disk diffusion method consists in cutting approximately 1 cm² discs from the films to be evaluated and placing them on the surface of solidified agar (previously inoculated with specific microorganisms) contained in Petri dishes. The petri dishes with the disks and inoculated agar are then incubated at the optimum growth temperature for microorganisms for a set time, after which the areas or zones of inhibition caused by the action exerted by the antimicrobial agents are measured. Padgett et al. (1998), Cagri et al. (2001), Cha et al. (2002), Rojas-Graü et al. (2006), Seydim and Sarikus (2006) and Rosales-Oballos et al. (2012) all used this method and found that it was useful to evaluate antimicrobial activity at different concentrations of antimicrobials, since this enabled researchers to pinpoint the optimum concentration for each one, based on the measurement of the zone of inhibition of microorganism growth around the discs.

As a general rule, the antimicrobial activity of coatings and films based on functional polymers can be determined by two methods: dilution and the disk diffusion method.

4.1 Dilution Method

This method consists in placing different concentrations of the antimicrobial in a liquid or solid medium, which is then inoculated with the microorganism under study. For example, Rojas-Graü et al. (2007) evaluated the antimicrobial activity of an edible film-forming solution prepared from alginate and apple puree against *E. coli* O157:H7. The solution also contained oregano, cinnamon, and lemon grass essential oils and/or their active components: carvacrol, cinnamaldehyde, and citral. Film-forming solutions containing one or more of the essential oils or their active components were diluted with saline solution at pH 3.3, and placed in microplate wells which were then inoculated with *E. coli* O157:H7. The concentration of each compound capable of reducing the population of the microorganism to 50%, denominated bactericidal activity 50 (BA50), was then determined.

4.2 Disk Diffusion Method

The disk diffusion method consists in placing discs of the films containing different concentrations of the antimicrobial substance to be evaluated on agar plates



Fig. 2 Representation of the disk diffusion method from functional biopolymers

previously inoculated with the microorganism to be studied (Fig. 2). Padgett et al. (1998), Cagri et al. (2001), Cha et al. (2002), Seydim and Sarikus (2006) and Rojas-Graü et al. (2006) all used this method and found that it was useful to evaluate antimicrobial activity at different concentrations of antimicrobials, since this enabled researchers to pinpoint the optimum concentration for each one, based on the detection and measurement of the zone of inhibition of microorganism growth around the discs.

5 Edible Films and Coatings with Antimicrobial Effects Applied to Foodstuffs

The main purpose of food packaging is to preserve the quality and safety of foods, from the time of manufacture to the moment of consumption. Thus, packaging materials must act as a barrier to the passage of food contaminating agents. The best-known packaging materials that meet this objective are polyethylene or copolymer-based materials, which have been used by the food industry for over 60 years (Cutter 2006). Nonetheless, one of the limitations of these materials is that they are not biodegradable, which means that they represent a source of

environmental pollution. This has motivated scientists to develop packaging materials made from biodegradable substances that may also be edible, thus reducing environmental pollution while ensuring that the packaging meets the principal objective of food protection.

A novel alternative to traditional packaging materials has been the use of edible films, which can provide barrier properties and limit the passage of oxygen, thus preventing the contamination and deterioration of foodstuffs. The growth of microorganisms can be inhibited by simply suppressing oxygen entry, although films may also be prepared from matrices with antimicrobial properties such as chitosan. In addition, these functional biopolymers can serve as carriers of antimicrobial substances of either natural or synthetic origin (Rojas-Graü et al. 2009). One of the advantages of incorporating antimicrobial agents into biopolymer-based films is the reduction in the rate of diffusion of these compounds from foods, thus guaranteeing their action over a longer period of time on the surface of the food, where the greatest contamination usually occurs (Cagri et al. 2004).

5.1 Meat Products

The contamination of meat products usually starts from their external surface due to the microbial load coming from improper handling, processing machinery, and packaging. Antimicrobial films can prevent the contamination of meat and meat products during refrigerated storage, but can also be used to inhibit microbial growth on the surface of processed fresh products, consequently extending their useful life (Cagri et al. 2004).

According to the literature, antimicrobial films applied to meat products have been developed mainly from polysaccharides (alginate, cellulose, methylcellulose, and hydroxypropylmethylcellulose) and proteins (zein, caseinate, whey, soy, and gelatin) (Thakur et al. 2016; Thakur and Kessler 2014a, b; Voicu et al. 2016; Corobea et al 2016).

Oussalah et al. (2004) evaluated the antimicrobial effects of edible films prepared from milk protein containing oregano essential oil (1%) and/or pepper essential oil (1%) against *E. coli* O157:H7 and *Pseudomonas* spp. inoculated on beef steaks stored for 7 days at 4 °C. These authors found that the films containing oregano essential oil were the most effective, with a reduction in microbial populations of about 1 log cycle compared to control samples and films containing pepper essential oil. Oussalah et al (2006a) also determined the effect of alginate-based films containing 1% oregano, cinnamon, or savory (*Satureja* spp.) essential oils on populations of *Salmonella typhimurium* or *E. coli* O157:H7 inoculated into beef filets stored for 5 days at 4 °C. The authors reported that the films containing oregano or cinnamon essential oils were most effective against *S. typhimurium* (causing a decrease in the population of about 1 log cycle), while films made with oregano essential oil were the most effective against *E. coli* O157:H7 (population decreased

by 1.97 log cycles). Millette et al. (2007) evaluated the antimicrobial effect of an alginate-based film incorporating two different amounts of nisin (500 and 1000 IU) to control the growth of *S. aureus* inoculated onto beef steaks stored for 14 days at 4 °C. After 7 days, reductions in microorganism populations of 0.91 and 1.86 CFU/cm² on the beef steaks covered with the films containing 500 or 1000 IU/mL of nisin, respectively, were observed. Studies done by Zinoviadou et al. (2010) on fresh beef covered with films made from whey protein isolate containing either sodium lactate (NaL) or e-polylysine (e-PL), showed a reduction in the growth rate of total native flora and a total inhibition in the growth of lactic acid bacteria when a concentration of 0.75% of e-PL was added to the films. In addition, the growth of the total flora and *Pseudomonas* spp. was significantly inhibited with the addition of 2% NaL. Ouattara et al. (2002) achieved a slight reduction (by 0.5 log cycles) in the total counts of microorganisms naturally present in ground beef during the first 4 days of storage at 4 °C, after covering with a film prepared from a mixture of proteins (calcium caseinate and soy protein isolate) and 3% powdered thyme, sage, and rosemary. Nevertheless, populations of *Brochothrix thermosphacta*, *Staphylococcus* spp., lactic acid bacteria, coliforms, enterobacteriaceae, and *Pseudomonas* were not significantly affected by the use of this antimicrobial film.

On the other hand, Seol et al. (2009) were able to reduce populations of total microorganisms and *E. coli* by 1.8 and 2.7 CFU/g, respectively, in chicken breast covered by a zein-based film containing EDTA (5 mM) and ovotransferrin (25 mg), stored for 7 days at 5 °C. Similarly, Janes et al. (2002) found that populations of *Listeria monocytogenes* decreased by 1.69 or 2.03 log cycles in ready-to-eat chicken stored for 8 days at 4 °C, by incorporating either nisin (1000 UI/g), or nisin (1000 UI/g)—calcium propionate (1%), respectively, into a zein-based film used to cover the chicken. In addition, the antimicrobial effect of nisin alone in the edible film was intensified (by up to 2.59 log reductions) when the storage temperature was increased to 8 °C.

In other studies, Hong et al. (2009) covered pork loin with a film based on a gelatin/red algae agarose mixture containing grapefruit seed extract (0.08%) or green tea extract (2.8%). The antimicrobial action of the film inhibited the growth of *E. coli* O157:H7 and reduced populations of *L. monocytogenes* by about 1 log cycle after 7 days of storage at 4 °C. Similarly, Kang et al. (2007) evaluated the effect of an edible coating prepared from pectin containing green tea powder (0.5%) on the quality of pork burgers packaged in air or under vacuum and stored for 14 days at 10 °C. The authors reported that the initial population of total aerobic microorganisms (10⁴ CFU/mg) declined to undetectable levels after 7 days under vacuum conditions. However, under normal atmosphere (air) it rose to 10⁵ CFU/mg, and after 7 days at 10 °C reached 10⁸ CFU/mg.

Dawson et al. (2007) evaluated the antimicrobial effectiveness of soy protein-based films containing lauric acid (8%) and nisin (400 IU/g), against *L. monocytogenes* inoculated into turkey mortadella. The *L. monocytogenes* population was successfully reduced by 1 log cycle after 21 days at 4 °C. An even greater antimicrobial effect was observed by Santiago-Silva et al. (2009) who showed that

pediocin (25% or 50%) incorporated into an emulsion for cellulose-based films lead to a reduction in the populations of the pathogens *Listeria* and *Salmonella* inoculated into ham slices. These antimicrobial films were, however, more effective against *Listeria* than *Salmonella*: 50% pediocin reduced *Listeria* populations by 2 log cycles but *Salmonella* populations by only 0.5 log cycles compared to the control. Similarly, Gadang et al. (2008) found that populations of *L. monocytogenes* and *E. coli* O157:H7 inoculated into Frankfurt-type sausages stored at 4 °C for 28 days, decreased by 2 log cycles and populations of *S. typhimurium* by 1 log cycle when covered with edible films prepared from whey protein containing a combination of nisin (6,000 IU/g), malic acid (1%), and grape seed extract (0.5%), plus EDTA (1.6 mg/mL) for *S. typhimurium* and *E. coli* O157:H7. Similar results were reported by Theivendran et al. (2006) who evaluated the bactericidal effect of nisin (10,000 IU/g) combined with grape seed extract (1%) or green tea extract (1%) against *L. monocytogenes* inoculated into Frankfurt-type sausages submerged in film-forming solutions prepared from soy protein. These authors observed a decrease the population of *L. monocytogenes* by more than 2 log cycles after 28 days of storage at 4 or 10 °C. Similarly, Franklin et al. (2004) achieved a reduction in populations of *L. monocytogenes* in hot dog-type sausage stored for 28 days at 4 °C by more than 2 log cycles using 2,500 IU/mL of nisin, and the same result at a lower concentration with films made from methylcellulose/hydroxypropylmethylcellulose. Finally, Marcos et al. (2008) achieved a bacteriostatic effect against *L. monocytogenes* inoculated into cooked ham during the first 8 days at 1 °C, after incorporating enterocins A and B into alginate-based films.

5.2 Fishery Products

Films applied to fishery products have been developed mainly using gelatin, either alone or in combination with chitosan. Gelatin has been widely studied for its ability to form films and its capacity to protect food from dehydration, light and oxygen when used as an external cover. It is also one of the first materials proposed as a carrier of bioactive compounds (Gómez-Guillén et al. 2009). The most abundant sources of gelatin are the skin and bones of pigs and cattle. However, in recent years gelatin extracted from fish has become an important alternative.

López-Caballero et al. (2005) evaluated the preservative effect of a coating made from a mixture of chitosan and fish (*Lepidohombus boschii*) skin gelatin on cod burgers. These researchers found that the coating protected the burgers from microbial spoilage when they were refrigerated and stored for 8 or 11 days, reporting microorganism counts about 2 log cycles lower than those of control samples. The coatings were especially effective against Gram-negative bacteria such as *Enterobacteriaceae* and *Pseudomonas* spp. In addition, Gómez-Estaca et al. (2007) showed that gelatin/chitosan-based edible films containing rosemary and

oregano extract lead to a decrease in the total counts of aerobic and sulfide-reducing bacteria from 2 to 3 log cycles on cold-smoked sardines after 16 days at 5 °C.

In the same way, Datta et al. (2008) reported that coatings derived from calcium alginate with incorporated oyster lysozyme or hen egg lysozyme applied to smoked ham was effective in reducing levels of inoculated *Salmonella* var. Anatum (about 2.2 log cycles) and *L. monocytogenes* (about 2.7 log cycles).

5.3 Cheese

Fresh cheeses may suffer deterioration through the action of Gram-negative psychrotrophic bacteria (*Pseudomonas*, *Flavobacterium*, and *Alcaligenes*), coliforms, yeasts, and molds that reach them as postprocessing contaminants. The spoilage of ripened cheeses, however, is generally due to the surface growth of molds and yeasts, particularly if they are exposed to oxygen. Furthermore, the use of a slow growing starter culture can allow the development of pathogenic microorganisms such as *Staphylococcus*, *Salmonella*, *Listeria*, and enteropathogenic *E. coli*, which may either come from raw milk or postprocessing contamination.

A novel alternative to avoid this deterioration, and thus both extend the useful life of cheeses and ensure the safety of these products, is the use of antimicrobial films. Cao-Hoang et al. (2010) demonstrated that the application of sodium caseinate-based films, with the addition of sorbitol as a plasticizer and nisin (1,000 IU/cm²) as an antimicrobial, reduced a population of *Listeria innocua* inoculated onto the surface of ripened cheese by 1.1 log cycles after a storage period of 7 days at 4 °C.

5.4 Fruits and Vegetables

Edible coatings with antimicrobial agents have gained importance as a new technology to reduce the deleterious effects produced during the storage of processed and whole fruits and fresh-cut vegetables. These effects are more severe in the latter, as the cut damages the cell structure of the tissues. This causes the cell constituents to leak out, resulting in changes to the color and texture, and shortening useful microbiological life. In these situations, edible coatings and films can function as carriers of different preservation agents such as antioxidants, antimicrobials, and textural and nutritional preservatives, as well as vitamins and minerals that counteract the effects of pathogenic and deteriorative microorganisms.

Valencia-Chamorro et al. (2009) studied the antifungal effect of hydroxypropyl methylcellulose-based coatings containing different mixtures of potassium sorbate (2%), sodium benzoate (2.5%) and sodium propionate (0.5%) on the postharvest conservation of whole “Valencia” oranges. The authors observed that the coatings significantly reduced the effects caused by strains of *Penicillium digitatum* and

Penicillium italicum inoculated onto the surface of oranges stored at 20 °C. In addition they showed that edible coatings with potassium sorbate combined with sodium propionate were the most effective after a storage period of 60 days at 5 °C. Park et al. (2005) evaluated the antifungal effects of coatings prepared from chitosan (2%) and hydroxypropyl methylcellulose (1%) with or without added potassium sorbate (0.3%) on fresh strawberries inoculated with strains of *Cladosporium* sp. or *Rhizopus* sp. and stored for 23 days at 5 °C. The authors reported that the incorporation of potassium sorbate had no significant additive effect against the inoculated molds compared to the chitosan coatings alone. However, all the coatings studied decreased total aerobic and coliform counts.

Caillet et al. (2006) found that carrots inoculated with *L. innocua* (10^3 CFU/g) and covered with an antimicrobial coating prepared from a combination of calcium caseinate, whey protein isolate, carboxymethylcellulose, and pectin containing trans-cinnamaldehyde (0.025%) showed a slight reduction (0.5 log cycles) in the population of the microorganism after 21 days at 4 °C.

Rojas-Graü et al. (2007) evaluated the antimicrobial effect of lemongrass (1 and 1.5%), oregano (0.1 and 0.5%), and vanillin (0.3 and 0.6%) essential oils incorporated into film-forming solutions made from alginate and apple puree on native flora (psychrophilic aerobic, molds, and yeasts) and *L. innocua* inoculated into fresh-cut apples. They found that all the antimicrobials studied significantly inhibited the native flora during 21 days of storage at 4 °C. The lemongrass and oregano essential oils exerted a greater antimicrobial effect than the vanillin on *L. innocua*, however, producing a reduction in its population of up to 4 log cycles. Likewise, Raybaudi-Massilia et al. (2008a) covered fresh melon pieces inoculated with *S. enteritidis* with alginate-based edible coatings containing malic acid, either alone or combined with cinnamon leaf, palamarosa, and lemongrass essential oils at 0.3 and 0.7%, or their active components (eugenol, geraniol, and citral) at 0.5%. The coatings significantly reduced the populations of *S. enteritidis* by about 3–5 log cycles and inhibited the growth of native flora after storage for more than 21 days at 5 °C. Raybaudi-Massilia et al. (2008b) obtained similar results for fresh apple pieces inoculated with *E. coli* O157:H7, this time coated with alginate-based films containing malic acid, and/or cinnamon bark, clove and lemongrass essential oils at 0.3 and 0.7%, or their active components (cinnamaldehyde, eugenol, and citral) at 0.5%. In this case, the authors achieved population reductions of more than 4 log cycles after 30 days of refrigerated storage. The growth of the native flora was also inhibited for over more than 30 days of storage at 5 °C.

Chien et al. (2007) evaluated the effects of edible coatings derived from chitosan (0.5, 1 and 2%) on the growth of native flora for fresh-cut mango stored for 7 days at 6 °C. Populations, expressed as the total count of microorganisms, were inhibited in samples coated with different concentrations of chitosan (5.53, 5.41, 5.30 CFU/g) compared to the control (6.41 CFU/g). Nevertheless, a greater effectiveness of chitosan-based coatings was observed by González-Aguilar et al. (2009), who found that populations of mesophilic aerobics on fresh-cut papayas, covered with low molecular weight (2%) and medium molecular weight (1 and 2%) chitosan coatings, decreased from 2.8 CFU/g to undetectable levels after 14 days

storage at 5 °C. These authors also reported that the growth of molds and yeasts was inhibited on coated papayas compared to the controls. These differences in the effectiveness of chitosan-based coatings may be due mainly to the type of fruit studied and the initial microbial load.

Finally, Sangsuwan et al. (2008) evaluated the effectiveness of chitosan/methylcellulose coatings. These authors observed that populations of inoculated *E. coli* in coated fresh-cut melon pieces (5.18 UFC/piece) significantly decreased during storage to undetectable levels, while populations of *Saccharomyces cerevisiae* only slightly decreased in coated fresh-cut melons, but significantly decreased in coated fresh-cut pineapples, compared to the controls. These authors also found that the addition of vanillin to the chitosan/methylcellulose coatings increased their effectiveness against both the inoculated microorganisms.

6 Impacts on Sensory Attributes

Edible films and coatings are generally consumed while still in place. It is thus important that the incorporation of compounds such as antimicrobials, antioxidants, and nutraceuticals does not affect consumer acceptance (Rojas-Graü et al. 2009). However, some authors have indicated that adding antimicrobial agents to edible coatings could affect the sensory attributes of food, especially when plant essential oils are used (Burt 2004). For example, Rojas-Graü et al. (2007) observed that the sensory attributes of fresh-cut apples were negatively affected when covered with a coating prepared from alginate-apple puree containing 0.1% (v/v) of oregano essential oil. Similarly, Raybaudi-Massilia et al. (2008a, b) found that fresh-cut apple and melon pieces wrapped in coatings derived from alginate and containing cinnamon, lemongrass, palmarosa, and nail essential oils at 0.7% affected sensory attributes such as texture, color, and flavor. In order to reduce these effects, it is thus recommended that essential oils be used only at very low concentrations and possibly in combination with alternative preservatives. Nevertheless, Raybaudi-Massilia et al. (2008a) reported that the addition of 0.3% (v/v) of palmarosa essential oil to alginate-based films coating fresh-cut melon pieces actually turned out to be promising, since this combination was well accepted by the panelists, despite being perceived by them.

In another study, Eswaranandam et al. (2006) found that antimicrobial coatings derived from soy protein containing the organic acids malic and lactic acid at 2.6% (w/v) did not affect the sensory properties of fresh-cut melon.

Rojas-Graü et al. (2007) evaluated the sensory quality of fresh-cut apples covered with an alginate-apple puree film containing vanillin at 0.3% (w/w), finding that the taste of the coated product was acceptable to the panelists. In contrast, Walton et al. (2003) noted that a limitation of vanillin, despite being a GRAS substance, is the strong flavor it imparts when used at the minimum inhibitory

concentrations (>0.2%) required in some foods. These variations in the results reported by researchers are probably influenced by the type of food coated.

The effects of other antimicrobial composites such as chitosan, used as a base for the formulation of antimicrobial coatings, has also been evaluated as regards their sensory attributes. For example, the sensory qualities of fresh strawberries covered with chitosan (0.6%) were not significantly affected after 7 days storage at 2 °C (Han et al. 2005). Similarly, Chien et al. (2007) reported that the sensory attributes of fresh-cut mango coated with 0.5, 1, and 2% chitosan did not vary significantly after 3 days of storage at 6 °C, but were significantly altered after 7 days for the mangos coated with 1 and 2% chitosan.

7 Toxicological Aspects of Composite Biopolymers with Antimicrobial Effects

Most scientific studies focusing on the development of functional biopolymers made from natural fillers with antimicrobial effects have been undertaken, fundamentally, for their application in the food industry. Nonetheless, there is still a great vacuum in relation to the toxicological characteristics of these materials. The application of antimicrobial agents derived from inorganic nanocomposites in food has been particularly questioned, since they can penetrate the intestinal wall, with smaller particles tending to spread more quickly through the mucus layer than larger particles. The rate of diffusion also depends on the charge of the particle; anionic particles have been shown to traverse the epithelial surface more easily, while cationic particles remain trapped in the mucus (Szentkuti 1997). In addition, ligand binding or coating with surfactants can affect the transcellular absorption of particles in the gastrointestinal tract (Russell-Jones et al. 1999; Hoet et al. 2004). Furthermore, if encapsulated particles or NPs are protected or sterically hindered, this can facilitate or inhibit their entry into the bloodstream, resulting in an either homogeneous or heterogeneous distribution in the human body (Gabor et al. 2004).

Once nano-encapsulated or NP antimicrobials pass through the gastrointestinal epithelium and into the bloodstream, they may interact with various components of the blood, such as plasmatic proteins, coagulation factors, platelets, and red and white blood cells (Nemmar et al. 2002). These interactions can have a substantial effect on the distribution and excretion of NPs (Dobrovolskaia 2007). For example, the hydrophobic surfaces of nanospheres are highly susceptible to opsonization and deuration by the reticulo-endothelial system, resulting in the kidnapping of particles within organs such as the liver and spleen (Letchford and Burt 2007).

Borm and Kreyling (2004), Oberdorster et al. (2005a), Nel et al. (2006), Powers et al. (2006), Hagens et al. (2007) and Oberdorster et al. (2007a, b) have observed that the functionalities of NPs, e.g., particle size, size distribution, potential agglomeration and surface charge, can change in different biological matrices, and that this depends on compounds that are present in the matrix and thermodynamic

conditions. Interactions between the matrix and the NP's can also change as a result of dilution. In practice this means that the appearance of a NP can be expected to change following sample processing (e.g., freeze-thaw cycles, heating, dilution). It has, therefore, so far not been possible to establish a single parameter that describes the possible toxicity of an antimicrobial compound, in particular depending on the amount employed (SCENIHR 2007). Several authors have indicated that toxicity tests will have to be undertaken on a case-by-case basis using different dose-describing parameters (Oberdorster et al. 2005b; Thomas and Sayre 2005; Powers et al. 2006). In order to give an idea of the magnitude of the studies that need to be carried out to determine the toxicity of an antimicrobial packaging material, some toxicological aspects are discussed in Table 4.

Table 4 Toxicological studies in functional biopolymers made from inorganic nanocomposites

Toxicology study	Effect of inorganic nanocomposites	References
In vitro toxicity	NPs may trigger the release of reactive species and thereby cause oxidative stress and subsequent inflammation through interaction with the reticulo-endothelial system	Nel et al. (2006), Donaldson et al. (2007), Donaldson and Seaton (2007), Oberdorster et al. (2007b)
Toxicokinetics	There are experimental data so far suggesting that the characteristics of NPs (e.g., size, surface charge, functionalized groups) can influence the absorption, distribution, metabolism, and excretion (ADME) of NPs present in food. However, not much is known about the relationship between these physicochemical characteristics and the behavior of NPs in the body	Jani et al. (1990), Ballou et al. (2004), Florence (2005), Roszek et al. (2005), des Rieux et al. (2006), Singh et al. (2006), Hagens et al. (2007)
Neurotoxicity	Several studies have indicated that NPs can pass the blood–brain barrier following systemic availability of PNs. Nevertheless, it is not clear if this is a generic effect of all NPs or only a subgroup. This highlights the need of kinetic studies, and increased attention toxicologists to neurotoxicity in their search for possible effects on target tissues. Therefore, this fact is highly relevant for its consideration	Hillyer and Albrecht (2001), Borm et al. (2006), Silva (2007)

(continued)

Table 4 (continued)

Toxicology study	Effect of inorganic nanocomposites	References
Acute toxicity	In the past decade, the toxicological results made orally have noted that depending on the particle size (e.g., copper, selenium, zinc, and zinc oxide and titanium dioxide NPs), the matrix in which this content and the chemical composition of the NPs, the acute toxicity may occur at higher doses	Jia et al. (2005), Zhang et al. (2005), Chen et al. (2006), Wang et al. (2006, 2007, 2008)
Long term toxicity	Nowadays there is no data on the toxicity after chronic or acute low dose oral exposure. Although inorganic nanocomposites can have effects on the immune and inflammatory and cardiovascular system, including may provoke oxidative stress and/or activation of pro-inflammatory cytokines in the liver, lungs, brain, and heart. There could also be effects on the cardiovascular system, which in turn may have pro-thrombotic effects and adverse effects on the cardiac function (acute myocardial infarction and adverse effects on heart rate). Furthermore, they possibly may produce genotoxicity, carcinogenesis, and teratogenicity, but no data on these latter points that are still available	Wang et al. (2006, 2007, 2008)
Reprotoxicity	Another aspect to consider and that cannot be excluded is the transfer of NPs through the placenta, including excretion via breast milk, which could lead to embryotoxicity as a result of exposure to NPs. Data addressing the distribution of NPs to the reproductive cells is currently unavailable. Besides, there are no clear data showing the distribution of PNs in the fetus. This leads to the recommendation that reprotoxicity needs to be carefully considered when there is evidence that NPs pass into the placenta	Fujimoto et al. (2005), Tran et al. (2005)

(continued)

Table 4 (continued)

Toxicology study	Effect of inorganic nanocomposites	References
Allergenicity (or sensitization)	Even for conventional chemicals little is known on the induction of food allergy and the type of exposure required inducing such responses. In the case of NPs, this becomes extra prominent for two reasons. First of all, it is the possible adjuvant activity of NPs that introduces additional uncertainty. And second, because of the actively charged surfaces of NPs it can absorb biomolecules as they pass through the GI tract. This might result in changed exposure of the cellular lining of the intestine. In addition, the surface properties, e.g., coatings are important determinants for the active uptake of encapsulates, but might also be a reason for concern. For example, lectins used for coatings are highly immunogenic, can be cytotoxic or induce inflammatory responses and gastrointestinal irritation	Govers et al. (1994), Borm and Kreyling (2004), Gabor et al. (2004), des Rieux et al. (2006), Hong et al. (2006), Kabanov (2006), Dobrovolskaia (2007)

8 Regulatory Status

Edible films and coatings can be classified, according to European and American regulations, as food products, food ingredients, and substances in contact with food, or food packaging materials (ED 1995, 1998; USFDA 2006a, b). Nevertheless, because films and coatings constitute an integral part of the edible portion of food they should be subject to the same regulations as those governing food ingredients (Guilbert and Gontard 1995). The main government agencies responsible for dealing with issues related to food additives are the U.S. Food and Drug Administration (USFDA), the European Committee for Standardization (CEN), *Codex Alimentarius*, the Food and Agriculture Organization (FAO) of the United Nations and the World Health Organization (WHO) (Raju and Bawa 2006).

The USFDA states that any compound to be included in a formulation should be “Generally Recognized as Safe” (GRAS) or regulated as a food additive and used within specific limits (USFDA 2006a, b, 2009, 2010). In Europe, the ingredients that may be incorporated into film-forming solutions are recognized primarily as food additives and are named in the list of additives for general purposes, although pectins, beeswax, polysorbates, fatty acids, lecithin, and arabic and karaya gums, are mentioned separately as coating applications (ED 1995). In any case, the use of

these film-forming substances is permitted as long as the principle of *quantum satis* is respected. Recently, the CEN introduced specific purity criteria for food additives (ED 2008).

Due to the fact that edible films and coatings may have ingredients with a functional effect, the inclusion of these compounds should be mentioned on the label. In Europe, the use of food additives should always be labeled on the packaging according to their category, for example, antioxidants, preservatives, colorings, among others. In the corresponding regulations of most countries, chemical substances added as antimicrobials are considered as food additives if their main purpose is the extension of the useful life of the food (Table 5). However, each country has its own regulations and lists of approved additives (ED 1995, 1998, 2008; USFDA 2006a, b, 2009).

Another important point within the regulatory status is the presence of allergens. Many edible films and coatings are made from ingredients that could cause allergic reactions.

Among the substances identified as allergens, those derived from milk, soybeans, marine foods (fish, shellfish, crustaceans, etc.), peanuts, walnuts, and wheat are the most important. Several edible films and coatings are composed of milk proteins (whey, casein), wheat protein (gluten), soy protein, and peanut protein. The presence of a known allergen incorporated into an edible film and/or food coating should thus be very clearly labeled (Franssen and Knochta 2003).

Table 5 Regulatory status of the main antimicrobials incorporated into edible films and coatings to obtain functional biopolymers

Antimicrobial agent	Regulatory status	Amount permitted	References
Chitosan	GRAS, GRN 73, GRN 170	GMP	USFDA (2010)
Essential oils of plants and their active compounds (carvacrol, cinnamon, cinnamaldehyde, citral, cinnamic acid, citric acid, clove, eugenol, garlic, geraniol, lemon, lime, lemongrass, mandarin, oregano, palmarosa)	GRAS, 21 CFR 182.10, 21 CFR 182.20, 21 CFR 184.1317, 21 CFR 182.60, 21 CFR 184.1257	GMP	USFDA (2010)
Grape seed extract	CAS-RN 085594-37-2, 21 CFR 182.20	GMP	USFDA (2009)

(continued)

Table 5 (continued)

Antimicrobial agent	Regulatory status	Amount permitted	References
Grapefruit seed extract	CAS-RN 090045-43-5	GMP	USFDA (2009)
Green tea extract	GRN 259	GMP, up to 540 mg/per portion in juice	USFDA (2006a, b)
Lysozyme	GRAS, GRN 64, E-1105	GMP, ≤ 5.5 mg/kg in Frankfurt-type sausages, ≤ 4.4 mg/kg in chicken and beef products	Losso et al. (2000), USFDA (2006a, b, 2010)
Nisin	GRAS, GRN 65, 21 CFR 184.1538, E-234, A565, Codex standard A-8	GMP, ≤ 6.9 mg/kg in Frankfurt-type sausages, 5.5–12.5 mg/kg in chicken and beef products	USFDA (2010), FSANZ (2007)
Vanillin	GRAS, 21 CFR 182.60	GMP	USFDA (2010)
Organic acids (acetic, lactic, malic, propionic, benzoic, and their salts)	GRAS, 21 CFR 184.1005, 21 CFR 184.1021, 21 CFR 184.1221, 21 CFR 184.1069, 21 CFR 182.3640	GMP	Doores (1993)
Inorganic nanocomposites (zinc oxide, titanium oxide silver)	EU No. 10/2011	In Europe, the legislation currently applies an overall migration limit of 10 mg constituent per dm ² surface area to all substances that can migrate from food contact materials up to foodstuffs. For a liter cubic packaging containing 1 kg of food, this equates to a	EU No. 10/2011, Silvestre et al. (2011)

(continued)

Table 5 (continued)

Antimicrobial agent	Regulatory status	Amount permitted	References
		migration of 60 mg of substance per kg of food. However, with the exception of a few materials (specifically listed in Annex 1 of the legislation) nanomaterial risk assessment has to be performed on a case-by-case basis	

GRAS generally recognized as safe, *GRN GRAS* news according to USFDA, *A* Application according to FSANZ, 21 CFR: title 21 code of regulations of the United States, *E* code number of food additives in the European Union, *CAS-RN* chemical abstract service-registration number, *GMP* according to good manufacturing practices

Hen egg proteins such as ovotransferrin (Gal d 3) and lysozyme (Gal d 4), which reside in the egg white fraction and are used as antimicrobials in edible films, have traditionally been involved in the development of food allergies. However, clinical reactions to ovotransferrin and lysozyme have rarely been reported. Nonetheless, a hypersensitive reaction mediated by immunoglobulin E (IgE) may occur in people allergic to these enzymes (Pérez-Calderón et al. 2007). Thus, to make the use of lysozyme and ovotransferrin safe, their presence should be clearly identified on the product label (USDA 2010).

9 Conclusions and Future Perspectives

It has been amply demonstrated that films and coatings with antimicrobial properties can be developed as novel alternative packaging materials that ensure the safety of different food types, including meat, fish, fruits, vegetables, and dairy products such as cheese, as well as extending their useful life. Nonetheless, for these materials to be successfully applied the following aspects should be taken into account: food composition, identification of the active component for forming the film or coating, the antimicrobial to use, the type and number of microorganisms to control, and the intrinsic, extrinsic, and processing factors that may affect the product characteristics. In addition, antimicrobial agents should be incorporated in moderate amounts in order to prevent their negative impact on the sensory characteristics of foods, thus ensuring consumer acceptance.

In the future we expect that materials currently underutilized or discarded by the food industry, such as vegetable waste, plants, and crustacean shells, among others, will be used to obtain base materials such as cellulose and chitosan for the formulation of films and coatings, thus producing biodegradable materials that aid environmental conservation.

In recent years there have been a number of research studies on naturally occurring compounds such as plant extracts that show functional and antimicrobial properties when tested *in vitro* against pathogenic microorganisms of importance in foods, such as *L. monocytogenes*, *E. coli* O157:H7, *Salmonella* spp., *S. aureus* among others. Nevertheless, their direct application in foods or as components of films and coatings has not been fully investigated. For this reason, we expect to see the continuing emergence of new proposals for the formulation of packaging materials including natural antimicrobial agents.

Acknowledgements The authors would like to thank National Council of Scientific and Technical Research (CONICET) (Postdoctoral fellowship internal PDS-Resolution 2417) and National University of Mar del Plata (UNMdP) for the financial support.

References

- Abee T, Rombouts FM, Hugenholtz J, Guihard G, Letellier L (1994) Mode of action of nisin Z against *Listeria monocytogenes* Scott A grown at high and low temperatures. *Appl Environ Microb* 60(6):1962–1968
- Almajano MP, Carbo R, Jiménez JAL, Gordon MH (2008) Antioxidant and antimicrobial activities of tea infusions. *Food Chem* 108(1):55–63
- Ammendolia MG, Iosi F, De Berardis B, Guccione G, Superti F, Conte MP, Longhi C (2014) *Listeria monocytogenes* behaviour in presence of non-UV-irradiated titanium dioxide nanoparticles. *PLoS ONE* 9(1):e84986
- Ayala-Zavala JF, Villegas-Ochoa MA, Cuamea-Navarro F, González-Aguilar GA (2005) Compuestos volátiles de origen natural. Nueva alternativa para la conservación. En: Nuevas tecnologías de conservación de productos vegetales frescos cortados. González-Aguilar GA, Gargea AA, Cuamea-Navarro F (ed). Sonora, Mexico: CIAD AC, pp 314–338
- Ballou B, Lagerholm BC, Ernst LA, Bruchez MP, Waggoner AS (2004) Noninvasive imaging of quantum dots in mice. *Bioconj Chem* 15(1):79–86
- Becheri A, Dürr M, Nostro PL, Baglioni P (2008) Synthesis and characterization of zinc oxide nanoparticles: application to textiles as UV-absorbers. *J Nanopart Res* 10(4):679–689
- Bégin A, Van Calsteren M-R (1999) Antimicrobial films produced from chitosan. *Int J Biol Macromol* 26(1):63–67
- Beuchat LR (1996) Pathogenic microorganisms associated with fresh produce. *J Food Prot* 59(2):204–216
- Bhunia AK, Johnson MC, Ray B, Kalchayanand N (1991) Mode of action of pediocin AcH from *Pediococcus acidilactici* H on sensitive bacterial strains. *J Appl Bacteriol* 70(1):25–33
- Bogdan J, Jackowska-Tracz A, Zarzyńska J, Pławińska-Czarnak J (2015) Chances and limitations of nanosized titanium dioxide practical application in view of its physicochemical properties. *Nanoscale Res Lett* 10(1):1–10
- Borm PJA, Kreyling W (2004) Toxicological hazards of inhaled nanoparticles—potential implications for drug delivery. *J Nanosci Nanotechnol* 4(5):521–531
- Borm P, Klaessig FC, Landry TD, Moudgil B, Pauluhn J, Thomas K, Trottier R, Wood S (2006) Research strategies for safety evaluation of nanomaterials, part V: role of dissolution in biological fate and effects of nanoscale particles. *Toxicol Sci* 90(1):23–32
- Božanić DK, Djoković V, Dimitrijević-Branković S, Krsmanović R, McPherson M, Nair PS, Georges MK, Radhakrishnan T (2011) Inhibition of microbial growth by silver–starch nanocomposite thin films. *J Biomat Sci Polym E* 22(17):2343–2355

- Burt S (2004) Essential oils: their antibacterial properties and potential applications in foods—a review. *Int J Food Microbiol* 94(3):223–253
- Cagri A, Ustunol Z, Ryser ET (2001) Antimicrobial, mechanical, and moisture barrier properties of low pH whey protein-based edible films containing p-aminobenzoic or sorbic acids. *J Food Sci* 66(6):865–870
- Cagri A, Ustunol Z, Ryser ET (2004) Antimicrobial edible films and coatings. *J Food Prot* 67(4):833–848
- Caillet S, Millette M, Salmieri S, Lacroix M (2006) Combined effects of antimicrobial coating, modified atmosphere packaging, and gamma irradiation on *Listeria innocua* present in ready-to-use carrots (*Daucus carota*). *J Food Prot* 69(1):80–85
- Cao-Hoang L, Grégoire L, Chaîne A, Waché Y (2010) Importance and efficiency of in-depth antimicrobial activity for the control of *listeria* development with nisin-incorporated sodium caseinate films. *Food Control* 21(9):1227–1233
- Cha DS, Choi JH, Chinnan MS, Park HJ (2002) Antimicrobial films based on Na-alginate and κ -carrageenan. *LWT Food Sci Technol* 35(8):715–719
- Chawengkijwanich C, Hayata Y (2008) Development of TiO₂ powder-coated food packaging film and its ability to inactivate *Escherichia coli* in vitro and in actual tests. *Int J Food Microbiol* 123(3):288–292
- Chen Z, Meng H, Xing G, Chen C, Zhao Y, Jia G, Wang T, Yuan H, Ye C, Zhao F, Chai Z, Zhu C, Fang X, Ma B, Wan L (2006) Acute toxicological effects of copper nanoparticles in vivo. *Toxicol Lett* 163(2):109–120
- Chien PJ, Sheu F, Yang FH (2007) Effects of edible chitosan coating on quality and shelf life of sliced mango fruit. *J Food Eng* 78(1):225–229
- Commission Regulation (EU) No. 10/2011 of 14 of January 2011 on plastic materials and articles intended to come in contact with food. *Off J Eur Un*
- Corobea MC, Muhulet O, Miculescu F, Antoniac IV, Vuluga Z, Florea D et al (2016) Novel nanocomposite membranes from cellulose acetate and clay-silica nanowires. *Polym Adv Technol* 27(12):1586–1595
- Crandall AD, Montville TJ (1998) Nisin resistance in *Listeria monocytogenes* ATCC 700302 is a complex phenotype. *Appl Environ Microb* 64(1):231–237
- Cutter CN (2006) Opportunities for bio-based packaging technologies to improve the quality and safety of fresh and further processed muscle foods. *Meat Sci* 74(1):131–142
- Cutter CN, Siragusa GR (1997) Growth of *Brochothrix thermosphacta* in ground beef following treatments with nisin in calcium alginate gels. *Food Microbiol* 14(5):425–430
- Dallas P, Sharma VK, Zboril R (2011) Silver polymeric nanocomposites as advanced antimicrobial agents: classification, synthetic paths, applications, and perspectives. *Adv Colloid Interface* 166(1):119–135
- Datta S, Janes ME, Xue QG, Losso J, La Peyre JF (2008) Control of *Listeria monocytogenes* and *Salmonella anatum* on the surface of smoked salmon coated with calcium alginate coating containing oyster lysozyme and nisin. *J Food Sci* 73(2):M67–M71
- Davidson PM, Parish ME (1989) Methods for testing the efficacy of food antimicrobials. *Food Technol Chicago* 43:148–155
- Davidson PM, Zivanovic S (2003) The use of natural antimicrobials. In: Zeuthen P, BoghSorensen L (eds) *Food preservation techniques*. CRC Press LLC, Boca Ratón, pp 5–30
- Davidson PM, Taylor TM, Schmidt SE (2013) Chemical preservatives and natural antimicrobial compounds. In: Doyle MP, Beuchat LR (eds) *Food microbiology. Fundamentals and frontiers*, 4a edn. ASM Press, Washington, pp 765–801
- Dawson PL, Carl GD, Acton JC, Han IY (2007) Efecto de películas a base de soya impregnadas con ácido láurico y nisina sobre el crecimiento de *Listeria monocytogenes* en mortadella de pavo. *Mundo lácteo y cárnico mayo/junio* 13–21
- des Rieux A, Fievez V, Garinot M, Schneider YJ, Preat V (2006) Nanoparticles as potential oral delivery systems of proteins and vaccines: a mechanistic approach. *J Control Release* 116(1): 1–27

- Devlieghere F, Vermeulen A, Debevere J (2004) Chitosan: antimicrobial activity, interactions with food components and applicability as a coating on fruit and vegetables. *Food Microbiol* 21 (6):703–714
- Díaz-Cinco ME, Acedo-Félix E, García-Gálaz A (2005) Principales microorganismos patógenos y de deterioro. In: González-Aguilar GA, Gardea AA, Cuamea-Navarro F (eds) *Nuevas tecnologías de conservación de productos vegetales frescos cortados*. CIAD, México, pp 216–240
- Dobrovolskaia M (2007) Immunological properties of engineered nanomaterials. *Nat Nanotechnol* 2(8):469–478
- Donaldson K, Seaton A (2007) The Janus faces of nanoparticles. *J Nanosci Nanotechnol* 7 (12):4607–4611
- Donaldson K, Faus S, Borm PJA, Stone V (2007) Approaches to the toxicological testing of particles. In: Donaldson K, Borm PJA (eds) *Particle toxicology*. CRC Press, Taylor and Francis Group, London, pp 299–316
- Dong H, Cheng L, Tan J, Zheng K, Jiang Y (2004) Effects of chitosan coating on quality and shelf life of peeled litchi fruit. *J Food Eng* 64(3):355–358
- Doores S (1993) Organic acids. In: Davidson PM, Branen AL (eds) *Antimicrobials in food*. Marcel Dekker, Nueva York, pp 95–136
- Duan J, Park S, Daeschel M, Zhao Y (2007) Antimicrobial chitosan-lysozyme (CL) films and coatings for enhancing microbial safety of mozzarella cheese. *J Food Sci* 72(9):M355–M362
- Dutta PK, Tripathi S, Mehrotra GK, Dutta J (2009) Perspectives for chitosan based antimicrobial films in food applications. *Food Chem* 114(4):1173–1182
- El Saeed AM, El-Fattah MA, Azzam AM (2015) Synthesis of ZnO nanoparticles and studying its influence on the antimicrobial, anticorrosion and mechanical behavior of polyurethane composite for surface coating. *Dyes Pigments* 121:282–289
- Eswaranandam S, Hettiarachchy NS, Meullenet JF (2006) Effect of malic and lactic acid incorporated soy protein coatings on the sensory attributes of whole apple and fresh-cut cantaloupe. *J Food Sci* 71(3):S307–S313
- European Parliament and Council Directive N_98/72/EC (ED) (1998) Food additive other than colors and sweeteners. http://ec.europa.eu/Food/fs/sfp/addit_Flavor/flav11_en.pdf
- European Parliament and Council Directive N_2008/84/EC (ED) (2008) Laying down specific purity criteria on food additives other than colours and sweeteners. <http://eur-lex.europa.eu/lexUriServ/Lex-UriServ.do?url=1/4OJ:L2008:253:0001;0175:EN:PDF>
- European Parliament and Council Directive No. 95/2/EC (ED) (1995) Food additive other than colors and sweeteners. http://ec.europa.eu/Food/fs/sfp/addit_Flavor/flav11_en.pdf
- Fajardo P, Martins JT, Fuciños C, Pastrana L, Teixeira JA, Vicente AA (2010) Evaluation of a chitosan-based edible film as carrier of natamycin to improve the storability of Saloio cheese. *J Food Eng* 101(4):349–356
- Fitzgerald DJ, Stratford M, Gasson MJ, Ueckert J, Bos A, Narbad A (2004) Mode of antimicrobial action of vanillin against *Escherichia coli*, *Lactobacillus plantarum* and *Listeria innocua*. *J Appl Microbiol* 97(1):104–113
- Florence AT (2005) Nanoparticle uptake by the oral route: fulfilling its potential? *Drug Discov Today* 2(1):75–81
- Food Standards Australian New Zeland (FSANZ) (2007) Application A565. Use of nisin in processed meat product. <http://www.foodstandards.gov.au>
- Franci G, Falanga A, Galdiero S, Palomba L, Rai M, Morelli G, Galdiero M (2015) Silver nanoparticles as potential antibacterial agents. *Molecules* 20(5):8856–8874
- Franklin NB, Cooksey KD, Getty KJ (2004) Inhibition of *Listeria monocytogenes* on the surface of individually packaged hot dogs with a packaging film coating containing nisin. *J Food Prot* 67(3):480–485
- Franssen LR, Knocht JM (2003) Edible coatings containing natural antimicrobials for processed foods. In: Roller S (ed) *Natural antimicrobials for minimal processing of food*. CRC Press, Boca Ratón, pp 250–262

- Frei B, Higdon JV (2003) Antioxidant activity of tea polyphenols in vivo: evidence from animal studies. *J Nutr* 133(10):3275S–3284S
- Fujimoto A, Tsukue N, Watanabe M, Sugawara I, Yanagisawa R, Takano H, Yoshida S, Takeda K (2005) Diesel exhaust affects immunological action in the placentas of mice. *Environ Toxicol* 20(4):431–440
- Gabor F, Bogner E, Weissenboeck A, Wirth M (2004) The lectin-cell interaction and its implications to intestinal lectin-mediated drug delivery. *Adv Drug Deliver Rev* 56(4):459–480
- Gadang VP, Hettiarachchy NS, Johnson MG, Owens C (2008) Evaluation of antibacterial activity of whey protein isolate coating incorporated with nisin, grape seed extract, malic acid, and EDTA on a turkey frankfurter system. *J Food Sci* 73(8):M389–M394
- Gennadios A, Hanna MA, Kurth LB (1997) Application of edible coatings on meats, poultry and seafoods: a review. *LWT Food Sci Technol* 30(4):337–350
- Gómez-Estaca J, Montero P, Giménez B, Gómez-Guillén MC (2007) Effect of functional edible films and high pressure processing on microbial and oxidative spoilage in cold-smoked sardine (*Sardina pilchardus*). *Food Chem* 105(2):511–520
- Gómez-Guillén MC, Pérez-Mateos M, Gómez-Estaca J, López-Caballero E, Giménez B, Montero P (2009) Fish gelatin: a renewable material for developing active biodegradable films. *Trends Food Sci Tech* 20(1):3–16
- González-Aguilar GA, Monroy-García IN, Goycoolea-Valencia F, Díaz-Cinco ME, Ayala-Zavala JF (2005) Cubiertas comestibles de quitosano. Una alternativa para prevenir el deterioro microbiano y conservar la calidad de papayas frescas cortadas. In: González-Aguilar G, Cuamea-Navarro F (eds) *Nuevas tecnologías de conservación y envasado de frutas y hortalizas*. Hermosillo, México, CIAD, pp 121–133
- González-Aguilar GA, Valenzuela-Soto E, Lizardi-Mendoza J, Goycoolea F, Martínez-Téllez MA, Villegas-Ochoa MA, Monroy-García IN, Ayala-Zavala JF (2009) Effect of chitosan coating in preventing deterioration and preserving the quality of fresh-cut papaya ‘Maradol’. *J Sci Food Agric* 89(1):15–23
- Gould GW (1989) Introduction. In: Gould GW (ed) *Mechanisms of action of food preservation procedures*. Elsevier Applied Science, Londres, pp 1–42
- Govers M, Termont D, Vanaken GA, Vandermeer R (1994) Characterization of the adsorption of conjugated and unconjugated bile-acids to insoluble, amorphous calcium-phosphate. *J Lipid Res* 35(5):741–748
- Guilbert S, Gontard N (1995) Edible and biodegradable food packing. In: Ackermann P, Jägerstand M, Ohlsson T (eds) *Food and packing material—chemical interactions*. The Royal Society of Chemistry, London, pp 159–168
- Hagens WI, Oomen AG, de Jong WH, Cassee FR, Sips AJ (2007) What do we (need to) know about the kinetic properties of nanoparticles in the body? *Regul Toxicol Pharm* 49(3):217–229
- Han C, Lederer C, McDaniel M, Zhao Y (2005) Sensory evaluation of fresh strawberries (*Fragaria ananassa*) coated with chitosan-based edible coatings. *J Food Sci* 70(3):S172–S178
- Heggors JP, Cottingham J, Gusman J, Reagor L, McCoy L, Carino E, Cox R, Zhao JG (2002) The effectiveness of processed grapefruit-seed extract as an antibacterial agent: II. Mechanism of action and in vitro toxicity. *J Altern Complement Med* 8(3):333–340
- Helander IM, Mattila-Sandholm T (2000) Permeability barrier of the Gram-negative bacterial outer membrane with special reference to nisin. *Int J Food Microbiol* 60(2):153–161
- Hillyer JF, Albrecht RM (2001) Gastrointestinal persorption and tissue distribution of differently sized colloidal gold nanoparticles. *J Pharm Sci* 90(12):1927–1936
- Hoet P, Bruske-Hohlfeld I, Salata O (2004) Nanoparticles—known and unknown health risks. *J Nanobiotechnol* 2(1):12
- Hong S, Leroueil PR, Janus EK, Peters JL, Kober MM, Islam MT, Orr BG, Baker JR, Banaszak Holl MM (2006) Interaction of polycationic polymers with supported lipid bilayers and cells: nanoscale hole formation and enhanced membrane permeability. *Bioconj Chem* 17(3):728–734
- Hong YH, Lim GO, Song KB (2009) Physical properties of Gelidium corneum–gelatin blend films containing grapefruit seed extract or green tea extract and its application in the packaging of pork loins. *J Food Sci* 74(1):C6–C10

- Ibrahim HM (2015) Green synthesis and characterization of silver nanoparticles using banana peel extract and their antimicrobial activity against representative microorganisms. *J Radiat Res Appl Sci* 8(3):265–275
- Ibrahim HR, Sugimoto Y, Aoki T (2000) Ovotransferrin antimicrobial peptide (OTAP-92) kills bacteria through a membrane damage mechanism. *BBA Gen Subj* 1523(2):196–205
- Janes ME, Kooshesh S, Johnson MG (2002) Control of *Listeria monocytogenes* on the surface of refrigerated, ready-to-eat chicken coated with edible zein film coatings containing nisin and/or calcium propionate. *J Food Sci* 67(7):2754–2757
- Jani P, Halbert GW, Langridge J, Florence AT (1990) Nanoparticle uptake by the rat gastrointestinal mucosa: quantitation and particle size dependency. *J Pharm Pharmacol* 42(12):821–826
- Jayaprakasha GK, Selvi T, Sakariah KK (2003) Antibacterial and antioxidant activities of grape (*Vitis vinifera*) seed extracts. *Food Res Int* 36(2):117–122
- Jia X, Li N, Chen J (2005) A subchronic toxicity study of elemental Nano-Se in Sprague-Dawley rats. *Life Sci* 76(17):1989–2003
- Jiang Z, Neetoo H, Chen H (2011) Control of *Listeria monocytogenes* on cold-smoked salmon using chitosan-based antimicrobial coatings and films. *J Food Sci* 76(1):M22–M26
- Kabanov AV (2006) Polymer genomics: an insight into pharmacology and toxicology of nanomedicine. *Adv Drug Deliver Rev* 58(15):1597–1621
- Kahrilas GA, Haggren W, Read RL, Wally LM, Fredrick SJ, Hiskey M, Prieto AL, Owens JE (2014) Investigation of antibacterial activity by silver nanoparticles prepared by microwave-assisted green syntheses with soluble starch, dextrose, and arabinose. *ACS Sustain Chem Eng* 2(4):590–598
- Kang HJ, Jo C, Kwon JH, Kim JH, Chung HJ, Byun MW (2007) Effect of a pectin-based edible coating containing green tea powder on the quality of irradiated pork patty. *Food Control* 18(5):430–435
- Ko KY, Mendonca AF, Ahn DU (2008) Effect of ethylenediaminetetraacetate and lysozyme on the antimicrobial activity of ovotransferrin against *Listeria monocytogenes*. *Poult Sci* 87(8):1649–1658
- Krämer J, Brandis H (1975) Mode of action of two *Streptococcus faecium* bacteriocins. *Antimicrob Agents Chemother* 7(2):117–120
- Lan Y, Lu Y, Ren Z (2013) Mini review on photocatalysis of titanium dioxide nanoparticles and their solar applications. *Nano Energy* 2(5):1031–1045
- Latif U, Al-Rubeaan K, Saeb AT (2015) A review on antimicrobial chitosan-silver nanocomposites: a roadmap toward pathogen targeted synthesis. *Int J Polym Mater* 64(9):448–458
- Letchford K, Burt H (2007) A review of the formation and classification of amphiphilic block copolymer nanoparticulate structures: micelles, nanospheres, nanocapsules and polymersomes. *Eur J Pharm Biopharm* 65(3):259–269
- Lin D, Zhao Y (2007) Innovations in the development and application of edible coatings for fresh and minimally processed fruits and vegetables. *Compr Rev Food Sci F* 6(3):60–75
- Liu H, Du Y, Wang X, Sun L (2004) Chitosan kills bacteria through cell membrane damage. *Int J Food Microbiol* 95(2):147–155
- Liu Y, He L, Mustapha A, Li H, Hu ZQ, Lin M (2009) Antibacterial activities of zinc oxide nanoparticles against *Escherichia coli* O157:H7. *J Appl Microbiol* 107(4):1193–1201
- Llorens A, Lloret E, Picouet PA, Trbojevich R, Fernandez A (2012) Metallic-based micro and nanocomposites in food contact materials and active food packaging. *Trends Food Sci Technol* 24(1):19–29
- López-Caballero ME, Gómez-Guillén MC, Pérez-Mateos M, Montero P (2005) A chitosan-gelatin blend as a coating for fish patties. *Food Hydrocolloid* 19(2):303–311
- Losso JN, Nakai S, Charter EA (2000) Lysozyme. In: Naidu AS (ed) *Natural food antimicrobial systems*. CRC Press, Boca Raton, pp 185–210
- Marcos B, Aymerich T, Monfort JM, Garriga M (2008) High-pressure processing and antimicrobial biodegradable packaging to control *Listeria monocytogenes* during storage of cooked ham. *Food Microbiol* 25(1):177–182

- Marugg JD (1991) Bacteriocins, their role in developing natural products. *Food Biotechnol* 5 (3):305–312
- Michalska-Požoga I, Tomkowski R, Rydzkowski T, Thakur VK (2016) Towards the usage of image analysis technique to measure particles size and composition in wood-polymer composites. *Ind Crops Prod* 92:149–156
- Mild RM, Joens LA, Friedman M, Olsen CW, McHugh TH, Law B, Ravishankar S (2011) Antimicrobial edible apple films inactivate antibiotic resistant and susceptible *Campylobacter jejuni* strains on chicken breast. *J Food Sci* 76(3):M163–M168
- Millette MCLT, Le Tien C, Smoragiewicz W, Lacroix M (2007) Inhibition of *Staphylococcus aureus* on beef by nisin-containing modified alginate films and beads. *Food Control* 18(7): 878–884
- Mohanty S, Mishra S, Jena P, Jacob B, Sarkar B, Sonawane A (2012) An investigation on the antibacterial, cytotoxic, and antibiofilm efficacy of starch-stabilized silver nanoparticles. *Nanomed Nanotechnol* 8(6):916–924
- Natrajan N, Sheldon B (2000) Inhibition of Salmonella on poultry skin using protein and polysaccharide-based films containing a nisin formulation. *J Food Prot* 63(9):1268–1272
- Nel A, Xia T, Madler L, Li N (2006) Toxic potential of materials at the nanolevel. *Science* 311 (5761):622–627
- Nemmar A, Hoet PHM, Vanquickenborne B, Dinsdale D, Thomeer M, Hoylaerts MF, Vanbilloen H, Mortelmans L, Nemery B (2002) Passage of inhaled particles into the blood circulation in humans. *Circulation* 105(4):411–414
- Nguyen VT, Gidley MJ, Dykes GA (2008) Potential of a nisin-containing bacterial cellulose film to inhibit *Listeria monocytogenes* on processed meats. *Food Microbiol* 25(3):471–478
- Nikaido H (1996) Other membrane. In: Neidhardt FC (ed) *Escherichia coli* and *Salmonella cellular* and molecular biology. D.C. ASM Press, Washington, pp 29–47
- Nychas GJE, Skandamis PN, Tassou CC (2003) Antimicrobials from herbs and spices. In: Roller S (ed) *Natural antimicrobials for the minimal processing of foods*. CRC Press, Washington, pp 177–199
- Oberdorster G, Maynard A, Donaldson K, Castranova V, Fitzpatrick J, Ausman K, Carter J, Karn B, Kreyling W, Lai D (2005a) Principles for characterizing the potential human health effects from exposure to nanomaterials: elements of a screening strategy. Part Fibre Toxicol 2:8
- Oberdorster G, Oberdorster E, Oberdorster J (2005b) Nanotoxicology: an emerging discipline evolving from studies of ultrafine particles. *Environ Health Perspect* 113(7):823–839
- Oberdorster G, Oberdorster E, Oberdorster J (2007a) Concepts of nanoparticle dose metric and response metric. *Environ Health Perspect* 115(6):A290
- Oberdorster G, Stone V, Donaldson K (2007b) Toxicology of nanoparticles: a historical perspective. *Nanotoxicology* 1(1):2–25
- Othman SH, Abd Salam NR, Zainal N, Kadir Basha R, Talib RA (2014) Antimicrobial activity of TiO₂ nanoparticle-coated film for potential food packaging applications. *Int J Photoenergy*, pp 1–6
- Ouattara B, Simard RE, Piette G, Bejín A, Holler RA (2000) Inhibition of surface spoilage bacteria in processed meats by application of antimicrobial films prepared with chitosan. *Int J Food Microbiol* 62(1):139–148
- Ouattara B, Giroux M, Yefsah R, Smoragiewicz W, Saucier L, Borsa J, Lacroix M (2002) Microbiological and biochemical characteristics of ground beef as affected by gamma irradiation, food additives and edible coating film. *Radiat Phys Chem* 63(3):299–304
- Oussalah M, Caillet S, Salmiéri S, Saucier L, Lacroix M (2004) Antimicrobial and antioxidant effects of milk protein-based film containing essential oils for the preservation of whole beef muscle. *J Agric Food Chem* 52(18):5598–5605
- Oussalah M, Caillet S, Saucier L, Lacroix M (2006a) Antimicrobial effects of alginate-based film containing essential oils for the preservation of whole beef muscle. *J Food Prot* 69(10):2364–2369

- Oussalah M, Caillet S, Lacroix M (2006b) Mechanism of action of spanish oregano, chinese cinnamon, and savory essential oils against cell membranes and walls of *Escherichia coli* O157:H7 and *Listeria monocytogenes*. *J Food Prot* 69(5):1046–1055
- Oussalah M, Caillet S, Salmieri S, Saucier L, Lacroix M (2007) Antimicrobial effects of alginate-based film containing essential oils o *Listeria monocytogenes* and *Salmonella thyphimurium* present in bologna and ham. *J Food Prot* 70(4):901–908
- Padgett T, Han IY, Dawson PL (1998) Incorporation of food-grade antimicrobial compounds into biodegradable packaging films. *J Food Prot* 61(10):1330–1335
- Park SI, Stan SD, Daeschel MA, Zhao Y (2005) Antifungal coatings on fresh strawberries (*Fragaria × ananassa*) to control mold growth during cold storage. *J Food Sci* 70(4):M202–M207
- Pen LT, Jiang YM (2003) Effects of chitosan coating on shelf life and quality of fresh-cut Chinese water chestnut. *LWT Food Sci Technol* 36(3):359–364
- Pérez-Calderón R, Gonzalo-Garijo MA, Lamilla-Yerga A, Mangas-Santos R, Moreno-Gaston I (2007) Recurrent angioedema due to lysozyme allergy. *J Investig Allergol Clin* 17(4):264–266
- Powers KW, Brown SC, Krishna VB, Wasdo SC, Moudgil BM, Roberts SM (2006) Research strategies for safety evaluation of nanomaterials. Part VI. Characterization of nanoscale particles for toxicological evaluation. *Toxicol Sci* 90(2):296–303
- Pranoto Y, Salokhe VM, Rakshit SK (2005a) Physical and antibacterial properties of alginate-based edible film incorporated with garlic oil. *Food Res Int* 38(3):267–272
- Pranoto Y, Rakshit SK, Salokhe VM (2005b) Enhancing antimicrobial activity of chitosan films by incorporating garlic oil, potassium sorbate and nisin. *LWT Food Sci Technol* 38(8):859–865
- Rahman MAA, Mahmud S, Alias AK, Nor AFM (2013) Effect of nanorod zinc oxide on electrical and optical properties of starch-based polymer nanocomposites. *J Phys Sci* 24(1):17–28
- Raji V, Chakraborty M, Parikh PA (2012) Synthesis of starch-stabilized silver nanoparticles and their antimicrobial activity. *Part Sci Technol* 30(6):565–577
- Raju PS, Bawa AS (2006) Food additives in fruit processing. In: Hui YH (ed) *Handbook of fruits and fruit processing*. Blackwell Publishing, Ames, pp 145–170
- Ravishankar S, Zhu L, Olsen CW, McHugh TH, Friedman M (2009) Edible apple film wraps containing plant antimicrobials inactivate foodborne pathogens on meat and poultry products. *J Food Sci* 74(8):M440–M445
- Raybaudi-Massilia RM, Mosqueda-Melgar J (2012) Polysaccharides as carriers and protectors of additives and bioactive compounds in foods. In: Karunarathn DN (ed) *The complex world of polysaccharides*. Editorial InTech, Rijeka, pp 429–454
- Raybaudi-Massilia RM, Mosqueda-Melgar J, Martín-Belloso O (2008a) Edible alginate-based coating as carrier of antimicrobials to improve shelf-life and safety of fresh-cut melon. *Int J Food Microbiol* 121(3):313–327
- Raybaudi-Massilia RM, Rojas-Graü MA, Mosqueda-Melgar J, Martín-Belloso O (2008b) Comparative study on essential oils incorporated into an alginate-based edible coating to assure the safety and quality of fresh-cut fuji apples. *J Food Prot* 71(6):1150–1161
- Raybaudi-Massilia RM, Mosqueda-Melgar J, Soliva-Fortuny R, Martín-Belloso O (2009) Control of pathogenic and spoilage microorganisms in fresh-cut fruits and fruit juices by traditional and alternative natural antimicrobials. *Compr Rev Food Sci F* 8(3):157–180
- Rojas-Graü MA, Avena-Bustillos RJ, Friedman M, Henika PR, Martín-Belloso O, McHugh TH (2006) Mechanical, barrier, and antimicrobial properties of apple puree edible films containing plant essential oils. *J Agric Food Chem* 54(24):9262–9267
- Rojas-Graü MA, Raybaudi-Massilia RM, Soliva-Fortuny RC, Avena-Bustillos RJ, McHugh TH, Martín-Belloso O (2007) Apple puree-alginate edible coating as carrier of antimicrobial agents to prolong shelf-life of fresh-cut apples. *Postharvest Biol Technol* 45(2):254–264
- Rojas-Graü MA, Soliva-Fortuny R, Martín-Belloso O (2009) Edible coatings to incorporate active ingredients to fresh-cut fruits: a review. *Trends Food Sci Technol* 20(10):438–447
- Rosales-Oballos Y, Raybaudi-Massilia R, Mosqueda-Melgar J, Tapia de Daza MS, Tomé-Boschian E (2012) Propiedades mecánicas, de barrera y antimicrobianas de películas de

- quitosano y películas de alginato de sodio con aceites esenciales y nisina. *Revista de la Facultad de Farmacia y Bioquímica Universidad de los Andes, Venezuela* 54(1):12–16
- Roszek B, de Jong W, Geertsma R (2005) Nanotechnology in medical applications: state-of-the-art in materials and devices. RIVM report. 265001001/2005
- Rozes N, Peres C (1998) Effects of phenolic compounds on the growth and the fatty acid composition of *Lactobacillus plantarum*. *Appl Microbiol Biotechnol* 49(1):108–111
- Russell-Jones GJ, Veitch H, Arthur L (1999) Lectin-mediated transport of nanoparticles across Caco-2 and OK cells. *Int J Pharm* 190(2):165–174
- Saito M, Hosoyama H, Ariga T, Kataoka S, Yamaji N (1998) Antiulcer activity of grape seed extract and procyanidins. *J Agric Food Chem* 46(4):1460–1464
- Salunke GR, Ghosh S, Kumar RS, Khade S, Vashisth P, Kale T, Chopade S, Pruthi V, Kundu G, Bellare JR, Chopade BA (2014) Rapid efficient synthesis and characterization of silver, gold, and bimetallic nanoparticles from the medicinal plant *Plumbago zeylanica* and their application in biofilm control. *Int J Nanomed* 9:2635
- Sangsuwan J, Rattanapanone N, Rachtanapun P (2008) Effect of chitosan/methyl cellulose films on microbial and quality characteristics of fresh-cut cantaloupe and pineapple. *Postharvest Biol Technol* 49(3):403–410
- Santiago-Silva P, Soares NF, Nóbrega JE, Júnior MA, Barbosa KB, Volp ACP, Zerdas ERMA, Würllitzer NJ (2009) Antimicrobial efficiency of film incorporated with pediocin (ALTA[®] 2351) on preservation of sliced ham. *Food Control* 20(1):85–89
- Sayanjali S, Ghanbarzadeh B, Ghiassifar S (2011) Evaluation of antimicrobial and physical properties of edible film based on carboxymethyl cellulose containing potassium sorbate on some mycotoxigenic *Aspergillus species* in fresh pistachios. *LWT Food Sci Technol* 44(4):1133–1138
- Scientific Committee on Emerging and Newly Identified Health Risk (SCENIHR) (2007) Opinion on: the appropriateness of the risk assessment methodology in accordance with the technical guidance documents for new and existing substances for assessing the risks of nanomaterials European Commission Health and Consumer Protection Directorate-General. Directorate C—Public Health and Risk Assessment C7—Risk Assessment
- Sebti I, Martial-Gros A, Carnet-Pantiez A, Grelier S, Coma V (2005) Chitosan polymer as bioactive coating and film against *Aspergillus niger* contamination. *J Food Sci* 70(2):M100–M104
- Seol KH, Lim DG, Jang A, Jo C, Lee M (2009) Antimicrobial effect of κ -carrageenan-based edible film containing ovotransferrin in fresh chicken breast stored at 5 °C. *Meat Sci* 83(3):479–483
- Seydim AC, Sarikus G (2006) Antimicrobial activity of whey protein based edible films incorporated with oregano, rosemary and garlic essential oils. *Food Res Int* 39(5):639–644
- Shankar S, Teng X, Li G, Rhim JW (2015) Preparation, characterization, and antimicrobial activity of gelatin/ZnO nanocomposite films. *Food Hydrocolloid* 45:264–271
- Sharma VK, Yngard RA, Lin Y (2009) Silver nanoparticles: green synthesis and their antimicrobial activities. *Adv Colloid Interface* 145(1):83–96
- Shimamura T, Zhao WH, Hu ZQ (2007) Mechanism of action and potential for use of tea catechin as an anti-infective agent. *Anti Infective Agents Med Chem* 6(1):57–62 (Formerly Current Medicinal Chemistry-Anti-Infective Agents)
- Silva GA (2007) Nanotechnology approaches for drug and small molecule delivery across the blood-brain barrier. *Surg Neurol* 67(2):113–116
- Silvera-Almirán C, Escobar-Giannini D, Repiso-Ibáñez L, Márquez-Romero R (2012) Aplicaciones de películas y cubiertas comestibles y métodos combinados para mejorar sus propiedades. In: Olivas-Orozco GI, González-Aguilar GA, Martín-Belloso O, Soliva-Fortuny R (eds) *Películas y recubrimientos comestibles. Propiedades y aplicaciones en alimentos*. Clave Editorial, México, pp 497–518
- Silvestre C, Duraccio D, Cimmino S (2011) Food packaging based on polymer nanomaterials. *Prog Polym Sci* 36(12):1766–1782

- Singh R, Pantarotto D, Lacerda L, Pastorin G, Klumpp C, Prato M, Bianco A, Kostarelos K (2006) Tissue biodistribution and blood clearance rates of intravenously administered carbon nanotube radiotracers. *Proc Natl Acad Sci USA* 103(9):3357–3362
- Siripatrawan U, Noipha S (2012) Active film from chitosan incorporating green tea extract for shelf life extension of pork sausages. *Food Hydrocolloid* 27(1):102–108
- Sobrinho-López A, Martín-Belloso O (2008) Use of nisin and other bacteriocins for preservation of dairy products. *Int Dairy J* 18(4):329–343
- Sondi I, Salopek-Sondi B (2004) Silver nanoparticles as antimicrobial agent: a case study on *E. coli* as a model for Gram-negative bacteria. *J Colloid Interface Sci* 275(1):177–182
- Stratford M, Eklund T (2003) Organic acids and esters. In: Russell NJ, Gould GW (eds) *Food preservatives*. Kluwer Academic/Plenum Publishers, Londres, pp 48–84
- Szentkuti L (1997) Light microscopical observations on luminally administered dyes, dextrans, nanospheres and microspheres in the pre-epithelial mucus gel layer of the rat distal colon. *J Control Release* 46(3):233–242
- Taheri S, Baier G, Majewski P, Barton M, Förch R, Landfester K, Vasilev K (2014) Synthesis and antibacterial properties of a hybrid of silver–potato starch nanocapsules by miniemulsion/polyaddition polymerization. *J Mater Chem* 2(13):1838–1845
- Taylor PW, Hamilton-Miller JM, Stapleton PD (2005) Antimicrobial properties of green tea catechins. *Food Sci Technol Bull* 2:71
- Thakur VK, Kessler MR (2014a) Free radical induced graft copolymerization of ethyl acrylate onto SOY for multifunctional materials. *Mater Today Commun* 1(1–2):34–41
- Thakur VK, Kessler MR (2014b) Synthesis and characterization of AN-g-SOY for sustainable polymer composites. *ACS Sustain Chem Eng* 2(10):2454–2460
- Thakur VK, Thakur MK (2014) Recent advances in graft copolymerization and applications of chitosan: a review. *ACS Sustain Chem Eng* 2(12):2637–2652
- Thakur VK, Voicu SI (2016) Recent advances in cellulose and chitosan based membranes for water purification: a concise review. *Carbohydr Polym* 146:148–165
- Thakur VK, Thunga M, Madbouly SA, Kessler MR (2014a) PMMA-g-SOY as a sustainable novel dielectric material. *RSC Adv* 4(35):18240–18249
- Thakur VK, Grewell D, Thunga M, Kessler MR (2014b) Novel composites from eco-friendly soy flour/SBS triblock copolymer. *Macromol Mater Eng* 299(8):953–958
- Thakur VK, Vennerberg D, Kessler MR (2014c) Green aqueous surface modification of polypropylene for novel polymer nanocomposites. *ACS Appl Mater Interfaces* 6(12):9349–9356
- Thakur MK, Thakur VK, Gupta RK, Pappu A (2016) Synthesis and applications of biodegradable soy based graft copolymers: a review. *ACS Sustain Chem Eng* 4(1):1–17
- Theivendran S, Hettiarachchy NS, Johnson MG (2006) Inhibition of *Listeria monocytogenes* by nisin combined with grape seed extract or green tea extract in soy protein film coated on turkey frankfurters. *J Food Sci* 71(2):M39–M44
- Thomas K, Sayre P (2005) Research strategies for safety evaluation of nanomaterials, part I: evaluating the human health implications of exposure to nanoscale materials. *Toxicol Sci* 87(2):316–321
- Thomas LV, Clarkson MR, Delves-Broughton J (2000) Nisin. In: Naidu AS (ed) *Natural food antimicrobial systems*. CRC Press, Boca Raton, pp 463–524
- Tran CL, Danaldson K, Stones V, Fernandez T, Ford A, Christofi N, Ayres JG, Steiner M, Hurley JF, Aitken RJ, Seaton A (2005) A scoping study to identify hazard data needs for addressing risks presented by nanoparticles and nanotubes. Institute of Occupational Medicine (IOM) research report, Edinburgh, United Kingdom
- US Food and Drug Administration (USFDA) (2006a) Food additives permitted for direct addition to food for human consumption 21CFR172, subpart C. Coatings, films and related substances
- US Food and Drug Administration (USFDA) (2006b) GRAS substances (SCOGS) database. <http://www.fda.gov/Food/FoodIngredientsPackaging/GenerallyRecognizedasSafeGRAS/GRASSubstancesSCOGSDatabase/default.htm>

- US Food and Drug Administration (USFDA) (2009) Everything added to food in the United States. <http://www.fda.gov/Food/foodingredientspackaging/ucm115326.htm>
- US Food and Drug Administration (USFDA) (2010) Listing of food additive status Part I and Part II. <http://www.fda.gov/Food/FoodIngredientsPackaging/FoodAdditives/FoodAdditiveListings/ucm091048.htm>
- Valencia-Chamorro SA, Pérez-Gago MB, del Río MÁ, Palou L (2009) Effect of antifungal hydroxypropyl methylcellulose (HPMC)-lipid edible composite coatings on postharvest decay development and quality attributes of cold-stored 'Valencia' oranges. *Postharvest Biol Technol* 54(2):72–79
- Valodkar M, Sharma P, Kanchan DK, Thakore S (2010) Conducting and antimicrobial properties of silver nanowire-waxy starch nanocomposites. *Int J Green Nanotechnol Phys Chem* 2(1): P10–P19
- Vargas M, Chiralt A, Albors A, González-Martínez C (2009) Effect of chitosan-based edible coatings applied by vacuum impregnation on quality preservation of fresh-cut carrot. *Postharvest Biol Technol* 51(2):263–271
- Voicu SI, Condruz RM, Mitran V, Cimpean A, Miculescu F, Andronesu C, Thakur VK (2016) Sericin covalent immobilization onto cellulose acetate membrane for biomedical applications. *ACS Sustain Chem Eng* 4(3):1765–1774
- Walton NJ, Mayer MJ, Narbad A (2003) Vanillin. *Phytochemistry* 63(5):505–515
- Wang B, Feng WY, Wang TC, Jia G, Wang M, Shi JW, Zhang F, Zhao YL, Chai ZF (2006) Acute toxicity of nano- and micro-scale zinc powder in healthy adult mice. *Toxicol Lett* 161(2): 115–123
- Wang J, Zhou G, Chen C, Yu H, Wang T, Ma Y, Jia G, Gao Y, Li B, Sun J (2007) Acute toxicity and biodistribution of different sized titanium dioxide particles in mice after oral administration. *Toxicol Lett* 168(2):176–185
- Wang B, Feng WY, Wang M, Wang TC, Gu YQ, Zhu MT, Ouyang H, Shi JW, Zhang F, Zhao YL (2008) Acute toxicological impact of nano- and submicroscaled zinc oxide powder on healthy adult mice. *J Nanopart Res* 10(2):263–276
- Wang J, Dong Z, Huang J, Li J, Liu K, Jin J, Ma J (2013) Synthesis of Ag nanoparticles decorated multiwalled carbon nanotubes using dialdehyde starch as complexant and reductant for antibacterial purposes. *RSC Adv* 3(3):918–922
- Wang B, Mireles K, Rock M, Li Y, Thakur VK, Gao D, Kessler MR (2016) Synthesis and preparation of bio-based ROMP thermosets from functionalized renewable isosorbide derivative. *Macromol Chem Phys* 217(7):871–879
- Wist J, Sanabria J, Dierolf C, Torres W, Pulgarin C (2002) Evaluation of photocatalytic disinfection of crude water for drinking-water production. *J Photoch Photobiol A* 147(3): 241–246
- Ye M, Neetoo H, Chen H (2008) Effectiveness of chitosan-coated plastic films incorporating antimicrobials in inhibition of *Listeria monocytogenes* on cold-smoked salmon. *Int J Food Microbiol* 127(3):235–240
- Yoksan R, Chirachanchai S (2010) Silver nanoparticle-loaded chitosan-starch based films: fabrication and evaluation of tensile, barrier and antimicrobial properties. *Mater Sci Eng C* 30 (6):891–897
- Zhang J, Wang H, Yan X, Zhang L (2005) Comparison of short-term toxicity between Nano-Se and selenite in mice. *Life Sci* 76(10):1099–1109
- Zinoviadou KG, Koutsoumanis KP, Biliaderis CG (2010) Physical and thermo-mechanical properties of whey protein isolate films containing antimicrobials, and their effect against spoilage flora of fresh beef. *Food Hydrocolloid* 24(1):49–59

Chapter 4

Functional Biocomposites of Calcium Phosphate–Chitosan and Its Derivatives for Hard Tissue Regeneration Short Review

L. Pighinelli, D. Wawro, M.F. Guimarães, R.L. Paz, G. Zanin, M. Kmiec, M.F. Tedesco, M. Silva and O.V. Reis

Abstract This short review presents an actual innovation in functional biopolymers related with a research and developments in chitosan/calcium phosphate composites studies. It is a promising biomaterial to face new problems and challenges in the field of materials science, biology, and medicine, related with musculoskeletal tissues, bones, and cartilage which are under extensive investigation in regenerative medicine and advanced biomaterials research. A growing number of cases requiring medical devices, which is related with many factor such as bone fractures, defects, or diseases in addition to other various problems which need to be cured, make the scientist research and develop a great number of biodegradable and bioresorbable biocomposites. New developments in this interdisciplinary and multidisciplinary field related with new materials, new methods possibly, will increase in the near future the feasibility to design a new biocomposite tailored for specific patients and disease treatment. The global socioeconomic situation of the modern world has raised the interest in renewable materials to use in regenerative medicine. The generation of functional biocomposites from chitosan and calcium phosphates is derived from two or more different organic and inorganic materials, keeping the main characteristics of both materials like bioactivity and biodegradability and biocompatibility of the physiological environment of the human tissues. The chemical characteristics of the micro- and nano-chitosan and ceramic formation between nano-B-TCP/HAp complex showed any secondary products formation in the biocomposite, with a good stability of the nano-ceramic formation in the chitosan salt solutions. This research showed also a new method of preparations

L. Pighinelli (✉) · M.F. Guimarães · R.L. Paz · G. Zanin · M. Kmiec · M.F. Tedesco · M. Silva · O.V. Reis
Biomatter Lab, Lutheran University of Brazil,
Av. Farroupilha, no. 8001, Canoas, RS 92425-900, Brazil
e-mail: luciano.pighinelli@ulbra.br; pighinelli@gmail.com

D. Wawro
Institute of Biopolymers and Chemical Fibers—IBWCh,
Sklodowskiej-Curie 19/27, 90-570 Lodz, Poland

nanoparticles of the commercial calcium phosphates founded in micro-size in chitosan solution. These materials can be used in future for medical applications as a base for scaffolds production in regenerative medicine and for drug delivery.

Keywords Biocomposites · Micro- and nano-chitosan · Nano-ceramic Functional biomaterial

1 Introduction

In the last 20 years, research and development of different biomaterials are created to improve cell adhesion, proliferation, and/or differentiation, and have been broadly explored for regenerative medicine and tissue engineering (Voicu et al. 2016; Trache et al. 2017; Corobea et al. 2016). Biomaterial is a multi- and interdisciplinary fields that have been increasing significantly in medicine, biology, chemistry, and materials science (Huipin et al. 2001; Maachou et al. 2008).

In this field, relevant results have been developed by different types of biomaterials from chitosan and its derivatives, basically because this polysaccharide has suitable properties, very important to develop biomaterials like nontoxicity, biocompatibility, biodegradability and high porosity for cell penetration and diffusion of nutrients, osteoconductive, resorbable, and osteoinductive (Thakur and Thakur 2014; Thakur and Voicu 2016).

Human skeleton provides support for the soft tissues and organs and gives shape to the body, providing also an excellent network between all physiological environmental of the human body. Many problems are related with hard tissue rising from bone fractures, imperfections, or diseases. The composition of the bones takes place with 69% calcium phosphate (mainly hydroxyapatite), 21% collagen, 9% water, and 1% other constituents. It is a natural functional biocomposite, with a complex hierarchical micro- and nanostructure very difficult to imitate providing superior mechanical properties to support all the body and extra daily forces (Huipin et al. 2001; Maachou et al. 2008; Clayton et al. 2006; Cancedda et al. 2003).

The process to develop new biomaterials to use as an artificial bone is classified as surface-active materials [hydroxyapatite (HAp)], resorbable materials [β -tricalcium phosphate (β -TCP)], also with very important characteristics such as bioactive and biodegradable material in this research (chitosan and its derivatives) (Fathi et al. 2008; Rho et al. 1998; Sathirakul et al. 1995). The composition and production of functional biomaterials composed of ceramic and polymers have a reasonable approach, and same advantages and drawbacks need to be considered and more clear per example: the biointeraction between the organic and inorganic parts with the human tissues, associated with the mechanical properties of polymers and ceramics, is considered producing composite materials that have a reasonable approach (Maachou et al. 2008; Pighinelli and Kucharska 2013).

The development of biomaterials in general has been used for several applications in the medical area, such as joint replacements, bone plates, bone cement, artificial ligaments and tendons, dental implants for tooth fixation, blood vessel prostheses, heart valves, artificial tissue, contact lenses, and breast implants (Huipin et al. 2001; Qun and Ajun 2006; Thakur et al. 2016). In the future, biomaterials are expected to enhance the regeneration of natural tissues, thereby promoting the restoration of structural, functional, metabolic, and biochemical behavior as well as biomechanical performance (Huipin et al. 2001; Maachou et al. 2008; Muzzarelli 1993).

The design of novel, inexpensive, biocompatible materials is crucial to the improvement of the living conditions and welfare of the population in view of the increasing number of people who need implants. Most of scaffolds can be classified based on their component materials: natural scaffolds, synthetic scaffolds, and mineral-based scaffolds.

Natural scaffolds, natural materials such as collagen, alginate, silk, cellulose, chitin, and chitosan, provide desirable properties very important to design biomaterials to use in regenerative medicine such as biodegradability, biocompatibility, and bioactivity, and stimulate new tissue growth (Huipin et al. 2001; Maachou et al. 2008; Muzzarelli 1995).

Synthetic scaffolds came from synthetic source biomaterials like polyglycolide (PGA), polylactides (PLA), polycaprolactone (PCL), and polydioxanone (PDS) (Maachou et al. 2008).

Mineral-based scaffolds, the apatite family such hydroxyapatite (HAp) and tricalcium phosphate (TCP), are the most used mineral to prepare biomaterials to replicate the calcium phosphate found in the extracellular matrix of normal bone, providing a high bioactivity and biocompatibility working as a substrate for bone formation (Maachou et al. 2008; Clayton et al. 2006; Pighinelli et al. 2012).

Chitin–chitosan is a family of nitrogen containing polysaccharide-based biopolymers derived from a range of natural resources, i.e., exoskeletons of crustaceans, insects, and cell walls of fungi. The structure of chitin and chitosan is very similar composed by *N*-acetyl-glucosamine and glucosamine repeating units. The difference is the number of those two repeating units. Conveniently, the structure with glucosamine units until 50% is chitin and over 50% is chitosan. Several methodologies have been utilized for the preparation of new bioactive, biocompatible materials with osteoconductivity, osteoinductivity, and chitosan, and its derivatives have received a great attention in the field of materials science and tissue engineering. Additionally, the cationic character of the amino substitutions of glucosamine residues also allows for electrostatic bindings with several negatively charged molecules such as fats, lipids, and proteins (Maachou et al. 2008; Clayton et al. 2006; Cancedda et al. 2003; Puttipipatkachorn et al. 2001; Pospieszny and Folkman 2004).

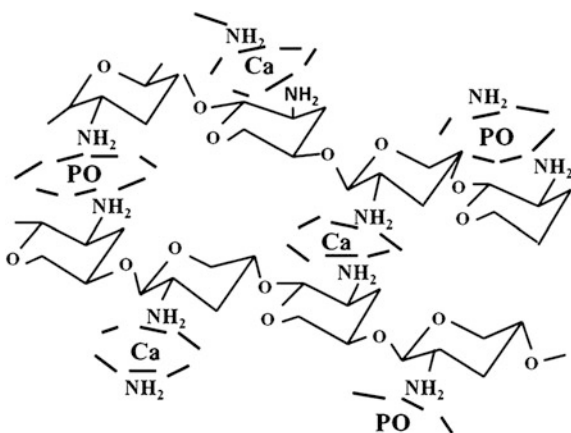
Some of the recent researches showed how the surface-active biomaterials such calcium phosphates bind to the bone through the apatite layer formation; the speed of the layer formation correlates with bioactivity, correlated with the interaction of amino groups from chitosan and phosphate ions, from the calcium phosphates using

the calcium as a crosslinking agent to reinforce the biomaterial and increase the interaction with the human tissues. It is assumed that the velocity of layer formation correlates with bioactivity (Pighinelli and Kucharska 2013; Qun and Ajun 2006; Muzzarelli 1993; Jue-Yeon et al. 2002; Muzzarelli 2009).

The apatite family is the major inorganic materials currently in use in reconstructive and regenerative medicine; the most used members this family are hydroxyapatite (HAp) with lower absorption and β -tricalcium phosphate (β -TCP) that is faster absorption compared with Hap. They are considered bioceramics and started to be used in early 1980s to now (Pighinelli and Kucharska 2013). On the other hand, both ceramics show a number of drawbacks that reduce their clinical performance such the low biodegradation of HAp in physiological (Qun and Ajun 2006), and the β -TCP shows fast release of Ca^{2+} and PO_4^{3-} ions when exposed to physiological fluids, the B-TCP contact with bone directly, suggesting mainly mechanical bonding (Muzzarelli 1995; Snel and McClure 2004, Qun and Ajun 2006, Muzzarelli 2011).

Natural or synthetic tricalcium phosphate (β -TCP), $\text{Ca}_3(\text{PO}_4)_2$ and hydroxyapatite (HAp), $\text{Ca}_{10}(\text{PO}_4)_6(\text{OH})_2$, are inorganic compounds with a high potential for bio-applications. This research is used to develop biocomposites made of nano- β -TCP and HAp, so-called nano-biphasic calcium phosphates ceramic or nano-ceramic, combining the bioactivity of HAp and the fast bioresorbability of β -TCP (Muzzarelli 1993, 1995; Dorozhkin 2009). The biological performance is related with dissolution control and the rate of the mixture. The appropriate blend is related with gradually dissolution of the apatites in the physiological environment controlling the Ca^{2+} and PO_4^{3-} ions release inducing and increasing the biodegradation, biocompatibility, and bioactivity properties (Qun and Ajun 2006; Muzzarelli 1993; Rinaudo 2006; Pighinelli and Kucharska 2014). Figure 1 showed the schematic illustration of the interaction mechanism between chitosan and calcium/phosphate ions.

Fig. 1 Schematic illustration of the mechanism between chitosan and calcium/phosphate ions [30]



2 Bones

The bone behaves like a composite material. Aging is a more general deteriorative process associated with side effects of the time, quality of life, disease, and so on, which increase affects reducing the biochemical and biomechanical properties of bone in a number of ways.

Natural bone is an inorganic–organic composite consisting mainly of nanohydroxyapatite and collagen fibers. Hydroxyapatite (HA), $\text{Ca}_{10}(\text{PO}_4)_6(\text{OH})_2$, is a major CaP mineral found in native bone. Hybridization of HA with different biopolymeric matrices like chitosan has been obtained by the sol–gel route combining the advantages of both organic and inorganic properties showing a good support bone regeneration and tissue stimulation (Fathi et al. 2008).

Fractures in the natural bones increase rapidly with age (Zioupos 2001). This is partly due to extra osseous factors such as the impaired reflexes of the elderly.

The bone changes can be divided into quantity effects such as bone mass loss and porosity related with age, gender, and other side effects; the quality effects are related with changes in the chemical composition and physical factors such as fractures diseases of the bones (Barbosa et al. 2005; Wang 2006; Qiaoling et al. 2004; Cyster et al. 2005; Porter et al. 2006).

One of the most important mechanical properties of the natural bones is the toughness that is directly related with age, and is defined in terms of the amount of energy absorbed by the bone required for fracture. The problem to absorb this external energy is related with the form of diffusion crack or “pre-fracture” (Muzzarelli 1978; Qiaoling et al. 2004; Zioupos 2001; Hutmacher 2000).

The mechanical properties of natural bones are shown in Table 1. The properties change when the tissue maturity is increased (age-dependent), its related with many factors such as demineralization, intrinsic fractures, changes in the structure of the bones caused by diseases, fractures, and defects which are directed related with mechanical properties (Niekraszewicz et al. 1998, 2004).

Table 1 The mechanical properties of human compact bone [5]

Properties	Test direction	
	Parallel	Normal
Tensile strength (MPa)	124–174	49
Compressive strength (MPa)	170–193	133
Bending strength (MPa)	160	–
Shear strength (MPa)	54	–
Young’s modulus (GPa)	17.0–18.9	11.5
Work of fracture (J/m^2)	6000 (low strain rate)	–
	98 (high strain rate)	
Ultimate tensile strain	0.014–0.031	0.007
Ultimate compressive strain	0.0185–0.026	0.028
Yield tensile strain	0.007	0.004
Yield compressive strain	0.010	0.011

Bone is a very difficult natural structure to imitate, because of many material structures, length scales, properties, and process of growing tissue related with a great interaction perform of diverse mechanical, biological, and chemical functions (Niekraszewicz et al. 2004; Struszczyk 2006).

Many factors are important in the mechanical properties studies such scale, porosity, morphology and concentration of inorganic and organic parts, quality of life, age, and diseases. The mass and strength of bones in normal individuals is ultimately determined by the need to resist the loads and deformations resulting from the normal activities.

The literature of bones shows a great number of publications making a strong relationship between mechanical properties and the component phases, and the structural relationship (Fathi et al. 2008; Rho et al. 1998; Struszczyk 2003):

(1) the macrostructure: cortical bones; (2) the microstructure (from 10 to 500 μm): Haversian systems (the osteon, or Haversian system, is the fundamental functional unit of much compact bone. Osteons, roughly cylindrical structures that are typically several millimeters long and around 0.2 mm in diameter, are present in many of the bones of most mammals, birds, reptiles, and amphibians), single trabeculae; (3) the sub-microstructure (1–10 μm): lamellae; (4) the nanostructure (from a few hundred nanometers to 1 μm): fibrillar collagen and embedded mineral; and (5) the subnanostructure (below a few hundred nanometers): molecular structure of constituent elements such as mineral, collagen, and non-collagenous organic proteins.

3 Chitosan

Polysaccharides such as chitosan and its derivatives biomaterials have a biochemical significance not encountered in other polysaccharides, natural polymers, promoting a new tissue formation, vascularization, and a continuous supply of chito-oligomers that stimulating the regeneration instead of cicatrization and orientation of collagen fibrils incorporated into the extracellular matrix components (Sathirakul et al. 1995; Muzzarelli 2009; Snel and McClure 2004; Kong et al. 2006).

A great number of articles show the use of polysaccharide such as chitosans (poly(β -(1,4)-2-amino-2-deoxy-D-glucopiranoose)) as safe biopolymer to develop biomaterials; the main reason is related with the biostimulation properties, increasing the speed of reconstruction, cell adhesion, cells reproduction, nutrient flow, and vascularization of damage tissues (Puttipipatkachorn et al. 2001).

Every year many articles related with chitin and chitosan and its derivatives are published providing a great knowledge of use of chitosan and its derivatives for variety of applications in different fields such as water treatment, agribusiness, food industry, pharmaceutical, cosmetics, textile, and more. The main reason for that is

the low toxicity and allergenicity, natural biodegradable, bioactive, and biocompatible (Muzzarelli 2009; Pramanik et al. 2009; Puttipipatkachorn et al. 2001; Pospieszny and Folkman 2004; Snel and McClure 2004; Muzzarelli 2001; Klinkaewnarong 2009).

Chitosan is a glucose-based unbranched polysaccharide derived from the *N*-deacetylation of chitin. The most of the reactions happen at the C-2 carbon by the presence of amino groups and the structure of this copolymer is a combination of glucosamine and *N*-acetylglucosamine. The chitosan polymer is positively charged and solubilized by protonation at environmental pH values of <6 in place.

The most important parameters of chitosan are the degree of acetylation which vary from (>50 to 95%) that is directly related with the degree of crystallinity, and the molecular weight range from 10,000 to 2 million Dalton. Both parameters have effects in the characteristic of the hydrogen bonding and ionic strength in this biopolymer, affecting its structure, process, and properties like hydrophilic characteristics that can retain water in its structure, solubility, degradability, biocompatibility, reactivity, viscosity, and mechanical properties (Pighinelli and Kucharska 2013).

Chitosan is insoluble at neutral and alkaline pH, but forms water-soluble salts with inorganic and organic acids, the most common including phosphoric, sulfuric, hydrochloric, acetic, and lactic acids protonating the amino groups of the polymer. One of the most promising derivatives of chitosan is the nano-chitosan (NCh) and microcrystalline chitosan (MCCh) because of their significantly different physico-chemical properties and inner surface formation increasing the amorphous part making the polymer more reactive (Pighinelli and Kucharska 2013; Qun and Ajun 2006; Jue-Yeon et al. 2002; Wang 2006).

Chemical modification as derivatives of chitosan provides and promotes new properties such as biological activities related with the primary amino groups that provide a mechanism for side-group attachment with a variety of inorganic and organic elements, substances, and tissues (Muzzarelli 1993, 1995; Pospieszny and Folkman 2004; Qiaoling et al. 2004). It behaves as a pseudo-plastic material exhibiting a decrease in viscosity with increasing rates of shear, directed dependent of temperature and degree of deacetylation, which have influence in physiochemical, mechanical, and biological properties such as wound-healing properties, enzymatically degradation by chitinase, chitosanase, and pectinase. Table 2 shows the chitosan and its derivatives used in regenerative medicine and tissue engineering.

A common sense in the literature about the higher degree of deacetylation produces a lower rate of degradation and average molecular weight demonstrated the highest level of activity (Pighinelli et al. 2012; Puttipipatkachorn et al. 2001; Jue-Yeon et al. 2002).

Tissue regeneration is related with cellular interactions using the same cell to repair the tissue and promote the new cells formation, different than healing that use fibroblast cells to promote the tissue repair living marks after this process (Muzzarelli 2009; Snel and McClure 2004; Cyster et al. 2005).

Table 2 Chitosan and its derivatives used in regenerative medicine and tissue engineering [16, 17]

Artificial skin
Surgical sutures
Artificial blood vessels
Controlled drug release
Contact lens
Eye humor fluid
Bandages, sponges
Burn dressings
Blood cholesterol control
Anti-inflammatory
Tumor inhibition
Antiviral
Dental plaque inhibition
Bone healing treatment
Wound-healing accelerator
Hemostatic
Antibacterial
Antifungal
Weight loss effect

Table 3 Characteristics and properties of the different natural biopolymers used in regenerative medicine, tissue engineering [18]

Chitosan	Hydrophilic surface, biocompatible, bioactive, and biodegradable, bactericidal/bacteriostatic activity. Low mechanical properties. Promote a high ionic and hydrogen bonds. Easy to process. Variety of structures
Silk fibroin	Slow degradability, versatility in processing, great mechanical properties. Lower biocompatibility, good bioactivity, and biodegradable
Alginate	Easy to crosslinking. Lower mechanical properties. Difficulties to sterilize. Variety of structures
Starch	Inexpensive. In vivo degradation has not been fully assessed yet
Bacterial cellulose	High purity, variety of Structures, good mechanical properties, and biocompatibility

Table 3 compares the characteristic and properties of the different natural biopolymers with great potential to use in regenerative medicine and tissue engineering.

Chitosan is a copolymer containing acetamino and primary amino groups, which can be protonated to produce polyammonium salts, the pH for the amino groups present in chitosan is between 6.0 and 7.0, and they can be protonated in very dilute acids or even close to neutral conditions, rendering a cationic nature to this biopolymer (Dorozhkin 2009; Rinaudo 2006).

The primary amine group (NH₂) of chitosan is protonated, so there is a strong electrostatic interaction in inter/intra-molecules; it is obvious that the ionic strength and pH value of chitosan solution have an effect on this interaction (Dorozhkin 2009; Xianmiao et al. 2009; Zioupos 2001).

While the ionic strength increases, the counter-ions would screen the protonated amine group and make the molecule contracted. Strong intra-molecular hydrogen bonding was formed in solution because of the large number of OH and acetyl groups on the chitosan molecular chains (Dorozhkin 2009; Rinaudo 2006; Porter et al. 2006).

The chitosan and its derivatives like microcrystalline chitosan (MCCh) have excellent biostimulation properties providing a new cell formation which facilitates regeneration with a small scar forming and vascularization (Pighinelli and Kucharska 2014; Brugnerotto et al. 2001).

Instead of biomedical application, chitosan and its derivatives have other applications such as water treatment, cosmetics, pharmaceutical, food additives, and paper industry (Snel and McClure 2004; Muzzarelli 2011; Dorozhkin 2009).

Chitosan is a promising biomaterial as a base for tissue engineering and scaffold devices and as modification tools for currently medical devices improving tissue regeneration efficacy. Also, it can expand the feasibility of combinative strategy of controlled drug release concept and tissue engineered and tissue formation in reconstructive therapy in the different medical areas (Dorozhkin 2009; Rinaudo 2006; Pighinelli and Kucharska 2014; Hutmacher 2000).

4 Medical Applications for Chitosan

The medical application is one of the most exciting research areas of the materials science. Many products were developed in recent years to improve the quality of life and well-being of the people that needs to use, such as catheters, heart valves, pacemakers, breast implants, fracture fixation plates, nails and screws in orthopedics, dental filling materials, and orthodontic wires, as well as total joint replacement prostheses.

Chitosan and its derivatives provide great properties such as nontoxicity, water solubility, high swelling, stability to pH variations, biodegradable, and bioactive. On the other hand, it had shown some weak points of chitosan and its derivatives that limited the usage of this material such as low mechanical properties, temperature and chemical instability, microbial, and enzymatic degradation (Muzzarelli 1993).

The world interest to use chitosan for medical applications is related with several properties such great bioactivity, biodegradability, biocompatibility, antibacterial, antifungal and antiviral activity, high adhesivity, film-fiber forming, no toxicity, and high miscibility (Barbosa et al. 2005; Muzzarelli 1978).

The development of new biomaterials for regenerative medicine and tissue engineering in different forms such injectable, films, fibers, powders, and sponge is

directed related with the place to use; different places have different properties and responses (Niekraszewicz et al. 1998; Struszczyk 2003, 2006).

There are few limitations in those days to produce and design biomaterials using chitosan as a substrate as follows (Muzzarelli 1978; Niekraszewicz et al. 2004; Vert et al. 1992):

Standardization to select the raw material and the process to obtain reproducible products;

- the cost of production and the biopolymer manufacture.

5 Micro- and Nanocrystalline Chitosan (MCCH and NCh)

Different biomaterials for regenerative medicine and tissue engineering using chitosan derivatives are elaborated in different forms in combination with other biomaterials. The microcrystalline chitosan (MCCh) and nano-chitosan (NCh) is a modification of the structure of the original chitosan but keep the main properties of the original material. The method to obtain the microcrystalline chitosan is aminoglucose macromolecule aggregation method increasing the amorphous part and reducing the size of the crystal.

Microcrystalline chitosan is often used to prepare biodegradable biomaterials used in wound dressing and drug delivery. The application of the microcrystalline form of this biopolymer reduces the size of the chitosan crystals with a great increase of the amorphous part improving the hydrophilic character resulting in an inner surface formation, resistance to pH variation, prolongation of biodegradation, and increase the antimicrobial activity. It is very helpful to produce effective, simple, and inexpensive wound dressings. Moreover, chitosan is well-known as a substance which indicates the absence of risk of transferring animal pathogen onto humans (Pighinelli and Kucharska 2013; Qun and Ajun 2006; Muzzarelli 1993, 1995; Oktay 2004).

Struszczyk HM 2003 showed the effects of acids used during coagulation of MCCh and NCh and no significant changes in DD and M_v were notified, besides that an improvement in water retention value (WRW) was noticed.

Due to its properties in hard tissue regeneration as a resorbability and re-mineralization, the MCCh and NCh complex with TCP was also mixed with HAp to make biphasic calcium phosphate ceramics (tricalcium phosphate/hydroxyapatite ceramic), including the properties of the MCCh and NCh in the complex as a biocompatibility and biodegradability, the composites complex with different rates were prepared. The biodegradability and dissolution of calcium phosphate biomaterials is beneficial to bone formation realizing Ca_2^{++} and phosphate ions that have been considered as the origin of bioactivity encouraging a new bone formation (Pighinelli et al. 2012; Pighinelli and Kucharska 2014; Struszczyk 2003).

In hard tissue regeneration, enzymatic degradability associated with scaffold structure similar to extracellular matrix with glucosamine groups and calcium phosphates makes both material composites very attractive biopolymer for hard tissue repair (Pighinelli and Kucharska 2014; Muzzarelli 1995).

6 Calcium Phosphate (HAp, B-TCP)

Mineral material such as hydroxyapatite (HAp) is one of the main bone filler materials, which has been widely used to manufacture various bone repairing scaffolds.

The apatite family materials had been incorporated into a wide of biomedical materials and devices for regenerative medicine and tissue engineering such as dental application, orthopedic implants, bone defects, fracture treatment, cranio-maxillofacial reconstruction, otolaryngology, ophthalmology, and spinal surgery (Huipin et al. 2001; Dorozhkin 2009; Kong et al. 2006).

The apatite families such as hydroxyapatite and tricalcium phosphate are very compatible with the physiological environment and have proven excellent biocompatibility and bioactivity in bone replacement and new tissue formation. Enabling rates of resorption/replacement could present a favorable micro-environment for protein adhesion, osteoconductive, and osteoinductive. The HAp is founded in natural bone than another calcium phosphate like β -TCP; however, the resorption of HAp is extremely low compared with that of β -TCP (Dorozhkin 2009; Pramanik et al. 2009; Jue-Yeon et al. 2002).

The biodegradation of apatite family has same characteristics such as physical and chemical methods to obtain biologics (Dorozhkin 2009; Kong et al. 2006; Misiek et al. 1984).

Surface-active materials bind to bone through an apatite layer improving the bioactivity and promoting a new tissue grow. It has not been made clear whether the apatite layer can be formed only under the influence of the bone tissue (Dorozhkin 2009; Kong et al. 2006). Table 4 shows the most usage of calcium phosphate in medical area.

Table 4 Calcium phosphates of biomedical application [19]

CaP	Compositional formula	Acronym
Amorphous calcium phosphate	$\text{Ca}_3(\text{PO}_4)_2 \cdot 3\text{H}_2\text{O}^a$	ACP
Mono calcium phosphate	$\text{Ca}(\text{H}_2\text{PO}_4)_2$	MCP
Dicalcium phosphate anhydrous	CaHPO_4	DCPA
Dicalcium phosphate dihydrate	$\text{CaHPO}_4 \cdot 2 \text{H}_2\text{O}$	DCPD
Tricalcium phosphate	$\text{Ca}_3(\text{PO}_4)_2$	TCP
Octacalcium phosphate	$\text{Ca}_8\text{H}_2(\text{PO}_4)_6 \cdot 3\text{H}_2\text{O}$	OCP
Hydroxyapatite	$\text{Ca}_{10}(\text{PO}_4)_2(\text{OH})_2$	HAP

The bioactivity and performance of ceramic composites need to be controlled especially by the speed of dissolution phases in the physiological environment, releasing Ca^{2+} and PO_4^{3-} ions; the interaction between apatite layer and the tissues is related with the ratio between the compounds mixed, crystalline, and amorphous part. Figure 1 shows a schematic interaction between chitosan and calcium/phosphate ions (Klinkaewnarong 2009).

The calcium phosphate such as HAp or β -TCP that remains during dissolution works as a template for the newly formed bone tissue (Huipin et al. 2001; Fathi et al. 2008; Pighinelli and Kucharska 2014; Muzzarelli 2011).

7 Infrared Spectroscopy Fourier Transformation (FTIR) of the Commercial Calcium Phosphate Powders

Infrared Spectroscopy Fourier Transformation (FTIR) is mostly used to identify the functional groups through their characteristic chemical bonds and each connection type to verify the presence of functional characteristic groups of β -TCP, HAp. The mostly used infrared analysis works in the range of $500\text{--}4000\text{ cm}^{-1}$ and the resolution of 4.0 cm^{-1} .

Figure 2 shows the infrared spectroscopy Fourier transformation identified in the β -TCP and HAp; the main characteristic functional groups are orthophosphate (PO_4^{3-}), hydroxyl (OH^-), and phosphate (HPO_4^{2-}); the latter one, in trace amount, shows the characteristics of commercial calcium phosphates material. The presence of carbonate group, in traces, showed in the commercial β -TCP and HAp indicates that CaO and $\text{Ca}(\text{OH})_2$ are commonly used to find the ideal stoichiometric relation between Ca/P (1:1.67), and the samples were prepared in atmospheric conditions with the presence of carbon dioxide and air.

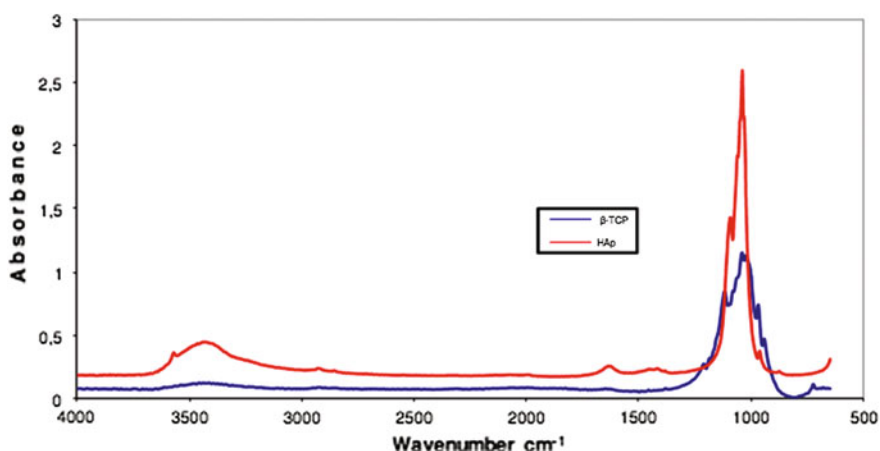


Fig. 2 FTIR spectrum of the commercial HAp and β -TCP

The FTIR results of the commercial β -TCP showed the absence of band at 740 (cm^{-1}), indicating that the only material is β -TCP and not a mixture of α -TCP, which shows also traces of a small amount of CO_3^{2-} in 1428 cm^{-1} , presenting a broad band in 900–1200 cm^{-1} ; the peak at 724 cm^{-1} is a characteristic of the symmetric mode (P–O–P) assigned to distortion of P–O. The peak at 1211 cm^{-1} is characteristic of a nondegenerate deformation of hydrogen groups— OPO_3 , $-\text{H}$, $\text{O}-\text{PO}_3$, and common ions HPO_4^{2-} (Dorozhkin 2009; Pighinelli and Kucharska 2014; Shinn-Jyh 2006; Rinaudo 2006; Majeti and Kumar 2000).

The infrared spectroscopy Fourier transformation results of the commercial HAp is shown in Fig. 2, a characteristic peak of 839 (cm^{-1}) that corresponds to deformation modes of phosphate groups (O–P–H) bonds. In bands 3570 and 3464 cm^{-1} , the OH^- group peak is also observed indicating one of the main characteristics of the calcium phosphates, the water absorption. The bands 1040 and 1093 (cm^{-1}) represent the asymmetric stretch modes, respectively, the P–O bonds of phosphate groups (Dorozhkin 2009; Pighinelli and Kucharska 2014; Ratajska et al. 2008; Bodek 2002; Wawro et al. 2011).

8 Morphology and Determination of Particles Size in Commercial HAp and β -TCP Powders

The morphology studies were directed by scanning electron microscopy [(SEM)—FEI Quanta 200, USA], to determine the morphology of the commercial HAp and β -TCP in the form of powder. Figure 3a, b illustrates β -TCP and HAp, respectively.

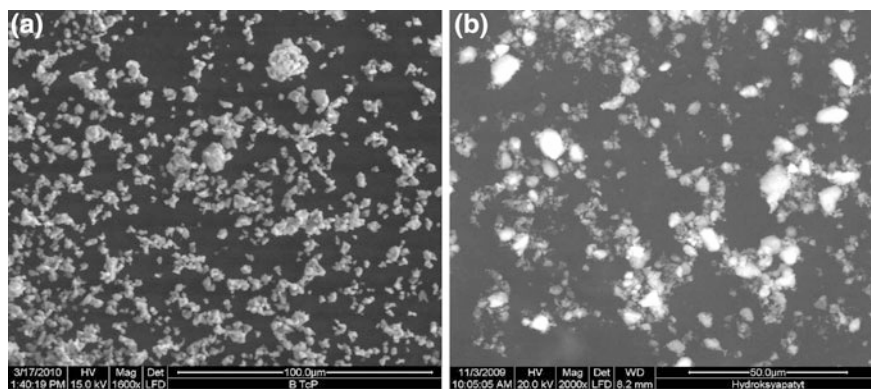


Fig. 3 The β -TCP and HAp, respectively

The morphologies of the calcium phosphates particles have one big difference: difference in shape; the β -TCP particles are more spherical than HAp powder. In both cases, the calcium phosphate particles showed great ability to agglomeration and cluster formation, that is, characteristics of the apatite family, taking place in a heterogeneous charge distribution on the surfaces, plus a great ability for water adsorption.

The literature showed that the performance of biomaterials made with calcium phosphates depends on the particles size and shape (aspect relation). There is a common sense in the literature about the shape showing that more round shape has a better performance in dissolution process, biocompatibility, biodegradability, bioactivity, and mechanical properties, but about the size of particles, still in discussion and more studies are needed to relate what is a better size of calcium phosphate particles for a biomaterial performance; same literature indicates that particle size around 50 to 150 micrometers has a better performance even in mechanical properties.

In the case of technique used to measure the particle size of the commercial calcium phosphate, it was directed by laser particles sizer by Sympatec Hellos H1330, type BF (sympatec GmbH, Clausthal, Germany). The analysis was performed in collaboration Thuringian Institute of Textile and Plastics Research, Rudolstadt, Germany.

The distribution covers only a narrow part, for instance 2–5 μm ; then the deviation is lower than 10%. However, the measurement itself is very precise. The measurement of the powders used in this research had procedure of three times for each sample and receives deviations of results lower than 2%; the samples of both powders had a range from 0.5 to 50 μm . The analysis showed that a β -TCP grain size fits in the range of 4.48.0–12.78 μm and grain size of HAp fits mainly in the range of 3.16–8.81 μm . The particle size distributions of HAp and β -TCP are shown in Fig. 4a, b, respectively.

The measurements of particles size by laser particles size gave a specified surface area covered by each powder: HAp is 3.41 e+04 cm^2/g and β -TCP is 2.53 e+04 cm^2/g . Also, it was found that around 10% of the calcium phosphate particles (HAp and β -TCP) were nano-size (Rinaudo 2006; Muzzarelli 1978; Sarkar et al. 2007). The research and development of biomaterials or functional biocomposites are related with so many factors that are directed related with performance of the materials involved in the tissue regeneration; the factors involved are as follows: preparation of suspension, mechanical properties, calcium and phosphate ions in the physiological environmental, particles size, shape, particles distribution, and ratio of inorganic parts in the polymer matrix (Rinaudo 2006; Muzzarelli 1978; Sarkar et al. 2007).

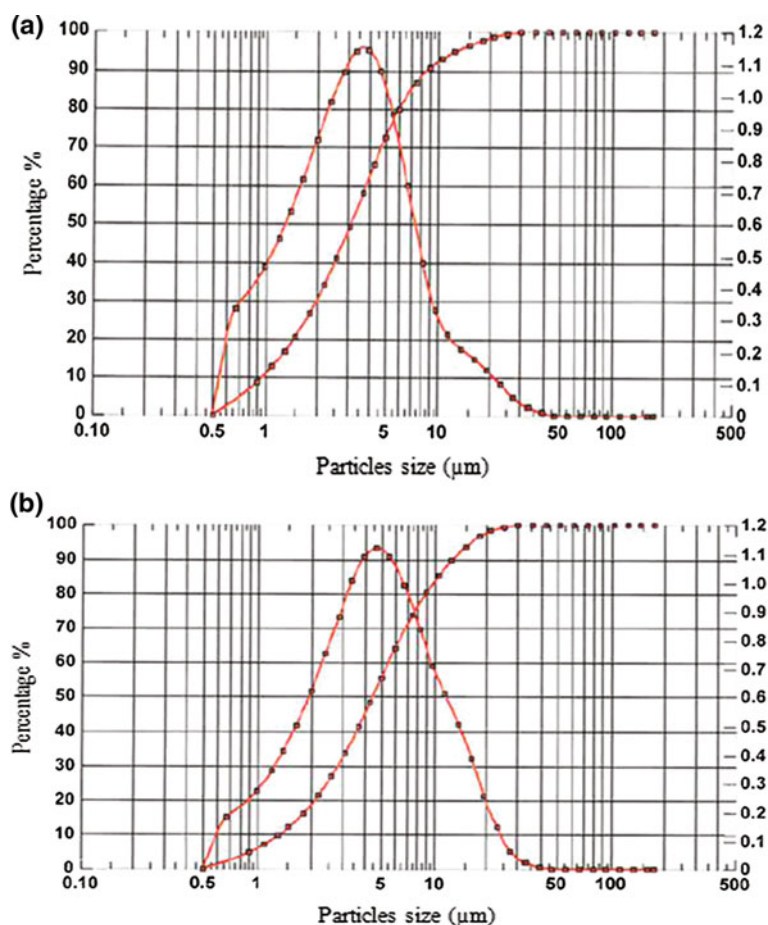


Fig. 4 a Grain size and distribution of synthetic HAP powder. b Grain size and distribution of synthetic β -TCP powder

9 Preparation of Chitosan Solutions Containing β -TCP, HAp, and HAp/ β -TCP

The preparation of hydrochloric chitosan/ β -TCP complex solution was prepared according to a method elaborated in the Institute of Biopolymers and Chemical Fibers, Poland (Snel and McClure 2004; Dorozhkin 2009) (Table 5).

The quantitative and qualitative compositions of biocomposite are shown in Table 6. The chitosan solutions were to elaborate a qualitative and quantitative composition of chitosan/ β -TCP complex with HAp to obtain a homogenous hydrochloric chitosan solution with nano-ceramic shown in Table 6.

Table 5 Particles size of commercial HAp and β -TCP

Powders	HAp	β -TCP
Particles size (90%), (μm)	8.81	12.78
Particles size (50%), (μm)	3.16	4.48
Particles size (10%), (μm)	0.97	1.35
Superficial area (cm^2/g)	3.41 e+04	2.53 e+04

Table 6 The formulation characteristic of hydrochloric chitosan solutions

Symbol of samples	Chitosan (%)	B-TCP (%)	HAp (%)	HCl (%)
Solution B	2	2.0	0	0.9
Solution C	2	0	0.5	0.9
Blend B/C 2:1 ratio	2	2.0	0.5	0.9

Dry polymer content 2.0%

The determination of particles size and zeta potential of hydrochloric chitosan solution with nano-ceramic was measured using a ZETASIZER 2000 (Malvern Instruments) apparatus.

The hydrochloric acid was used to dissolve the apatites family, the β -TCP and HAp; however just the small amount of calcium phosphate was used to obtain a homogenous complex chitosan solution that is used to prepare chitosan salt modified with nano-ceramic. Figure 5 shows a step-by-step dissolution process of the 2 wt% of the initial chitosan, including 2 wt% of microparticles of β -TCP dissolved in 0.9 wt% of hydrochloric acid. This process reduced the β -TCP particles size from micro- to nano-size, resulting in a clear solution of hydrochloric chitosan salt modified with β -TCP nanoparticles and this solution is called as solution B.

The literature shows that hydroxyapatite is less soluble than β -TCP; it was very clear in the preparation of the solution C when only a small amount 0.5 wt% of HAp was added in the chitosan (2 wt%) solution dissolved with 0.9 wt% of hydrochloric acid; the final solution was an opalescent suspension (Fig. 6).

Figure 7 shows the range of particle sizes of the calcium phosphates in the solutions and the stability of the solution by zeta potential. The blend of chitosan solutions contains two parts of the solution B (with β -TCP) and one part of the solution C (with HAp), that is, 2:1 of solution B and solution C, respectively, provided adequate conditions for the total dissolution of HAp, increasing the ionic bond between a negative surface charge of the β -TCP and a positive surface charge of the HAp, creating a clear and homogenous solution and all calcium phosphates in nanoparticles, the size of the nanoparticles within the range of 12.8–58.0 nm with great stability of the blend compared with the solutions B and C.

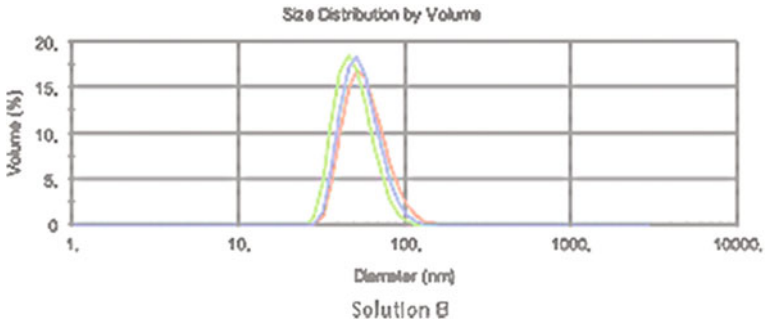


Fig. 5 Particle size distribution of β -TCP in chitosan solution in hydrochloric acid

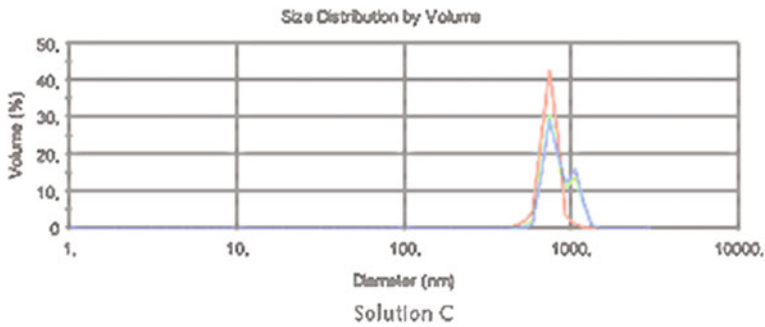


Fig. 6 HAP particles in chitosan hydrochloric solution (solution C)

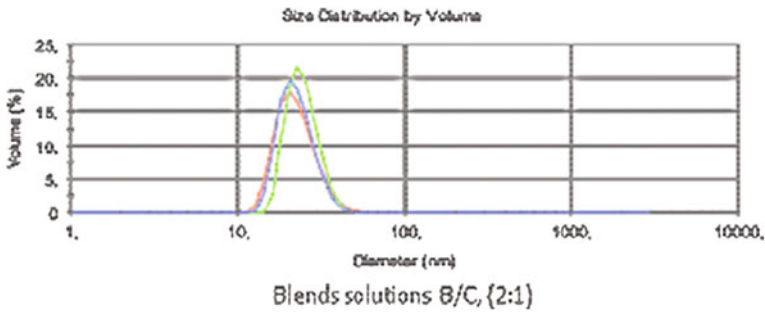


Fig. 7 The HAP/ β -TCP blend in chitosan (solution B/C)

10 Calcium Phosphate–Chitosan Biocomposites in Multifilament Fibers Form

This part of the chapter describes a method for preparing chitosan fibers modified with HAp/ β -TCP nanoparticles. The properties of the spinning solutions and the wet spinning process were included here as well. Chitosan fibers modified with nanoparticles of HAp/ β -TCP were characterized by a level of tenacity and calcium content and showed one hundred times higher than that of regular chitosan fibers.

One of the most common biocomposites is with inorganic/organic parts that are biomaterials widely used in regenerative medicine and tissue engineering. The biomaterial studies are multidisciplinary field and many characteristics needs to be considered in a fabrication of biocomposites such a structure of the polymer, shape, place to use, porosity and surface properties, texture, rigidity, bioactivity, and biodegradability process because all characteristics have more or less inflammatory response to also the type of injury, location of the injury, and health of the patient (Pighinelli and Kucharska 2013; Dorozhkin 2009; Strobin et al. 2007; Heineman et al. 2009).

Polymer–hydroxyapatite blends have been reported to be easily prepared and handled during surgery because they are easy to mold plastic material being more easily applied than pure hydroxyapatite powder or granules. Major disadvantages of those biodegradable systems are their considerably inferior mechanical strength, when compared to natural bone. This limits their application to low load-bearing parts of the human skeleton (Pighinelli and Kucharska 2014; Niekraszewicz et al. 1998, 2004; Klinkaewnarong 2009). Figure 8 shows the hydrogen bonds between chitosan and hydroxyapatite (β -hydrogen bonds) (Xianmiao et al. 2009). The biomaterials discipline is founded on the knowledge of the synergistic interface of material science, biology, chemistry, medicine, and mechanical science and requires the input of comprehension from all these areas so that implanted biomaterials.

The main characteristic of biomaterials when compared with other materials is their ability to remain in a biological environment without damaging the surroundings health tissues (Wang 2006; Heineman et al. 2010).

The aim of the use of these biocomposites has two characteristics to improve the tissue regeneration (Dorozhkin 2009; Tuzlakoglu et al. 2004):

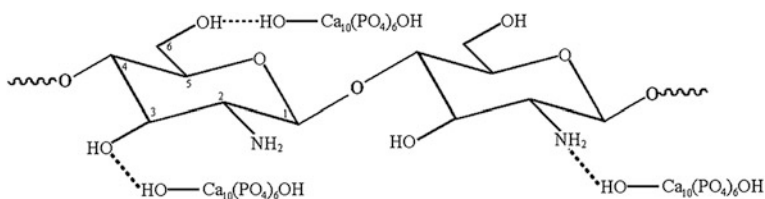


Fig. 8 Hydrogen bonds between chitosan and hydroxyapatite (β -hydrogen bonds) [34]

1. give support permissive for nutrient flow, cell migration, adhesion, and growth increasing the regeneration;
2. vehicle for controlled release of drugs.

The biological response and structural configuration of ceramic composites with natural polymers including calcium phosphate–chitosan biocomposites are related with the size and morphology of the pores to fabricated scaffold (Cyster et al. 2005; Xianmiao et al. 2009; Zioupos 2001). The challenge to create a new generation of implantable biomaterials is to develop a suitable bone scaffold with sufficient porosity and mechanical strength to allow cell adhesion, migration, growth resulting in good integration, and regeneration (Klinkaewnarong 2009; Xianmiao et al. 2009).

Figure 9 shows the schema of the most important interaction between chitosan and hydroxyapatite and interaction between Ca(II) of hydroxyapatite and -NH_2 of chitosan (Xianmiao et al. 2009).

The research and development of biomaterials and biocomposites for regenerative medicine and tissue engineering is still very promising field of studies, and every person during the life will be in contact with biomaterials to replace and/or restore the damage tissue and/or organs or in a part of treatment of several diseases. Making pressure on health and welfare systems of our countries starts rise up even further. Aging, diseases, fractures, and defects are also related with musculoskeletal disorder, when combined with other skeletal complications such demineralization,

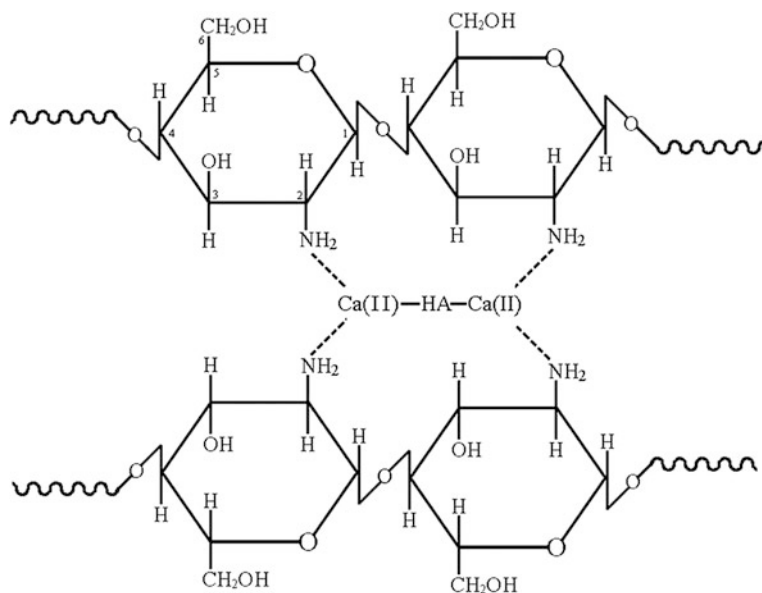


Fig. 9 Interaction between Ca(II) of hydroxyapatite and -NH_2 of chitosan (- coordination bonds) [34]

contribute and improve the research and developments of biocomposites for tissue engineering and regenerative medicine.

Biomaterials containing bioactive bioceramics and polymers should serve two purposes: (a) Increase the bioactivity promoting the new cells and (b) reinforce the scaffolds. The most common strategy used to obtain those biomaterials are

- (1) Incorporating bioceramic particles in the scaffold through a variety of techniques;
- (2) Coating a polymer scaffold with a thin layer of apatite through biomimetic processes;
- (3) Preparing a complex polymer/calcium phosphate.

One of the manufacturing processes to produce 3D interconnected porous scaffolds is freeze-drying method which is used for final stage to produce the porous structure in polymer/calcium phosphate composites, but some factors need to be considered such as polymer solution concentration, ratio of inorganic/organic parts. The porous type and size can be changed in the freeze-drying method. Same parameters such as pressure, temperature, and time play very important roles in forming the scaffolds of desired porous structures (pore geometry, pore size and size distribution, pore interconnectivity, thickness of pore walls, etc.) and hence the mechanical performance (Wang 2006; Qiaoling et al. 2004; Tuzlakoglu and Reis 2007).

Biocomposite materials are designed to increase the relationship between strength and toughness reflecting the balance between the rates of new bone deposition, bone resorption, and bone formation with two major characteristics, biodegradable and biocompatible (Porter et al. 2006).

The inorganic part of the biocomposite, usually made from apatite family (calcium phosphate), and the organic part (polymers) are ductile but may not have enough mechanical properties to withstand the load.

Definitions given by Vert are as follows (Brugnerotto et al. 2001).

Biodegradables are solid polymeric materials which break down due to macromolecular degradation by biological elements with dispersion in vivo but no proof for the elimination from the body.

Bioresorbable are solid polymeric materials which show bulk degradation and further resorb in vivo, i.e., polymers which are eliminated through natural pathways.

Bioresorption/Bioerosion is thus a concept which reflects total elimination of the initial foreign material with no residual side effects.

A biocomposite material including hydroxyapatite [$\text{Ca}_{10}(\text{PO}_4)_6(\text{OH})_2$; HAp and β -TCP ($\text{Ca}_3(\text{PO}_4)_2$)] with chitosan improves the biocompatibility between hard and soft tissue integrations and allows to increase initial fast spread of serum proteins compared to the more hydrophobic polymer surface; they have been introduced clinically for applications such as spinal fusions, bone tumors, fractures, and in the replacement of failed or loose joint prostheses (Zioupou 2001; Porter et al. 2006; Hutmacher 2000).

Natural bones are organized into 3-D structures in the body. The three-dimensional (3-D) structure provides the necessary support for cells adhesion, proliferation, diffusion of nutrients, and gas exchange (Brugnerotto et al. 2001; Lian et al. 2007).

Micro- and nano-chitosan fibers can be made by electrospinning (Huipin et al. 2001), pseudo-dry-spun fibers (Maachou et al. 2008) or wet spinning, multi-filaments fibers (Clayton et al. 2006; Cancedda et al. 2003). Chitosan fibers are widely used to prepare biomaterials for many applications, because it is easy to get different shapes. This research was based by to use a simple wet spinning process from a polymer solution to obtain multifilament chitosan fibers. Wet spinning from a solution of the polymer enables modifications by adding various functional substances to the solution, notably nanoparticles including pharmaceutical drugs for different diseases: carbon nanotubes (CNT) (Fathi et al. 2008; Rho et al. 1998; Sathirakul et al. 1995), nanosilver (Pighinelli and Kucharska 2013), calcium phosphates (Qun and Ajun 2006), calcium sulphite (Muzzarelli 1993), and a number of other polymers such as proteins and keratin proteins (Muzzarelli 1995; Pighinelli et al. 2012).

Chitosan lends itself to be used in biomaterials, thanks to properties such as its biodegradability, biosorption, and ability to accelerate wound healing.

To confer functionality upon chitosan fibers, they are frequently coated with other biomaterials such as collagen or calcium phosphates (Puttipipatkachorn et al. 2001; Pospieszny and Folkman 2004; Jue-Yeon et al. 2002; Muzzarelli 2009; Snel and McClure 2004). Following coating, they are used to reinforce composite implants containing hydroxyapatites (HAp) (Muzzarelli 2011). Calcium phosphates are known for their compatibility, osteoconductivity, and easy absorption by the human body, which makes them suitable for the preparation of composite dental implants (Dorozhkin 2009) and in combination with chitosan and artificial bones (Rinaudo 2006; Pighinelli and Kucharska 2014).

Multifilament chitosan fibers are used in many fields of applications such as tissue engineering, culture medium for cell growth, substrate for drug delivery, to construct a substrate. Adding calcium phosphates like HAp or β -TCP can be used for many medical applications such as artificial bones, cement, cartilage, and glues for hard tissue engineering (Clayton et al. 2006; Puttipipatkachorn et al. 2001; Pospieszny and Folkman 2004; Jue-Yeon et al. 2002; Rinaudo 2006; Pighinelli and Kucharska 2014; Barbosa et al. 2005; Muzzarelli 1978).

Calcium phosphate is very difficult to dissolve in chitosan solutions. The dissolution depends basically on the acid used to dissolve the primer chitosan, also the crystallinity grade of the chitosan and the calcium phosphate. Beta chitosan and amorphous calcium phosphates dissolve faster and easier compared with the high crystallinity raw material and also the dissolving conditions and process.

Apatite family have different dissolving properties such as HAp and β -TCP, related with dissolution process involved. Materials like hydrochloric and nitric acids show in the literature the best acids to dissolve apatite's family. The most favorable ratio between calcium and phosphorus is 1.67 (Niekraszewicz et al. 2004; Murugan and Ramakrishna 2004; Niekraszewicz et al. 1998).

The preparation of novel chitosan fibers containing calcium phosphates nanoparticles for medical use by the wet spinning process has many influences such as spinning conditions, mechanical properties, ratio of HAp/ β -TCP, morphology, fishing agent for the multifilament fibers, and stability of the chitosan solution modified with nano-calcium phosphate.

11 Preparation of Chitosan Solutions Modified with HAp/ β -TCP Nanoparticles to Prepare Multifilament Fibers by Wet Spinning

The preparation of chitosan solutions starts dissolving 5.16 wt% of chitosan in 3 wt% of the acetic acid. This aqueous solution, called solution A (code Chit-58), showed a solution clear and optically pure. Another solution was prepared dissolving 2 wt% of chitosan in 0.9 wt% of hydrochloric acid containing 2 wt% of β -TCP solution B (code MCT-6) presents β -TCP nanoparticles and also appear clear and optically pure.

The preparation of the solution C (code MCT-7) takes place dissolving 2 wt% of chitosan in 0.4 wt% of acetic acid, adding 0.5 wt% of HAp. The acetic acid did not dissolve HAp and was easy to see not clear solution like solution B. Hydroxyapatite is less soluble than β -TCP. This was apparent in the course of preparing solution C (code MCT-7) the solution appeared as an opalescent suspension showing a negative influence the quality of the prepared calcium-containing fibers (Table 7).

The solutions B and C were blended admixing in the ratio 2:1 to obtain solution (code MCT-11). Notice during the blending of the HAp and β -TCP particle containing chitosan solutions, the HAp particles dissolved immediately improving the solubility of HAp in the final chitosan solution providing adequate conditions for the complete dissolution of HAp, making the solution easier for wet spinning process. The solution (code MCT-11) was clear, homogenous, and stable chitosan solution and suitable for wet spinning process. Table 8, presents the qualitative and quantitative composition of the chitosan solutions.

Table 7 Selected parameters of chitosan solutions containing HAp, β -TCP, and HAp/ β -TCP

Chitosan solution	Range of particles size (nm)	Size of fraction with highest content (nm)	Percentage of volume (%)	Potential zeta (mV)
Solution B	28.9–164.9	65.2	11.5	43.0 \pm 2.3
Solution C	417.3–1495	745.4	34.2	45.3 \pm 2.3
Blend of solution B/C 2:1 ratio	12.8–58	22.9	19	52.9 \pm 4.0

Table 8 Some properties of chitosan solutions containing hydroxyapatite (HAp) and tricalcium phosphate (β -TCP) particles phosphate (β -TCP) particles

Solution code	Percentage of solution used (%)			Concentration of				Dynamic viscosity/temp.
				β -TCP	HAp	Acetic acid chitosan		
	A	B	C	wt%	wt%	wt%	wt%	Pa/°C
Chit 58	100	–	–	–	–	3.00	5.16	19,000/52
MCT 6	83.3	16.7	–	0.333	–	2.75	4.50	7500/49
MCT 7	83.3	–	16.7	–	0.330	2.75	4.63	9250/49
MCT 8	71.4	14.3	14.3	0.286	0.283	2.36	4.46	4500/52
MCT 11	62.5	25.0	12.5	0.707	0.252	2.10	4.01	1750/51

It was noticed that the presence of the chitosan acetate solution contains HAp particles (code MCT-7) with microparticles not suitable for wet spinning process showing a negative influence on the quality of the prepared calcium-containing fibers. Same problems were observed like decrease of the acid concentration and the dynamic viscosity of the final solution resulted by the calcium phosphates addition.

The solution (code MCT-8) was a blend mixing the solutions B and C in the ratio of 1:1; notice that blend did not dissolve HAp and founded agglomerations and cluster formation in the solution (MCT-8) with a size of 1500 nm that is present in the spinning solution provoking a negative influence of the mechanical properties and the spinning process of the fibers.

Analyzing the particles size of the solution MCT-11 showed that mixing process of the chitosan solutions had a beneficial effect by limiting the size of the calcium phosphate nanoparticles within the range of 12.8–58.0 nm with a great stability of the solutions.

Table 7 and Fig. 10 present the particle size distributions of the solutions MCT-6, MCT-7, and MCT-11, respectively.

12 Rheology Studies of Chitosan Solution (MCT 11) Modified with HAp/ β -TCP Nanoparticles

The dynamic viscosity of chitosan solution MCT-11 modified with nano-B-TCT/HAp is shown in Fig. 11. The flow curves were drawn in different temperatures at 20, 25, 30, 35, and 40 °C and in different shearing speeds.

The dynamic viscosity curves of chitosan solution MCT-11 showed a non-Newtonian fluid, expressing the direct relation with the viscosity decreasing when increasing the shearing speed, characterizing the chitosan solution as a pseudo-plastic fluid typical of natural semi-crystalline polymer, which was noticed when increased the temperature and the shearing speed drastically to the viscosity.

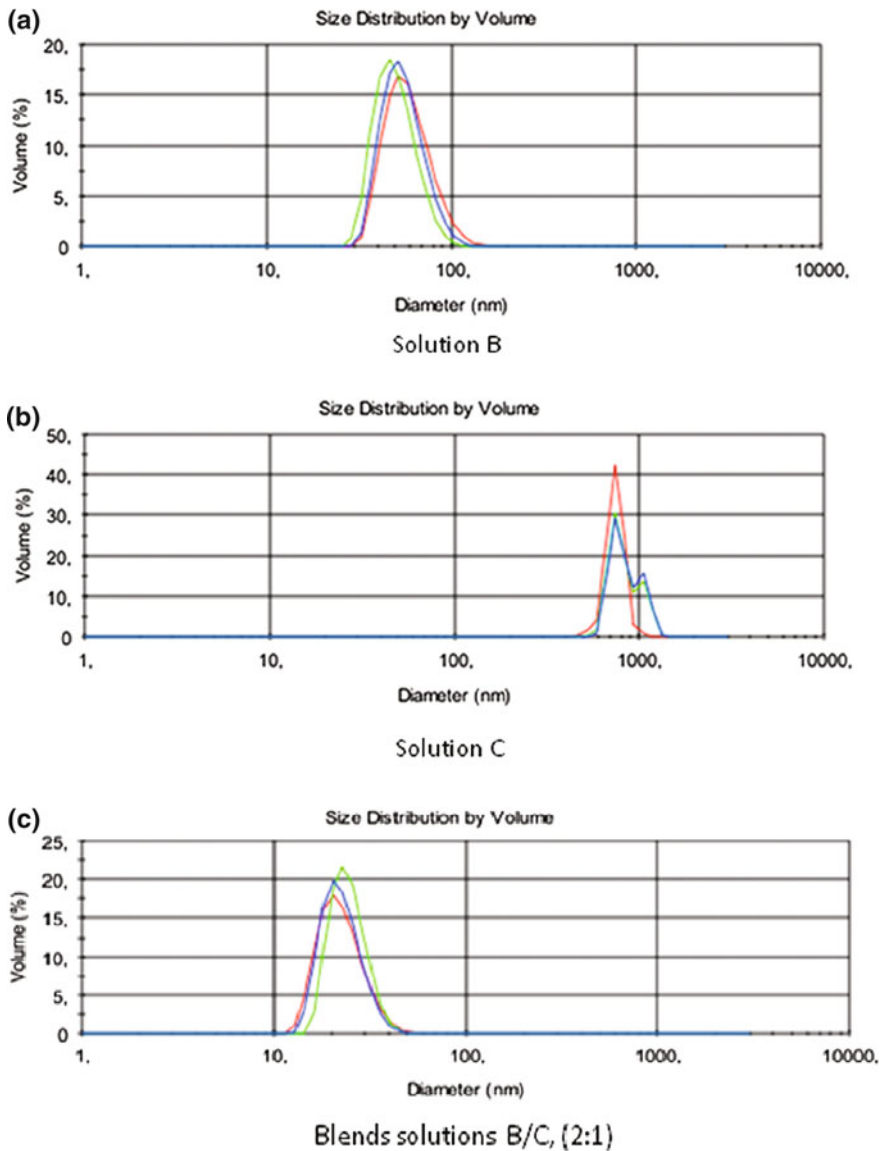


Fig. 10 **a** Particle size distribution of β -TCP in chitosan solution in hydrochloric acid (solution B); **b** HAp particles in chitosan acetate solution (solution C); **c** the HAp/B-TCP blend in chitosan (solution B/C)

This also can be considered as a limitation of the wet spinning process making more difficult and taking more time to set the parameters of the process. The stability of solutions is a very important parameter to be considered in the wet spinning process.

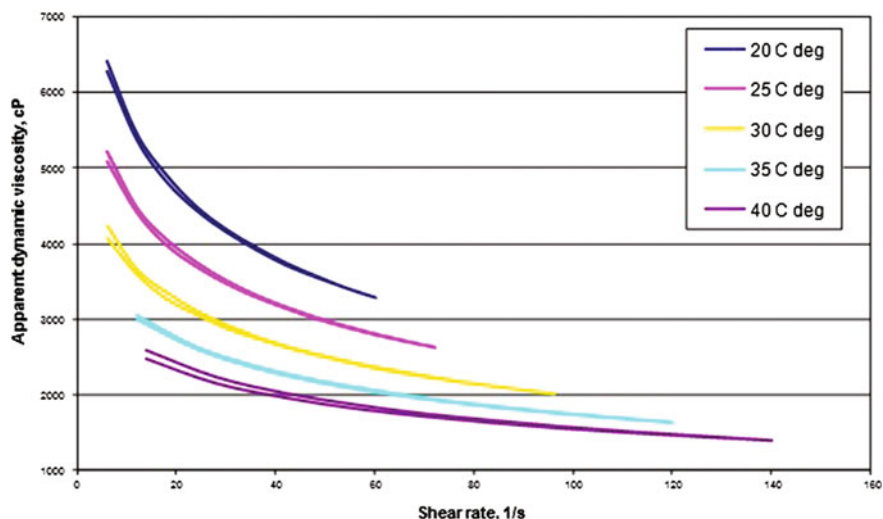


Fig. 11 Dependence of the apparent dynamic viscosity on the shearing rate and temperature of the acetate chitosan solution modified with HAp/ β -TCP (MCT 11)

13 Spinning Process of Chitosan Multifilament Fibers Modified with Nano-ceramics

To set the wet spinning process of chitosan (MCT-11) modified with HAp/ β -TCP, nanoparticles were found in the following conditions: at a spinning speed of 31.0 m/min, draw ratio of 34%, and temperature of around 25–30 °C. The multifilament fibers were passed into a coagulation bath containing aqueous 3.0% NaOH. The spinning process was smooth and easy to control, better than a normal chitosan fiber without nano-calcium phosphate particles; the nano-ceramic addition in the chitosan solution has a beneficial effect on spinning stability making the process more stable and regular. Also notice that no finishing agent is required in this process making also faster and more attractive for the industry.

14 Mechanical Properties of Multifilament Chitosan Fibers Modified with Nano-ceramics

Table 9 shows the mechanical properties of multifilament chitosan fibers modified with nano-ceramic (HAp/ β -TCP) related with the amount of organic and inorganic parts of the biomaterial in study that also related with the stretching of the wet spinning process and additives added during the manufacturing of fibers by wet spinning. In the solution, MCT-6 and MCT-7 notice a little effect on tenacity. The

Table 9 Impact of HAp, β -TCP, and HAp/ β -TCP concentration in the chitosan solution on the mechanical properties of fibers

Parameter		MCT 58	MCT 6	MCT 7	MCT 8	MCT 11
Linear density	dtex	4.39	4.48	5.14	5.41	4.16
Coefficient of variability of linear density	%	1.25	2.48	1.93	3.57	1.64
Confidence interval of linear density	%	± 1.55	± 3.08	± 2.40	± 4.43	± 2.04
Breaking force	cN	3.61	3.51	2.46	2.91	3.35
Coefficient of variability of breaking force (conditioned)	%	14.6	14.0	32.2	28.6	19.5
Confidence interval of breaking force	%	± 6.02	± 5.77	± 13.3	± 11.8	± 8.03
Tenacity (cond)	cN/tex	8.22	7.83	4.79	5.38	8.05
Elongation at break (cond)	%	17.0	22.0	9.9	11.0	12.0
Breaking force (wet)	cN	2.80	2.21	1.78	2.48	2.25
Coefficient of variability of breaking force (wet)	%	36.8	31.9	49.9	33.4	18.3
Tenacity (wet)	cN/tex	6.38	4.93	3.46	4.58	6.86
Elongation at break (wet)	%	7.8	7.3	7.8	6.1	8.00

mechanical properties are directed related with the calcium phosphate agglomeration and cluster formation, and we can see in the sample MCT-8 (1:1). In the SEM studies, a non-homogenous distribution of the calcium phosphates in the polymer matrix showing up a small amount of agglomeration and cluster formation related with the HAp and β -TCP involved in the solution probably related with some of the HAp particles is not dissolved completely by the concentration of the hydrotropic acid, the higher amount of calcium phosphates effect, and slight increase in fiber tenacity.

When increasing the concentration of hydrochloric acid by the amount of solution B (code MCT-6), notice that the de-agglomeration and cluster formation disappear showing a homogeneous distribution of the calcium phosphate in the polymer matrix (MCT-11). The reflection of this can be seen in a better distribution of the nano-ceramic and can be noticed in the mechanical properties with nanoparticles along with the highest level of calcium phosphates and resulted in fibers with the same tenacity as that of regular chitosan fibers.

The MCT-11 with a higher concentration of nano-ceramic HAp/ β -TCP avoids an effect that the fibers did not stick to each other. Effect can be seen in the normal chitosan fibers without nano-ceramics modification. Instead of that, no finishing agent is required in the wet spinning process. The advantage of chitosan fibers containing nano-ceramics (MCT 11) can be noticed in the higher tenacity and lower coefficient of variability of breaking force in wet conditions when compared with regular chitosan fibers.

15 Infrared Spectroscopy Fourier Transformation (FTIR) of the Chitosan Fibers Modified with Nano-ceramics

Infrared Spectroscopy Fourier Transformation (FTIR) is mostly used to identify the functional groups through their characteristic chemical bonds, and each connection type is used to verify the presence of functional characteristic groups of β -TCP, HAp, explained in the item 7 in this chapter and confirmed as shown in Figs. 12 and 13. The most infrared analysis used works in the range of $500\text{--}4000\text{ cm}^{-1}$ and resolution of 4.0 cm^{-1} .

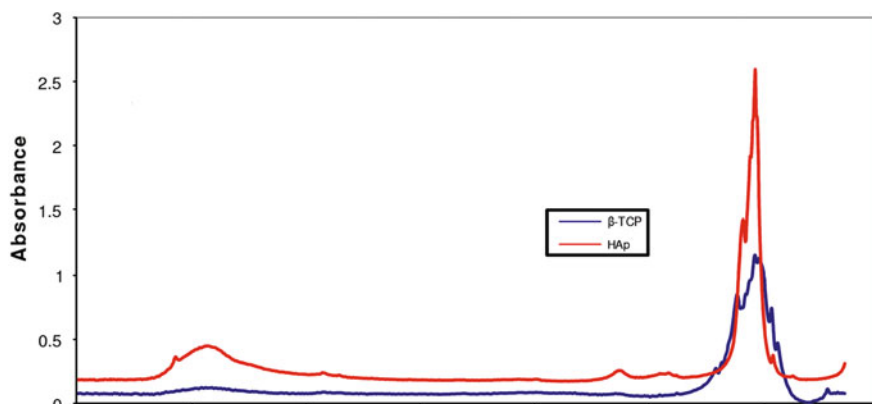


Fig. 12 FTIR spectrum of the commercial HAp and β -TCP

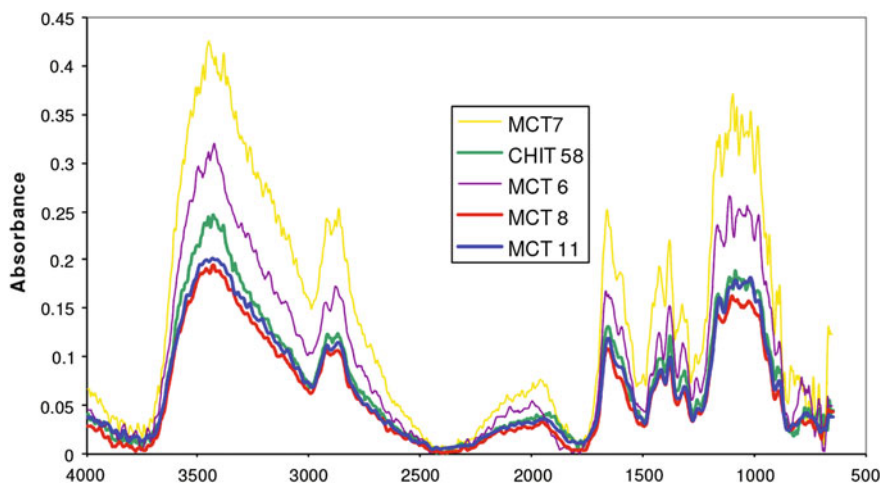


Fig. 13 FTIR spectra of chitosan fibers (Chit 58) and modified β -TCP (MCT 6), and those modified with HAp (MCT 7), HAp/ β -TCP (1:1) (MCT 8) and HAp/ β -TCP (1:2) (MCT 11)

Figure 12 shows the infrared spectroscopy Fourier transformation identified in the β -TCP and HAp; the main characteristic functional groups are orthophosphate (PO_4^{3-}), hydroxyl (OH^-), and phosphate (HPO_4^{2-}); the latter one in trace amount shows the characteristics of commercial calcium phosphates material (Muzzarelli 1978; Niekraszewicz et al. 2004; Kong et al. 2006; Pramanik et al. 2009; Klinkaewnarong 2009).

The infrared spectroscopy Fourier transformation results of the commercial β -TCP show the absence of band at 740 cm^{-1} . Indicating that the only raw material was β -TCP and not a mixture of α -TCP, it shows also the traces of a small amount of CO_3^{2-} in 1428 cm^{-1} , presenting a broad band in the range of $900\text{--}1200\text{ cm}^{-1}$ and the peak at 724 cm^{-1} , which is a characteristic of the symmetric mode (P–O–P) assigned to distortion of P–O. The peak at 1211 cm^{-1} is the characteristic of a nondegenerate deformation of hydrogen groups $-\text{OPO}_3$, $-\text{H}$, $\text{O}-\text{PO}_3$, and common ions HPO_4^{2-} (Dorozhkin 2009; Pighinelli and Kucharska 2014; Shinn-Jyh 2006; Rinaudo 2006; Majeti and Kumar 2000).

The infrared spectroscopy Fourier transformation results of the commercial HAp is explained in the item 7 in this chapter and confirmed as shown in Figs. 12 and 13 (Muzzarelli 1978; Wang 2006; Qiaoling et al. 2004; Cyster et al. 2005; Xianmiao et al. 2009).

Figure 13 shows the infrared spectroscopy Fourier transformation of the MCT 6, MCT-7, MCT-8, and MCT-11, and shows a characteristic vibration peaks of the composite with chitosan/HAp/ β -TCP: the peaks between 1032 , 1086 , and 1160 cm^{-1} reflect the skeletal vibrations of the saccharide structure and at 1559 , 1543 cm^{-1} is related with the free primary amino group (NH_2), amide I (1637 cm^{-1}), indicating that chitosan used in this research is partially deacetylated (83.2%), amide II (1559 cm^{-1}) and amide III (1319 cm^{-1}). The C–O–C can be seen at (1160 cm^{-1}), N–H (3298 , 3500 cm^{-1}), and O–H (3445 cm^{-1}), identifying the chitosan in the composite. The peak at 1243 cm^{-1} represents the free amino groups and the C2 position of glucosamine (Muzzarelli 1978; Niekraszewicz et al. 2004; Struszczyk 2003; Klinkaewnarong 2009; Wang 2006; Qiaoling et al. 2004; Zioupos 2001; Brugnerotto et al. 2001). The HAp infrared spectroscopy Fourier transformation was explained in the beginning of this chapter shown in Figs. 12 and 13.

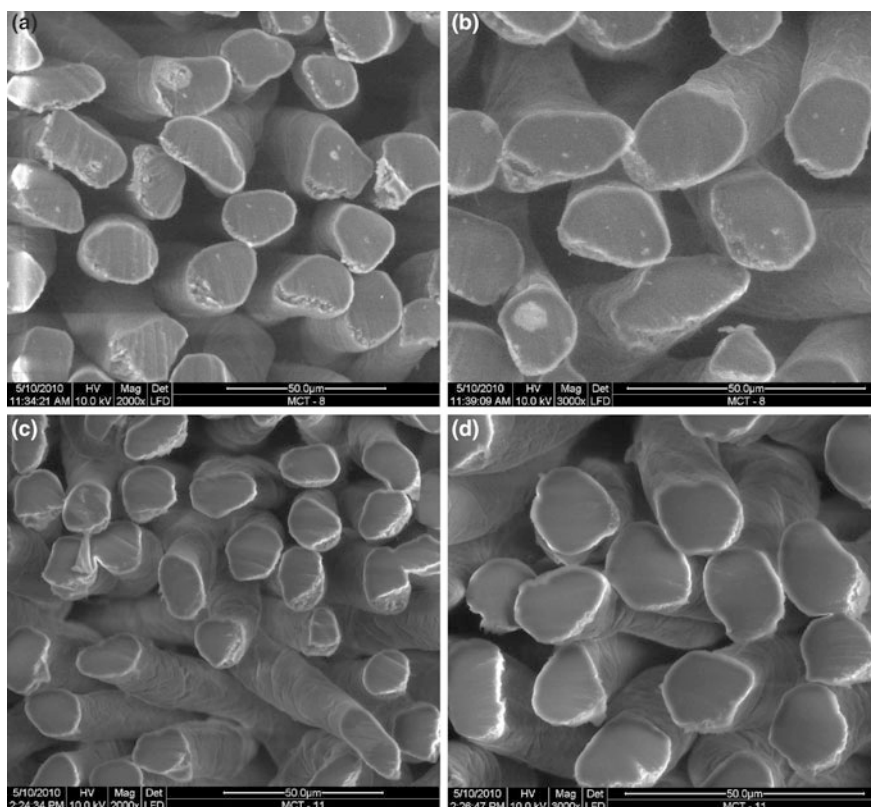
16 Morphology and Chemistry of Chitosan Fibers Modified with HAp, β -TCP and HAp/ β -TCP Nanoparticles

One analysis very important to identify how much your biomaterial increase the hydrophilic character and see how suitable hydrolytic and enzymatic degradation will affect this biomaterial is the water retention value (WRV).

Table 10 presents the range of the WRV of the samples from 150 to 331%; the variation is directed related with the amount of calcium phosphate added to the

Table 10 Water retention value (WRV) content of calcium and ash in HAp/ β -TCP-modified chitosan fibers

Fiber code	WRV (%)	Ash (%)	Calcium content (g/kg)
Chit 58	158	0.1	0.14
MCT 6	163	0.4	0.35
MCT 7	154	3.2	8.45
MCT 8	331	4.8	9.95
MCT 11	210	4.8	14.35

**Fig. 14** a, b SEM images of the surface and cross section of chitosan fibers modified with HAp/ β -TCP (MCT 8); c, d chitosan fibers modified with HAp/ β -TCP nanoparticles (MCT 11)

samples. Figure 14 shows the SEM images that illustrate the calcium phosphate distribution in the polymer matrix, identifying the HAp/ β -TCP agglomeration and cluster formation.

MCT-11 can notice a lower WRV because of the higher amount of the calcium phosphate and also can be seen in the SEM study a little difference in the shape of the fiber, more oval than others and a much better calcium phosphate distribution in the polymer matrix with no agglomeration and cluster formation shown in the cross-sectional images by SEM. Figure 14a–d shows that nanoparticles in the ratio 2:1 (MCT-11) are beneficial and increase the interaction between free amino groups of the chitosan and phosphate ions from the calcium phosphate, also a better ionic interaction between different calcium phosphates with different surface charges.

17 Preparation of Chitosan Spinning Solution Containing HAp, β -TCP and HAp/ β -TCP Nanoparticles

The preparation of chitosan solutions starts dissolving 5.16 wt% of chitosan in 3 wt% of the acetic acid. This aqueous solution called solution A (code Chit-58) shows a clear and optically pure solution. Another solution was prepared dissolving 2 wt% of chitosan in 0.9 wt% of hydrochloric acid containing 2 wt% of β -TCP; solution B (code MCT-6) presents β -TCP nanoparticles and also appears clear and optically pure.

The preparation of the solution C (code MCT-7) takes place by dissolving 2 wt% of chitosan in 0.4 wt% of acetic acid, adding 0.5 wt% of HAp. The acetic acid did not dissolve HAp and was not easy to see a clear solution like solution B. Hydroxyapatite is less soluble than β -TCP. This was apparent in the course of preparing solution C (code MCT-7), the solution appeared as an opalescent suspension showing a negative influence by the quality of the prepared calcium-containing fibers.

The MCT-11 is a blend using two parts of solution B (MCT-6) and one part of solution C (MCT-7). Notice that all solutions even before and after blend need to be deaerated at room temperature.

18 Wet Spinning Process of Chitosan Fibers Containing Nano-ceramics

Wet spinning process of chitosan fibers containing calcium phosphates (HAp/ β -TCP) nanoparticles was prepared using a spinning head holding a rhodium/platinum spinneret with 150 holes, each having a diameter of 0.08 mm, using at 35 °C. The first step after spinning process was to pass the fiber into the first bath for coagulation (aqueous 3.0 wt%, sodium hydroxide at 35 °C).

The second step after coagulation bath is to pass the fiber into the second bath to remove the sodium hydroxide surplus on the fibers washed in a water bath at 40 °C

and after then in a water–ethanol (60% v/v). It is a continuous process of spun wet spinning; the multifilament fibers need to be dried without tension and the speed process at 31 m/min.

Chitosan fibers modified with HAp, β -TCP and HAp/ β -TCP nanoparticles were prepared by wet spinning on a pilot line equipped with the spinning solution, the same as a coagulation bath. The spun fibers were bath and were then dried without tension in a loose bundle. The spinning speed for the chitosan fibers modified with HAp/ β -TCP nanoparticles was 31 m/min.

19 Conclusions

Addition of nano-ceramics, composed of HAp/ β -TCP nanoparticles, shows the preparation of multifilament fibers by wet spinning process, a beneficial effect. Then it can be noticed in infrared spectroscopy Fourier transformation (FTIR) that identifies the presence of the main functional groups of HAp/ β -TCP and chitosan and no secondary groups were founded.

The sample MCT-11 was founded more homogenous distribution of the nano-ceramic in the polymer matrix and no agglomeration and cluster formation were founded. Also, increase in the water retention value that is related with the hydrophilic character suggests more susceptible to hydrolytic, and enzymatic degradation will affect this biomaterial by the water retention value (WRV).

The mechanical properties showed that addition of ceramics decreases a little the tenacity of the chitosan fibers. This result can also be seen by the ash content of the sample MCT-11 showing a calcium content of 14.35 g/kg and an ash content of 4.8%.

The wet spinning process was smooth with speed of 31 m/min, and no finishing agent was required because the multifilament chitosan fibers modified with nano-ceramics did not stick from each other.

The multi- and interdisciplinary fields related with research and development of biocomposites are growing and new biomaterials, methods, and knowledge make possible to increase the applications that can contribute to design a new generation of biomaterials for regenerative medicine and tissue engineering.

Acknowledgements Lutheran University of Brazil, Biomatter lab, Post-Graduation program of Toxicology and Genetic and Materials Engineering. Ministry of Science and Higher Education in 2009–2012 as research project no: N N508 445636. European Community's Seventh Framework Program (Marie-Curie), FP7/2007–2013 under grant agreement no: PITN-GA-2008-214015. Institute of Polymer and Dye Technology of the Technical University, Lodz, Poland. Institute of Biopolymers and Chemical Fibres, Lodz, Poland. Thuringian Institute of Textile and Plastics Research, Rudolstadt, Germany (TITK).

References

- Barbosa MA, Granja PL, Barrias CC, Amaral IF (2005) Polysaccharides as scaffolds for bone regeneration. *ITBM-RBM* 26:212–217
- Bodek KH (2002) Evaluation of properties microcrystalline chitosan as a drug carrier *Acta Polonica pharmaceutic. Drug Res* 57(6):431–441
- Brugnerotto J, Lizardi J, Goycoolea FM, ArguÉelles-Monal W, DesbrieÁres J, Rinaudo M (2001) An infrared investigation in relation with chitin and chitosan characterization. *Polymer* 42:3569–3580
- Cancedda R, Dozin B, Giannoni P, Quarto R (2003) Tissue engineering and cell therapy of cartilage and bone. *Matrix Biol* 22:81–91
- Clayton EW, Moyo CK, de Bruijn JD, van Blitterswijk CA, Cumhur Oner F, Verbout AJ, Dhert Wouter JA (2006) A new in vivo screening model for posterior spinal bone formation: comparison of ten calcium phosphate ceramic material treatments. *Biomaterials* 27:302–314
- Corobea MC, Muhulet O, Miculescu F, Antoniac IV, Vuluga Z, Florea D et al. (2016) Novel nanocomposite membranes from cellulose acetate and clay-silica nanowires. *Polym Adv Technol* 27(12):1586–1595
- Cyster LA, Grant DM, Howdle SM, Rose FRAJ, Irvine DJ, Freeman D, Scotchford CA, Shakesheff KM (2005) The influence of dispersant concentration on the pore morphology of hydroxyapatite ceramics for bone tissue engineering. *Biomaterials* 26:697–702
- Dorozhkin SV (2009) Nanodimensional and nanocrystalline apatites and other calcium orthophosphates in biomedical engineering, biology and medicine. *Materials* 2:1975–2045
- Fathi MH, Hanifi A, Mortazavi V (2008) Preparation and bioactivity evaluation of bone-like hydroxyapatite nanopowder. *J Mater Process Technol* 202:536–542
- Heineman C, Heineman S, Bernhard A, Lode A, Worch H, Hanke T (2009) In vitro evaluation of textile chitosan scaffolds for tissue engineering using human bone marrow stromal cells. *Biomacromol* 10:1305–1310
- Heineman C, Heineman S, Bernhard A, Lode A, Worch H, Hanke T (2010) In vitro osteoclastogenesis on textile chitosan scaffolds. *Eur Cell Mater* 19:96–106
- Huipin Y, Bruijn JD, Yubao L, Feng J, Yang Z, Groot K, Zhang X (2001) Bone formation induced by calcium phosphate ceramics in soft tissue of dogs: a comparative study between porous a-TCP and b-TCP. *J Mater Sci - Mater Med* 12:7–13
- Hutmacher DW (2000) Scaffolds in tissue engineering bone and cartilage. *Biomaterials* 21:2529–2543
- Jue-Yeon L, Sung-Heon N, Su-Yeon I, Yoon-Jeong P, Yong-Moo L, Yang-Jo S, Chong-Pyoung C, Seung-Jin L (2002) Enhanced bone formation by controlled growth factor delivery from chitosan-based biomaterials. *J Controlled Release* 78:187–197
- Klinkaewnarong J (2009) Nanocrystalline hydroxyapatite powders by a chitosan–polymer complex solution route: synthesis and characterization. *Solid State Sci* 11:1023–1027
- Kong L, Yuan G, Guangyuan L, Yandao G, Nanming Z, Xiufang Z (2006) A study on the bioactivity of chitosan/nano-hydroxyapatite composite scaffolds for bone tissue engineering. *Eur Polymer J* 42:3171–3179
- Kwon SH, Jun YK, Hong SH, Kim HE (2003) Synthesis and dissolution behavior of β -TCP and HA/ β -TCP composite powder. *J Eur Ceram Soc* 23:1039–1045
- Lee CY, Lee JS, Chen SC (2010) Dechlorinating chitosan fibers and method for manufacturing the same. U.S. 2010/0084336 A1
- Lian Q, Li DC, He JK, Wang Z (2007) Mechanical properties and in-vivo performance of calcium phosphate cement-chitosan fiber composite. *Proc Inst Mech Eng H* 222:347–353
- Maachou H, Bal KE, Bal Y, Chagnes A, Cote G, Alliouche D (2008) Characterization and in vitro bioactivity of chitosan/hydroxyapatite composite membrane prepared by freeze-gelation method. *Trends Biomater Artif Organs* 22:16–27
- Majeti NV, Kumar R (2000) A review of chitin and chitosan applications. *React Funct Polym* 46:1–27

- Matsumoto T, Okazaki M, Inoune M, Hamada Y, Taira M, Takahashi J (2002) Crystallinity and solubility characteristics of hydroxyapatite adsorbed amino acid. *Biomaterials* 23:2241–2247
- Misiek DJ, Kent JM, Carr RF (1984) Soft tissue responses to hydroxyapatite particles of different shapes. *J Oral Maxillofac Surg* 42:150–160
- Murugan R, Ramakrishna S (2004) Bioresorbable composite bone paste using polysaccharide based nano hydroxyapatite. *Biomaterials* 25:3829–3835
- Muzzarelli RAA (1978) Chitin. Pergamon Press, Oxford
- Muzzarelli RAA (1993) Biochemical significance of exogenous chitins and chitosans in animals and patients. *Carbohydr Polym* 20:7–16
- Muzzarelli RAA (1995) Chitin and the human body. In: First international conference of the European Chitin Society, *Advances in Chitin Science*, Brest, pp 448–461
- Muzzarelli RAA (2009) Chitins and chitosans for the repair of wounded skin, nerve, cartilage and bone. *Carbohydr Polym* 76:167–182
- Muzzarelli RAA (2011) Chitosan composites with inorganic, morphogenetic proteins and stem cells for bone regeneration. *Carbohydr Polym* 83:1433–1445
- Niekraszewicz A, Kucharska M, Wisniewska-Wrona M (1998) Some aspects of chitosan degradation. In: Struszczyk H (ed) *Progress on chemistry and application of chitin and its derivatives*, vol IV. PTChit., pp 55–63
- Niekraszewicz A, Kucharska M, Wisniewska-Wrona M, Wesolowska E, Struszczyk H (2004) Chitosan in medical application. In: *Progress on chemistry and application of chitin and its derivatives*, vol X. PTChit., pp 13–17
- Oktay Y (2004) Preparation and characterization of chitosan/calcium phosphate based composite biomaterials. Master of science dissertation, zmir Institute of Technology zmir, Turkey
- Pighinelli L, Kucharska M (2013) Chitosan-hydroxyapatite composites. *Carbohydr Polym* 93:256–262
- Pighinelli L, Kucharska M (2014) Properties and structure of microcrystalline chitosan and hydroxyapatite composites. *J Biomater Nanobiotechnol* 05:128–138
- Pighinelli L, Kucharska M, Gruchala B, Wisniewska-Wrona M, Brzoza-Malczewska K (2012) Biodegradation study of microcrystalline chitosan and microcrystalline chitosan/ β -TCP complex composites. *Int J Mol Sci* 13:7617–7628
- Porter AE, Buckland T, Hing K, Best SM, Bonfield W (2006) The structure of the bond between bone and porous silicon-substituted hydroxyapatite bioceramic implants. *J Biomed Mater Res, Part A* 78:25–33. doi:10.1002/jbm.a
- Pospieszny H, Folkman W (2004) Factors modifying a biological activity of chitin derivatives. In: *Progress on chemistry and application of chitin and its derivatives*, vol X. PTChit., pp 7–12
- Pramanik N, Mishra D, Banerjee I, Maiti TK, Bhargava P, Pramanik P (2009) Chemical synthesis, characterization, and biocompatibility study of hydroxyapatite/chitosan phosphate nanocomposite for bone tissue engineering applications. *Int J Biomater*. doi:10.1155/2009/512417
- Puttipipatkachorn S, Nunthanid J, Yamamoto K, Peck GE (2001) Drug physical state and drug-polymer interaction on drug release from chitosan matrix films. *J Controlled Release* 75: 143–153
- Qiaoling H, Baoqiang L, Mang W, Jiacong S (2004) Preparation and characterization of biodegradable chitosan/hydroxyapatite nanocomposite rods via in situ hybridization: a potential material as internal fixation of bone fracture. *Biomaterials* 25:779–785
- Qun G, Ajun W (2006) Effects of molecular weight, degree of acetylation and ionic strength on surface tension of chitosan in dilute solute. *Carbohydr Polym* 64:29–36
- Ratajska M, Haberkowicz K, Cienchanska D, Niekraszewicz A, Kucharska M (2008) Hydroxyapatite-chitosan biocomposites. In: *Progress on chemistry and application of chitin and its derivatives*, vol XIII. PTChit, pp 89–94
- Rho J-Y, Kuhn-Spearing L, Zioupos P (1998) Mechanical properties and the hierarchical structure of bone. *Med Eng Phys* 20:92–102
- Rinaudo M (2006) Chitin and chitosan: properties and applications. *Prog Polym Sci* 31:603–632
- Sarkar S, Jana AD, Samanta SK, Mostafa G (2007) Facile synthesis of silver nanoparticles with highly efficient antimicrobial property. *Polyhedron* 26:4419–4426

- Sathirakul K, How NC, Stevens WF, Chandkrachang S (1995) Applications of chitin and chitosan bandages for wound-healing. In: First international conference of the European Chitin Society, Advances in Chitin Science, Brest, pp 490–492
- Shinn-Jyh D (2006) Preparation and properties of chitosan/calcium phosphate composites for bone repair. *Dent Mater J* 25(4):706–712
- Snel S, McClure SJ (2004) Potential applications of chitosan in veterinary medicine. *Adv Drug Deliv Rev* 56:1467–1480
- Strobin G, Ciecchańska D, Wawro D, Steplewski W, Józwicka J, Sobczak S, Haga A (2007) Chitosan fibers modified by fibroin. *Fibers Text East Eur* 15:64–65
- Struszczyk HM (2003) The effect of the preparation method on the physicochemical properties of microcrystalline chitosan (MCCh). In: Progress on chemistry and application of chitin and its derivatives, vol IX. PTChit., pp 179–186
- Struszczyk HM (2006) Global requirements for medical applications of chitin and its derivatives. In: Progress on chemistry and application of chitin and its derivatives, vol XI. PTChit., pp 95–102
- Thakur VK, Thakur MK (2014) Recent advances in graft copolymerization and applications of chitosan: a review. *ACS Sustain Chem Eng* 2(12):2637–2652
- Thakur VK, Voicu SI (2016) Recent advances in cellulose and chitosan based membranes for water purification: a concise review. *Carbohydr Polym* 146:148–165
- Thakur MK, Thakur VK, Gupta RK, Pappu A (2016) Synthesis and applications of biodegradable soy based graft copolymers: a review. *ACS Sustain Chem Eng* 4(1):1–17
- Trache D, Hazwan Hussin M, Mohamad Haafiz MK, Kumar Thakur V (2017) Recent progress in cellulose nanocrystals: sources and production. *Nanoscale* 9(5):1763–1786
- Tuzlakoglu K, Reis RL (2007) Formation of bone-like apatite layer on chitosan fiber mesh scaffolds by a biomimetic spraying process. *J Mater Sci Mater Med* 18:1279–1286
- Tuzlakoglu K, Alves CM, Mano JF, Reis RL (2004) Production and characterization of chitosan fibers and 3-D fiber mesh scaffolds for tissue engineering applications. *Macromol Biosci* 4:811–819
- Vert M, Li MS, Spenlehauer G, Guerin P (1992) Bioresorbability and biocompatibility of aliphatic polyesters. *J Mater Sci* 3:432–446
- Voicu SI, Condruz RM, Mitran V, Cimpean A, Miculescu F, Andronesu C, Thakur VK (2016) Sericin covalent immobilization onto cellulose acetate membrane for biomedical applications. *ACS Sustain Chem Eng* 4(3):1765–1774
- Wang M (2006) Composite scaffolds for bone tissue engineering. *Am J Biochem Biotechnol* 2(2):80–84 (ISSN 1553-3468)
- Wawro D, Krucińska I, Ciecchańska D, Niekraszewicz A, Steplewski W (2011) Some functional properties of chitosan fibers modified with nanoparticles. In: Proceedings of the 10th international conference of the European Chitin Society, EUCHIS'11, St. Petersburg, Russia
- Wilsonjr O, Hull JR (2008) Surface modification of nanophased hydroxyapatite with chitosan. *Mater Sci Eng, C* 28:434–437
- Xianmiao C, Yubao L, Zuo Y, Zhang L, Jidong L, Huanan W (2009) Properties and in vitro biological evaluation of nano-hydroxyapatite/chitosan membranes for bone guided regeneration. *Mater Sci Eng, C* 29:29–35
- Zargarian SS, Haddadi-Asl V (2010) A nanofibrous composite scaffold of PCL/hydroxyapatite-chitosan/PVA prepared by electrospinning. *Iran Polym J* 19:457–468
- Zioupou P (2001) Ageing human bone: factors affecting its biomechanical properties and the role of collagen. *J Biomater Appl* 15:187–229. doi:[10.1106/5JUJ-TFJ3-JVVA-3RJO](https://doi.org/10.1106/5JUJ-TFJ3-JVVA-3RJO)

Chapter 5

Surface Properties of Thermoplastic Starch Materials Reinforced with Natural Fillers

Tomy J. Gutiérrez, Romina Ollier and Vera A. Alvarez

Abstract The self-association force of water on the surface of a composite polymeric material is a physicochemical process dominated by cohesive forces and van der Waals-type interactions existing below the material surface. Perturbations in the chemical potential of water, brought about by the interaction between it and a polymeric surface, induce compensatory structural changes. Thus, the structure of water on the surface of a composite polymeric material reveals the hydrogen bond interactions taking place beneath it, which are key to understanding the properties of thermoplastic starch (TPS) materials. In the literature, there is a broad consensus based on empirical results that a contact angle (θ) greater than 65° defines a hydrophobic surface. These findings suggest that there are at least two different types of water structures that exist as a response to interactions occurring within the composite polymers. One of these is formed when there is a low density of “Lewis sites”, and the other when there is a high density of “Lewis sites” on the surface of the thermoplastic materials. This second scenario produces the collapse of the water structure, i.e., the collapse of the hydrogen-bonded network. In spite of the physicochemical response of water to the intra- and intermolecular interactions that occur on composite materials, these have not been studied as a means to modify the surface behavior of TPS materials. This could be achieved by incorporating natural fillers that have a plasticizer or crosslinking effect on their structure. In this chapter, we analyze the surface properties of starch-based composite materials as an indirect

T.J. Gutiérrez (✉) · R. Ollier · V.A. Alvarez (✉)
Thermoplastic Composite Materials (CoMP) Group, Faculty of Engineering,
Institute of Research in Materials Science and Technology (INTEMA),
National University of Mar del Plata (UNMdP) and National Council
of Scientific and Technical Research (CONICET), Colón 10850,
7600 Mar del Plata, Buenos Aires, Argentina
e-mail: tomy.gutierrez@fi.mdp.edu.ar; tomy_gutierrez@yahoo.es

V.A. Alvarez
e-mail: alvarezvera@fi.mdp.edu.ar; alvarezvera@gmail.com

measure of the interactions that occur within them, mainly as regards plasticizing effects and crosslinking reactions.

Keywords Composite materials · Natural fillers · Surface properties
Thermoplastic starch

1 Introduction

The surface properties of thermoplastic starch (TPS) used to pack food are key variables for food packaging designers and engineers as they influence product shelf life, appearance, and quality control.

Materials made using TPS often contain fillers such as nanoparticles, microcapsules, cellulose, and clay, among others, which have all been extensively studied (Trache et al. 2017; Voicu et al. 2016; Miculescu et al. 2016). Because they are highly susceptible to humidity, the starches used are usually modified in order to improve their physicochemical properties (Wang et al. 2016). However, although there have been many efforts made to develop materials from biomacromolecules, especially starch, their surface properties have received relatively little attention.

Surface composition and morphology are commonly determined by means of several techniques such as electron spectroscopy for chemical analysis (ESCA or XPS), secondary ion mass spectrometry (SIMS), scanning electron microscopy (SEM), atomic force microscopy (AFM), and contact angle (Peeling et al. 1976; Varma 1984; Russell et al. 1987; Baldwin et al. 1997, 1998; Michalska-Požoga et al. 2016). In particular, this last technique is increasingly being used in the academic and scientific worlds, as well as at an industrial level, since the table-top equipment now on offer can cost as little as 150 dollars. The instruments are also more portable and robust (Fig. 1a) than more traditional equipment (Fig. 1b) and can produce higher quality images (Fig. 1c, d).

The contact angle (θ) is defined as the angle formed by the intersection of the tangent lines of the liquid and solid surfaces at the three-phase boundary between these two phases and the third surrounding phase (generally air or vapor) (Wong et al. 1992). A schematic representation of a contact angle (θ) is shown in Fig. 2. One of the primary characteristics of any immiscible two- or three-phase system made up of two condensed phases, at least one of which is a liquid, is the contact angle of that liquid on the other condensed phases (solid or liquid surfaces) (Ghanbarzadeh et al. 2013). These phases can be as follows:

- liquid–vapor–solid: for example, water on an edible film.
- liquid–liquid–solid: for example, water–oil–protein in an emulsion.
- liquid–liquid–vapor: for example, an oil drop on a water surface.

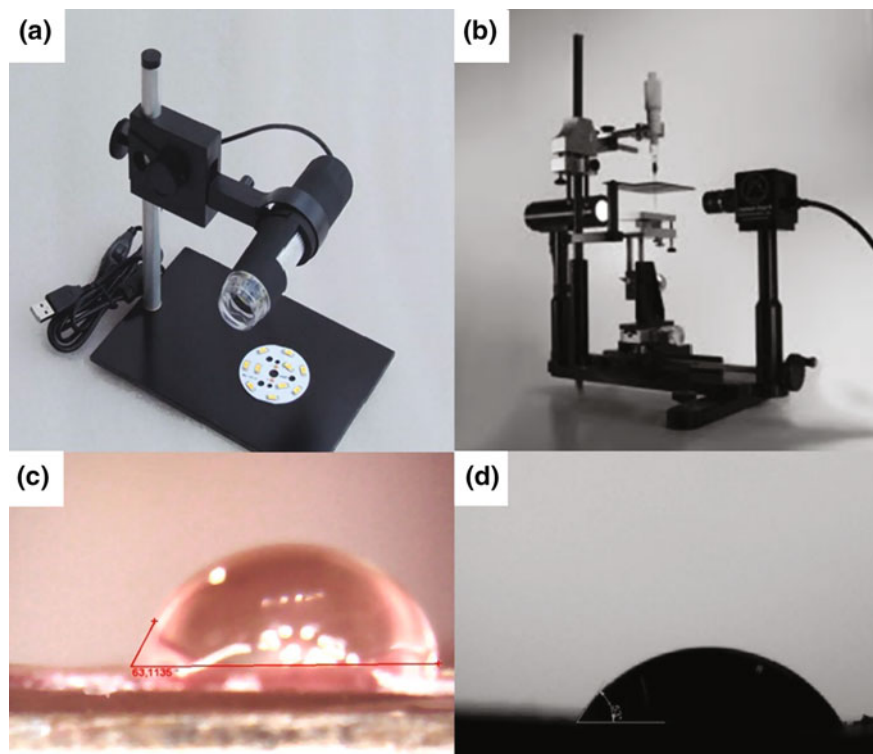
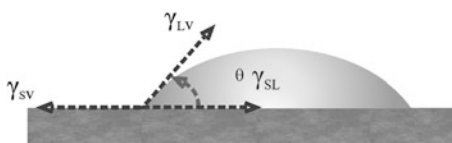


Fig. 1 **a** USB digital microscope (model DIGMIC200X, China) equipped with Image Analysis Software 220X 2.0MP video, with 0.0001° precision, **b** Ramé-Hart instrument co. (USA, Succasunna), **c** image taken with a USB digital microscope, and **d** image taken with a Ramé-Hart instrument

Fig. 2 Contact angles formed by pure liquid drops on a surface



To summarize, the contact angle is the angle, conventionally measured through the liquid, where a liquid–vapor interface meets a solid surface. It quantifies the wettability of a solid surface by a liquid via the Young equation (Fig. 2). Any solid, liquid, and vapor system at a given temperature and pressure will have a unique equilibrium contact angle. However, in practice, contact angle hysteresis is observed, ranging from the so-called advancing (maximal) contact angle to the receding (minimal) contact angle. The equilibrium contact lies between these values and can be calculated from them. The equilibrium contact angle reflects the relative strength of the liquid, solid, and vapor molecular interaction. Contact angles are

extremely sensitive to contamination: values reproducible to less than a few degrees are generally only obtained under laboratory conditions with purified liquids and very clean solid surfaces. If the liquid molecules are strongly attracted to the solid molecules, then the liquid drop will completely spread out on the solid surface, giving a contact angle of 0° .

In essence, the contact angle may be explained as the physicochemical response of a pure solvent drop on a surface. This is related to the surface tension produced by the unbalanced forces of the liquid molecules on that surface (Fig. 3). Wettability studies of a surface are usually performed by determining contact angles using distilled and deionized water. In this regard, there is a broad consensus in the literature, based on empirical results, than a contact angle (θ) greater than 65° defines a hydrophobic surface when water is used as a solvent (Fig. 4) (Vogler 1998). It is well known that the contact angle of water increases with an increase in surface hydrophobicity (Ojagh et al. 2010). Karbowski et al. (2006) suggested that an increase in the water contact angle of biopolymers could be due to strong intermolecular hydrogen bonding under the film surface. The most polar sites (Lewis sites) would be affected by these interactions, thus generating a reduction in the surface polarity of biopolymer films. Starch film surfaces with higher contact angles do not contain the energy required to break the cohesive force of water (Vogler 1998). Thus, a droplet with high surface tension resting on a low-energy solid tends to adopt a spherical shape due to the establishment of a high contact angle with the surface. Conversely, when the surface energy of the solid exceeds the liquid surface tension, the droplet tends to adopt a flatter shape due to the establishment of a low contact angle with the surface (Fig. 5).

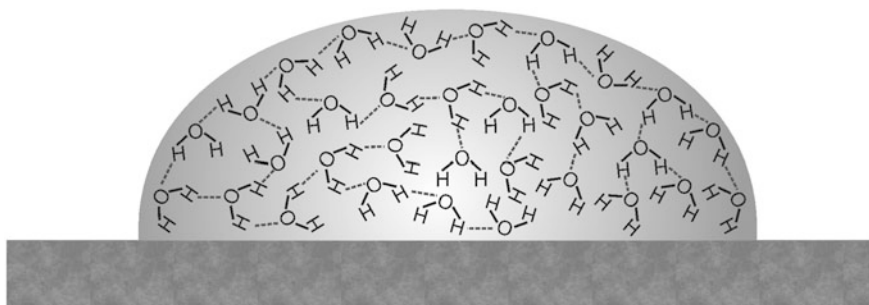


Fig. 3 Surface tension caused by the unbalanced forces of the liquid molecules at the surface

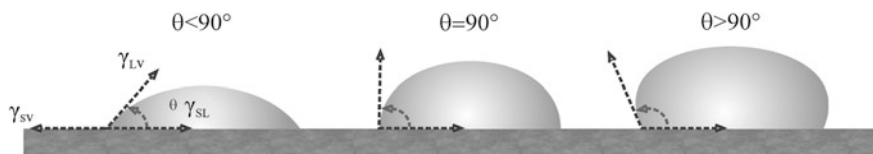


Fig. 4 Contact angle on the gauge of wettability of a solid surface with a specific liquid

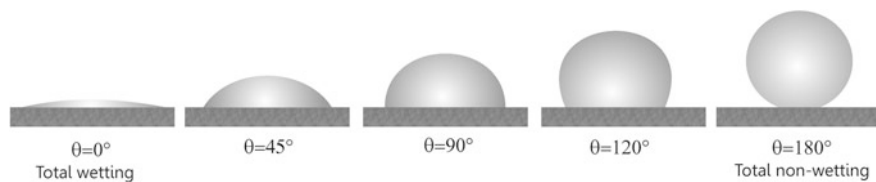


Fig. 5 Wettability of starch films

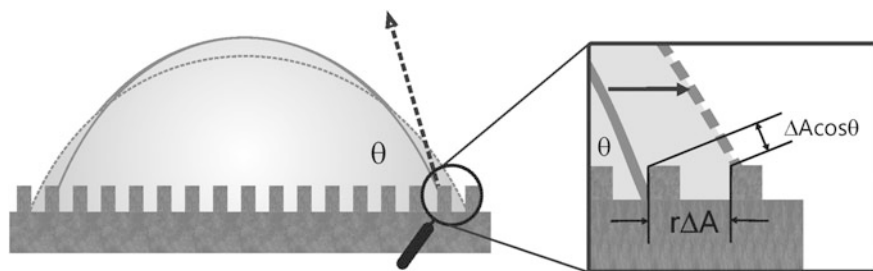


Fig. 6 Contact angle on rough surface using Wenzel's equation

Interestingly, this kind of water structure requires that the hydrogen bond network of water directly adjacent to a nonpolar surface is interrupted yielding “dangling hydrogen bonds”. These dangling hydrogen bonds have been theoretically predicted (Lee et al. 1984) and spectroscopically resolved from hydrogen bonds in bulk water (Du et al. 1993, 1994a, b).

Contact angles have also been associated with the surface characteristics of starchy materials through the well-known Wenzel equation (Wenzel 1936):

$$\cos \theta_w = r \cos \theta. \quad (1)$$

In Wenzel's equation, the roughness factor (r) acts to amplify the surface chemistry-determined term $\cos \theta$. Thus, small changes in θ translate to larger changes in θ_w , provided complete contact is maintained between the liquid and the solid (Fig. 6). The importance of $\theta = 90^\circ$ is the changeover in the sign of the cosine term. When $\theta < 90$, the effect of increasing roughness (r) is to further reduce the Wenzel contact angle toward 0. However, when $\theta > 90$, the effect of increasing r is to further increase the Wenzel contact angle toward 180. Thus, Wenzel roughness emphasizes the intrinsic tendency of a surface to have either complete wetting or complete non-wetting properties.

Conversely, a liquid may form bridges between surface features and no longer penetrate through the spaces separating them; a simplified example of a flat-topped surface is shown in Fig. 7. In this example, it is assumed that the liquid only makes contact with the flat parts of the surface and that the meniscus below the drop is flat. This implies that the gaps between the features are much smaller than the curvature

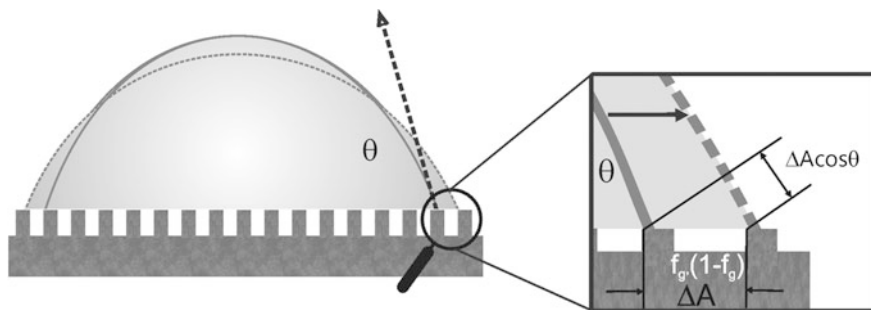


Fig. 7 Contact angle on rough surface using Cassie–Baxter equation

of the meniscus due to the weight of the liquid and the pressure exerted by the top meniscus. As the contact line advances by ΔA only a fraction, $f_s \Delta A$, of the solid makes contact with the liquid, and the remainder $(1 - f_s) \Delta A$ is the area bridged between surface features in contact with the air. Thus, this remainder involves the creation of a liquid vapor interface. The surface free energy change is given by Eq. 2:

$$\Delta F = (\gamma_{SL} - \gamma_{SV})f_s \Delta A + (1 - f_s) \Delta A \gamma_{LV} + \gamma_{LV} \cos \theta \Delta A. \quad (2)$$

Based on these concepts, in this chapter, we discuss the surface properties of TPS materials reinforced with natural fillers as an indirect measure of interactions in starch-based composite materials, mainly with regard to plasticizing effects and crosslinking reactions.

2 Effect of the Amylose/Amylopectin Ratio on the Surface Properties of TPS

Starch is a polysaccharide composed of the essentially (1-4)-linked linear amylose and the extensively (1-6)-branched amylopectin, and occurs naturally in plants in the form of granules. The film formation process is important for film structure and crystallinity. Previous studies undertaken by Stading et al. (2001) and Rindlav-Westling et al. (2002) have shown that amylopectin films are totally amorphous without any visible structure, and this is reflected by a smooth surface. In contrast, amylose films are semicrystalline (Stading et al. 2001, Rindlav-Westling et al. 2002) giving rise to a rougher surface.

Rindlav-Westling and Gatenholm (2003) analyzed the surfaces of starch solution cast films prepared from amylose and amylopectin by scanning electron microscopy (SEM), atomic force microscopy (AFM), electron spectroscopy for chemical

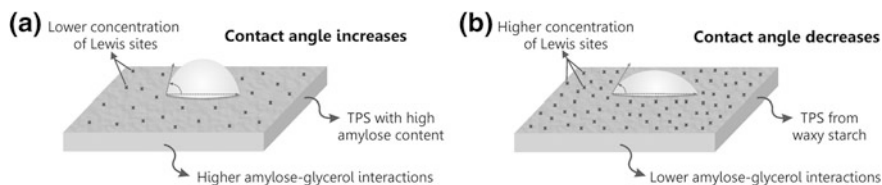


Fig. 8 Wettability from **a** amylose films and **b** amylopectin films

analysis (ESCA), and time-of-flight secondary ion mass spectrometry (ToF-SIMS). They found that the surface (as visualized by SEM) of amylopectin films was very smooth, whereas that of amylose films was rougher. A possible explanation for this is the higher crystallinity of the amylose films due to starch retrogradation, which affects their topography (Fig. 8). Moreover, the amylopectin films appeared to be flat even at the high magnifications obtained with atomic force microscope (AFM). Using this technique, small protrusions were also observed on top of the surface structures of the much rougher amylose films.

The authors also examined the starch films using a light microscope and found that most showed phase separation. This result could be related to the fact that under certain conditions, amylose and amylopectin are incompatible in aqueous solutions (Kalichevsky and Ring 1987) producing phase separation during film formation (Rindlav-Westling et al. 2002). In addition, differences in the crystalline structures of the films also appeared to influence their surface topography.

As an initial conclusion, we can say that the surfaces of starch films reflect the effects of retrogradation and phase separation. Smooth surfaces are associated with amylopectin films, whereas amylose film surfaces are much rougher.

The topic of wetting has sparked a great deal of interest both from the fundamental and the applied point of view (Yuan and Lee 2013). Wettability studies usually involve the measurement of contact angles as the primary data, as this indicates the degree of wetting when a solid and a liquid interact. Small contact angles ($\ll 90^\circ$) correspond to high wettability, while large contact angles ($\gg 90^\circ$) denote low wettability.

Phan et al. (2005) prepared edible films made from agar (AG), cassava starch (CAS), normal rice starch (NRS), and waxy (glutinous) rice starch (WRS), and tested them for their potential use as edible packaging or coatings. Among other properties, the surface hydrophobicity and wettability of these films were investigated using the sessile drop contact angle method. SEM micrographs of the cross sections of the prepared films showed an irregular and rough topography, suggesting a heterogeneous structure due to the retrogradation and partial crystallization of the gelatinized starch before the formation of the films. The water vapor permeability (WVP) of the films was directly proportional to their amylopectin content. Similar results on the better barrier properties of amylose films compared with those of amylopectin films were reported by Stading et al. (1998). It can thus

be said that films with poor water vapor barrier properties will show high hydrophilicity. Stading et al. (1998) evaluated the sensitivity of films to liquid moisture transfer by determining the adsorption rate of water droplets, finding that, in general, a higher contact angle indicated a lower adsorption rate. Nevertheless, this characteristic might be affected by the evaporation of excess water during the measurement period. Gutiérrez and González (2016) prepared edible films from cassava (*Manihot esculenta* C.) and taro (*Colocasia esculenta* L. Schott) starch plasticized with glycerol, as packaging materials. A comparison of these two starches revealed that the taro starch had a lower amylose content than the cassava starch (15.1 and 19.9%, respectively). Weak amylopectin–glycerol interactions facilitate water absorption, which could explain the higher moisture content of the taro starch films. Under weak starch–glycerol interactions, water can act as a plasticizer, a phenomenon commonly known as moisture plasticization. Glycerol–amylose interactions produce a reduction in the intra- and intermolecular interactions between the starch macromolecules increasing the movement and rearrangement of the chains. XRD diffraction patterns have shown that the areas under the crystalline peaks are larger in cassava starch films than in taro starch films, which correlates with the higher amylose content of cassava starch. In addition, SEM images showed that the cassava starch films had more compact structures, possibly associated with their high amylose content (Miles et al. 1985a, b). It has been previously established that a more compact structure leads to lower water adsorption as it makes interactions between the starch–glycerol and water less likely, leading to a decrease in the polar glycerol–starch character of the films (García-Tejeda et al. 2013; Pelissari et al. 2013) (Fig. 8).

Gutiérrez and González (2016) studied the color of cassava and taro starch films and found that the indexes evaluated were higher for the cassava films than the taro films. They also found that cassava starch films were whiter and more opaque than taro starch films, confirming that materials with a lower amylose content are more transparent.

Following on from this, AFM studies showed that films made from cassava starch (with a higher amylose content) have a rougher surface than those made from taro starch. This agrees with the luminosity data: films with a high roughness profile are more opaque, i.e., less transparent (Reyes 2013). Apparently, the greater tendency to retrogradation of starch-based films with a higher amylose content creates torsional forces on the macromolecules, which generates a rougher surface.

Regarding wettability, the contact angles of the cassava starch films were higher than those of the taro starch films, which can be associated with their higher surface hydrophobicity (Ojagh et al. 2010). An increase in the water contact angle of biopolymers has been related to stronger intermolecular hydrogen bonding under the film surface (Karbowiak et al. 2006). Thus, a decrease in the number of Lewis sites could generate a decrease in the surface polarity of biopolymer films. This produces dry cassava starch film surfaces, since they do not contain enough energy to break the cohesive force of water (Vogler 1998). Gutiérrez and González (2016)

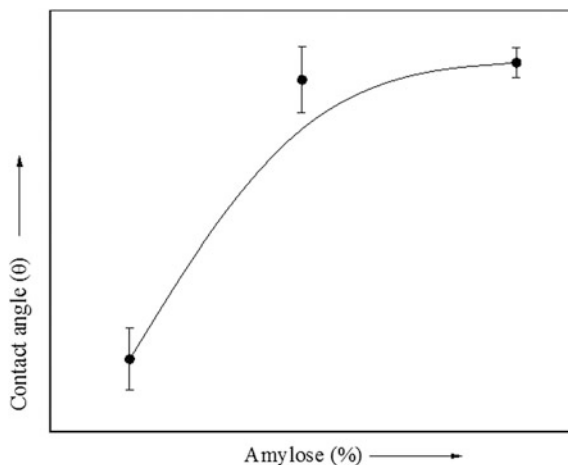


Fig. 9 Effect of amylose content on contact angle values of starch-based films

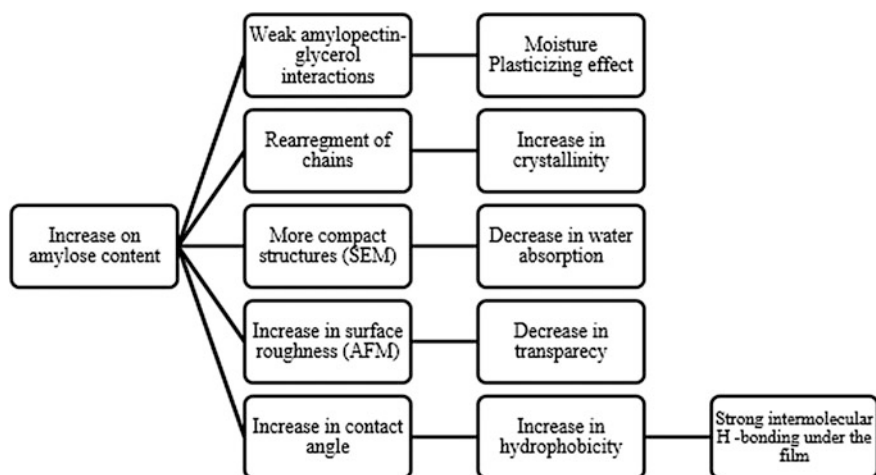


Fig. 10 Graphic summary of the properties of TPS films due to the amylose content

claim that films derived from starches with a lower amylose content show a lower plasticizer–polymer compatibility. This allows the plasticizer to migrate toward the surface of the film, thereby increasing the number of Lewis sites and reducing the water contact angle (Fig. 8b). Higher contact angle values are thus recorded for films with a higher amylose content (Fig. 9). A diagrammatic summary of the surface properties of TPS films associated with their amylose content effects is provided in Fig. 10.

3 Effect of Exposure to Pulsed Light on the Surface Properties of TPS

Crosslinking technologies have been used to modify TPS and other starch-based blends in order to improve their physical and mechanical properties (Zhou et al. 2009). As regards UV photo-crosslinking, photo-sensitizers or photo-initiators are generally incorporated into the materials during processing to produce reactive radicals that subsequently initiate crosslinking reactions under UV irradiation. This treatment generally produces a reduction in surface hydrophilicity and improved water resistance (Gutiérrez and González 2016).

Zhou et al. (2009) prepared crosslinked surfaces from TPS/PVA blends by applying ultraviolet (UV) irradiation, and using sodium benzoate as a photosensitizer. They then analyzed several physical properties of the films, such as the water contact angle, moisture absorption, degree of swelling, and water solubility. Mechanical properties were also measured to characterize the influence of the photo-crosslinking modification on the film surface. These authors observed that crosslinking considerably reduced the hydrophilic character of the TPS/PVA film surfaces, as well as enhancing water resistance. The tensile strength and Young's modulus also increased, but the elongation at break of the films was lowered. These results were attributed to the increase in the crosslinking density of the macromolecular chains on the surface of the films.

Zhou et al. (2009) also found a direct correlation between the surface contact angle and surface roughness. In addition, the orientation of the polar hydroxyl groups on the contact surface had a significant influence on the contact angle measurements. An increase in the water contact angle indicates an enhancement of the hydrophobic character of the surface and a lower value for the polar component of the surface energy.

These same authors found that after surface photo-crosslinking, the water contact angle of the TPS/PVA films, jumped significantly and continued to rise with an increasing UV irradiation dose until 20 J/cm². In contrast, a decrease in the water contact angle as a function of the UV irradiation dose was observed on the photo-crosslinked surface of corn starch sheets (Zhou et al. 2008). These authors proposed that as the crosslinking reaction progresses, more and more hydroxyl groups on the surface layer, either from TPS or PVA molecular chains, are consumed and are thus not available to water. In addition, they found that as the UV irradiation dose increased, the resulting crosslinked structure caused both the degree of swelling and the water solubility to decrease, thus these crosslinking points restrict the molecular mobility of the polymer chains.

Gutiérrez and González (2016) evaluated the effects of pulsed light (PL) treatment, as a crosslinking method, on some properties of edible films derived from cassava (*Manihot esculenta* C.) and taro (*Colocasia esculenta* L. Schott) starch plasticized with glycerol, relevant to their use as packaging materials. They found that samples deteriorated after PL treatment compared to control films as demonstrated by an increase in the contact angle, roughness, and crystallinity, and a

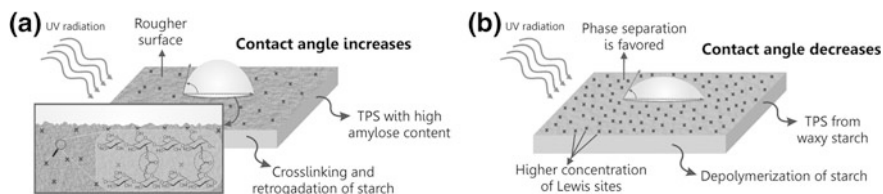


Fig. 11 Effect of UV radiation on **a** amylose films and **b** amylopectin films

decrease in the tensile strength, transparency, and water content regardless of the amylose content of the starch used to develop the films. In addition, the degree of crystallinity of the films exposed to PL was slightly higher than that of the untreated ones, a phenomenon that can be associated with the retrogradation of starch during aging or by the deterioration process, which reduces chain mobility (García-Tejeda et al. 2013, Bertuzzi et al. 2007). They also found that films treated with PL showed a significant reduction in the moisture content, possibly due to the crosslinking caused by the UV radiation on the films treated with PL (Andrady et al. 1998, Cui et al. 2013). After PL treatments, the films displayed a more compact structure reflecting their lower moisture content. It is worth noting that the molecular weight of the cassava starch-based films (with a higher amylose content) decreased, whereas the molecular weight of the taro starch films (with less amylose content) slightly increased. Based on this, Gutiérrez and González (2016) suggested that the crosslinking reaction in taro starch films produced a slightly more pronounced increase in the water contact angle than the cassava starch films. In the cassava starch films, the decrease in their molecular weight suggests the de-polymerization of their biopolymer chains. This exposes the amylose chains resulting in a less conspicuous increase in the contact angle (Fig. 11). A diagrammatic summary of the properties of TPS films modified by PL is provided in Fig. 12.

4 Effect of the Chemical Modification of Starch on the Surface Properties of TPS

Two of the main advantages starch has over other materials are its low cost and availability in very large amounts from renewable resources. These aspects, together with the fact that starch may be used in thermoplastic formulations, make it one of the best options for preparing biodegradable polymers. However, the use of starch as a substitute for conventional petroleum-based plastics has been limited by its brittleness and hydrophilicity (Shogren et al. 1998). This has meant that TPS compositions developed thus far cannot be used for many applications, including packaging, and intensive work has been done to overcome these drawbacks (Dufresne and Vignon 1998, Averous et al. 2000, 2001; Curvelo et al. 2001, Carvalho et al. 2005). Several strategies have been attempted in order to widen the

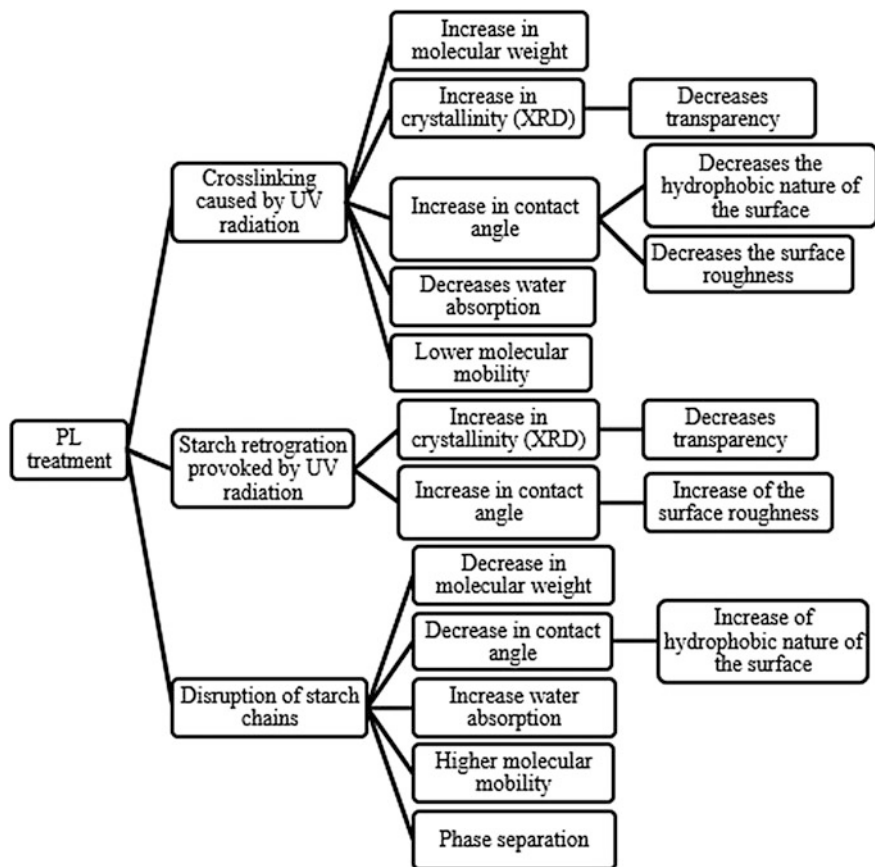


Fig. 12 Graphic summary of the properties of TPS films due to pulsed light

usability of starch as a biodegradable thermoplastic material suitable for packaging applications. One possibility is to modify the starch. Chemical modification involves the introduction of functional groups into the starch molecule by phosphorylation, acetylation, and oxidation, among others. Starches can also be physically modified by heat-moisture treatment and annealing. Chemical modification causes changes in the molecular structure or introduces functional groups, thus improving the applicability of plant-derived materials in both the food and non-food industries (Xia et al. 2005; Bertolini 2010; Nafchi et al. 2013).

Carvalho et al. (2005) prepared TPS films plasticized with 20 and 30 wt% glycerol. The materials obtained were treated with various reagents (phenyl isocyanate (PhNCO), a phenol blocked polyisocyanate of trimethylol propane and toluene diisocyanate (TMP-TDI-Phenol), a styrene-co-glycidyl methacrylate (PS-GMA) copolymer and stearoyl chloride (StCl)) in order to make their surfaces less sensitive to moisture. In addition, two different techniques were used to

produce the modifications: (a) suspension at room temperature and (b) dipping in the reactant solution followed by heating under reflux.

Carvalho et al. (2005) found that the polar contribution was drastically reduced in the modified polymers, indicating that the surfaces had become more hydrophobic. The treatment with phenyl isocyanate in xylene proved the most effective.

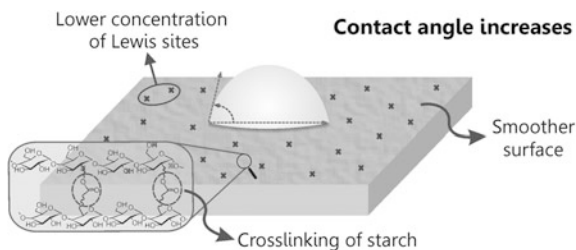
In addition, all the chemical treatments carried out produced an increase in the contact angle values with water, together with a decrease in the purely dispersive liquids, confirming that coupling reactions took place. In particular, the phenyl isocyanate produced some excellent results, probably because of the very high reactivity of this compound, which gave rise to the formation of a densely packed monolayer of phenyl moieties on the surface. Treatment with stearyl chloride also gave some interesting results (very low values for the polar component). However, the formation of HCl in the coupling reaction with the OH groups might limit its practical use.

Carvalho et al. (2005) concluded that the use of these polymeric reagents offers a further advantage in that a given macromolecule can couple with OH groups coming from both the starch and the glycerol simultaneously, thus immobilizing the latter species. The dipping + heating treatment was found to be the most appropriate for practical applications.

Gutiérrez and González (2017) prepared films from plantain flour with the incorporation of different concentrations of *Aloe vera* (Av) gel. They found that the Av gel produced crosslinking of the starch found in the flour, resulting in films that were smoother, more transparent, more rigid and plastic, dryer, and with increased hydrophobicity (Fig. 13).

As already mentioned, the Av gel produced a decrease in the moisture content of the plantain flour films. This could be associated with strong starch–glycerol interactions, which inhibit water absorption (Cyras et al. 2006; Flores et al. 2007; Hu et al. 2009; Gutiérrez et al. 2015). In addition, color testing (opacity of the film) revealed that films with a lower Av gel content showed a tendency to retrograde. AFM studies also showed that the surface roughness of films made from plantain flour with a higher Av gel content tended to decrease, which is consistent with the luminosity results (high roughness profiles were more opaque, i.e., less transparent). In addition, the contact angle increased as a function of Av content, which agrees with all the previous results, and also with the fact that the organic acids present in

Fig. 13 Implications of effect of crosslinking on the surface properties of TPS films



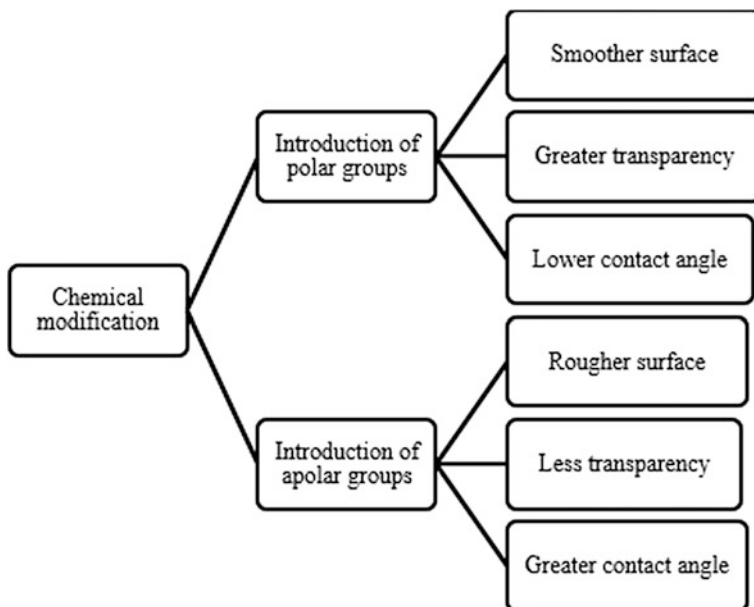


Fig. 14 Graphic summary of the properties of TPS films due to chemical modification of the starch

Av gel produce stronger hydrogen bond interactions between the starch and the glycerol, probably due to the crosslinking of the former. The SEM images were also consonant with the other results: the plantain flour-based films with higher Av gel content had the most closed structures, which act as a physical barrier to water.

Similarly, the incorporated Av gel had a positive effect on all the mechanical parameters measured: films with higher Av gel content were markedly more rigid, showed a greater strain at break, and had higher enthalpy (ΔH) and glass transition temperatures (T_g). This last is further evidence of the crosslinking of the starch in the presence of the Av gel: crosslinking limits the movement of the molecular segments, resulting in an increase in T_g . A diagrammatic summary of the properties of chemically modified TPS films is provided in Fig. 14.

5 Effect of Plasticizers on the Surface Properties of TPS

In general, plasticization refers to a change in the thermal and mechanical properties of a given polymer which involves the following:

- A decrease in stiffness at room temperature.
- A decrease in the temperature at which substantial deformations can be produced with moderate forces.

- An increase in the elongation to break at room temperature.
- An increase in the toughness (impact strength) at the lowest serviceable temperature.

These effects can be achieved by combining the polymer of interest with a low molecular weight compound or another polymer, or by introducing a co-monomer into the original polymer to reduce crystallinity and increase chain flexibility.

Medina et al. (2015) prepared cassava starch-based films with different amounts of *yerba mate* (Y) extract as an antioxidant (0–20 wt%). They found that films with 5 wt% of the extract (TPS-Y5) showed a lower loss of antioxidant than films with 20 wt% (TPS-Y20). In addition, the incorporation of the Y extract led to increased values of surface roughness and contact angle, indicating an increase in the hydrophobicity of the film surface. This was confirmed by a decrease in water vapor permeability and water content values. The greater hydrophobicity of the Y extract-containing films is due to the fact that covalent and hydrogen interactions between the polysaccharide network and the polyphenol compounds limit the availability of the hydrogen groups to form hydrophilic bonds, thus reducing the affinity of the films to water (Siripatrawan and Harte 2010). Previous studies have positively correlated the surface roughness of a material with its hydrophobicity (Erbil et al. 2003). The contact angle of a material is also related to the roughness and hydrophobicity: a rougher surface increases the contact angle and therefore, the hydrophobicity of the material (Erbil et al. 2003). This is because a rougher surface increases the fraction of trapped air and thereby the water contact angle (Kim et al. 2014). Regarding mechanical properties, Medina et al. (2015) found that the addition of the Y extract resulted in a decrease in the elastic modulus and tensile strength, but a significant increase in the strain at break values. This resulted in more flexible materials as the relaxation processes took place at lower temperatures compared to the matrix without Y extract. Other mechanical properties of the extract-containing films were also typical of plasticized films. Finally, cassava starch films containing Y appear promising as coatings for retarding the oxidation of food products, thus increasing their shelf life. In addition, according to Medina et al. (2016), films with a smoother surface are apparently more biodegradable.

Gutiérrez et al. (2016a) prepared films from native and modified plantain flour, plasticized with glycerol, with or without the addition of beet flour. Analysis of the prepared flours showed that the fiber content of the modified plantain flour increased by about 20%, possibly as a result of the leaching of proteins and fatty material during its modification. The phosphorus content, degree of substitution (DS), and apparent amylose content also decreased by about 50% in the modified flour, due to the crosslinking of the amylose.

Gutiérrez et al. (2016a) observed that the incorporation of beet flour resulted in an increase in water solubility that became significant when combined with the modified flour. This behavior was associated with the sugars contained in beet flour, which conferred a more polar character to the films. In contrast, native plantain flour-based films exhibited higher contact angles, reflecting an increase in surface hydrophobicity. The surface of these films was dryer as they do not have enough

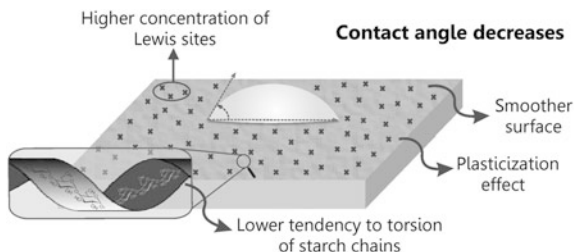
energy to break the cohesive force of water (Vogler 1998). These types of hydrophobic surfaces require Lewis sites for surface wetting to occur. In addition, their higher amylose content gives them a closed structure (observed by SEM) resulting in a further, physical impediment to wetting. Conversely, phosphated plantain flour-based films showed a lower contact angle. This could be related to the addition of phosphate groups that strengthen the polar character of the surface, increasing the density of Lewis sites. These sites would be close to the hydrogen bond network of water, and would thus compete with the cohesive forces, leading to the collapse of water structure on the hydrophilic surface and decreasing the contact angle. The incorporation of beet flour produced a decrease in the contact angle for both native and modified plantain flour as a consequence of the polar character of the sugars contained within it.

Gutiérrez et al. (2016a) found that the incorporation of beet flour also enabled the preparation of intelligent films sensitive to alkaline pH changes. In addition, they demonstrated that betalains found in the beet flour interacted more efficiently with the phosphated plantain flour, limiting its immediate response to pH changes.

In addition, other components (proteins and sugars) in the beet flour produced more flexible films (an increase in the elongation at break: plasticizing effect). This can be associated with hydrogen bond interactions between these components and the plantain flours, which could explain the decrease in the contact angle together with the increase in the thickness and solubility of these films.

Furthermore, Gutiérrez et al. (2016b) found that beet flour incorporated into edible films prepared from native and phosphate-modified plantain flour acted as a plasticizer, producing smoother, wetter, and more transparent films. The beet flour also improved the transmittance of the films and their thermodynamic stability. According to the results obtained from differential scanning calorimetry (DSC), the addition of beet flour destroys the intra- and intermolecular interactions between starch–starch chains, thus strengthening hydrogen bonding interactions between the hydroxyl groups of the starch chains and the polar compounds of the beet flour. This enables the starch chains to become more mobile and produces a reduction in the T_g confirming the plasticizer effect. The increase in the transmittance of the films (more evident in the case of the phosphate-modified plantain flour) produced by the plasticizing effect of the beet flour could be related to an increase in the degrees of freedom of the OH groups, which itself is a consequence of the greater mobility of the starch chains (Medina et al. 2016). Thus, an increase in transmittance is related to a decrease in the T_g . The SEM images taken were consistent with these results and revealed the plasticizer effect of the beet flour, which inhibited the recrystallization of the starch. AFM images showed that films made from native plantain flour (with a higher amylose content) displayed greater surface roughness than those made from phosphated plantain flour: a rougher surface gives more opaque (less transparent) films. This is probably due to the fact that a rougher surface texture does not permit the reflection of light which is thus absorbed by the film (Reyes 2013, Gutiérrez and González 2016, 2017). The incorporation of the beet flour generated a smoother surface due to its plasticizing effect. This inhibited

Fig. 15 Implications of plasticizing effect on the surface properties of TPS films



starch retrogradation thereby avoiding the creation of holes. Similarly, a smoother surface was related to an increase in the transparency of these systems (Fig. 15).

Gutiérrez et al. (2016a, b) also showed that modified plantain flour crosslinked with sodium trimetaphosphate produced more transparent, smoother, more plastic, and biodegradable films. The decrease in the moisture content of the phosphated plantain flour films was associated with the strong hydrogen bond interactions between the phosphated flour and the plasticizer, which limits possible water adsorption by these polar compounds (Gutiérrez et al. 2015). XRD results also suggest an increase in the number of hydrogen bond interactions, caused by the plasticizer effect of beet flour (Gutiérrez et al. 2016b).

After analyzing their results, Gutiérrez et al. (2016a, b) concluded that the minor interaction between the starch–starch chains produced more transparent, less crystalline, smoother, more plastic, and biodegradable films. A diagrammatic summary of the effects of plasticizers on the surface properties of TPS films is provided in Fig. 16.

6 Effect of Composites on the Surface Properties of TPS

TPS on its own often cannot meet all the requirements of a packaging material. However, the incorporation of environmentally acceptable reinforcing materials has proved an effective method to obtain starch-based biocomposites with improved physical and mechanical properties (Cyras et al. 2008). In this section, we discuss the surface properties of TPS materials with added fillers.

6.1 Effect of Clay/Starch Composite Materials

The incorporation of clays has been reported as a good approach to improve polysaccharide-based film properties. Kaolinite, smectite, and sepiolite are the most frequently used clays in polymer nanocomposite studies. These clays are environmentally friendly, naturally abundant, and economical. Smectites, in particular, are often chosen for the preparation of polymer-based nanocomposites. The most

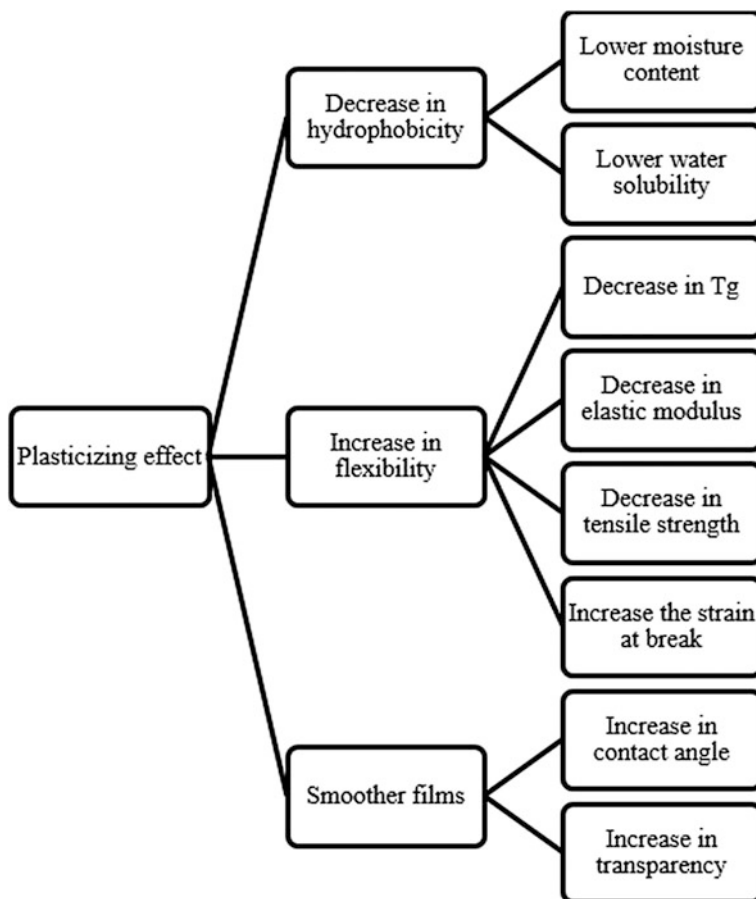


Fig. 16 Graphic summary of the properties of TPS films due to the plasticizing effect

widely studied smectite clay filler is montmorillonite (Mnt) (de Azeredo 2009). Mnt is a hydrated alumina-silicate-layered clay consisting of two-dimensional layers, 1 nm thick, made up of two silica tetrahedrals fused to an edge-shared octahedral sheet of either aluminum or magnesium hydroxide (Ray and Bousmina 2005). The imbalance of the negative surface charges is compensated by exchangeable cations (typically Na^+ and Ca^{+2}). The parallel layers are stacked together by weak electrostatic forces leading to a regular van der Waals gap between the layers called the interlayer or gallery. As the forces that hold the stacks together are relatively weak, the intercalation of small molecules between the layers is straightforward. Thus, in addition to their low cost, high surface area, and large aspect ratio, the rich intercalation chemistry of these clays enables them to be easily chemically modified.

In order to obtain nanocomposites with improved final properties, the clay layers must be highly dispersed in the polymer matrix (intercalated or exfoliated) as

opposed to being aggregated as tactoids (Ray and Okamoto 2003). The major problem in preparing these composites is thus to separate the layers of the clay as they are initially agglomerated. The most significant challenges in the development of well-dispersed clay/polymer nanocomposites are as follows (Ollier et al. 2014):

- The maximization of chemical compatibility between the clay surface and the polymer matrix, i.e., how to make the clay more compatible with starch, which facilitates the dispersion of the clay layers.
- The selection of the most appropriate processing method in order to provide optimal conditions for the dispersion of the clay platelets.

The presence of exfoliated clay layers in polymer structures has been shown to greatly improve barrier properties since they obstruct diffusion gases and water molecules forcing them to follow a tortuous path, and thus minimizing one of the main limitations of biopolymer films (de Azeredo 2009). The clay layers also induce changes in the molecular mobility of the polymer matrix, which may enhance its thermal and mechanical properties as well as oxidation stability, among other advantages. It is important to mention that all these improvements can be achieved with low amounts of Mnt (below 10 wt%).

Mnt has been extensively employed to reinforce native starch (Slavutsky et al. 2012), derivative starch (Gao et al. 2012), carboxymethyl cellulose (CMC) (Gutiérrez et al. 2012), starch/CMC (Almasi et al. 2010; Ghanbarzadeh et al. 2013), and starch/chitosan films (Ghani et al. 2013). However, very few of the studies concerned with clay/starch nanocomposites have analyzed in detail the surface properties of these materials.

Aouada et al. (2013) prepared Mnt/TPS bionanocomposite films. They employed a pristine Mnt and focused on the processing procedure of the materials. The composites were prepared by intercalation from solution followed by melt processing, with 1 and 5 wt% Mnt. The authors affirmed that the intercalation/exfoliation of the clay into TPS is achieved when the shear rate increases. Additionally, swelling may expand the clay galleries, thus facilitating their dispersion (Paul and Robeson 2008). Measurements of water absorption confirmed the stability of the nanocomposites and showed that the addition of natural Mnt reduced the bulk hydrophilicity of the TPS matrix. A decrease in water absorption after increasing the clay content of the TPS matrix was associated with the following phenomena: (1) the migration of a fraction of the glycerol plasticizer to the clay phase, which reduces the glycerol content of the polymeric matrix and (2) the reinforcement effect of the clay due to high interaction between the clay and the TPS matrix, which makes the matrix three-dimensionally more stable with limited expansion. Furthermore, water contact angle measurements showed that the addition of clay also reduced the surface hydrophilicity of the nanocomposites. The authors associated this improvement with the novel methodology used to prepare the TPS bionanocomposites. Cyras et al. (2008) observed a different behavior when they dispersed Mnt into TPS by the casting method. In their case, the clay nanolayers formed an intercalated structure but not complete exfoliation. The

nanocomposites were also more hydrophilic than the neat starch due to their high surface polarity, as measured by the contact angle. This can be attributed to the non-exfoliated structure of the clay in the starch matrix, which causes lower hydrogen bonding interactions compared to materials developed by Aouada et al. (2013) (obtained by a different processing protocol). However, maximum water absorption as well as the rate of water absorption was reduced by the addition of clay to the TPS. This behavior was attributed to the formation of a tortuous pathway due to the presence of the clay layers.

Wilpiszewska et al. (2015) prepared carboxymethyl starch (CMS)-based biodegradable films with calcium-rich montmorillonite (Ca-Mnt) by the casting method; glycerol and citric acid were used as the plasticizer and crosslinking agents, respectively. CMS is a derivative starch obtained by the Williamson process, by which ionic substituents are introduced into the starch structure through reactions with monochloroacetic acid sodium salt (Yanli et al. 2009). The intercalated structure of Ca-Mnt was observed in all composites; however, the most efficient clay platelet dispersion was noted for the 5 wt% Ca-Mnt/CMS film. The introduction of Ca-Mnt into CMS produced an increase in the water contact angle from 70° for the neat CMS films, to 107° for the films containing 5 wt% Ca-Mnt/CMS, i.e., the surface became more hydrophobic. A lower contact angle value for the 7 wt% Ca-Mnt/CMS films compared to the 5 wt% Ca-Mnt/CMS films indicated that clay dispersion was less effective in the former. This was confirmed by XRD. In addition, there was a negative correlation between clay content and water absorption. The higher Ca-Mnt content in this composite could lead to stronger hydrogen bonding between the hydroxyl groups of the starch, and the hydroxyl or carboxylic groups of the CMC and ^-OH of the clay layers (Huang et al. 2004). This would result in a stronger structure with fewer active sites for water absorption.

Although clays are naturally compatible with starch, they can be chemically modified to obtain composites with improved properties. Kampeerapappun et al. (2007) prepared Mnt/cassava starch composite films, with chitosan, a natural cationic polysaccharide, as a compatibilizing agent for Mnt modification and glycerol as a plasticizer. Chitosan is compatible with the starch matrix as it has amine and hydroxyl groups which can interact via hydrogen bonding, as well as being ion-exchangeable with clay (Darder et al. 2003). As a result, the average particle size of chitosan-treated Mnt was notably smaller than that of pristine Mnt/starch film. Improvements in the physical properties include reduced surface wettability and a decrease in the water vapor transmission rate and moisture absorption. An interesting finding was that the addition of neat Mnt did not affect film surface hydrophobicity. However, at a fixed clay content, an increase in the percentage of added chitosan produced a significant increase in the water contact angle values of the composite films. Moreover, chitosan content had a significant effect on the moisture uptake values (which is related to the bulk hydrophobicity) of the composite films compared with neat Mnt composites. The authors suggested that the contribution of chitosan to the surface and bulk hydrophobicity was associated with the role of available hydrophobic acetyl groups present in the structure of incompletely deacetylated

chitosan chains. In addition, the tensile properties of the composite films were improved by the addition of both chitosan and Mnt.

Abreu et al. (2015) developed Mnt modified with a quaternary ammonium salt C30B/starch nanocomposite (C30B/ST-NC), silver nanoparticles/starch nanocomposite (Ag-NPs/ST-NC), and both silver nanoparticles/C30B/starch nanocomposites (Ag-NPs/C30B/ST-NC) films by the solution casting procedure. The silver nanoparticles (Ag-NPs) were incorporated and synthesized in situ by the chemical reduction method. The incorporation of both types of nanoparticles, Ag-NPs and C30B, had a synergetic effect, resulting in a material with greater homogeneity and better clay dispersion, as demonstrated by SEM and XRD. In addition, the Ag-NPs/C30B/ST-NC film exhibited an increase in the storage modulus value (calculated from DMA measurements) compared to the starch film. It is known that the effect of clay in polymer matrices is to increase the modulus or stiffness via reinforcement mechanisms described by composite theories (Fornes and Paul 2003). The incorporation of C30B by itself, however, caused a significant decrease in the water contact angle value. This suggests that there was an increase in the polarity, which can be attributed to the incorporation of more hydrophilic groups in the clay. More hydrophobic surfaces were achieved when both nanoparticles were added. Abreu et al. (2015) also found that the composite films they obtained showed antimicrobial activity against *Staphylococcus aureus*, *Escherichia coli*, and *Candida albicans*. Furthermore, the migration of components from the nanostructured starch films was minor and under the legal limits. Thus, according to the authors, starch films loaded with C30B and Ag-NPs have the potential to be used as nanostructured packaging materials.

6.2 Effect of Natural Fibers/Starch Composite Materials

Adding natural fibers to starch-based composites in order to obtain more resistant and stable films has given some promising results. Moreover, natural fibers provide positive environmental benefits regarding ultimate disposability and the use of raw materials (Singha and Thakur 2008a, b, c; Thakur et al. 2013a, b, c, d). Generally speaking, the properties of natural fibers, such as a high aspect ratio, low cost, renewability, biodegradability, high specific strength and modulus, low density, and reactive surface sites that facilitate grafting chemical species to achieve other useful surface properties, make them a very attractive alternative (Singha and Thakur 2009a, b, c, d; Faruk et al. 2012, López et al. 2015). Several types of natural fibers such as cotton, hemp, sisal, jute, flax, ramie, coir, and cellulose have been explored (Faruk et al. 2012; Pappu et al. 2016). Natural fibers can be processed in different ways to yield reinforcing elements with different properties (Corobea et al. 2016).

Cellulose is a very abundant natural polysaccharide, composed of linear chains of β -1,4 linked glucopyranose units. These polymer chains are associated by hydrogen bonds forming bundles of fibrils, also called microfibrillar aggregates, with high axial stiffness. Within cellulose microfibrils there are highly ordered

regions (crystalline phases) alternating with disordered domains (amorphous phases) (Azizi Samir et al. 2005). The crystalline regions contained within the cellulose microfibrils can be extracted by various methods, resulting in cellulose nanocrystals (Moon et al. 2011).

Cao et al. (2008) prepared nanocomposite films made from plasticized starch (PS) reinforced with hemp cellulose nanocrystals (HCNs). Loadings were between 0 and 30 wt%, and prepared by casting from aqueous suspensions. A homogeneous distribution of the HCNs in the PS matrix was observed, indicating strong adhesion between the fillers and matrix. The uniform distribution of the fillers in the matrix played an important role in improving the mechanical performance of the resulting nanocomposite films. With the incorporation of HCN fillers into the PS matrix, the contact angle of the nanocomposites significantly increased. This behavior was associated with the highly crystalline hydrophobic cellulose compared with the hydrophilic starch. Moreover, the presence of HCNs caused a reduction in the rate of water adsorption by the PS/HCN nanocomposites. The authors concluded that the improvements in the performance of the nanocomposites were due to chemical similarities between the starch and cellulose, the nanometric size effect of the HCNs, and the hydrogen bonding interactions between the fillers and the matrix.

Spiridon et al. (2013) prepared starch–cellulose composite materials from modified starch microparticles, synthesized from starch previously crosslinked by reaction with tartaric acid. These starch–cellulose materials were then used as fillers within a glycerol plasticized-corn starch matrix prepared by the casting technique. Cellulose fibers, obtained from bleached birch industrial pulp, were also incorporated into the polymeric matrix. The crosslinked starch microparticles produced an increase in the water contact angle due to the fact that OH groups on the surface of the material were less available to establish hydrogen bonds with the water molecules. The addition of cellulose fibers increased the hydrophobic properties of the starch-based films even further. This effect was limited to low cellulose contents, but at high cellulose contents, poor wetting properties of the films were observed. The presence of the cellulose fibers also enhanced the water resistance of the films although there was a slight decrease in transparency. Although cellulose is a hydrophilic polymer, the high degree of crystallinity and tight structure of the microfibrils within the fibers tended to decrease the water adsorption capacity of the composite compared with that of amorphous starch. The hydrogen bonding interactions between the starch and cellulose stabilized the starch matrix even when it was placed in a highly moisturized environment. Due to the strong intermolecular hydrogen bonds, the thermal stability and mechanical properties of the starch–cellulose composite films were improved compared with the neat matrix. The T_g increased with increasing amounts of cellulose in the composites. This was associated with the anti-plasticization of amylopectin-rich domains by the presence of the cellulose fibers.

López et al. (2015) prepared biocomposite films from TPS containing 0.5% w/w fibrous residue obtained from *Pachyrhizus ahipa* starch extraction (PASR) by melt-mixing and compression molding. PASR is mainly constituted by the remaining cell walls and natural fibers. Chemical analysis of the residue indicated that fiber and starch were the principal components. A continuous PASR-TPS

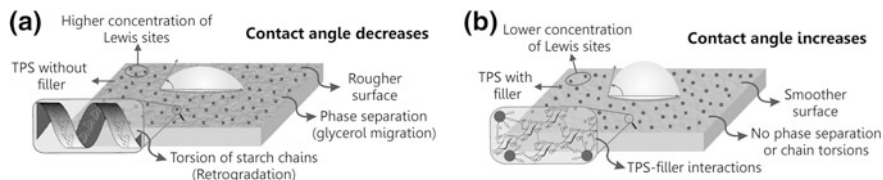


Fig. 17 Implications of fillers on the surface properties of TPS films

interface was observed by SEM, confirming the good adhesion of the fibrous residue to the starch matrix. SEM micrographs of the TPS surfaces revealed the presence of some non-molten starch granules and micropores, as well as numerous superficial micro-cracks. Films containing PASR showed fewer superficial cracks than neat TPS, but their fracture surfaces were more irregular. Films with the filler also showed far fewer non-molten starch granules. The authors associated this effect with the fact that starch granular fusion was affected by the presence of the fibers during the thermo-plastic processing of the TPS (Ma et al. 2005; Luna et al. 2009), i.e., the filler had an effect on the plasticization of the corn starch (Martins et al. 2009). Based on previous research, the authors mentioned that the presence of the filler during thermo-mechanical processing lead to improved melting of the starch granules. AFM images also demonstrated the effect of PASR on starch melting and plasticization during TPS processing. In addition, the presence of PASR increased the surface roughness of the starch films, due to randomly oriented fiber agglomerates, and PASR-TPS films showed significantly lower water vapor permeability values. Finally, the PASR filler increased the maximum tensile strength and Young's modulus of the TPS films, indicating that these matrices were more resistant.

In conclusion, we can say that the strong hydrogen bonding interactions between fillers and TPS prevent phase separation with the plasticizer. This decreases the number of Lewis sites on the surface of these materials, since the plasticizer cannot migrate to the surface. The water contact angle is thus increased, and the surface roughness decreased (Fig. 17).

7 Conclusions and Future Perspectives

Up until now, the surface properties of TPS have been little studied with regard to the inter- and intramolecular interactions that occur within biopolymer films, although theoretical information on this topic is available in the literature. Nevertheless, interest in the surface effects of these types of materials is surging, since they can serve as a support for biocatalysts (enzymes). This line of research could enable the development of innovative active packaging systems, which can remove substrates such as lactose. Thus, lactose-free products, for example, could be obtained by the use of active packaging with the appropriate surface properties. With this in mind, our research group is currently developing a standard

methodology based on the measurement of the contact angle of starch-based materials. This would enable us to determine the degree of aging in these types of materials, and the extent of the loss of their surface properties during storage. This could help to rapidly evaluate these materials in an easy and economical way that would also be applicable at an industrial scale. Finally, the study of the surface properties of TPS materials is promising for the development of other products that will surely have a major impact on future society.

Acknowledgements The authors would like to thank National Council of Scientific and Technical Research (CONICET) (Postdoctoral fellowship internal PDTs-Resolution 2417) and National University of Mar del Plata (UNMdP) for the financial support.

References

- Abreu AS, Oliveira M, de Sá A, Rodrigues RM, Cerqueira MA, Vicente AA, Machado AV (2015) Antimicrobial nanostructured starch based films for packaging. *Carbohydr Polym* 129:127–134
- Almasi H, Ghanbarzadeh B, Entezami AA (2010) Physicochemical properties of starch-CMC-nanoclay biodegradable films. *Int J Biol Macromol* 46:1–5
- Andrady AL, Hamid SH, Hu X, Torikai A (1998) Effects of increased solar ultraviolet radiation on materials. *J Photochem Photobiol, B* 46(1):96–103
- Aouada FA, Mattoso LH, Longo E (2013) Enhanced bulk and superficial hydrophobicities of starch-based bionanocomposites by addition of clay. *Ind Crops Prod* 50:449–455
- Averous L, Fringant C, Moro L (2001) Plasticized starch–cellulose interactions in polysaccharide composites. *Polymer* 42(15):6565–6572
- Averous L, Moro L, Dole P, Fringant C (2000) Properties of thermoplastic blends: starch–polycaprolactone. *Polymer* 41(11):4157–4167
- Azizi Samir MAS, Alloin F, Dufresne A (2005) Review of recent research into cellulosic whiskers, their properties and their application in nanocomposite field. *Biomacromol* 6(2):612–626
- Baldwin PM, Adler J, Davies MC, Melia CD (1998) High resolution imaging of starch granule surfaces by atomic force microscopy. *J Cereal Sci* 27(3):255–265
- Baldwin PM, Melia CD, Davies MC (1997) The surface chemistry of starch granules studied by time-of-flight secondary ion mass spectrometry. *J Cereal Sci* 26(3):329–346
- Bertolini AC (2010) Trends in starch applications. *Starches: characterization, properties, and applications*. Taylor and Francis Group, LLC, Abingdon, pp 1–20
- Bertuzzi MA, Vidaurre EC, Armada M, Gottifredi JC (2007) Water vapor permeability of edible starch based films. *J Food Eng* 80(3):972–978
- Cao X, Chen Y, Chang PR, Stumborg M, Huneault MA (2008) Green composites reinforced with hemp nanocrystals in plasticized starch. *J Appl Polym Sci* 109(6):3804–3810
- Carvalho AJF, Curvelo AAS, Gandini A (2005) Surface chemical modification of thermoplastic starch: reactions with isocyanates, epoxy functions and stearoyl chloride. *Ind Crops Prod* 21(3):331–336
- Cui H, Hanus R, Kessler MR (2013) Degradation of ROMP-based bio-renewable polymers by UV radiation. *Polym Degrad Stab* 98(11):2357–2365
- Curvelo AAS, De Carvalho AJF, Agnelli JAM (2001) Thermoplastic starch–cellulosic fibers composites: preliminary results. *Carbohydr Polym* 45(2):183–188
- Corobea MC, Muhulet O, Miculescu F, Antoniac IV, Vuluga Z, Florea D et al. (2016) Novel nanocomposite membranes from cellulose acetate and clay-silica nanowires. *Polym Adv Technol* 27(12):1586–1595

- Cyras VP, Tolosa Zenklusen MC, Vazquez A (2006) Relationship between structure and properties of modified potato starch biodegradable films. *J Appl Polym Sci* 101(6):4313–4319
- Cyras VP, Manfredi LB, Ton-That MT, Vázquez A (2008) Physical and mechanical properties of thermoplastic starch/montmorillonite nanocomposite films. *Carbohydr Polym* 73(1):55–63
- Darder M, Colilla M, Ruiz-Hitzky E (2003) Biopolymer-clay nanocomposites based on chitosan intercalated in montmorillonite. *Chem Mater* 15(20):3774–3780
- de Azeredo HM (2009) Nanocomposites for food packaging applications. *Food Res Int* 42(9):1240–1253
- Du Q, Freysz E, Shen YR (1994a) Surface vibrational spectroscopic studies of hydrogen bonding and hydrophobicity. *Science* 264(5160):826–828
- Du Q, Freysz E, Shen YR (1994b) Vibrational spectra of water molecules at quartz/water interfaces. *Phys Rev Lett* 72(2):238
- Du Q, Superfine R, Freysz E, Shen YR (1993) Vibrational spectroscopy of water at the vapor/water interface. *Phys Rev Lett* 70(15):2313
- Dufresne A, Vignon MR (1998) Improvement of starch film performances using cellulose microfibrils. *Macromolecules* 31(8):2693–2696
- Erbil HY, Demirel AL, Avcı Y, Mert O (2003) Transformation of a simple plastic into a superhydrophobic surface. *Science* 299(5611):1377–1380
- Faruk O, Bledzki AK, Fink HP, Sain M (2012) Biocomposites reinforced with natural fibers: 2000–2010. *Prog Polym Sci* 37(11):1552–1596
- Flores S, Famá L, Rojas AM, Goyanes S, Gerschenson L (2007) Physical properties of tapioca-starch edible films: influence of filmmaking and potassium sorbate. *Food Res Int* 40(2):257–265
- Fornes TD, Paul DR (2003) Modeling properties of nylon 6/clay nanocomposites using composite theories. *Polymer* 44(17):4993–5013
- Gao W, Dong H, Hou H, Zhang H (2012) Effects of clays with various hydrophilicities on properties of starch–clay nanocomposites by film blowing. *Carbohydr Polym* 88:321–328
- García-Tejeda YV, López-González C, Pérez-Orozco JP, Rendón-Villalobos R, Jiménez-Pérez A, Flores-Huicochea E, Solorza-Feria J, Bastida CA (2013) Physicochemical and mechanical properties of extruded laminates from native and oxidized banana starch during storage. *LWT Food Sci Technol* 54(2):447–455
- Ghanbarzadeh B, Almasi H, Oleyaei SA (2013) A novel modified starch/carboxymethyl cellulose/montmorillonite bionanocomposite film: structural and physical properties. *Int J Food Eng* 10:121–130
- Ghani SWA, Bakar AA, Samsudin SA (2013) Mechanical properties of chitosan modified montmorillonite filled tapioca starch nanocomposite films. *Adv Mat Res* 686:145–154
- Gutiérrez MQ, Echeverría I, Ihl M, Bifani V, Mauri AN (2012) Carboxymethylcellulose-montmorillonite nanocomposite films activated with murta (*Ugni molinae* Turcz) leaves extract. *Carbohydr Polym* 87:1495–1502
- Gutiérrez TJ, González G (2016) Effects of exposure to pulsed light on surface and structural properties of edible films made from cassava and taro starch. *Food Bioproc Tech* 9(11):1812–1824
- Gutiérrez TJ, González, G (2017) Effect of cross-linking with Aloe vera gel on surface and physicochemical properties of edible films made from plantain flour. *Food Biophys* 12(1):11–22
- Gutiérrez TJ, Guzmán R, Medina C, Famá L (2016a) Effect of beet flour on films made from biological macromolecules: native and modified plantain flour. *Int J Biol Macromol* 82:395–403
- Gutiérrez TJ, Suniaga J, Monsalve A, García NL (2016b) Influence of beet flour on the relationship surface-properties of edible and intelligent films made from native and modified plantain flour. *Food Hydrocoll* 54:234–244
- Gutiérrez TJ, Morales NJ, Pérez E, Tapia MS, Famá L (2015) Physico-chemical properties of edible films derived from native and phosphated cush-cush yam and cassava starches. *Food Packag Shelf Life* 3:1–8

- Hu G, Chen J, Gao J (2009) Preparation and characteristics of oxidized potato starch films. *Carbohydr Polym* 76(2):291–298
- Huang MF, Yu JG, Ma XF (2004) Studies on the properties of montmorillonite-reinforced thermoplastic starch composites. *Polymer* 45:7017–7023
- Kalichevsky MT, Ring SG (1987) Incompatibility of amylose and amylopectin in aqueous solution. *Carbohydr Res* 162(2):323–328
- Kampeerappun P, Aht-ong D, Pentrakoon D, Srikulkit K (2007) Preparation of cassava starch/montmorillonite composite film. *Carbohydr Polym* 67(2):155–163
- Karbowiak T, Debeaufort F, Champion D, Voilley A (2006) Wetting properties at the surface of iota-carrageenan-based edible films. *J Colloid Interface Sci* 294(2):400–410
- Kim SI, Lee BR, Lim JI, Mun CH, Jung Y, Kim JH, Kim SH (2014) Preparation of topographically modified poly(L-lactic acid)-b-poly(ϵ -caprolactone)-b-poly(L-lactic acid) tri-block copolymer film surfaces and its blood compatibility. *Macromol Res* 22(11):1229–1237
- Lee CY, McCammon JA, Rossky PJ (1984) The structure of liquid water at an extended hydrophobic surface. *J Chem Phys* 80(9):4448–4455
- López OV, Versino F, Villar MA, García MA (2015) Agro-industrial residue from starch extraction of *Pachyrhizus ahipa* as filler of thermoplastic corn starch films. *Carbohydr Polym* 134:324–332
- Luna G, Villada H, Velasco R (2009) Fique's fiber reinforced thermoplastic starch of cassava: preliminary. *Dyna* 159:145–151
- Ma X, Yu J, Kennedy JF (2005) Studies on the properties of natural fibers-reinforced thermoplastic starch composites. *Carbohydr Polym* 62(1):19–24
- Martins IMG, Magina SP, Oliveira L, Freire CSR, Silvestre AJD, Neto CP, Gandini A (2009) New biocomposites based on thermoplastic starch and bacterial cellulose. *Compos Sci Technol* 69(13):2163–2168
- Medina C, González P, Goyanes S, Bernal C, Famá L (2015) Biofilms based on cassava starch containing extract of *yerba mate* as antioxidant and plasticizer. *Stärke* 67(9–10):780–789
- Medina C, Gutiérrez TJ, Goyanes S, Bernal C, Famá L (2016) Biodegradability and plasticizing effect of *yerba mate* extract on cassava starch edible films. *Carbohydr Polym* 151:150–159
- Miles MJ, Morris VJ, Orford PD, Ring SG (1985a) The roles of amylose and amylopectin in the gelation and retrogradation of starch. *Carbohydr Res* 135(2):271–281
- Miles MJ, Morris VJ, Ring SG (1985b) Gelation of amylose. *Carbohydr Res* 135(2):257–269
- Miculescu M, Thakur VK, Miculescu F, Voicu SI (2016) Graphene-based polymer nanocomposite membranes: a review. *Polym Adv Technol* 27(7):844–859
- Michalska-Požoga I, Tomkowski R, Rydzkowski T, Thakur VK (2016) Towards the usage of image analysis technique to measure particles size and composition in wood-polymer composites. *Ind Crops Prod* 92:149–156
- Moon RJ, Martini A, Nairn J, Simonsen J, Youngblood J (2011) Cellulose nanomaterials review: structure, properties and nanocomposites. *Chem Soc Rev* 40(7):3941–3994
- Nafchi AM, Tabatabaei RH, Pashania B, Rajabi HZ, Karim AA (2013) Effects of ascorbic acid and sugars on solubility, thermal, and mechanical properties of egg white protein gels. *Int J Biol Macromol* 62:397–404
- Ojagh SM, Rezaei M, Razavi SH, Hosseini SMH (2010) Development and evaluation of a novel biodegradable film made from chitosan and cinnamon essential oil with low affinity toward water. *Food Chem* 122(1):161–166
- Ollier R, Lanfranchi M, Alvarez V (2014) Chemical modifications of natural clays: strategies to improve the polymeric matrix/clay compatibility. In: Wythers Maryann C (ed) *Advances in materials science research*. Nova Science Publishers, Hauppauge, NY, pp 55–82
- Paul DR, Robeson LM (2008) *Polymer nanotechnology: nanocomposites*. *Polymer* 49:3187–3204
- Pappu A, Saxena M, Thakur VK, Sharma A, Haque R (2016) Facile extraction, processing and characterization of biorenewable sisal fibers for multifunctional applications. *J Macromol Sci Part A* 53(7):424–432

- Peeling J, Clark DT, Evans IM, Boulter D (1976) Evaluation of the ESCA technique as a screening method for the estimation of protein content and quality in seed meals. *J Sci Food Agric* 27(4):331–340
- Pelissari FM, Andrade-Mahecha MM, do Amaral Sobral PJ, Menegalli FC (2013) Comparative study on the properties of flour and starch films of plantain bananas (*Musa paradisiaca*). *Food Hydrocoll* 30(2):681–690
- Phan TD, Debeaufort F, Luu D, Voilley A (2005) Functional properties of edible agar-based and starch-based films for food quality preservation. *J Agric Food Chem* 53(4):973–981
- Ray SS, Bousmina M (2005) Biodegradable polymers and their layered silicate nanocomposites: in greening the 21st century materials world. *Prog Mater Sci* 50(8):962–1079
- Ray SS, Okamoto M (2003) Polymer/layered silicate nanocomposites: a review from preparation to processing. *Prog Polym Sci* 28(11):1539
- Reyes LR (2013) Caracterización de dispersiones filmogénicas a base de almidón de maíz y ácido oleico en nanoemulsión con capacidad de formación de recubrimientos comestibles activos. Tesis de Maestría. Facultad de Química. Universidad Autónoma de Querétaro, México
- Rindlav-Westling Å, Gatenholm P (2003) Surface composition and morphology of starch, amylose, and amylopectin films. *Biomacromol* 4(1):166–172
- Rindlav-Westling Å, Stading M, Gatenholm P (2002) Crystallinity and morphology in films of starch, amylose and amylopectin blends. *Biomacromol* 3(1):84–91
- Russell PL, Gough BM, Greenwell P, Fowler A, Munro HS (1987) A study by ESCA of the surface of native and chlorine-treated wheat starch granules: the effects of various surface treatments. *J Cereal Sci* 5(1):83–100
- Shogren RL, Lawton JW, Tiefenbacher KF, Chen L (1998) Starch–poly (vinyl alcohol) foamed articles prepared by a baking process. *J Appl Polym Sci* 68(13):2129–2140
- Siripatrawan U, Harte BR (2010) Physical properties and antioxidant activity of an active film from chitosan incorporated with green tea extract. *Food Hydrocoll* 24(8):770–775
- Singha AS, Thakur VK (2008a) Synthesis and characterization of *Grewia optiva* fiber-reinforced PF-based composites. *Int J Polym Mater Polym Biomater* 57(12):1059–1074
- Singha AS, Thakur VK (2008b) Synthesis and characterization of pine needles reinforced RF matrix based biocomposites. *J Chem* 5(S1):1055–1062
- Singha AS, Thakur VK (2008c) Fabrication and study of lignocellulosic hibiscus *sabdariffa* fiber reinforced polymer composites. *BioResources* 3(4):1173–1186
- Singha AS, Thakur VK (2009a) Fabrication and characterization of *H. sabdariffa* fiber-reinforced green polymer composites. *Polym Plast Technol Eng* 48(4):482–487
- Singha AS, Thakur VK (2009b) *Grewia optiva* fiber reinforced novel, low cost polymer composites. *J Chem* 6(1):71–76
- Singha AS, Thakur VK (2009c) Mechanical, thermal and morphological properties of *grewia optiva* fiber/polymer matrix composites. *Polym Plast Technol Eng* 48(2):201–208
- Singha AS, Thakur VK (2009d) Study of mechanical properties of urea-formaldehyde thermosets reinforced by pine needle powder. *BioResources* 4(1):292–308
- Slavutsky AM, Bertuzzi MA, Armada M (2012) Water barrier properties of starch-clay nanocomposite films. *Braz J Food Technol* 15:208–218
- Spiridon I, Teacă CA, Bodîrlău R, Bercea M (2013) Behavior of cellulose reinforced cross-linked starch composite films made with tartaric acid modified starch microparticles. *J Polym Environ* 21(2):431–440
- Stading M, Hermansson AM, Gatenholm P (1998) Structure, mechanical and barrier properties of amylose and amylopectin films. *Carbohydr Polym* 36(2):217–224
- Stading M, Rindlav-Westling Å, Gatenholm P (2001) Humidity-induced structural transitions in amylose and amylopectin films. *Carbohydr Polym* 45(3):209–217
- Thakur VK, Thakur MK, Gupta RK (2013a) Graft copolymers from cellulose: synthesis, characterization and evaluation. *Carbohydr Polym* 97:18–25
- Thakur VK, Thakur MK, Gupta RK (2013b) Rapid synthesis of graft copolymers from natural cellulose fibers. *Carbohydr Polym* 98:820–828

- Thakur VK, Singha AS, Thakur MK (2013c) Synthesis of natural cellulose-based graft copolymers using methyl methacrylate as an efficient monomer. *Adv Polym Technol* 32(S1):E741–E748
- Thakur VK, Thakur MK, Gupta RK (2013d) Graft copolymers from natural polymers using free radical polymerization. *Int J Polym Anal Charact* 18(7):495–503
- Trache D, Hazwan Hussin M, Mohamad Haafiz MK, Kumar Thakur V (2017) Recent progress in cellulose nanocrystals: sources and production. *Nanoscale* 9(5):1763–1786
- Varma AJ (1984) Photoelectron spectroscopic studies of cellulose, starch and their oxidation products, in powdered form. *Carbohydr Polym* 4(6):473–479
- Voicu SI, Condruz RM, Mitran V, Cimpean A, Miculescu F, Andronesu C, Thakur VK (2016) Sericin covalent immobilization onto cellulose acetate membrane for biomedical applications. *ACS Sustain Chem Eng* 4(3):1765–1774
- Vogler EA (1998) Structure and reactivity of water at biomaterial surfaces. *Adv Colloid Interface* 74(1):69–117
- Wang B, Mireles K, Rock M, Li Y, Thakur VK, Gao D, Kessler MR (2016) Synthesis and preparation of bio-based ROMP thermosets from functionalized renewable isosorbide derivative. *Macromol Chem Phys* 217(7):871–879
- Wenzel RN (1936) Resistance of solid surfaces to wetting by water. *Ind Eng Chem* 28(8):988–994
- Wilpiszewska K, Antosik AK, Szychaj T (2015) Novel hydrophilic carboxymethyl starch/montmorillonite nanocomposite films. *Carbohydr Polym* 128:82–89
- Wong DWS, Gastineau FA, Gregorski KS, Tillin SJ, Pavlath AE (1992) Chitosan-lipid films: microstructure and surface energy. *J Agric Food Chem* 40:540–544
- Xia X, Hu Z, Marquez M (2005) Physically bonded nanoparticle networks: a novel drug delivery system. *J Control Release* 103(1):21–30
- Yanli W, Wenyuan G, Xia L (2009) Carboxymethyl Chinese yam starch: synthesis, characterization, and influence of reaction parameters. *Carbohydr Res* 344:1764–1769
- Yuan Y, Lee TR (2013) Contact angle and wetting properties. In: Bracco G, Holst B (eds) *Surface science techniques*. Springer, Berlin, pp 3–34
- Zhou J, Ma Y, Ren L, Tong J, Liu Z, Xie L (2009) Preparation and characterization of surface crosslinked TPS/PVA blend films. *Carbohydr Polym* 76(4):632–638
- Zhou J, Zhang J, Ma Y, Tong J (2008) Surface photo-crosslinking of corn starch sheets. *Carbohydr Polym* 74(3):405–410

Chapter 6

Functional Biopolymer Composites

Sarat K. Swain, Adrushya J. Pattanayak and Amrita P. Sahoo

Abstract In the current era, there is a burgeoning demand for clean, pollution-free environment and high urgency for minimizing fossil fuel. This leads to an increasing demand for manufacture of high performing cultured products from biological and renewable resources. Polymer biocomposites are the suitable alternate to fulfil such alarming urgency. These have properties of high mechanical resistance, thermogravimetric, oxygen barrier, biodegradation and chemical resistance. There is no single material which can achieve such wide range of properties for which design of composites, in particular with biopolymers, is an attempt for substantial improvement of properties. The biopolymers can be functionalized for better compatibility during preparation of composites. In this chapter, study of biopolymers and their composites is presented along with some critical issues, advantages and disadvantages. A brief discussion about preparation of bio-nanocomposites by in situ reaction, solution casting method and melt mixing technique is discussed. The interaction between components and characterisation of biocomposites has been presented through various spectroscopic analyses such as FTIR, XRD, SEM and TEM. The mechanical, thermal, biodegradable and antimicrobial properties of functional polymer-based biocomposites are compared. Finally biomedical, packaging and environmental applications of biocomposites are presented along with their future prospect.

Keywords Biopolymers · Biocomposites · Packaging · Biomedical applications

Abbreviations

PA	Polyamide
PC	Polycarbonates
PCL	Polycaprolactone
PDS	Polydioxanone suture

S.K. Swain (✉) · A.J. Pattanayak · A.P. Sahoo
Department of Chemistry, Veer Surendra Sai University of Technology,
Burla, Sambalpur, Odisha 768018, India
e-mail: swainsk2@yahoo.co.in

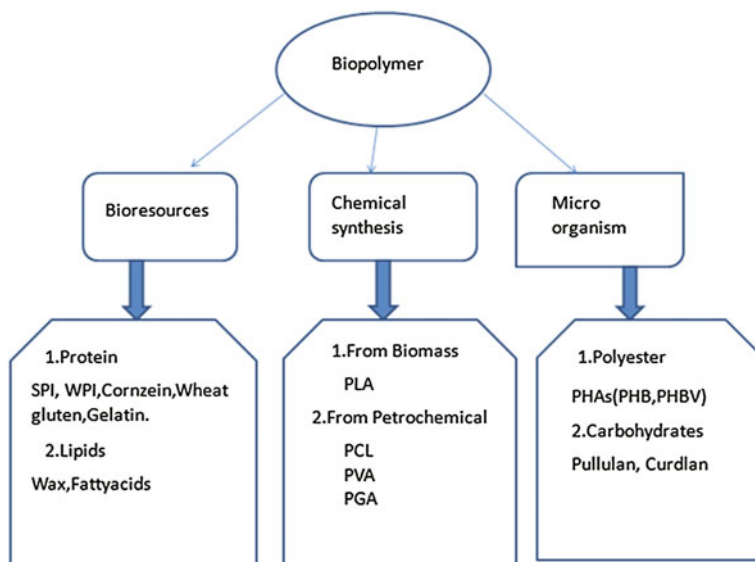
PGA	Polyglycolic acid
PHB	Polyhydroxybutyrate
PLA	Polylactic acid
PMMC	Polymethyl methacrylate
PP	Polypropylene
PTFE	Polytetrafluoroethylene
PVC	Polyvinyl chloride

1 Introduction

Biopolymers are the polymers of biological origin. These may be linear or cross-linked combinations of their monomer units (Thakur et al. 2016; Thakur and Kessler 2014a, b). Biopolymers are classified as the following categories depending upon several factors such as (a) degradability (b) polymer backbone (c) monomers. Biodegradable polymers are typical type of polymers which degrade or break down after their intended purpose and form by-products like environmental gases (CO₂, N₂), water, biomass, and inorganic and organic salts such as PGA, PLA, PDS, PCL, PHB and PPF. Non-biodegradable polymers are the substances that do not break down to a natural, environmental safe condition over time by biological processes, for example, PP, PA, PVC, PC, PMMC and PTFE. Biopolymer may be of the following type depending upon backbone or skeletal framework, examples—polyesters, polysaccharides, polycarbonates, polyamides and vinyl polymers. Depending upon monomer units like monosaccharides, amino acids, nucleotides natural biopolymer are of the following types, e.g.,—polysaccharides, proteins, nucleic acids. The broad classification of biopolymers may be represented in Scheme 1.

1.1 Biopolymers

These are obtained from renewable natural occurring biological matters (Kaplan 1998) which are often biodegradable and can be produced by biological system such as plant body, microorganisms like mushrooms, animals like crustaceans, etc. (Voicu et al. 2016; Wang et al. 2016). Nowadays, fossil fuel is reduced in alarming rate; to minimize dependencies on fossil fuel, few innovative technologies are introduced around biobased materials (Trache et al. 2017). Biopolymers are used as substitute because these are more sustainable, renewable and more importantly eco-friendly in nature (Thakur et al. 2013a, b, c, d, e, f, 2014a, b). Biopolymers are also biodegradable, biocompatible (Rinaudo 2006) and antimicrobial in nature. Therefore, these are globally used in various fields starting from agriculture to



Scheme 1 Schematic classification of biopolymers. *Reproduced with permission from Elsevier* [Progress in Polymer Science 38 (2013) 1629–1652] (Rhim et al. 2013a, b)

therapeutics (Kumar 2000; Berger et al. 2004; Mohanty et al. 2000; Uyama et al. 2003; Dodane and Vilivalam 1998; Subbiah et al. 2005), nevertheless working with biopolymers is challenging. For example, chitin is a derived product of crustacean shells (Kumar 2000; Tolaimate et al. 2000) insect cuticles, (Zhang et al. 2000) or fungal biomass (Wu et al. 2004; Pochanavanich and Suntornsuk 2002; Suntornsuk et al. 2002). From source to source there is a change in degree of deacetylation (DD), percentage of purity and spatial arrangement of charged group and functional group (Nwe and Stevens 2004; Teng et al. 2001) and crystalline (Jaworska et al. 2003; Ogawa et al. 2004). This variation is applicable to all polymers of biological origin (Daly and Noyles Chun 1991). Despite all the adverse challenges, we cannot ignore the profitable aspects of bionanocomposites. Hence, biopolymers have a vast impact on modern life (Fig. 1).

1.2 Biopolymer Composites

Composite means two or more materials having distinct constituents and phases. Polymer composite is a homogenous polymer-based material having specific properties (Pappu et al. 2016). In general composite consists of two phases (1) Phase with lower modulus and high elasticity is chosen as matrix phase during formation of composite polymers (2) Reinforcing phase has high load capacity. There are three types of composites. (a) Particle reinforcement composites formed

by suspending one material to another to form a strong matrix. (b) Structural composites or sandwich composites are two or different materials that bond one layer with another to form strong layers. (c) Fibre reinforcement composites, there are the composites in which materials embedded to other material and form long fibres of extremely strong matrix. Polymer nanocomposites bind with natural polymer to give biodegradable biocomposites (Subbiah et al. 2005; Singha and Thakur 2009a, b, c, d). Nowadays, environment is mostly polluted by non-degradable polymers so replacement with natural biopolymer to create a non-toxic material which is degradable by the nature is a matter of concern (Singha and Thakur 2008a, b, c). The composite of material mostly depends on micro- or nano-sized particle, because less the size more is its effectiveness for the formation of composites. In bionanocomposites materials, two phases are equally merged in the range of nanometer not exceeding 100 nm. The shape of nanoparticles like spherical or platy depends on polymeric composite. Polymer nanocomposites and nanoparticle in the form of inorganic and organic state formed mechanical, optical and electrical properties. Nanocomposite material causes barrier between the substances having composite material polymer. They are with high mechanical strength and increase heat resistance (Tolaimate et al. 2000). Plant-based, bacterial-based biodegradable cellulose polymer can be renewable in plants with high compatibility, to control the material in nanoscale in which the material should be micro or macroscopic properties (Entcheva et al. 2004; Klemm et al. 2011; Martson et al. 1999/1989). Bionanocomposites also be used in food packing, which means the food can be stored without leakage of oxygen and moisture. In this manner, the food can maintain its quality physically and chemically protected. The chemical component of bone called hydroxyl apatite (HAP) can cause many diseases such as bone grafting or bone defects. Bionanocomposites are a combination of new artificial bone materials and it looks like natural bone that can be used for this purpose. Plant reserves food such as starch consists of fossil resources which are easily available and highly water sensitive. Due to possession of unique characteristic properties and above-mentioned wide range of applications which are discussed in detail later on in this chapter, functional biopolymer composites are considered as subject matter for the present topic.

1.3 Functional Biopolymer Composites

Bionanocomposites synonymous to nanobiocomposites are the bio-hybrid composites materials of biological origin. These are an assembly of functionalized biopolymers with inorganic salts having a series of structures with diverse morphology in nanoscale regime. Due to their vast applications ranging from environmental pollution control to drug delivery in biomedical field, many scientists, researchers and engineers are getting attracted to do research work on biocomposites. This may be illustrated as follows:

1.3.1 Chitin and Chitosan as Biocomposites Sorbents

Recently, biosorption has become an emerging and effective waste water treatment technique to remove heavy metals like lead, cadmium, mercury, etc. Biopolymers are the basic constituent of biocomposites. Some of biopolymers such as alginate, micro-algal, chitin and chitosan are successfully examined for heavy metal removal. The advantages of chitin- and chitosan-based biocomposites are their natural abundance, non-toxicity, environment friendliness and cost effectiveness (Thakur and Voicu 2016; Thakur and Thakur 2014).

1.3.2 Cellulose and Cellulose Derivatives as Biocomposites Electrospun

Cellulose and derivatives of cellulose-based biocomposites are commonly applied for the fabrication of semi-permeable membranes. The fabricated semi-permeable membranes are used in dialysis, ultra-filtration and reverse osmosis process. Cellulose acetate is used as electrospun.

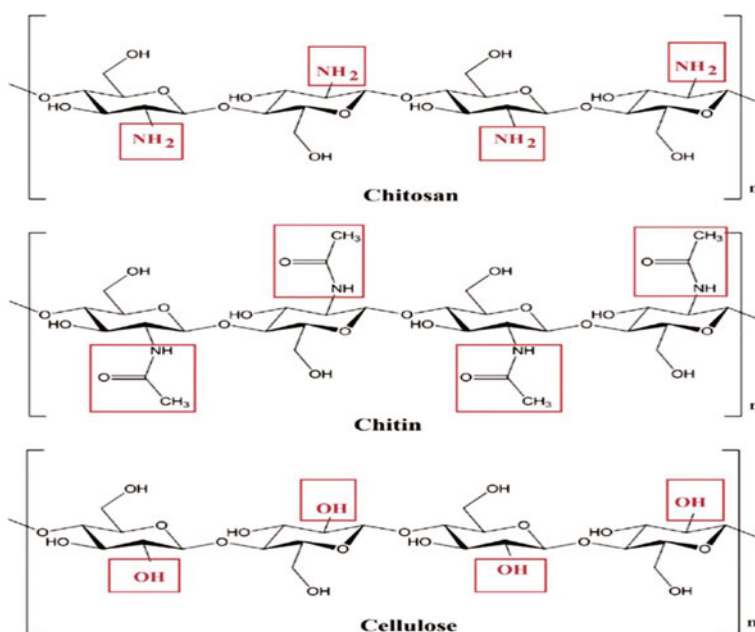


Fig. 1 Structure of few biopolymers used in bionanocomposites synthesis. *Reproduced with permission from Elsevier [Journal of Radiation Research and Applied Science (2015) 8:255–263] (Rahim and Haris 2015)*

1.3.3 Silver (Noble Metal) Decorated Biocomposites for Drug Delivery

Since ancient past heavy noble metals like copper, gold, silver and arsenic etc. are used in therapeutics for the treatment of contaminated diseases. Among these heavy metals, silver has antimicrobial, antibiotic and anti-resistant properties widely used in biomedical field (Silva et al. 2005). In the recent past, silver nanoparticle (AgNPs) has taken over the place metallic silver due to its high potency, hence used for making novel nano-medicine (Gibson 2003).

1.3.4 Lignocellulosic Biocomposites for Bone and Cartilage Tissue Regeneration

Lignocelluloses are a combination of lignin and cellulose. It is present in plant cell wall and similarly bones phosphates of calcium are present in skeletal connective tissue of animal. These provide pathway for exchange and transport of nutrient (Mano 2002). In plants, similar components to that of skeletal connective tissue are present on epidermis, e.g., bark (Gandini et al. 2006). Cork is also a lignocellulosic materials consisting of suber as chief component with concentration 30–50%

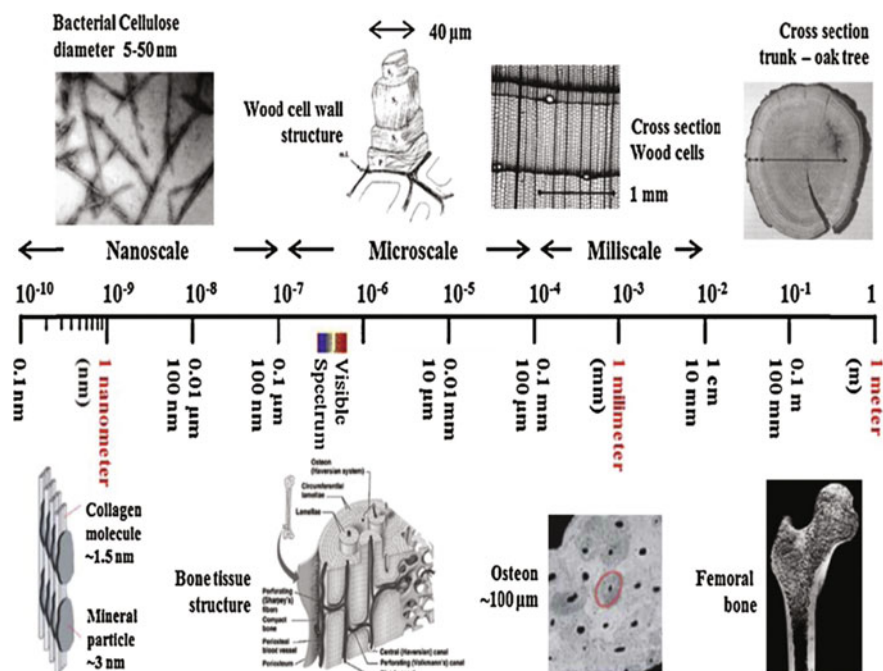


Fig. 2 Hierarchy of lignocellulosic materials and bone (Skeletal connective tissue) (Sinha Ray and Okamoto 2003a, b; Pavlidou and Paspaspyrides 2008; Paul et al. 2005; Zhou and Xanthos 2008). Reproduced with permission from Elsevier [Progress in polymer science (2013) 38:1415–1441] (Fernandes et al. 2013)

(Fernandes et al. 2010). Suberin is a low thermal conductive, fire resistant, low dense and viscoelastic material having very high coefficient of friction and nearly zero poisson ratio (Fernandes et al. 2011; Pires et al. 2011; Stokke and Gardner 2003). These unique properties of lignocelluloses biocomposites are used in different field (Beniash 2011; Sprio et al. 2011; Grunert and Winter 2002) (Fig. 2).

2 Methods of Preparation of Bionanocomposites

Bionanocomposites are prepared by several methods, out of which the following three methods of preparations are important. These methods are (1) in situ reaction, (2) solution casting method, (3) melt mixing technique

2.1 *In Situ Reaction*

In situ polymer techniques for the preparation of bionanocomposites are mostly carried out in the presence of suitable initiators like heat, radiation, etc. In this technique, the nanoparticle gets intermixed with liquid monomer or in monomer solution.

2.2 *Solution Casting Technique*

Solution casting technique is based on the principle of Stokes' law. Solution casting means polymer and prepolymer are equally soluble in the suitable solution. The polymer dissolved easily whereas the nanoparticles are dispersed in same solution or different solution before the two gets intermixed. To prepare clay-based bionanocomposites, the solution must be swell to clay (Fukushima et al. 2009). The clay dispersed due to weak force such that the layer filled one by one. Once solution swelling is over, the surface is then mixed in clay dispersion. The polymer chain breaks when it is put into a solvent. In this manner, solvent adsorbed on to silicate surface. In biopolymer clay solution, entropy is gained from desorption of solvent. In this manner, the entropy decreases to confine intercalated chain. The solvent gets evaporate to get nanocomposite structure (Sinha Ray et al. 2003a, b).

2.3 *Melt Mixing Technique*

In melt mixing technique, the nanoparticle mixed each other in the molten state. In this process, the mixing of particle and modified clay proceeded to degradation. The

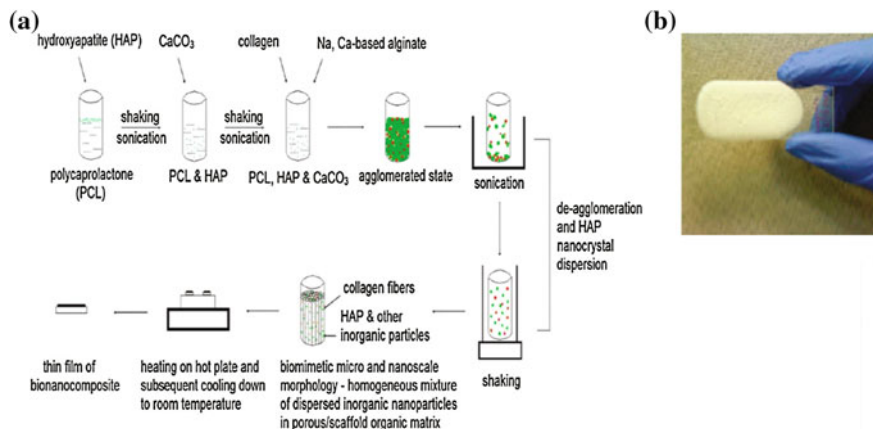


Fig. 3 **a** Schematic representation of the synthesis process of bionanocomposites. **b** Bionanocomposites bone material photograph. *Reproduced with permission from [Biomacromolecules (2010) 10:2545–2549] (Biswas et al. 2010)*

melted nanocomposite clay sustained long period which is called peeling of platelets. Certain nano-compounds like CNTS dispersed the nanoparticle which means the breakage of nanoparticle. In melting process, the agglomeration nanoscale dispersed the particle. The temperature and pressure depend on the degradation of biopolymer (Fig. 3).

3 Characterization Techniques

The characterization of bionanocomposites is carried out by the following techniques; it is explained briefly by taking the example of cellulose biocomposites fibre with nano-SiO₂ as filler.

3.1 Scanning Electron Microscopy (SEM)

The scanning electron micrographs of bionanocomposites were evaluated by JEOLSEM 6700 microscope operating at 5 kV. At first, fibres of biocomposites were frozen in inert atmosphere of liquid nitrogen, and then fractured biocomposite fibres were dried by vacuum distillation. A layer of platinum was coated over the dried fibre and supplied to microscope for observation, e.g., cellulose and cellulose/nano-SiO₂.

At first, cellulose fibres were fabricated with different wt% of nano-SiO₂ (2, 4, 6, 8, 10 and 12) by dry jet-wet spinning to form cellulose/nano-SiO₂ fibres. From

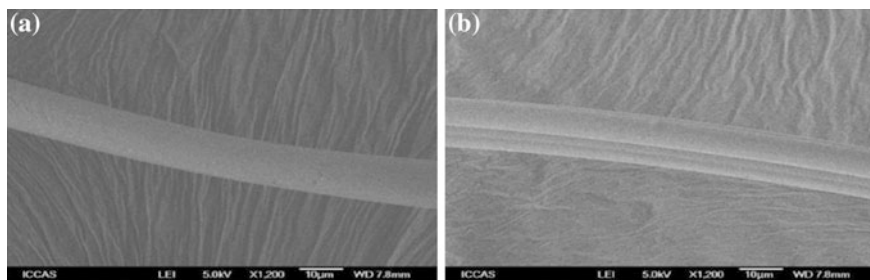


Fig. 4 **a** Images of Scanning electron micrograph of cellulose (Side surface view), **b** cellulose/nano-SiO₂ fibres with 8 wt% of nano-SiO₂. *Reproduced with permission from Elsevier [Carbohydrate polymer (2013) 98:161–167] (Song et al. 2013)*

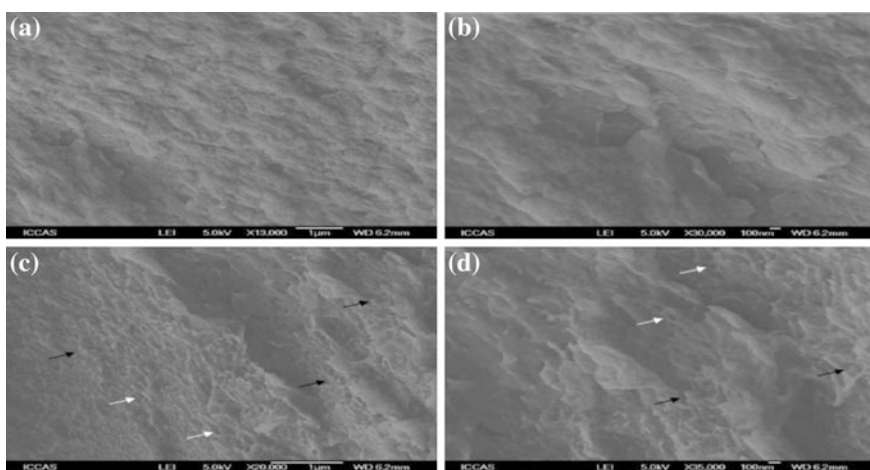
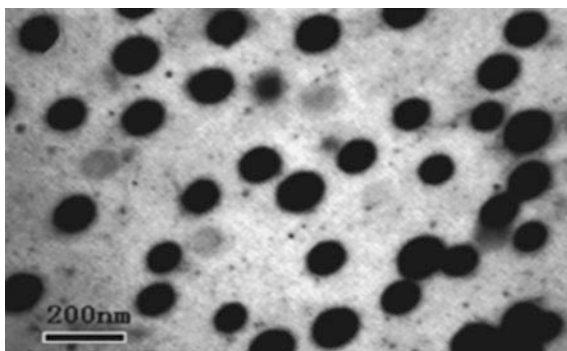


Fig. 5 **a, b** Scanning electron micrograph images of cross sections for cellulose fibres. **b, d** The magnified images of Cellulose/nano-SiO₂ fibres of **a** and **c** respectively. *Reproduced with permission from Elsevier [Carbohydrate polymer (2013) 98:161–167] (Song et al. 2013)*

Fig. 4a, b it is clear that both cellulose and its composites with nano-SiO₂ have smooth surface in side view, which indicates facile fabrication of cellulose nanocomposites fibres.

The cross-section SEM image micrographs are represented in Fig. 5a–d. The images are for cellulose and cellulose/nano-SiO₂ composite fibres with 8 wt% of nano-SiO₂ as filler component. From Fig. 5a, b, it is concluded that the cross-sectional area of cellulose is flat and featureless. In Fig. 5c, d cellulose/nano-SiO₂ SEM image indicates the presence of a large number of voids and roughness of the surface. As a result, the composite fibres have enhanced tensile strength, toughness, higher magnification as compared to cellulose counterpart alone. The filler particles form a strong interfacial bonding with cellulose which is clearly indicated in Fig. 5d.

Fig. 6 A TEM image micrograph of the nanocomposites fibre (e). Reproduced with permission from Elsevier [Carbohydrate polymer 98 (2013):161–167] (Song et al. 2013)



3.2 Transmission Electron Microscopy (TEM)

The nano-SiO₂ particles are dispersed in cellulose matrix which was investigated by taking ultrathin slices of composites fibre having thickness of approximately 70–90 nm and embedded into an epoxy resin by ultra-microscope (Leica EM UC6 & FC6) under cryogenic study condition followed by placing on to a carbon-coated copper grid, finally observed under JEOL JEM-2200 FS at an accelerating voltage of 220 kV. From the observation it was shown that the nanofiller particles were dispersed in the cellulose matrix in the absence of gravity (Fig. 6).

3.3 X-Ray Diffraction (XRD)

The structural analysis of a substance can be carried out by X-ray diffraction. Here we considered MCC/nano-SiO₂. The WXAD of both components were obtained by using an X-ray diffract metre (D/MAX-2500, Rigaku Denki, Japan) with Cu K_α radiation ($\lambda = 0.154$ nm) at 40 kV and 100 mA. The samples were scanned from 2θ from 5° to 40° at a rate of 1°/min and the WAXD sample were recorded at an interval of 0.02°. In Fig. 7, WAXD patterns of cellulose, cellulose fibre, and cellulose/nano-SiO₂ nanocomposites containing 8 wt% nano-SiO₂. From the observation, we can find out that the original cellulose powder belongs to cellulose I family, because it shows three numbers of crystalline peaks at 14.9°, 16.2° and 22.5°. Cellulose fibre showing a diffraction pattern with two broad peaks or weak crystalline peaks at 20.0° (110) and 21.6° (200) corresponds to typical cellulose II crystalline form. For cellulose composite fibre, two crystalline peaks appearing at 20.0° and 21.6° but the peak appearing at 20.0° becomes blunt and weak. From this, it was concluded that the silica nanoparticles at this size range is not crystalline.

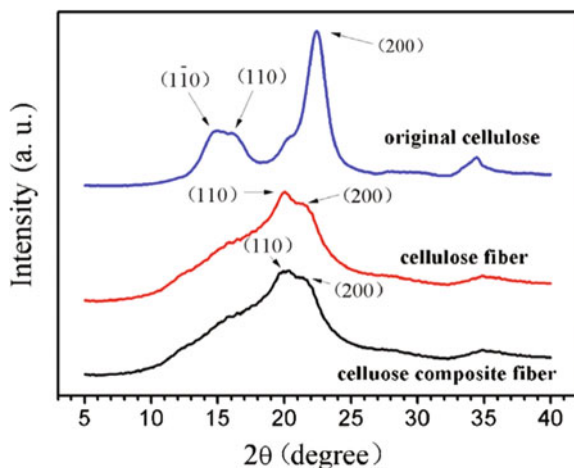


Fig. 7 WAXD patterns of original cellulose powder, regenerated cellulose fibre, and cellulose nanocomposites fibres containing 8 wt% nano-SiO₂. Reproduced with permission from Elsevier [Carbohydrate polymer (2013) 98:161–167] (Song et al. 2013)

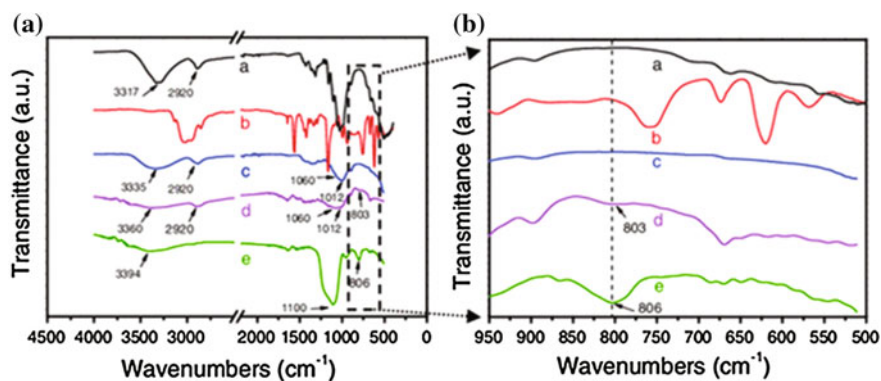


Fig. 8 FTIR patterns of *a* original MCC, *b* AMIMCl, *c* regenerated MCC, *d* regenerated MCC/nano-SiO₂ composite, and *e* pure nano-SiO₂. The *right* FTIR spectra are the magnified view. Reproduced with permission from Springer [Cellulose 20 (2013)1737–1746] (Song and Zheng 2013)

3.4 Fourier Transforms Infrared Spectroscopy (FTIR)

In Fig. 8 the FTIR spectra consists of having original MCC, ionic liquid AMIMCL, regenerate MCC, regenerate MCC/nano-SiO₂ composite and nano-SiO₂. In Fig. 8a regenerate MCC shows the strong band at 3350 cm⁻¹, which contains hydroxyl group of MCC. Another peak at 2920 cm⁻¹ is obtained showing C–H stretching vibration, again 1060 and 1012 cm⁻¹ peak are obtained to C–O–C and C–OH

respectively. Again Fig. 8b shows combination of both regenerate MCC and nano-SiO₂, which gives a broad absorption band at 3360 cm⁻¹ due to OH group in nano-SiO₂ and peak 1060 cm⁻¹ for C–O–C group in MCC, and at 803 cm⁻¹, a weak peak observed for Si–O bending vibration.

4 Properties

4.1 Thermogravimetric Analysis

TGA is the most important method for the characterization of thermal stability of polymers and polymer-based composites. The thermal degradation property of biocomposites was measured by the Perkin-Elmer Pyris 6 type thermo gravimetric analyzer (TGA) with heating rate 20°/min in an inert atmosphere of nitrogen. The thermal stability of biocomposites directly related to nature of nanofiller, i.e., nano-SiO₂. Figure 9 shows the effect of nano-SiO₂ on thermal stability of cellulose fibres. (T_{max}) is considered as degradation temperature which indicates the percentage wt loss with increase in temperature, obtained from DTG curve. The thermal stability of nanocomposites increases with content of nano-SiO₂. From the TG graph, it is also concluded that loss of nano-SiO₂ is very less as the amount of residue increased almost equal to amount of nano-SiO₂ incorporated during spinning.

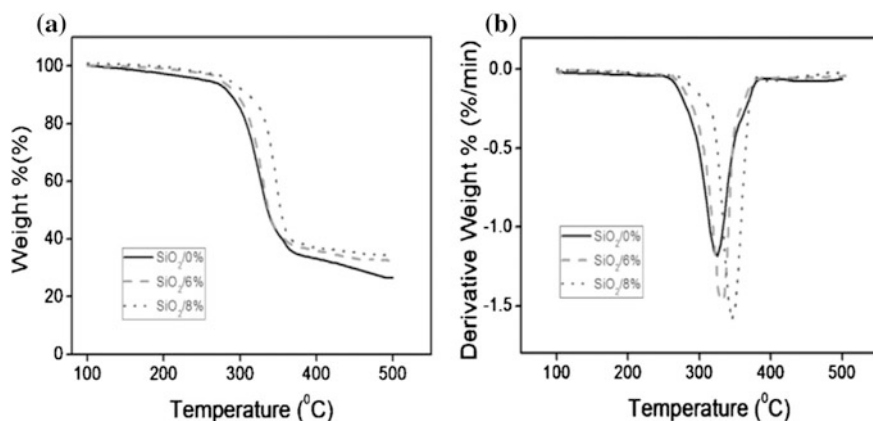


Fig. 9 a Thermogravimetric analysis curve. b Differential thermal gravimetric (DTG) curves for different cellulose nanocomposites fibres. *Reproduced with permission from Elsevier [Carbohydrate polymer 98 (2013):161–167] (Song et al. 2013)*

4.2 Mechanical Properties

The maximum amount of bearable stress that can withstand before failure is called tensile strength; by addition of inorganic filler, tensile strength or mechanical property of biocomposite as a whole increases, so mechanical property is very needful for the detailed study of biocomposites. Mechanical performance of the bionanocomposites is directly related to the nature of inorganic filler. The mechanical properties like tensile strength and elongation at break of bionanocomposites were measured using the TA AR2000 rheometer with a solid fixture. The tensile gauge length was 10 mm. The speed of tensile testing was 10 m/s and three specimens with dimension of 20 mm in length, 3 mm in width, and 45 ± 6 mm in thickness were used for each sample group. The stress and strain were calculated through the machine-recorded force and displacement based on the initial cross-section area and gauge length, respectively. The Young's modulus was calculated through the linear regression analysis of the initial linear portion of the stress–strain curves. It can be explained from Fig. 10. From the graph, it is concluded that below 8 wt%, tensile strength is directly proportional to amount of nanofiller, i.e., nano-SiO₂. At exactly 8 wt% of nano-SiO₂, the mechanical strength increased nearly by 21%. However beyond 8 wt% of nanofiller, the tensile strength is inversely related to the amount of filler.

On the other hand, when we consider elongation at break it increases with addition of nano-SiO₂ from 0 wt% up to 6 wt% in pure cellulose fibre, the reason behind it is that a strong intermolecular force of attraction occurs between pure

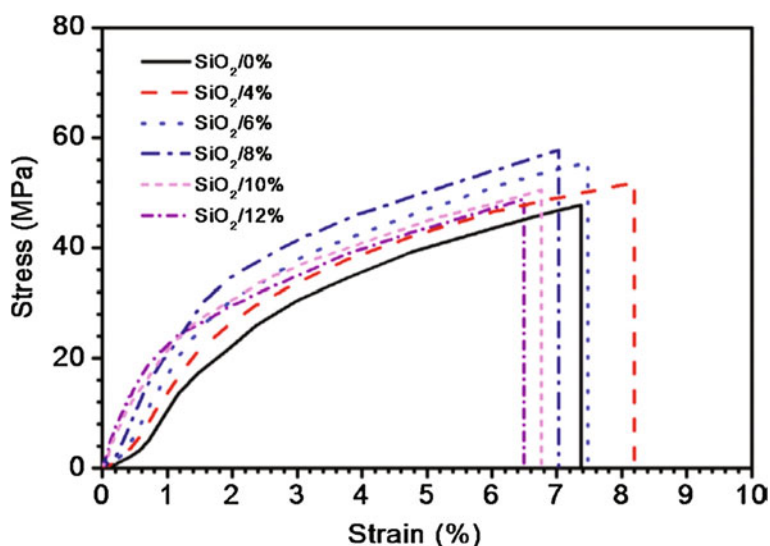


Fig. 10 Stress versus strain graphs of regenerated MCC/nano-SiO₂ composite fibres with proportion of nano-SiO₂. *Reproduced with permission from Elsevier [Carbohydrate polymer 98 (2013):161–167] (Song et al. 2013)*

cellulose fibre and nano-SiO₂. Substantially, we can say that the improvement in mechanical properties like elongation at break, tensile strength are due to high surface area to volume ratio or aspect ratio and rigidity, and most importantly the interfacial interaction between polymer matrix and dispersed nanofiller like nano-SiO₂.

4.3 Biodegradation Properties

Biodegradation of biocomposites means fragmentation and loss of its mechanical properties. It is carried out often by microorganisms like bacteria, algae and fungi. Biodegradation of polymer is either a complex oxidative or hydrolysis process catalyzed by enzyme (Nieddu et al. 2009). Biodegradability was first tested on PCL-based nanocomposites; it is the main reason for using biopolymer for the preparation of bionanocomposites. A series of biodegradation experiment was carried out for PLA-based nanocomposites (Nieddu et al. 2009; Damm et al. 2008; Cioffi et al. 2005; Hong and Rhim 2008; Bi et al. 2011; Wang et al. 2006) in the environment by Sinha Ray et al. (Bi et al. 2011; Wang et al. 2006; Rhim et al.) and found that PLA/organo-clay nanocomposites is completely degraded by compost resulting in evolution of CO₂ (Wang et al. 2006), CO₂ and H₂O (Quintavalla and Vicini 2002). Similar experiment was done. Hence, the presence of terminal hydroxylated edge group plays a significant role for the process of biodegradation.

4.4 Antimicrobial Properties of Bionanocomposites

Bionanocomposites are generally having high aspect ratio which tremendously increases the surface activity and antimicrobial property; the larger surface will be able to inactivate microorganisms more effectively compared to its micro- or macro-scale counterparts (Takahashi and Yamaguchi 1991). A wide range of materials are tested to prepare nanocomposites with antimicrobial function which includes (a) metal and metal ions, e.g., silver, copper, etc. (b) Oxides of metal, e.g., TiO₂, ZnO, etc. (c) modified organic nanoclay, e.g., Ag-zeolite (d) natural biopolymers, e.g., chitin, chitosan, etc. (e) natural antimicrobial agents, e.g., nisin, thymol, etc. (f) enzymes, e.g., peroxidase, lysozyme, etc. and (g) cultured antimicrobial agents, e.g., tetra alkyl or aryl ammonium salts, propionic acid. Antimicrobial properties of bionanocomposites have been implemented as growth inhibitor (Viseras et al. 2008), antimicrobial agent (Emamifar et al. 2011), antimicrobial carrier (Xu et al. 2006), antimicrobial packaging film (Faraji and Wipf 2009; Luckham and Rossi 1999), and packaging sector (Emamifar et al. 2011; Friedman and Junesa 2010; Carlson et al. 2008; Rhim et al. 2006; Choy et al. 2007; Viseras et al. 2008; Xu et al. 2006; Faraji and Wipf 2009; Takahashi and Yamaguchi 1991; Carretero and Pozo 2009). Figures 11 and 12 show antimicrobial agent and antiviral agent in Ag NPs.

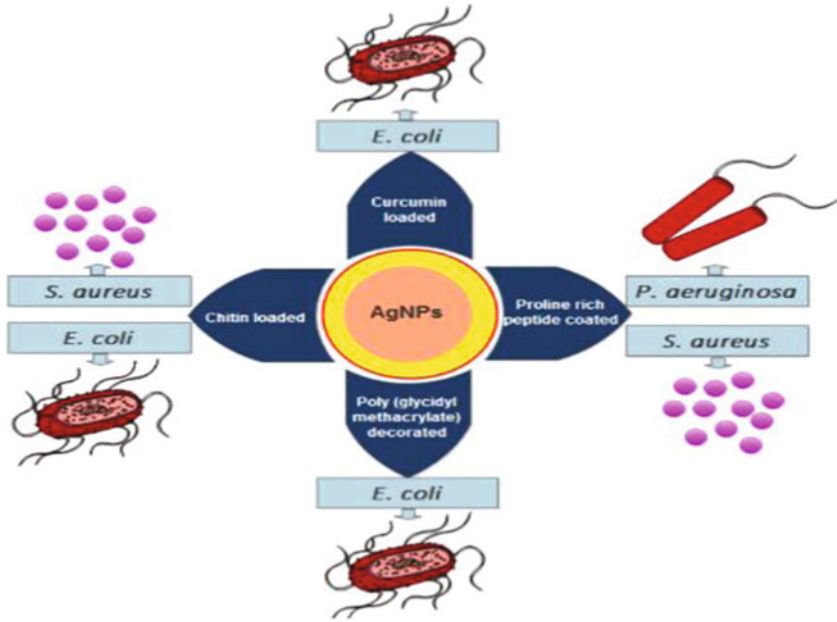


Fig. 11 Antibacterial properties of composite loaded with AgNPs. *Reproduced with permission from Elsevier [International Journal of (2015) 496:159–172] (Rai et al. 2015)*

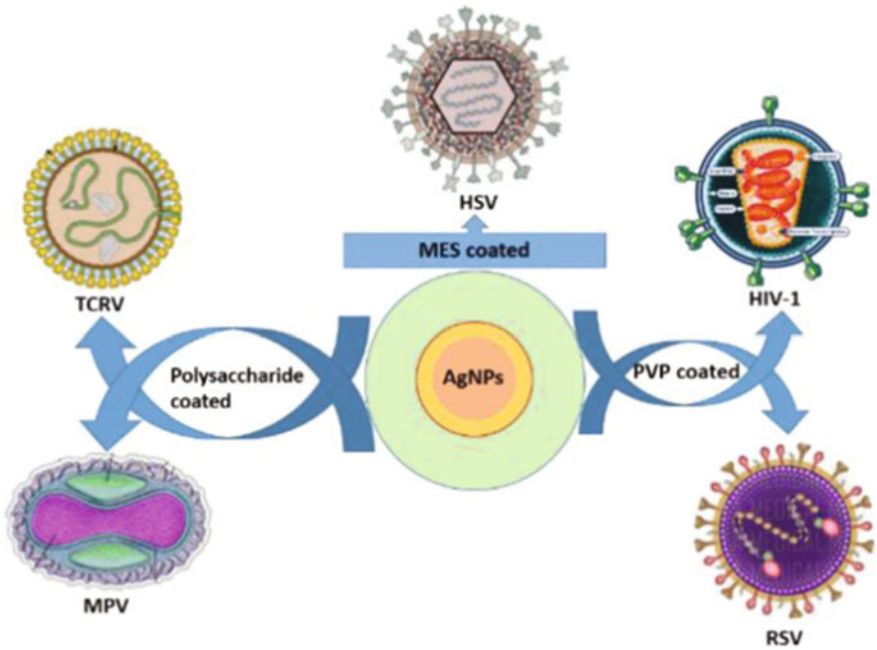


Fig. 12 Antiviral activity of composite loaded with *Pharmaceutics* AgNPs. *Reproduced with permission from Elsevier [International Journal of (2015) 496:159–172] (Rai et al. 2015)*

5 Applications of Functional Biopolymer Composites

5.1 Biomedical Application

In biomedical sector, the clay-based bio-hybrids nanocomposite has been used. In biomedical, the bionanocomposites are mostly used in tissue engineering, vaccination, drug delivery. The materials are mostly biocompatible so these are non-toxic in nature (Temenoff et al. 2008). The other properties of nanoclay are density, surface charge and adsorbed bimolecular hydrophilicity which are favourable for drug delivery and target drug delivery; and during drug delivery control, for avoiding overdosing and underdosing. The biocomposites are used in pharmaceuticals where the clay minerals can be used to inherent of low toxicity, biocompatibility (Choy et al. 2007; Viseras et al. 2008). Currently, the polymeric or viral vectors delivery system are completely different in above properties (Xu et al. 2006; Faraji and Wipf 2009). Traditionally, the clay is used in pharmaceutical like smectites, kaolinite or fibrous clays, as their rheological properties, which is used for their emulsifiers and stabilizers and also acts as suspended agents for hydrophobic drugs (Takahashi and Yamaguchi 1991; Carretero and Pozo 2009). The nanoclay used in drug delivery has a major issue for flocculate of high ionic strength (Luckham and Rossi 1999). Biopolymer clay composite has colloidal properties; so it absorbs polymers towards itself and also has swelling and film forming ability (Viseras et al. 2008). The research focused on silicates layer and minerals clay fibres, as these carryout drug delivery. The biocompatibility of polyvinyl alcohol polymer were controlled by rifampicin (Viçosa et al. 2009). This work can be done when sepiolite fibres dispersed into a drug-loaded polymer, then it reduces swelling capacity at that time water migrates into PVA as release rifampicin. In tissue engineering application, the bionanocomposites are used for hard tissue replacement and bone transplant.

5.2 Packaging Applications

In food packing industries, the main aim is properly pack the material and their properties must include thermal stability, chemical stability, water vapour, loss of gas, high mechanical strength, biodegradability, heat resistance, good optical clarity, developed antimicrobial and anti-fungal surface. In packing performance, polymer nanoclay composite is used in variety of food packing application. In food packing application, various review articles were published (Sorrentino et al. 2007; Rhim and Ng 2007; Akbari et al. 2007; Arora and Padua 2010; Smolander and Chaudhry 2010; Johansson 2011; Hatzigrigoriou and Papaspyrides 2011; de Azeredo 2009; Duncan 2011). The main application to concentrate nanocomposite made up of thermoplastic and thermo set. This idea is used in various industries to improve barrier properties of the biocomposites material. Traditionally four layers

of barrier properties are used, first is the multilayer of one middle and outside structure layer, and second is middle layer in which reinforced with nanocomposites film to enhance the properties. Third layer is having active surface barrier properties made up of gas (O_2) which acts as scavenger and fourth one consists of both active and passive layer with barrier property. For example, Nylon-6 which is used in plastic materials to provide strength and toughness of the structure and it also has high barrier properties in packing materials. The main aim of the nanocomposites polymer is to reduce packing waste and efforts to recycle the material; but without barrier properties of oxygen in food packing cause nutrient losses, microbial growth, colour change, etc. Bionanocomposites with antimicrobial activities are used to reduce the growth of contaminated microorganisms; improve the food quality and safety measures. The food packing bionanocomposites film are used in packing of meat, fish, bread, fruits and vegetables (Moreira et al. 2011; Kerry et al. 2006). The coating of nanoparticle in biocomposites materials are used to create scratch resistance, corrosion resistance, antimicrobial activity. Biocomposite having better future prospects means lower production and high cost restriction. The water resistance capacity of bionanocomposites is too poor but in environment safety condition, it is widely used. The most important factor used in bionanocomposites is to improve the optimum formulation and desired properties of its wide range application, as well as less cost effectiveness of bionanocomposite materials. Another application of nanocomposite is starch; starch is most abundant biopolymeric material on earth and also it is expensive. It is used in packing material to increase the mechanical strength. Mostly starch contains α -D glucan amylase having amyl pectin. It forms poor mechanical properties and high water affinity, so nanomaterial and particle are used to increase the properties. The starch clay nanocomposites have intermolecular hydrogen bond between chain which helps starch to melt often at higher than degradation temperature. Organic-based clay material has been used to protect the environment. Clay is most abundant, non-toxic and low-cost natural product; it can reduce the hazardous materials from the soil (Gatica and Vidal 2010). So the research mostly focused the drinking water treatment (Rajamohan and Al-Sinani 2016). The modified clay biopolymer is more interesting to remove the pollutants in water (Ruiz-Hitzky et al. 2010). Due to adsorbent properties in clay biocomposites materials have removed heavy metals ion in water and also recovers of azodyes particle. Earlier, the fibrous clay incorporates into carbon paste electrodes that are used in the determination of drugs in biological samples.

5.3 *Environmental Applications*

In environmental protection, clay and soil combined to enhance efficiency in laundry process (Ruiz-Hitzky et al. 2010). Clays, due to its low cost, non-toxicity and abundant material and less hazardous nature, can be used for drinking water treatment (Gatica and Vidal 2010; Srinivasan 2011). The biopolymer modified clay

is mostly used pollutants removal (Ruiz-Hitzky et al. 2010). Chitosan/clay bionanocomposites are used to recover azo dyes and heavy metal as in combination of ion exchange capacity and adsorbent properties (Darder et al. 2012). The nanoclay-based bionanocomposites are mostly used in adsorption and absorption properties based system. In case of sepiolite and polygorskite nanocomposite, which consists of polyacrylic acid and polyacrylamide, their derivatives are dispersion in nanometre scale with the polymer. This product has super absorbency ability due to high water adsorption capacity (Ruiz-Hitzky et al. 2011). Biopolymer such as polyacrylic acid and polyacrylamide, starch is biodegradable and eco-friendly with environment. The above biopolymer due to their good absorbent capacity and reswelling cycles, therefore is mostly applicable for agriculture and horticulture (Wang et al. 2008). Biopolymer incorporation material also used environmental remediation. The bionanocomposites CMC-g-PAA/polygorskite are applicable for heavy metal and metal cation like Pb(II) (Liu et al. 2010) due to their super absorbents capacity, i.e., remove Cu(II) (Wang et al. 2009). Hg(II) (Wang and Wang 2010) (Table 1).

Table 1 Application of different biocomposites with reinforcements of nanofiller

Biopolymer	Filler	Application	References
Keratin	Acrylonitrile-butadiene	Rubber	Prochoń and Przeórkowska (2013)
Starch	Clay	Food packing	Tang et al. (2008)
	Silicate nanoclay	Food packaging	Rhim et al. (2013a, b)
	Cellulose	Food packing	Neumann and Seib US 5185382A
	Lignocellulose fibres	Food packing	Averous and Boquillon (2004)
Polyacetic acid	Silver, copper, gold, platinum	Food packing	Fortunati et al. (2012)
Polycaprolactone, Poly (hydroxyl butyrate-Co-Valerate) (PHBV)	TiO ₂	Food packing	Mofokeng and Luyt (2015)
Cellulose	Polypropylene	Food packing	Laka et al. (2011)
	High density polyethylene	Food packing	Pasquini et al. (2008)
Chitosan	Poly vinyl pyrrolidone	Food packing	Abdelarzek et al. (2010)
	PVA	Food packing	Abdelarzek et al. (2010)

(continued)

Table 1 (continued)

Biopolymer	Filler	Application	References
Poly-L-lactic acid	β -Tricalcium phosphate	Biomedical	Damadzadeh et al. (2010)
Poly-L-lactic-Co-glycolic acid	β -Tricalcium phosphate	Biomedical	Kasuga et al. (2003)

6 Conclusion

In this chapter, a brief explanation about bionanocomposites has been presented which are the biobased hybrid materials combinations of biopolymer with organic and inorganic solid like metals, metal oxides, and organic nanoclay at molecular level. These have better tensile strength, mechanical resistance and thermal properties as compared to its individual components. Bionanocomposites have diverse applications in various fields like tissue engineering, biomedical, food packaging as well packing in general. In future, attempt would be stressed to explore new starting material or process for the synthesis of novel multi-component bionanocomposites with multifunctional aspects. Care should be taken towards synthesis of smart responsive bionanocomposites for target drug delivery in therapeutics.

Acknowledgements Authors express their thanks to Department of Science and Technology (Biotechnology), Government of Odisha, India for financial support.

References

- Abdelarzek EM, Elashmawi IS, Labeeb S (2010) Chitosan filler effects on the experimental characterization, spectroscopic investigation and thermal studies of PVA/PVP blend films. *Physics B* 405:2017–2021
- Akbari Z, Ghomashchi T, Moghadam S (2007) Improvement in food packaging industry with biobased nanocomposites. *Int J Food Eng* 4(3):1–24
- Arora A, Padua GW (2010) Review: nanocomposite in food packaging. *J Food Sci* 75(1):R43–R49
- Averous L, Boquillon N (2004) Biocomposites based on plasticized starch: thermal and mechanical behaviours. *Carbohydr Polym* 56(2):111–122
- Beniash E (2011) Biomaterials—hierarchical nanocomposites: the example of bone. *Wiley Interdiscip Rev Nanomed Nanobiotechnol* 3:47–69
- Berger J, Reist M, Mayer JM, Felt O, Peppas NA, Gurny R (2004) Structure and interactions in covalently and ionically crosslinked chitosan hydrogels for biomedical applications. *Eur J Pharm Biopharm* 57:19–34
- Bi L, Yang L, Narsimhan G, Bhunia AK, Yao Y (2011) Designing carbohydrate nanoparticles for prolonged efficacy of antimicrobial peptide. *J Control Release* 150:1506
- Biswas A, Bayer IS, Zhao H, Wang T, Watanabe F, Biris AS (2010) Design and synthesis of biomimetic multicomponent all-bone minerals bionano composites. *Biomacromolecules* 11:2545–2549

- Carlson C, Hussain SM, Schrand AM, Braydich-Stolle LK, Hess KL, Jones RL, Schlager JJ (2008) Unique cellular interaction of silver nanoparticles: size-dependent generation of reactive oxygen species. *J Phys Chem B* 112:13608–13619
- Carretero MI, Pozo M (2009) Clay and non-clay minerals in the pharmaceutical industry Part I. Excipients and medical applications. *Appl Clay Sci* 46:73–80
- Choy JH, Choi SJ, Oh JM, Park T (2007) Clay minerals and layered double hydroxides for novel biological applications. *Appl Clay Sci* 36:122–132
- Cioffi N, Torsi L, Ditaranto N, Tantillo G, Ghibelli L, Sabbatini L, Blevè-Zacheo T, D'alesio M, Zambonin PG, Traversa E (2005) Copper nanoparticle/polymer composites with antifungal and bacteriostatic properties. *Chem Mater* 17:5255–5262
- Daly WH, Chun Noyles, HL (1991) *Polymers from biobased materials*. Data Corporation: Park Ridge 81–89
- Damadzadeh B, Jabari H, Skrifvars M, Airola K, Moritz N, Vallittu PK (2010) Effect of ceramic filler content on the mechanical and thermal behaviour of poly-L-lactic acid and poly-L-lactic-co-glycolic acid composites for medical applications. *J Mater Sci Mater Med* 21:2523–2531
- Damm C, Münsted H, Rösch A (2008) The antimicrobial efficacy of polyamide 6/silver nano- and microcomposites. *Mater Chem Phys* 108:61–66
- Darder M, Aranda P, Ruiz-Hitzky E (2012) Chitosan-clay bionanocomposites. In: Avérous L, Pollet E (eds) *Environmental silicate nano-biocomposites*. Springer, London, pp 365–391
- de Azeredo HMC (2009) Nanocomposites for food packaging applications. *Food Res Int* 42: 1240–1253
- Dodane V, Vilivalam VD (1998) Pharmaceutical applications of chitosan. *Pharm Sci Technol Today* 1:246–253
- Duncan TV (2011) Applications of nanotechnology in food packaging and food safety: barrier materials, antimicrobials and sensors. *J Colloid Interface Sci* 363:1–24
- Emamifar A, Kadivar M, Shahedi N, Soleimani-Zad S (2011) Effect of nanocomposite packaging containing Ag and ZnO on inactivation of *Lactobacillus plantarum* in orange juice. *Food Control* 22:408–413
- Entcheva E, Bien H, Yin LH, Chung CY, Farrell M, Kostov Y (2004) Functional cardiac cell constructs on cellulose-based scaffolding. *Biomaterials* 25:5753–5762
- Faraji AH, Wipf P (2009) Nanoparticles in cellular drug delivery. *Bioorg Med Chem* 17: 2950–2962
- Fernandes EM, Correlo VM, Chagas JAM, Mano JF, Reis RL (2010) Cork based composites using polyolefin's as matrix: morphology and mechanical performance. *Compos Sci Technol* 70:2310–2318
- Fernandes EM, Correlo VM, Chagas JAM, Mano JF, Reis RL (2011) Properties of new cork-polymer composites: advantages and drawbacks as compared with commercially available fibreboard materials. *Compos Struct* 3:120–3129
- Fernandes EM, Pires RA, Mano JF, Reis RL (2013) Bionanocomposites from lignocellulosic resources: properties, applications and future trends for their use in the biomedical field. *Prog Polym Sci* 38:1415–1441
- Fortunati E, Armentano I, Zhou Q, Iannoni A, Saino E, Visai L, Kenny JM (2012) Multifunctional bionanocomposite films of poly (lactic acid), cellulose nanocrystals and silver nanoparticles. *Carbohydr Polym* 87:1596–1605
- Friedman M, Junesa VK (2010) Review of antimicrobial and antioxidative activities of chitosans in food. *J Food Prot* 73:1737–1761
- Fukushima K, Abbate C, Tabuani D, Gennari M, Camino G (2009) Biodegradation of poly(lactic acid) and its nanocomposites. *Polym Degrad Stab* 94:1646–1655
- Gandini A, Neto CP, Silvestre AJD (2006) Suberin: a promising renewable resource for novel macromolecular materials. *Prog Polym Sci* 31:878–892
- Gatica JM, Vidal H (2010) Non-cordierite clay-based structured materials for environmental applications. *J Hazard Mater* 181:9–18
- Gibson LJ (2003) Cellular solids. *MRS Bull* 28:270–274

- Grunert M, Winter WT (2002) Nanocomposites of cellulose acetate butyrate reinforced with cellulose nanocrystals. *J Polym Environ* 10:27–30
- Hatzigrigoriou NB, Papaspyrides CD (2011) Nanotechnology in plastic food-contact materials. *J Appl Polym Sci* 122:3720–3739
- Hong SI, Rhim JW (2008) Antimicrobial activity of organically modified nanoclays. *J Nanosci Nanotechnol* 8:5818–5824
- Jaworska M, Sakurai K, Gaudon P, Guibal E (2003) Influence of chitosan characteristics on polymer properties. I: crystallographic properties. *Polym Int* 52:198–205
- Johansson C (2011) Bio-nanocomposites for food packaging applications. In: Mittal V (ed) *Nanocomposites with biodegradable polymers*. Oxford University Press, New York, pp 348–367
- Kaplan DL (1998) *Biopolymers from renewable resources*. Springer, New York
- Kasuga T, Maeda H, Kato K, Nogami M, Hata KI, Ueda M (2003) Preparation of poly(lactic acid) composites containing calcium carbonate (vaterite). *Biomaterials* 24:3247–3253
- Kerry JP, O’Grady MN, Hogan SA (2006) Past, current and potential utilization of active and intelligent packaging systems for meat and muscle-based products: a review. *Meat Sci* 74: 113–130
- Klemm D, Kramer F, Moritz S, Lindstrom T, Ankerfors M, Gray D, Dorris A, (2011) Nanocelluloses: A new family of nature based materials. *Angew Chem Int Ed* 50:5438–5466
- Kumar MNVR (2000) A review of chitin and chitosan applications. *React Funct Polym* 46:1–27
- Laka M, Chernyavskaya S, Shulga G, Shapovalov V, Valenkov A, Tavroginskaya M (2011) Use of cellulose-containing fillers in composites with polypropylene. *Mater Sci (Mediziagotyra)* 17 (2):150–154. ISSN 1392-1320
- Liu Y, Wang WB, Wang AG (2010) Adsorption of lead ions from aqueous solution by using carboxymethyl cellulose-g-poly (acrylic acid)/attapulgite hydrogel composites. *Desalination* 259:258–264
- Luckham PF, Rossi S (1999) The colloidal and rheological properties of bentonite suspensions. *Adv Coll Interface Sci* 82:43–92
- Mano JF (2002) The viscoelastic properties of cork. *J Mater Sci* 37:257–263
- Martson M, Viljanto J, Hurme T, Laippala P, Saukko P (1999/1989) Is cellulose sponge degradable or stable as implantation material? An in vivo subcutaneous study in the rat. *Biomaterials*. 20:95
- Mofokeng JP, Luyt AS (2015) Morphology and thermal degradation studies of melt-mixed poly (hydroxybutyrate-co-valerate)(PHBV)/poly(ϵ -caprolactone)(PCL) biodegradable polymer blend nanocomposites with TiO₂ as filler. *J Mater Sci* 50:3812–3824
- Mohanty AK, Misra M, Hinrichsen G (2000) Biofibres, biodegradable polymers and biocomposites: an overview. *Macromol Mater Eng* 24:276–277
- Moreira MR, Pereda M, Marcovich NE, Roura SI (2011) Antimicrobial effectiveness of bioactive packaging materials from edible chitosan and casein polymers: assessment on carrot, cheese, and salami. *J Food Sci* 76(1):54–63
- Neumann PE, Seib PA (1993) Starch-based biodegradable packing filler and method of preparing same. US 5185382A
- Nieddu E, Mazzucco L, Gentile P, Benko T, Balbo V, Mandrile R, Ciardelli G (2009) Preparation and biodegradation of clay composite of PLA. *React Funct Polym* 69:371–379
- Nwe N, Stevens WF (2004) Effect of urea on fungal chitosan production in solid substrate Fermentation. *Process Biochem* 39:1639–1642
- Ogawa K, Yui T, Okuyama K (2004) Three D structures of chitosan. *Int J Biol Macromol* 34:1–8
- Pappu A, Saxena M, Thakur VK, Sharma A, Haque R (2016) Facile extraction, processing and characterization of biorenewable sisal fibers for multifunctional applications. *J Macromol Sci Part A* 53(7):424–432
- Pasquini D, de Moraes Teixeira E, da Silva Curvelo AA, Belgacem MN, Dufresne A (2008) Surface esterification of cellulose fibres: processing and characterisation of low-density polyethylene/cellulose fibres composites. *Compos Sci Technol* 68:193–201

- Paul MA, Delcourt C, Alexandre M, Degée Ph, Monteverde F, Dubois Ph (2005) Poly(lactide)/montmorillonite nanocomposites: study of the hydrolytic degradation. *Polym Degrad Stab* 87:535–542
- Pavlidou S, Papispyrides CD (2008) A review on polymer-layered silicate nanocomposites. *Prog Polym Sci* 33:1119–1198
- Pires RA, Aroso IM, Silva SP, Mano JF, Reis RL (2011) Isolation of fiedelin from black condensate of cork. *Nat Prod Commun* 6:1577–1579
- Pochanavanich P, Suntornasuk W (2002) Fungal chitosan production and its characterization. *Lett Appl Microbiol* 35:17–21
- Prochoń M, Przepiórkowska A (2013) Innovative application of biopolymer keratin as a filler of synthetic acrylonitrile-butadiene rubber NBR. *J Chem* 2013:8
- Quintavalla S, Vicini L (2002) Antimicrobial food packaging in meat industry. *Meat Sci* 62:373–380
- Rahim M, Haris MRHM (2015) Application of biopolymer composites in arsenic removal from aqueous medium: a review. *J Radiat Res Appl Sci* 8:255–263
- Rai M, Ingle AP, Gupta I, Brandelli A (2015) Bioactivity of noble metal nanoparticles decorated with biopolymers and their application in drug delivery. *Int J Pharm* 496:159–172
- Rajamohan N, Al-Sinani J (2016) Removal of boron using clay-effect of process parameters, kinetic and isotherm studies. *J Eng Sci Technol* 11(3):311–326
- Rhim JW, Ng PK (2007) Natural biopolymer-based nanocomposite films for packaging applications. *Crit Rev Food Sci Nutr* 47:411–433
- Rhim JW, Hong SI, Park HM, Ng PKW (2006) Preparation and characterization of chitosan-based nanocomposite films with antimicrobial activity. *J Agric Food Chem* 54:5814–5822
- Rhim JW, Park HM, Ha CS (2013a) Bio-nanocomposites for food packaging applications. *Prog Polym Sci* 38(10):1629–1652
- Rhim JW, Park HM, Ha CS (2013b) Bio-nanocomposites for food packaging applications. *Prog Polym Sci* 38:1629–1652
- Rinaudo M (2006) Chitin and chitosan: properties and applications. *Prog Polym Sci* 31:603–632
- Ruiz-Hitzky E, Aranda P, Darder M, Rytwo G (2010) Hybrid materials based on clays for environmental and biomedical applications. *J Mater Chem* 20(42):9306–9321
- Ruiz-Hitzky E, Aranda P, Alvarez A, Santarén J, Esteban-Cubillo A (2011) Advanced materials and new applications of sepiolite and Palygorskite. In: Galán E, Singer A (eds) *Developments in Palygorskite-sepiolite research. A new outlook on these nanomaterials*. Elsevier, Oxford, pp 393–452
- Silva SP, Sabino MA, Fernandes EM, Correló VM, Boesel LF, Reis RL (2005) Cork: properties, capabilities and applications. *Int Mater Rev* 50:345–365
- Singha AS, Thakur VK (2008a) Synthesis and characterization of pine needles reinforced RF matrix based biocomposites. *J Chem* 5(S1):1055–1062
- Singha AS, Thakur VK (2008b) Synthesis and characterization of *Grewia optiva* fiber-reinforced PF-based composites. *Int J Polym Mater Polym Biomater* 57(12):1059–1074
- Singha AS, Thakur VK (2008c) Fabrication and study of lignocellulosic *Hibiscus sabdariffa* fiber reinforced polymer composites. *BioResources* 3(4):1173–1186
- Singha AS, Thakur VK (2009a) *Grewia optiva* fiber reinforced novel, low cost polymer composites. *J Chem* 6(1):71–76
- Singha AS, Thakur VK (2009b) Fabrication and characterization of *H. sabdariffa* fiber-reinforced green polymer composites. *Polym-Plast Technol Eng* 48(4):482–487
- Singha AS, Thakur VK (2009c) Study of mechanical properties of urea-formaldehyde thermosets reinforced by pine needle powder. *BioResources* 4(1):292–308
- Singha AS, Thakur VK (2009d) Mechanical, thermal and morphological properties of *Grewia optiva* fiber/polymer matrix composites. *Polym-Plast Technol Eng* 48(2):201–208
- Sinha Ray S, Okamoto M (2003a) Polymer/layered silicate nanocomposites: a review from preparation to processing. *Prog Polym Sci* 28:1539–1641
- Sinha Ray S, Okamoto M (2003b) New poly(lactide)/layered silicate nanocomposites: open a new dimension for plastics and composites. *Macromol Rapid Commun* 24:815–840

- Sinha Ray S, Yamada K, Okamoto M, Ueda K (2003a) Biodegradable poly(lactide)/montmorillonite nanocomposites. *J Nanosci Nanotechnol* 3:503–510
- Sinha Ray S, Yamada K, Okamoto M, Ueda K (2003b) New poly(lactide)-layered silicate nanocomposites. 2. Concurrent improvements of materials properties, biodegradability and melt rheology. *Polymer* 44:857–866
- Smolander M, Chaudhry Q (2010) Nanotechnologies in food packaging. In: Chaudhry Q, Castle L, Watkins R (eds) *Nanotechnologies in food*. RSC Publishing, Cambridge, pp 86–101
- Song H, Zheng L (2013) Nanocomposite films based on cellulose reinforced with nano-SiO₂: microstructure, hydrophilicity, thermal stability, and mechanical properties. *Cellulose* 20:1737–1746
- Song HZ, Luo ZQ, Wang CZ, Hao XF, Gao JG (2013) Preparation and characterization of bionanocomposite fiber based on cellulose and nano-SiO₂ using ionic liquid. *Carbohydr Polym* 98:161–167
- Sorrentino A, Gorrasi G, Vittoria V (2007) Potential perspectives of bionanocomposites for food packaging applications. *Trends Food Sci Technol* 18:84–95
- Sprio S, Ruffini A, Valentini F, D'Alessandro T, Sandri M, Panseri S, Tampieri A (2011) Biomimesis and biomorphic transformations: new concepts applied to bone regeneration. *J Biotechnol* 156:347–355
- Srinivasan R (2011) Advances in application of natural clay and its composites in removal of biological, organic, and inorganic contaminants from drinking water. *Adv Mater Sci Eng* 2011:17. Article ID 872531
- Stokke DD, Gardner DJ (2003) Fundamental aspects of wood as a component of thermoplastic composites. *J Vinyl Addit Technol* 9:96–104
- Subbiah T, Bhat GS, Tock RW, Parameswaran S, RamKumar SS (2005) Electrospinning of nanofibers. *J Appl Polym Sci* 96:557–569
- Suntornsuk W, Pochanavanich P, Suntornsuk L (2002) Fungal chitosan production on food processing by-products. *Process Biochem* 37:727–729
- Takahashi T, Yamaguchi M (1991) Host-guest interaction between swelling clay-minerals and poorly water-soluble drugs. 1. Complex-formation between a swelling clay mineral and griseofulvin. *J Incl Phenom Mol Recognit Chem* 10:283–297
- Tang X, Alavi S, Herald TJ (2008) Barrier and mechanical properties of starch clay nanocomposite film. *Cereal Chem* 85(3):433–439
- Temenoff JS, Mikos Antonios G (2008) *Biomaterials: the intersection of biology and materials science*. Pearson/Prentice Hall, Upper Saddle River, N.J
- Teng WL, Khor E, Tan TK, Lim LY, Tan SC (2001) Concurrent production of chitin from shrimp shells and fungi. *Carbohydr Res* 332:305–316
- Thakur VK, Kessler MR (2014a) Free radical induced graft copolymerization of ethyl acrylate onto SOY for multifunctional materials. *Mater Today Commun* 1(1–2):34–41
- Thakur VK, Kessler MR (2014b) Synthesis and characterization of AN-g-SOY for sustainable polymer composites. *ACS Sustain Chem Eng* 2(10):2454–2460
- Thakur VK, Thakur MK (2014) Recent advances in graft copolymerization and applications of chitosan: a review. *ACS Sustain Chem Eng* 2(12):2637–2652. doi:10.1021/sc500634p
- Thakur VK, Voicu SI (2016) Recent advances in cellulose and chitosan based membranes for water purification: a concise review. *Carbohydr Polym* 146:148–165
- Thakur VK, Thakur MK, Gupta RK (2013a) Graft copolymers from cellulose: synthesis, characterization and evaluation. *Carbohydr Polym* 97:18–25
- Thakur VK, Singha AS, Thakur MK (2013b) Synthesis of natural cellulose-based graft copolymers using methyl methacrylate as an efficient monomer. *Adv Polym Technol* 32 (S1):E741–E748
- Thakur VK, Thakur MK, Gupta RK (2013c) Graft copolymers from natural polymers using free radical polymerization. *Int J Polym Anal Charact* 18(7):495–503
- Thakur VK, Thakur MK, Gupta RK (2013d) Rapid synthesis of graft copolymers from natural cellulose fibers. *Carbohydr Polym* 98:820–828

- Thakur VK, Singha AS, Thakur MK (2013e) Ecofriendly biocomposites from natural fibers: mechanical and weathering study. *Int J Polym Anal Charact* 18(1):64–72
- Thakur VK, Singha AS, Thakur MK (2013f) Fabrication and physico-chemical properties of high-performance pine needles/green polymer composites. *Int J Polym Mater Polym Biomater* 62(4):226–230
- Thakur VK, Thakur MK, Gupta RK (2014a) Graft copolymers of natural fibers for green composites. *Carbohydr Polym* 104:87–93
- Thakur VK, Thunga M, Madbouly SA, Kessler MR (2014b) PMMA-g-SOY as a sustainable novel dielectric material. *RSC Adv* 4(35):18240–18249
- Thakur MK, Thakur VK, Gupta RK, Pappu A (2016) Synthesis and applications of biodegradable soy based graft copolymers: a review. *ACS Sustain Chem Eng* 4(1):1–17
- Tolaimate A, Desbrieres J, Rhazi M, Alagui A, Vincendon M, Vottero P (2000) On the Influence of deacetylation process on the physicochemical characteristics of chitosan from squid chitin. *Polymer* 41:2463–2469
- Trache D, Hazwan Hussin M, Mohamad Haafiz MK, Kumar Thakur V (2017) Recent progress in cellulose nanocrystals: sources and production. *Nanoscale* 9(5):1763–1786
- Uyama H, Kuwabara M, Tsujimoto T, Kobayashi S (2003) Enzymatic synthesis and curing of biodegradable epoxide-containing polyesters from renewable resources. *Biomacromolecules* 4:211–215
- Viçosa AL, Gomes ACO, Soares BG, Paranhos CM (2009) Effect of sepiolite on the physical properties and swelling behavior of rifampicin-loaded nanocomposite hydrogels. *Express Polym Lett* 3:518–524
- Viseras C, Aguzzi C, Cerezo P, Bedmar MC (2008) Biopolymer-clay nanocomposites for controlled drug delivery. *Mater Sci Technol* 24:1020–1026
- Voicu SI, Condruz RM, Mitran V, Cimpean A, Miculescu F, Andronesu C, Thakur VK (2016) Sericin covalent immobilization onto cellulose acetate membrane for biomedical applications. *ACS Sustain Chem Eng* 4(3):1765–1774
- Wang XH, Wang AQ (2010) Adsorption characteristics of chitosan-g-poly(acrylic acid)/attapulgitic hydrogel composite for Hg(II) ions from aqueous solution. *Sep Sci Technol* 45:2086–2094
- Wang X, Du Y, Yang J, Wang X, Shi X, Hu Y (2006) Preparation, characterization and antimicrobial activity of chitosan/layered silicate nanocomposites. *Polymer* 47:6738–6744
- Wang WB, Zheng YA, Wang AQ (2008) Syntheses and properties of superabsorbent composites based on natural guar gum and attapulgitic. *Polym Adv Technol* 19:1852–1859
- Wang XH, Zheng Y, Wang AQ (2009) Fast removal of copper ions from aqueous solution by chitosan-g-poly(acrylic acid)/attapulgitic composites. *J Hazard Mater* 168:970–977
- Wang B, Mireles K, Rock M, Li Y, Thakur VK, Gao D, Kessler MR (2016) Synthesis and preparation of bio-based ROMP thermosets from functionalized renewable isosorbide derivative. *Macromol Chem Phys* 217(7):871–879
- Wu T, Zivanovic S, Draughon FA, Sams CE (2004) Chitin and chitosan-value-added products from mushroom waste. *J Agric Food Chem* 52:7905–7910
- Xu ZP, Zeng QH, Lu GQ, Yu AB (2006) Inorganic nanoparticles as carriers for efficient cellular delivery. *Chem Eng Sci* 61:1027–1040
- Zhang M, Haga A, Sekiguchi H, Hirano S (2000) Structure of insect chitin isolated from beetle larva cuticle and silkworm (*Bombyx mori*) pupa exuvia. *Int J Biol Macromol* 27:99–105
- Zhou Q, Xanthos M (2008) Nanoclay and crystallinity effects on the hydrolytic degradation of polymers. *Polym Degrad Stab* 93:1450–1459

Chapter 7

Cellulose-Enabled Polylactic Acid (PLA) Nanocomposites: Recent Developments and Emerging Trends

Wei Dan Ding, Muhammad Pervaiz and Mohini Sain

Abstract Environmental consciousness, technology improvement, and stringent regulations have significantly increased the interest of biodegradable polymers in the industry in the past decade and polylactic acid (PLA) represents one of the most promising biopolymers. However, compared to the conventional petroleum-based polymers, owing to its inherent chemistry, PLA has relatively poor mechanical and thermal properties. To broaden its application, it becomes necessary to introduce inorganic/organic fillers into the biopolymer to meet the performance requirements and facilitate the processing. The use of nanoscale fillers is the strategy by exploiting the nature and properties of the nanoparticulates, such as huge surface area per mass, high aspect ratios, and low percolation threshold. Different inorganic particulates (e.g., nanoclay, nanosilica, carbon nanotubes, etc.) have been extensively studied. However, these added nanoparticulates are inorganic and pose considerable health risks from the manufacturing process to their final disposal. In contrast, nanocellulose, produced from renewable resources, has attracted great interest in recent years due to their sustainability and natural abundance. The combination of PLA and nanocelluloses results in a novel class of fully biorenewable resource-based composites. The recent developments and future trends (i.e., processing methods, various properties, and potential applications) of this novel nanocomposite have been discussed in this chapter.

Keywords Cellulose nanofibers · Cellulose nanocrystals · Polylactic acid Nanocomposites · Thermal properties · Crystallization · Barrier properties Mechanical properties

W.D. Ding (✉)

Department of Mechanical and Industrial Engineering, University of Toronto,
Toronto, ON M5S 3G8, Canada
e-mail: wd.ding@mail.utoronto.ca

W.D. Ding · M. Pervaiz · M. Sain

Centre for Biocomposites and Biomaterials Processing, Faculty of Forestry,
University of Toronto, Toronto, ON M5S 3B3, Canada

M. Sain

Centre of Advanced Chemistry, King Abdulaziz University, Jeddah, Saudi Arabia

1 Introduction

Petrochemical-based plastic products have brought numerous benefits in our daily life due to their low density, easy machining and processing, durability, and acceptable performance. However, massive use of these plastics in recent decades has resulted in extraordinary accumulation of plastic waste in landfills and in maritime environments, causing serious disposal and environmental challenges (Pervaiz et al. 2014; Michalska-Požoga et al. 2016). These plastics are usually non-biodegradable (Wang et al. 2016). It takes years to break down in the soil if the waste ends up in landfills. In case of incineration, high costs and serious air pollution are involved (Voicu et al. 2016; Miculescu et al. 2016; Corobea et al. 2016). Either way may pose significant risks to human health and the environment. In light of this, researchers have been pushed to develop biodegradable plastics from renewable resources, such as polylactic acid (PLA), polyhydroxyalkanoates (PHAs), and poly(butylene succinate) (PBS) etc. (Zhang et al. 2012). These polymers can be produced via fermentation process of sugar from renewable feedstock such as corns, sugar beets or animal fat (Drumright et al. 2000; Jacquel et al. 2008; Keshavarz and Roy 2010; Xu and Guo 2010). Among these, PLA has comparable mechanical strength to many petrochemical-based plastics (Auras et al. 2004; Drumright et al. 2000; Jamshidian et al. 2010). Besides, the process improvement has reduced the manufacturing cost of PLA significantly (Drumright et al. 2000; Dusselier et al. 2015; Jamshidian et al. 2010; Vink and Davies 2015), making it relatively inexpensive in the market. Therefore, PLA is considered as one of the most promising alternatives to conventional petrochemical-based plastics. However, PLA has some intrinsic drawbacks (e.g., low heat resistance, slow crystallization rate, brittleness, etc.) which prevent it to be used in wider applications (Drumright et al. 2000; Zhang et al. 2012). To broaden PLA's application, various fillers or reinforcements have been used to tailor its properties, including inorganic (e.g., talc, clay, graphene, carbon nanotubes, etc.) and organic materials (e.g., natural cellulose, other polymers, etc.)

In the context of sustainable biomaterials, natural celluloses are often used as fillers or reinforcements to replace inorganic materials in thermoplastic composites in many fields, including packaging, construction, furniture, and automotive industries (Faruk et al. 2007; Holbery and Houston 2006; Singha and Thakur 2008a, b, c, 2009a, b, c, d). Cellulose is the most abundant organic polymers on earth (Thakur et al. 2013a, b, c, d, e, f; Pappu et al. 2016). It is a linear polysaccharide consisting of many D-glucose monosaccharide units and the major component of cell walls in plants. Cellulose can also be biosynthesized by other living organisms, such as marine animals, algae, bacteria, and fungi (Raquez et al. 2013; Zhao and Li 2014). The basic cellulose chain is schematically shown in Fig. 1. These 30–100 cellulose chains are assembled together to form an elementary fibril (or microfibril), which has a cross-dimensional thickness of 2–5 nm (Ng et al. 2015; Nishiyama 2009; Raquez et al. 2013). The linear cellulose chains are packed in a parallel manner and bonded by Van der Waals forces and inter- and intra-molecular hydrogen bonds (Nishiyama 2009; Raquez et al. 2013; Trache et al. 2017). The

elementary fibrils consist of both crystalline and amorphous regions. In the crystalline region, cellulose chains are highly ordered packed through strong hydrogen bonds; while in the amorphous segments, there are mainly disordered holocellulose segments which bond with crystalline region (Ng et al. 2015; Pappu et al. 2016). The elementary fibrils are aggregated laterally to form large-size fibers. These fibers, including wood flour (WF), cellulose fiber (CF), and microcrystalline cellulose (MCC), have been proposed and used to enhance the performance of the polymers, such as their mechanical strength, heat deflection temperature, thermal properties, crystallization kinetics, biodegradation rate, and foaming behaviors.

Recently, nanocellulose, which has at least one dimension in the range of 1–100 nm, has drawn much attention. The nanocellulose is either a bundle of elementary fibrils or a crystalline rod-like nanoparticle. The bundles of elementary fibrils are commonly known as cellulose nanofibers (or microfibrillated cellulose) and are referred hereafter as CNFs. The crystalline nanoparticles are named as cellulose nanocrystals and are referred hereafter as CNs. A schematic of cellulosic fiber structure from the plant source to nanocellulose is illustrated in Fig. 2. CNFs or CNs have many attractive features such as nanoscale dimension, huge surface area per mass, high mechanical strength, low percolation threshold, and often high aspect ratios (length/width). Compared to micro-size cellulose, nanocellulose can improve the aforementioned plastics' properties much more significantly (Ding et al. 2012, 2014, 2015a, b; Iwatake et al. 2008; Jonoobi et al. 2010; Kose and Kondo 2013; Lee et al. 2014; Mathew et al. 2005, 2006; Matuana and Faruk 2010; Song et al. 2013; Wu et al. 2013). Besides, the potentials of cellulosic nanoparticles have been exploited for some functional applications, such as in electrochemical, optical, cosmetic, and biomedical applications (Charreau et al. 2013; Darder et al. 2007; Domingues et al. 2014; Walther et al. 2011; Yanamala et al. 2014). Since the first introduction of CNFs by Turbak et al. in 1980s (Turbak et al. 1983), a large amount of research work has been carried out on the subject of nanocellulose materials, especially in the past decade. Given the rapid progress in this field, in this chapter, we mainly focus on the recent development of PLA/nanocellulose composites from 2010 to 2015.

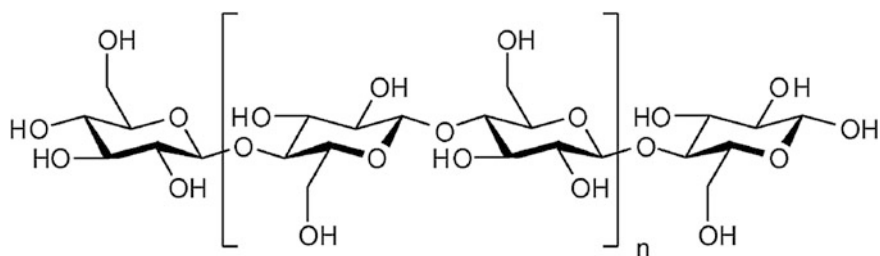


Fig. 1 Chemical structure of cellulose

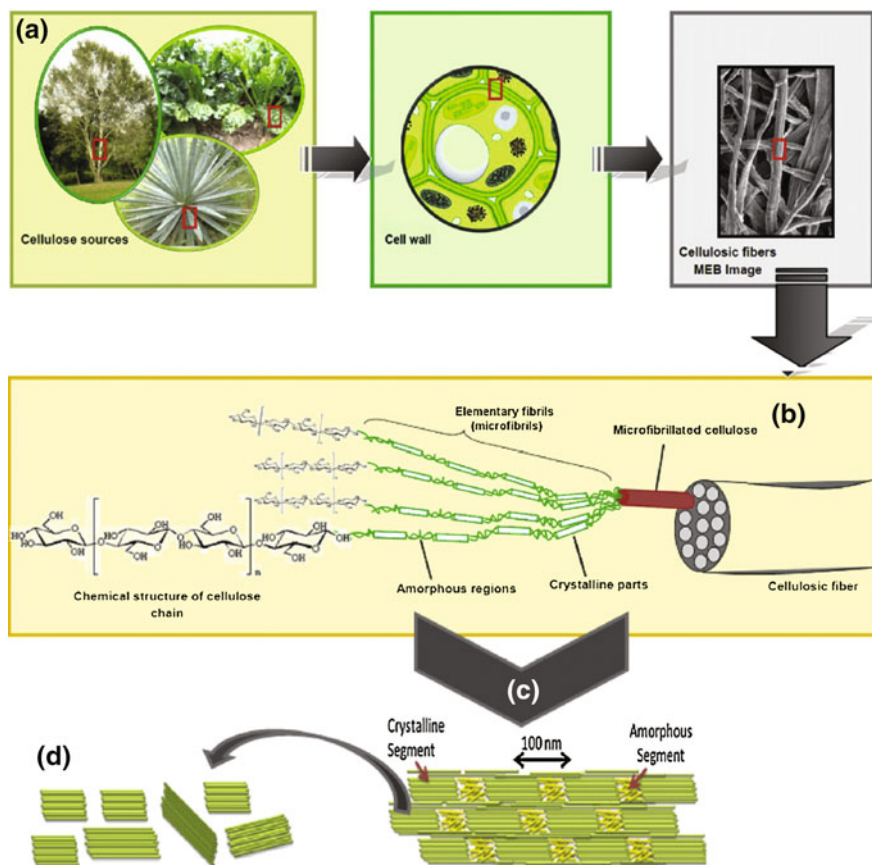


Fig. 2 A schematic of cellulosic fiber structure from the plant to the nanocellulose. Reprinted from Ng et al. (2015), Copyright (2015), with permission from Elsevier

2 Nanocelluloses

2.1 Cellulose Nanofibers (CNFs)

Cellulose nanofibers (CNFs) can be extracted from cellulose fibers in a number of ways including solely mechanical treatment (Chakraborty et al. 2005; Nair and Yan 2015a, b), chemical or enzymatic pretreatment followed by mechanical process (Henriksson et al. 2007; Pääkkö et al. 2007; Saito et al. 2006, 2007; Wågberg et al. 2008) or high-intensity ultrasonication process (Chen et al. 2011a, b, c; Wang and Cheng 2009). In general, solely mechanical defibrillation process requires tremendous shearing force to overcome the strong hydrogen bonding and thus, disintegrate macrofibers into sub-structural fibrils with high aspect ratios. This is a high-energy demanding process. Many techniques had been developed for the fiber

fibrillation process including high pressure homogenizer (Alemdar and Sain 2008b; Nakagaito and Yano 2005; Wang and Sain 2007a), cryocrushing (Alemdar and Sain 2008b; Bhatnagar and Sain 2005), grinder (Abe et al. 2007; Cheng et al. 2014a, b), SuperMassColloider (Nair and Yan 2015a, b), high speed blending (Uetani and Yano 2011), high-intensity ultrasonication (Wang and Cheng 2009), and a combination of two or several above techniques. Despite the high-energy input, it is difficult to obtain individual microfibrils using a solely mechanical process and most of the resultant products consist of bundles of microfibrils. An example of CNF morphology from unbleached lodgepole pine bark after 1, 5, and 15 passes of solely mechanical fibrillation is shown in Fig. 3. To improve the uniform of CNFs' morphology, multiple passes through defibrillation equipment are often needed. However, too high number of passes significantly reduced the degree of crystallinity and the degree of polymerization, thereby enhancing CNFs' thermal expansion and degrading the mechanical properties of their composites (Cheng et al. 2014a; Iwamoto et al. 2008; Panthapulakkal and Sain 2013).

To facilitate the defibrillation process, chemical modification or enzymatic pretreatment prior to the mechanical process has been introduced (Henriksson et al. 2007; Pääkkö et al. 2007; Panthapulakkal and Sain 2013; Saito et al. 2006, 2007; Wågberg et al. 2008). It has been reported that carboxylated cellulose fibers by 2,2,6,6-tetramethylpiperidine-1-oxyl radical (TEMPO) oxidation (Saito et al. 2006, 2007) (Fig. 4a) or carboxymethylated fibers by sodium hydroxide and monochloroacetic acid (Wågberg et al. 2008) helped defibrillation process effectively. The introduced carboxyl or carboxymethyl groups made the surface of microfibrils negatively charged and the electrostatic repulsions reduced the interaction between microfibrils, thus facilitating the disintegration process. Pretreatment of cellulose fibers with sodium hydroxide or enzymatic hydrolysis has also been studied and these treatments assist the homogenizing process to generate CNFs successfully (Bhatnagar and Sain 2005; Cheng et al. 2014a; Henriksson et al. 2007; Pääkkö et al. 2007; Panthapulakkal and Sain 2013). The primary purpose of these pretreatments is to reduce the bonding strength or linkages between microfibrils so that a much lower amount of energy, less number of passes, and less processing time are needed to

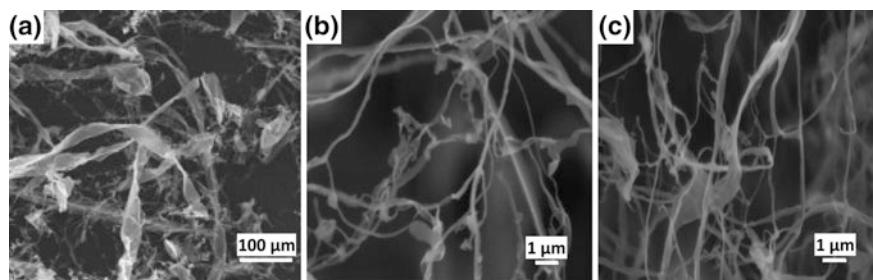


Fig. 3 SEM images of CNFs from unbleached lodgepole pine bark after 1, 5, and 15 passes of mechanical fibrillation. Reprinted from Nair and Yan (2015b), Copyright (2015), with permission from Elsevier

produce CNFs (Saito et al. 2006, 2007). Individual microfibrils with uniform lateral size are often produced in this manner (Pääkkö et al. 2007; Saito et al. 2006, 2007; Wågberg et al. 2008). After chemical treatment, high-intensity ultrasonication has also been developed to manufacture CNFs. The high-frequency ultrasound transfers energy to the cellulose fibers by acoustic cavitation (Chen et al. 2011a, b, c). The violent collapse of micro-voids generates micro-jets or shock waves on the surface of the fibers, which lead to a gradual disintegration (Chen et al. 2011a, c). The transferred energy is in the range of hydrogen bonding energy, about 10–100 kJ/mol (Chen et al. 2011a).

Depending on the biological origin of cellulose fiber, the pretreatment, and the number of defibrillation passes through the machine, the CNFs' morphology (i.e., the diameter and aspect ratio), degree of crystallinity, and chemical compositions are different. Figure 5 shows some examples of CNFs extracted from different sources.

2.2 Cellulose Nanocrystals (CNs)

CNFs consist of long-ordered crystalline segment and shorter disordered amorphous segments. Compared to the crystalline segments, the amorphous segments have a loosely packed structure which endows them a lower density and greater chance for hydroxyl groups to react with other molecules. Upon contact with strong acid, amorphous segments are more susceptible to hydrolysis, whereas crystalline domains remain intact since they have a higher resistance to the acid attack (Habibi et al. 2010; Vazquez et al. 2015). Acid hydrolysis of the amorphous segments involves a rapid decrease of the degree of polymerization (Habibi et al. 2010). Thus, by taking advantage of their differences in chemical resistance, researchers can isolate rod-like cellulose nanocrystals (CNs) with high degree of crystallinity from cellulose fibers by a combination of acid hydrolysis and mechanical refining. The CNs, also called nanocrystalline cellulose or cellulose whiskers, in general, have diameters in the range of 2–20 nm and lengths of tens of nanometers to

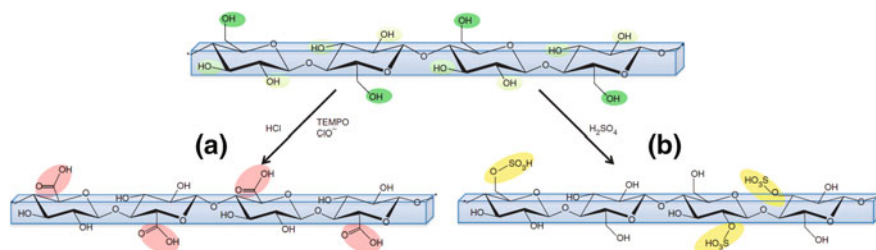


Fig. 4 Schematic of **a** TEMPO-mediated oxidation process and **b** the hydrolysis with sulfuric acid for producing nanocelluloses. Reprinted by permission from Macmillan Publishers Ltd: [NPG Asia Materials] (Lagerwall et al. 2014), Copyright (2014)

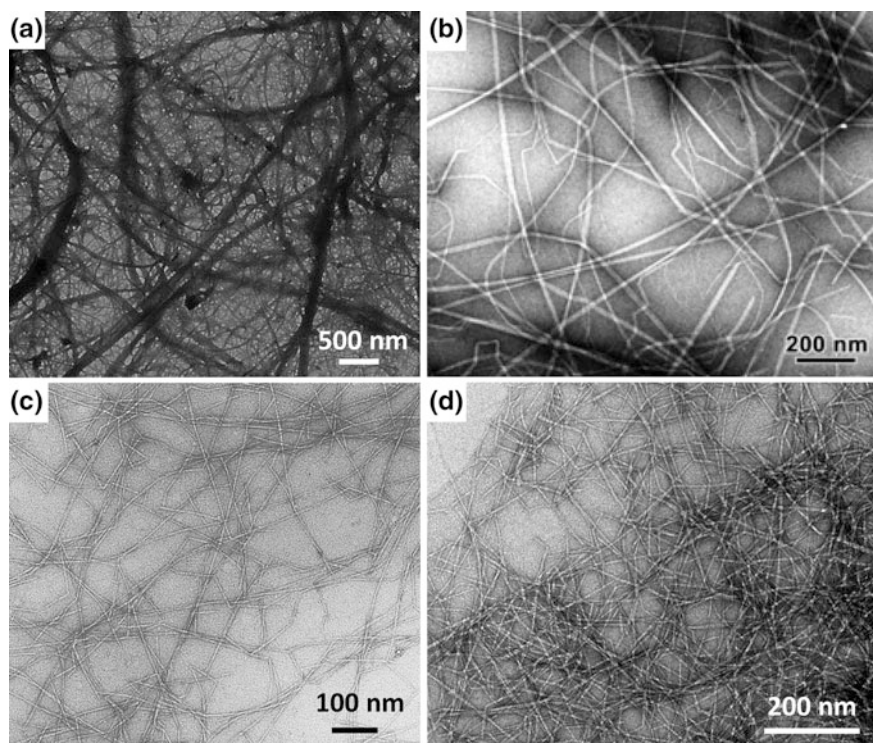


Fig. 5 Transmission Electron Micrographs of CNFs extracted from different sources by various treatments prior to the mechanical process, **a** sodium hydroxide treated wheat straw. Reprinted from Alemdar and Sain (2008a), Copyright 2008, with permission from Elsevier; **b** TEMPO oxidized tunicin. Reprinted with permission from Saito et al. (2006), Copyright (2006) American Chemical Society; **c** TEMPO oxidized hardwood bleached kraft pulp. Reprinted with permission from Saito et al. (2007), Copyright (2007) American Chemical Society; and **d** enzymatic treated softwood pulp. Reprinted with permission from Wågberg et al. (2008), Copyright (2008) American Chemical Society

several micrometers depending on the source of the cellulose fibers and extraction conditions (Beck-Candanedo et al. 2005; Habibi et al. 2010; Ng et al. 2015). Typical geometrical characteristics and morphologies of CNs extracted from different sources by various techniques are summarized in Table 1 and Fig. 6, respectively. The acid types (hydrochloric vs. sulfuric), acid concentration, hydrolysis reaction condition (temperature and time), mixing condition (agitation speed and time) can affect the final dimensions, morphologies, and surface charges of CNs. For instance, if the CNs is prepared through hydrochloric acid hydrolysis, their aqueous suspension tends to flocculate (Habibi et al. 2010; Raquez et al. 2013). In the case of sulfuric acid, the formed negatively charged sulfate esters on CNs' surface through the reaction between the sulfuric acid and hydroxyl groups of cellulose can facilitate their dispersion in water (Fig. 4b) (Habibi et al. 2010;

Raquez et al. 2013). Consequently, sulfuric acid has been extensively used for CN production in most studies. Many raw materials have been used for producing CNs includes wood pulp, ramie, sisal, cotton, MCC, bacterial cellulose, and tunicates. The CNs from plants often has short lengths compared to the ones from bacterial cellulose and tunicate (Araki and Kuga 2001; Elazzouzi-Hafraoui et al. 2008). It has also been reported that CNs from plant are needle-shaped, while tunicate CNs exhibited a ribbon-like shape and a kinked structure (Elazzouzi-Hafraoui et al. 2008). The aspect ratios of NCs are normally lower than that of CNFs and span a broad range from 10 for cotton to around 100 for tunicate. The aspect ratio and the length are important parameters governing their reinforcement capacity in polymers. These will be discussed in the following sections.

Table 1 Examples of the dimensions of cellulose nanocrystals from various sources by different techniques

Source	Length (nm)	Diameter (nm)	Technique	References
Wood	100–200	10	Sulfuric acid/TEM	Landry et al. (2011)
	195–470	2–5	Hydrochloric acid/AFM and TEM	Salajková et al. (2012)
	100–300	3–5	Sulfuric acid/AFM	Beck-Candanedo et al. (2005)
MCC	195–290	7–12	Sulfuric acid/FESEM	Espino-Pérez et al. (2013)
Ramie	75–190	6–15	Sulfuric acid/TEM	Junior de Menezes et al. (2009)
	150–250	6–8	Sulfuric acid/TEM	Habibi et al. (2008)
Sisal	50–600	2–7	Sulfuric acid/TEM	Garcia de Rodriguez et al. (2006)
	150–280	3.5–6.5	Sulfuric acid/TEM	Siqueira et al. (2009)
Cotton	100–300	10–30	Sulfuric acid/AFM	Lin and Dufresne (2014)
	200–300	10–20	Sulfuric acid/TEM	Lin et al. (2011, 2015)
	150–250	10–20	Sulfuric acid/TEM	Hu et al. (2015)
Tunicate	500–2000	~ 10	Sulfuric acid/TEM	Anglès and Dufresne (2000)
	400—a few micron	16–23	Enzymatic, TEMPO, sulfuric acid/AFM and SEM	Zhao et al. (2015)
Bacterial cellulose	100–2000	10–40	Sulfuric acid/TEM	Araki and Kuga (2001)
Bagasse	350 ± 153	33 ± 13	Sulfuric acid/AFM	Robles et al. (2015)

3 Poly(lactic Acid) (PLA)

Poly(lactic acid) (PLA) is a bio-based, linear aliphatic polyester derived entirely from annually renewable resources such as corn starch and sugar beets (Drumright et al. 2000). Compared to traditional petrochemical-based plastics (e.g., polypropylene (PP), low-density polyethylene, polystyrene (PS), nylon, etc.), PLA consumes 50% less nonrenewable energy during production and is readily biodegradable for waste disposal purposes (Vink and Davies 2015). PLA has good physical and mechanical properties which are comparable to many petrochemical-based plastics (Auras et al. 2004; Drumright et al. 2000; Jamshidian et al. 2010). Meanwhile, improvements in PLA manufacturing processes have made it a commercially available and large-volume plastic at competitive market prices (Drumright et al. 2000; Jamshidian et al. 2010; Vink et al. 2004). The current industrial practice for producing high-molecular weight PLA is ring-opening polymerization of lactide (Fig. 7). It consists of: (1) polycondensation of aqueous lactic acid to produce

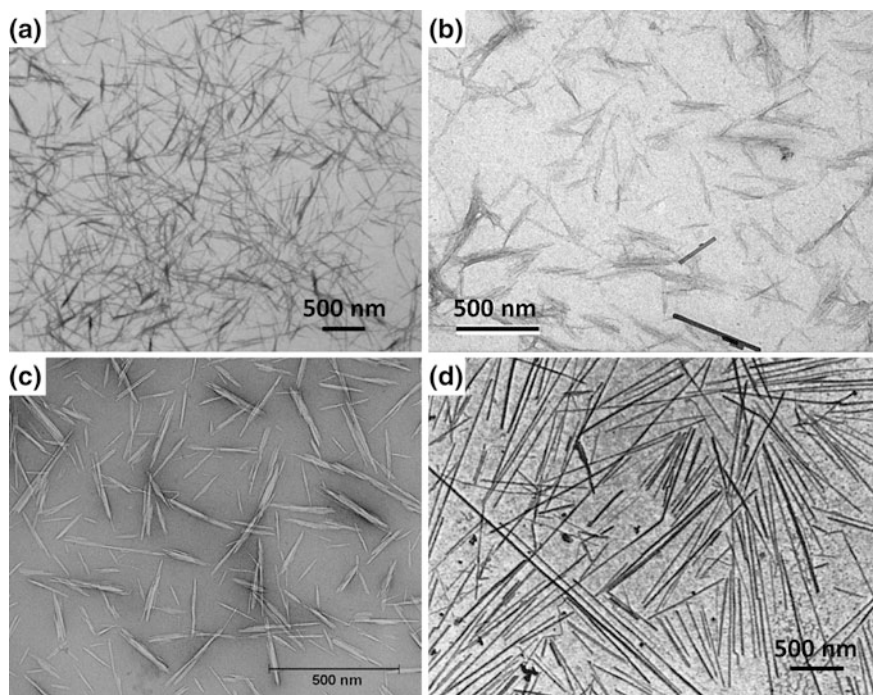


Fig. 6 Transmission Electron Micrographs of CNFs extracted from different sources: **a** softwood pulp. Reproduced from Salajková et al. (2012) with permission from RSC; **b** cotton. Reprinted from Lin et al. (2015), Copyright 2015, with permission from Springer Publishing; **c** Ramie. Reprinted from Junior de Menezes et al. (2009), Copyright (2009), with permission from Elsevier; and **d** Tunicate. Reprinted with permission from Anglès and Dufresne (2000), Copyright (2000) American Chemical Society.

low-molecular weight PLA prepolymer; and (2) depolymerization of the prepolymer into a mixture of lactide stereoisomers prior to ring-opening lactide polymerization (Drumright et al. 2000; Dusselier et al. 2015; Jamshidian et al. 2010). This two-step process is relatively time- and energy-intensive and involves strenuous downstream purification. Recently, a direct zeolite-based catalytic process which converts aqueous lactic acid to lactide has been proposed (Dusselier et al. 2015). It is forecasted that the highly productive process can further simplify PLA's manufacturing process and thereby, improving the production efficiency and reducing the cost (Dusselier et al. 2015). PLA has become one of the most promising sustainable alternatives to its petrochemical-based counterparts and is suitable for a wide range of products including food packaging, nonwoven fabrics, and electronics (Auras et al. 2004; Jamshidian et al. 2010; Vink et al. 2004). It has also been widely used in biomedical applications due to its biodegradability and biocompatibility (Auras et al. 2004; Ma et al. 2011).

Due to an asymmetric carbon atom, the monomer, lactic acid has two stereoisomeric forms, L-lactic acid and D-lactic acid. Consequently, three stereoisomers of lactide can be generated, namely L-lactide, D-lactide, and meso-lactide (a combination of one L- and one D-lactic acid) (Saeidlou et al. 2012). The polymers synthesized from pure L- or pure D-lactide are referred to as PLLA or PDLA; while polymerization of a mixture of L- and D-lactide (at least 10% or more in one stereoisomer content) usually leads to a fully amorphous PLA. The industrial production of lactic acid is generally through bacterial homofermentation of carbohydrates since the homofermentative method yields L-lactic acid predominately and low level of by-products (Jamshidian et al. 2010). Most commercial grades of PLA are usually L-rich mixture

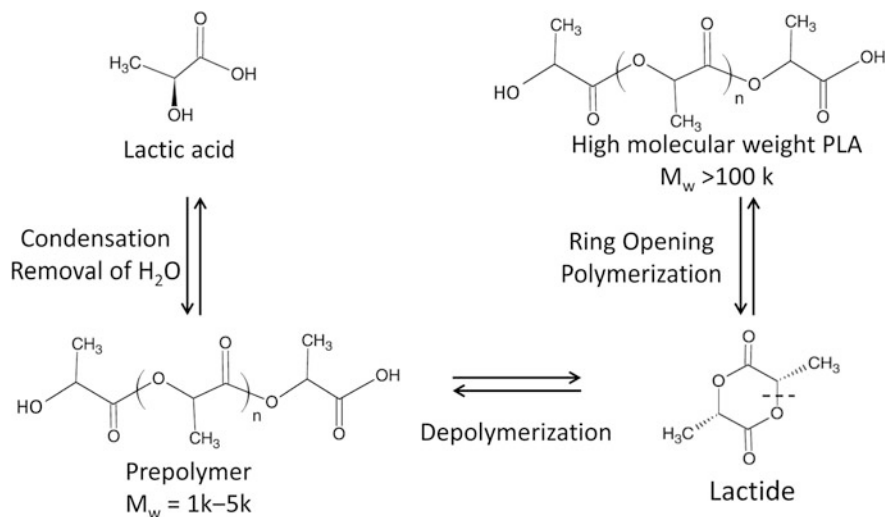


Fig. 7 Schematic of PLA production via ring-opening polymerization process Reprinted from Drumright et al. 2000, Copyright (2000), with permission from John Wiley & Sons Publisher

with D-unit content range of 1–5%. These PLAs are semicrystalline polymers. The mechanical properties, degradation rate, and thermal properties of PLA can be tailored to a large extent based on the stereochemistry. A semicrystalline PLA can be crystallized to various degrees of crystallinity depending on the processing conditions. Compared with PDLLA, semicrystalline PLLA has higher tensile strength and modulus (2.7 vs. 1.9 GPa), and lower elongation because formed crystallites (highly ordered molecular chains) act as crosslinks between chains (Middleton and Tipton 2000). The homopolymer PLLA has a longer degradation time of the order of over 2 years, whereas amorphous PDLLA has only 12–16 months (Middleton and Tipton 2000). The co-crystallization of PLLA and PDLA can form a stereocomplex with a melting point around 220 °C, which is about 50 °C higher than PLA homopolymer (Saeidlou et al. 2012).

4 PLA/Nanocellulose Biocomposites

4.1 Processing Techniques

The incorporation of nanocelluloses in PLA not only endows the resulting composites with fully biodegradable properties, but also gives those significantly improved mechanical properties, enhanced crystallization, and rheological and thermal properties over the neat PLA. The improvements on these properties have been largely dependent on the nanocomposite preparation methods. Various methods have been developed to disperse the nanocelluloses in PLA. In general, these methods can be classified into three categories: solvent casting, emulsion filtration/freeze drying, and direct melt-compounding process. Table 2 shows some examples of the processing methods and surface functionalization methods that have been used for CNFs/CNs in PLA nanocomposite preparation conducted between 2011 and 2015.

4.1.1 Solvent Casting

Solvent casting is one of the most common methods used to produce the PLA/nanocellulose biocomposites. In this process, solvent exchange method is first applied to aqueous nanocelluloses to extract CNFs/CNs by a series of centrifuging and re-dispersing processes. The solvent(s) should be miscible with water and can dissolve PLA resin, such as acetone (Ding et al. 2015a, b; Dlouhá et al. 2012; Jonoobi et al. 2010), dichloromethane (Lin et al. 2009; Suryanegara et al. 2009), or chloroform (Braun et al. 2012; Espino-Pérez et al. 2013; Fortunati et al. 2012a; Fujisawa et al. 2013; Liu et al. 2010; Lizundia et al. 2015; Pei et al. 2010; Petersson et al. 2007; Tingaut et al. 2010). The PLA resin is then added into the nanocellulose solvent suspension to produce a homogeneous mixture. After, the mixture is casted

Table 2 Examples of processing methods and surface functionalization of CNFs/CNs in PLA nanocomposite preparation conducted between 2011 and 2015

CNF/CN	Treatment	Fabrication method	Investigated properties	References
CNF	Untreated	Solvent casting	Foaming, rheological and thermal properties	Ding et al. (2015a)
CNF	Untreated	Solvent casting	Thermal properties	Ding et al. (2015b)
CNF	Untreated	Direct melt blending (liquid feeding)	Tensile and thermal properties	Herrera et al. (2015)
CNF	Acetylation	Solvent casting	Foaming, rheological and tensile properties	Dlouhá et al. (2012, 2014)
CNF	Acetylation	Solvent casting	Tensile and thermal properties, WVP	Abdulkhani et al. (2014)
CNF	PEG-grafted	Solvent casting	Tensile and thermal properties	Fujisawa et al. (2013)
CNF	Untreated	Emulsion filtration	Crystallization	Kose and Kondo (2013)
CNF	Silanization	Direct melt blending (dry feeding)	Thermal properties	Frone et al. (2013)
CNF	Acetylation	Solvent casting followed by melt blending	Tensile and thermal properties, DMA, contact angle	Jonoobi et al. (2012)
CNF	Carboxymethylation	Solvent casting followed by melt blending	Tensile properties, DMTA, MFI	Eyholzer et al. (2012)
CNF	Silanization	Solvent casting	Tensile and thermal properties	Qu et al. (2012)
CNF	Untreated	Emulsion filtration	Flexural and thermal properties, DMTA	Wang and Drzal (2012)
CNF	Untreated	Emulsion filtration followed by melt blending	Foaming behavior	Boissard et al. (2012)
CNF	Untreated	Solvent casting followed by melt blending	Thermal properties, DMTA, crystallization	Kowalczyk et al. (2011)
CN	PLLA-grafted	Solvent casting	Thermal properties	Lizundia et al. (2015)
CN	Esterification	Oven-dried CNs and melt blending	Thermal properties, DMTA, HDT	Spinella et al. (2015)
CN	Esterification	Oven-dried CNs and melt blending	Thermal and tensile properties	Robles et al. (2015)
CN	GMA-grafted	Oven-dried CNs and melt blending		Pracella et al. (2014)

(continued)

Table 2 (continued)

CNF/CN	Treatment	Fabrication method	Investigated properties	References
			Thermal and mechanical properties, DMTA	
CN	ICN-grafted	Solvent casting	Thermal and tensile properties, barrier properties	Espino-Pérez et al. (2013)
CN	Acetylation	Oven-dried CNs and melt blending	Interfacial tension	Khoshkava and Kamal (2013)
CN	PDLA-grafted	Oven-dried CNs and melt blending	Thermal properties, DMTA	Habibi et al. (2013)
CN	Acetylation and PLLA-grafted	Solvent casting	Crystallization, DMTA	Braun et al. (2012)
CN	Surfactant-coated	Solvent casting	Thermal and tensile properties, DMA	Fortunati et al. (2012a)
CN	Surfactant-coated	Solvent casting	Barrier and migration properties	Fortunati et al. (2012b)
CN	PLLA-grafted	Oven-dried CNs and melt blending	Thermal property, DMTA	Goffin et al. (2011)
CN	Acetylation	Oven-dried CNs and solvent casting	DMTA, Tensile, contact angle	Lin et al. (2011)

DMTA dynamic mechanical thermal analysis, *GMA* glycidyl methacrylate, *ICN* *n*-octadecyl isocyanate, *MFI* melt flow index, *PEG* poly(ethylene glycol), *WVP* water vapor permeability

on a flat surface and dried. Finally, the dried PLA/nanocellulose composites are hot-pressed to the specimen size for various experiments or serve as masterbatch for melt-compounding process. Due to the solvent exchange process and some pre-treatments on the nanocelluloses, CNFs/CNs can be well dispersed in the polymer matrix without many agglomerations (Iwatake et al. 2008). As a result, the effect of these nanocelluloses on the thermal and mechanical properties of PLA is more pronounced than that from direct mixing methods (Iwatake et al. 2008). Solvent casting method is normally used to develop an understanding of PLA/CNF(CN) composites and can provide valuable insights into the continuous processes. However, this approach is impractical due to a large quantity of solvent required and a long processing time.

4.1.2 Emulsion Filtration/Emulsion Freeze-Drying

Emulsion filtration/Emulsion freeze-drying has also been explored to mix PLA microparticles with nanocelluloses (Kose and Kondo 2013; Nakagaito et al. 2009; Wang and Drzal 2012). In general, a low-molecular weight PLA is used to produce

the particles or fibers with diameters below 15 μm (Nakagaito et al. 2009; Wang and Drzal 2012). These PLA microparticles are added to aqueous nanocellulose suspension to obtain an emulsion. The emulsion is then filtered with a sieve/membrane, similar to a papermaking process (Boissard et al. 2012; Nakagaito et al. 2009; Wang and Drzal 2012), or freeze-dried (Kose and Kondo 2013). These thin films can be stacked and hot-pressed to make composite with various thicknesses. In general, water is used as the mixing medium, no solvent or only a small amount is involved in this process. Also, higher nanocellulose content composites can be produced using this method. Consequently, the mechanical properties can be improved substantially. Due to the presence of water during the filtration process, CNFs are connected by strong hydrogen bonding and also by mutual entanglement (Nakagaito et al. 2009). This is one of the main reasons that, at the same fiber content, emulsion filtration method offers higher reinforcing efficiency in comparison with solvent casting method.

4.1.3 Direct Melt-Compounding

For industrial-scale production, direct melt-compounding of PLA and nanocelluloses is preferred due to simplified procedure and economic purpose. Melt compounding is a traditional processing technique to produce polymer composites and it is a cheap and fast processing method. The idea is to feed the dried nanocellulose particles or pump the nanocellulose suspension directly into the PLA melt during extrusion process. To obtain CNFs/CNs in dried form, surface modification of CNFs/CNs is often required prior to drying processes (freeze or oven drying) (Eyholzer et al. 2012; Frone et al. 2013; Goffin et al. 2011; Habibi et al. 2013; Robles et al. 2015; Spinella et al. 2015; Wang and Sain 2007b). The surface modification is to improve the compatibility between the CNFs/CNs and polymer matrix, improve the fiber dispersion in the matrix, and prevent the irreversible agglomeration of CNFs/CNs upon drying, thereby, enhancing the properties of the resultant composites. In general, the reinforcing efficiency of the nanocelluloses is dependent on many factors including functionality of the chemicals used, degree of substitution, nanoparticulate morphology, and processing conditions. For dried CNF/CN particles, one of the challenges is how to feed them into the extruder. The dried particles are lightweight and fluffy, which make accurate feeding problematic.

The concept of direct liquid feeding is more appealing than dry feeding from a cost perspective. The drying processes in the dry feeding, such as freeze-drying or vacuum oven drying, involve additional cost for time, equipment, and energy input. In liquid feeding, water, solvent, plasticizer or a combination of those are used as the dispersing medium (Herrera et al. 2015; Oksman et al. 2006). The selected liquid medium must not degrade PLA during the process. The nanocellulose solution is pumped directly into the polymer melt in the extruder. If the dispersing medium includes water or solvent, they should be removed later during the process. Figure 8 shows a schematic of the extrusion process using liquid feeding. In the process, co-rotating twin-screw extruders (TSE) are often selected over

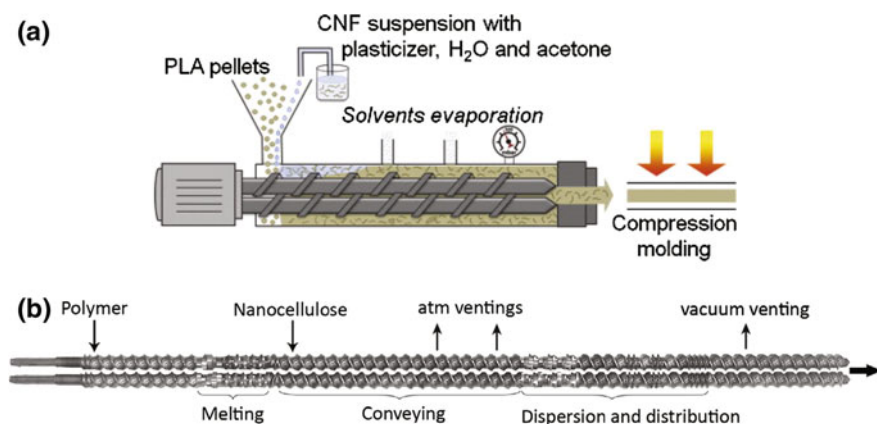


Fig. 8 **a** Schematic illustration of liquid feeding during compounding process. Reprinted from Herrera et al. (2015), Copyright (2015), with permission from Elsevier; and **b** screw configuration of the twin-screw extruder for different processing zones. Reprinted from Oksman et al. (2016), Copyright (2016), with permission from Elsevier

counter-rotating extruders because of their flexible screw design and arrangement of the processing zone, resulting in better dispersion and distribution (Oksman et al. 2006; Oksman and Mathew 2014).

Direct liquid feeding shows a great promise for large-scale manufacturing of PLA/nanocellulose composites. However, it presents several challenges: (i) feeding the CNF/CN solution into extruder; (ii) dispersing and distribution of nanocelluloses in the polymer matrix; (iii) avoiding the thermal degradation of the polymer and fibers, and (iv) removing the water and/or solvent efficiently during the process. So far only a few researchers have studied the direct mixing using liquid feeding to produce the cellulose nanocomposites (Herrera et al. 2015; Iwatake et al. 2008; Oksman et al. 2006). Oksman et al. was the first research group to study the feasibility of using direct liquid feeding during the melt-compounding process with the aim to develop a large-scale production of cellulose nanocomposites (Oksman et al. 2006). CN suspension, pretreated with swelling/separation agents of *N, N*-Dimethyl acetamide (DMAc) and lithium chloride (LiCl), was pumped into the TSE. PEG and maleated PLA (PLA-MA) were also added as a processing aid and compatibilizer during the process, respectively. Compared to the nanocomposites prepared by solvent casting, the CNFs or CNs were only partially dispersed in the PLA matrix at a low filler content (1–10 wt%) from direct mixing and many agglomerations were observed (Herrera et al. 2015; Iwatake et al. 2008; Oksman et al. 2006), as shown in Fig. 9.

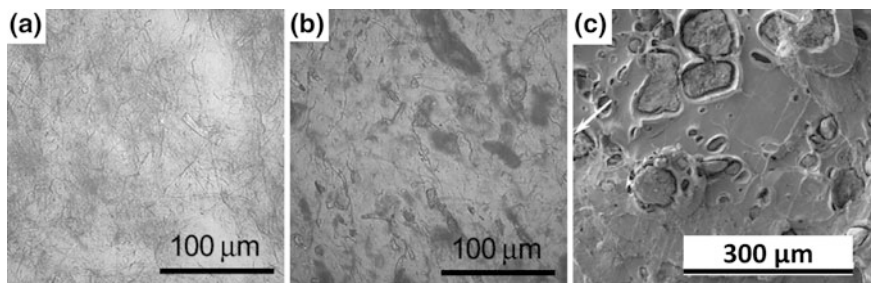


Fig. 9 Micrographs of PLA/CNF composites prepared by **a** solvent casting method and **b** direct mixing method. Reprinted from Iwatake et al. (2008), Copyright (2008), with permission from Elsevier; and **c** direct feeding with oven-dried carboxymethylated CNFs. Reprinted from Eyholzer et al. (2012), Copyright 2012, with permission from Springer Publishing

4.2 Properties of PLA/Nanocellulose Biocomposites

4.2.1 Thermal Properties

One of the goals is to broaden service temperature range where PLA can be used when incorporating nanocelluloses into PLA. Thermogravimetric analysis (TGA), differential scanning calorimeter (DSC), and dynamic mechanical thermal analysis (DMTA) are normally used to investigate the thermal properties of nanocelluloses and their PLA nanocomposites. As aforementioned, due to different pretreatments prior to the defibrillation process, the onset degradation temperature for CNFs is higher than that of CNs (~ 290 °C vs. 240 °C) (Alemdar and Sain 2008a; Spinella et al. 2015; Tingaut et al. 2010). The sulfuric acid hydrolysis results in decreased thermal stabilities of CNs due to the presence of acid sulfate groups on their surface (Habibi et al. 2010; Roman and Winter 2004). However, if the CNs are prepared using hydrochloric acid, the thermal stability is improved, e.g., compared to the CNs prepared from sulfuric acid, around 30 °C higher in thermal degradation temperature was found at first 10% of the material had decomposed (Spinella et al. 2015). The surface treatment can also affect the thermal stability of the nanocelluloses. Tingaut et al. revealed that acetylation enhanced the thermal stability of the CNFs considerably and the temperature at 5% weight loss increased with the acetyl content up to 10.5 wt% (55 °C increment) (Tingaut et al. 2010); while Jonoobi et al. discovered that acetylated CNFs started to degrade earlier (~ 20 °C) than the untreated ones and attributed the decrease to the lower degree of crystallinity by the acetylation process (Jonoobi et al. 2012). Silanization of CNFs seems to have little influence on the onset decomposition temperature (Qu et al. 2012). However, the surface modification by surfactant coating and esterification has been found to improve the thermal stability of the CNs. Compared to the untreated CNs, the BeycoStat A B09 surfactant treated CNs started to degrade at a much higher temperature (~ 40 °C higher) (Pettersson et al. 2007). The esterified CNs with lactic

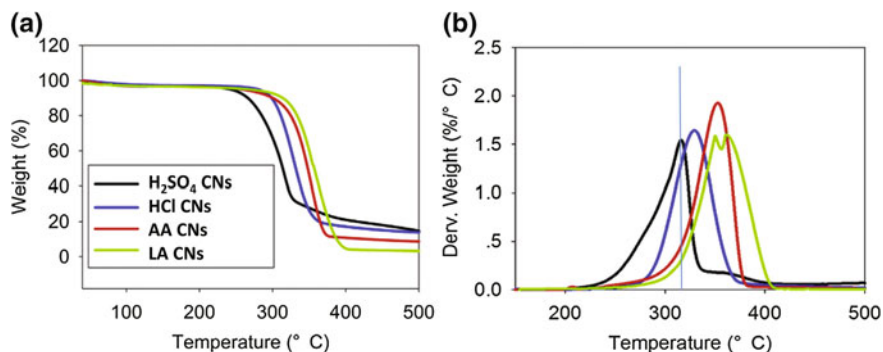


Fig. 10 Thermal stability of sulfuric acid (*dark*) and hydrochloric acid (*blue*) hydrolyzed CNs, and CNs after acetic acid (*red*) and lactic acid (*green*) surface treatment. Reprinted from Spinella et al. (2015), Copyright (2015), with permission from Elsevier

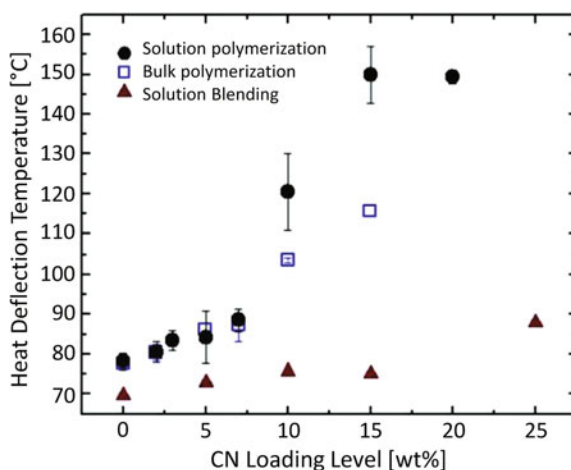
acid (LA) can further increase their thermal stability by 15 °C, but only a slight improvement with acetic acid (AA) (Fig. 10) (Spinella et al. 2015).

Generally, the incorporation of untreated (Ding et al. 2015a, b; Frone et al. 2013; Wang and Drzal 2012), silanized (Frone et al. 2013; Robles et al. 2015), or esterified (Abdulkhani et al. 2014; Espino-Pérez et al. 2013; Lin et al. 2011) nanocelluloses at low loading levels have very limited influences on the glass transition temperature (T_g) of PLA at the atmospheric pressure. In these studies, either no significant or only slight improvements in T_g (<2 °C) were observed due to the inhabitation of PLA chains' motion by well-dispersion CNs. Despite a better dispersion of CNs in the PLA matrix, the chemical treatments by surfactant coating and polymer grafting generally have a negative effect on PLA's T_g . The higher content of these surfactants or grafted polymers, the greater decrease of T_g is shown. Fortunati et al. showed a decrease up to 11 °C in PLA's T_g when 5 wt% Beycostat A B09 surfactant-coated CNs were added in PLA (Fortunati et al. 2012a). Incorporation of a low-molecular-weight polymer grafted nanocelluloses into PLA also decreases T_g , for instance, over 5 °C decrease was found when 8 wt% of polycaprolactone (PCL)-grafted CNs (85 wt% PCL) were added (Lin et al. 2009), 4 °C for 3 wt% glycidyl methacrylate (GMA)-grafted CNs (63 wt% GMA) (Pracella et al. 2014), around 5 °C for 0.1–1 wt% PEG-grafted CNFs (Fujisawa et al. 2013), and 7 °C for 8 wt% PLLA-grafted CNs (14 wt% PLA) (Goffin et al. 2011) compared to their unreinforced counterparts. Although PDLA-grafted CNs helped to form the stereocomplex when mixed with PLLA, a decrease in T_g (3 °C) was still observed (Habibi et al. 2013). These results suggest that the motion of PLA segments in the amorphous region is improved by the presence of low-molecular-weight grafted polymers or oligomers which act as plasticizers (Goffin et al. 2011; Lin et al. 2009). When a large amount of plasticizer (20 wt%) was used to assist the dispersion of CNFs into PLA during the melt compounding, the T_g was not even detected (Herrera et al. 2015). The α relaxation temperature at loss (Tan δ) peak from dynamic mechanical thermal analysis corroborated the T_g measured from DSC. The addition of surfactant in the PLA/nanocellulose composites affected Tan δ peak

position, which was shifted towards lower temperatures with increased surfactant content (Bondeson and Oksman 2007). 10 wt% Beycostat A B09 surfactant showed a threefold decrease in molecular weight compared to the neat PLA under the same processing condition (Bondeson and Oksman 2007). It is believed that the surfactant not only degrades the PLA, but also facilitates the segmental mobility of the polymer chains (Bondeson and Oksman 2007). $\tan \delta$ of PLA was also shifted to a lower temperature when PCL or PLLA was used to graft CNs prior to being mixed with PLA matrix, indicating the improvement of the motion for the PLA segments by PCL and PLLA component (Goffin et al. 2011; Lin et al. 2009).

One of the major drawbacks prohibiting PLA's usage at high temperature is its low heat deflection temperature (HDT) which is around 55–60 °C. The esterified CNs with lactic acid (LA-CNs) has been reported to increase PLA's HDT. The HDT was increased from 55 °C for the neat PLA to 65 °C when 5 wt% LA-CNs were added and the value was further increased to 75 °C at 20 wt% (Spinella et al. 2015). It is attributed to the better dispersion of CNs and enhanced interfacial adhesion between PLA matrix and LA-CNs even at high CN content. The surface grafted high-molecular-weight PLA had a much profound impact on PLA's HDT. The HDTs were increased to 120 and 150 °C, which were more than 40 and 70 °C increment, when 10 and 15 wt% CNs were added, respectively, (Braun et al. 2012) (Fig. 11). However, increasing the CNs to 20 wt% did not further enhance the heat resistance. The HDT change is also associated with the composite preparation method which determines the distribution and dispersion quality of CNs in PLA. Solution polymerized nanocomposites showed significant higher HDTs than the bulk polymerized ones. Individualization of CNs is the key factor contributing to the exceptional increase in PLA's heat resistance. The author speculated that, during the solution polymerization process, CNs formed a percolating network which improved the modulus substantially in the temperature range of 40–160 °C (Braun et al. 2012). Both studies showed that the increase in HDT

Fig. 11 Heat deflection temperature as a function of CN content for PLA nanocomposites prepared by in situ polymerization in solution and bulk compared with solution-blended nanocomposites. Reprinted with permission from Braun et al. (2012), Copyright (2012) American Chemical Society



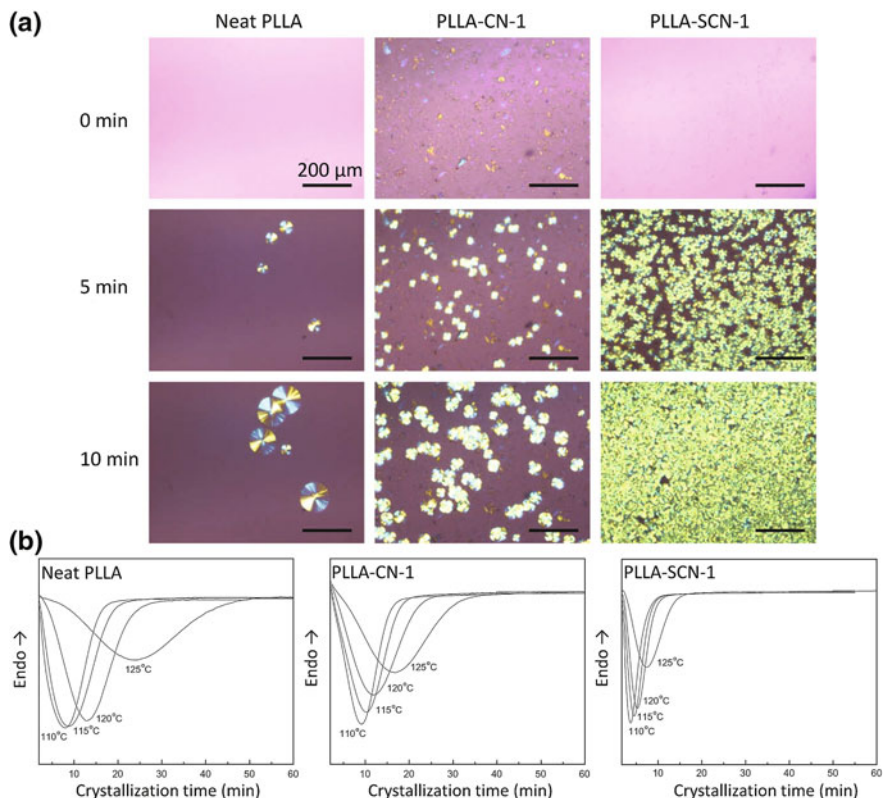


Fig. 12 **a** Polarized optical microscope images of neat PLLA, PLLA-CN-1 (1 wt%) and PLLA-SCN-1 (silylated, 1 wt%) at isothermal crystallization of 125 °C after 5 and 10 min (quenching from the 210 °C). **b** isothermal crystallization exotherms of neat PLLA, PLLA-CN-1, and PLLA-SCN-1 at various crystallization temperatures. Reprinted from Pei et al. (2010), Copyright (2010), with permission from Elsevier

was highly dependent on the nanocellulose content. A linear relationship with a high regression coefficient ($r^2 = 0.994$) was established between HDT and CN content (Spinella et al. 2015).

4.2.2 Crystallization Behaviors

Slow crystallization rate is another drawback of PLA. In general, the incorporation of nanocelluloses promotes PLA's crystallization significantly. These nanocelluloses serve as heterogeneous crystal nucleating agents to accelerate the crystallization process by providing more number of crystal nuclei and decreasing crystallization half-time (Ding et al. 2015a, b; Espino-Pérez et al. 2013; Frone et al. 2013; Habibi et al. 2013; Kamal and Khoshkava 2015; Kose and Kondo 2013; Pei et al. 2010;

Song et al. 2013) (Fig. 12). Kamal and Khoshkava reported that PLA's crystallization time was reduced remarkably to 10 min from 30 min by the addition of 1.5 wt% of spray freeze-dried CNs and the $t_{1/2}$ showed a 5–8 fold decrease during the isothermal crystallization process between 100 and 120 °C (Kamal and Khoshkava 2015). 1 wt% surface silylated CNs increased PLA's crystallinity significantly, from 14.3 to 30.4% (Pei et al. 2010). This result is comparable to the PLA composites containing 25 wt% micro-size cellulose fibers where an increase from 19.2 to 35.3% was reported (Mathew et al. 2006). Due to the slow crystallization nature of PLA, the final crystallinity during the non-isothermal crystallization process is affected by the cooling rate and nanocellulose content. Adding even 0.5 wt% CNFs in PLA increased the crystallinity from 8.2% for the neat PLA to 31.4% at 1 °C/min cooling rate (Ding et al. 2015b). Incorporating PDLA-grafted CNs into PLLA could co-crystallize and form a stereocomplexation which showed a single melting peak at 202 °C compared to a melting temperature (T_m) of 150 °C for the neat PLLA (Habibi et al. 2013). When the PDLA-grafted CNs was increased from 2.5 to 10 wt%, the cold crystallization temperature (T_{cc}) was shifted to a lower temperature, from 105.4 to 95.4 °C, and the crystallinity of PLLA was significantly increased, from 7.3 to around 32% (Habibi et al. 2013). The presence of PDLA-grafted CNs also changed PLLA from a single-peak (150 °C) to a double-peak melting behavior (160 and 170 °C) (Habibi et al. 2013). The double-melting peak behavior was attributed to the co-existence of two crystalline structures with the low-melting peak corresponding to the loosely packed crystals and high-melting peak to the more perfect crystals and/or the crystals re-crystallized from the low-melting temperature crystals (Ding et al. 2015b; Habibi et al. 2013). Similar phenomena were observed for surfactant treated CNs (Fortunati et al. 2012a), isocyanate treated CNs (Espino-Pérez et al. 2013), PLA-grafted CNs (Braun et al. 2012; Goffin et al. 2011). On the contrary, some researchers claimed that untreated CNs, LA-CN, GMA-grafted CNs, silanized CNFs, or esterified CNs did not show obvious nucleating effects, that is, the T_{cc} , the crystallinity, and the T_m were not notably affected (Pei et al. 2010; Pracella et al. 2014; Robles et al. 2015; Spinella et al. 2015). Moreover, some studies have shown that well-dispersed CNFs even delayed PLA's crystallization and increased its crystallization half-time (Zhang et al. 2013) and decreased the final crystallinity (Frone et al. 2013). However, it is worthy to note that it is difficult to compare the results reported in the literature. This is because the crystallization kinetics is strongly dependent on the crystallization temperature, processing condition, D-lactic acid content, molecular weight and distribution of the PLA matrix, and the morphology, surface chemistry, and weight content of the nanocelluloses.

4.2.3 Barrier Properties

Nanocelluloses have been used to enhance the water vapor and gas barrier properties of PLA. Neat PLA has relatively poor water vapor and gas barrier properties compared to the other benchmark packaging polymers such as polyethylene (PE), PP, and polyethylene terephthalate (PET). The water vapor permeability (WVP) coefficient of the

neat PLA has been reported between 1.04 and 4.66×10^{-14} kg m/s m² Pa depending on the film preparation method, the test conditions, and PLA resin grade (Auras et al. 2003; Fortunati et al. 2012b; Rhim et al. 2006; Sanchez-Garcia and Lagaron 2010). The oxygen (O₂) permeability coefficient of PLA ($1.21\text{--}2.77 \times 10^{-18}$ kg m/s m² Pa at 25 °C and 70% RH) is about one order of magnitude lower than the value for PS, but one order higher than PET at the same condition (Auras et al. 2003).

The effect of nanocelluloses on the WVP of PLA film has been studied intensively in recent years. Both freeze-dried and solvent-exchanged CNs have been used to decrease PLA's WVP, and the PLA composites containing freeze-dried CNs showed better results (Sanchez-Garcia and Lagaron 2010). The reductions of PLA's WVP were about 64, 78, 82, and 81% when 1, 2, 3, and 5 wt% freeze-dried CNs were incorporated, respectively. Fortunati et al. observed that unmodified 1 or 5 wt% CNs showed little improvement on the WVP of the PLA (Fortunati et al. 2012b). Espino-Pérez et al. found that the WVP values of PLA nanocomposites increased with CN content, for instance, increases by 21.3, 42.4, and 195.8% when 2.5, 7.5, and 15 wt% CNs were added (Espino-Pérez et al. 2013). Many authors attributed the increased permeability to the poor interface between polymer and CNs and the CNs' agglomeration (Abdulkhali et al. 2014; Espino-Pérez et al. 2013; Fortunati et al. 2012b). As a result, surface-modified nanocelluloses have been used to improve their dispersion and reduce their hygroscopic property. 1 wt% surface modified CNs with a surfactant of Beycostat A B09 showed a reduction of 34% in water permeability compared to the neat PLA (Fortunati et al. 2012b). But lower reductions in WVP were detected in the case of nanocomposites reinforced with 5 wt% of modified CNs. It was attributed to the agglomeration of CNs. In contrast, *n*-octadecyl-isocyanate grafted CNs (Espino-Pérez et al. 2013) and acetylated CNFs (Abdulkhali et al. 2014) had no significant effect on PLA film's WVP.

Similarly to PLA's WVP, the oxygen permeability of PLA film by the inclusion of nanocelluloses showed no consistency. Sanchez-Garcia and Lagaron reported oxygen permeability reductions of 83, 90, 90 and 88% for the PLA film with 1, 2, 3 and 5 wt% freeze-dried CNs, respectively (Sanchez-Garcia and Lagaron 2010). Fortunati et al. also observed improved O₂ barrier properties up to 48% when 5 wt% surfactant modified CNs were added (Fortunati et al. 2012b). However, no significant improvement on the O₂ permeability were recorded for both pristine and isocyanate grafted CNs even when the quantity of CNs was increased to 15 wt% (Espino-Pérez et al. 2013). It is believed that the transport properties are influenced by a number of factors including the shape, aspect ratio, and surface chemistry of the fillers, degree of dispersion, filler content, filler-induced crystallinity, polymer-filler interaction, plasticizer content, and porosity (Espino-Pérez et al. 2013; Fortunati et al. 2012b; Petersson and Oksman 2006; Sanchez-Garcia and Lagaron 2010). The improvement of PLA's barrier properties by nanocellulose addition is mostly due to the increased tortuosity for a gas molecule to go through the film.

4.2.4 Foaming Behaviors

Development of PLA foams is desirable and promising because they have huge potentials not only to replace current widely used nonbiodegradable PS and non-recyclable polyurethane foams, but also to be used in tissue engineering applications. The strategy of combing biodegradable polymer with nanocelluloses offers the possibility of generating a new class of fully biorenewable resource-based and biodegradable composites. Moreover, nanocelluloses have significantly less cytotoxicity and genotoxicity compared with inorganic nanoparticulates (Clift et al. 2011; De Lima et al. 2012; Domingues et al. 2014).

Nanocelluloses have been used to improve PLA's foamability by enhancing its melt strength and crystallization kinetics and providing cell nucleating sites during foaming (Ding et al. 2012, 2015a, b; Dlouhá et al. 2012, 2014). Ding et al. used an in situ foaming visualization system to understand the role of CNFs in the initial foaming process of PLA (Fig. 13) (Ding et al. 2015a). They found that CNFs, serving as effective cell nucleating agents, enhanced cell nucleation and suppressed the cell growth rate, cell coalescence, and cell coarsening significantly due to the considerable increase in the PLA's melt strength by the addition of CNFs. In the solid state batch foaming, well-dispersed CNFs resulted in a higher cell density and a smaller cell size compared with neat PLA foam (Ding et al. 2015a; Dlouhá et al. 2012, 2014). It was attributed to the cell nucleating effects of the CNFs and the formed crystals, as well as the suppressed cell deterioration through the increased melt strength of PLA with added CNFs and crystals (Ding et al. 2015a). The fiber

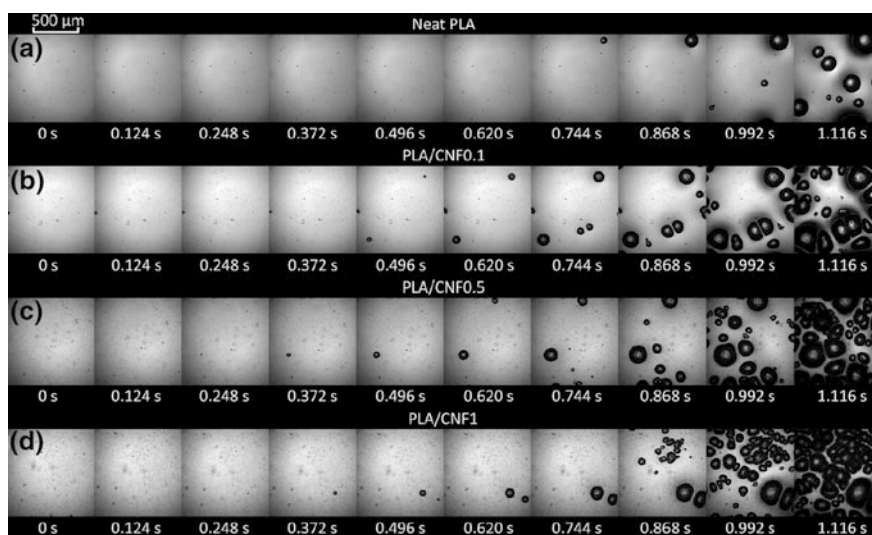


Fig. 13 Snapshots of the PLA/CNF nanocomposite foaming video with various CNF contents, **a** neat PLA, **b** 0.1 wt%, **c** 0.5 wt%, and **d** 1 wt%. Reproduced from (Ding et al. 2015a), with permission from RSC

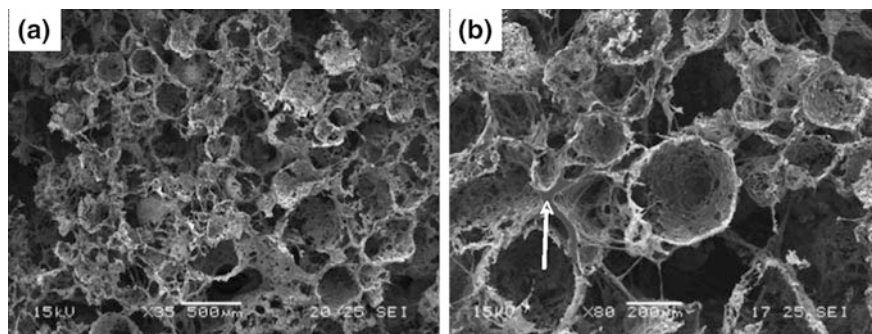


Fig. 14 PLA foams containing 30 wt% bacterial CNs and 20 vol% ice microspheres as a template for scaffolds. Reprinted from Blaker et al. (2010), Copyright (2010), with permission from Elsevier

content and dispersion level also have a profound influence on the PLA's foam morphology. In general, as the CNF content increases, the cell nucleating power and the resulting cell density increase and the cell sizes become more uniform (Ding et al. 2015a; Dlouhá et al. 2012). However, in the studies conducted by Boissard et al. (2012) and Cho et al. (2013), only a slight improvement, or even a deteriorated cell structure, was observed due to the fiber aggregation (Boissard et al. 2012; Cho et al. 2013). The effects of CNFs on the specific tensile strength and modulus and strain at break were remarkably improved by foaming when compared to their effects on the solid counterparts (Dlouhá et al. 2014). The specific modulus increased with increasing CNF content, but specific strength was independent on the fiber content. Strain at break was increased up to 31.5 times by foaming with the addition of only 3 wt% of CNFs. The surface modification showed much pronounced effect on the toughness with a high CNF content. The acetylated CNF foams exhibited higher strength and modulus over native CNF foams (Dlouhá et al. 2014).

The major challenge concerning the use of PLA/nanocellulose biocomposites in commercial application is their low production efficiency. With the potential of nanocelluloses to generate open-cell micro- or nano- porous structure in PLA using solvent-free fabrication techniques, the relatively high cost of batch foaming of PLA could be justified in biomedical applications (Domingues et al. 2014). The blowing agents could be inert gas such as carbon dioxide and/or nitrogen. The cell opening can be controlled by ultrasound treatment after the foaming process (Wang et al. 2006). This is completely different from the current methods which involve organic solvents or porogen for producing open-cell structure and the residues can affect biological cells' bioactivities. Figure 14 presents a highly porous and interconnected 3D scaffolds for tissue engineering produced with PLA and bacterial CNs.

4.2.5 Mechanical Properties

The nanosize dimension, nontoxicity, large surface area, and outstanding mechanical properties of nanocelluloses make them attractive components for high performance polymer nanocomposites, especially with biopolymers such as PLA, PHAs, and PBS. Nanocellulose possesses a Young's modulus of 115–150 GPa in the longitudinal direction and a tensile strength of up to 2 GPa (Diddens et al. 2008; Nakagaito and Yano 2005; Nishiyama 2009; Wang and Sain 2007a), very low thermal expansion coefficients (10^{-7} K^{-1}) (Nishino et al. 2004), a large surface area per mass ($\sim 1000 \text{ m}^2 \text{ g}^{-1}$) (Saito et al. 2013). The mechanical properties are comparable to or even higher than those of high-strength glass fibers.

Compared with CNs, CNFs have a better reinforcing ability due to their higher aspect ratios (over 100) and their entanglement (Alemdar and Sain 2008a; Wang and Sain 2007c; Xu et al. 2013, 2014). Reinforcing PLA with CNFs at a fiber content of 20 wt% produced by solvent exchange method increased its tensile strength and modulus by about 22 and 58%, respectively (Suryanegara et al. 2009). The storage modulus of the PLA composites at 120 °C was also improved about 3.5 fold with a fiber content of 20 wt% (Suryanegara et al. 2009). Using the same processing method, Iwatake et al. reported that 5 wt% CNFs increased the PLA's tensile strength and modulus by about 17 and 26%, respectively (Iwatake et al. 2008). In another study, PLA's tensile strength was increased by 25 and 59% and tensile modulus by 42 and 47%, respectively, even when 2.5 and 5 wt% of CNFs prepared from flax fiber were added (Liu et al. 2010). In contrast, the addition of CNs in PLA showed only little improvements or even decreases in the mechanical properties (Pei et al. 2010; Pracella et al. 2014; Robles et al. 2015; Sanchez-Garcia and Lagaron 2010). At low CN contents (1–5 wt%), some researchers found that the addition of CNs slightly increased (up to 11%) or maintained the tensile strength and modulus of PLA owing to the high modulus of the CNs (Espino-Pérez et al. 2013; Fortunati et al. 2012a; Pracella et al. 2014). While some others reported a decrease when 5 wt% or a higher CN content was added. Sanchez-Garcia and Lagaron claimed that 5 wt% CNs reinforced PLA nanocomposites obtained by solvent exchange with chloroform presented a reduction in tensile strength and modulus by 38 and 52%, respectively, (Sanchez-Garcia and Lagaron 2010). Espino-Pérez et al. showed that the addition of 7.5–15 wt% of CNs in PLA reduced the tensile strength by up to 63% and elongation at break up to 21% (Espino-Pérez et al. 2013). Using the same processing method, Petersson and Oksman reported that 5 wt% CNs improved tensile strength by 12%, but decreased tensile modulus and elongation at break by 12 and 16%, respectively (Petersson and Oksman 2006). These slight increases or obvious decreases in the tensile strength and modulus are mainly attributed to the incompatibility between PLA matrix and CNs (Espino-Pérez et al. 2013; Sanchez-Garcia and Lagaron 2010). As a result, the elongation at break of the PLA nanocomposites is normally reduced compared to the neat PLA. Although a few studies argued that PLA nanocomposites processed

by solvent casting showed a ductile behavior at a low nanocellulose content, the improved elongation at break was probably due to the residual solvent which acted as a plasticizer (Fortunati et al. 2012a). At the same CNF or CN loading rate, various degrees of improvements on PLA's mechanical properties origin have been reported. These differences are ascribed to the origin of the nanocelluloses and defibrillation methods, which determine the morphologies, surface chemistry, degree of crystallinity, and aspect ratios of nanocelluloses (Habibi et al. 2010; Peng et al. 2011).

The reinforcement of CNFs and CNs is highly dependent on the composite processing methods. In general, the solvent casting method produces better results than the direct melt-compounding process due to the good dispersion of nanocelluloses in PLA matrix. Iwatake compared the mechanical properties of PLA/CNF nanocomposites prepared by solvent exchange followed by melt kneading process, solvent method without the kneading process, and direct melt-compounding method (Iwatake et al. 2008). The results showed that solvent exchange coupled with melt kneading produced the best mechanical properties, followed by the simple solvent method without the kneading process and the direct melt-compounding method. To their best, 10 wt% of CNFs increased the PLA's tensile strength and modulus by about 33 and 38%, respectively, while the direct melt-compounding method led to a reduction of tensile strength by 10% and yield strain by almost 50% (Iwatake et al. 2008). Ding et al. measured the flexural properties of PLA/CNF composites by solvent exchange method and found that 5 wt% of CNFs enhanced the flexural strength and modulus by 11.3 and 22.3%, respectively, while retaining the yield strain around 3.2% (Ding et al. 2012).

Emulsion filtration process makes it possible to produce high-fiber-content PLA with exceptional improvements on its mechanical properties. Nakagaito et al. first developed a papermaking-like process to produce PLA/CNF nanocomposites (Nakagaito et al. 2009). The tensile strength and modulus, strain at break all increased with CNF content with strength tripled and modulus doubled as CNF content increased from 10 to 70 wt%. The storage modulus above T_g also increased as the CNF content increased (Nakagaito et al. 2009). The storage modulus was sustained up to 250°C at CNF contents of 70 and 90 wt%. A similar filtration process has been used by Wang et al. to fabricate PLA nanocomposites with 8–32 wt% CNFs (Wang and Drzal 2012). The flexural strength and modulus increased almost linearly with CNF content from 3.8 GPa and 26 MPa for the neat PLA to 6.0 GPa and 78 MPa for 32 wt% CNF reinforced PLA, respectively. The greater improvement in mechanical properties by emulsion filtration process is primarily due to the percolated CNF network structure at high CNF contents which acts as a load bearing framework and maintains the network structure even at high temperature (Nakagaito et al. 2009; Wang and Drzal 2012).

Direct melt-compounding process either by feeding liquid or dried nanocelluloses into melted PLA usually results in a decreased mechanical strength compared to the neat PLA (Herrera et al. 2015; Oksman et al. 2006; Robles et al. 2015). This is due to

one or more combined factors as follows: thermal degradation of PLA by moisture and/or heat (Boissard et al. 2012), incorporated plasticizer or surfactant (Herrera et al. 2015; Oksman et al. 2006), or a large amount of agglomerations (Bondeson and Oksman 2007; Robles et al. 2015; Sanchez-Garcia and Lagaron 2010). Using nanocelluloses in dried form, only slight improvements in tensile strength and modulus and dynamic modulus were found (Goffin et al. 2011; Wang and Sain 2007b). Others found no improvement or even decreases in mechanical properties after the incorporation of CNFs (Bondeson and Oksman 2007; Eyholzer et al. 2012; Robles et al. 2015). However, if PLA/nanocellulose materbatch prepared by solvent casting is used to mix with PLA, the resultant composites showed a comparable or slight increase in mechanical properties (Jonoobi et al. 2010, 2012; Pracella et al. 2014). Oksman et al. first attempted to prepare PLA/CN nanocomposites using a direct liquid feeding method where 20 wt% DMAc/LiCl, a swelling and pumping medium, and 10 wt% PLA-MA, a compatibilizer, were added in the composites (Oksman et al. 2006). Each individual additive had a negative effect on the tensile properties of the neat PLA. However, the addition of 5 wt% CNs improved the tensile strength and modulus and elongation to break compared to the PLA with DMAc/LiCl. The addition of PEG further increased the elongation to break of the composites by about 560%. The same group also melt-compounded PLA and CNFs using direct liquid feeding with glycerol triacetate (GTA) as a processing aid to facilitate CNF dispersion (Herrera et al. 2015). The addition of 20% of GTA reduced the tensile strength and modulus by more than 60% compared to the neat PLA, but increased the elongation at break by 678% and the work to fracture by 389%.

In general, the mechanical properties of PLA/CNF composites increased with CNF content up to a certain value (Abdulkhani et al. 2014; Fujisawa et al. 2013; Iwatake et al. 2008; Jonoobi et al. 2010; Suryanegara et al. 2009). Overloading of CNFs can adversely affect these properties (Iwatake et al. 2008). In solvent casting, CNFs' interaction by hydrogen bonding is limited because polymer chains hinder the CNF rearrangement; therefore, the CNF network is primarily based on entanglement (Nakagaito et al. 2009). In case of CNs, untreated CNs showed no significant increase in tensile strength and modulus due to the weak interaction between CNs and PLA (Pei et al. 2010; Petersson et al. 2007; Pracella et al. 2014). In contrast, the tensile strength of the PLA was enhanced by 61.3% and the tensile Young's modulus was 1.5-fold greater than those of the neat PLA when 6 wt% acetylated CNs were added (Lin et al. 2011). The addition of 1 wt% silylated CNs resulted in a 21 and 27% increase in tensile strength and modulus, respectively (Pei et al. 2010). When CNs are surface grafted with nonpolar polymer chains, these polymer not only help disperse the CNs, but also act as compatibilizer to improve the interfacial adhesion. In particular, when the grafted polymers are of the same nature as the PLA matrix, the compatibility between the nanocelluloses and PLA can be maximized. Lin et al. incorporated PCL-grafted CNs into PLA matrix to produce nanocomposites with better mechanical performance (Lin et al. 2009). The tensile strength and elongation at break increased with increasing treated CN

content up till 8 wt% and then they decreased. The dependence of tensile modulus on the CN content was the opposite of that of elongation at break. The optimal content of 8 wt% of PCL-grafted CNs resulted in simultaneous enhancements of the strength and elongation of approximately 1.9- and 10.7-fold, respectively, compared to the neat PLA (Lin et al. 2009). In another study, Pracella et al. incorporated 3 wt% GMA-grafted CNs which increased the tensile strength and modulus of PLA by 9 and 16%, respectively (Pracella et al. 2014).

5 Conclusions and Outlook

Nanocelluloses, the most abundant and renewable biopolymers, have been the focus of advanced research for a wide range of consumer applications in recent times. Their nanoscale dimension, excellent reinforcing ability, hydrophilic surface nature, biodegradability, and biocompatibility make them unique biomaterials for the development of advanced functional bionanocomposites. In this context, PLA represents one of the most promising biopolymers in the market to replace petroleum-based polymers in many applications including food packing, nonwoven fabrics, electronic and electrical devices, and biomedical applications. However, to meet the end-user demands, PLA's deficiencies must be mitigated in terms of slow crystallization rate, low melt strength, low heat deflection temperature, and brittleness. The combination of PLA and nanocelluloses not only endows the resulting composites with fully biodegradable feature, but also gives them significantly improved performance properties.

This chapter has attempted to provide a broad vista of nanocelluloses' fundamental properties and fabrication methods, recent development of processing techniques for producing PLA/CNF nanocomposites, and some important properties of the PLA improved by nanocelluloses for different applications. The solution casting, emulsion filtration/emulsion freeze-drying, and direct melt-compounding are the most common techniques to develop PLA/cellulose nanocomposites. Among those, solvent casting still remains one of widely used laboratory processing methods to produce the nanocomposites with the best possible dispersion of CNFs in PLA, while direct melt-compounding demonstrates a great promise for large-scale industrial production. The majority of the research has been focused on the effect of nanocelluloses on the thermal properties, crystallization kinetics, barrier properties, foaming behaviors, and mechanical performance of PLA. Despite various research efforts in this area, there still remains a number of issues to deal with prior to any commercial application of such composite materials. One of the key challenges is to further optimize the surface functionalization of nanocellulose entities to enable their uniform dispersion into PLA at a reasonable cost, and secondly, enhancing thermal integrity of PLA itself can boost versatility of these products to a larger extent.

References

- Abdulkhani A, Hosseinzadeh J, Ashori A, Dadashi S, Takzare Z (2014) Preparation and characterization of modified cellulose nanofibers reinforced polylactic acid nanocomposite. *Polym Test* 35:73
- Abe K, Iwamoto S, Yano H (2007) Obtaining cellulose nanofibers with a uniform width of 15 nm from wood. *Biomacromolecules* 8:3276
- Alemdar A, Sain M (2008a) Biocomposites from wheat straw nanofibers: morphology, thermal and mechanical properties. *Compos Sci Technol* 68:557
- Alemdar A, Sain M (2008b) Isolation and characterization of nanofibers from agricultural residues—wheat straw and soy hulls. *Bioresour Technol* 99:1664
- Anglès MN, Dufresne A (2000) Plasticized starch/tunicin whiskers nanocomposites. 1. Structural analysis. *Macromolecules* 33:8344
- Araki J, Kuga S (2001) Effect of trace electrolyte on liquid crystal type of cellulose microcrystals. *Langmuir* 17:4493
- Auras RA, Harte B, Selke S, Hernandez R (2003) Mechanical, physical, and barrier properties of poly(lactide) films. *J Plast Film Sheeting* 19:123
- Auras R, Harte B, Selke S (2004) An overview of polylactides as packaging materials. *Macromol Biosci* 4:835
- Beck-Candanedo S, Roman M, Gray DG (2005) Effect of reaction conditions on the properties and behavior of wood cellulose nanocrystal suspensions. *Biomacromolecules* 6:1048
- Bhatnagar A, Sain M (2005) Processing of cellulose nanofiber-reinforced composites. *J Reinf Plast Compos* 24:1259
- Blaker JJ, Lee KY, Mantalaris A, Bismarck A (2010) Ice-microsphere templating to produce highly porous nanocomposite PLA matrix scaffolds with pores selectively lined by bacterial cellulose nano-whiskers. *Compos Sci Technol* 70:1879
- Boissard CIR, Bourban PE, Plummer CJG, Neagu RC, Månson JAE (2012) Cellular biocomposites from polylactide and microfibrillated cellulose. *J Cell Plast* 48:445
- Bondeson D, Oksman K (2007) Dispersion and characteristics of surfactant modified cellulose whiskers nanocomposites. *Compos Interfaces* 14:617
- Braun B, Dorgan JR, Hollingsworth LO (2012) Supra-molecular ecobionanocomposites based on polylactide and cellulosic nanowhiskers: synthesis and properties. *Biomacromolecules* 13:2013
- Chakraborty A, Sain M, Kortschot M (2005) Cellulose microfibrils: a novel method of preparation using high shear refining and cryocrushing. *Holzforschung* 59:102
- Charreau H, Foresti ML, Vázquez A (2013) Nanocellulose patents trends: a comprehensive review on patents on cellulose nanocrystals, microfibrillated and bacterial cellulose. *Recent Pat Nanotechnol* 7:56
- Chen W, Yu H, Liu Y, Chen P, Zhang M, Hai Y (2011a) Individualization of cellulose nanofibers from wood using high-intensity ultrasonication combined with chemical pretreatments. *Carbohydr Polym* 83:1804
- Chen W, Yu H, Liu Y, Hai Y, Zhang M, Chen P (2011b) Isolation and characterization of cellulose nanofibers from four plant cellulose fibers using a chemical-ultrasonic process. *Cellulose* 18:433
- Chen W, Yu H, Liu Y (2011c) Preparation of millimeter-long cellulose I nanofibers with diameters of 30–80 nm from bamboo fibers. *Carbohydr Polym* 86:453
- Cheng S, Panthapulakkal S, Ramezani N, Asiri AM, Sain M (2014a) Aloe vera rind nanofibers: effect of isolation process on the tensile properties of nanofibre films. *BioResources* 9:7653
- Cheng S, Panthapulakkal S, Sain M, Asiri A (2014b) Aloe vera rind cellulose nanofibers-reinforced films. *J Appl Polym Sci* 131:40592
- Cho S, Park H, Yun Y, Jin H-J (2013) Influence of cellulose nanofibers on the morphology and physical properties of poly(lactic acid) foaming by supercritical carbon dioxide. *Macromol Res* 21:529

- Clift MJD, Foster EJ, Vanhecke D, Studer D, Wick P, Gehr P, Rothen-Rutishauser B, Weder C (2011) Investigating the interaction of cellulose nanofibers derived from cotton with a sophisticated 3D human lung cell coculture. *Biomacromolecules* 12:3666
- Corobea MC, Muhulet O, Miculescu F, Antoniac IV, Vuluga Z, Florea D et al (2016) Novel nanocomposite membranes from cellulose acetate and clay-silica nanowires. *Polym Adv Technol* 27(12):1586
- Darder M, Aranda P, Ruiz-Hitzky E (2007) Bionanocomposites: a new concept of ecological, bioinspired, and functional hybrid materials. *Adv Mater* 19:1309
- De Lima R, Feitosa LO, Maruyama CR, Barga MA, Yamawaki PC, Vieira IJ, Teixeira EM, Corrêa AC, Caparelli Mattoso LH, Fraceto LF (2012) Evaluation of the genotoxicity of cellulose nanofibers. *Int J Nanomed* 7:3555
- Diddens I, Murphy B, Krisch M, Müller M (2008) Anisotropic elastic properties of cellulose measured using inelastic X-ray scattering. *Macromolecules* 41:9755
- Ding WD, Kuboki T, Zhao N, Malm T, Park CB, Sain M (2012) Mechanical properties of cellulose nanofiber reinforced poly(lactic acid) biocomposites and their foams. *CSME International Congress*, Winnipeg
- Ding WD, Kuboki T, Wong A, Park CB, Sain M (2015a) Rheology, thermal properties, and foaming behavior of high d-content poly(lactic acid)/cellulose nanofiber composites. *RSC Adv* 5:91544
- Ding WD, Chu RKM, Mark LH, Park CB, Sain M (2015b) Non-isothermal crystallization behaviors of poly(lactic acid)/cellulose nanofiber composites in the presence of CO₂. *Eur Polym J* 71:231
- Dlouhá J, Suryanegara L, Yano H (2012) The role of cellulose nanofibres in supercritical foaming of poly(lactic acid) and their effect on the foam morphology. *Soft Matter* 8:8704
- Dlouhá J, Suryanegara L, Yano H (2014) Cellulose nanofibre-poly(lactic acid) microcellular foams exhibiting high tensile toughness. *React Funct Polym* 85:201
- Domingues RMA, Gomes ME, Reis RL (2014) The potential of cellulose nanocrystals in tissue engineering strategies. *Biomacromolecules* 15:2327
- Drumright RE, Gruber PR, Henton DE (2000) Poly(lactic acid) technology. *Adv Mater* 12:1841
- Dusselier M, Van Wouwe P, Dewaele A, Jacobs PA, Sels BF (2015) Shape-selective zeolite catalysis for bioplastics production. *Science* 349:78
- Elazzouzi-Hafraoui S, Nishiyama Y, Putaux J-L, Heux L, Dubreuil F, Rochas C (2008) The shape and size distribution of crystalline nanoparticles prepared by acid hydrolysis of native cellulose. *Biomacromolecules* 9:57
- Espino-Pérez E, Bras J, Ducruet V, Guinault A, Dufresne A, Domenek S (2013) Influence of chemical surface modification of cellulose nanowhiskers on thermal, mechanical, and barrier properties of poly(lactide) based bionanocomposites. *Eur Polym J* 49:3144
- Eyholzer C, Tingaut P, Zimmermann T, Oksman K (2012) Dispersion and reinforcing potential of carboxymethylated nanofibrillated cellulose powders modified with 1-hexanol in extruded poly(lactic acid) (PLA) composites. *J Polym Environ* 20:1052
- Faruk O, Bledzki AK, Matuana LM (2007) Microcellular foamed wood-plastic composites by different processes: a review. *Macromol Mater Eng* 292:113
- Fortunati E, Armentano I, Zhou Q, Puglia D, Terenzi A, Berglund LA, Kenny JM (2012a) Microstructure and nonisothermal cold crystallization of PLA composites based on silver nanoparticles and nanocrystalline cellulose. *Polym Degrad Stab* 97:2027
- Fortunati E, Peltzer M, Armentano I, Torre L, Jiménez A, Kenny JM (2012b) Effects of modified cellulose nanocrystals on the barrier and migration properties of PLA nano-biocomposites. *Carbohydr Polym* 90:948
- Frone AN, Berlioz S, Chailan JF, Panaitescu DM (2013) Morphology and thermal properties of PLA-cellulose nanofibers composites. *Carbohydr Polym* 91:377
- Fujisawa S, Saito T, Kimura S, Iwata T, Isogai A (2013) Surface engineering of ultrafine cellulose nanofibrils toward polymer nanocomposite materials. *Biomacromolecules* 14:1541
- García de Rodríguez NL, Thielemans W, Dufresne A (2006) Sisal cellulose whiskers reinforced poly(vinyl acetate) nanocomposites. *Cellulose* 13:261

- Goffin AL, Raquez JM, Duquesne E, Siqueira G, Habibi Y, Dufresne A, Dubois P (2011) From interfacial ring-opening polymerization to melt processing of cellulose nanowhisker-filled polylactide-based nanocomposites. *Biomacromolecules* 12:2456
- Habibi Y, Goffin A-L, Schiltz N, Duquesne E, Dubois P, Dufresne A (2008) Bionanocomposites based on poly(ϵ -caprolactone)-grafted cellulose nanocrystals by ring-opening polymerization. *J Mater Chem* 18:5002
- Habibi Y, Lucia LA, Rojas OJ (2010) Cellulose nanocrystals: chemistry, self-assembly, and applications. *Chem Rev* 110:3479
- Habibi Y, Aouadi S, Raquez JM, Dubois P (2013) Effects of interfacial stereocomplexation in cellulose nanocrystal-filled polylactide nanocomposites. *Cellulose* 20:2877
- Henriksson M, Henriksson G, Berglund LA, Lindström T (2007) An environmentally friendly method for enzyme-assisted preparation of microfibrillated cellulose (MFC) nanofibers. *Eur Polym J* 43:3434
- Herrera N, Mathew AP, Oksman K (2015) Plasticized polylactic acid/cellulose nanocomposites prepared using melt-extrusion and liquid feeding: mechanical, thermal and optical properties. *Compos Sci Technol* 106:149
- Holbery J, Houston D (2006) Natural-fiber-reinforced polymer composites in automotive applications. *JOM* 58:80
- Hu F, Lin N, Chang PR, Huang J (2015) Reinforcement and nucleation of acetylated cellulose nanocrystals in foamed polyester composites. *Carbohydr Polym* 129:208
- Iwamoto S, Abe K, Yano H (2008) The effect of hemicelluloses on wood pulp nanofibrillation and nanofiber network characteristics. *Biomacromolecules* 9:1022
- Iwatake A, Nogi M, Yano H (2008) Cellulose nanofiber-reinforced polylactic acid. *Compos Sci Technol* 68:2103
- Jacquel N, Lo C-W, Wei Y-H, Wu H-S, Wang SS (2008) Isolation and purification of bacterial poly(3-hydroxyalkanoates). *Biochem Eng J* 39:15
- Jamshidian M, Tehrani EA, Imran M, Jacquot M, Desobry S (2010) Poly-lactic acid: production, applications, nanocomposites, and release studies. *Compr Rev Food Sci Food Saf* 9:552
- Jonoobi M, Harun J, Mathew AP, Oksman K (2010) Mechanical properties of cellulose nanofiber (CNF) reinforced polylactic acid (PLA) prepared by twin screw extrusion. *Compos Sci Technol* 70:1742
- Jonoobi M, Mathew AP, Abdi MM, Makinejad MD, Oksman K (2012) A Comparison of modified and unmodified cellulose nanofiber reinforced polylactic acid (PLA) prepared by twin screw extrusion. *J Polym Environ* 20:991
- Junior de Menezes A, Siqueira G, Curvelo AAS, Dufresne A (2009) Extrusion and characterization of functionalized cellulose whiskers reinforced polyethylene nanocomposites. *Polymer* 50:4552
- Kamal MR, Khoshkava V (2015) Effect of cellulose nanocrystals (CNC) on rheological and mechanical properties and crystallization behavior of PLA/CNC nanocomposites. *Carbohydr Polym* 123:105
- Keshavarz T, Roy I (2010) Polyhydroxyalkanoates: bioplastics with a green agenda. *Curr Opin Microbiol* 13:321
- Khoshkava V, Kamal MR (2013) Effect of surface energy on dispersion and mechanical properties of polymer/nanocrystalline cellulose nanocomposites. *Biomacromolecules* 14:3155
- Kose R, Kondo T (2013) Size effects of cellulose nanofibers for enhancing the crystallization of poly(lactic acid). *J Appl Polym Sci* 128:1200
- Kowalczyk M, Piorkowska E, Kulpinski P, Pracella M (2011) Mechanical and thermal properties of PLA composites with cellulose nanofibers and standard size fibers. *Compos A* 42:1509
- Lagerwall JPF, Schütz C, Salajkova M, Noh J, Park JH, Scalia G, Bergström L (2014) Cellulose nanocrystal-based materials: from liquid crystal self-assembly and glass formation to multifunctional thin films. *NPG Asia Mater* 6:e80
- Landry V, Alemdar A, Blanchet P (2011) Nanocrystalline cellulose: morphological, physical, and mechanical properties. *Forest Prod J* 61:104

- Lee K-Y, Aitomäki Y, Berglund LA, Oksman K, Bismarck A (2014) On the use of nanocellulose as reinforcement in polymer matrix composites. *Compos Sci Technol* 105:15
- Lin N, Dufresne A (2014) Surface chemistry, morphological analysis and properties of cellulose nanocrystals with gradiented sulfation degrees. *Nanoscale* 6:5384
- Lin N, Chen G, Huang J, Dufresne A, Chang PR (2009) Effects of polymer-grafted natural nanocrystals on the structure and mechanical properties of poly(lactic acid): a case of cellulose whisker-graft-polycaprolactone. *J Appl Polym Sci* 113:3417
- Lin N, Huang J, Chang PR, Feng J, Yu J (2011) Surface acetylation of cellulose nanocrystal and its reinforcing function in poly(lactic acid). *Carbohydr Polym* 83:1834
- Lin N, Chen Y, Hu F, Huang J (2015) Mechanical reinforcement of cellulose nanocrystals on biodegradable microcellular foams with melt-compounding process. *Cellulose* 22:2629
- Liu DY, Yuan XW, Bhattacharyya D, Eastale AJ (2010) Characterisation of solution cast cellulose nanofibre—reinforced poly(lactic acid). *Express Polym Lett* 4:26
- Lizundia E, Vilas JL, León LM (2015) Crystallization, structural relaxation and thermal degradation in poly(L-lactide)/cellulose nanocrystal renewable nanocomposites. *Carbohydr Polym* 123:256
- Ma Z, Chen F, Zhu YJ, Cui T, Liu XY (2011) Amorphous calcium phosphate/poly(D, L-lactic acid) composite nanofibers: electrospinning preparation and biomineralization. *J Colloid Interface Sci* 359:371
- Mathew AP, Oksman K, Sain M (2005) Mechanical properties of biodegradable composites from poly lactic acid (PLA) and microcrystalline cellulose (MCC). *J Appl Polym Sci* 97:2014
- Mathew AP, Oksman K, Sain M (2006) The effect of morphology and chemical characteristics of cellulose reinforcements on the crystallinity of polylactic acid. *J Appl Polym Sci* 101:300
- Matuana LM, Faruk O (2010) Effect of gas saturation conditions on the expansion ratio of microcellular poly (lactic acid)/wood-flour composites. *Express Polym Lett* 4:621
- Michalska-Požoga I, Tomkowski R, Rydzkowski T, Thakur VK (2016) Towards the usage of image analysis technique to measure particles size and composition in wood-polymer composites. *Ind Crops Prod* 92:149
- Miculescu M, Thakur VK, Miculescu F, Voicu SI (2016) Graphene-based polymer nanocomposite membranes: a review. *Polym Adv Technol* 27(7):844
- Middleton JC, Tipton AJ (2000) Synthetic biodegradable polymers as orthopedic devices. *Biomaterials* 21:2335
- Nair S, Yan N (2015a) Effect of high residual lignin on the thermal stability of nanofibrils and its enhanced mechanical performance in aqueous environments. *Cellulose* 22:3137
- Nair SS, Yan N (2015b) Bark derived submicron-sized and nano-sized cellulose fibers: from industrial waste to high performance materials. *Carbohydr Polym* 134:258
- Nakagaito AN, Yano H (2005) Novel high-strength biocomposites based on microfibrillated cellulose having nano-order-unit web-like network structure. *Appl Phys A Mater Sci Process* 80:155
- Nakagaito AN, Fujimura A, Sakai T, Hama Y, Yano H (2009) Production of microfibrillated cellulose (MFC)-reinforced polylactic acid (PLA) nanocomposites from sheets obtained by a papermaking-like process. *Compos Sci Technol* 69:1293
- Ng H-M, Sin LT, Tee T-T, Bee S-T, Hui D, Low C-Y, Rahmat AR (2015) Extraction of cellulose nanocrystals from plant sources for application as reinforcing agent in polymers. *Compos Part B Eng* 75:176
- Nishino T, Matsuda I, Hirao K (2004) All-cellulose composite. *Macromolecules* 37:7683
- Nishiyama Y (2009) Structure and properties of the cellulose microfibril. *J Wood Sci* 55:241
- Oksman K, Mathew AP (2014) Melt compounding process of cellulose nanocomposites. In: Oksman K, Mathew AP, Bismarck A, Rojas O, Sain M (eds) *Handbook of green materials*, vol 2. World Scientific Publishing, Singapore, pp 53–68
- Oksman K, Mathew AP, Bondeson D, Kvien I (2006) Manufacturing process of cellulose whiskers/polylactic acid nanocomposites. *Compos Sci Technol* 66:2776

- Oksman K, Aitomäki Y, Mathew AP, Siqueira G, Zhou Q, Butylina S, Tanpichai S, Zhou X, Hooshmand S (2016) Review of the recent developments in cellulose nanocomposite processing. *Compos A* 83:2
- Pääkkö M, Ankerfors M, Kosonen H, Nykänen A, Ahola S, Österberg M, Ruokolainen J, Laine J, Larsson PT, Ikkala O, Lindström T (2007) Enzymatic hydrolysis combined with mechanical shearing and high-pressure homogenization for nanoscale cellulose fibrils and strong gels. *Biomacromolecules* 8:1934
- Panthapulakkal S, Sain M (2013) Isolation of nano fibres from hemp and flax and their thermoplastic composites. *Plast Polym Technol* 2:9
- Pappu A, Saxena M, Thakur VK, Sharma A, Haque R (2016) Facile extraction, processing and characterization of biorenewable sisal fibers for multifunctional applications. *J Macromol Sci Part A* 53:424
- Pei A, Zhou Q, Berglund LA (2010) Functionalized cellulose nanocrystals as biobased nucleation agents in poly(L-lactide) (PLLA)—crystallization and mechanical property effects. *Compos Sci Technol* 70:815
- Peng BL, Dhar N, Liu HL, Tam KC (2011) Chemistry and applications of nanocrystalline cellulose and its derivatives: a nanotechnology perspective. *Can J Chem Eng* 89:1191
- Pervaiz M, Oakley P, Sain M (2014) Extrusion of thermoplastic starch: effect of “green” and common polyethylene on the hydrophobicity characteristics. *Mater Sci Appl* 5:845
- Petersson L, Oksman K (2006) Biopolymer based nanocomposites: comparing layered silicates and microcrystalline cellulose as nanoreinforcement. *Compos Sci Technol* 66:2187
- Petersson L, Kvien I, Oksman K (2007) Structure and thermal properties of poly(lactic acid)/cellulose whiskers nanocomposite materials. *Compos Sci Technol* 67:2535
- Pracella M, Haque MM-U, Puglia D (2014) Morphology and properties tuning of PLA/cellulose nanocrystals bio-nanocomposites by means of reactive functionalization and blending with PVAc. *Polymer* 55:3720
- Qu P, Zhou Y, Zhang X, Yao S, Zhang L (2012) Surface modification of cellulose nanofibrils for poly(lactic acid) composite application. *J Appl Polym Sci* 125:3084
- Raquez J-M, Habibi Y, Murariu M, Dubois P (2013) Polylactide (PLA)-based nanocomposites. *Prog Polym Sci* 38:1504
- Rhim J-W, Mohanty AK, Singh SP, Ng PKW (2006) Effect of the processing methods on the performance of polylactide films: thermocompression versus solvent casting. *J Appl Polym Sci* 101:3736
- Robles E, Urruzola I, Labidi J, Serrano L (2015) Surface-modified nano-cellulose as reinforcement in poly(lactic acid) to conform new composites. *Ind Crops Prod* 71:44
- Roman M, Winter WT (2004) Effect of sulfate groups from sulfuric acid hydrolysis on the thermal degradation behavior of bacterial cellulose. *Biomacromolecules* 5:1671
- Saeidlou S, Huneault MA, Li H, Park CB (2012) Poly(lactic acid) crystallization. *Prog Polym Sci* 37:1657
- Saito T, Nishiyama Y, Putaux J-L, Vignon M, Isogai A (2006) Homogeneous suspensions of individualized microfibrils from TEMPO-catalyzed oxidation of native cellulose. *Biomacromolecules* 7:1687
- Saito T, Kimura S, Nishiyama Y, Isogai A (2007) Cellulose nanofibers prepared by TEMPO-mediated oxidation of native cellulose. *Biomacromolecules* 8:2485
- Saito T, Kuramae R, Wohlert J, Berglund LA, Isogai A (2013) An ultrastrong nanofibrillar biomaterial: the strength of single cellulose nanofibrils revealed via sonication-induced fragmentation. *Biomacromolecules* 14:248
- Salajková M, Berglund LA, Zhou Q (2012) Hydrophobic cellulose nanocrystals modified with quaternary ammonium salts. *J Mater Chem* 22:19798
- Sanchez-Garcia M, Lagaron J (2010) On the use of plant cellulose nanowhiskers to enhance the barrier properties of polylactic acid. *Cellulose* 17:987
- Singha AS, Thakur VK (2008a) Synthesis and characterization of grewia optiva fiber-reinforced pf-based composites. *Int J Polym Mater Polym Biomater* 57:1059

- Singha AS, Thakur VK (2008b) Synthesis and characterization of pine needles reinforced RF matrix based biocomposites. *J Chem* 5(S1):1055
- Singha AS, Thakur VK (2008c) Fabrication and study of lignocellulosic hibiscus sabdariffa fiber reinforced polymer composites. *BioResources* 3:1173
- Singha AS, Thakur VK (2009a) Fabrication and characterization of *H. sabdariffa* fiber-reinforced green polymer composites. *Polym Plast Technol Eng* 48:482
- Singha AS, Thakur VK (2009b) *Grewia optiva* fiber reinforced novel, low cost polymer composites. *J Chem* 6:71
- Singha AS, Thakur VK (2009c) Mechanical, Thermal and morphological properties of *grewia optiva* fiber/polymer matrix composites. *Polym Plast Technol Eng* 48:201
- Singha AS, Thakur VK (2009d) Study of mechanical properties of urea-formaldehyde thermosets reinforced by pine needle powder. *BioResources* 4:292
- Siqueira G, Bras J, Dufresne A (2009) Cellulose whiskers versus microfibrils: influence of the nature of the nanoparticle and its surface functionalization on the thermal and mechanical properties of nanocomposites. *Biomacromolecules* 10:425
- Song Y, Tashiro K, Xu D, Liu J, Bin Y (2013) Crystallization behavior of poly(lactic acid)/microfibrillated cellulose composite. *Polymer* 54:3417
- Spinella S, Lo Re G, Liu B, Dorgan J, Habibi Y, Leclère P, Raquez J-M, Dubois P, Gross RA (2015) Poly(lactide)/cellulose nanocrystal nanocomposites: efficient routes for nanofiber modification and effects of nanofiber chemistry on PLA reinforcement. *Polymer* 65:9
- Suryanegara L, Nakagaito AN, Yano H (2009) The effect of crystallization of PLA on the thermal and mechanical properties of microfibrillated cellulose-reinforced PLA composites. *Compos Sci Technol* 69:1187
- Thakur VK, Singha AS, Thakur MK (2013a) Ecofriendly biocomposites from natural fibers: mechanical and weathering study. *Int J Polym Anal Charact* 18:64
- Thakur VK, Singha AS, Thakur MK (2013b) Fabrication and physico-chemical properties of high-performance pine needles/green polymer composites. *Int J Polym Mater Polym Biomater* 62:226
- Thakur VK, Singha AS, Thakur MK (2013c) Synthesis of natural cellulose-based graft copolymers using methyl methacrylate as an efficient monomer. *Adv Polym Technol* 32(S1):E741
- Thakur VK, Thakur MK, Gupta RK (2013d) Graft copolymers from natural polymers using free radical polymerization. *Int J Polym Anal Charact* 18:495
- Thakur VK, Thakur MK, Gupta RK (2013e) Graft copolymers from cellulose: synthesis, characterization and evaluation. *Carbohydr Polym* 97:18
- Thakur VK, Thakur MK, Gupta RK (2013f) Rapid synthesis of graft copolymers from natural cellulose fibers. *Carbohydr Polym* 98:820
- Tingaut P, Zimmermann T, Lopez-Suevos F (2010) Synthesis and characterization of bionanocomposites with tunable properties from poly(lactic acid) and acetylated microfibrillated cellulose. *Biomacromolecules* 11:454
- Trache D, Hazwan Hussin M, Mohamad Haafiz MK, Kumar Thakur V (2017) Recent progress in cellulose nanocrystals: sources and production. *Nanoscale* 9:1763
- Turbak AF, Snyder FW, Sandberg KR (1983) Microfibrillated cellulose, a new cellulose product: properties, uses, and commercial potential. *J Appl Polym Sci Appl Polym Symp* 37:815
- Uetani K, Yano H (2011) Nanofibrillation of wood pulp using a high-speed blender. *Biomacromolecules* 12:348
- Vazquez A, Foresti ML, Moran J, Cyrus V (2015) Extraction and production of cellulose nanofibers. In: Pandey JK, Takagi H, Nakagaito AN, Kim H-J (eds) *Handbook of polymer nanocomposites. Processing, performance and application*. Springer, Berlin, pp 81–118
- Vink ETH, Davies S (2015) Life cycle inventory and impact assessment data for 2014 Ingeo® polylactide production. *Ind Biotechnol* 11:167
- Vink ETH, Rábago KR, Glassner DA, Springs B, O'Connor RP, Kolstad J, Gruber PR (2004) The sustainability of Natureworks™ polylactide polymers and Ingeo™ polylactide fibers: an update of the future. *Macromol Biosci* 4:551

- Voicu SI, Condruz RM, Mitran V, Cimpean A, Miculescu F, Andronesu C, Thakur VK (2016) Sericin covalent immobilization onto cellulose acetate membrane for biomedical applications. *ACS Sustain Chem Eng* 4:1765
- Wågberg L, Decher G, Norgren M, Lindström T, Ankerfors M, Axnäs K (2008) The build-up of polyelectrolyte multilayers of microfibrillated cellulose and cationic polyelectrolytes. *Langmuir* 24:784
- Walther A, Timonen JVI, Díez I, Laukkanen A, Ikkala O (2011) Multifunctional high-performance biofibers based on wet-extrusion of renewable native cellulose nanofibrils. *Adv Mater* 23:2924
- Wang S, Cheng Q (2009) A novel process to isolate fibrils from cellulose fibers by high-intensity ultrasonication, part 1: process optimization. *J Appl Polym Sci* 113:1270
- Wang T, Drzal LT (2012) Cellulose-nanofiber-reinforced poly(lactic acid) composites prepared by a water-based approach. *ACS Appl Mater Interfaces* 4:5079
- Wang B, Sain M (2007a) Isolation of nanofibers from soybean source and their reinforcing capability on synthetic polymers. *Compos Sci Technol* 67:2521
- Wang B, Sain M (2007b) The effect of chemically coated nanofiber reinforcement on biopolymer based nanocomposites. *BioResources* 2:371
- Wang B, Sain M (2007c) Dispersion of soybean stock-based nanofiber in a plastic matrix. *Polym Int* 56:538
- Wang X, Li W, Kumar V (2006) A method for solvent-free fabrication of porous polymer using solid-state foaming and ultrasound for tissue engineering applications. *Biomaterials* 27:1924
- Wang B, Mireles K, Rock M, Li Y, Thakur VK, Gao D, Kessler MR (2016) Synthesis and preparation of bio-based ROMP thermosets from functionalized renewable isosorbide derivative. *Macromol Chem Phys* 217:871
- Wu JH, Kuo MC, Chen CW, Kuan PH, Wang YJ, Jhang SY (2013) Crystallization behavior of α -cellulose short-fiber reinforced poly(lactic acid) composites. *J Appl Polym Sci* 129:3007
- Xu J, Guo B-H (2010) Poly(butylene succinate) and its copolymers: Research, development and industrialization. *Biotechnol J* 5:1149
- Xu X, Liu F, Jiang L, Zhu JY, Haagenson D, Wiesenborn DP (2013) Cellulose nanocrystals vs. cellulose nanofibrils: a comparative study on their microstructures and effects as polymer reinforcing agents. *ACS Appl Mater Interfaces* 5:2999
- Xu X, Wang H, Jiang L, Wang X, Payne SA, Zhu JY, Li R (2014) Comparison between cellulose nanocrystal and cellulose nanofibril reinforced poly(ethylene oxide) nanofibers and their novel shish-kebab-like crystalline structures. *Macromolecules* 47:3409
- Yanamala N, Farcas MT, Hatfield MK, Kisin ER, Kagan VE, Geraci CL, Shvedova AA (2014) In vivo evaluation of the pulmonary toxicity of cellulose nanocrystals: a renewable and sustainable nanomaterial of the future. *ACS Sustain Chem Eng* 2:1691
- Zhang K, Mohanty AK, Misra M (2012) Fully biodegradable and biorenewable ternary blends from polylactide, poly(3-hydroxybutyrate-co-hydroxyvalerate) and poly(butylene succinate) with balanced properties. *ACS Appl Mater Interfaces* 4:3091
- Zhang X, Li W, Ye B, Lin Z, Rong J (2013) Studies on confined crystallization behavior of nanobiocomposites consisting of acetylated bacterial cellulose and poly(lactic acid). *J Thermoplast Compos Mater* 26:346
- Zhao Y, Li J (2014) Excellent chemical and material cellulose from tunicates: diversity in cellulose production yield and chemical and morphological structures from different tunicate species. *Cellulose* 21:3427
- Zhao Y, Zhang Y, Lindström ME, Li J (2015) Tunicate cellulose nanocrystals: preparation, neat films and nanocomposite films with glucmannans. *Carbohydr Polym* 117:286

Chapter 8

Epoxidized Vegetable Oils for Thermosetting Resins and Their Potential Applications

Carmen-Alice Teacă, Dan Roșu, Fulga Tanasă, Mădălina Zănoagă
and Fănică Mustață

Abstract In the recent decades, bio-based polymers have gained increasing interest, especially for composite materials. These polymers and their respective monomers are derived from renewable resources, being thermoplastics or thermosetting resins which are biodegradable or non-biodegradable. Thermosettings are strong, rigid polymer materials and cannot be easily processed by melting after their hardening. At present, thermosetting resins are obtained using highly toxic and volatile petrochemicals, which require human and environmental safety monitoring. Considering the wide range of diverse renewable monomers available, vegetable oils (VOs) are especially well-suited when it comes to the synthesis of thermosetting resins due to their carbon-carbon double bonds, highly desirable for this type of application as these unsaturated bonds can be chemically modified in order to increase reactivity toward further polymerization. Thus, epoxidation, which consists of introducing a single oxygen atom to each non-saturated bond to yield in an epoxidic cycle, is a simple, effective method to modify these VOs. The resulted thermosetting resins exhibit improved toughness and environmental-friendly behavior. VOs, especially soybean oil which is abundant and cheap, are typically mixtures of unsaturated fatty acids with numerous bonds that can be easily converted into the more reactive oxirane rings through the reaction with peracids or

C.-A. Teacă (✉) · D. Roșu

Advanced Research Center for Bionanoconjugates and Biopolymers,
“Petru Poni” Institute of Macromolecular Chemistry, 41A Gr. Ghica-Voda Alley,
700487 Iasi, Romania
e-mail: cateaca14@yahoo.com

F. Tanasă · M. Zănoagă

Polyaddition and Photochemistry Department, “Petru Poni” Institute of Macromolecular
Chemistry, 41A Gr. Ghica-Voda Alley, 700487 Iasi, Romania

F. Mustață

Physical Chemistry of Polymers Department, “Petru Poni” Institute of Macromolecular
Chemistry, 41A Gr. Ghica-Voda Alley, 700487 Iasi, Romania

peroxides. The present chapter focuses on composites obtained from epoxidized vegetable oils (EVOs) and epoxy resins and their properties in correlation with their envisaged applications.

Keywords Vegetable oils · Epoxidation · Thermosetting resins · Applications

1 Introduction

In recent decade, there has been noticed an increasing research interest for using vegetable oils in obtainment of valuable polymer materials (Gan and Jiang 2015; Paluvai et al. 2015a, b; Mustață et al. 2013; Stemmelen et al. 2011; Raquez et al. 2010; Guner et al. 2006). These bio-based polymer materials are usually designed for technical applications. Considering their different uses, for example, biomedical purposes, or surface coatings applications (such as paint and printing ink formulations), these materials should have specific features including good thermal stability and significant ability to resist damage by chemical reactivity or solvent reaction.

As these materials are biodegradable being resulted from renewable raw materials, they should be also biocompatible in terms of their physical and chemical properties, mainly when they are used for medical applications. Other technical usefulnesses should require electrical conductive, non-flammable, gas permeable properties, or materials with good adhesion to metallic substrates (Guner et al. 2006).

Vegetable oils derived from seeds of oil-type plants and separated through extraction procedures are natural, environmental friendly and renewable raw materials with large availability, low cost, and functionality readily to be significantly improved in order to obtain novel bio-based functional polymers and polymer materials (Gan and Jiang 2015; Quirino et al. 2014; Lligadas et al. 2013). The structural constituents of vegetable oils are triglycerides, resulted from glycerol and fatty acids by esterification reaction. Oils are in fact a complex mixture of such esters with different saturation levels. Fatty acids content is specific for each vegetable oil and they confer many reactive sites (e.g. double bonds, ester groups, epoxy groups) suitable for modification approaches in order to obtain new synthesized structures.

Most of the present literature data focused on the use of vegetable oils and their functionalized derivatives for either linear structures, three dimensional networks, or matrices for thermoplastic and thermosetting-based composites, biocomposites and hybrid materials (Paluvai et al. 2015a, b; Altuna et al. 2015; Quirino et al. 2014; Ding and Matharu 2014; Miao et al. 2014; Lligadas et al. 2013; Biermann et al. 2011; Raquez et al. 2010; Guner et al. 2006).

Among vegetable oils, the most used for tailoring oil-modified polymers with different potential applications include linseed (Pin et al. 2015a, b; Ding et al. 2015; Luo et al. 2013; Henna et al. 2008; Lligadas et al. 2006a Miyagawa et al. 2005a),

sunflower (Taghizadeh et al. 2008), castor (Echeverri et al. 2015; Rosu et al. 2015; Paluvai et al. 2015a, b; Ray et al. 2012; Sharmin et al. 2011; Mulazim et al. 2011), soybean (Roşu et al. 2016; Tsujimoto et al. 2015; Echeverri et al. 2015; Altuna et al. 2015; Hosoda et al. 2014; Pan and Webster 2011; Adekunle et al. 2010; Tsujimoto et al. 2003; Uyama et al. 2003; Gerbase et al. 2002), palm (Jusoh et al. 2012), pine (Abdelwahab et al. 2015), tall (Liu et al. 2015), corn (Mustață et al. 2013), rapeseed (Wu et al. 2000), grapeseed (Stemmelen et al. 2011), and tung (Meiorin et al. 2015; Luo et al. 2013) oils.

Thermosetting resins are valuable products for industrial applications (Raquez et al. 2010; Thakur et al. 2013a, b; Pappu et al. 2016) considering their versatile properties that can be tailored as desired, for example enhanced strength, and high modulus, improved stability (e.g. chemical, thermal) and durability. All these desirable properties are conferred by the high cross-linking density exhibited by thermosetting resins (Yousefi et al. 1997; Feldman 1996; Krawczak and Pabiot 1995; Singha and Thakur 2008a, b, c, 2009a, b, c, d), but there are also some inherent disadvantages including reduced impact properties and not being reshapable after curing/polymerization process (Carfagna et al. 1997). Fibers type fillers including glass, carbon, aramid or natural ones (intact or shredded), and clay type fillers are often used as additives in resin formulations to produce composite materials (Paluvai et al. 2014; Shibata et al. 2009; Miyagawa et al. 2005b; Uyama et al. 2003; Hayes and Seferis 2001).

2 Thermosetting Resins from Renewable Resources and Their Applications

The use of vegetable oils, an important class of renewable raw materials, readily available for the synthesis of different monomers and polymeric materials with many applications, was briefly presented as reviewed (Xia and Larock 2010). The resulted polymer materials, converting soft, flexible rubbers into hard, rigid plastics, display a large range of beneficial properties, the main important being the mechanical, and thermal ones, and constitute potential promising alternatives to classic oil-based materials. A thermosetting polymer material results as a solid state from liquid solution (comprising mainly a mixture of co-monomers) through curing process in an irreversible way, under heating or UV irradiation. It is essential that one or more of the monomers have at least three or more reactive groups in the molecular structure, which further generates tri-dimensional cross-linked networks with no ability to reshape after the reaction ending. Usually, thermosetting materials are obtained using a resin, a curing agent, a catalyst or initiator, and sometimes a solvent (Auvergne et al. 2014; Raquez et al. 2010).

Thermosetting polymer materials, representing less than 20% of plastic products, have many industrial applications. The most important examples are represented by phenolic resins, urea formaldehyde resins, unsaturated polyesters, and epoxy resins.

Epoxy resins are low molecular mass monomers containing at least two epoxide groups (glycidyl or oxirane group type). These epoxy monomers can interact with themselves through homo-polymerization reactions (anionic or cationic), or in the presence of a large range of co-reactants (polyfunctional amines, acids, anhydrides, phenols, alcohols, thiols) that are usually called hardeners. Blending with some additives and fillers is also applied when reduction of costs or achieving desirable processing and/or properties are envisaged (Auvergne et al. 2014). An effective approach to generate oxirane groups is represented by peroxidation of double bonds which, in the case of aliphatic chains, is a simple oxidation process by using hydrogen peroxide (e.g. epoxidation of vegetable oils). Vegetable oils comprise varied fatty acids structures which present naturally occurring functional groups (carbon-carbon double bonds, hydroxyl groups, even epoxy groups). The first mentioned ones, with reduced reactivity, can generate new functional groups capable to be easily polymerized. Some of the most significant applications of thermosetting resins from epoxidized vegetable oils will be further presented.

2.1 Coatings

Epoxidized vegetable oils (EVOs)-based polymers have been extensively used as coatings, given their superior mechanical properties, processing ability, and chemical resistance, in various applications: electrical engineering, electronics, automotive and even aeronautics, biomedical and food packaging (Auvergne et al. 2014). Thus, commercial products are readily available on various markets. Functionalized vegetable oils can be employed in coatings made of epoxidized linseed oil (ELO) and epoxidized soybean oil (ESO), the most common and widely used (Miyagawa et al. 2006). The synthesis approach may vary to a large extent. ESO is known to undergo both cationic and thermal processing (Raghavachar et al. 2000) while epoxidized palm oil (EPO) have been used for UV-curable coatings (Wan et al. 2003; Raghavachar et al. 2000), as well as the vernonia oil, which naturally contains epoxide groups that made it fit for such applications (Thames and Yu 1999). Since each type of application sets its own performance requirements, all formulations are target-oriented. As for the coatings, the processing techniques, along with the complex chemistry characteristic for a multi-component polymer system, are a key factor. Temperature, pressure, reaction rate and visco-elastic behaviour can influence the properties of the materials during each stage of processing, and even afterwards (delamination, debonding or even post-processing reactions (Pascault and Williams 2013)).

Complex coating formulations may also include additives of various types aimed to improve mechanical and thermal properties, specifying that they may also undesirably increase the viscosity. Initiators having cationic structure are inert under normal conditions (ambient temperature and illumination), but they exhibit activity under external stimulus (heating or photo-irradiation). They are used not only for epoxidized vegetable oils-based coatings, but also for adhesives, paintings,

inks and photoresists. The preparation of epoxy-modified cyclohexene-containing linseed oil (ECLo) was reported and the kinetics of photo-polymerization was studied in comparison with the corresponding compound without epoxy groups (Zou and Soucek 2005; Zong et al. 2003). The epoxy conversion and the polymerization reaction rate, as well as the mechanical properties of the coatings, were proven to depend on the reduced viscosity of the system.

Other kinetic studies were focused on the polymerization of EVOs bearing benzyl alcohols units (Ortiz et al. 2005). The effect of the both cationic and anionic initiators on the rate of the photo-polymerization of epoxidized triglycerides was evaluated. The raw material used was vernonia oil, known to naturally contain epoxy moieties, and the resulted coatings exhibited high flexibility and impact strength (Crivello and Narayan 1992). UV-curable coatings with an interesting supramolecular architecture were obtained using vernolic acid units grafted onto a functionalized hyperbranched polyether (Samuelsson et al. 2004).

Fundamental studies were also performed on different triglyceride-initiator systems aiming to optimize them. For ESO, which is considered a representative green monomer, it was found that silyl radical chemistry used for promoting the free-radical cationic polymerization was highly efficient, even in air and upon natural irradiation: after 1 h exposure, a tack-free uncolored coating yielded in with a conversion of 60% (Tehfe et al. 2010).

An epoxidized derivative of anacardic acid was reported to yield in thin films by cationic photo-polymerization (Pascualt and Williams 2010) in the presence of a solution of triaryl sulfonium hexafluoroantimonate salt in propylene carbonate. The coatings exhibited surface with enhanced hydrophobicity due to the achieved long, hydrophobic alkyl chain localized at the coating-air interface. (Chen et al. 2009; Huang et al. 2012). These epoxidized vegetable oils may be used as reactive additives in UV curable materials by cationic photo-polymerization (“humidity blockers”).

The use of hardeners, either from renewable resources or synthetic, is aimed to improve the properties of coatings. The literature is scarce concerning epoxidized vegetable oils formulated with bio-based hardeners. Still, data on the properties of ESO-based coatings cured in the presence of maleinated soybean oil (Warth et al. 1997) or terpene derived acid anhydride (Takahashi et al. 2008) were communicated. Resins obtained from epoxidized linseed oil using a vegetable oil polyamine prepared by thiol-ene chemistry as cross-linker (Stemmelen et al. 2011) were reported to exhibit elastomeric properties and low glass transition temperatures. Other coatings were obtained using bio-based hardeners formulated with synthetic commercially available epoxy ethers, namely glycerol polyglycidyl ether (GPE; epoxy functionality 2) and polyglycerol polyglycidyl ether (PGPE; epoxy functionality 4.1) (Shibata and Nakai 2010; Takada et al. 2009).

Coatings properties may be upgraded by applying different methods, one of them being the increase of the epoxydic precursor functionality. Such an example is the synthesis of new epoxy monomers, namely epoxidized sucrose esters of fatty acids (ESEFAs) (Pan et al. 2011), that reacted with a cycloaliphatic anhydride (4-methyl-1,2-cyclohexanedicarboxylic anhydride, MHHPA) in the presence of an

initiator (1,8-diazabicyclo[5.4.0]undec-7-ene, DBU). Their properties as coatings for steel were studied in comparison with a commercially available ESO-based coating and the data collected from various measurements indicated these ESEFAs-based materials as high performance thermoset coatings in correlation with their high content (approx. 75%) of vegetable component. The high modulus values of these coatings, their hardness and ductility can be explained considering the structure of ESEFAs and their enhanced functionality. These monomers may be of further use for composites and adhesives, as well.

Other thermosetting coatings were obtained by substituting in a certain degree synthetic prepolymers (i.e., diglycidyl ether of bisphenol A DGEBA) with EVO commonly used as reactive diluents and/or agents for improved flexibility (Czub 2006). Thus, formulations containing DGEBA and ESO, including methyl tetrahydrophthalic anhydride (MTHPA) as hardener and 1-methylimidazole (1-MI) as an initiator (Altuna et al. 2011), yielded in coatings reported to have decreasing T_g values along with the increasing amount of ESO and a good balance between composition and properties was reached for a ratio DGEBA/ESO = 40/60 (wt%). When soybean (Miyagawa et al. 2005b) or linseed oil (Miyagawa et al. 2005c) was used in combination with diglycidyl ether of bisphenol F (DGEBF), employing the same hardener and initiator, the properties of the resulted coatings were comparable.

Another approach to enhance the properties of EVOs-based coatings consists of chemical modifications performed to the EVO precursors. In example, grafting phenol units (such as bisphenol A) onto EVOs (epoxidized soybean, rapeseed, linseed, and sunflower oils) yielded in prepolymers that may be further cross-linked in the presence of various hardeners (2-methylimidazole, dicyanodiamide, hexahydrophthalic anhydride, and triethylenetetramine) (Czub 2009).

The new materials were reported to have improved mechanical strength. When reagents bearing phosphorus moieties were employed to modify EVO, coatings with flame retardant properties were obtained. Thus, a diepoxy monomer was synthesized starting from 10-undecenoyl chloride and a diphenol resulted from the reaction of 9,10-dihydro-9-oxa-10-phosphaphenanthrene-10-oxide and benzoquinone; subsequently, the double bonds were oxidized (Lligadas et al. 2006b, c). Then methylene dianiline (MDA) or bis(m-aminophenyl)methylphosphine oxide (BAMPO) was used for the cross-linking reaction. It was proven the material achieved a diminished flammability.

Coatings with tailored properties, such as biocide, biocompatible, biodegradable, anti-corrosion, low emission of volatiles, were designed for special applications, namely decorative, protective and architectural layers, electrically insulations, films for paper packaging or having self-healing properties (Alam et al. 2014).

Coatings having paint properties were obtained from EVOs containing oxazoline units (Trumbo and Otto 2008). Pure vegetable oils and in blends with polymethylmethacrylate and polystyrene have been used as anticorrosive coatings with high flexibility (Ahmad et al. 2006a, b). Coatings obtained from EVOs blended with polyvinyl chloride and polyvinyl alcohol, respectively, have achieved biodegradable character and may be used as films for food packaging (Riaz et al.

2010, 2011). Naturally-containing epoxy moiety vernonia oil, as well as epoxidized vegetable oils (ESO and ELO) have been used as reactive diluents, the resulting coatings showing improved properties and zero emission of volatiles (Das and Karak 2009).

When employing epoxidized 10-undecenoic acid triglyceride, cured in the presence of amines, coatings with high UV-stability, good adhesion, solvent resistance and toughness were obtained (Earls et al. 2004).

2.2 *EVO Based Composites*

Fiber reinforced composites are materials that may be used in automotive and aircraft industry, as structural materials, with good results. Manufactured generally starting from natural (flax, hemp) and synthetic (glass, short carbon fibers, as well as mineral fibers, such as surface-modified wollastonite) fibers, they employ polymeric matrices which can be made also from renewable resources, as in the case of epoxidized vegetable oils. The growing interest in the use of such materials is a mark of the last decades, considering the global environmental movement and green policy.

The epoxidized soybean oil (ESO) based composites are an example of epoxidized vegetable oils successfully used as matrices (Meier et al. 2007; Kayode and Adekunle 2015; Petrovic et al. 2004). Reinforced with glass and carbon fibers (Liu et al. 2002, 2007), these composites proved thermal, mechanical and physical properties comparable to classic oil-based elastic polymeric materials. The formulations included some well-chosen curing agents and epoxy resins to enable the final composite to fit a wide range of end-user requirements. The method of manufacturing was also a new approach, as the solid free from fabrication (SFF—a method of producing objects without molds, best known from stereo lithography as a method to rapidly obtain prototypes) is not commonly used to produce fiber reinforced composites. Experimental results showed, as follows: glass and carbon fibers exerted a better reinforcing effect as compared to mineral fibers; the composite modulus depended on the fibers orientation, aspect ratio and volume fraction; the reinforcement effect is enhanced at higher temperature; it is possible to use the SFF method to obtain end products based on such composites when other manufacturing approaches cannot be employed.

Further functionalization of vegetable oils yielded in valuable compounds that were used as matrix for fiber-reinforced composites with either natural or synthetic fibers. This is the case of acrylated epoxidized soybean oil (AESO), maleinized soy oil monoglyceride (SOMG/MA) and maleinized hydroxylated oil (HO/MA) synthesized from the triglyceride oil, or even maleinated acrylated epoxidized soybean oil (MAESO) (Campanella et al. 2015).

When glass fibers (QM6408 E-Glass) were employed, AESO-based composites containing up to 50% fibers showed excellent mechanical properties (Khot et al. 2001). The addition of natural fibers (flax and hemp) in various ratios induced

improved elastic properties. These properties exhibited by composites with combined natural and synthetic fibers can be furthermore exploited, since they are combining advantages from the both classes of fiber composites (i.e., the low cost of natural fibers and the high performance of the synthetic ones).

Lignocellulosic materials (flax, cellulose, pulp, hemp, wheat straw fibers) were also used to produce AESO-based composites. For this purpose, flax fibers were mixed with butyrate kraft lignin (Thielemans and Wool 2004) which acted as compatibilizing agent between matrix (AESO and styrene) and fibers by improving the adhesion at the interface. This behaviour was evidenced by SEM images illustrating that fibers fractured along with the matrix, without pulling out. When short wheat straw fibers were employed, the effect of butyrate kraft lignin was most evident in the tensile strength improvement, as the system enabled a better interaction between matrix and fibers, given the enhanced fibers wettability. All these composites were made by the vacuum assisted transfer molding process which granted a good permeation of the matrix around and within the fibers.

Another approach in this field was the production of fiber-reinforced composites directly as end-products. Thus, panels for in-door applications (housing, structural materials, furniture, automotive parts, etc.) were made from AESO and natural fiber mats (flax, cellulose, pulp and recycled paper, hemp) up to 10–50% (O'Donnell et al. 2004). Vacuum-assisted resin transfer molding or resin vacuum infusion process were used to obtain such panels. All these materials showed good mechanical properties as compared to woven E-glass fibers reinforced AESO composites, with different values of the flexural modulus depending on the nature of fibers, but the production costs were lower.

The maleinated acrylated epoxidized soybean oil (MAESO) is another example of functionalized vegetable oil that can be used in fiber-reinforced composites production (Campanella et al. 2015).

Composites panels were made of both glass fibers and natural fibers (flax), and using MAESO along with wisely chosen reactive diluents (styrene, vinyl-toluene, divinyl-benzene, methyl methacrylate and methacrylated fatty acid—MFA) as matrices. The end-products proved to have good mechanical characteristics and physical properties close to those made of oil-based polymers. It was shown that tuning the amount of MFA versus MAESO, it was possible to increase the amount of natural fibers in the formulation, but given their lower density, the composites remained lighter as compared with glass fiber reinforced ones. At the same time, the flax containing composites displayed enhanced elastic properties, despite their lower strength, which makes them fit for lightweight applications in automotive industry. The experimental data confirmed that MAESO is a versatile compound fit for further processing in order to obtain multi-component systems with tailored properties. Since the presence of MFA in formulations reduced the modulus but increased the elongation for equivalent strength, it is beneficial to combine MAESO and MFA to obtain lightweight composite products with high content of natural fibers.

Other ESO-based resins were also tested to be further used in the production of fiber-reinforced composites. Thus, a combination of epoxidized soybean oil ESO

and diglycidyl ether of bisphenol A DGEBA was formulated and cured in the presence of *p*-aminobenzoic acid (*p*-ABA). The influence of ESO on the curing kinetics and thermal properties of the cured resin was investigated (Mustață et al. 2011). The results confirmed that ESO contributed to improve the resin toughness, as well as its biocompatibility. The morphology study of the cross-linked system showed a smooth fracture surface and cracks uniformly spread in the entire sample, indication of the enhanced toughness due to the reactive epoxidic groups of ESO and DGEBA cross-linked to yield larger network structures. This phenomenon was enabled by the good dispersion of ESO in the resin bulk.

Other inexpensive composites with glass fibers were made by using renewable resources, namely epoxidized allyl soyate (EAS), a soy-based resin produced starting from unsaturated soybean oil (Chandrashekhara et al. 2005). EAS consists of mixtures of epoxidized fatty acid esters and it was expected to yield a highly dense intermolecular cross-linking given its superior reactivity and, subsequently produce materials with better mechanical properties than those of materials resulted from unmodified ESO. Data collected for the pultruded glass fiber reinforced composites indicated good values for flexural strength, modulus and impact resistance, confirming the possibility to use these composites as structural materials. The decrease in the pull force during the pultrusion process was noticeable, as expected, given the unctuousity of the soybean oil. These results validated the potential of EAS to environmentally friendly and low cost structural applications.

Keratin fibers were also considered when it came to the development of novel bio-based composite materials with specific properties (Hong and Wool 2005). Keratin fibers originating from feathers are tough, despite their lightweight and hollow structure and, given their chemical proteic nature, are compatible with acrylated epoxidized soybean oil (AESO). Since the fibers are not filled with resin during the processing, the final composites contain a high amount of air inside the hollow structure of fibers and the density barely reach 1 g/cm^3 for 30% (volume fraction) keratin fibers content. Therefore, the values of the dielectric constant are lower than silicon dioxide or epoxy, or polymer dielectric insulators. At the same time, the value of the coefficient of thermal expansion is also low enough, and that makes these composites fit for electronics. Another property evaluated was the water sorption which is correlated with the amount of keratin fibers and their wettability by AESO. The mechanical properties (storage modulus, fracture toughness, flexural strength) were dramatically increased due to the presence of keratin fibers. Even more significant improvements may be achieved by wisely select the matrix in terms of compatibility with the reinforcement and strictly sort the fibers.

Particulate composites using EVO as matrices are found to be of high interest in structural materials, depending on the amount and type of particles, as well as mechanical level of performance of the considered resins. It is well known that the best mechanical properties in particulate composites are achieved when particles with different size, from coarse particles to fine particles, are mixed previously. This protocol enables an enhanced reinforcement of the final composite as each dimensional fraction of particles occupy a specific volume and contributes to the formation of a rigid “skeleton” inside the matrix. Under these circumstances, the

higher the compatibility between matrix and filler, the better the wettability, the better elasticity to strength ratio of the composite.

An interesting study on composites made of epoxidized castor oil (ECO) and mixtures of inorganic fillers in different ratios evidenced this assessment (Balo 2011). The filling materials (coal fly ash, clay, perlite and pumice) were selected due to their characteristics, mainly their pozzolanic effect, and local availability. The pozzolans are siliceous materials with no cementitious properties by themselves, but added in controlled ratios and in finely ground state to classic formulations may react with calcium hydroxide in the presence of water, at ambient temperature, to yield in compounds with remarkable cementitious properties. Thus, it is possible to estimate the pozzolanic activity (Snellings et al. 2012). The coal fly ash is currently a municipal waste commonly disposed of in landfill or ash deposits, with noticeable negative environmental impact. It is already used in low amounts in some applications, such as component in concrete used for grouting and other stabilizing operations in mining, as well as filling material in civil engineering (Horiuchi et al. 2000). The clay used in these formulations was commercially available. Pumice is a glassy volcanic rock (rhyolitic or dacitic magma) with high porosity which grants a specific density lower than 1 and enables it to float. In civil engineering applications as structural materials, pumice proved to be easy processable and to contribute to the heat and sound insulation, and fireproofing (Shrew and Brink 1977). Perlite is an amorphous volcanic glass which contains high amount of water and may be expanded to 7–16 times its original volume upon heating at 850–900 °C, when its density becomes 0.03–0.15 g/cm³ (Maxim et al. 2014). In natural state, perlite has a good pozzolanic effect and it is used in concrete formulations to improve their mechanical properties, mainly the compressive strength (Mo and Fournier 2007; Demirboğa et al. 2001).

The experimental results indicated that the fly ash and ECO contributed to the decrease of the compressive-tensile strength and thermal conductivity, but the lowest values were obtained in samples containing pumice and expanded perlite (5% each); same for the abrasive loss and water sorption. The thermal conductivity of samples increased along with the increasing density of materials, but decreased when the water sorption enhanced. It was also proven that the presence of clay caused an improved abrasion resistance. It is noticeable that these composites are able to incorporate high amounts of filler, while maintaining low density and high structural performance, which recommends them for lightweight applications.

2.3 Nanocomposites with EVO Matrices

Polymer nanocomposites are multi-component systems and basically consist of nanofillers (particles of different shape, platelets, fibers and fibrils, etc.) dispersed in a polymeric matrix made of one polymer or a mixture of polymers. The transition from micrometer to nanometer scale entails changes in both physical and chemical

properties of the materials. Since the nanofillers are affecting the behaviour of the nanocomposite, it is of interest to consider two structural aspects of the filler: the increased surface area:volume ratio, and the size of the particle. The smaller the particles, the higher the surface area:volume ratio, which shifts the interest from the atom interactions inside the particle to the ones at the exterior surface of the particle, or, more specifically, at the interface between matrix and particle.

Typical nanofillers are considered silica (SiO_2) nanoparticles, metal-oxo clusters ($-\text{O}-\text{Ti}-\text{O}-$, zirconia, etc.), clays in native state or organically modified, etc. Polymers reinforced with well-defined nanosized inorganic clusters, including ceramers (IUPAC 1997), have attracted a great interest due to their versatility in terms of properties and applications.

Polyhedral oligomeric silsesquioxane (POSS) compounds have a unique cage-like structure (1–3 nm in diameter) where the ratio between oxygen and silicon is $(\text{SiO}_{1.5})_n$, $n = 8, 10, \text{ or } 12$. Various POSS were used to obtain nanocomposites by copolymerization with different organic monomers (Kannan et al. 2005); even epoxidic resins were employed to prepare such nanocomposites (Abad et al. 2003).

Generally, the presence of POSS renders improved thermal and mechanical properties, as well as reduced flammability. When the structure contains POSS pendant on a network chain, the $(\text{SiO}_{1.5})_n$ clusters exhibit a trend to aggregate, depending on the nature of organic ligands, and the POSS-POSS interactions become the network structuring driving force. Even more, the extent of POSS aggregation increases along with the decrease of the POSS crosslinking functionality (Matějka et al. 2004).

An excellent example of biobased POSS-nanocomposites from plant oil derivatives is represented by the epoxidized linseed oil (ELO) and 3-glycidylpropylheptaisobutyl- T_8 -polyhedral oligomeric silsesquioxane (G-POSS) in different amounts (2, 5, and 10 wt%) that were cross-linked (Lligadas et al. 2006d). At low amounts of G-POSS (2 wt%), no aggregates were observed, but for higher contents clusters having several nanometers in diameter were noticed. The glass transition temperatures were higher and storage moduli of the networks in the glassy state were improved as compared to those of pure ELO network. A rubber plateau was also observed to be higher than that of the pure resin. These findings were attributed to the reinforcing effect of the G-POSS clusters.

Novel biobased hybrid organic-inorganic materials were obtained using several polyfunctional hydrosilylating agents, such as 1,4-bis(dimethylsilyl)benzene (DMSB), tetrakis(dimethylsilyloxy)silane (TKDS) and 2,4,6,8-tetramethylcyclotetrasiloxane (TMCTS) (Galià et al. 2010). Other several inorganic precursors, namely 3-glycidoxypropyl-trimethoxysilane (GPTMS), 2-(3,4-epoxycyclohexyl)-ethyl-trimethoxysilane (ECTMS), 3-aminopropyl-trimethoxysilane (APTEOS), and 2-aminoethyl-3-aminopropyltrimethoxysilane (AEPTEOS), were also employed in order to obtain hybrid materials (Tsujimoto et al. 2010).

Biodegradable nanocomposites were successfully prepared starting from epoxidized soybean and linseed oils (ESO and ELO) and 3-glycidoxypropyltrimethoxysilane (GPTMS) (Tsujimoto et al. 2003). The nanocomposites were obtained in situ by an

acid-catalyzed reaction and this allowed the simultaneous formation of both resin matrix and silica network. The covalently bonded organic and inorganic structures enabled a highly organized architecture that entailed improved film properties. Thus, the hardness and tensile strength were enhanced, as well as the flexibility of the nanocomposites. The reinforcing effect of the silica network was also substantiated by the rheologic behaviour of the novel materials, which were also tested for their biodegradation susceptibility with good results: after 2 months in an activated sludge, the samples degraded over 50%.

On the other hand, using the same ELO and ESO, and GPTMS, it was possible to obtain nanocomposites by an acid-catalyzed curing reaction, these being able to form highly glossy, transparent films, with good coating characteristics, while maintaining their biodegradability (Tsujiimoto et al. 2010). Besides the improvement of the mechanical strength and thermal stability, the reinforcing effect of the silica network was also confirmed by the dynamic visco-elasticity analysis.

Other ceramers were prepared by sol-gel processes using an inorganic precursor, namely tetraethoxysilane (TEOS), and epoxidized castor oil (ECO), in various ratios, aiming to reach an optimum between composition and properties (de Luca et al. 2006). The morphology of the materials was characteristic to homogeneous films when the inorganic component was in low amounts. Unlike simple castor oil-based nanocomposites, the ceramers made of ECO may include higher amounts of inorganic component without any occurrence of phase separation, which is an indication of the wettability of the inorganic network, hence, the compatibility of the two components. Mechanical properties (hardness and tensile strength) improved along with the increasing amount of TEOS, though the swelling in toluene diminished. All considered samples have showed good adhesive properties, which recommend them for coating applications.

Another inorganic precursor, namely 3-aminopropyltriethoxysilane (APTES), was employed for ceramers preparation due to its structural and functional features. This bifunctional precursor, containing an amine group supplemental to the silane moiety, is able to yield 3D silicon oxide networks where -NH_2 and -Si-OH groups can be crosslinked. Therefore, in a wisely chosen reaction system it may act as reagent, contributing to the inorganic network, as well as a coupling agent, linking the organic and inorganic components. Thus, hybrid homogeneous films were obtained using ECO and mixtures of APTES and TEOS in various ratios (Becchi et al. 2011). It was proven that additional APTES did not enhanced the thermal stability of the nanocomposites, as compared to ECO-TEOS ones, but contributed to the increase of the hardness and tensile strength values. Given the thermal data achieved for the ECO-APTES-TEOS systems, it was suggested that the conversion of the inorganic precursors into pure silica was not complete, as expected, but they also yielded in some amorphous silicon oxycarbide ($\text{SiC}_x\text{O}_{4-x}$). The samples studied have proved competitive adhesive properties toward aluminum surfaces and, consequently, these materials may be considered for anti-corrosive protection coatings.

Ceramers containing metal-oxo clusters were designed to yield materials with beneficial properties derived from both organic and inorganic phases; they may be

prepared through sol-gel processes, as the inorganic phase can generate self-assembled networks and, at the same time, react with the organic phase by cross-linking via hydrolysis and condensation reactions (Wold and Soucek 2000).

Thus, ceramer coatings intended for electronics applications were obtained with good results using linseed and sunflower oil, as the organic phase, and titanium (IV) *i*-propoxide (TIP), titanium (IV) di-*i*-propoxide bis-acetoacetate (TIA), and zirconium *n*-propoxide (ZRP), as the inorganic phase (Tuman and Soucek 1996; Tuman et al. 1996).

Given the reactivity of the EVO and considering the conditions of the sol-gel process, it was suggested that better results might be obtained by replacing blown or bodied vegetable oils with the epoxidized ones. Thus, the sol-gel precursors proved to be more reactive in the presence of EVO, bonding with both hydroxyl and epoxide groups in their structure. Even more, a certain catalytic effect of the inorganic precursor on the homo-polymerization of the epoxidized oil was assumed (Chen and Chen 1997). A significant improvement was noticed in terms of mechanical properties in the ceramers obtained from ESO and inorganic precursors, such as titanium (IV) *i*-propoxide (TIP), titanium (IV) di-*i*-propoxide bis-acetoacetate (TIA), and zirconium *n*-propoxide (ZRP) (Teng and Soucek 2000). The tensile modulus, strength, and hardness varied depending on the nature of the precursor, thus supporting the hypothesis of different interactions between organic and inorganic phases. The improvement in mechanical properties (tensile modulus and strength, and hardness) might be attributed to the formation of both inorganic rigid clusters and organic high density cross-linked network. At the same time, the higher the amount of inorganic component, the lower the elasticity of the ceramer films is.

The use of clays (either in native state or organically modified) as nanosized fillers for EVO-based nanocomposites was considered as an alternate pathway to achieve not only enhanced mechanical properties, but reduced flammability and significantly improved biodegradability, as well. Thus, starting from ESO and ELO as organic components, it was possible to obtain nanocomposites using an organically modified montmorillonite (containing an octadecylammonium tail, 30 wt%), by thermal curing in the presence of a benzylsulfonium hexafluoroantimonate derivative, as a thermally latent cationic catalyst (Uyama et al. 2003). The ESO containing nanocomposites yielded in homogeneous, resilient, highly elastic films, due to the decrease of the cross-linking density of ESO when the clay was dispersed in the matrix and the reinforcing effect of clay platelets. The ELO-based nanocomposites have showed a higher cross-linking density, given the greater number of epoxide moieties. These data suggested that these materials are expected to be used in applications as coatings and biodegradable plastics.

A mixture of ESO and diglycidyl ether of bisphenol-A (DGEBA) was also considered as matrix for bio-based nanocomposites with organically modified montmorillonite (OMM) (Aboobucker Sithique and Alagar 2010). The morphology analysis (wide angle X-ray diffraction WAXD and scanning electron microscopy SEM) proved that the clay tactoids exfoliated up to a high extent inside the matrix, which explained the significant improvement in tensile strength and modulus,

flexural strength and modulus (up to 24% for 7 wt% OMM content), and impact strength. The increased tortuosity of the system, granted by the clay platelets, restricted the chains mobility so that the diffusion of volatiles lowered, while the overall thermal stability increased.

Aiming to obtain green composites, different matrix formulations were designed, including further modified EVO, such as acrylated epoxidized soybean oil (AESO) (Thielemans et al. 2005) or acrylated epoxidized castor oil (AECO), or even mixed matrices, namely AECO-DGEBA (diglycidyl ether of bisphenol A) (Paluvai et al. 2015a, b). The organically modified clay used in this case was Cloisite 30B—montmorillonite functionalized with bis(2-hydroxyethyl) quaternary ammonium salt- and the transmission electron microscopy TEM and X-ray diffraction XRD analysis results confirmed exfoliated structure of the nanocomposites. The cross-linking density increased along with the amount of clay, because the alkylammonium groups reacted with the AECO-DGEBA system and contributed to the tensile and flexural properties. At the same time, a certain degree of ductility was noticed evidencing the plasticization effect of clay platelets, although higher amounts of clay entailed some brittleness.

The same Cloisite 30B was used for other mixed matrices, namely anhydride-cured epoxidized linseed oil (AELO) or octyl epoxide linseedate (OEL) and diglycidyl ether of bisphenol F (DGEBF) (Miyagawa et al. 2005a, b, c). The advisedly chosen curing agent and bio-based epoxies yielded in matrices displaying high values for elastic modulus, glass transition temperature, and heat distortion temperature. The addition under sonication of the functionalized clay produced nanocomposites with almost completely exfoliated structure, as evidenced through morphology studies. Thus, they achieved a higher storage modulus as compared to the initial resin. Given the value of the heat distortion temperature (100 °C) as well, it is possible to consider these materials as promising options for industrial applications.

Interesting result were achieved when the classic montmorillonites were replaced with other silicates, such as attapulgite (ATT—derived from the US town Attapulgis, in SW Georgia, where is abundant) or palygorskite (after the name of the first described deposit at Palygorskaya, in 1862, on the Popovka river, in Middle Urals, region Permskaya, Russia). This is a magnesium aluminium phyllosilicate that consists of bundles of acicular bristle-like crystals, having 2–3 µm in length and <3 nm in diameter (www.handbookofmineralogy.com), although other sources indicated 20 nm in diameter and few micrometers in length (Zhao et al. 2008), hence, a fiber-like morphology. The bundles are wetted by a slightly swellable smectite matrix. When added to metakaolin mortars, it may be used for period-correct restoration of mortars in heritage sites (Andrejkovičová et al. 2013).

Neat ATT was used as reinforcement in epoxy resins (Lu et al. 2005), but further modification of the clay surface was expected to improve the compatibility between matrix and filler, with beneficial effects on the mechanical, thermal and flame retardant properties of the nanocomposites (Shen et al. 2006; Xue et al. 2006). Thus, poly(ethylene oxide) (PEO) has been used to functionalize the surface of layered nanoparticles, due to its interactions with metal ions (Tunney and Detellier

1996), but another reagent, namely poly(ethylene glycol) diglycidyl ether (PEGDE), proved to be a better choice (Zhang et al. 2013). The clay surface functionalization was confirmed by FTIR spectroscopy: a novel absorption band was identified and attributed to the newly formed hydrogen bonds and chelation phenomena that occurred. This filler was further employed in different matrix formulations containing epoxidized soybean oil (ESO) and cyanate ester resin (CE) in order to obtain bio-based nanocomposites with enhanced properties. It was shown that a moderate degree of ATT functionalization had entailed the highest improvement in terms of storage modulus, as compared to neat or highly functionalized ATT.

When these nanocomposites are intended for applications that require higher levels of performance, such as structural applications, the clays are mixed with high-performance fillers, such as glass fibers or carbon fibers (CF). The processing of such multi-component systems must take into consideration the compatibility between partners, as well as the most suitable methods. Thus, new nanocomposites based on ELO, Cloisite 30B and carbon fibers were obtained in stages (Miyagawa et al. 2006), as follows. First, the ELO-Cloisite 30B nanocomposite was prepared by the sonication technique that allowed exfoliated structures, evidenced by the enhanced modulus and strength, and the homogeneous dispersion was confirmed by TEM. In the second stage, CF-reinforced materials were obtained through compression molding. The elastic modulus of unidirectional carbon fiber reinforced polymers (CFRP) made with different matrices (DGEBF, DGEBF-ELO, ELO-Cloisite 30B exfoliated or intercalated) was consistent regardless the matrix, due to the fact that the flexural test for the unidirectional CFRP is highly depending on the fibers characteristics. The inter-laminar shear strength tests indicated that the failure occurred in the ELO-Cloisite 30B phase (matrix) or at the matrix-fibers interface.

3 Conclusions and Future Perspective

In recent decade, there has been noticed an increasing research interest for using vegetable oils in obtainment of valuable polymer materials usually designed for technical applications. Considering their different uses, for example, biomedical purposes, or surface coatings applications, these polymer materials should have specific features including good thermal stability and significant ability to resist damage by chemical reactivity or solvent reaction. Vegetable oils are natural, environmental friendly and renewable raw materials with large availability, low cost, and functionality readily to be significantly improved for obtainment of bio-based functional polymers and polymeric materials (e.g. linear structures, three dimensional networks, and matrices for thermoplastic and thermosetting materials, biocomposites and organic-inorganic hybrid materials). An effective approach to generate epoxy resin moieties (e.g. with oxirane groups) is represented by epoxidation of vegetable oils (namely, peroxidation of double bonds which, in the case of

aliphatic chains, is a simple oxidation process by using hydrogen peroxide). Some of the most significant applications of thermosetting resins from epoxidized vegetable oils (EVOs) include coatings, fiber reinforced composites, and nanocomposites. As for the coatings, the processing techniques, along with the complex chemistry characteristic for a multi-component polymer system, are a key factor. Coatings properties may be improved by applying different methods, an effective one being the synthesis of new epoxy monomers by increasing functionality of the epoxy precursor. Further functionalization of vegetable oils (e.g. acrylated epoxidized soybean oil, maleinated acrylated epoxidized soybean oil) can generate valuable compounds to be employed as matrices for fiber-reinforced composites with either natural or synthetic fibers. Particulate composites using EVO as matrices are found to be of high interest in structural materials, depending on the amount and type of particles, as well as mechanical level of performance of the considered resins. Polymer nanocomposites are multi-component systems and basically consist of nanofillers (particles of different shape, platelets, fibers and fibrils, etc.) dispersed within a polymeric matrix made of one polymer or a mixture of polymers. Polymers reinforced with well-defined nanosized inorganic fillers (e.g. silica SiO₂ nanoparticles, metal-oxo clusters, clays in native state or organically modified) including ceramers have attracted a great interest given their versatility in terms of properties-application relationship. The resulted organic—inorganic hybrid materials may exhibit enhanced mechanical properties, but reduced flammability and significantly improved biodegradability, as well. Nevertheless, an increasing interest for bio-based, sustainable materials, with significant performance and endurance features, and not quite biodegradable, is observed. The future of bio-based polymers, including precursors for thermosetting epoxy resins, is strongly dependent on the future of different biorefinery strategies.

References

- Abad MJ, Barral L, Fasce DP, Williams RJ (2003) Epoxy networks containing large mass fractions of a monofunctional polyhedral oligomeric silsesquioxane (POSS). *Macromolecules* 36:3128–3135
- Abdelwahab MA, Misra M, Mohanty AK (2015) Epoxidized pine oil-siloxane: crosslinking kinetic study and thermomechanical properties. *J Appl Polym Sci* 132:42451–42462
- Aboobucker Sithique M, Alagar M (2010) Preparation and properties of bio-based nanocomposites from epoxidized soy bean oil and layered silicate. *MPJ* 5:151–161
- Adekunle K, Akesson D, Skrifvars M (2010) Biobased composites prepared by compression molding with a novel thermoset resin from soybean oil and a natural-fiber reinforcement. *J Appl Polym Sci* 116:1759–1765
- Adekunle KF (2015) A review of vegetable oil-based polymers: synthesis and applications. *OJPChem* 5:34–40. doi:[10.4236/ojpchem.2015.53004](https://doi.org/10.4236/ojpchem.2015.53004)
- Ahmad S, Ashraf SM, Alam M (2006a) Studies on melamine modified polyesteramide as anticorrosive coatings from linseed oil: a sustainable resource. *J Macromol Sci Part A Pure Appl Chem* 43:773–783

- Ahmad S, Ashraf SM, Hasnat A, Kumar GS, Sharmin E (2006b) Studies on epoxy-butylated melamine formaldehyde-based anticorrosive coatings from a sustainable resource. *Prog Org Coat* 56:207–213
- Alam M, Akram D, Sharmin E, Zafar F, Ahmad S (2014) Vegetable oil based eco-friendly coating materials: a review article. *Arab J Chem* 7:469–479
- Altuna FI, Esposito LH, Ruseckaite RA, Stefani PM (2011) Thermal and mechanical properties of anhydride-cured epoxy resins with different contents of biobased epoxidized soybean oil. *J Appl Polym Sci* 120:789–798
- Altuna FI, Ruseckaite RA, Stefani PM (2015) Biobased thermosetting epoxy foams: mechanical and thermal characterization. *ACS Sustain Chem Eng* 3:1406–1411
- Andrejkovičová S, Velosa A, Gameiro A, Ferraz E, Rocha F (2013) Palygorskite as an admixture to air lime–metakaolin mortars for restoration purposes. *Appl Clay Sci* 83–84:368–374
- Auvergne R, Caillol S, David G, Boutevin B, Pascault J-P (2014) Biobased thermosetting epoxy: present and future. *Chem Rev* 114:1082–1115
- Balo F (2011) Castor oil-based building materials reinforced with fly ash, clay, expanded perlite and pumice powder. *CERAM-SILIKÁTY* 55:280–293
- Becchi DM, de Luca MA, Martinelli M, Mitidieri S (2011) Organic–inorganic coatings based on epoxidised castor oil/APTES/TEOS. *J Am Oil Chem Soc* 88:101–109
- Biermann U, Bornscheuer U, Meier MAR, Metzger JO, Schafer HJ (2011) Oils and fats as renewable raw materials in chemistry. *Angew Chem Int Ed* 50:3854–3871
- Campanella A, Zhan M, Watt P, Grous AT, Shen C, Wool RP (2015) Triglyceride-based thermosetting resins with different reactive diluents and fiber reinforced composite applications. *Compos A* 72:192–199
- Carfagna C, Amendola E, Giamberini M (1997) Liquid crystalline epoxy based thermosetting polymers. *Prog Polym Sci* 22:1607–1647
- Chandrasekhara K, Sundararaman S, Flanigan V, Kapila S (2005) Affordable composites using renewable materials. *Mater Sci Eng A* 412:2–6
- Chen X, Chen Y (1997) Studies on active center concentration in photopolymerization of cyclohexene oxide initiated with iron-arene complex. *J Appl Polym Sci* 66:2551–2554
- Chen Z, Chisholm BJ, Webster DC, Zhang Y, Patel S (2009) New aromatic amine based on cardanol giving new bio-based epoxy networks. *Prog Org Coat* 65:246–250
- Crivello JV, Narayan R (1992) Epoxidized triglycerides as renewable monomers in photoinitiated cationic polymerization. *Chem Mater* 4:692–699
- Czub P (2006) Application of modified natural oils as reactive diluents for epoxy resins. *Macromol Symp* 242:60–64
- Czub P (2009) Synthesis and modification of epoxy resins using recycled poly(ethylene terephthalate). *Polym Adv Technol* 20:183–193
- Das G, Karak N (2009) Epoxidized *Mesua ferrea* L. seed oil-based reactive diluent for BPA epoxy resin and their green nanocomposites. *Prog Org Coat* 66:59–64
- de Luca MA, Martinelli M, Jacobi MM, Becker PL, Ferrão MF (2006) Ceramer coatings from castor oil or epoxidized castor oil and tetraethoxysilane. *JAOCS* 83:147–151
- Demirboğa R, Orung I, Gul R (2001) Effects of expanded perlite aggregate and mineral admixtures on the compressive strength of low-density concretes. *Cem Concr Res* 31:1627–1632
- Ding C, Matharu AS (2014) Recent developments on biobased curing agents: a review of their preparation and use. *ACS Sustain Chem Eng* 2:2217–2236
- Ding C, Shuttleworth PS, Makin S, Clark JH, Matharu AS (2015) New insights into the curing of epoxidized linseed oil with dicarboxylic acids. *Green Chem* 17:4000–4008
- Earls JD, White JE, Dettloff ML, Null MJ (2004) Development and evaluation of terminally epoxidized triglycerides for coatings applications. *J Coat Technol Res* 1:243–245
- Echeverri DA, Rios LA, Rivas BL (2015) Synthesis and copolymerization of thermosetting resins obtained from vegetable oils and biodiesel-derived crude glycerol. *Eur Polym J* 67:428–438
- Feldman D (1996) Composites, thermosetting polymers. In: Salamone JC (ed) *Polymeric materials encyclopedia*. CRC Press, Boca Raton, pp 277–278

- Galià M, Montero de Espinosa L, Ronda JC, Lligadas G, Cádiz V (2010) Vegetable oil-based thermosetting polymers. *Eur J Lipid Sci Technol* 112:87–96
- Gan Y, Jiang X (2015) Photo-cured materials from vegetable oils, Chapter 1. In: Liu Z, Kraus G (eds) *Green materials from plant oils*. RSC Green Chemistry (Book 29), The Royal Society of Chemistry, pp 1–27
- Gerbase AE, Petzhold CL, Costa APO (2002) Dynamic mechanical and thermal behavior of epoxy resins based on soybean oil. *JAOCS* 79:797–802
- Guner FS, Yagci Y, Erciyes AT (2006) Polymers from triglyceride oils. *Prog Polym Sci* 31:633–670
- Hayes BS, Seferis JC (2001) Modification of thermosetting resins and composites through preformed polymer particles: a review. *Polym Comp* 22:451–467
- Henna PH, Kessler MR, Larock RC (2008) Fabrication and properties of vegetable-oil-based glass fiber composites by ring-opening metathesis polymerization. *Macromol Mater Eng* 293:979–990
- Hong CK, Wool RP (2005) Development of a bio-based composite material from soybean oil and keratin fibers. *J Appl Polym Sci* 95:1524–1538
- Horiuchi S, Kawaguchi M, Yasuhara K (2000) Effective use of fly ash slurry as fill material. *J Hazard Mater* 76:301–337
- Hosoda N, Tsujimoto T, Uyama H (2014) Plant oil-based green composite using porous poly (3-hydroxybutyrate). *Polym J* 46:301–306
- Huang K, Zhang Y, Li M, Lian J, Yang X, Xia J (2012) Preparation of a light color cardanol-based curing agent and epoxy resin composite: cure-induced phase separation and its effect on properties. *Prog Org Coat* 74:240–247
- IUPAC Compendium of Chemical Terminology (1997) *The gold book*, 2nd edn. In: McNaught AD, Wilkinson A (eds). Blackwell Scientific Publications, Oxford, ISBN 0-9678550-9-8. doi:10.1351/goldbook.CT07539
- Kannan RY, Salacinski HJ, Butler PE, Seifalian AM (2005) Polyhedral oligomeric silsesquioxane nanocomposites: the next generation material for biomedical applications. *Acc Chem Res* 38:879–884
- Jusoh ER, Ismail MHS, Abdullah LC, Yunus R, Rahman WAWA (2012) Crude palm oil as a bioadditive in polypropylene blown films. *BioResources* 7:859–867
- Khot SN, Lascala JJ, Can E, Morye SS, Williams GI, Palmese GR, Kusefoglu SH, Wool RP (2001) Development and applications of triglyceride-based polymers and composites. *J Appl Polym Sci* 82:703–723
- Krawczak P, Pabiot J (1995) Fracture mechanics applied to glass fibre/epoxy matrix interface characterization. *J Compos Mat* 29:2230–2253
- Liu K, Madbouly SA, Schrader JA, Kessler MR, Grewell D, Graves WR (2015) Biorenewable polymer composites from tall oil-based polyamide and lignin-cellulose fiber. *J Appl Polym Sci* 132:42592
- Liu ZS, Erhan SZ, Xu J, Calvert PD (2002) Development of soybean oil-based composites by solid freeform fabrication method: epoxidized soybean oil with bis or polyalkyleneamine curing agents systems. *J Appl Polym Sci* 85:2100–2107
- Liu ZS, Erhan SZ, Calvert PD (2007) Solid freeform fabrication of epoxidized soybean oil/epoxy composite with bis or polyalkyleneamine curing agents. *Compos A* 38:87–93
- Lligadas G, Ronda JC, Galià M, Cádiz V (2006a) Bionanocomposites from renewable resources: epoxidized linseed oil-polyhedral oligomeric silsesquioxanes hybrid materials. *Biomacromol* 7:3521–3526
- Lligadas G, Ronda JC, Galià M, Cadiz V (2006b) Synthesis and properties of thermosetting polymers from a phosphorous-containing fatty acid derivative. *J Polym Sci Part A Polym Chem* 44:5630–5644
- Lligadas G, Ronda JC, Galià M, Cadiz V (2006c) Development of novel phosphorous-containing epoxy resins from renewable resources. *J Polym Sci Part A Polym Chem* 44:6717–6727

- Lligadas G, Ronda JC, Galia M, Cádiz V (2006d) Bionanocomposites from renewable resources: epoxidized linseed oil polyhedral oligomeric silsesquioxanes (POSS) hybrid materials. *Biomacromolecules* 7:3521–3526
- Lligadas G, Ronda JC, Galia M, Cadiz V (2013) Renewable polymeric materials from vegetable oils: a perspective. *Mater Today* 16:337–343
- Lu HB, Shen HB, Song ZL, Shing KS, Tao W, Nutt S (2005) Rod-like silicate-epoxy nanocomposites. *Macromol Rapid Commun* 26:1445–1450
- Luo C, Grigsby WJ, Edmonds NR, Al-Hakkak J (2013) Vegetable oil thermosets reinforced by tannin–lipid formulations. *Acta Biomater* 9:5226–5233
- Matějka L, Strachota A, Pleštil J, Whelan P, Steinhart M, Šlouf M (2004) Epoxy networks reinforced with polyhedral oligomeric silsesquioxanes (POSS). Structure and morphology. *Macromolecules* 37:9449–9456
- Maxim LD, Niebo R, McConnell EE (2014) Perlite toxicology and epidemiology—a review. *Inhal Toxicol* 26:259–270
- Meier MAR, Metzger JO, Schubert US (2007) Plant oil renewable resources as green alternatives in polymer science. *Chem Soc Rev* 36:1788–1802
- Meiorin C, Aranguren MI, Mosiewicki MA (2015) Polymeric networks based on tung oil: reaction and modification with green oil monomers. *Eur Polym J* 67:551–560
- Miao S, Wang P, Su Z, Zhang S (2014) Vegetable oil-based polymers as future polymeric biomaterials. *Acta Biomater* 10:1692–1704
- Miyagawa H, Misra M, Drzal LT, Mohanty AK (2005a) Biobased epoxy/layered silicate nanocomposites: thermophysical properties and fracture behavior evaluation. *J Polym Environ* 13:87–96
- Miyagawa H, Misra M, Drzal LT, Mohanty AK (2005b) Novel biobased nanocomposites from functionalized vegetable oil and organically-modified layered silicate clay. *Polymer* 46:445–453
- Miyagawa H, Misra M, Drzal LT, Mohanty AK (2005c) Fracture toughness and impact strength of anhydride-cured bio-based epoxy. *Polym Eng Sci* 45:487–495
- Miyagawa H, Jureka RJ, Mohanty AK, Misra M, Drzal LT (2006) Biobased epoxy/clay nanocomposites as a new matrix for CFRP. *Compos A* 37:54–62
- Mo X, Fournier B (2007) Investigation of structural properties associated with alkali–silica reaction by means of macro and micro structural analysis. *Mater Charact* 58(2):79–189
- Mulazim Y, Cakmakc E, Kahraman MV (2011) Preparation of photo curable highly hydrophobic coatings using a modified castor oil derivative as a sol–gel component. *Prog Org Coat* 72:394–401
- Mustață F, Tudorachi N, Rosu D (2011) Curing and thermal behavior of resin matrix for composites based on epoxidized soybean oil/diglycidyl ether of bisphenol A. *Compos B* 42:1803–1812
- Mustață F, Tudorachi N, Bicu I (2013) Biobased epoxy matrix from diglycidyl ether of bisphenol A and epoxidized corn oil, cross-linked with Diels–Alder adduct of levopimaric acid with acrylic acid. *Ind Eng Chem Res* 52:17099–17110
- O'Donnell A, Dweib MA, Wool RP (2004) Natural fiber composites with plant oil-based resin. *Compos Sci Technol* 64:1135–1145
- Ortiz RA, López DP, Cisneros MLG, Valverde JCR, Crivello JV (2005) A kinetic study of the acceleration effect of substituted benzyl alcohols on the cationic photopolymerization rate of epoxidized natural oils. *Polymer* 46:1535–1541
- Pappu A, Saxena M, Thakur VK, Sharma A, Haque R (2016) Facile extraction, processing and characterization of biorenewable sisal fibers for multifunctional applications. *J Macromol Sci Part A* 53(7):424–432
- Paluvai NR, Mohanty S, Nayak SK (2014) Synthesis and modifications of epoxy resins and their composites: a review. *Polym Plast Technol Eng* 53:1723–1758
- Paluvai NR, Mohanty S, Nayak SK (2015a) Epoxidized castor oil toughened diglycidyl ether of bisphenol A epoxy nanocomposites: structure and property relationships. *Polym Adv Technol* 26:1575–1586

- Paluvai NR, Mohanty S, Nayak SK (2015b) Fabrication and evaluation of acrylated epoxidized castor oil-toughened diglycidyl ether of bisphenol A nanocomposites. *Can J Chem Eng* 9999:1–10
- Pan X, Webster DC (2011) Impact of structure and functionality of core polyol in highly functional biobased epoxy resins. *Macromol Rapid Commun* 32:1324–1330
- Pan X, Sengupta P, Webster DC (2011) High bio-based content epoxy-anhydride thermosets from epoxidized sucrose esters of fatty acids. *Biomacromolecules* 12:2416–2428
- Pascault J-P, Williams RJJ (2010) Conclusions and perspectives. In: Pascault J-P, Williams RJJ (eds) *Epoxy polymers*. Wiley, Hoboken, pp 347–355
- Pascault JP, Williams RJJ (2013) Thermosetting polymers, chapter 28. In: Salvidar-Guerra E, Vivaldo-Lima E (eds) *Handbook of polymer, synthesis, characterisation and processing*. Wiley, New York, pp 519–534
- Petrovic ZS, Guo A, Javni I, Zhang W (2004) Plastics and composites from soybean oil. In: Wallenberger FT, Weston N (eds) *Natural fibers, plastics and composites*. Springer, New York, pp 167–192
- Pin JM, Sbirrazzuoli N, Mija A (2015a) From epoxidized linseed oil to bioresin: an overall approach of epoxy/anhydride cross-linking. *Chemsuschem* 8:1232–1243
- Pin J-M, Guigo N, Vincent L, Sbirrazzuoli N, Mija A (2015b) Copolymerization as a strategy to combine epoxidized linseed oil and furfuryl alcohol: the design of a fully bio-based thermoset. *Chemsuschem* 8:4149–4161
- Quirino RL, Garrison TF, Kessler MR (2014) Matrices from vegetable oils, cashew nut shell liquid, and other relevant systems for biocomposite applications. *Green Chem* 16:1700–1715
- Raghavachar R, Sarnecki G, Baghdachi J, Massingill J (2000) Cationic, thermally cured coatings using epoxidized soybean oil. *J Coat Technol* 72:125–133
- Ray D, Ghorui S, Bandyopadhyay NR, Sengupta S, Kar T (2012) New materials from maleated castor oil/epoxy resin blend reinforced with fly ash. *Ind Eng Chem Res* 51:2603–2608
- Raquez J-M, Deléglise M, Lacrampe M-F, Krawczak P (2010) Thermosetting (bio)materials derived from renewable resources: a critical review. *Prog Polym Sci* 35:487–509
- Riaz U, Vashist A, Ahmad SA, Ahmad S, Ashraf SM (2010) Compatibility and biodegradability studies of linseed oil epoxy and PVC blends. *Biomass Bioenergy* 34:396–401
- Riaz U, Ashraf SM, Sharma HO (2011) Mechanical, morphological and biodegradation studies of microwave processed nanostructured blends of some bio-based oil epoxies with poly(vinyl alcohol). *Polym Degrad Stab* 96:33–42
- Rosu D, Mustata F, Tudorachi N, Musteata VE, Rosu L, Varganici C-D (2015) Novel bio-based flexible epoxy resin from diglycidyl ether of bisphenol A cured with castor oil maleate. *RSC Adv* 5:45679–45687
- Roşu D, Bodîrlău R, Teacă C-A, Roşu L, Varganici C-D (2016) Epoxy and succinic anhydride functionalized soybean oil for wood protection against UV light action. *J Clean Prod* 112:1175–1183
- Samuelsson J, Sundell PE, Johansson M (2004) Synthesis and polymerization of a radiation curable hyperbranched resin based on epoxy functional fatty acids. *Prog Org Coat* 50:193–198
- Sharmin E, Akram D, Ghosal A, Rahman O, Zafar F, Ahmad S (2011) Preparation and characterization of nanostructured biohybrid. *Prog Org Coat* 72:469–472
- Shen L, Lin YJ, Du QG, Zhong W (2006) Studies on structure–property relationship of polyamide-6/attapulgite nanocomposites. *Compos Sci Technol* 66:2242–2248
- Shibata M, Teramoto N, Someya Y, Suzuki S (2009) Bio-based nanocomposites composed of photo-cured epoxidized soybean oil and supramolecular hydroxystearic acid nanofillers. *J Polym Sci Part B Polym Phys* 47:669–673
- Shibata M, Nakai K (2010) Preparation and properties of biocomposites composed of bio-based epoxy resin, tannin acid, and microfibrillated cellulose. *J Polym Sci Part B Polym Phys* 48:425–433
- Singha AS, Thakur VK (2008a) Synthesis and characterization of pine needles reinforced RF matrix based biocomposites. *J Chem* 5(S1):1055–1062

- Singha AS, Thakur VK (2008b) Fabrication and study of lignocellulosic hibiscus sabdariffa fiber reinforced polymer composites. *BioResources* 3(4):1173–1186
- Singha AS, Thakur VK (2008c) Synthesis and characterization of grewia optiva fiber-reinforced PF-based composites. *Int J Polym Mater Polym Biomater* 57(12):1059–1074
- Singha AS, Thakur VK (2009a) Fabrication and characterization of *H. sabdariffa* fiber-reinforced green polymer composites. *Polym Plast Technol Eng* 48(4):482–487
- Singha AS, Thakur VK (2009b) Grewia optiva fiber reinforced novel, low cost polymer composites. *J Chem* 6(1):71–76
- Singha AS, Thakur VK (2009c) Study of mechanical properties of urea-formaldehyde thermosets reinforced by pine needle powder. *BioResources* 4(1):292–308
- Singha AS, Thakur VK (2009d) Mechanical, thermal and morphological properties of grewia optiva fiber/polymer matrix composites. *Polym Plast Technol Eng* 48(2):201–208
- Snellings R, Mertens G, Elsen J (2012) Supplementary cementitious materials. *Rev Mineral Geochem* 74:211–278. doi:10.2138/rmg.2012.74.6
- Shrew RN, Brink JA (1977) *Chemical process industries*, 4th edn. McGraw-Hill Kogakusha, Tokyo
- Stemmelen M, Pessel F, Lapinte V, Caillol S, Habas JP, Robin JJ (2011) A fully biobased epoxy resin from vegetable oils: from the synthesis of the precursors by thiol-ene reaction to the study of the final material. *J Polym Sci A Polym Chem* 49:2434–2444
- Taghizadeh MT, Nalbandi N, Bahadori A (2008) Stabilizing effect of epoxidized sunflower oil as a secondary stabilizer for Ca/Hg stabilized PVC. *Express Polym Lett* 2:65–76
- Takada Y, Shinbo K, Someya Y, Shibata M (2009) Preparation and properties of bio-based epoxy montmorillonite nanocomposites derived from polyglycerol polyglycidyl ether and ϵ -polylysine. *J Appl Polym Sci* 113:479–484
- Takahashi T, Hirayama K-I, Teramoto N, Shibata M (2008) Biocomposites composed of epoxidized soybean oil cured with terpene-based acid anhydride and cellulose fibers. *J Appl Polym Sci* 108:1596–1602
- Tehfe MA, Lalevée J, Gigmes D, Fouassier JP (2010) Green chemistry: sunlight induced cationic polymerization of renewable epoxy monomer under air. *Macromolecules* 43:1364–1370
- Teng G, Soucek MD (2000) Epoxidized soybean oil-based epoximer coatings. *JAOCs* 77:381–387
- Thames S, Yu H (1999) Cationic UV-cured coatings of epoxide-containing vegetable oils. *Surf Coat Technol* 115:208–214
- Thakur VK, Singha AS, Thakur MK (2013a) Ecofriendly biocomposites from natural fibers: mechanical and weathering study. *Int J Polym Anal Charact* 18(1):64–72
- Thakur VK, Singha AS, Thakur MK (2013b) Fabrication and physico-chemical properties of high-performance pine needles/green polymer composites. *Int J Polym Mater Polym Biomater* 62(4):226–230
- Thielemans W, Wool RP (2004) Butyrate kraft lignin as compatibilizing agent for natural fiber reinforced thermoset composites. *Compos Part A* 35:327–338
- Thielemans W, McAninch IM, Barron V, Blau WJ, Wool RP (2005) Impure carbon nanotubes as reinforcements for acrylated epoxidized soy oil composites. *J Appl Polym Sci* 98:1325–1338
- Trumbo DL, Otto JT (2008) Epoxidized fatty acid-derived oxazoline in thermoset coatings. *J Coat Technol Res* 1–8:107–111
- Tsujimoto T, Uyama H, Kobayashi S (2003) Green nanocomposites from renewable resources: biodegradable plant oil-silica hybrid coatings. *Macromol Rapid Commun* 24:711–714
- Tsujimoto T, Uyama H, Kobayashi S (2010) Synthesis of high-performance green nanocomposites from renewable natural oils. *Polym Degrad Stab* 95:1399–1405
- Tsujimoto T, Takayama T, Uyama H (2015) Biodegradable shape memory polymeric material from epoxidized soybean oil and polycaprolactone. *Polymer* 7:2165–2174
- Tuman SJ, Soucek MD (1996) Novel inorganic/organic coatings based on linseed oil and sunflower oil with sol-gel precursors. *J Coat Technol* 68:73–81
- Tuman SJ, Chamberlain D, Scholsky KM, Soucek MD (1996) Metal alkoxides as precursors for electronic and ceramic materials. *Prog Org Coat* 28:251–258

- Tunney JJ, Detellier C (1996) Aluminosilicate nanocomposite materials. Poly(ethylene glycol)-kaolinite intercalates. *Chem Mater* 8:927–935
- Uyama H, Kuwabara M, Tsujimoto T, Nakano M, Usuki A, Kobayashi S (2003) Green nanocomposites from renewable resources: plant oil-clay hybrid materials. *Chem Mater* 15:2492–2494
- Wan RW, Kumar R, Mek ZS, Hilmi MM (2003) UV radiation curing of epoxidized palm oil-cycloaliphatic diepoxide system induced by cationic photoinitiators for surface coatings. *Eur Polym J* 39:593–600
- Warth H, Mühlhaupt R, Hoffmann B, Lawson S (1997) Polyester networks based upon epoxidized and maleinated natural oils. *Angew Makromol Chem* 249:79–92
- Wold CR, Soucek MD (2000) Viscoelastic and thermal properties of linseed oil-based ceramer coatings. *Macromol Chem Phys* 201:382–392
- Wu X, Zhang X, Yang S, Chen H, Wang D (2000) The study of epoxidized rapeseed oil used as a potential biodegradable lubricant. *JAACS* 77:561–563
- Xia Y, Larock RC (2010) Vegetable oil-based polymeric materials: synthesis, properties, and applications. *Green Chem* 12:1893–1909
- Xue SQ, Reinholdt M, Pinnavaia TJ (2006) Palygorskite as an epoxy polymer reinforcement agent. *Polymer* 47:3344–3350
- Yousefi A, Lafleur PG, Gauvin R (1997) Kinetic studies of thermoset cure reactions: a review. *Polym Comp* 18:157–168
- Zhang J, Hu S, Zhan G, Tang X, Yu Y (2013) Biobased nanocomposites from clay modified blend of epoxidized soybean oil and cyanate ester resin. *Prog Org Coat* 76:1683–1690
- Zhao L, Zhan GZ, Yu YF, Tang XL, Li SJ (2008) Influence of attapulgites on cure-reaction-induced phase separation in epoxy/poly(ether sulfone) blends. *J Appl Polym Sci* 108:953–959
- Zong Z, Soucek MD, Liu Y, Hu JJ (2003) Cationic photopolymerization of epoxynorbornane linseed oils: the effect of diluents. *J Polym Sci Part A Polym Chem* 41:3440–3456
- Zou K, Soucek MD (2005) UV-curable cycloaliphatic epoxide based on modified linseed oil: synthesis, characterization and kinetics. *Macromol Chem Phys* 206:967–974

Chapter 9

Philosophical Study on Composites and Their Drilling Techniques

Sikiru Oluwarotimi Ismail and Hom Nath Dhakal

Abstract Due to the advancement in the properties, design and manufacturing of fibre-reinforced polymer composite materials, especially the natural or bio-based types, their wide applications have been significantly enhanced compared to the conventional materials (metals and alloys). With this trend, there is a strong interest and importance in understanding the machinability of these materials. Machinability of these materials depends, among other parameters, on properties of fibres and matrices, drilling conditions, parameters and techniques. Among the machining operations of these composites, drilling is the most crucial and common operation. Hence, this chapter focuses on better understanding of biocomposites and various composite conventional and non-conventional drilling techniques. The primary aim of this chapter, therefore, is to provide comparative analysis between conventional and non-conventional drilling of composite materials.

Keywords Composite materials · Machinability · Drilling techniques
Fibres · Matrices

1 Introduction

The increasing application of the fibre-reinforced polymer (FRP) composites, as an effective engineering materials to meet the human insatiable needs in various areas, has encouraged many industrial sectors. The exhausting crude oil resources and quest for a perfect substitute for non-renewable (synthetic) composites have necessitated the advancing research on and use of FRP composites, most importantly, the renewable (natural) composites (Scarponi et al. 2015; Ismail et al. 2015). The list of the areas of application is not exhaustive, as it involves both commercial

S.O. Ismail (✉) · H.N. Dhakal
School of Engineering, University of Portsmouth, Portsmouth
PO1 3DJ, England, UK
e-mail: sikiru.ismail@port.ac.uk; ismailrotimi@gmail.com

© Springer International Publishing AG 2018
V.K. Thakur and M.K. Thakur (eds.), *Functional Biopolymers*,
Springer Series on Polymer and Composite Materials,
https://doi.org/10.1007/978-3-319-66417-0_9

and industrial uses such as aerospace, defense, marine, automotive, civil infrastructure/building construction, oil and gas, sports, leisure and recreation, medical science, electrical and electronics.

Drilling is a machining process that involves the cutting out or enlargement of holes in a solid material. It is a versatile manufacturing operation which forms an integral part of any machine assembly and component mating. Mostly used as a finishing process, drilling requires a great deal of precision and accuracy for effective usage. The functionality of any mechanical structure is largely dependent on the quality of mating between its interconnecting parts, which is achieved through the use of mechanical fasteners such as rivets, pins, screws, among others. However, in order to achieve the effective mating of machine parts through the use of fasteners, proper provision of grooves/holes for their installation must be adequately made, and this can only be achieved through drilling.

Mechanical fasteners, usually available in standard sizes, are required to create perfect fit into grooves for which they are designated for use. Therefore, it is necessary to ensure that bolted or riveted joints are accurately drilled, so as to prevent the slackness of the fasteners on the machine members or their excessive tightness. Consequently, drilling is a crucial machining operation which constitutes largely to the success or failure of any machine assembly (Makhdum et al. 2014). Drilling plays a major role in various industries, from automotive to aerospace and a whole lot of other manufacturing industries. It is the most common composite machining operation, since many holes are required for the installation of mechanical fasteners towards component assembly. Reports showed that approximately 25% of the machining operations used among manufacturing industries are drilling-associated, with an estimate of about 55,000 drilled holes used to assemble the numerous parts of the Airbus A350 aircraft (Faraz et al. 2009).

Different engineering materials such as metals, woods, plastics, polymers and composites have all been machined through drilling. More so, a variety of drilling processes are available in the world today, depending on the target finish and the nature of the workpiece. Furthermore, drilling engineering is not limited to the aforementioned engineering materials and industries, as it is also a major operation used in the Oil and Gas industry. Drilling operations in the Oil and Gas industry take the form of well drilling for potential exploration sites; the earth crust being the workpiece in this regard. As a result, drilling is a versatile manufacturing operation which spans across a vast majority of the engineering world.

2 Types of Fibre-Reinforced Composites

Fibre-reinforced composites are normally grouped on the basis of the nature of their reinforcement (fibres), and not the matrix. The naming convention for each type follows after the source of the reinforcement. As a result, there are basically two

types of fibre-reinforced composites namely: Natural fibre-reinforced composites (NFRC) and Synthetic fibre-reinforced composites (SFRC). Mainly, emphasis will be on NFRC, while both will be considered under drilling techniques.

2.1 Natural Fibre-Reinforced Composites

Natural fibre-reinforced composites are otherwise referred to as green composites or biocomposites, these are composites which contain embedded reinforcements of biofibres. In this type of composite, the fibre reinforcements are sourced from natural means of plants, animals and minerals, as shown in Fig. 1.

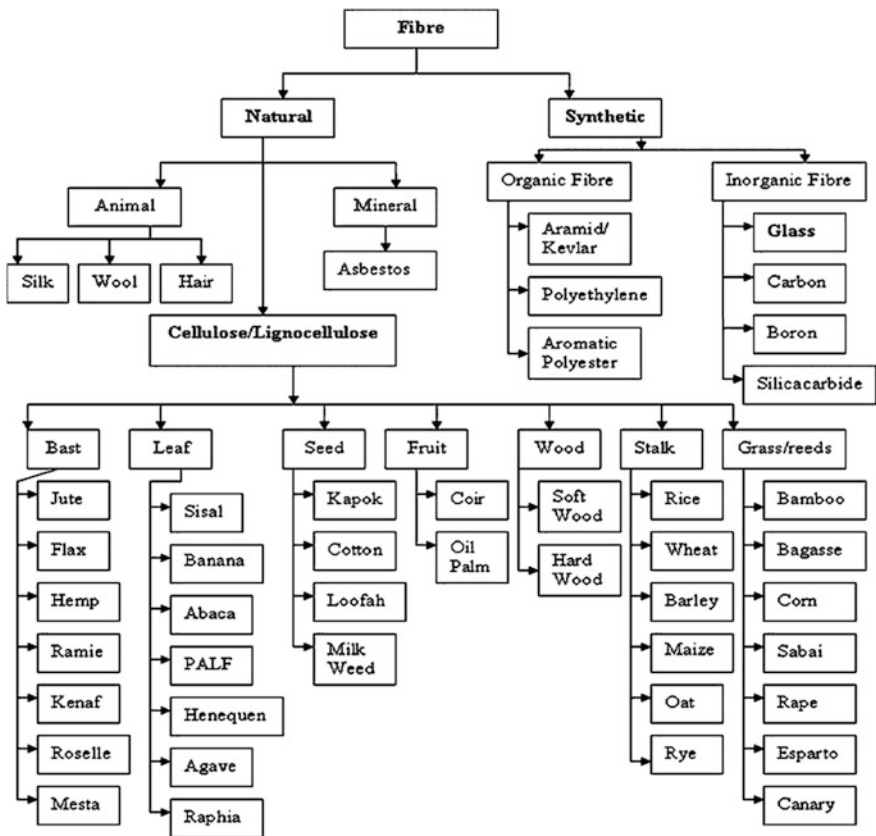


Fig. 1 Classification of FRP composite fibres (Jawaid and Abdul Khalil 2011)

2.1.1 Historical Background of Natural Fibre-Reinforced Composites

The utilization of natural fibres as reinforcement in composites has its history well documented. It is generally believed that composite materials evolved as biomaterials which had natural fibres as their primary reinforcement. As far back as the era of the Stone Age (6500 BC), history has it that hemp and linen textiles were utilized as fillers for ceramics (Pickering 2008). Similarly, dating back as 3000 years ago, the Egyptians used straws and grasses as reinforcement for making clay bricks used for wall building (Bledzki et al. 2002). In the last century (1950), a major pick of product development was the manufacturing of an East German Trabant car, which had its frame constructed from cotton fibre-reinforced polyesters (Jawaid and Abdul Khalil 2011).

2.1.2 Plant or Vegetable Fibres

Among all the sources of natural fibres used in the reinforcement of composites, plant fibres are mostly employed (Jawaid and Abdul Khalil 2011). Commonly referred to as lignocellulosic fibres, these natural fibres are gaining research recognition in recent years due to a number of impressive advantages they possess over their synthetic counterparts. The mechanical properties of natural fibre-reinforced composite are largely depended on the chemical composition and physical properties of the embedded natural fibres. In the selection of natural fibres as choice materials for composite reinforcement, the most important mechanical properties of interest are the density, Young modulus and the tensile strength.

2.1.3 Chemical Properties of Plant Fibres

The chemical composition of plant fibres is notably made up of atoms of cellulose and lignin. The lignin acts as the glue which binds the fibre cells or cellulose together, thus having a direct bearing on the shape, structure and properties of any natural fibre (Terzopoulou et al. 2015). While the cellulose level in a natural fibre dictates the mechanical properties, the nature of the lignin layer accounts for the level of its chemical reactivity (Nirmal et al. 2015).

Natural fibres are selective in their matrix choice. This is due to their hydrophilic nature, i.e. a strong affinity for water absorption and the hydrophobic quality of most composite matrices. As a result of these contrasting properties between the fibres and the binders, there is usually a high tendency for the formation of aggregates at the interfacial boundary; a condition which puts the composite's interfacial bonding at a failure threat (Kocsis et al. 2015). In the selection of matrices for biofibres, thermoplastic materials are usually preferred to their thermosetting counterparts due to their high toughness and resilience properties. Up to 30% of NFRCs with plant fibre reinforcement operate on thermosetting plastic matrices, while the rest are based on thermoplastics (Shah 2013). Commonly used

thermoplastic polymers for this purpose are the polypropylene (PP), polyethylene and poly vinyl chloride (PVC); while phenolic, epoxy and polyester resins are the notably used thermosetting matrices (Puglia et al. 2004; Ku et al. 2011).

2.1.4 Physical Properties of Plant Fibres

The physical properties of plant fibres emanate from the variation of its sizes, shapes and cell wall thickness. The aspect ratio (implies length to width ratio) is a crucial factor in evaluating the mechanical strength of natural fibres. A central hollow cavity known as “lumen” exists in the transverse axis of lignocellulosic fibres, which further translates to the reduction of the fibre’s bulk density. While the hollow cavity accounts for the good thermal and acoustical insulation qualities of the fibres, the density reduction translates to their lightweight properties.

In a study conducted by Sapuan et al. (2011), 29 samples of natural fibres were weighed with respect to a number of design criteria such as Young Modulus, density and tensile strength. The results gotten from the study indicated the suitability of natural fibres for manufacturing the dashboard panel of automotives. Similarly, Cheung et al. (2009) studied the application potential of natural fibres of plants and animal residues in biomedical, with regards to their mechanical and thermal strengths. The results achieved in the study showed that these natural fibres can be effectively employed in manufacturing materials suitable for biomedical applications.

Graupner et al. (2009) studied extensively on the mechanical properties of various renewable fibres. The major evaluation criteria used for these natural fibres were the tensile strength, Young modulus, elongation at break and the Charpy impact tests. The results obtained from the study showed the superiority of kenaf and hemp fibres in tensile strength and Young modulus values; as well as cotton exhibiting good impact strength, while lyocell fibres had the combination of high tensile strength, Young modulus and impact strength.

The mechanical properties of NFRCs are influenced by a number of parameters such as fibre weight, processing techniques, fibre quality and the adhesive matrix employed (Ku et al. 2011). The most common processing techniques for NFRCs are the extrusion–injection moulding and the compression moulding. Tungjitpornkull and Sombatsompop (2009) researched on the variation of tensile properties of an E-glass fibre (GF) reinforced wood/PVC (WPVC) manufactured by the injection moulding and compression methods, respectively. The results obtained from this study showed that a better tensile modulus of the composite was achieved in compression moulding technique, compared to its injection–extrusion counterpart, as shown in Fig. 2.

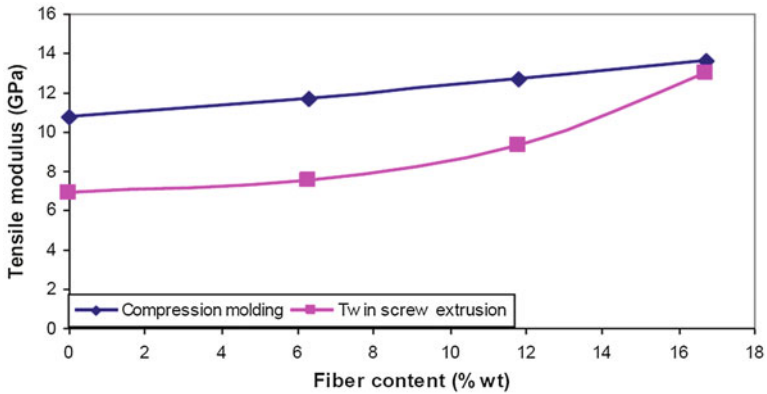


Fig. 2 Tensile modulus variation for compression moulding and injection–extrusion processing techniques (Tungjitpornkull and Sombatsompop 2009)

2.1.5 Examples of Natural Fibre-Reinforced Composites

Considering the wealth of natural fibres available for use in composite reinforcements, notable ones commonly employed in the manufacturing industries are as listed:

- (i) Hemp fibre-reinforced composites.
- (ii) Sisal fibre-reinforced composites.
- (iii) Date-palm fibre-reinforced composites.
- (iv) Coir fibre-reinforced composites.

2.1.6 Advantages of Natural Fibre-Reinforced Composites

Today, the applications of natural fibre-reinforced polymer (NFRP) composites are increasing more than the uses of synthetic composites such as carbon and glass fibre-reinforced composites, mostly in the automotive company. This increase is based on the following highlighted merits:

- (i) Relatively lesser production cost due to their universal availability and ease of processing or machining: less drill wear.
- (ii) Greater modulus-weight ratio compared to E-glass fibres, resulting in greater specific strength and stiffness
- (iii) Reduced risk of environmental pollution through their biodegradability, reusability and recyclability properties, including possibility of thermal recycling. Environmental friendliness due to their biodegradability and lower CO₂ emission.

- (iv) Irritation effects of composites on dermal and respiratory organs are not applicable to natural fibre composites.
- (v) Lower density of $1.25\text{--}1.50\text{ g cm}^{-3}$ compared to $1.80\text{--}2.10\text{ g cm}^{-3}$ and 2.54 g cm^{-3} for carbon and glass fibres, respectively.
- (vi) Tool resistance, degradation and wear commonly encountered in the machining of composites are largely reduced in the case of natural fibre composites.
- (vii) Better electrical resistance, good thermal stability and acoustical balance makes them suitable for the automotive industry. Greater acoustic damping property/suitability for noise diminution (reduction).
- (viii) Smaller energy consumption during production.
- (ix) Minimal or no global warming potential, due to their enhanced carbon (iv) Oxide sequestration ability (Pickering 2008; Wambua et al. 2003; Faruk et al. 2012).
- (x) Carbon and glass fibres are much expensive than natural fibres (Mallick 2008; Jawaid and Abdul Khalil 2011).

2.1.7 Disadvantages of Natural Fibre-Reinforced Composites

Conversely, natural fibres have some setbacks which limit their structural application in some engineering components. These disadvantages include:

- (i) Non-uniformity in fibre geometry can result in structural instability of the finished composite.
- (ii) Fibre breakage and thermal degradation during manufacturing processes.
- (iii) Poor interfacial adhesion between hydrophilic reinforcing fibres and hydrophobic matrices often lead to poor mechanical properties of composite and fibre swelling (Yan et al. 2013). High rate of moisture absorption (in some cases), which consequently resulted in product failure (Kabir et al. 2012). This implies weak fibre-matrix interface due to poor adhesion between fibre and matrix (Dhakal et al. 2007).
- (iv) Susceptibility to pest infestation if not treated properly, as well as degradation by other natural interferences such as fire.
- (v) Unsuitability for high-temperature applications due to their low degradation temperatures ($<200\text{ }^{\circ}\text{C}$) makes them limited in effective usage (Abiola et al. 2014). It has been reported that the thermal degradation or decomposition of natural fibres begins at temperature just above $200\text{ }^{\circ}\text{C}$ (Mallick 2008), while carbon fibres start at a temperature greater than $900\text{ }^{\circ}\text{C}$ (Wang et al. 2013).
- (vi) Inability to resist fire.
- (vii) Negative impacts of harvest results on price fluctuation (Jawaid and Abdul Khalil 2011). Also, there is an instability of cost by harvest, being an agricultural produce unpredictably and easily affected by bad weather.

In summary, natural fibre composites are considered eco-friendly materials which are crucial to a sustainable product development, as a means of properly harnessing the potentials of the supposed waste materials of natural fibres, which will also aid in their complete disposal.

3 Types of Drilling Processes

There are basically two types of drilling processes under which all drilling techniques and methods can be appropriately classified. These are:

- Conventional or traditional drilling (CD), and
- Non-conventional or non-traditional drilling (NCD).

3.1 Conventional Drilling

Advancement in materials science over the years has prompted the evolution of new tools and the discovery of newer energy sources for effective materials processing. While tools made from crude materials of stone and iron were effective in materials processing some decades ago, twentieth century products featured sophisticated, durable and consequently the most difficult materials to the machine using the pre-existing tools. Therefore, in order to overcome the challenges posed by these materials, new processing tools such as carbide, diamond and steel were introduced, while new methods of machining were developed to ensure satisfactory levels of materials processing.

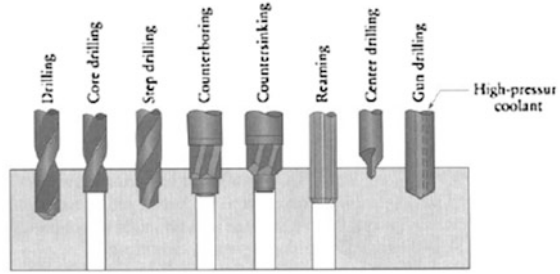
Initially, conventional or traditional techniques were pioneering methods used in the drilling of materials. These techniques usually involve the use of prime movers to mechanically energize crude cutting tools against a workpiece material surface. Typical prime movers used in these pre-existing techniques were electric motor, gravity and hydraulics, with iron-made materials being the main cutting tools.

3.1.1 Mechanics of Conventional Drilling

The conventional drilling operation is actualized by the high-speed rotary impact of a cutting tool; the drill bit, against the surface of a workpiece, which is guided by the influence of a mechanical thrust for the generation of drilling effects. The cutting edge of the drill bit which rotates at high speed; usually in the range of hundreds to thousands of revolutions per minute then cuts off chips from the workpiece material by shear deformation.

Various drill bits are available in the manufacturing world of today, such as the twist drill bit, step drill bit, hole saws, among others, for different drilling

Fig. 3 Various types of drills and drilling operations (Kalpakjian and Schmid 2003)



operations, as depicted in Fig. 3. However, the twist drill bit remains the most common type of drill bit used for drilling purposes, with reports which showed that the United States’ manufacturing industries consume about 250 million twist drills per annum (DeGarmo et al. 2003). The twist drill bit is made up of a cylindrical shaft with helical flutes and a cutting edge at its end, with other designed geometry (Fig. 4). The drilling effect of the twist drill bit is achieved by the rotary action of the cylindrical shaft against the workpiece, primarily caused by the impact of the helical flutes with the sharp cutting edge.

Furthermore, the governing parameters of drilling mechanics are the cutting speed, feed rate, cutting force and the material removal rate (MRR). These are further discussed as thus:

Cutting Speed This is the rate at which the outside or the periphery of the tool moves relative to the workpiece, usually measured in mm/min. It is the largest of all the relative velocities developed in the drilling operation. Respectively, the peripheral and rotational velocities of a cutting tool are given by the relations:

$$V = \frac{\pi DS}{1000} \tag{1}$$

where V is the peripheral velocity measured in mm/s, D is the diameter of the drill bit in mm and N is the rotational speed; otherwise referred to as spindle speed, measured in revolutions per minute (rpm).

Consequently, the spindle speed

$$S = \frac{1000 V}{\pi D} \tag{2}$$

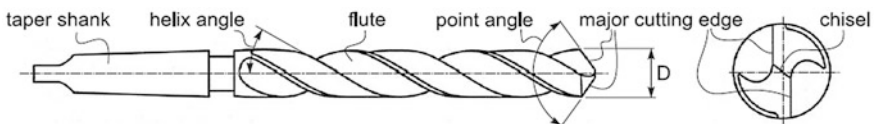


Fig. 4 Standard geometry of a twist drill (Marinov 2010)

The optimum cutting speeds can be adjusted for better performance, depending on factors as follows:

- Material composition, hardness and thermal stability.
- Nature of cutting fluid.
- Depth of hole, as well as the finish quality desired.
- Stiffness of cutting tool and orientation.

Feed Rate This refers to the rate at which the drilling tool advances along the workpiece geometry, usually measured in mm/min. It signifies the rate at which the workpiece material is fed into the drill bit without causing a jam, and is given by the equation:

$$F = S \times f \times N \quad (3)$$

where S = spindle speed, f = feed per tooth and N is the number of flutes on the cutting tool.

Furthermore, the feed rate is a standardized parameter for different drill diameters, and highly dependent on the strength nature of the workpiece material. A good rule of thumb for drilling operation is to use lower feed rates for harder materials, and higher feed rates for their softer counterparts.

Cutting Force This refers to the contact force generated by the tool tip against the workpiece surface, as shown in Fig. 5.

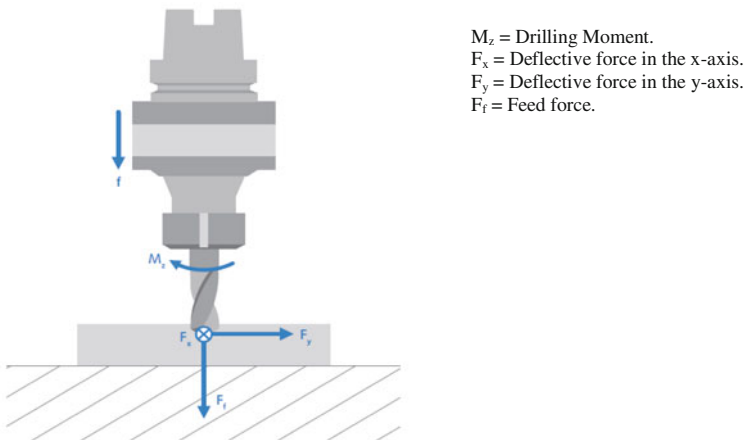


Fig. 5 Cutting forces in drilling operation

Thrust Force This is the normal force exerted by the cutting tool on the work-piece, for the generation of drilling effects. It can be estimated according to the equation:

$$F = \frac{k' \times k_c \times f \times D}{2} \tag{4}$$

where

k_c specific cutting force, measured in N/mm^2 , depending on the material being drilled.

f feed per rotation (mm),

D tool diameter (mm), and

k is a drilling coefficient, depending on the tool tip geometry (typically considered as an average of 0.5).

Material Removal Rate This is the volume of workpiece material removed per minute, given by

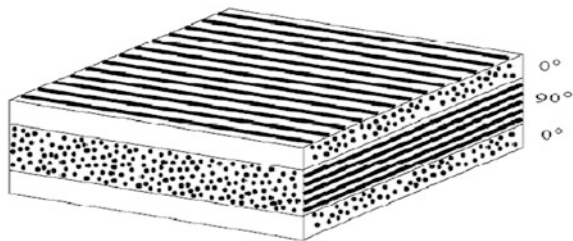
$$MRR = V \times f \times D \tag{5}$$

3.2 Drilling of Fibre-Reinforced Polymer (FRP) Composites

Fibre-reinforced polymer composites are special materials developed from the combination of different conventional materials, as depicted in Fig. 6. Over the last decade, the increasing demand for high-performance lightweight materials in manufacturing industries has prompted the evolution of these composite materials.

Owing to their unique mechanical properties of high strength to weight ratio, these materials are fast becoming the manufacturer’s choice in aerospace, defense, automotive and sporting goods industries. However, a great deal of limitations attached to their industrial usage; notably the high production cost, complexity and machining-related damage, have raised research concerns over the past years

Fig. 6 A typical composite laminate (Sankar et al. 2014)



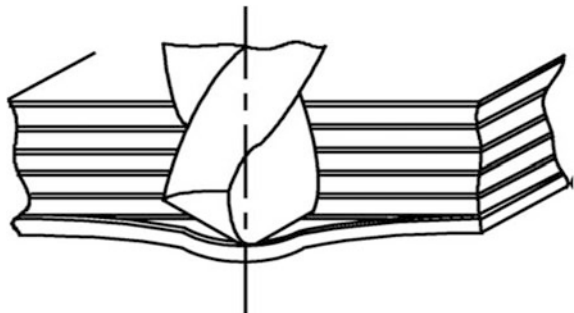
(Durão et al. 2014). Besides their production costs, the unpredictable reactions of these materials to machining operations, particularly drilling, have been worrisome to the manufacturing world. However, the structural and mechanical damages commonly encountered in the drilling operation of composites have been attributed to the variance that exists in the chemical and mechanical compositions of their reinforcements (fibres) and binders (polymer matrices), usually exhibited at the interfacial boundaries.

Drilling of a natural or biocomposites has not been well studied, compared with other synthetic fibre-reinforced polymer composites such as glass and carbon FRP composites. The reasons could be traced to the new advent of some eco-friendly composites that require the application of non-conventional drilling techniques so that the hole quality and structural integrity of the biocomposite materials could be protected both during machining and in service. In addition, the lower decomposition and melting temperatures of natural fibres and biodegradable thermoplastic matrices such as hemp and polycaprolactone resin, respectively, compared with synthetic fibres and thermoset matrices such as carbon and epoxy resin, has necessitated a careful choice of drilling technique for NFRP composites due to the high tool-workpiece interface temperature.

More so, since drilling is often the final machining operation on composite laminates before machine assembly, its associated damage on composites often results in expensive losses for manufacturing industries (Fig. 7). Of all the composites available today, the carbon fibre polymer composites (CFRPs) and glass fibre polymer composites (GFRPs) are the commonly used laminates, due to their high mechanical properties (Liu et al. 2012).

Different techniques and methodologies to achieve a damage-free drilling output of these composites have been studied in extant literatures, such as conventional drilling (Abrate and Walton 1992; Tagliaferri et al. 1990; Bongiorno et al. 1998), high-speed drilling (HSS) (Rubio et al. 2008; Arul et al. 2006) vibration-assisted drilling (VAD) (Arul et al. 2006; Sakthivel et al. 2015; Ramkumara et al. 2004), grinding drilling (Park et al. 1995) and other specially designed non-conventional drilling techniques (Abrate and Walton 2016).

Fig. 7 Schematics of drilling in composite materials (Hocheng and Tsao 2005)



3.2.1 Conventional Drilling of Fibre-Reinforced Polymer Composites

Conventional drilling refers to any material removal process for hole generation, which involves the formation of chips from a workpiece by the direct contact of a wedge shaped cutting tool which is harder than the workpiece material, under machining conditions. It is characterized by a macroscopic chip formation; achieved by the shear deformation of the workpiece material, a mechanical energy domain for cutting effects and a tool which is stronger than the workpiece at room temperature and machining conditions.

The thrust and torque applied to a bit during drilling operation are dependent on the drilling speed, feed rate, tool geometry and the rate of tool wear, as illustrated in Table 1 (Abrate and Walton 1992). Wong et al. (1982) reported that the thrust increases steadily at the entrance until a constant value necessary to initiate drilling is ultimately reached, followed by a sharp decrease in the thrust value, as the tool finally exits the opposite side of the workpiece. As a result, there is a sharp decline in the feed force at the entrance of the workpiece, resulting in a “peeling-out” phenomenon; commonly referred to as delamination. Owing to the abrasive, inhomogeneity and anisotropic nature of FRPs, the actualization of a damage-free output in their conventional drilling approach has proven quite ineffective (Arul et al. 2006).

Table 1 Typical machining parameters for drilling composite materials (Abrate and Walton 1992)

Workpiece material	Tool material	Hole diameter (mm)	Material thickness (mm)	Cutting speed (m min ⁻¹)	Feed rate (mm rev ⁻¹)
Unidirectional graphite-epoxy	Carbide	4.85–7.92	0–12.7	42.7	0.0254–0.0508
		4.85–7.92	12.7–19.1	33.5	0.0254
	PCD	4.85–7.92	0–12.7	61.0	0.0508–0.0889
		4.85–7.92	12.7–19.1	51.8	0.0508–0.0889
Multidirectional graphite-epoxy	Carbide	4.85–7.92	0–12.7	61.0	0.0254–0.0508
		4.85–7.92	12.7–19.1	42.7	0.0254
	PCD	4.85–7.92	0–12.7	68.6	0.0508–0.0889
		4.85–7.92	12.7–19.1	61.0	0.0508–0.0889
Graphite-epoxy	Carbide	4.85	6.35	60.9	0.0254
Glass-epoxy	HSS	–	12.5	15.0	0.028
Glass-epoxy	HSS	3	10	33.0	0.05
Carbon-epoxy	Carbide	3	10	33.0	0.05
Glass-epoxy	HSS	8	1.2	0–40.2	20–460 mm min ⁻¹
Boron-epoxy	PCD	6.35	2.0	91–182	25.4 mm min ⁻¹
		6.35	25.4	91–181	25.4 mm min ⁻¹
MMC	PCD	6	19.2	15–75	0.05
	Carbide				
Boron-epoxy	PCD	6.35	10.4	79	41.91 mm min ⁻¹
Kevlar-epoxy	Carbide	5.6	–	158	0.05

3.3 Failure Modes of FRPs in Conventional Drilling

Conventional drilling of FRPs often results in a variety of damage on the composite laminates, which affects the load-bearing capacity of the composite joints, and consequently leads to their eventual discard. Due to the complex nature of the materials, some of these damages may not be observable by visual inspection, thus leading to the need for conducting non-destructive testing (NDT) of the composite materials, in order to assess their safety towards industrial usage (Durão et al. 2014). Notable material damage and tool effects commonly encountered in the conventional drilling of composite materials are outlined.

3.3.1 Delamination

This is a drilling-induced damage on composites, typically exhibited at the inter-laminar boundaries between the adjacent fibres. Consequently, its occurrence during drilling is dependent on the nature of composite fibres, the polymer matrix and the mechanical properties; such as toughness, Poisson ratio, or the elastic modulus of the interfacial boundaries. It is the major drilling damage on composite materials (Kavad et al. 2014). Reports from Wong et al. (1982) and Sakthivel et al. (2015) also showed that about 60% of composite rejects in the aerospace industry are traceable to delamination defects, as highlighted in Fig. 8.

3.3.2 Mechanics of Delamination

Delamination is caused by a number of drilling parameters, namely the thrust force, feed and the thermal stress mode on the material. Experimentally proven by Stone and Krishnamurthy (1996) as well as Tsao (2012), the delamination potential is directly related to the thrust force developed during drilling (Fig. 9). Khashaba (2004) showed that delamination size increased linearly with feed, and inversely with cutting speed. The thrust force; being the normal force on the drill bit, is the major cause of delamination, and a critical thrust force is usually reached before the onset of crack propagation. While the ability to transmit the thrust force developed

Fig. 8 Composite rejection reasons in the aerospace industry (Sakthivel et al. 2015)

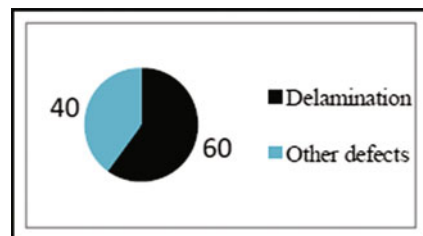
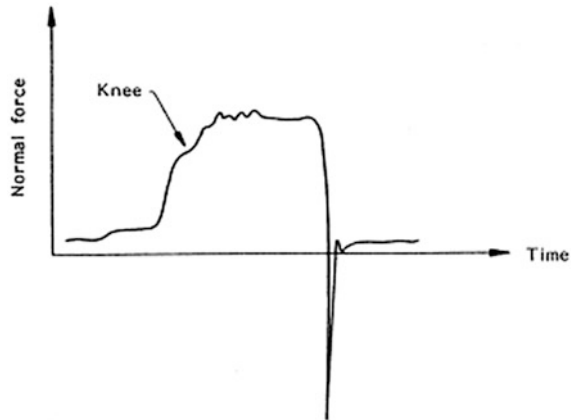


Fig. 9 Typical axial force history during composite drilling (Abrate and Walton 1992)



during drilling from the tool to the composite material is dependent on the tool geometry (Fig. 10), the evaluation of delamination onset is also subject to the type of drill bit employed in the drilling operation.

Numerical models to evaluate the relationship between thrust force and delamination damage during drilling have been developed (Hocheng and Tsao 2005; Hocheng and Dharan 1988; Upadhyay and Lyons 1999). The first model which was developed by Hocheng and Dharan (1988) assumed a circular delaminated region, and a rigid circular plate which was clamped on its contour to the cut portion of the laminate. More so, they treated the critical thrust as a single concentrated load through the drill tip, and found that it was dependent on the composite properties (quasi-isotropic), and the thickness of the uncut plies. However, Hocheng and Tsao (2005) developed a more comprehensive model by considering the influence of tool geometry (across a variety of drill bits such as brad point, slot, step and core drill bits) in the generation of the critical thrust. Further mathematical models are presented in Table 2. Similarly, Upadhyay and Lyons (1999) improved the model by Hocheng and Dharan (1988) by treating the thrust force as a uniformly distributed load, rather than a single concentrated. This is because, the thrust force does not act as a single concentrated load through the tool tip, but as a distributed load over the entire chisel edge of the drill bit.

3.3.3 Delamination Assessment

In the evaluation of delamination damage in drilled materials, a number of assessment models have been developed to measure the extent of the material damage. The most common evaluation is shown in Fig. 11. For clear understanding, they are clearly illustrated in Table 3.

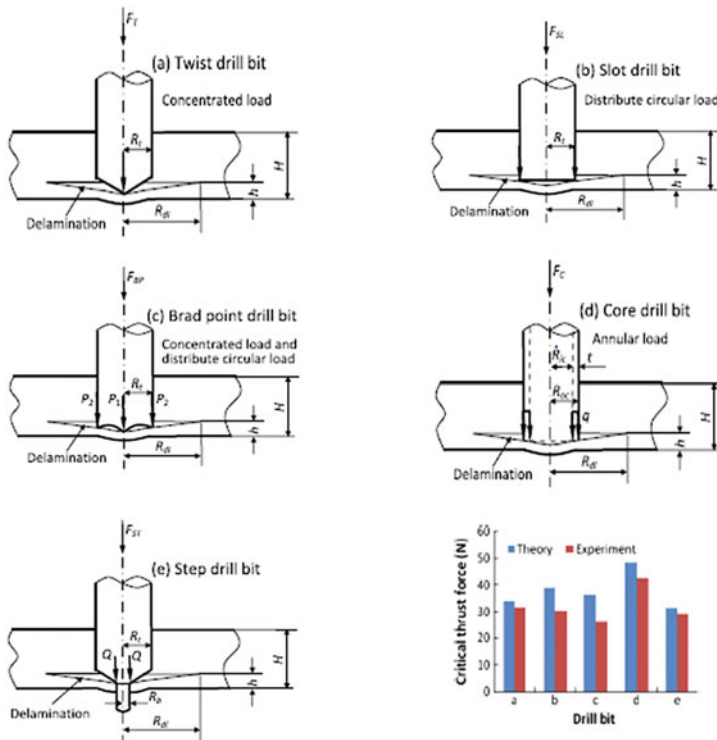


Fig. 10 Schematics of delamination for various drill bits (Liu et al. 2012)

3.3.4 Types of Delamination

Delamination effects can be classified into two, depending on the side of its occurrence and the nature of force involved in its mechanics. They are:

Peel-Up Delamination This type of delamination effect is caused by the tensile impact of the cutting thrust which pulls the laminate surface towards the helical flutes of the drill bit at hole entrance, as shown in Fig. 12. Consequently, this results in the separation of the upper laminate surface from the adjacent layers beneath, leading to a cavity within the composite material. The peel-up delamination is dependent on the tool geometry and the friction between the tool and workpiece.

Push-Out Delamination The push-out delamination is generated by the compressive action of the drill bit on the adjacent layers of the laminate, usually at the exit side of the composite material (Fig. 13). It is the most prominent and severe delamination damage in composite machining (Khashaba 2004; Hejjaji et al. 2016). As the drill bit approaches the exit side of the laminate, the uncut plies gradually become thinner and more prone to deformation. With constant thrust force coupled

Table 2 Critical thrust force models for delamination onset in various drill bits

S/N	Drill bit type	Critical thrust force model	Remarks	Author
1	Twist drill	$F_{CT} = \pi \left[\frac{8G_c E t^3}{3(1-\nu^2)} \right]^{1/2}$	E = Elastic modulus, G_c = Critical strain energy, t = uncut plies thickness under drill bit	Hocheng and Dharan (1988), Abrate and Walton (1992) and Sakthivel et al. (2015)
2	Brad drill bit	$F_{CSL} = \frac{1}{\sqrt{1-2S^2+S^4}} F_{CT}$	$S = R_i/R_{di}$, where R_i = drill bit radius, and R_{di} = Delamination radius	Hocheng and Tsao (2005)
3	Slot drill bit	$F_{CBP} = \frac{1+\alpha}{\sqrt{1+\alpha(1-2S^2+S^4)}} F_{CT}$	α = Ratio of concentrated load (P_1) and peripheral circular load (P_2)	
4	Step drill bit	$F_{CBP} = \frac{\beta(2-\beta)}{\sqrt{[1-(1-\beta)^4]-(1/2)S^2[1-(1-\beta)^4]}} F_{CT}$	$S = R_{oc}/R_{di}$, and $\beta = t/R_{oc}$ t = Thickness of core drill bit, and R_{oc} = Outer radius of core drill bit	
5	Core drill bit	$F_{CST} = \left\{ \frac{[(1-\nu)+2(1+\nu)\xi^2]^2}{\sqrt{(1+\nu)[2(1-\nu)(1+2\nu^2)-12(12-4\nu+3\nu^2+3\nu^3)\xi^2 \ln \xi]}} \right\}^{1/2} F_{CT}$, $\xi = R_o/R_i$		

Fig. 11 Surface image of delamination in CFRP drilling (Liu et al. 2012)

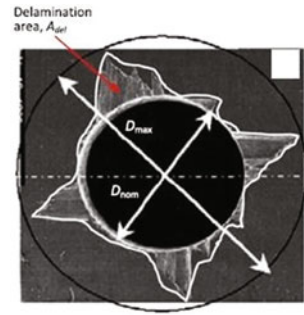
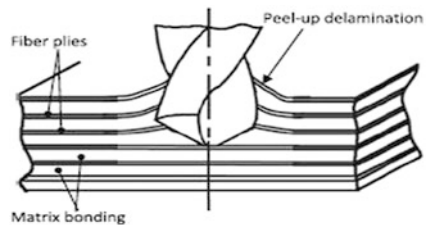


Table 3 Delamination factor assessment models

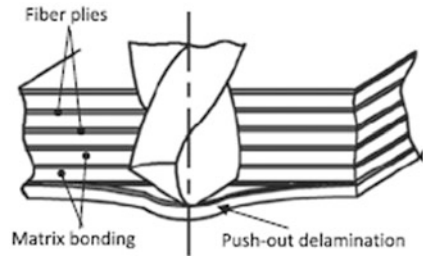
S\N	Delamination factor (D_f) assessment	Analysis	Remarks	Author
1.	$\frac{D_{max}}{D_{min}}$	One dimensional	D_{max} major diameter D_{min} minor diameter	Arul et al. (2006), Sakthivel et al. (2015), Abrate and Walton (1992)
2.	$\frac{D_{MAR}}{A_{AVG}}$	Two dimensional	D_{MAR} hole peripheral damage area A_{AVG} nominal drilled hole area	Mehta et al. (1992)
3.	$\left(\frac{A_{del}-A_{nom}}{A_{nom}}\right)$	Two dimensional	A_{del} damaged area A_{nom} nominal area of hole	Faraz et al. (2009)
4.	$\alpha \frac{D_{max}}{D_{nom}} + \beta \frac{A_{max}}{A_{nom}}$	Adjusted two dimensional	A_{max} area of maximum diameter in delamination zone α and β are delamination coefficients	Davim et al. (2008)

Fig. 12 Peel-up delamination in FRP composite laminate (Liu et al. 2012)



with reduced laminate thickness, the interfacial bonding strength of the composite is eventually exceeded by the thrust, leading to the push-out delamination at the periphery of exit.

Fig. 13 Push-out delamination in FRP composite laminate (Liu et al. 2012)



Temperature-induced damage in conventional drilling techniques takes the form of localized heating which results in burning, melting, or micro-cracks within the composite structure. Due to the highly abrasive nature of FRPs, high thermal energy resulting from excess friction is usually developed at the interface between the tool tip and the composite. While it is not recommended to employ cutting fluids during composite drilling due to the nature of their fibres, the distribution of the generated heat becomes quite concentrated (Durão 2005).

Basically, the heat distribution during drilling operation differs with workpiece materials. For metals, 75% of the heat generated during drilling is eliminated by the chips, 7% is absorbed by the workpiece material and 18% by the tool. However, in the case of carbon–epoxy composites, half the heat generated is absorbed by the tool, while the other half is trapped within the composite and conveyed by the chips. With machining temperatures reaching as high as 200 °C during composite drilling, and in the absence of cutting fluids, the risk of thermal damage via localized heating increases significantly (König and Graß 1989).

Matrix Debonding and Fibre Pull-out Due to the quasi-isotropic nature of FRPs, the high cutting thrust developed during their drilling operation destroys the interfacial adhesion energy between the fibres and the matrix, resulting in matrix debonding, and eventually fibre pull-out.

Tool Wear Conventional drilling of composite materials is usually accompanied by relatively higher cutting thrust sufficient to damage the tool tip by flaking and chipping mechanisms. Tool damage is usually characterized by excessive wear and frictional heat; in cases of composites with hard and abrasive fibres, and tool edge dull by clogging; in cases of soft and sticky polymer matrix (Chen 1997). Experimental investigations on the wear mechanisms of drill bits such as high-speed steel (HSS), cemented carbide and diamond coated carbides have been extensively studied (Abrão et al. 2007; Rawat and Attia 2009) to prove this subject.

Table 4 Summary of differences between CD and NCD techniques

S \N	Conventional drilling	Non-conventional drilling
1.	Energy domain for drilling effects is solely mechanical	Drilling energy can be sourced from mechanical, chemical, electrical, or thermal means
2.	A sharp solid cutting tool is required for material removal	Cutting tool could be solid, liquid, or gaseous
3.	Chip formation is visible with macroscopic volumes	Chip formation is microscopic in size, or completely dissolved at atomic levels

4 Non-conventional Drilling

With regards to the sophisticated characteristics of the new age materials, the conventional drilling techniques became relatively ineffective in materials processing. More so, a great deal of restrictions associated with the use of traditional drilling techniques for materials processing rendered them relatively unsatisfactory for reliable usage, as outlined:

- Very hard fragile materials difficult to clamp are unsuitable for traditional drilling methods.
- Extremely slender or flexible workpiece are prone to failure in traditional drilling.
- The inability to satisfactorily drill complex shaped workpiece materials; particularly fibre-reinforced composites.

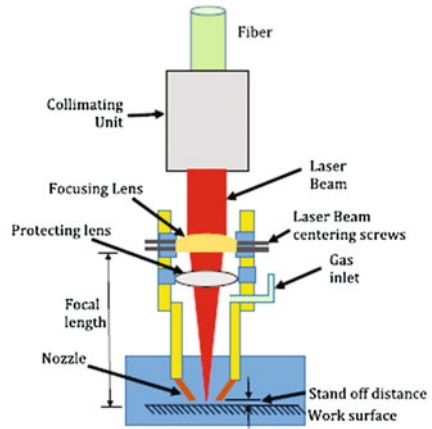
As a result of the aforementioned limitations of traditional drilling, there arose the need to develop better, sustainable and reliable processing techniques, which are collectively referred to as the non-conventional drilling (NCD) processes.

Non-Conventional Drilling refers to a group of advanced drilling processes employed to remove excess material by various individual or combinatory techniques of mechanical, electrical, chemical or thermal energy domains, usually in the absence of a sharp cutting tool which is typical of the conventional counterparts. Unlike the conventional drilling processes, chip formation in non-conventional drilling is not achieved solely by shear deformation which results in macroscopic chip volumes. Rather, chips formed in these advanced drilling processes are microscopic in size, or completely dissolute at atomic levels. Other differences are summarized in Table 4.

4.1 Classification of Non-conventional Drilling Processes

Non-Conventional Drilling processes are classified based on the nature of their energy domains, under which we have the mechanical, electrical, thermal and chemical:

Fig. 14 Schematics of laser head and workpiece arrangement in LBD (Hejjaji et al. 2016)



Mechanical Energy Water jet drilling (WJD), abrasive jet drilling (AJD), ultrasonic-assisted drilling (UAD).

Electrical Energy Electrical discharge drilling (EDD).

Thermal Energy Laser beam drilling (LBD), plasma arc drilling (PAD).

Chemical Energy Chemical and electro-chemical drilling (ECD).

4.2 Types of Non-conventional Drilling Methods

4.2.1 Laser Beam Drilling (LBD)

The LBD is an advanced drilling technique, as depicted in Fig. 14, which utilizes high-temperature radiation to produce drilling effects. It is a non-conventional technique, one of the few used for drilling high aspect holes with depth-to-diameter ratio greater than 10:1 (Forsmann et al. 2007).

Mechanics of Laser Beam Drilling

The term LASER is an acronym for Light Amplification by Stimulated Emission of Radiation. In this technique, drilling is achieved by the impact of a short laser pulse with high power density on the workpiece surface. The process is based on the conversion of electrical energy to light energy, and then to heat energy. Typically generated by a transducer, the laser beam transmits high heat energy sufficient to thermally degrade the workpiece, and then cuts through the material by melting and vapourisation mechanisms. The power developed by the laser (P) is thus given as

$$P = \delta V_m \delta t \quad (6)$$

where δ is the material parameter, which depends on the specific heat of vapourization, the specific heat and the vapourization temperature of the material, V_m is the maximum transverse speed and δt is the material thickness.

Lasers are promising alternatives in composite machining processes. The chips formed are expelled from the hole by the generated vapour pressure, usually in dissolved gaseous forms. While air is mostly used as the assist gas; due to its ability to neutralize oxidation, other gases such as CO₂ and helium have been used for glass and boron–epoxy composites, respectively.

Chips are formed by material melting and expelled via vapourisation from the drilled region. 90% of the drilled material is removed as small particles of diameter less 0.1 μm . The vapourization of carbon–epoxy composites at temperatures of about 4000 °C produces CO and CO₂ gases, while aramid–epoxy composites produced fragments of diameter range 50–100 μm , with 35% of the removed material being recovered as gases with high amounts of hydrogen cyanide (HCN) gas, and small amounts of organic compounds. Lasers can be focused to a spot of about 0.018–0.30 mm in diameter, with beam power output as high as 125–20,000 W. However, a spot size of 0.013 mm in diameter can be achieved in laser cuts, while a hole diameter of as low as 0.005 mm can be produced in LBD, which may be unachievable by other drilling techniques.

Heat Affected Zone (HAZ) This is defined as the region in which the localized temperature exceeds the vapourization temperature of the polymer matrix (Abrate and Walton 2016). It is the major defect of LBD technique, particularly with thermoset polymers. In most cases, the HAZ can be eliminated by post-heat treatment, but there is a risk of distortion.

Kerf This is the portion of the material removed by the laser when it cuts through a workpiece. Usually, it ranges from 0.08 to 0.45 mm, depending on the type of material and other conditional factors.

Laser Beam Drilling of FRPs

The applicability of the laser drilling technology to a material is dependent on the microstructural interactions within the material's lattice. With regards to composite materials, the workability of FRPs with lasers is subject to the type of polymer matrix used for interfacial bonding. Generally, lasers are effective for drilling plastics; due to their high absorptivity for infra-red radiation and low thermal conductivity which allows high heat retention (Abrate and Walton 2016). As a result, the LBD technique is best used for drilling composites with thermoplastic polymer matrices, as opposed to their thermosetting counterparts. This is because thermoplastics have a linear chain of monomers with a simpler lattice fusion, while thermosets have a three-dimensional lattice structure. Therefore, in order to break the strong fusion bond present in the lattice structure of thermosetting plastics,

Table 5 (a) Typical thermal properties of fibre-reinforced material constituents and (b) unidirectional composites (Komanduri 1997)

Material	ρ (g cm ⁻³)	K (W m ⁻¹ km ⁻¹)	C (J kg ⁻¹ K ⁻¹)	κ (cm ² s ⁻¹) 10 ⁻³	T (°C)	H_v (J g ⁻¹)
(a)						
Resin	1.25	0.20	1200	1.30	450	1000
Aramid fibres	1.44	0.05	1420	0.24	950	4000
Carbon fibres	1.85	50	710	380	3300	43,000
Class	2.55	1.0	850	4.6	2300	31,000
Composite	ρ (g cm ⁻³)	K (W m ⁻¹ km ⁻¹)	C (J kg ⁻¹ K ⁻¹)	κ (cm ² s ⁻¹) 10 ⁻³		
(b)						
Aramid/resin	135	0.13	1300	0.74		
Graphite/resin	1.55	25	950	170		
Glass/resin	1.90	0.60	1000	3.2		

relatively higher energy levels (vapourisation temperatures of about 3000 °C for thermosets, compared to 1000 °C for thermoplastics) are required. However, with higher energy levels in laser drilling, there is a greater risk of HAZ formation and thermal degradation via burnout (Caiazzo et al. 2005).

In addition, the wide differences in the thermal conductivities, vapourisation temperatures, and heat of vapourisation of the constituents of a composite make laser drilling complicated (Table 5). Generally, polymer resins; which make up for about 50–60% of FRPs, usually have low thermal properties, when compared to the reinforcing fibres. However, in order to use the LBD technique on FRPs, the laser power requirements need to be based on the type and volume of fibres used, thus leading to high energy levels which can chemically degrade the polymer resins.

Taking reference from the numerical differences in the vapourisation temperatures of the prominent resins and fibres above, it can be inferred that the laser drilling of aramid FRPs will produce lesser HAZ effects than the glass and carbon counterparts. Conclusively, in the laser drilling of FRPs, the order of workability (measured with respect to HAZ effects) goes from Aramid to Glass to Carbon composites (Komanduri 1997).

Caiazzo et al. (2005) investigated the applicability of CO₂ laser for cutting three polymeric thermoplastics; namely polyethylene (PE), polypropylene (PP) and polycarbonate (PC). Using a thickness range of 2–10 mm, the obtained results which showed that high cutting speeds are not always related to good process efficiency, as there exist optimum values of cutting speeds for each material type. Similarly, using a wide range of power settings (200–1400 W), he discovered that the use of CO₂ with the laser beam was quite unnecessary, as the same cutting effects on the thermoplastics could have been achieved with a few hundred watts. From the results achieved, the workability of the polymers; measured relative to

their kerf widths, melted transverse area, melted volume per unit time, surface roughness values, was ranked as PC-high, PP-medium high and PE-lower.

In a similar research by Davim et al. (2008), the effect of laser processing parameters on the quality of cut (HAZ dimension and surface finish) for several thermoplastic polymers; namely PP, PC and Polymethyl methacrylate (PMMA), was conducted. Using a CO₂ laser, the obtained results which ranked the workability of the polymers as PMMA-very high, PC-high and PP-high/medium, and thus confirmed the results by Caiazzo et al. (2005). It was found that the HAZ increases with laser power and decreases with cutting velocity. Consequently, attempts to apply the laser cutting technique on thermosetting plastics produced results with high HAZ effect and surface burnout.

Choudhury and Shirley (2010) also investigated the use of CO₂ laser to cut PP, PC and PMMA thermoplastics. The workability of each polymer; measured relative to the HAZ, roughness and dimensional accuracy, presented results which showed close conformity with that by Davim et al. (2008). From the results, PMMA had the least HAZ, followed by PC and PP. However, in terms of dimensional accuracy,

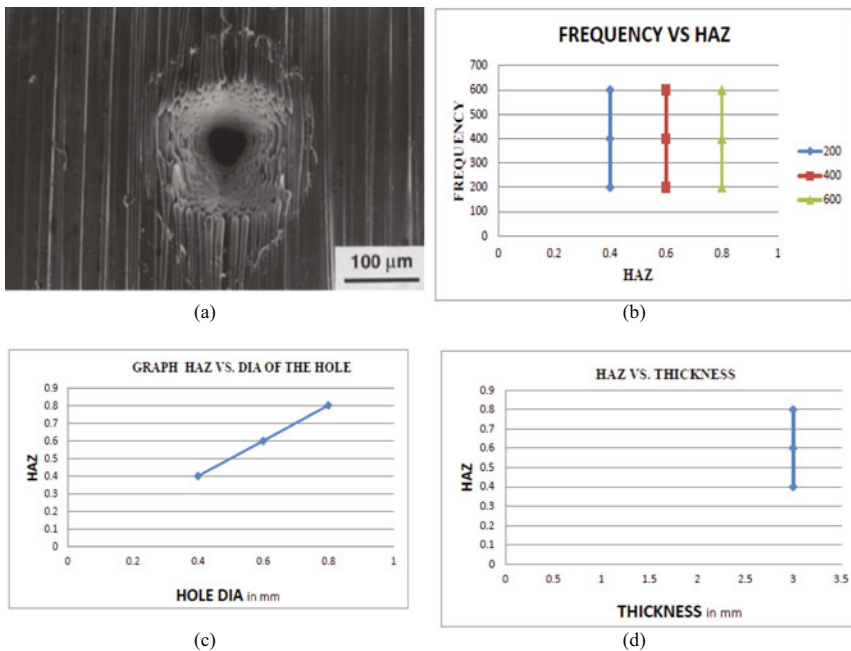


Fig. 15 a Scanning electron microscope (SEM) of a laser drilled hole; b graph of frequency versus HAZ; c graph of HAZ versus hole diameter; and d graph of HAZ versus laminate thickness (Anarghya et al. 2015)

PMMA had the best surface finish, followed by PP and PC. For all the three polymers investigated, it was also found that the HAZ dimension was directly proportional to the laser power, and inversely proportional to the cutting speed and compressed air pressure.

A research study by Anarghya et al. (2015) explored the use of lasers in the drilling operation of CFRPs. Using a series of Scanning Electron Microscope (SEM) images, he obtained the optimum machining parameters which produced a good surface finish with the least HAZ effects. Results from the research study showed that the HAZ effect increases proportionally with the increase in laser frequency, hole diameter and laminate thickness as shown in Fig. 15. The optimum machining parameters obtained are:

1. Frequency range: 200–250 Hz.
2. Diameter of the hole: 0.4 mm.
3. Drilling speed: 200 m/s.
4. Thickness of specimen: 3 mm.

Advantages of Laser Beam Drilling

1. Relatively lesser cutting thrust is developed in this technique, leading to reduced delamination potential. Hejjaji et al. (2016) studied the damage characterization of FRPs comparatively in conventional and fibre laser drilling techniques. While the CD technique produced a finer finish quality on the composite, the machining damage, measured with respect to the delamination effect on the composite, was relatively greater in CD than the laser counterpart.
2. Fragile, slender and delicate materials can be conveniently drilled because of the non-contact relationship between laser and workpiece (Chryssoulouris et al. 2014).
3. High aspect ratio holes, as high as 30:1 depth-to-diameter ratios can be drilled.
4. It is accurately fast, and can be easily automated.
5. Beveled holes; that is, holes at shallow angles from the workpiece surface are best achieved with this technique.



Fig. 16 Rounded-corner effects in excessive-power laser drilling of FRPs (Abrate and Walton 2016)

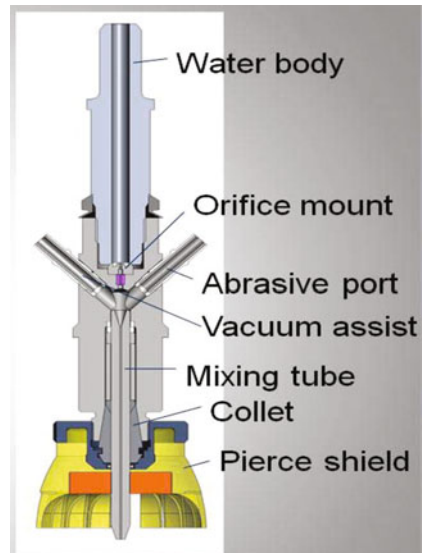
Disadvantages of Laser Beam Drilling

1. LBD requires a huge capital investment to set-up.
2. Accumulation of dross build-up at hole entry and exit may be present, due to the melting and vapourisation mechanisms. Consequently, this defect reduces the hole quality.
3. A considerable taper may be present in holes with large depth-to-diameter ratios.
4. Unsuitability for drilling thermoset FRPs; such as glass and carbon-epoxies, makes it limited for wider usage in composite machining.
5. The thermal energy often induces a HAZ around the drilled hole, leading to micro-cracks in some materials. Abrate and Walton (2016) studied the applicability of laser drilling on composites, and obtained results which highlighted the major setbacks of this advanced technology as HAZ formation, and the destructive interference of material thickness on laser beam focus. Consequently, this causes higher energy levels and results in charring (Fig. 16).

4.2.2 Water Jet and Abrasive Jet Drilling

The AJD is an advanced drilling technique which employs extremely high fluid pressures to mechanically energize a jet of abrasive particles on to a material surface for drilling effects (Fig. 17). The high velocity impact of the abrasive jet produces a micro-cutting action which automatically erodes the material surface for drilling to occur. The abrasive particles are typically in the range of 10–50 μm in size, with flow velocity reaching as high as 300 m/s, depending on the MRR desired.

Fig. 17 Schematic of the abrasive water jet drilling tool (Mohamed 2014)



Mechanics of Abrasive Jet Drilling

A nozzle of injection diameter of about 0.5 mm, positioned at a stand-off distance in the range of 0.5–15 mm, and at a deflection angle of 60°–90° is used to supply the pressure needed to drive the abrasive jet to the workpiece surface. The kinetic energy developed by the abrasive particles in the transport process is then converted to produce the drilling effects, via erosion degradation and brittle fracture of the workpiece. Notable transport fluids commonly employed in the AJD technique are air, carbon (iv) oxide, Nitrogen gas, inert gases and in some cases water. In processes where water is used as the transport fluid, the technique is otherwise known as abrasive water jet drilling (AWJD). Similarly, in the absence of abrasives, the technique is referred to as water jet drilling (WJD).

AWJD is a relatively new manufacturing technology which addresses various limitations of pre-existing techniques. In AWJD, material removal rate (MRR) depends on the operating parameters and the properties of the target material. Similarly, the taper of machined surface increases with a decrease in hardness of abrasives. However, abrasives with a high level of hardness have detrimental effects like accelerating tool wear. Thus, garnet abrasives are the often used in AWJ machining industries due to their favourable effects like low nozzle wear rate, good machinability and economical availability (Doreswamy et al. 2015). Other commonly used abrasives are Al_2O_3 , silicon carbide and glass beads.

Abrasive Jet Drilling of FRPs

Hocheng (1990) investigated the mechanics of exit-ply delamination during WJD of graphite–epoxy composite laminates. Using fracture mechanics and plate theory, he developed a numerical model to optimize the water pressure needed for zero delamination effects in WJD.

While the water jet force was adjudged to be the most significant factor towards the onset of delamination, it was noticed that at some points during WJD, the water jet force appears bent. Therefore, as the water jet continues drilling towards exit, the decrease in thickness of the uncut plies resulted in lesser resistance to deformation. Consequently, the interfacial bonding strength breaks off, and delamination sets in. Conclusively, a better machining performance on FRPs is possible with WJD, given that the significant process parameters such as water jet pressure and jet diameter are optimized.

Shaikh and Jain (2012) studied the cutting mechanisms of FRPs (such as cotton fibre polyester composites), using CO_2 laser, water jet and diamond saw cutting techniques. Results obtained from experimental analysis showed the preference of laser cutting over water jet and diamond saw cutting, due to failure effects; such as fibre pull-out during diamond saw cutting, and fibre pull-out in many directions and fibre curling experienced during water jet machining of composites. More so, the tendency of degradation of reinforcing fibres; in this case, cotton fibres with moisture, automatically limits the applicability of water jet cutting technique.

In a recent research by Unde et al. (2014), the machinability of FRPs using AWJ technique was critically reviewed. They discovered that the most important process parameters for tuning purposes in AWJ machining are the transverse speed, stand-off distance, abrasive water pressure and the mass flow rate. Due to the absence of HAZ via thermal distortion in AWJ machining of FRPs, he concluded that it is the most suitable method for machining composite materials. More so, the prevalent problems of other machining techniques, such as burr formation and delamination were found to be almost negligible in AWJ machining, thus making it a good preference for composite machining.

Furthermore, Ramulu and Arola (1993) investigated the micromechanical behaviour of the reinforcing fibres and matrix of a unidirectional graphite–epoxy composite, to water jet machining (WJM) and abrasive water jet machining (AWJM) techniques. Results obtained from the experimental analysis showed that the AWJM produced a finer surface finish than WJM, due to its combinatory material removal mechanisms of shearing, erosion and micro-machining. Consequently, AWJM was considered feasible for machining FRPs.

Advantages of Abrasive Jet Drilling

1. Complex, intrinsic mechanical parts can be easily drilled using this advanced technique.
2. Material wastage is largely reduced by the smaller kerf size.
3. Requires no secondary finishing operation.
4. Strain hardening effects; typical of conventional methods, is minimally reduced due to the cooling effects of the transport fluids.
5. Absence of thermal distortion via HAZ.
6. Chip formation is microscopic and unattached to material surface, due to the cleaning effects of the transport fluid. Consequently, this aids drilling performance and enhances tool life.
7. Low cutting thrust levels in this technique reduce tool wear and delamination damage.

Disadvantages of Abrasive Jet Drilling

1. High capital investment is required to set-up this advanced technique.
2. Noise levels during operation are relatively high.
3. Unsuitability for materials with high moisture degradation potential.
4. Inability to drill flat bottomed holes.

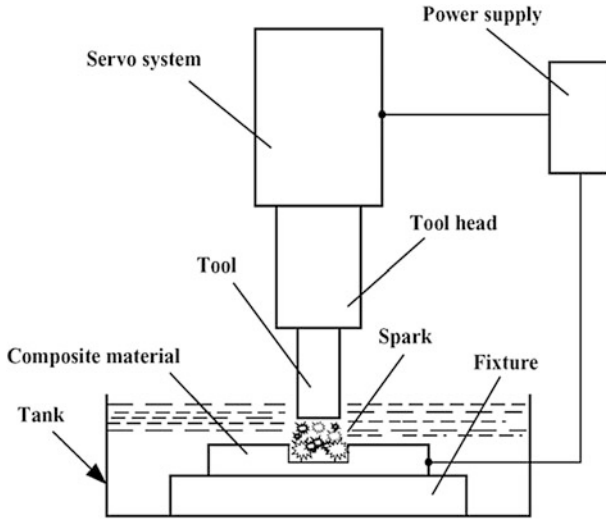
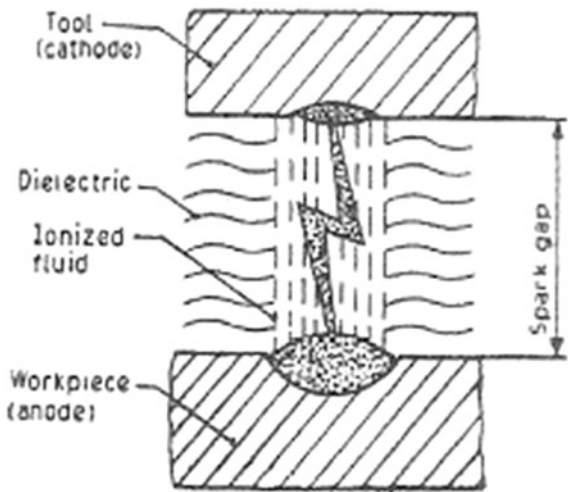


Fig. 18 Schematics of electrical discharge machining (Hocheng and Tsao 2005)

Fig. 19 Basic EDM system (Khan and Ndaliman 2011)



4.2.3 Electrical Discharge Drilling (EDD)

EDD is thermoelectric material removal process between a tool and the workpiece, usually in the presence of a dielectric fluid (Fig. 18). It is a non-conventional drilling technique that is largely dependent on electrical conductivity.

Mechanics of EDD

In this technique, drilling is achieved by the impact of recurring electrical sparks used to thermally erode the workpiece surface in order to remove the undesired materials. While the tool serves as the electrode in this technique, the workpiece is deployed for use as the anode, along with a conductive dielectric fluid (Fig. 19). The cathode; in this case, the tool, gradually erodes the anode until the desired material geometry is ultimately achieved.

At the start of the EDD process, a high voltage electric spark is applied across the small gap between the tool and workpiece, in the presence of a dielectric fluid. This voltage creates an electric field which agitates the particles within the dielectric fluid, and causes them to settle at the points where the electrical field is strongest. As the potential difference between the tool and the workpiece becomes considerably high, the dielectric fluid breaks down and recurring sparks which gradually removes material from the workpiece surface are discharged through the dielectric fluid. Material removal rate (MRR) in EDD process is given by the formula:

$$\text{MRR} = 40I/T_m^{1.23} \quad (7)$$

where I is the current ampere and T_m is the melting temperature of workpiece.

In EDD process, the dielectric fluid serves three purposes, as described:

- Acts as an insulator between the tool and workpiece.
- Regulates the temperature generated at the tool–workpiece interface, by acting as a coolant.
- Acts as a flushing medium for chip removal.

Typical dielectric fluids commonly used in EDM processes are hydrocarbon oils, kerosene and deionised water.

Electrical Discharge Drilling of FRPs

Vaxevanidis et al. (2006) investigated the applicability of EDD to FRPs, using PAN–epoxy, Hexcel satin carbon–epoxy and PAN–carbon composites with copper electrodes. From the experimental results obtained, the feasibility of EDD to FRPs was found to be largely dependent on the selection of optimum machining parameters, namely positive tool polarity, small pulse-on times and small pulse currents. Also, the surface finish of the hole entrance was better than the exit in this technique due to the influence of the small pulse-on times, while machining damage on the composites was reported as craters, valleys as well as delamination and cracking.

Guu et al. (2001) investigated the feasibility of machining CFRPs by electrical discharge machining (EDM) technique. Using a series of generated empirical formulas for process assessment, they obtained the optimized machining parameters for the composite under test.

$$D_f = 0.815I_p^{0.0681}\tau_{on}^{0.0579} \tag{8}$$

$$d_t = 13.696I_p^{0.534}\tau_{on}^{0.204} \tag{9}$$

$$MRR = 0.378I_p^{0.216}\tau_{on}^{0.041} \quad \tau_{on} \leq 100 \mu s \tag{10}$$

$$MRR = 4.400I_p^{0.134}\tau_{on}^{-0.428} \quad \tau_{on} > 100 \mu s \tag{11}$$

$$R_a = 1.326I_p^{0.224}\tau_{on}^{0.216} \tag{12}$$

where D_f is the delamination factor, d_t is the recast layer thickness, MRR is the material removal rate, R_a is the surface roughness, I_p is the pulse current and τ_{on} is the pulse duration.

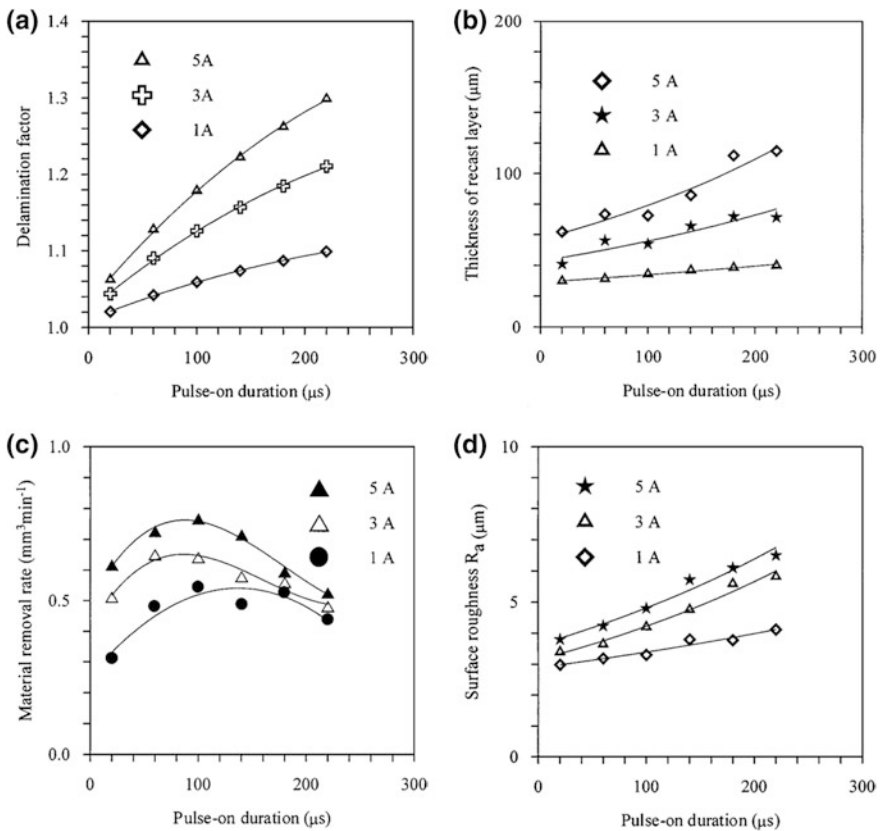


Fig. 20 Graphs of correlation between **a** delamination factor and machining conditions; **b** recast layer under various machined conditions; **c** material removal rates for various pulse current and duration; **d** surface roughness against various pulse durations (Guu et al. 2001)

From the results obtained (Fig. 20), it was found that both peel-up and push-out delamination defects can be prevented by using smaller pulse energy for electrical discharge. Similarly, higher discharge energy was characterized with high temperatures which constituted to surface roughness, larger recast layer and delamination on the cutting edge.

Using the optimized pulse current of 5 A, and pulse-on duration of 100 μ s, MRR was found to be as high as 0.768 mm³/min in this technique. Conclusively, and with the selection of appropriate process parameters, the EDM technique was considered feasible for machining CFRPs.

Advantages of Electrical Discharge Drilling

1. Thin and fragile workpiece materials can be accurately drilled without distortion, using EDD.
2. Absence of burrs on machined surface.
3. Electrically conductive materials of any hardness can be machined using EDD.

Limitations of Electrical Discharge Drilling

1. EDD is limited to machining electrically conductive materials only.
2. Low MRR makes it relatively slow to conventional techniques.
3. Increased MRR can lead to rough surface finish.
4. Higher risk of erosion and over cutting is a major concern in this technique.

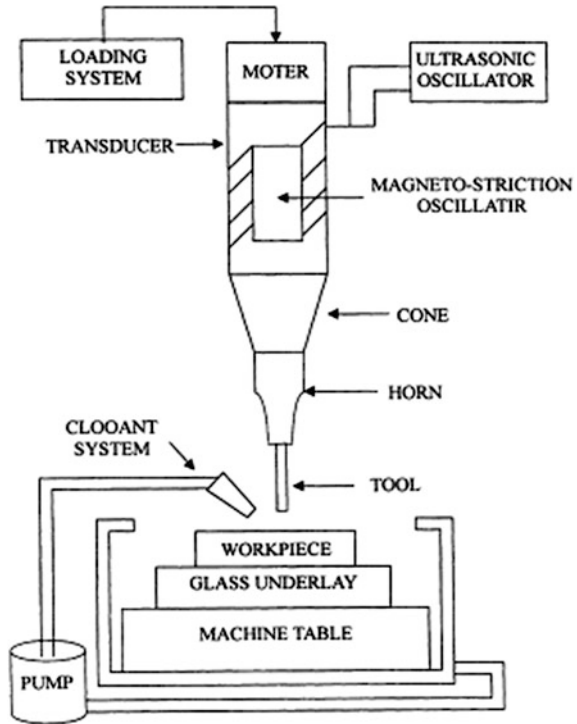
4.2.4 Ultrasonic-Assisted Drilling (UAD)

This is a non-conventional drilling technique which utilizes high mechanical vibration to produce drilling effects. It involves the superimposition of a high-frequency vibration on a drill bit at the feed direction.

Mechanics of UAD

In this technique, the drill bit is mechanically excited in the torsional or axial direction by the superimposed vibration (the axial excitation being preferred in many applications) to remove undesired materials. It involves the combinatory mechanisms of conventional drilling and ultrasonic oscillation (Fig. 21), and is applicable to drilling both ductile and brittle materials (Azarhoushang and Akbari 2007).

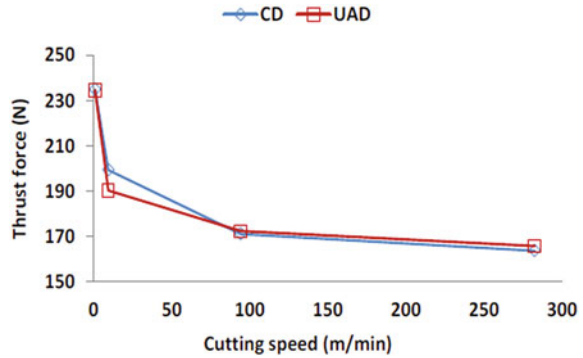
Fig. 21 Set-up of ultrasonic machining (Hocheng et al. 2000)



The ultrasonic vibration (with frequency typically in excess of 20 kHz, and balanced with a low amplitude of tens of micrometers) can be sourced from piezoelectric actuators such as transducers. The use of ultrasonic vibration in machining operations has its history documented for more than 50 years (Graf 1975). Results obtained from this technology over the years of discovery has proven successful in applications where conventional drilling techniques were ineffective.

Fundamentally, UAD being an advanced technology, has different mechanics of material removal compared to CD. While material removal is continuous in CD, UAD utilizes the impact of a low amplitude intermittence between the tool and workpiece interface to achieve high deformation rates. Consequently, the drilling process in UAD is achieved by the high-frequency hammering effect of the abrasive grains at the tool’s cutting edge on the surface of the workpiece (Hocheng et al. 2000).

Fig. 22 Average thrust force recorded in CD and UAD (Gupta et al. 2014)



Drilling Parameters in UAD

Thrust Force and Torque The thrust force developed in UAD has an optimal value, and is significantly lower than that of CD techniques at all vibration frequencies (Thomas and Babitsky 2007; Makhdum et al. 2014). In some cases, such as reports from Gupta et al. (2014), thrust force in CD and UAD techniques are nearly equal at all cutting speeds with constant feed rates (in the absence of cutting fluids), but with slight reduction in the thrust force during UAD at specific lower cutting speeds. Similarly, the torque on the tool in UAD is comparatively lower than that developed during CD techniques over the period of tool engagement.

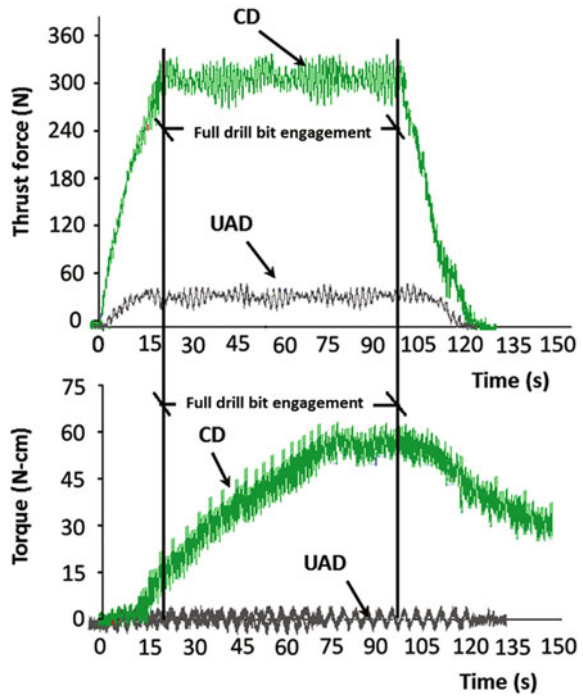
Cutting Speed The cutting speed varies linearly with thrust force in UAD, and is similar to that of CD. The thrust force reaches its maximum value at the lowest cutting speed and vice versa, as shown in Fig. 22. Consequently, it is recommended to employ high cutting speeds during UAD (Phadnis et al. 2012a, b).

Feed Rate Feed rate varies linearly with MRR in UAD, as well as to the amount of workpiece material removed by one abrasive grain (Cong et al. 2012).

Cutting Temperature The temperature developed at the tool–workpiece interface during UAD is similar to that of CD at lower cutting speeds (<10 m/min), but greater in UAD at higher cutting speeds (<200 m/min) (Gupta et al. 2014). However, while the cutting temperature increases linearly with feed rate in CD, the high temperature in UAD remains constant irrespective of the feed rate (for <20 mm/min), due to the repeated vibratory cycles to which the drill bit is constantly subjected. Using a feed rate of 16 mm/min, cutting temperatures of 90.2 and 290.8 °C were, respectively, reported for CD and UAD technologies by Makhdum et al. (2014).

Comparatively with CD, Pujana et al. (2009) reported that tool tip temperature was relatively higher in the UAD of Ti₆Al₄V material, and observed the linear relationship between vibration amplitude and tool tip temperature.

Fig. 23 a Cutting forces history in UAD and CD; and **b** drilling torque history in UAD and CD (Makhdum et al. 2014)



Ultrasonic-Assisted Drilling of FRPs

Phadnis et al. (2012a, b) investigated the drilling of CFRP laminate using UAD and CD techniques. Results obtained from the experimental analysis showed the effectiveness of UAD over CD in terms of reduction in the average thrust force. An excellent correlation between experimental data and numerical analysis models portrayed the feasibility of UAD over CD techniques in composites machining.

At certain drilling conditions, comparative reduction in the average thrust force was as high as 30%. Considering the linear relationship between thrust force and delamination potential in drilling operation, the safe workability of composites with UAD was thus verified.

Similarly, the relationship between cutting speed and thrust force was studied in both UAD and CD techniques by Phadnis et al. (2012a, b), using both experimental data and numerical analysis on a CFRP composite. Results showed that thrust force decreased with increase in cutting speed, as decrease in thrust force was considerably higher in UAD than CD (31.1% at 1700 rpm against 15.8% at 216 rpm) at higher cutting speeds.

Furthermore, the intermittent vibration oscillation in UAD was adjudged to reduce the frictional effect at the tool–workpiece interface, by increasing the sliding velocity. This translated into a tangible reduction in the overall thrust force at the tool–workpiece interface, and thus suggested the need to employ higher rotational speeds during the UAD of CFRPs.

Makhdum et al. (2014) studied the mechanics involved in the UAD of CFRPs. Using a combination of experimental data and mathematical models, the drilling forces, cutting temperature, chip formation, surface finish, circularity, delamination and tool wear were investigated. Results from the study showed a significant reduction in drilling forces during UAD, as high as 80% for aluminium workpiece (Fig. 23), as well as general improvements in the drilling output, relative to conventional drilling. Furthermore, the softening effects of UAD on CFRPs was accounted for in the numerical model of this research, and the results obtained from this demonstrated the reason behind the much desired reduction of thrust forces in this advanced method of drilling.

Advantages of Ultrasonic-Assisted Drilling

1. Ability to drill any type of materials, irrespective of their electrical conductivity.
2. UAD can be used to machine hard materials of 40 HRC to 60 HRC like carbides, ceramics and industrial diamonds.
3. Aspect ratio of about 40:1 can be achieved using UAD.
4. Holes of 76 μm diameter with 51 mm depth can be conveniently drilled.
5. Produces surface integrity and finish.
6. Absence of thermal, electrical and chemical effects.
7. Can be conjunctively used with other non-conventional techniques like EDD.

Disadvantages of Ultrasonic-Assisted Drilling

1. UAD is an advanced technology, and so requires huge capital investment to set-up.
2. High power consumption with unpredictable results is often gotten from the application of this technology, due to the misunderstanding of the working process.
3. High rate of tool wear may result from chipping effects, leading to premature tool failure (Thomas and Babitsky 2007).

Summary of Ultrasonic-Assisted Drilling

Below are the documented summaries of the characteristics of the ultrasonic-assisted drilling over conventional drilling:

1. Reduced drilling reaction force and torque: this enhances the ease of drilling thin structures without deformation.
2. Increased positional accuracy; better precision.

Table 6 Summary of differences in process capabilities of NCD and CD techniques (Singh 2008)

S\N	Process	MRR (mm ³ /min)	Tolerance (μ)	Surface finish (μ)	Depth of surface damage (μ)	Power consumption (W)
1	USD	300	7.5	0.2–0.5	25	2400
2	AJD	0.8	50	0.5–1.2	2.5	250
3	EDD	800	15	0.2–1.2	125	2700
4	LBD	0.1	25	0.5–1.2	125	2 (average)
5	Conventional drilling	50,000	50	0.5–50	25	3000

Table 7 Summary of material applicability for various NCD techniques (Singh 2008)

S\N	Process	Steel	Ceramics	Plastics	Glass	Refractory material
1	USD	Fair	Good	Fair	Good	Good
2	AJD	Fair	Good	Fair	Good	Good
3	EDD	Good	–	–	–	Good
4	LBD	Fair	Good	Fair	Fair	Poor

3. Improved chip expulsion.
4. Reduced or eliminated burr formation on the exit side of drilled holes.
5. Improved hole roundness and size.
6. Extended drill bit life due to the reduction in the rate of tool wear.
7. Increased material removal rate.
8. Improved hole surface finish.
9. Reduced or eliminated built up edge.

As a result, UAD has proven to be better than conventional drilling techniques because of the following under-listed reasons:

1. No de-burring operations are required after drilling,
2. No spot drilling operation is required when drilling into an inclined surface,
3. Improved hole quality/roundness automatically eliminates the need for subsequent reaming operations, and thus saves production cost.

Lastly, Tables 6 and 7 summarize the differences in process capabilities of the two techniques and material applicability for various NCD techniques.

5 Conclusions and Future Perspective

A comprehensive philosophical study has been reported in this chapter, in which emphasis was on various aspects of natural (bio) composites. These included, but are not limited to, uses, properties, classifications, advantages and limitations. Also,

the workability of FRPs with various non-conventional drilling technologies has been discussed in this chapter. Decisions on process suitability for machining FRPs were based on the ability to produce a damage-free drilled laminate, measured with respect to the delamination potential, thermal degradation effects and operational costs involved. Among all the five processes discussed in this chapter, abrasive jet and ultrasonic-assisted drilling demonstrated capabilities for effective machining of FRPs. This is reflected in their quality of machined holes, coupled with their flexibility in the choice of workpiece materials.

Laser beam technology proved highly promising due to the ease of process automation, but with limited applicability to FRPs due to the tendency of HAZ formation, and unsuitability for thermosetting polymer matrices such as epoxy and polyester resins. Abrasive jet drilling showed lesser delamination damage on FRPs, but with undue high noise level during operation and process costs involved in setting up this technology. Water jet drilling, though extensively used in manufacturing industries, has restrictions due to its possibility of introducing delamination, and its incompatibility for materials with water degradation potential; of which some FRPs, such as natural (cotton, hemp, jute, to mention but a few) fibre-reinforced composites are inclusive. Electrical discharge drilling technology, though most suitable for generating precision holes (holes without distortion), has its applicability to FRPs reduced by the total dependence on materials' electrical conductivity and low material removal rates. However, Ultrasonic-assisted drilling proved highly applicable to FRPs by its relatively lesser delamination potential and lower thermal build-up at tool–workpiece interface. While operational costs for this technology were reportedly high comparing with other non-conventional processes, favourable results obtained from this technology suggests its suitability for machining several FRP composite materials, regardless of their electrical conductivity levels, hardness or slenderness. Conclusively, non-conventional drilling technologies showed greater effectiveness towards machining FRPs over their conventional counterparts.

The scope of this chapter does not cover much about the application of analytical, numerical and finite element modellings of machining (drilling) of FRP composite materials. Also, drilling of natural FRP composite materials is not well covered. These highlighted areas are the prospective focus of research towards recent and furtherance of FRP composite materials manufacturing technology.

References

- Abiola OS, Kupolati WK, Sadiku ER, Ndambuki JM (2014) Utilisation of natural fibre as modifier in bituminous mixes: A review. *Const Build Mater* 54:305–312
- Abrão AM, Faria PE, Rubio JCC, Reis P, Davim JP (2007) Drilling of fibre reinforced plastics: A review. *J Mater Proc Technol* 186(1–3):1–7
- Abbate S, Walton D (2016) Machining of composite materials. Part II: non-traditional methods. *Compos manuf* 3(2):85–94

- Abrate S, Walton DA (1992) Machining of composite materials Parts I: traditional methods. *Compos Manuf* 3(2):75–94
- Anarghya A, Yatheesha RB, Gurumurthy BM, Rao N, Ranjith BS (2015) Drill-ability studies of laser drilled micro holes on CFRP composites. In: *New developments in biology, biomedical and chemical engineering and materials science. International conference proceedings, Vienna, Austria, 15–17 March*
- Arul S, Vijayaraghavan L, Malhotra SK, Krishnamurthy R (2006) The effect of vibratory drilling on hole quality in polymeric composites. *Int J Mach Tools Manuf* 46:252–259
- Azarhoushang B, Akbari J (2007) Ultrasonic-assisted drilling of Inconel 738-LC. *Int J Mach Tools Manuf* 47:1027–1033
- Bledzki A, Sperber VE, Faruk O (2002) Natural wood and fibre reinforcement in polymers. *Rapra Review Reports, Rapra Technology Ltd, Shrewsbury*
- Bongiorno A, Capello E, Copani G, Tagliaferri V (1998) Drilled hole damage and residual fatigue behaviour of GFRP, ECCM-8, Naples, Italy II, pp 525–532
- Caiazzo F, Curcio F, Daurelio G, Memola FCM (2005) Laser cutting of different polymeric plastics (PE, PP and PC) by a CO₂ laser beam. *J Mater Process Technol* 159(3):279–285
- Chen WC (1997) Some experimental investigations in the drilling of carbon fibre-reinforced plastic (CFRP) composite laminates. *Int J Mach Tools Manuf* 37:1097–1108
- Cheung HY, Ho MP, Lau KT, Cardona F, Hui D (2009) Natural fibre reinforced composites for bioengineering and environmental engineering applications. *Compos Part B Eng* 40(7):655–663
- Choudhury IA, Shirley S (2010) Laser cutting of polymeric materials: an experimental investigation. *Opt Laser Technol* 42:503–508
- Chryssolouris G, Stavropoulos P, Salonitis K (2014) Process of laser machining. In: *Handbook of manufacturing energy and technology*, pp 1–25
- Cong WL, Pei ZJ, Feng Q, Deines TW, Treadwell C (2012) Rotary ultrasonic machining of CFRP: a comparison with twist drilling. *J Reinf Plast Compos* 31(5):313–321
- Davim JP, Barricas N, Conceicao M, Oliveira C (2008) Some experimental studies on CO₂ laser cutting quality of polymeric materials. *J Mater Proc Technol* 198:99–104
- DeGarmo EP, Black JT, Kohser RA (2003) *Materials and processes in manufacturing*, 9th edn. Wiley, New York
- Dhakal HN, Zhang ZY, Richardson MOW (2007) Effect of water absorption on the mechanical properties of hemp fibre reinforced unsaturated polyester composites. *Compos Sci Technol* 67 (7–8):1674–1683
- Doreswamy D, Shivamurthy B, Anjaiah D, Sharma NY (2015) An investigation of abrasive water jet machining on graphite/glass/epoxy composite. *Int J Manuf Eng* 2015:1–11
- Durão LMP (2005) Machining of hybrid composite. Ph.D. Thesis, Faculty of Engineering, University of Porto
- Durão MLP, Tavares JMRS, de Albuquerque VHC, Marques JFS, Andrade ONG (2014) Drilling damage in composite material. *Open Access Mater* 7:3802–3819
- Faraz A, Biermann D, Weinert K (2009) Cutting edge rounding: an innovative tool wear criterion in drilling CFRP composite laminates. *Int J Mach Tools Manuf* 49:1185–1196
- Faruk O, Bledzki AK, Fink HP, Sain M (2012) Biocomposites reinforced with natural fibers: 2000–2010. *Prog Poly Sci* 37(11):1552–1596
- Forsmann AC, Lundgren EH, Dodell AL, Komashko AM, Armas MS (2007) Double pulse format for laser drilling. *Photonics Spectra* 1–9
- Graf K (1975) *Macrosclerosis in industry: 5. Ultrasonic machining. Ultrasonics* 13(3):103–109
- Graupner N, Herrman AS, Mussig J (2009) Natural and man-made cellulose fibre reinforced poly (lactic acid) (PLA) composites: an overview about mechanical characteristics and application areas. *Compos Part A Appl Sci Manuf* 40(6–7):810–821
- Gupta A, Barnes S, McEwen I, Kourra N, Williams MA (2014) Study of cutting speed variation in the ultrasonic assisted drilling of carbon fibre composites. In: *Proceedings of the ASME 2014 international mechanical engineering congress and exposition*, 37046

- Guu YH, Hocheng H, Tai NH, Liu SY (2001) Effect of electrical discharge machining on the characteristics of carbon fibre reinforced carbon composites. *J Mater Sci* 36:2037–2043
- Hejjaji A, Singh D, Kubher S, Kalyanasundaram D, Gururaja S (2016) Machining damage in FRPs: laser versus conventional drilling. *Compos Part A Appl Sci Manuf* 82:42–52
- Hocheng H (1990) A failure analysis of water jet drilling in composite laminate. *Int J March Tools Manufact* 30(3):423–429
- Hocheng H, Dharan CKH (1988) Delamination during drilling in composite laminates. In: Proceedings of the conference on machining composites, Winter Annual Meeting, American Society of Mechanical Engineers (PED-35/MD-12), pp 39–44
- Hocheng H, Tai NH, Liu CS (2000) Assessment of ultrasonic drilling of C/SiC composite material. *Compos Part A Appl Sci Manuf* 31:133–142
- Hocheng H, Tsao CC (2005) The path towards delamination-free drilling of composite materials. *J Mater Process Technol* 167:251–264
- Ismail SO, Dhakal HN, Popov I, Beaugrand J (2015) Experimental analysis of drilling-induced damage of lignocelulosic 19/hemp fibre reinforced PCL and MTM 44-1/carbon fibre reinforced epoxy resin composites. In: Proceedings of 5th international conference on natural fibre composites for industrial applications, Sapienza Universita de Roma, Rome, Italy, 15–16 October, pp 1–4
- Jawaid M, Abdul Khalil HPS (2011) Cellulosic/synthetic fibre reinforced polymer hybrid composites: a review. *Carbohydr Polym* 86(1):1–18
- Kabir MM, Wang H, Lau KT, Cardona F (2012) Chemical treatments on plant based natural fibre reinforced polymer composites: an overview. *Compos Part B: Eng* 43(7):2883–2892
- Kalpakjian S, Schmid SR (2003) Manufacturing processes for engineering materials, 4th edn. Prentice-Hall, New York
- Kavad BV, Pandey AB, Tadavi MV, Jakharia HC (2014) A review paper on effects of drilling on glass fibre reinforced plastic. *Procedia Technol* 14:457–464
- Khan AA, Ndaliman BM (2011) An introduction to electrical discharge machining. *Adv Mach Process*: 65–69
- Khashaba UA (2004) Delamination in drilling GFR-thermoset composites. *Compos Struct* 63(3–4):313–327
- Kocsis J, Mahmood H, Pegoretti A (2015) Recent advances in fiber/matrix interphase engineering for polymer composites. *Prog Mater Sci* 73:1–43
- Komanduri R (1997) Machining fibre-reinforced composites. *Mach Sci Tech* 1(1):113–152
- König W, Graß P (1989) Quality definition and assessment in drilling of fibre reinforced thermosets. *CIRP Ann Manuf Technol* 38(1):119–124
- Ku H, Wang H, Pattarachaiyakoo N, Trada M (2011) A review on the tensile properties of natural fibre reinforced polymer composites. *Compos Part B Eng* 42(4):856–873
- Liu D, Tang Y, Cong WL (2012) A review of mechanical drilling for composite laminates. *Compos Struct* 94(4):1265–1279
- Makhadm F, Phadnis AA, Roy A, Silberschmidt VV (2014) Effect of ultrasonically-assisted drilling on carbon fibre-reinforced plastics. *J Sound Vib* 333(23):5939–5952
- Mallick PK (2008) Fibre-reinforcement composites, materials, manufacturing and design, 3rd edn. CRC Press, Taylor and Francis Group, New York
- Marinov V (2010) Manufacturing processes for metal products, 1st edn. Kendall/Hunt Publishing Company, Dubuque
- Mehbudi P, Baghlani V, Akbari J, Bushroa AR, Mardi NA (2013) Applying ultrasonic vibration to decrease drilling-induced delamination in GFRP laminates. *Procedia Soc Behav Sci* 6:577–582
- Mehta M, Reinhart TJ, Soni AH (1992) Effect of fastener hole drilling anomalies on structural integrity of PMR-15/Gr composite laminates. In: Proceedings of the machining composite materials symposium, ASM Materials Week, Chicago, IL, USA, 1–5 November, pp 113–126
- Mohamed AH (2014) Waterjet trimming and drilling of CFRP components for advanced aircraft. Flow International Corporation, SME Technical Paper, Kent, WA
- Nirmal U, Hashim J, Ahmed MMHM (2015) A review on the tribological performance of natural fibre polymeric composites. *Tribol Int* 83:77–104

- Park KY, Choi JH, Lee DG (1995) Delamination-free and high efficiency drilling of carbon fibre reinforced plastics. *J Compos Mater* 29(15):1988–2002
- Phadnis VA, Makhдум F, Roy A, Silberschmidt VV (2012a) Experimental and numerical investigations in conventional and ultrasonically assisted drilling of CFRP laminate. *Procedia CIRP* 1:455–459
- Phadnis VA, Makhдум F, Roy A, Silberschmidt VV (2012b) Ultrasonically-assisted drilling in CFRP composites. In: *ECCM15—15th European conference on composite materials*, pp 24–28
- Pickering K (ed) (2008) *Properties and performance of natural fibre composites*. CRC Press LLC, Boca Raton
- Puglia D, Biagiotti J, Kenny JM (2004) Application of natural reinforcements in composite materials, Part II: Application of natural reinforcements in composite materials for automotive industry. *J Nat Fib* 1(3):23–65
- Pujana J, Rivero A, Celaya A, López de Lacalle LN (2009) Analysis of ultrasonic-assisted drilling of Ti6Al4V. *Int J Mach Tools Manuf* 49:500–508
- Ramkumara J, Malhotra SK, Krishnamurthy R (2004) Effect of work piece vibration on drilling of GFRP laminates. *J Mater Proc Technol* 152:329–332
- Ramulu M, Arola D (1993) Water jet and abrasive water jet cutting of unidirectional granite/epoxy composite. *Composites* 24:299–308
- Rawat S, Attia H (2009) Wear mechanisms and tool life management of WC–Co drills during dry high speed drilling of woven carbon fibre composites. *Wear* 267(5–8):1022–1030
- Rubio JC, Abrao AM, Faria PE, Correia AE, Davim JP (2008) Effects of high speed in the drilling of glass fibre reinforced plastic: evaluation of the delamination factor. *Int J Mach Tools Manuf* 48:715–720
- Sakthivel M, Vijayakumar S, Channankaiah RM (2015) A review on delamination in conventional and vibrated assisted drilling in glass fibre reinforced polymer composites. *Int J ChemTech Res* 7(6):2794–2801
- Sankar BR, Umamaheswarrao P, Reddy AVA, Kumar PK (2014) Drilling of composite laminates: a review. *J Basic Appl Eng Res* 1(3):19–24
- Sapuan SM, Kho JY, Zainudin ES, Leman Z, Ali BAA, Hambali A (2011) Material selection for natural fiber reinforced polymer composites using analytical hierarchy process. *Ind J Eng Mater Sci* 18(4):255–267
- Scarponi C, Sarasini F, Tirillo J, Lampani L, Valente T, Gaudenzi P (2015) Low-velocity impact response of hemp fibre reinforced bio-based epoxy laminates. In: *Proceedings of 5th conference on natural fibre composites for industrial applications*, Sapienza Università de Roma, Rome, Italy, 15–16 October, pp 1–4
- Shah DU (2013) Developing plant fibre composites for structural applications by optimising composite parameters: a critical review. *J Mater Sci* 48:6083–6107
- Shaikh AA, Jain PS (2012) Experimental study of various technologies for cutting polymer matrix composites. *Int J Adv Eng Technol* 2(1):81–88
- Singh MK (2008) *Unconventional manufacturing processes*, 1st edn. New Age International, London
- Stone R, Krishnamurthy K (1996) A neural network thrust force controller to minimize delamination during drilling of graphite–epoxy laminates. *J Mach Tools Manuf.* 36(9):985–1003
- Tagliaferri V, Caprino G, Diterlizzi A (1990) Effect of drilling parameters on the finish and mechanical properties of GFRP composites. *Znt J Mach Tools Manu* 30(1):77–84
- Terzopoulou ZN, Papageorgio GZ, Papadopoulou E, Athanassiadou E, Alexopoulou E, Bikiaris DN (2015) Green composites prepared from aliphatic polyesters and bast fibers. *Indust Crops Sci* 68:60–79
- Thomas PNH, Babitsky VI (2007) Experiments and simulations on ultrasonically assisted drilling. *J Sound Vib* 3(8):3–5
- Tsao CC (2012) *Drilling processes for composites, machining technology for composite materials*. Woodhead Publishing, Cambridge

- Tungjitpornkull S, Sombatsompop N (2009) Processing technique and fibre orientation angle affecting the mechanical properties of E-glass reinforced wood/PVC composites. *J Mater Process Technol* 209(6):3079–3088
- Unde PD, Gayakwad MD, Ghadge RS (2014) Abrasive water jet machining of composite materials: a review. *Int J Innov Res in Sci Eng Technol* 3(4):6–8
- Upadhyay PC, Lyons JS (1999) On the evaluation of critical thrust for delamination-free drilling of composite laminates. *J Rein Plast Compos* 18(14):1287–1303
- Vaxevanidis NM, Gourgouletis K, Galanis NI, Manolakos DE (2006) Electrical discharge drilling of carbon fibre reinforced composite materials. *Int J Mach Machinab Mater* 10(3):187–201
- Wambua P, Ivens J, Verpoest I (2003) Natural fibres: can they replace glass in fibre reinforced plastics. *Compos Sci Technol* 63(9):1259–1264
- Wang H, Guo Q, Yang J, Liu Z, Zhao Y, Li J, Feng Z, Liu L (2013) Microstructural evolution and oxidation resistance of polyacrylonitrile-based carbon fibers doped with boron by the decomposition of B₄C. *Carbon* 56:296–308
- Wong TL, Wu SM, Croy GM (1982) An analysis of delamination in drilling composite material. In: 14th national SAMPE technology conference, Atlanta, pp 471–483
- Yan Z, Zhang J, Zhang H, Wang H (2013) Improvement of mechanical properties of noil hemp fiber reinforced polypropylene composites by resin modification and fiber treatment. *Adv Mater Sci Eng* 2013:1–7

Chapter 10

Multicomponent, Semi-interpenetrating-Polymer-Network and Interpenetrating-Polymer-Network Hydrogels: Smart Materials for Biomedical Applications

Nazire Deniz Yilmaz

Abstract Multicomponent, semi-IPN, or IPN hydrogels are interesting materials which are composed of at least two different components and are able to respond to various stimuli, that is the change in certain properties of the medium such as temperature, pH, ion concentration, and so on. Based on this unique feature, these environmentally responsive materials may find use in biomedical applications in terms of changes in the properties of the medium in the human organism which occur naturally or induced by an outside source. Environmentally responsive hydrogels respond to changes in the physical, chemical, or biological properties of the medium by exhibiting a change in their size, shape, color, solubility, and so on. They can be fabricated from natural or synthetic components by a number of production methods including physical cross-linking and chemical cross-linking techniques as well as other novel fabrication methods such as cross-linking with genetically engineered protein domains. Environmentally responsive hydrogels have found in various subfields of the biomedical research area including drug delivery, biosensors, tissue engineering, actuators, and so on. Whereas hydrogels are promising materials, there are some drawbacks which should be overcome before these materials can be used clinically. To address the major concerns, the response rates should be increased while maintaining the necessary mechanical performance. Biodegradability and biocompatibility are other development fields. Environmentally responsive hydrogels with the desired properties can be prepared by use of the right components, production methods and forming the right polymer architecture.

Keywords Hydrogels · Smart materials · Environmentally-responsive
Stimuli-responsive · Environmental-sensitive · Biomedical materials

N.D. Yilmaz (✉)

Department of Textile Engineering, Pamukkale University, Denizli, Turkey
e-mail: naziredyilmaz@gmail.com

1 Introduction

Classically, there are three states of matter on Earth: solid, liquid, and gas. If sufficient changes of temperature or pressure take place, transitions between phases may occur. To give an example, due to drop of temperature to subzero Celsius degrees, liquid water turns to solid ice (Paleos 2012).

There are some matters that cannot be classified in one of the mentioned three phases. Gelatin powder is solid. Nevertheless, when mixed with water it is not either solid or liquid or gas, but a hydrogel. Similar to solid materials, a hydrogel does not flow. But at the same time, as if a liquid, small-size molecules can diffuse through hydrogels (Paleos 2012).

Hydrogels are cross-linked 3D polymer chain networks which are insoluble in water. The cross-linking renders the hydrogel water-insoluble and imparts mechanical strength and structural integrity. A hydrogel can imbibe significant amount of water (Paleos 2012) or body fluids (Sandeep et al. 2012), the mass fraction of which may be far higher compared to that of polymer, due to hydrophilic character of the hydrogel (Paleos 2012).

An example of hydrogels is gelatin—a mixture of proteins and peptides—which is produced by partially hydrolyzing collagen protein that is obtained from different animal tissues (Khan et al. 2016). As the gelatin dissolves in hot water, the long chains of the protein polymer move freely in the aqueous solution. When the solution is cooled, this movement slows down and the chains get entangled with each other. As the extent of entanglement rises, a certain amount of water gets trapped in the polymer chain network and becomes immobile. Thus, it can be said that the hydrogels behave like a liquid in some ways and like a solid in other ways (Paleos 2012).

Some changes in the external media including minute changes in temperature, pH, pressure, ionic strength, chemical and biological agents, light, and electric and magnetic fields trigger sharp and great changes in swelling behavior, solubility, shape or pore structures of hydrogels in great degrees (Kopeček 2007; Kumar, n.d.; Peppas 2004; Paleos 2012; Ebara et al. 2014). Thus, these hydrogels are also named as smart, stimuli-responsive, or environmentally sensitive. The changes that the smart hydrogels exhibit may be observed at the macroscopic level and may be reversible as the smart hydrogel returns to its initial form when the stimulus is ceased (Kumar n.d.; Peppas 2004). These external stimuli can be classified as physical (pressure, temperature, electrical field, magnetic field, and ultrasound), chemical (pH, solvent composition, ion type, and ionic strength), and biological stimuli (glucose, enzyme, and antibody) (Lee et al. 2013).

The most common stimuli that the smart hydrogels are responsive to are: pH, temperature, and ionic strength (Paleos 2012). The mechanisms that take part in the changes the hydrogels undergo are varied. It can be the neutralization of charged groups due to change in pH or inclusion of oppositely charged polymers or change in the hydrogen bond strength resulting in the collapse of hydrogel networks upon a change in temperature (Kumar, n.d.). For most of the hydrogels, a critical point is present where the transition in property change takes place (Peppas 2004).

As biomimetic systems, smart hydrogels have been the focus of intense attraction (Lim et al. 2014). Hydrogels show similarities to some components of body tissues. They can be injected into the organism by causing minimal invasive effects and adjust their shapes to the host tissue (Smart Hydrogels for Biomedical Applications 2015). Furthermore high water content, as well as rubbery soft structure of hydrogels, also resembles soft body tissues (Sandeep et al. 2012). In fact, human body naturally utilizes hydrogels. Examples include blood clots, cartilage, and mucin (lining the bronchial tubes, stomach, and intestines) (Paleos 2012).

Exhibiting multicomponent structure, hydrogels consists of three different phases: 3D solid cross-linked polymer network, interstitial fluid, and ion species (Hua 2009). When in aqueous solutions, hydrogels can absorb water or physiological fluids as much as thousand times their dry mass while not dissolving in water (Khodamoradi and Khodamoradi 2014; Paleos 2012; Maziad et al. 2015). The hydrophilicity is due to the fact that the polymer network includes hydrophilic polymers containing water solubilizing groups like $-OH$, $-COOH$, and $-CONH$, whereas the insolubility comes from the complex 3D network structure. The hydrophilic polymers are cross-linked via chemical or physical bonds (Maziad et al. 2015).

Hydrogels can be classified into two groups, as natural and synthetic hydrogels, according to their origin (Ebara et al. 2014). Natural hydrogels have attracted intense research interest (Khodamoradi and Khodamoradi 2014) due to their low toxicity and biocompatibility. Natural hydrogels may contain proteins including gelatin and collagen, and polysaccharides like agarose and alginate. The chemical structures of natural hydrogels show similarities to glycosaminoglycan (GAG) molecules (e.g., hyaluronan, chondroitin sulfate, and heparin sulfate). GAG is naturally found in the extracellular matrix (ECM) (Ebara et al. 2014).

Synthetic hydrogels are conventionally produced via chemical polymerization methods (El-Sherbiny and Yacoub 2013; Thakur et al 2016). Novel hydrogel production methods include genetic engineering and biosynthetic techniques to obtain hydrogels with special characteristics (Ebara et al. 2014).

The hydrogel, in the current sense, for biomedical application was initially developed by Wichterle and Lim (Wichterle and Lim 1960; Lee et al. 2013). They proposed using poly (2-hydroxyethyl methacrylate) (PHEMA) hydrophilic networks in contact lenses (Sandeep et al. 2012; Lee et al. 2013). Since then, the hydrogel technology advanced greatly as a class of biomaterials in the biomedical field (Khodamoradi and Khodamoradi 2014).

Their structures including lower interfacial tension, native tissue-like characteristics, permeability to small molecules, and controlled release of entrapped molecules have rendered smart hydrogels a focus of interest for various biomedical applications including sustained drug delivery (Jafari et al. 2011; Tanigo et al. 2010), tissue engineering (Langer and Vacanti 1993; El-Sherbiny and Yacoub 2013), biosensors (Miyata et al. 2002; Moschou et al. 2008), actuators (Asoh et al. 2008; Maeda et al. 2007) and so on. Among these various fields of the biomedical research area, the use of hydrogels is particularly explored in drug delivery systems

as hydrogels protect the drug from hostile environments and release them in a controlled manner based on their response to external stimuli (Ebara et al. 2014).

Research on smart hydrogel also attracts support from international bodies. For examples, European Commission supports research on hydrogels via Horizon 2020 Marie Skłodowska-Curie actions, under the training network BIOGEL for a period of four years with a total budget of 3.5 Million Euros. BIOGEL network includes 13 research institutes and enterprises from Europe, Japan, and the United States (Smart Hydrogels for Biomedical Applications 2015).

This work has been written in order to investigate smart hydrogels in terms of their use in the biomedical area. This chapter provides an overview of different classes of smart hydrogels, their structures, and production methods. The response mechanisms are described, performance characteristics and characterization methods are explained, and application areas are investigated. The chapter ends with a discussion on some future development areas of hydrogels for their use in the biomedical area.

2 Classification of Environmental-Responsive Hydrogels

Hydrogels can be classified in terms of various parameters such as the synthesis route, hydrogel structure and cross-link types which are in turn reflected in the performance characteristics. Different classifications are found in the literature (Khodamoradi and Khodamoradi 2014; El-Sherbiny and Yacoub 2013; Peppas 2004; Sandeep et al. 2012). First, in terms of synthesis route, the hydrogels can be classified as (Khodamoradi and Khodamoradi 2014; Peppas 2004):

- Homopolymer hydrogels (cross-linked structures including only one type of hydrophilic monomer)
- Copolymer hydrogels (cross-linked structures of two types of monomers, at least one of which is hydrophilic)
- Multipolymer hydrogels (composed of three or more types of monomers)
- Interpenetrating polymeric (IPN) hydrogels (manufactured first by forming a polymer network which is then allowed to swell in a monomer. The second monomer reacts to produce a second interpenetrating network structure (Khodamoradi and Khodamoradi 2014; Peppas 2004), where no covalent bonds form between the two polymeric networks (Paleos 2012).

Hydrogels can also be classified based on their ionic charges as (Khodamoradi and Khodamoradi 2014):

- Anionic hydrogels (negative charge) including carrageenan (Paleos 2012), anionic thermo-associative carboxymethyl and pullulan hydrogels (Khodamoradi and Khodamoradi 2014).

- Cationic hydrogels (positive charge) including chitosan (Paleos 2012) (novel thermosensitive cationic *N*-isopropylacrylamide (NIPAM) and (3-acrylamidopropyl) trimethylammonium chloride hydrogels (Khodamoradi and Khodamoradi 2014).
- Neutral hydrogels (miscible blends of polymers that are insoluble in water such as poly (2,4,4-trimethylhexamethylene terephthalamide) (Khodamoradi and Khodamoradi 2014).
- Ampholytic hydrogels (can behave like charged either positively or negatively (Paleos 2012) like collagen, ampholytic hydrogels based on acrylamide).

Thirdly, hydrogels can be classified in terms of their physical fine structures as (Khodamoradi and Khodamoradi 2014; Peppas 2004):

- Amorphous hydrogels (composed of randomly arranged macromolecular chains).
- Semi crystalline hydrogels (including dense regions composed of macromolecular chains of a high order).
- H-bonded or complexation structures (the 3-D network).
- Super molecular structures.
- Hydrocolloidal aggregates (Sandeep et al. 2012).

Another classification may be made based on the physical forms of the hydrogels:

- Solid molded form (soft contact lenses)
- Pressed powder matrix (capsules or pills for oral administration)
- Microparticle (bioadhesive carriers)
- Coating (on implants or oral administration drugs)
- Membrane (electrophoresis gels),
- Encapsulated solid (osmotic pumps)
- Liquid (shows gelling when the temperature is increased or decreased) (Hoffman 2002; Ebara et al. 2014).

The hydrogels can also be classified according to their origin as:

- Natural hydrogels
- Synthetic hydrogels (Paleos 2012).

2.1 *Natural Hydrogels*

Hydrogels of natural origin have certain advantages including biocompatibility, biodegradability and supporting of cellular activities (Paleos 2012). Furthermore, natural materials may receive approval to be used in clinical studies easier compared to their synthetic counterparts. Nevertheless, they also entail some drawbacks such as contamination with biological pathogens, the risk of evoking an immune response. Two other drawbacks can be given as moderate mechanical strength and

high variability (Paleos 2012) which is common in materials of natural origin in comparison to synthetic ones (Yilmaz 2009).

Some examples of hydrogels of natural origin can consist of proteins like gelatin and collagen; and polysaccharides such as chitosan, dextran, alginate (Paleos 2012), pectin (Maziad et al. 2015), psyllium (Thakur and Thakur 2014a, b) and hyaluronan (Sandeep et al. 2012); and also from lignin (Thakur and Thakur 2015). Hydrogels of natural origin may include pectin which is a natural biopolymer presenting a biodegradable and biocompatible nature (Maziad et al. 2015). Pectin is a polysaccharide of plant origin presenting a linear molecular chain configuration. It is hydrophilic and soluble in water. Pectin possesses the gelling ability and depending on its degree of esterification (DE), the gelling behavior depends on medium pH or presence of Ca^{2+} or other divalent cations (Yilmaz et al. 2015). Cross-linked polymers of pectin can form hydrogels which can imbibe and hold water that is hundreds of times of their dry weight and known as superabsorbents. Pectin has been increasingly used in pharmaceutical applications. It is also used as a carrier for drug entrapment and targeted drug delivery. Pectin is degraded by the activity of colonic microorganisms; hence, it stands as a promising carrier to be utilized in colon-targeted drug delivery systems (Maziad et al. 2015).

Pullulan is another polysaccharide used in hydrogel preparation. Hydrogel nanoparticles were obtained via self-aggregation of pullulan in water (Gupta and Gupta 2004; Na and Bae 2004; Morimoto et al. 2013). Cholesterol-bearing pullulan is a natural homopolysaccharide of glucose obtained from different fungus species. It is soluble in aqua and forms viscous solutions (Yilmaz et al. 2015). Pullulan-based pH-responsive nanogels were developed for use as protein carriers (Morimoto et al. 2013) for detection of tumor extracellular pH (Na and Bae 2004). Hydrogels prepared from Chitosan were also proposed (Naderi-Meshkin et al. 2014). Chitosan is a polysaccharide that is obtained via alkalization of chitin (Thakur and Voicu 2016; Thakur and Thakur 2014a, b). It is soluble in water in contrast to chitin and is the mere natural polymer that possesses a positive charge. It is strongly polycationic and dissolves in acidic media. Hydrogels of Chitosan is generally prepared by using glutaraldehyde as a cross-linker (Yilmaz et al. 2015). Chitosan solutions incorporating glycerol-2-phosphate (β -GP) that presents a pH-dependent sol-gel transition at body temperature have been proposed (Chenite et al. 2000; Molinaro et al. 2002). Various studies related to use of hydrogels based on chitosan and other polymers in injectable applications of controlled drug release and tissue engineering have taken place (Naderi-Meshkin et al. 2014; Tan et al. 2009; Ta et al. 2008; Kim and Park 2012; Yanga et al. 2014; Jin et al. 2009).

Hydrogels incorporating functional proteins are also promising for biomedical applications. Hydrogels based on polypeptides include block copolypeptides, recombinant natural protein [such as elastin (Kim 2013) and silk (Khan et al. 2016; Nagarkar et al. 2010)] segments, tandemly repeated blocks of silk-like and elastin-like peptides (Megeed et al. 2002), as well as coiled-coil block flanked random polypeptide sequenced recombinant triblock copolymers (Xu et al. 2005; Kopeček 2007; Banta et al. 2010).

An example of the protein-incorporating hydrogel is calmodulin-phenothiazine hydrogels where calmodulin (CaM) protein is the biological element in response to stimuli (Ehrick et al. 2005). Modified calmodulin and polymerizable phenothiazine were entrapped inside the hydrogel polymer network. When Ca^{2+} was present in the environment, the immobilized derivative of phenothiazine was bound to CaM via physical bonds within the network structure of the hydrogel. When Ca^{2+} was removed from the environment, the immobilized derivative of phenothiazine was released from the site that bound CaM, and CaM, in turn, undergoes a transition from a constrictive configuration to its natural configuration, resulting in the swelling of the hydrogel. This hydrogel was claimed to be promising for use as a valve in a microfluidic device (Ehrick et al. 2005; Banta et al. 2010).

Another example of hydrogels that includes a protein is a resilin-dityrosine hydrogel. This hydrogel was reported to present resiliency comparable to unfilled polybutadiene to exhibit negligible hysteresis when compressed (Kopeček 2007; Elvin et al. 2005).

2.2 Synthetic Hydrogels

Synthetic hydrogels can be produced from various monomers like vinyl acetate, ethylene glycol, acrylamide, lactic acid (Paleos 2012), vinyl pyrrolidone, acrylic acid, and methacrylate (Sandeep et al. 2012) where methacrylate derivatives play a very significant role (Kopeček 2007). Most synthetic hydrogels are prepared via or vinyl-activated monomer polymerization. It should be noted that not all synthetic polymers are derived from petroleum-based monomers; to give an example, lactic acid can be obtained from plants such as corn and sugarcane (Paleos 2012) and can form a biologically degradable polymer, poly(lactic acid) (Yilmaz and Powell 2015). Polymer synthesis can be closely controlled and fine-tuned to obtain desired features. The risks related to the presence of biological pathogen presence and immune response evoking are also low. The entailed drawbacks are low biodegradability and bioactivity as well as the probability of toxicity (Paleos 2012). Table 1 presents a list of monomers used in the production of synthetic hydrogels.

An important member of synthetic hydrogels is polyacrylic acid (PAAc)-based hydrogels. They are formed by polymers of cross-linked PAAc or combined with other comonomers. The water amount that is entrapped by the hydrogel should be controlled as it influences other performance characteristics such as the solute transport in the case of drug delivery systems. In relation to that, the permeation rate can be tailored by fine-tuning the density of cross-linking or by incorporation of a comonomer with lower hydrophilicity. Due to the presence of $-\text{COOH}$ groups, PAAc hydrogels can imbibe large amounts of water. Again, owing to these carboxylic acid groups, the swelling behavior is greatly influenced by the medium pH (Maziad et al. 2015).

Poly(ethylene glycol) (PEG) is also used in hydrogel formation. PEG exhibits some advantages for in vivo use in biomedical applications. PEG-based hydrogels

Table 1 Monomers used in synthetic hydrogel preparation to be used in biomedical applications (Sandeep et al. 2012)

Monomer/polymer abbreviation	Monomer/polymer
HEMA	Hydroxyethyl methacrylate
HEEMA	Hydroxyethoxyethyl methacrylate
HDEEMA	Hydroxydiethoxyethyl methacrylate
MEMA	Methoxyethyl methacrylate
MEEMA	Methoxyethoxyethyl methacrylate
MDEEMA	Methoxydiethoxyethyl methacrylate
EGDMA	Ethylene glycol dimethacrylate
NVP	<i>N</i> -vinyl-2-pyrrolidone
NIPAAm	<i>N</i> -isopropyl acrylamide
VAc	Vinyl acetate
AA	Acrylic acid
HPMA	<i>N</i> -(2-hydroxypropyl) methacrylamide
EG	Ethylene glycol
PEG	Poly(ethylene glycol)
PEGA	PEG acrylate
PEGMA	PEG methacrylate
PEGDA	PEG diacrylate
PEGDMA	PEG dimethacrylate
MAA	Methacrylic acid

With permission from Sandeep et al. (2012); Copyright 2012 IJRPC Pending

induce lower inflammatory response compared to other polymers such as PLGA. Besides, when used in protein delivery such as recombinant human growth hormone (rhGH), use of PEG enhances protein stability and decreases immunogenicity due to steric effects. Thus, hydrogels based on PEG are promising as carriers in protein release applications (Tae et al. 2005).

2.3 Hybrid Hydrogels

Hybrid hydrogels consist of components from synthetic polymers and biological macromolecules that form cross-linked structures due to chemical or physical bonding forces. Merging peptide/protein modules and synthetic polymers may result in new materials exhibiting performance characteristics surpassing those each constituent (Kopeček 2007).

In the literature, peptide/protein modules have been incorporated into hydrogel structures to impart biodegradability, temperature-responsive phase transition, and bioagent sensitivity. Hydrogel structures have been developed by cross-linking synthetic polymers, that are soluble in water, with molecules of biological origin

including oligodeoxyribonucleotides, oligopeptides, stereospecific D,L-lactic acid oligomers, intact native proteins; or via antigen-antibody binding (Kopeček 2007).

Hybrid hydrogels do not always contain protein/peptide domain as the bio-based portion, but it may contain other biological polymers like polysaccharides. An example to this is chitosan-based hydrogels. In such an example, a triblock copolymer structure of chitosan-beta glycerophosphate-hydroxyethyl cellulose was developed presenting a sol-gel transition temperature of 37 °C. This structure was planned to be used in injectable cartilage tissue engineering encapsulating mesenchymal stem cells or chondrogenic factors (Naderi-Meshkin et al. 2014).

3 Preparation of Hydrogels

Hydrogels can be classified according to their starting point in the course of production. They can be listed as:

1. Cross-linking copolymerization
2. Cross-linking of reactive polymer precursors (El-Sherbiny and Yacoub 2013)
3. Cross-linking via polymer-polymer reaction (Kopeček 2007).

In the first option, a polymer network may be formed from hydrophilic monomers by use of cross-linkers. Networks produced with polyethylene glycol (PEG) and polypropylene oxide (PPO) monomers may be given as examples. In the second route, a polymer network may be produced from oligomers which are polymers of low molecular weight and are able to polymerize further. Polyurethane networks can be produced by using oligomers. In the third class, networks may be produced by starting with polymers where the network structure is formed by cross-linking of hydrophilic polymer chains. An example can be given as is chitosan cross-linked with glutaraldehyde that finds use in tissue engineering (Paleos 2012).

Several preparation methods used for hydrogel formation can be listed as physical, chemical and radiation cross-linking and grafting polymerization as follows (Sandeep et al. 2012).

3.1 *Hydrogels Produced via Physical Cross-Linking Methods*

Production of hydrogels via physical cross-linking presents some advantages such as ease of manufacturing and avoiding the use of cross-linkers. These cross-linking agents which are necessary for chemical cross-linking may interfere with the integrity of substances to be entrapped in the hydrogel, such as cells or proteins, therefore, it may be necessary to remove them before intended use. Through a

selection of various types of hydrocolloids, concentration and pH of preparation, a wide range of hydrogel textures can be attained via physical cross-linking techniques. This area is the focus of intense interest, especially in the food industry. Various methods of physical cross-linking as given in the literature are as follows (Sandeep et al. 2012):

1. Heating/cooling a polymer solution
2. Ionic interaction
3. Complex coacervation
4. H-bonding
5. Maturation (heat induced aggregation)
6. Freeze-thawing

1. Heating/cooling a polymer solution

When hot solutions of carrageenan or gelatine are cooled down, gels which are physically cross-linked are formed. Various mechanisms may be in effect during gel formation such as the formation of helix configuration, association of the helices, and junction zone formation. In aqueous solutions, carrageenan is found in random coil conformation above the melting transition temperature. When cooled, the structure transforms to rigid helical rods. In the presence of salts of K^+ , Na^+ , double helices may aggregate to give stable hydrogels upon screening sulphonic group (SO^{-3}) repulsion. In other cases, the hydrogel can be produced by block copolymerization which takes place when polymer solutions are warmed. Polyethylene oxide (PEO), polypropylene oxide (PPO), polyethylene glycol (PEG), and polylactic acid (PLA) hydrogels may be given as examples (Sandeep et al. 2012).

2. Ionic interaction

By adding di- or tri-valent counter ions, ionic polymers can be cross-linked. An example of this technique is producing a hydrogel by the inclusion of a multivalent counter ion such as $Ca^{2+} + 2Cl^-$ into a polyelectrolyte solution like Na^+ alginate $^-$. Some other relevant examples may be listed as hydrogels of chitosan/dextran (Hennink and Nostrum 2002), chitosan/polylysine (Sandeep et al. 2012), and chitosan/glycerol phosphate salt (Zhao et al. 2009).

3. Complex coacervation

Complex coacervate hydrogels can be produced from polyanion and polycation mixtures. In this procedure, opposite charged polymers attract one another and hold together and form complexes which do or do not dissolve in water based on the solution concentration and pH (Sandeep et al. 2012). An example can be given as a coacervate polycationic chitosan/polyanionic xanthan hydrogel (Esteban and Severian 2000). Below their isoelectric points, proteins bear positive charges and tend to interact with anionic hydrocolloids and in turn produce polyion complex coacervate hydrogels (Magnin et al. 2004; Sandeep et al. 2012).

4. H-bonding

Hydrogen bonding is also used in hydrogel preparation. Hydrogen bonds are formed between polymer chains via interaction of hydrogen that is electron deficient and a highly electronegative functional group (El-Sherbiny and Yacoub 2013). H-bonded hydrogels can be produced by decreasing pH level of aqueous solutions of polymers incorporating ($-\text{COOH}$) carboxyl groups. An example can be given as a H-bonded CMC (carboxymethyl cellulose) network which was obtained by dispersing CMC in a HCl solution (Takigami et al. 2007). In course of the procedure, sodium in CMC is replaced with a hydrogen from the acid solution which in turn to promote H-bonding. Hydrogen bonding results in decreased water solubility of CMC and leads to the production of a hydrogel. Similarly, hydrogels of carboxymethylated chitosan can also be obtained via cross-linking by using acids or polyfunctional monomers. One other example is a hydrogel of polyethylene oxide and polyacrylic acid which was formed by reducing the pH of the aqueous solution (Hoffman 2002). In the case of a xanthan-alginate hydrogel, intermolecular H-bonding between xanthan and alginate leads to change in the matrix structure and a hydrogel that is insoluble in water is formed (Sandeep et al. 2012).

5. Maturation (heat induced aggregation)

Maturation can be explained as heat induced aggregation. Via this method, hydrogels from Gum Arabic can be produced. Gum arabic (also named as Gum Acacia) mainly presents a polysaccharide structure but it is also covalently bonded to a protein moiety that affects its surface activity (Yilmaz et al. 2015). Three major fractions have been detected in Gum Arabic which are arabinogalactan, arabinogalactan protein, and glycoprotein. By a thermal treatment, the proteinaceous components can be aggregated resulting in increased molecular weight and in turn, a hydrogel of good mechanical strength and water binding capability can be formed. Maturing of Gum Arabic leads to transfer of the protein corresponding to the components with a lower molecular weight which in turn results in higher concentrations of components with high molecular weight (arabinogalactan protein) (Aoki et al. 2007a, b). This procedure is also applicable to other gums like gum ghatti and Acacia kerensis for dental care applications (Al-Assaf et al. 2009; Sandeep et al. 2012).

6. Freeze-thawing (Cryogelation)

Hydrogels can also be obtained via freeze-thawing cycles where physical cross-linking of a polymer takes place. This procedure is also known as cryogelation. In the course of the method, a polymer or a monomer is added to an aqueous solution and kept in subzero temperature for cryopolymerization/gelation and crystal formation (Kumar and Srivastava 2010). The method is suitable for some polymers including PVA. An example can be given as a poly vinyl alcohol-based hydrogel produced by the freeze-thawing method for use in cell encapsulation (Vrana et al. 2009). PVA-bacterial cellulose hydrogels were also produced via

freeze-thawing method (Millon et al. 2008; Wan and Millon 2006; Millon and Wan 2006; Yilmaz 2015b).

3.2 Hydrogels Produced via Chemical Cross-Linking Methods

When monomers are grafted on the backbone of the polymers (Yilmaz 2015a; Thakur et al 2013a, b, c, d) or when cross-linking agent bonds two polymer chains, chemical cross-linking takes place (2014a, b). Polymers can be cross-linked via their reactive functional groups (hydroxyl (–OH), carboxyl (–COOH), amino groups (–NH₂),...) with cross-linking agents (like glutaraldehyde or adipic acid dihydrazide). Various techniques have been implemented to produce chemically cross-linked hydrogels in the literature (Peppas 2004; Sandeep et al. 2012). Besides other methods, interpenetrating net work (IPN) formation and hydrophobic interactions (Hennink and Nostrum 2002; El-Sherbiny and Yacoub 2013) have been investigated. In the former, a monomer is polymerized within another polymer to form an intermeshed network structure or an IPN, and in the case of the latter (Hennink and Nostrum 2002) a polar hydrophilic group is incorporated via oxidation or hydrolysis succeeded by cross-linking via covalent linkages have also been applied to prepare chemically cross-linked hydrogels (Sandeep et al. 2012). In the following sections, major hydrogel chemical cross-linking methods are introduced.

1. Chemical cross-linking

Cross-linking agents including glutaraldehyde, 2-acrylamido-2-methylpropanesulfonic acid, and epichlorohydrin have found wide use for obtaining various cross-linked networks of hydrogels from both natural and synthetic polymers. The method includes the addition of separate molecules between the polymeric chains in order to form cross-links. An example can be given as the corn starch—polyvinyl alcohol hydrogel where the cross-linking is achieved through the use of glutaraldehyde as a cross-linking agent. Hydrogels of CMC can be prepared by using 1,3-diaminopropane to form cross-links between CMC chains. In another example, xanthan-polyvinyl alcohol hydrogels were formed by using epichlorohydrin as a cross-linking agent. A hydrogel of κ -carrageenan-acrylic acid can be produced by incorporating the cross-linking agent: 2-acrylamido-2-methylpropanesulfonic acid (Pourjavadi and Zohuriaan-Mehr 2002). Hydrogels can also be prepared by using cellulose in aqueous solutions of NaOH/urea and the cross-linking agent, epichlorohydrin, and implementing freeze-thawing methods (Sandeep et al. 2012; Chang et al. 2010; Chang and Zhang 2011).

2. Grafting

In grafting a monomer is polymerized on the backbone of a polymer (Sandeep et al. 2012). Ionic, radical, and chemical initiators can be used to induce grafting (Yilmaz 2015a). Functional monomers that grow on activated macroradicals causes branch forming and then results in cross-linking (Sandeep et al. 2012). In another κ -carrageenan example, highly swellable hydrogels were produced using free-radical polymerization method in grafting cross-linked polyacrylic acid-*co*-poly-2-acrylamido-2-methylpropanesulfonic acid chains onto κ -carrageenan (Pourjavadi et al. 2007).

2.1 Chemical grafting

Chemical grafting involves the use of a chemical reagent to activate a macromolecular backbone to initiate grafting. In such an example a starch-*g*-poly(acrylic acid-*co*-2-hydroxy ethyl methacrylate) was prepared as a pH-responsive hydrogel, where ammonium persulfate was utilized as a thermally dissociating initiator. Ammonium persulfate produces sulfate anion radical when heated, which then abstracts hydrogen from hydroxyl groups of the starch in order to produce the corresponding radical. Then, these macroradicals initiate grafting of the monomer onto starch, resulting in a graft copolymer. Additionally, via use of a cross-linker, methylenebisacrylamide, cross-linking reaction was carried out forming a 3-D network (Sadeghi 2011).

2.2 Radiation grafting

High energy radiation like electron or gamma beams can also be utilized in grafting initiation (Sandeep et al. 2012; Peppas 2004; El-Sherbiny and Yacoub 2013). The advantage of this method is that hydrogel preparation can be conducted in aqueous solutions under mild conditions without needing a cross-linker. On the other hand, the bioactive material must be loaded after the hydrogel preparation has finished preventing the negative effects of irradiation on the agent. Besides, for some hydrogels including PEG and PVA-based gels, nonbiodegradable C–C bonds may take place in cross-links (Ebara et al. 2014). Furthermore, this method is not suitable for hydrogels from polymers that may degrade upon exposure to ionizing irradiation (El-Sherbiny and Yacoub 2013).

Radiation technique has been successfully applied in manufacturing hydrogels from acrylic acid and PEG-CMC chitosan that are responsive to medium pH (El-Sherbiny and Yacoub 2013). In a study, Said et al. (2004) produced CMC-acrylic acid hydrogel via grafting acrylic acid on CMC in an aqueous solution by using electron beam irradiation. The electron beam initiated free-radical polymerization of acrylic acid on CMC chain. Irradiation of CMC and acrylic acid caused the formation of free radicals that can bind together to form a hydrogel.

In another study, Poly(acrylic acid) and Poly(acrylic acid)/pectin hydrogels were produced via radiation-induced copolymerization of AAC in aqueous solutions at different concentrations. The solutions were exposed to N₂ exposure in order for O₂ removal and then irradiated at different doses of gamma rays from a source at 60 °

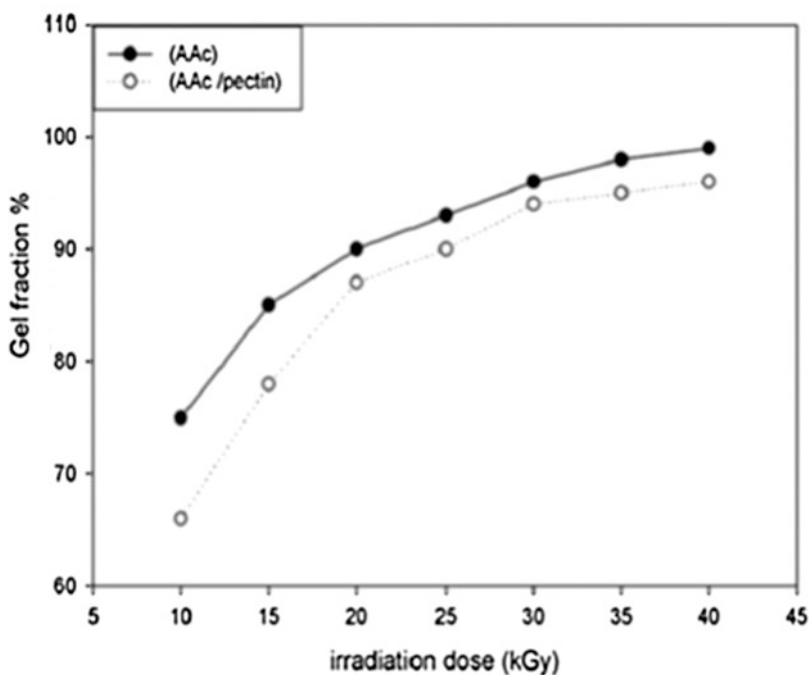


Fig. 1 The effect of irradiation dose (kGy) on gelation fraction of poly(acrylic acid) and poly(acrylic acid)-pectin hydrogels. With permission from Maziad et al. (2015); Copyright 2015 Asian Journal of Pharmaceutical and Clinical Research Pending

C. The hydrogel then was rinsed with excess distilled water in order to remove unreacted monomer and then it was allowed to dry under vacuum until a constant mass was attained. Figure 1 depicts the effect of irradiation dose on the gelation rate. The concentration of the acrylic acid solution was 30 wt%. An increase in gel fraction is seen with increment in irradiation dose for both Poly(acrylic acid) and Poly(acrylic acid)/pectin hydrogels due to increased cross-linking of polymer networks (Maziad et al. 2015).

4 Novel Hydrogel Preparation Methods

Conventional techniques of hydrogel production are restricted in terms of precise control on the fine structure. Because of side reactions, the chain networks include unreacted pendant groups, entanglements, and cycles. Other shortcomings of the conventional hydrogels can be given as insufficient mechanical performance and slow response to environmental stimuli. Traditional synthetic pathways do not

allow precise control on chain length, moiety sequence, and 3D conformation. However, novel hydrogel manufacturing techniques allow preparation of hydrogels with lower molecular weight variations. These techniques include controlled radical polymerization, such as atom transfer radical polymerization, nitroxide-mediated polymerization, and reversible addition-fragmentation transfer. Novel catalysts like transition metal complexes and new treatment techniques such as low-temperature or under-vacuum polymerization provide control of α -amino acid *N*-carboxyanhydrides polymerization and allow well-defined synthetic polypeptide manufacturing (Kopeček 2007).

Some remarkable advancements have broadened the benefits of hydrogels. Three recent advancements including introduction of sliding cross-linking agents (Okumura and Ito 2001), double-network (DN) hydrogels (Gong et al. 2003), and nanocomposite (NC) (clay-filled) hydrogels (Haraguchi and Takehisa 2002) have substantially enhanced the mechanical performance of hydrogels and have broadened their application areas as presented in Fig. 2 (Kopeček 2007).

Sliding Cross-Linking Agents Okumura and Ito (2001) introduced sliding cross-linking agents. They chemically cross-linked two cyclodextrin molecules. Each cyclodextrin molecule was threaded on a different PEG chain, the end of which was capped with a bulky group like adamantane, forming a sliding double-ring cross-linker. The resulting hydrogel was reported to present remarkable mechanical performance—a high level of swellability in aqua and a high elongation rate before breaking. The sliding cross-links apparently acted in a way that allowed equalizing the load among polymer chains (Kopeček 2007).

Double Networks (DN) Are a class of interpenetrating networks (IPNs). They consist of two hydrophilic networks: one of which is highly cross-linked, whereas the other is loosely cross-linked. An example of DN, poly(2-acrylamido-2-methylpropanesulfonic acid) and polyacrylamide, obtained by Gong et al. (2003) from two hydrophilic networks of low mechanical performance, exhibits good mechanical characteristics. The researchers reported that those DN hydrogels with

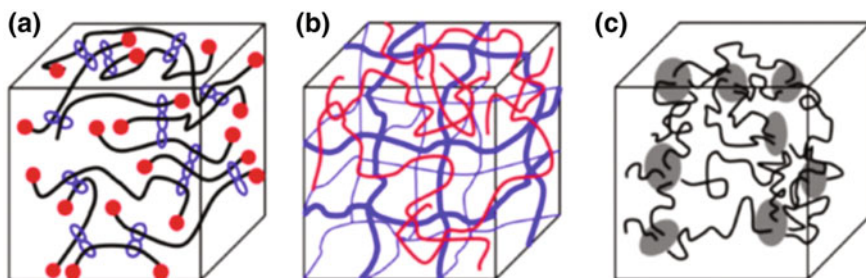


Fig. 2 a Sliding hydrogels consisting of chains of PEG threaded with α -cyclodextrin groups and cross-linked by freely moving trichlorotriazine, b DN hydrogels consisting one highly cross-linked and one loosely cross-linked hydrophilic polymer networks, c NC hydrogels composed of clay sheets grafted with polymer chains. With permission from Kopeček (2007); Copyright 2007 Elsevier

90% water content exhibited fracture strength values around 10 MPa, as well as high wear resistance. DN consisting of stiff/brittle and ductile/soft polymer networks result in stiff and ductile hydrogels, but not brittle and soft, due to efficient distribution of local stresses and absorption of fracture energy through a nonlinear binary combination of the dissimilar characteristics of the two polymer components.

Nanocomposite Hydrogels Hybrid hydrogels may incorporate organic and inorganic components at the same time. Hydrogels including clay platelets are among these hybrid materials. An example of these is an *n*-isopropylacrylamide (NIPAAm)-based hydrogel cross-linked with hectorite, $[\text{Mg}_{5.34}\text{Li}_{0.66}\text{Si}_8\text{O}_{20}(\text{OH})_4]\text{Na}_{0.66}$, developed by Haraguchi and Takehisa (2002). Here, a unique network configuration was prepared via in situ free-radical polymerization, where the chain lengths of the networks between cross-linking points presented a narrow range compared to wide distribution is observed in conventional hydrogels as shown in Fig. 3. The researchers reported structural homogeneity—as reflected in transparency levels—, nearly full recovery from the extension, good swellability, and fast deswelling induced by changes in the temperature.

Self-assembled Hydrogels may be obtained from graft and block copolymers where hydrophobic interactions are active. An example of this can be given as hydrogels of ABA triblock copolymer structure incorporating (short) hydrophobic

Fig. 3 Network structure of **a** nanocomposite (NC) gel composed of exfoliated organic clay on which flexible polymer chains are grafted **b** elongated form of the nanocomposite gel. **c** Network structure of the conventional gel. With permission from Haraguchi and Takehisa (2002); Copyright 2002 John Wiley and Sons

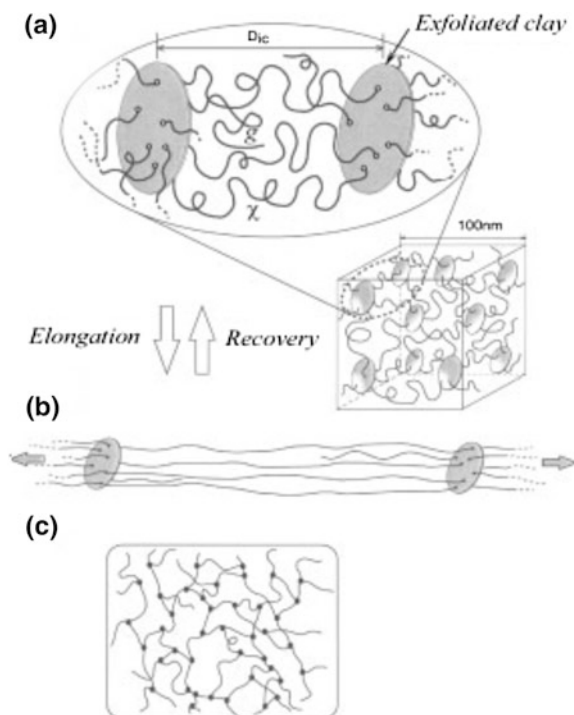
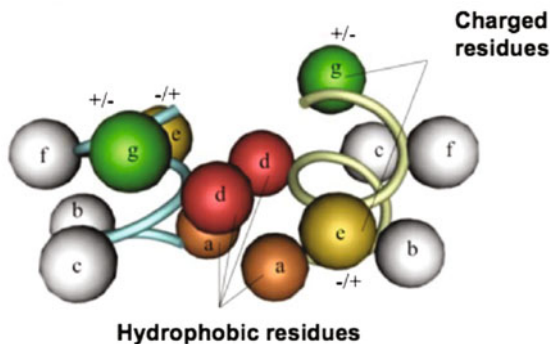


Fig. 4 A heptad repeat of a typical coiled-coil structure. With permission from Kopeček (2007); Copyright 2007 Elsevier



A blocks capping a hydrophilic B block (Kopeček 2007; Tae et al. 2005). In another class of self-assembled hydrogels, a biomimetic approach where configurations found in nature should be used, such as the coiled-coil structure. By designing copolymers in this configuration to form hydrogels, higher control of the 3D structure may be attained. As known, the coiled-coil structure is obtained from at least two α -helix strands. A standard coiled-coil consists of 7-residue repeats, called heptads, in each α -helices. The amino acid moieties can be named as a, b, c, d, e, f, and g as shown in Fig. 4. The inter-helical hydrophobic core that stabilizes the interface between the helices is obtained by hydrophobic moieties at a and d. The charged moieties at e and g enhance coiled-coil structure stability and provide interaction among helices by forming electrostatic interactions. By using this configuration, new hydrogels may be designed due to the versatility brought forward by the possibility of modifying the primary structure (Kopeček 2007; Kopeček and Yang 2009; Banta et al. 2010).

4.1 Self-assembly from Genetically Engineered Block Copolymers

Triblock copolymers in the sequence of ABA, wherein A (a coiled-coil forming peptide block) and B (a random coil), can self-assemble into hydrogels. During self-assembly, helical end oligomerization and central water-soluble polyelectrolyte swelling are counter-balanced. Minor modification of the coiled-coil structure may be strongly reflected in the resulting hydrogel properties such as response to temperature or pH. Such hydrogels disassemble upon denaturation and reassemble, once the denaturing agent, such as guanidine hydrochloride, is removed from the medium (Kopeček 2007; Xu and Kopeček 2008; Xu et al. 2005; Banta et al. 2010).

4.2 *Cross-Linking of Polymer Precursors with Genetically Engineered Protein Domains*

A novel technique of hydrogel preparation takes place by imposing a coiled-coil protein pattern onto a synthetic polymer main chain-containing hydrogels (Kopeček and Yang 2009). This can be achieved by attaching a genetically engineered coiled-coil protein motif to a hydrophilic synthetic copolymer primary chain. The self-assembly of the coiled-coil domains provided physical cross-linking. The transition of the coiled-coil domains from an elongated helix configuration to an unfolded conformation results in temperature-responsive hydrogel volume change (Kopeček 2007; Kopeček and Yang 2009).

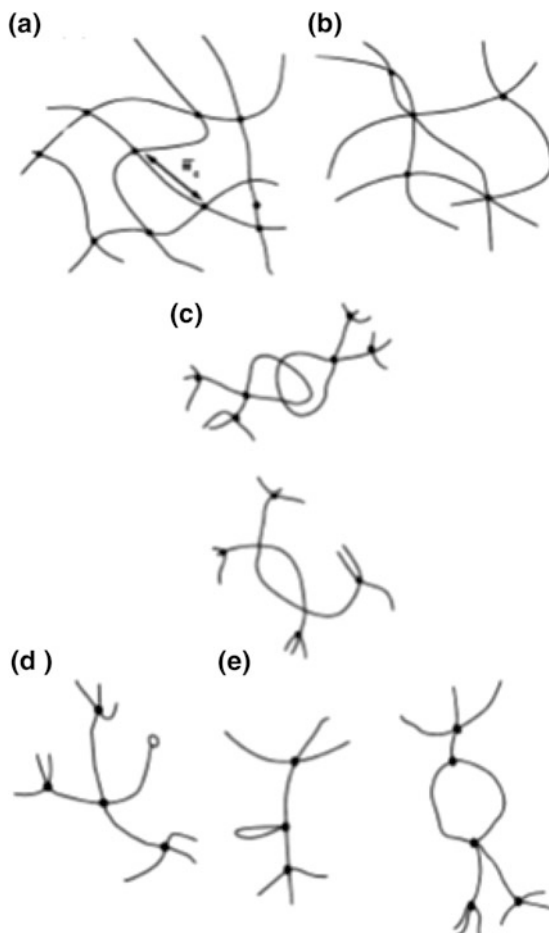
5 Structure of Hydrogels

Among the most important structural characteristics come effective molecular weight and correlation distance of the polymer between cross-linking points, as well as polymer content in the swollen state. These three parameters are interdependent and can be defined with rubber-elasticity theory and equilibrium-swelling theory based on Flory (1942) and Huggins (1942). Polymer chain structures and cross-linking characteristics determine the resultant hydrogel properties (Ebara et al. 2014).

Due to limited control on the precise configuration of hydrogels, “ideal” networks are seldom achieved. In Fig. 5a, an ideal hydrogel macromolecular network (hydrogel) which incorporates tetrafunctional covalent junctions are shown. However, multifunctional junctions (Fig. 5b) or physical entanglements (Fig. 5c) are also encountered in real networks. Hydrogels with molecular defects such as unreacted functional groups with partial entanglements (Fig. 5d) and chain loops (Fig. 5e) are also possible. These unreacted functionalities or chain loops do not contribute to the mechanical characteristics of hydrogels (Peppas 2004).

For some hydrogels, the swellability property comes from hydrophilic side groups like $-\text{OH}$, $-\text{CONH}-$, $-\text{CONH}_2-$, $-\text{SO}_3\text{H}$ (Khodamoradi and Khodamoradi 2014), and $-\text{COOH}$ groups which are attached to the polymer backbone. In case the side group of interest is a carboxyl ($-\text{COOH}$) group, upon immersion in water, the hydrogen of the carboxylic acid group may dissociate which leads to the formation of a carboxylate ion (RCOO^-) possessing a negative charge. If the medium is in favor of hydrogen dissociation, then the polymer chain becomes negatively charged throughout its backbone. These negative charges throughout the chain form a repelling force and the polymer chain uncoils. Furthermore, the negative charge also leads to increased affinity of the polymer to water. These combined effects, polymer chain uncoiling and increased affinity to water, results in hydrogel swelling (Paleos 2012).

Fig. 5 The network structure of **a** ideal hydrogel, **b** multifunctional junctions, **c** physical entanglements, **d** unreacted functional groups, and **e** chain loops in a hydrogel. Reprinted from *Biomaterials Science*, Nicholas A. Peppas, *Hydrogels*, 100–107, Copyright (2004)



Transition of RCOOH to RCOO^- is reversible. The medium is effective on the charge of the side groups, whether it is neutral or negative. Acidic media are in favor of a neutral charge and vice versa. Consequently, medium pH influences the shape/volume of a hydrogel. Besides pH, the salt concentration of the medium also affects hydrogel polymer network shape. As salt (NaCl) is poured into water, it dissociates into Na^+ and Cl^- ions. Na^+ ions associated with RCOO^- ions displacing some water molecules. Furthermore, the repelling force among negatively charged side groups become weaker and the polymer chains acquire a more coiled conformation. A minute variation in salt concentration may lead to a remarkable change in hydrogel swelling behavior (Paleos 2012).

6 Properties of Hydrogels Based on Cross-Linking Structure

As mentioned before, hydrogels can be classified based on the preparation methods in terms of the cross-linking structure such as physically and chemically cross-linked hydrogels. In chemically cross-linked hydrogels, polymer chains are bonded through covalent linkages. Thus, chemically cross-linked hydrogels present a stable structure and; provided that the covalent cross-linking points are not cleaved, they are not soluble in solvents. In terms of physically cross-linked hydrogels, physical interactions between polymer chains prevent dissolution (Ebara et al. 2014).

7 Properties of Physically Cross-Linked Hydrogels

The polymer chains in physically cross-linked hydrogels are linked through ionic bonding, hydrogen bonds, hydrophobic interactions, or molecular chain entanglements as shown in Fig. 6. In comparison to chemically cross-linked hydrogels, these connections are weaker and more reversible (Paleos 2012) and may be disrupted upon application of stress or changes occur in physical conditions (Khodamoradi and Khodamoradi 2014). In the physically cross-linked gels, the mentioned physical interactions between different polymer chains prevent dissolution (Hennink and Nostrum 2002).

Recently, physically cross-linked hydrogels have attracted remarkable interest due to their advantage that cross-linking agents are not needed during preparation. As mentioned in the section above, different techniques can be used to produce physically cross-linked hydrogels. For example, alginate which is a polysaccharide incorporating mannuronic and glucuronic acid residues can be cross-linked via Ca^{++} ions as shown in Fig. 6a at room temperature and at the physiological pH. This renders alginate appropriate for use as carriers of living cells and for protein release (Ebara et al. 2014; Yilmaz et al. 2015).

As shown in Fig. 6b hydrogels can be also cross-linked via hydrophobic interactions. An example can be given as hydrogels of amphiphilic block and graft copolymers. They can self-assemble in aqueous solutions to give ordered network structures including polymeric micelles and hydrogels where the hydrophobic portions are aggregated (Ebara et al. 2014).

Physically cross-linked hydrogels are commonly prepared from multiblock copolymers or graft copolymers. Hydrogels of graft polymers can be produced from polymer backbone that dissolves in water such as a polysaccharide, on which hydrophobic groups are adjoined. The reverse is also possible: hydrophobic chains where water-soluble groups are grafted. Two common examples of multiblock copolymer hydrogels are Pluronics[®] and Tetronics[®] (Ebara et al. 2014) which are poly(ethylene oxide) (PEO)-poly(propylene oxide) (PPO) block copolymers

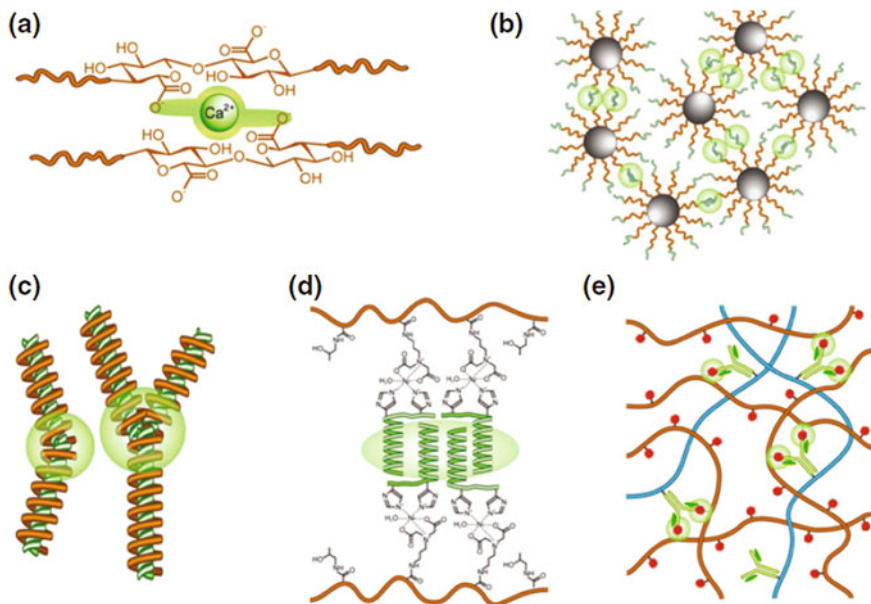


Fig. 6 Physically cross-linked hydrogel formation by **a** ionic interactions, **b** hydrophobic interactions, **c** self-assembly of stereocomplex formation, **d** coiled-coil associations, **e** specific molecular recognition. With permission from Ebara et al. (2014); Copyright 2014 Springer

(Fernandez-Tarrio et al. 2008). At low concentrations, micelles are obtained in water, whereas thermo-reversible gels are formed in the case of higher concentrations. Some variations of Plurionics[®] and Tetronics[®] have approval from FDA and EPA for use in food additives, pharmaceuticals, and agricultural products. To impart biodegradability, biodegradable poly(L-lactic acid) (PLLA) or poly(DL-lactic acid-co-glycolic acid) (PLGA) can replace the PPO segment in the PEO–PPO–PEO block copolymers (Ebara et al. 2014).

In terms of PEG–PLGA–PEG triblockpolymer, where PEG and PLGA exhibit lower and higher molecular weights, respectively, the structure is in the form of a solution at room temperature, whereas it rapidly gels when exposed to body temperature. The molecular configuration forms 3-D hyper-branched architectures like star-shaped structures. By varying the molecular weight and polymer architecture, different temperatures of phase transition can be achieved (Ebara et al. 2014; Kopeček and Yang 2009).

Among physically cross-linking mechanisms of hydrogel forming, hydrogen bonding interactions also take place. Accordingly, hydrogels of two or more natural polymers can be obtained. When polymer mixture exhibit rheological synergism, the viscoelastic properties of the polymer mixture present more gel-like behavior compared to those of individual polymers. Injectable hydrogels of various physically cross-linked polymers including gelatin–agar, starch–CMC, and hyaluronic

acid–methylcellulose can be obtained. Via hydrophobic interactions, physically cross-linked poly(acrylic acid)-PEG or poly(methacrylic acid)-PEG hydrogels may be formed through hydrogen linkages between the oxygen of the PEG and the carboxylic (–COOH) group of poly(acrylic acid)-PEG or poly(methacrylic acid) (Ebara et al. 2014; Bajpai and Shrivastava 2005).

Another method of forming physically cross-linked hydrogels is polymer crystallization. In such an example, poly(vinyl alcohol) is dissolved in water and is subjected to a freeze–thawing process, and subsequently, a hydrogel of high strength and elasticity was obtained. It was assumed that poly(vinyl alcohol) crystallites formed in the network and acted as cross-linking sites (Ebara et al. 2014; Sandeep et al. 2012).

An interesting method of physically cross-linked hydrogel formation is stereocomplex formation via self-assembly as shown in Fig. 6c. Tsuji et al. (1992) were the first to report stereocomplex formation ability of PLA. In a study, hydrogels were prepared by cross-linking via stereocomplex formation through coupling of lactic acid oligomers to dextran (de Jong et al. 2000). Formation of stereocomplexes takes place in mixtures of PLLA–PEG–PLLA and PDLA–PEG–PDLA triblock copolymers. Lim and Park (2000) studied bovine serum albumin (BSA) release behavior of microspheres based on PLLA–PEG–PLLA and PDLA–PEG–PDLA triblock copolymers. This system is advantageous due to the ease of hydrogel formation: a hydrogel can be simply manufactured by dissolving the components in aqua and mixing them. On the other hand, one critical drawback is a limited number of polymer compositions suitable for this technique (Ebara et al. 2014).

The noncovalent interactions, where chemical bonding or electron pairing are not altered, dominate biological systems. Via these interactions, the assembly and function of biological systems can be dynamically regulated. This mechanism can be implemented in the preparation of physically cross-linked hydrogels. Petka et al. (1998) was the first to develop hydrogels exhibiting the “leucine zipper” motif. Terminal domains produce coiled-coil aggregates in aqueous solutions at nearly neutral pH values, which in turn induce a 3-D polymer network formation. Here, the polyelectrolyte module retains solvent and do not allow the chain to precipitate. Upon an increase in pH or temperature, the coiled-coil aggregates dissociate which cause the transition of the gel form to solution phase (Banta et al. 2010; Petka et al. 1998). In a more recent study, Huang et al. (2014) prepared 3-D self-assembling leucine zipper hydrogel with adjustable pore size by altering peptide concentration for use in tissue engineering.

In another way of mimicking noncovalent biological interactions, proteins can be designed to self-assemble into a fibrous structure. By combining the knowledge on interactions among proteins and the ability of new protein synthesis, various physically cross-linked hydrogels can be produced (Ebara et al. 2014). In a study (Ogihara et al. 2001), heterodimeric proteins were designed to self-assemble into protein filaments with diameters lower than 100 nm. In another work, Wang et al. (1999). developed hydrogels by using natural as well as engineered proteins presenting coiled-coil associations and utilizing cross-linkers for poly(*N*-(2-hydroxypropyl)methacrylamide) (PHPMA) (Fig. 6d). the proteins were linked to

the polymer backbone through one end by metal complexes between histidine tags and metal-chelating ligands on the polymer. The hydrogel presented collapsing behavior triggered by temperature change near the melting point of the protein. This was ascribed to transition from elongated rod-like configuration to a coiled-coil form (Ebara et al. 2014; Wang et al. 1999).

Hydrogels can also be prepared through cross-linking interactions based on antigen–antibody binding. In a related study, Miyata et al. (1999) developed a hydrogel where network cross-linking occurred through the association between the grafted antigen and the corresponding antibody as shown in Fig. 6e. By changing the antigen/antibody concentration in the solution, reversible swelling and shrinking take place. Such hydrogels can be utilized in controlled drug release applications (Ebara et al. 2014) and diagnostic applications (Gerlach and Arndt 2009).

8 Properties of Chemically Cross-Linked Hydrogels

In chemically cross-linked hydrogels, the polymer chains are adjoined via permanent covalent linkages. In a covalent bond, electron pairs are shared between atoms (Paleos 2012). Chemical bonds are stronger than physical linkages (Hennink and Nostrum 2002; Khodamoradi and Khodamoradi 2014). Chemically cross-linked hydrogels can be prepared according to various methods such as radical polymerization, pendant functional group reaction, and radiation (Ebara et al. 2014; Sandeep et al. 2012).

Although physically cross-linked hydrogels exhibit certain advantages such as avoidance of chemical cross-linkers in the preparation stage, they entail some shortcomings. Physical hydrogels lack design flexibility due to their lower mechanical strength which limits variability in chemical functionalization, network pore size, gelation duration, and degradation time. To the contrary, chemically cross-linked hydrogels exhibit relatively higher mechanical strength and longer degradation durations (Ebara et al. 2014; Sandeep et al. 2012).

Chemically cross-linked hydrogels can be prepared via radical polymerization of monomers of low molecular weight by using a cross-linking agent (Fig. 7a). A commonly applied method of NIPAAm-based hydrogel preparation is by application of a redox polymerization process in the presence of an initiator (ammonium persulfate) and a catalyst (*N,N,N',N'*-tetramethylethylenediamine). The polymerization parameters including the concentrations of the monomer and cross-linking agent affect hydrogel characteristics. The mentioned procedure allows rapid hydrogel formation even under mild conditions and a number of stimuli-responsive hydrogels have been prepared via this technique (Miyata et al. 1999). Nevertheless, the unreacted initiator and catalyst reagents plus the degradation products should be removed from the hydrogel prior to in vivo application. Furthermore, this chemical can harm protein domains if present in the preparation stage (Ebara et al. 2014; Sandeep et al. 2012).

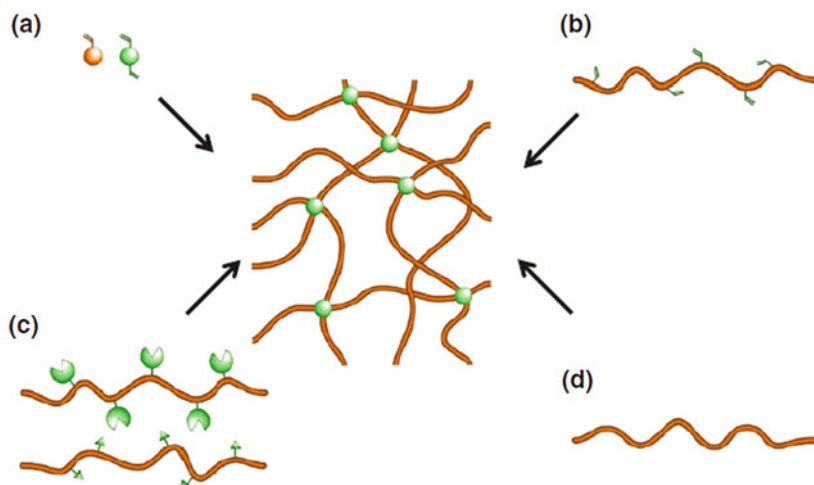


Fig. 7 Chemically cross-linked hydrogel formation by radical polymerization of **a** vinyl monomers and **b** macromonomers, **c** pendant functionality reactions, and **d** radiation (Ebara et al. 2014) With permission from Ebara et al. (2014); Copyright 2014 Springer

In another way of obtaining chemically cross-linked hydrogels, radical polymerization of polymers that are derivatized with groups capable of polymerizing (macromonomer) can be utilized as shown in Fig. 7b. By using polymers that are soluble in water such as methacrylic anhydride, methacryloyl chloride, and bromoacetyl bromide, methacrylate groups can be obtained. And after incorporation of initiator/catalyst, a hydrogel can be formed. For example, a hydrogel system was produced by introducing *N,N,N',N'*-tetramethylethylenediamine and ammonium persulfate to a *N'*-methylenebisacrylamide (MBAAm) aqueous solution containing methacryl-dextran. Apart from dextran, other water-soluble polymers including albumin, starch, hyaluronic acid and poly(vinyl alcohol) have also been derivatized with methacrylic groups to produce hydrogels (Ebara et al. 2014; Martens and Anseth 2000; Jin et al. 2001).

UV-induced polymerization method can be also used for producing chemically cross-linked hydrogels. Via this method, patterned architectures can be obtained. However, the adverse effects of UV radiation, as well as the utilized solvent and the formed radicals on the protein or drug which the hydrogel is associated with, should be carefully monitored (Ebara et al. 2014; El-Sherbiny and Yacoub 2013).

In another technique of obtaining chemically cross-linked hydrogels, polymers with functional pendant groups are used. These functional groups such as hydroxyl, carboxyl, and amine groups (e.g., OH, COOH, and NH₂) can form covalent bonds with functional groups with complementary reactivity like reactions between amine-carboxylic acid or an isocyanate-OH/NH₂, or by Schiff base reaction as shown in Fig. 7c. To give an example, hydroxyl group containing water-soluble polymers can be cross-linked by the use of glutaraldehyde (Dai and Barbari 1999).

Polymers which include amine groups can be cross-linked again with glutaraldehyde under mild conditions and Schiff base formation takes place. Via this method, a protein containing hydrogels may be produced. However, as glutaraldehyde exhibits toxic effects at low concentrations including inhibition of cell growth, alternatives have been developed (Ebara et al. 2014; Jameela and Jayakrishnan 1995). Schiff base reaction was also used in the preparation of hydrogels from starch-polyvinylamine (Li et al. 2014) and chitosan-alginate (Shi et al. 2014).

Via partial oxidation of dextran, gelatin was cross-linked with the use of polyaldehydes. Hydrogels based on hyaluronic acid were produced via derivatizing with adipic dihydrazide and cross-linking through the use of a macromolecular cross-linker. These hydrogels exhibited degradation in the presence of hyaluronidase and thus can be used in sustained drug release at wound sites (Ebara et al. 2014; Luo et al. 2000).

Hydrogels can be obtained from polymers that are soluble in water also by addition reactions. By changing the concentration of the polymers as well as the cross-linker, the resulting hydrogel characteristics can be fine-tuned. However, organic solvents rather than water are preferred as the cross-linker may react with water. Thus, the solvent and the unreacted cross-linking agent should be completely removed from the hydrogel to prevent toxic effects (Ebara et al. 2014; Hovgaard and Brondsted 1995).

The condensation reactions that occur between hydroxyl/amine groups with carboxylic acids and carboxylic acid derivatives can also be used in hydrogel preparation. The condensation reactions are generally utilized in polyester and polyamide production. *N,N*-(3-dimethylaminopropyl)-*N*-ethyl carbodiimide is used efficiently in cross-linking water-soluble polymers with amide bonds. Kuijpers et al. (2000) produced gelatin-based hydrogels by using the mentioned reagent. In another study, alginate and PEG-diamines were cross-linked using *N,N*-(3-dimethylaminopropyl)-*N*-ethyl carbodiimide and chemically cross-linked hydrogels of alginate were produced which exhibit better mechanical strength compared to alginate hydrogels prepared with ionic cross-linkages (Eiselt et al. 1999). Methods of producing polysaccharide-based hydrogels via various condensation reactions have been described in the literature de Nooy et al. (2000).

9 Classification of Environmental-Responsive Hydrogels on the Basis of Stimuli

Smart hydrogels can also be classified based on the nature of the stimuli that induce response. The stimuli can either be physical- or chemical. Physical stimuli can be temperature, electric or magnetic fields, and mechanical stress. The physical stimuli affect levels of different energy sources and modify molecular interactions. Chemical stimuli including pH, ionic factors, and chemical agents affect the molecular interactions at polymer–polymer or polymer–solvent level. A third class

of biochemical stimuli relates to biochemical agents such as antigens, enzymes, ligands. On the other hand, some hydrogel systems may respond to more than one type of stimulus (Ebara et al. 2014; Qiu and Park 2012).

9.1 Physical Stimuli

9.1.1 Temperature Responsive

A class of environmental-responsive hydrogels exhibits swelling/shrinking behavior induced by a change in the temperature. Temperature-responsive hydrogels generally present a lower critical solution temperature (LCST). In other words, such hydrogels present higher solubility/compatibility with water and undergo substantial swelling below this specific temperature, whereas it exhibits a hydrophobic characteristic and shrinking in water above LCST (Peppas 2004). This phenomenon is in contrary to most polymers which exhibit higher solubility with increasing temperature and is referred to as inverse (or negative) temperature-dependence (Qiu and Park 2012).

Temperature-responsive hydrogels are among the most widely investigated environmentally responsive polymer structures (Qiu and Park 2001). Chemical structures of some temperature-responsive polymers are depicted in Fig. 8. Temperature-responsive polymers generally contain hydrophobic sites including methyl, ethyl and propyl groups. Among different temperature-responsive polymers, poly(*N*-isopropylacrylamide) (PNIPAAm) is one of the most commonly studied one. Besides PNIPAAm, Poly(*N,N*-diethylacrylamide) (PDEAAm) is also widely studied due to its LCST, which is in the range of 25–32 °C, that is close to the body temperature. In order to change LCST, different copolymers of NIPAAm including monomers such as butyl methacrylate (BMA) can be produced (Qiu and Park 2012).

Another type of temperature-responsive hydrogels is obtained from poly(ethylene oxide) (PEO) and poly(propylene oxide) (PPO) block copolymers. They also

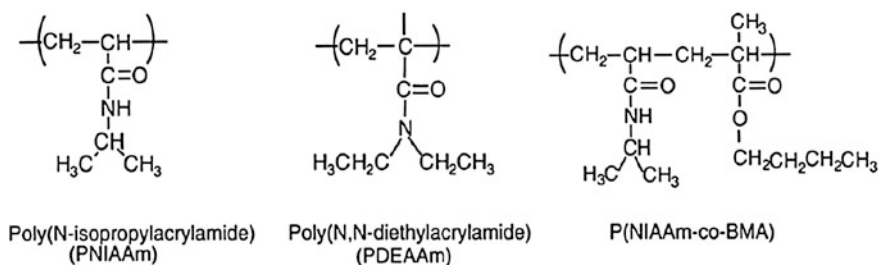


Fig. 8 Chemical structures of some temperature-responsive hydrogels. With permission from Qiu and Park (2012); Copyright 2012 Elsevier

exhibit inverse temperature sensitivity. Their LCST, which is around the body temperature, renders them suitable for biomedical applications. As mentioned before, various PEO–PPO block copolymers are available under the commercial names of Pluronics[®] (or Poloxamers[®]) and Tetronics[®] (Qiu and Park 2001).

The polymer chains of the temperature-responsive hydrogels contain moderately hydrophobic moieties (if the groups are strongly hydrophobic, the polymer chains will not show solubility in water at all) or include hydrophilic and hydrophobic parts together. At low temperatures, hydrogen bonding between hydrophilic groups in the chain and water molecules is dominant, which results in increased water solubility. Upon an increase in temperature, hydrophobic interactions among hydrophobic parts become dominant, whereas H-linkages becomes weaker. This situation leads to shrinking of the hydrogel. The LCST can be modified via changing hydrophilic/hydrophobic segment ratio. Generally, LCST decreases with the increase in the hydrophobic component. Temperature-responsive hydrogels may be obtained from copolymers of hydrophobic (such as NIPAAm) and hydrophilic (acrylic acid, etc.) monomers. If a small amount of ionizable groups are incorporated into the hydrogel network, the continuous phase transition of PNIPAAm (poly (*N*-isopropylacrylamide)) can be converted into a discontinuous transition mode; thus, a faster response behavior can be achieved (Qiu and Park 2012).

In the case the cross-links between the polymer chains are not covalent, i.e., the hydrogel is physically cross-linked, the response to change in the temperature will not be swelling/shrinking, but transition between sol–gel phases. Block copolymers of PEO and PPO show such behavior. Another method of obtaining temperature-sensitive hydrogels is via the use of temperature-sensitive cross-linking agents. Temperature-sensitive hydrogels can be classified as negatively thermosensitive, positively thermosensitive, and thermally reversible hydrogels (Qiu and Park 2001).

9.2 *Negatively Thermosensitive Hydrogels*

As mentioned before, negative thermosensitivity refers to swelling at a lower temperature and shrinking at a higher temperature. This behavior can be used in designing on–off drug release induced by a change in the temperature. In related studies, hydrogels based on P(NIPAAm–co-BMA), and IPNs of P(NIPAAm) and poly(tetramethylenether glycol) (PTMEG) were investigated. Incorporation of hydrophobic comonomer BMA into NIPAAm hydrogels resulted in improved mechanical strength. These hydrogels were studied in terms of use in drug delivery (Qiu and Park 2012).

In a study on negative thermosensitive hydrogels, Luchini et al. (2008) reported decreased particle size of NIPAm upon an increase in temperature (Fig. 9a). Whereas NIPAm/AAc (acrylic acid) particles exhibited similar temperature response, they also presented a pH-sensitivity (Fig. 9b).

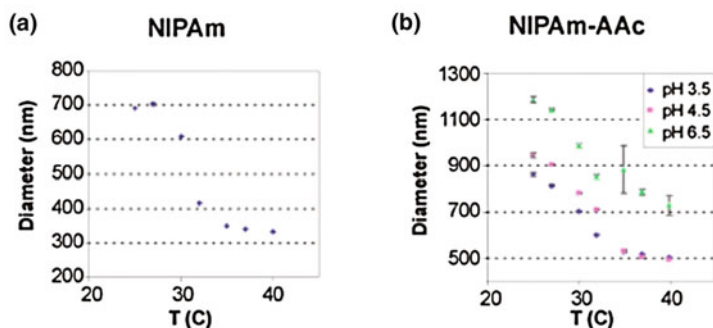


Fig. 9 Diameter of **a** NIPAm particle as a function of temperature **b** NIPAm/AAc particles as a function of temperature and pH. Reprinted permission from Luchini et al. (2008); Copyright 2008 American Chemical Society

9.3 Positively Thermosensitive Hydrogels

In contrary to negatively thermosensitive hydrogels, some hydrogels obtained from IPNs exhibit positive thermosensitivity that is swelling with increased temperature and shrinking with decreasing temperature (Qiu and Park 2001). Positively thermosensitive hydrogels possess upper critical solution temperature (UCST) in contrast to LCST of negatively thermosensitive hydrogels (Khodamoradi and Khodamoradi 2014). Hydrogels obtained from polymers with UCST show shrinking behavior below their UCST (Ebara et al. 2014). Hydrogels produced from IPNs of poly (acrylic acid) and polyacrylamide (PAAm) or poly(acrylamide-*co*-butyl methacrylate) can be given examples of such hydrogels. The temperature of transition can be increased with increment in BMA (butyl methacrylate) content (Qiu and Park 2001).

9.4 Thermo-reversible Hydrogels

Hydrogels that exhibit sol–gel transition induced by a change in temperature are referred to as thermo-reversible hydrogels. The most widely used ones of sub-hydrogels are Pluronic[®] and Tetronics[®]. The LCST can be adjusted by arranging the molecular weight and polymer network configuration. As most of the research on thermo-responsive hydrogels such as that made of NIPAAm and its derivatives have been conducted in vitro, there is not enough knowledge that they are biocompatible, that is not toxic, carcinogenic or teratogenic. Furthermore, NIPAAm and its derivatives are not biodegradable. Thus, further studies should also deal with novel thermo-responsive hydrogels based on biocompatible and biodegradable components such as PEO–PLA block copolymers (Qiu and Park 2012).

9.4.1 Photo-Responsive

Photo-responsive hydrogels can be used in ophthalmic drug delivery systems, display units, and optical switches. Photo-responsive hydrogels are advantageous in the sense that they can be exposed to a light stimulus in specific amounts instantly at high precision, whereas the sensitivity levels of thermal- and pH-responsive hydrogels are limited by thermal and ion diffusions, respectively. This advantage renders photo-responsive hydrogels promising for engineering and biomedical applications. Photo-responsive hydrogel activity can be induced by UV or visible light. In comparison to UV light, visible light is easier to obtain, more cost-efficient, safer and easier to manipulate (Qiu and Park 2001).

Photo-responsiveness can be imparted to hydrogels by incorporating photo-reactive agents such as azobenzene, triphenylmethane, and spiropyran groups via entrapping in, cross-linked with or introducing into the polymer chains in the network systems (Ebara et al. 2014; Sumaru et al. 2006).

UV-responsive hydrogels can be prepared by incorporating leuco derivative molecule, such as bis(4-dimethylamino)phenylmethyl leucocyanide, into the polymer chain network. Triphenylmethane leuco derivatives, which are neutral in their normal state, dissociate into ion pairs under UV irradiation generating triphenylmethyl cations as depicted in Fig. 10. These hydrogels exhibit discontinuous swelling behavior when exposed to UV irradiation and present continuous shrinking when the stimulus is off. The UV light-induced discontinuous swelling occurs on the basis of increment in osmotic pressure within the hydrogel upon formation of cyanide ions triggered by UV irradiation (Priya James et al. 2014).

In a study, Sumaru et al. (2006) developed a photo-responsive hydrogel obtained from NIPAAm, a spirobenzopyran residue-containing vinyl monomer, and a cross-linker. They reported a repeatable increase in permeability to an acidic solution induced by exposure to blue light (Ebara et al. 2014). By incorporating additional functional moieties, pH-responsiveness can also be imparted to the hydrogel (Qiu and Park 2001), whereas the reverse is also possible (Ebara et al. 2014). Techawanitchai et al. imparted photo-responsiveness to a pH-responsive hydrogel through the incorporation of o-nitrobenzaldehyde (NBA) which shows

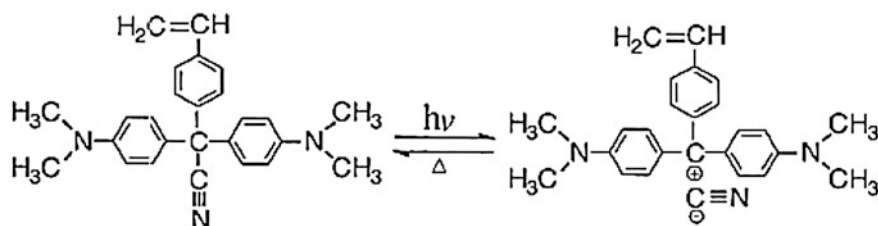


Fig. 10 Chemical structure of leuco derivative molecule bis(4-(dimethylamino)phenyl) (4-vinylphenyl)methylleucocyanide. With permission from Qiu and Park (2001); Copyright 2001 Elsevier

photo-induced proton release. When exposed to UV light, proton release took place decreasing pH inside the hydrogel below pKa level which in turn triggered volume change (Ebara et al. 2014; Techawanitchai et al. 2012a).

In an example of hydrogels that are responsive to both UV and visible light, Takashima et al. (2012) developed a photo-responsive actuator. The photo-responsive hydrogel contains α -cyclodextrin as the host and an azobenzene derivative as the photo-responsive guest. The hydrogel presented reversible macroscopical changes in shape and size upon exposure to UV at 365 nm wavelength or visible light at 430 nm wavelength. The observed changes were affected by the direction of incidence (Ebara et al. 2014; Takashima et al. 2012).

Photo-responsive hydrogels find use in photo-sensitive artificial muscles, switches, memory devices (Qiu and Park 2001), separation/recovery in bioMEMS (Micro-Electro-Mechanical Systems) systems, targeted drug delivery systems, and enzymatic bioprocessing (Ebara et al. 2014; Qiu and Park 2001; Priya James et al. 2014).

Even though the fact that the light stimulus is instantaneous, the hydrogel response can be still slow. In most of the examples, the light energy should be converted to heat energy resulting in increased response duration. Additionally, there is the risk of chromophore leaching out during swelling/shrinking cycles unless they are linked to the polymer chain network through covalent bonds (Qiu and Park 2012).

9.4.2 Electric Responsive

Among physical stimuli, electric current can also trigger a response of hydrogels. Electric-responsive hydrogels present some advantages such as control over current, electric pulse durations and intervals between pulses with high accuracy. Electro-responsive hydrogels generally include polyelectrolytes similar to pH-responsive hydrogels. Polyelectrolytes are polymers which present a high content of ionizable groups in their chains (Murdan 2003). Electro-responsive hydrogels present swelling/deswelling as well as eroding behavior induced by an electric field. Hydrogels may exhibit swelling behavior on one side and deswelling on the other side simultaneously which is observed as bending (Murdan 2003; Qiu and Park 2012). The bending behavior of hydrogels can be utilized in the manufacturing of mechanical devices including soft-actuators, switches, valves, artificial fingers/hands/muscles, and molecular machines, whereas swelling/deswelling and eroding responses is useful in drug release applications (Murdan 2003). The electro-responsive hydrogel may be in direct contact with an electrode or it may not touch the electrode but placed in an aqueous solution with or without electrolytes (Qiu and Park 2012).

Generally, polyanions are used in the preparation of electro-responsive hydrogels, but polycations and an amphoteric polyelectrolyte can also be utilized. Electro-responsive hydrogels may present natural, synthetic, as well as hybrid compositions. Examples of the natural polymers used in electro-responsive

hydrogels can be given as hyaluronic acid, chondroitin sulfate, agarose, carbomer, calcium alginate, and xanthan gum; whereas their synthetic counterparts include acrylate and methacrylate derivatives like partially hydrolyzed polyacrylamide, poly dimethylaminopropyl acrylamide. These hydrogels may be produced through irradiation, free-radical polymerization of monomers or via the use of cross-linkers as Ca^{2+} , ethylene glycol dimethacrylate ethylene diglycidylether, or *N,N'*-methylenebis acrylamide (Murdan 2003).

IPNs can also be used in electro-responsive hydrogel preparation. In an example hydrogels of sodium alginate and poly(diallyldimethylammonium chloride) were prepared via the use of the sequential IPN technique. The electrical-stimuli response of the IPN hydrogel, which is originally pH-responsive was studied. When the IPN hydrogel was positioned between a pair of electrodes in the swollen state, the IPN bent when exposed to an electric field (Kim et al. 2003).

Upon exposal to an electrical field over a threshold level, polyelectrolyte gels generally show shrinking behavior as shown in Fig. 11 via water syneresis. As the volume change is based on diffusion, the response is slow unless microparticle hydrogels are used. The shrinking may be observed visually and may occur concurrently with increment in hydrogel opacity. The hydrogel continues to shrink with the increase in the electrical field strength up to a point. As the exposal to the electrical field ceases, the hydrogel swells again. Although swelling/deswelling behavior is reversible, this response gets weaker with time and with increased cycle numbers as shown in Fig. 12 due to fatigue effect (Murdan 2003).

Low response rates, gel fatigue, and nonlinear relationship between the electrical field strength and response level are major drawbacks of electro-responsive hydrogels. The response rates can be increased via decreasing hydrogel dimensions, through the use of microspheres or by using super-porous hydrogels. As the use of electro-responsive in the biomedical area is mostly in the laboratory stage, where most of the research has been conducted in vitro, more research on live models is needed to fully understand their performance during targeted service (Murdan 2003).

Fig. 11 Shrinking of a hydrogel when exposed to electrical stimulation as a function of time. R_w : the proportion between the weight of the hydrogel after electro-stimulation and the weight of the hydrogel before electro-stimulation. With permission from Murdan (2003; Copyright 2003 Elsevier

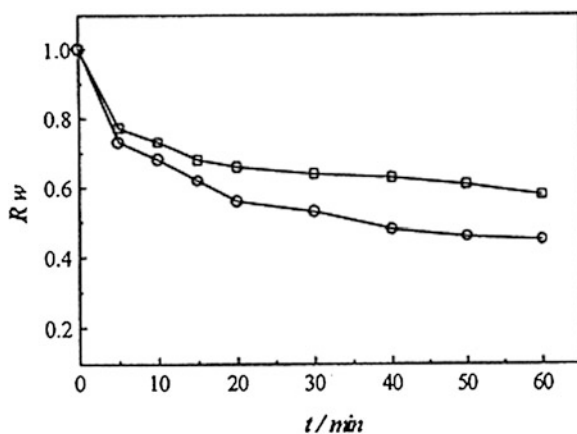
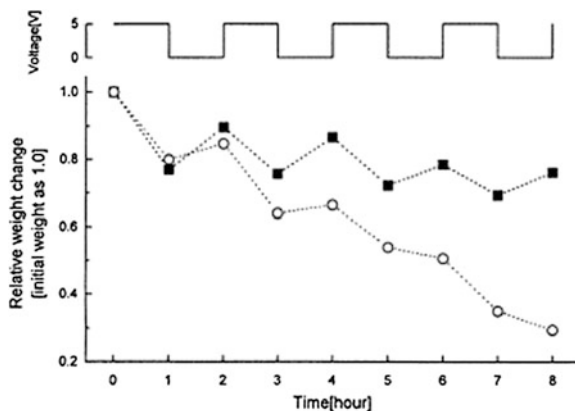


Fig. 12 Shrinking of hydrogel deswelling induced by electrical pulses (1 h, 5 V). With permission from Murdan (2003); Copyright 2003 Elsevier



9.4.3 Pressure Responsive

As a result of the thermodynamic calculations according to the uncharged hydrogel theory, hydrogels which collapse at low pressure should expand at higher pressure. Research on hydrogels based on PNIPAAm proved this expectation (Lee et al. 1990). Hydrogels exhibited greater swelling under pressure when the temperature is close to their LCST (Ebara et al. 2014). Pressure sensitivity is observed in thermo-responsive hydrogels. It is considered that applied pressure leads to increase in LCST point (Qiu and Park 2012).

9.5 Chemical Stimuli

pH Sensitive

Another class of smart hydrogels which have been the focus of common interest is pH-responsive hydrogels. The polymer chain networks of these hydrogels contain acidic (such as carboxylic and sulfonic acids) or basic (such as ammonium salts) pendant groups. At specific pH, the pendant groups ionize by accepting or releasing protons resulting in the formation of charges on the hydrogel. All ionic materials present sensitivity to pH and ionic strength. The swelling forces increased because of repulsion among localized fixed charges on the pendant groups. Consequently, minute changes in pH may trigger a significant change in volume (Peppas 2004; Qiu and Park 2012).

pH-responsive hydrogels can be classified into two groups: anionic and cationic hydrogels (Ebara et al. 2014). Examples of anionic and cationic electrolytes and their response to environmental pH are shown in Fig. 13. As it can be seen, poly (acrylic acid) becomes ionized at basic pH, while poly(*N,N*9-diethylaminoethyl meth acrylate) (PDEAEM) becomes ionized at acidic pH. PDEAEM, which is a cationic polyelectrolyte, dissolve/swell more at acidic pH upon ionization, whereas

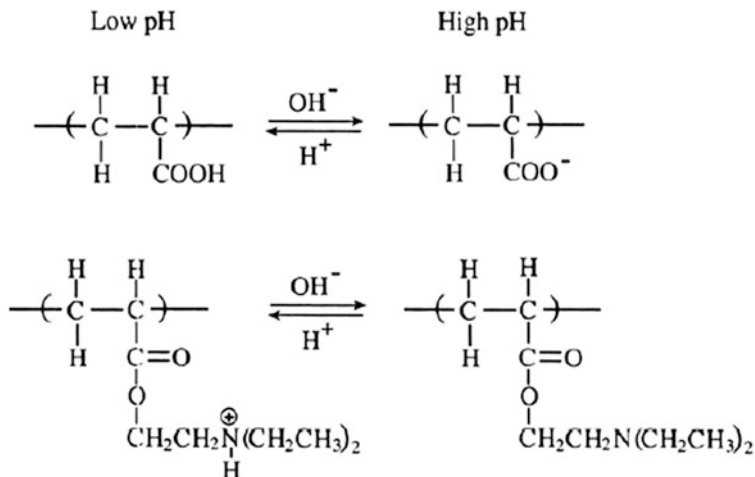


Fig. 13 Effect of pH on ionization of polyelectrolytes. **a** Poly(acrylic acid), **b** poly(*N,N'*-diethylaminoethyl methacrylate). With permission from Qiu and Park (2012); Copyright 2012 Elsevier

PAA, a polyanion, dissolves more at basic pH (Qiu and Park 2012). Such swelling behavior of hydrogels based on poly (acrylic acid) and poly(acrylic acid)-pectin is presented in Fig. 14.

As the swelling behavior of pH-responsive hydrogels is based on the electrostatic repulsion forces among charges on the polymer chain which are formed due to ionization, the level of swelling is affected by factors that are influential on electrostatic repulsion, including pH, ionic strength, and the presence of counterions. The swelling response can be altered via the introduction of neutral comonomers, including 2-hydroxyethyl methacrylate, methyl methacrylate, and maleic anhydride. Comonomers with different hydrophobicity levels result in different pH-responsive behavior (Qiu and Park 2001).

Poly(methacrylic acid)-poly(ethylene glycol) (PEG) hydrogels exhibit specific pH-responsive behavior. In acidic medium, the protons of the carboxyl (–COOH) groups of poly(methacrylic acid) associate with the ether oxygen of PEG via hydrogen bonds causing in hydrogel shrinking. And under basic conditions, the carboxyl groups of poly(methacrylic acid) become ionized and leading to decomplexation which in turn resulting in hydrogel swelling. Via this approach, novel pH-responsive hydrogels made of IPNs may be designed (Qiu and Park 2012; Peppas and Klier 1991). Table 2 lists some pH-responsive polymers and their threshold pH values.

pH-sensitive hydrogels can be used in drug delivery systems (Maziad et al. 2015). pH-responsive hydrogels have been investigated in terms of use in drug delivery for oral administration as different sections of the digestive tract exhibit different pH levels. Polycationic hydrogels undergo minimal swelling in neutral pH

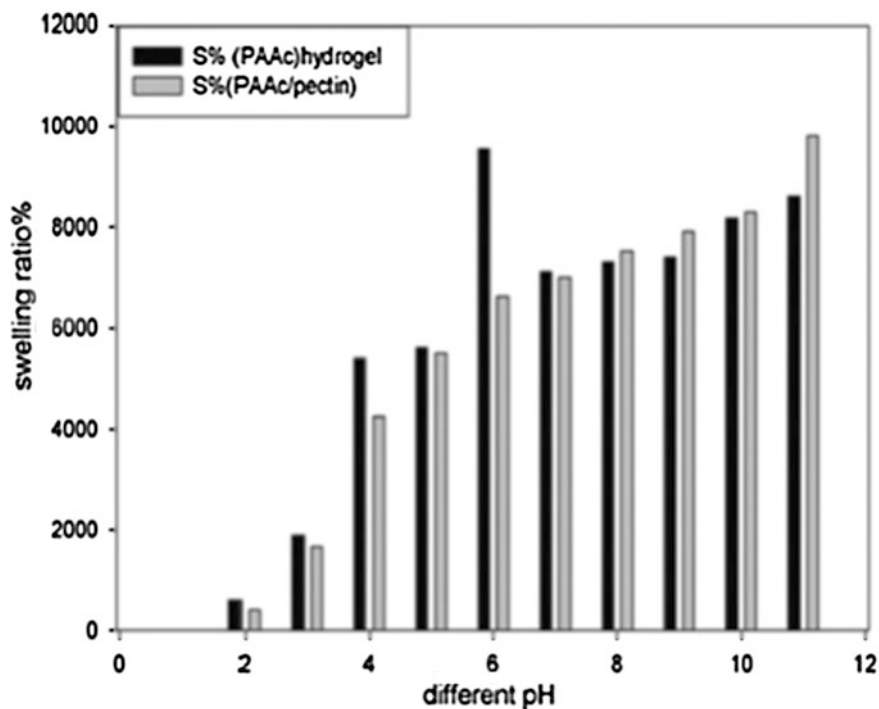


Fig. 14 Swelling of hydrogels based on poly(acrylic acid) and poly(acrylic acid)-pectin as a function of pH. With permission from Maziad et al. (2015); Copyright 2015 Asian Journal of Pharmaceutical and Clinical Research Pending

Table 2 pH-responsive polymers and their threshold pH (Sandeep et al. 2012)

Polymer name/commercial name	Threshold pH
Eudragit L 100	6
Eudragit L-30D	5.6
Eudragit S100	7
Eudragit FS30D	6.8
Eudragit L100-55	5.5
Polyvinyl acetate phthalate	5
Hydroxy propyl methyl cellulose phthalate	4.5–4.8
Hydroxy propyl methyl cellulose phthalate-50	5.2
HPMC55	5.4
Cellulose acetate trimellitate	4.8
Cellulose acetate phthalate	5

With permission from Sandeep et al. (2012); Copyright 2012 IJRPC pending

medium leading to decreased drug release. This behavior is utilized in the prevention of unpleasant tasting drugs from releasing in the mouth where the pH is neutral. For this, methyl meth(acrylate)-*N,N*9-dimethylaminoethylmethacrylate (DMAEM) copolymers were used, which exhibited no release at neutral pH and zero-order release at pH 3–5 DMAEM. Semi-IPN polycationic hydrogels, such as Chitosan-PEO, were investigated for use in targeted drug delivery in the stomach based on increased swelling in low pH levels (Qiu and Park 2001). On the other hand, hydrogels based on Poly(acrylic acid) or poly(methacrylic acid) may be utilized for drug release in neutral pH (Ebara et al. 2014).

Hydrogels based on polyanions such as poly(acrylic acid) prepared by using azoaromatic cross-linking agents were developed for colon-targeted drug delivery. As mentioned before polyanions undergo minimum swelling and drug release at low pH (such as that in the stomach), but exhibit higher swelling and resulting drug release at high pHs, such as that in intestines. However, the azoaromatic cross-links can only be degraded by azoreductase present in the flora of the colon (Akala et al. 1998; Qiu and Park 2012).

By introduction of ionizable and hydrophobic groups into the polymer chain networks, it is possible to obtain hydrogels which are pH- and thermo-responsive at the same time. If an anionic monomer, like acrylic acid, is introduced into a thermo-reversible polymer, the LCST is affected by the ionization of the pendant carboxyl groups, and the medium pH. If the medium pH exceeds the pK of the carboxyl groups of polyanions, LCST increases based on increment in hydrophilicity and repulsion of charges. Hydrogels prepared from NIPAAm, acrylic acid, and 2-hydroxyethyl meth acrylate presented pH- and temperature-induced volume change responses (Qiu and Park 2001; Vakkalanka et al. 1996; De La Rosa et al. 2016).

Apart from drug delivery systems, pH-responsive hydrogels have also been investigated for use in biosensors and permeation switch applications. For these applications, the hydrogels may be loaded with enzymes that lead to pH change. One example is glucose oxidase which transforms glucose to gluconic acid resulting in acidic pH and inducing the response of pH-sensitive hydrogels (Qiu and Park 2001; Hoffman 1997).

One of the major drawbacks of synthetic pH-responsive polymers is non-biodegradability. This makes it necessary to remove them from the body after use. Hence, research efforts have taken place to obtain biodegradable, pH-sensitive hydrogels by using peptides, proteins, and polysaccharides. In a related study, dextran was used as a hydrogel component of biological origin. However, dextran may not be biodegradable in vivo if the body does not possess enzymes which can degrade dextran molecules (Qiu and Park 2012). As not all bio-based polymers are biodegradable in nature (Yilmaz et al. 2016), polymers that are degradable in nature may also not be degradable in the human body (Yilmaz 2015b).

Another potential use of pH-responsive hydrogels can be related with therapeutic strategies targeting solid tumors which present low extracellular pH due to lactic acid accumulation. Other pathologic tissues, including ischemic or infected sites, also present lower pH, where pH-responsive hydrogels may find use. Accordingly,

pH-responsive hydrogels have been investigated for use in cytosolic nucleic acid, anticancer drugs, and internalizing antibody delivery systems (Ebara et al. 2014; Lee et al. 2008).

Ion-Sensitive Hydrogels

Whereas the effect of salt concentration on the volume transition behavior of neutral hydrogels is expected to be negligible, swelling/deswelling response of nonionic hydrogels may be induced by the presence of salt ions. In such an examples, a nonionic hydrogel based on poly(*N*-isopropylacrylamide) underwent sharp deswelling volume phase transition in an aqueous solution at a specific NaCl concentration. Under LCST, hydrogel water content is heavily related to NaCl concentration, where the critical concentration varies based on temperature. On the other hand, the LCST point also varies with changing salt concentration, as it decreases with increasing salt concentration (Gupta and Siddiqui 2012).

Biological responsive Glucose-responsive

Development of self-regulated (modulated) insulin delivery systems forms one of the holy grails in the field of controlled drug delivery. Insulin delivery differs from other drug delivery systems as insulin should be delivered at the right time at the exact quantity. Thus, delivery of insulin should be self-regulated with the ability to sense glucose level in the blood as well as be equipped with a shut-off mechanism to cease insulin release in order for prevention of hypoglycemia (Lee et al. 2013). A number of hydrogel systems were designed to be glucose-responsive to be used in insulin delivery systems. The hydrogels systems developed for insulin delivery can respond to glucose levels via swelling/deswelling, eroding or sol-gel transition. The glucose-sensing ability is imparted to hydrogels via use of enzymes like glucose oxidase (Kang and Bae 2003), lectins, which are proteins capable of selective and reversible binding of carbohydrates, such as concanavalin A (Con A) (Fig. 15) (Kim and Park 2001; Valuev et al. 2011), and phenyl boronic acid (Zhang et al. 2013).

pH-responsive hydrogels are used together with enzymes in the insulin-release systems. Among different enzymes, glucose oxidase is the most commonly used one, as it transforms glucose into gluconic acid, leading to increase in the acidity of the medium. This situation renders various pH-responsive hydrogels to be utilized in insulin delivery systems. When pH-responsive hydrogels based on polycations such as PDEAEM (poly(*N,N'*-diethylaminoethyl methacrylate)) are used, increased acidity triggers swelling response upon PDEAEM ionization. A swollen membrane may allow the release of more drugs, which is insulin, in this case (Qiu and Park 2012).

In the case of membranes made of hydrogels based on polyanions, insulin-release mechanisms differ. As polyanion-based pH-responsive hydrogels show shrinking response to decrease in pH levels due to the activity of immobilized

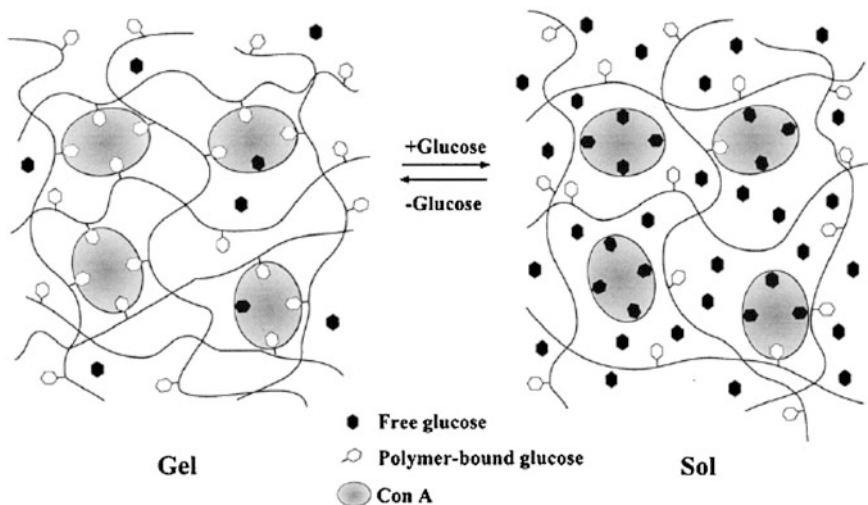


Fig. 15 A glucose-responsive hydrogel showing sol-gel phase transition. With permission from Qiu and Park (2001); Copyright 2001 Elsevier

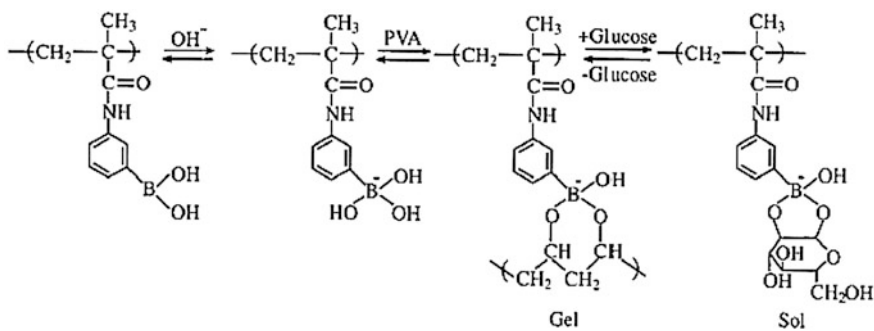


Fig. 16 Sol-gel phase transition of a glucose-responsive phenyl borate polymer. With permission from Qiu and Park (2001); Copyright 2001 Elsevier

glucose oxidase enzyme, this time the drug release mechanism can be designed according to “squeeze” effect upon collapsing (Hassan et al. 1997). To the contrary, pH-induced polymer eroding response also can be utilized for hydrogels which also contain the glucose oxidase enzyme (Qiu and Park 2012) (Fig. 16).

Similar to other hydrogel systems, glucose-responsive hydrogels should be improved in terms of response rate, biocompatibility/biodegradability, and reproducibility (Qiu and Park 2012).

Protein-Responsive

Similar to glucose-responsive hydrogels, protein-responsive hydrogels function based on biomolecular interactions (Yoshida and Okano 2010). Protein-responsive hydrogels can respond to enzymes, antigens as well as DNAs and RNAs. Enzymes can be used as signals for specific sites in the body as well as some physiological changes (Miyata et al. 2002).

As some enzymes are located at specific sites in the human body, they can be used as signals for targeted drug delivery. To give examples, microbial enzymes such as dextranases and azoreductases are predominantly present in the colon area; and thus may be utilized as signals for colon-targeted drug release. Hydrogels were developed that contain dextran (Rolinski et al. 2001) or azo aromatic bonds (Akala et al. 1998). Upon degradation by the enzymes, drug release can be achieved (Miyata et al. 2002; Mateescu et al. 2012; Pickup et al. 2005).

An antibody has the ability to bond with a specific antigen via noncovalent linkages. Through this immune system mechanism, the biological organism is tried to be protected from infections. This ability of antibodies to recognize and bind to antigens can be implemented into the design of responsive hydrogels (Miyata et al. 2002). In a related study, a hydrogel based on a semi-IPN structure was developed from two sets of polymers, where to one the antibody was grafted and to the other the corresponding antigen was bonded. The cross-linking occurred between the antibodies and antigens of the polymer chains. When the hydrogel was exposed to a medium including the specific antigen, hydrogel swelling occurred with a decrease in cross-linking density due to debonding of bound antigen to the bound antibody in the polymer network upon competition of free antigen present in the environment as shown in Fig. 17 (Miyata et al. 1999).

In a different study, Murakami and Maeda (2005) developed DNA-responsive hydrogels containing grafted single-stranded DNAs or conjugate of single-stranded DNA-polyacrylamide in the form of a semi-IPN that shows deswelling behavior in an environment including the specific DNA.

10 Characterization Methods

Hydrogels can be characterized based on their morphology, swelling property, water absorption capacity, mechanical, and optical properties. Here, morphology indicates the surface structure and porosity (Sandeep et al. 2012; Ebara et al. 2014).

10.1 Water in Hydrogels

As a hydrogel is immersed in water, the polar hydrophilic groups of its polymer chains will be hydrated initially and form “primary bound water.” This leads to hydrogel network swelling and exposal of hydrophobic groups with the capability

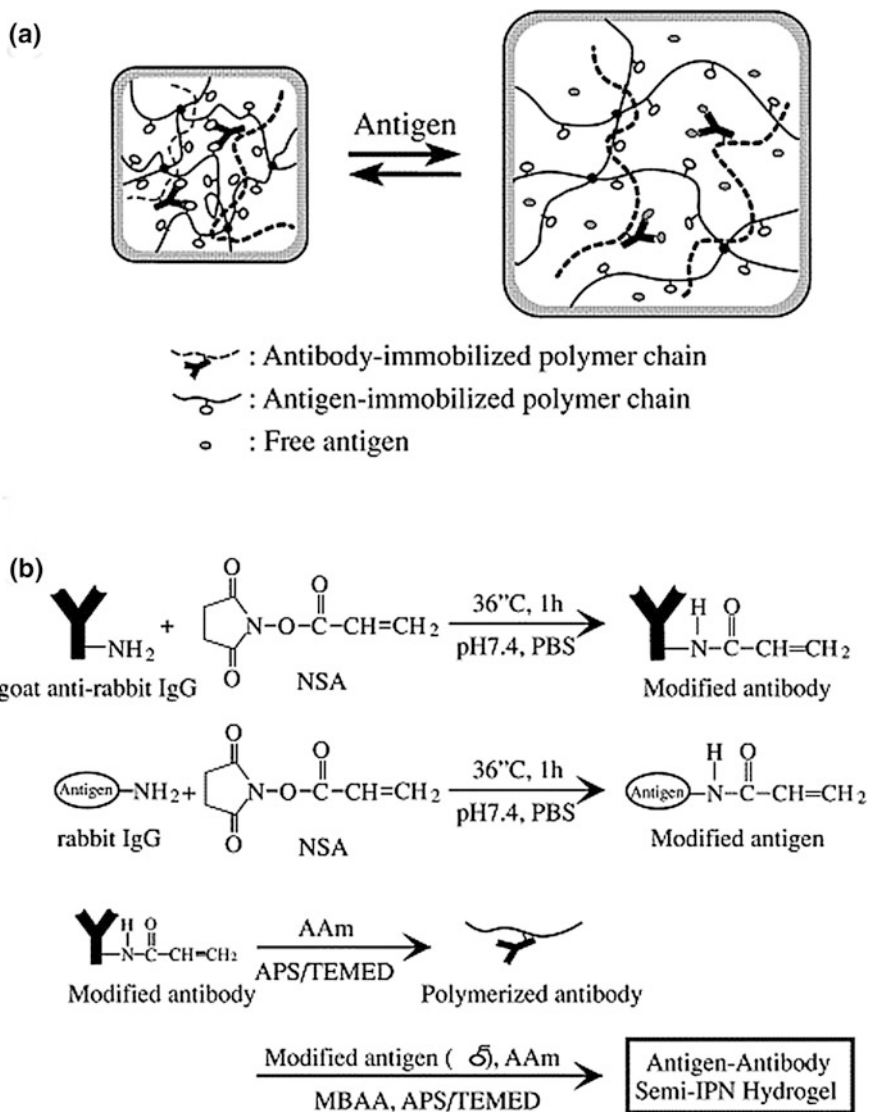


Fig. 17 Production route for an antigen-sensitive semi-IPN hydrogel (Miyata et al. 1999). With permission from Miyata et al. (1999); Copyright 1999 National Academy of Sciences pending

to associate with the water molecules. This results in hydrophobically bound water content referred to as “secondary bound water”. Primary bound water and secondary bound water constitute “total bound water”. The hydrogel continues to imbibe water driven by the osmotic force of the network toward infinite dilution. This extra swelling evokes elastic network retraction force exerted by the

cross-links. These two opposing effects lead the hydrogel to reach an equilibrium-swelling level. The additional imbibed water is referred to as “free water” or “bulk water” (Hennink and Nostrum 2002; Hoffman 2002; Khodamoradi and Khodamoradi 2014). A number of methods can be used to predict total bound water and free water amounts, including DSC, and NMR techniques (Ebara et al. 2014; Sandeep et al. 2012).

10.2 Thermodynamics of Hydrogel Swelling

In an early study, Dusek and Patterson (1968) have predicted the swelling phenomena of hydrogels induced by environmental stimuli and this theory has been verified by following experimental studies of other researchers (Tanaka 1978; Hrouz et al. 1981). The swelling behavior of hydrogels can be investigated as a combination of two components: equilibrium and dynamic swelling behavior in water. When a dry and hydrophilic cross-linked polymer network is immersed in a solvent such as water, the interaction between the molecules of the solvent and the polymers take place due to thermodynamic compatibility which results in volume expansion up to the solvated form (Peppas 2004).

10.3 Response Mechanism

As mentioned, hydrogels may undergo a volume phase transition between solvent-swollen and hydrophobic collapsed states as induced by external stimuli. In the collapsed state, interactions between polymer chains are dominant which leads to release of water from the hydrogel network Fig. 1. In the case of the swollen state, solvent-polymer interactions dominate (Khodamoradi and Khodamoradi 2014)

The Flory–Huggins theory can be utilized for understanding the swelling behavior of hydrogels. Flory (1942) and Huggins (1942) independently developed the initial theory for explaining cross-linked polymer gel swelling. In the model, the degree of polymer network swelling is postulated to be determined by the polymer chains’ elastic retractive forces and the thermodynamic compatibility between the molecules of the polymer and the solvent. When these two forces become equal to each other, the swelling equilibrium is attained. The volume degree of swelling, Q , can be given by the expression below (Peppas 2004):

$$\vartheta_{2,s} = \frac{\text{volume of polymer}}{\text{volume of swollen gel}} = \frac{V_p}{V_{\text{gel}}} = 1/Q \quad (1)$$

Swelling degree can be expressed by other terms such as the weight degree of swelling, Q , which is the ratio of the weight of the swollen sample to that of the dry sample, or hydration rate, H (Peppas 2004).

The hydrogels can be classified into two groups in terms of their swelling degrees such as highly swollen hydrogels (cellulose derivatives, poly(vinyl alcohol), poly(*N*-vinyl-2-pyrrolidone) (PNVP), and poly(ethylene glycol)), and moderately and poorly swollen hydrogels (poly(hydroxyethyl methacrylate) (PHEMA) and its derivatives). Normally the swelling degree can be arranged to a desired level by co-polymerizing highly hydrophilic monomers with less hydrophilic monomers. Via this method, hydrogels with a broad range of swelling degrees can be obtained. As swelling behaviors have an influence on certain properties of hydrogels such as solute diffusion through the hydrogels, surface characteristics, optical and mechanical properties, it is, of uttermost importance to possess sound knowledge pertaining to swelling properties of hydrogels (Peppas 2004).

Swelling of hydrogels can be measured according to different methods. Among different methods, the Japanese Industrial Standard K8150 method can be used. As stated in the standard method, a dry hydrogel is kept under deionized water for 48 h on a roller mixer at room temperature. Then, the hydrogel is filtered by a stainless steel net of 30 meshes (Sandeep et al. 2012). In Fig. 18, the effect of monomer concentration on swelling ratio of hydrogels based on poly(acrylic acid) is shown.

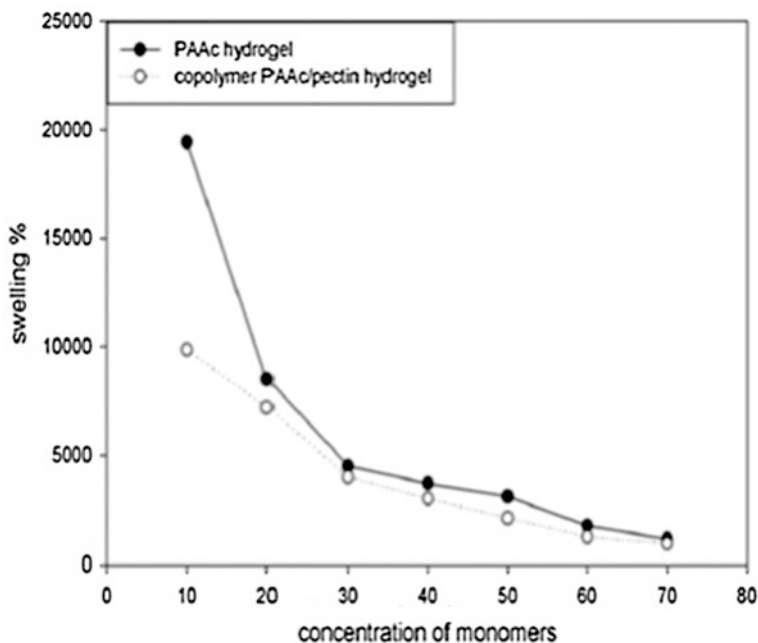


Fig. 18 Swelling ratio of poly(acrylic acid)-based hydrogels as a function of monomer concentration (Maziad et al. 2015). With permission from Maziad et al. (2015); Copyright 2015 Springer

11 Mechanical Properties

Similar to other materials, the mechanical characteristics of hydrogels are determined by their composition and structure. Polymer gels generally present low mechanical performance with their low tenacity, hardness, and capability to endure deformation values. This situation is based on the fact that the polymer networks are not completely connected while including various inhomogeneities, dangling chains, and loops. The strength and durability of hydrogels can be investigated in terms of their tensile, shearing and compression behaviors under static or dynamic loading conditions (Ebara et al. 2014).

The hydrogels may show viscoelastic or pure elastic characteristic based on the cross-links that bond polymer chains, which determine hardness, elasticity, and stickiness. The water content in hydrogels also contributes to its flexibility. Thus, by changing the polarity of the polymer chains, the surface properties and swelling behavior of hydrogels through arranging comonomer composition, polymerization parameters and cross-linking density, it is possible to tailor its mechanical performance (Khodamoradi and Khodamoradi 2014; Ebara et al. 2014). Especially in the swollen form, the strength of the hydrogel merely depends on cross-links, as the physical entanglements are almost totally cleaved. While it is possible to change the strength by modifying cross-linking properties, it should not be neglected that other hydrogel characteristics will be affected as well.

Novel hydrogel structures which result in unique mechanical behavior have been developed. In an example, a hydrogel with a slide-ring structure was obtained (Okumura and Ito 2001). This hydrogel was produced by cross-linking of polyrotaxane containing PEG threaded through a cyclodextrin ring molecule. As the cyclodextrins were not linked to the axis polymer with covalent linkages, the cross-links were capable of sliding along the axial chain, leading to specific mechanical and swelling behaviors. In another study, hydrogels possessing double network structure presenting good mechanical properties with a very high toughness that is energy dissipation capacity (Ebara et al. 2014; Gong et al. 2003).

11.1 Solubility

Hydrogels may consist of soluble and insoluble constituents. The soluble/insoluble content may be calculated based on different techniques. These techniques are generally based on immersing hydrogel in deionized water at high liquor ratios for a specific duration (16 or 48 h) at room temperature where the specimen is fully dispersed. The insoluble content may be determined by using the following formula (Sandeep et al. 2012):

$$\text{Insoluble gel fraction (hydrogel \%)} = (W_d/W_i) * 100. \quad (2)$$

Here, W_i stands for the initial weight of the dried sample and W_d represents the weight of the dried insoluble portion of the sample upon extracting with water (Sandeep et al. 2012).

11.2 Rheology

The rheological characteristics of materials are determined by the interactions within their structure such as association, entanglement, and cross-links. Polymer solutions generally present viscous behavior ($G' \sim \omega^2$ and $G'' \sim \omega$) for low frequencies and dominantly elastic behavior ($G' > G''$) at high-frequency regions. In terms of cross-linked microgel dispersions, G' and G'' are nearly independent of frequency (Ebara et al. 2014).

11.3 Morphological Characterization

A hydrogel may exhibit smooth, rough or stepped surface structure. Various techniques may be used for evaluating the surface property of hydrogels which include scanning electron microscopy (SEM), and atomic force microscopy (AFM). Via SEM method, information pertaining to the surface topography, network structure as well as electrical conductivity can be obtained. In AFM technique, the surface topography of a hydrogel may be imaged at the molecular level via the use of an indenting tip (Ebara et al. 2014; Sandeep et al. 2012).

11.4 Crystalline Structure

The network of a hydrogel may possess highly crystalline, disordered and inhomogeneous structures (Ebara et al. 2014) which may be deformed during different possesses. Via X-ray diffraction method, the presence, and properties of the crystalline structures can be characterized, deformations of these structures can be detected (Sandeep et al. 2012).

11.5 Chemical Characterization

FTIR (Fourier Transform Infrared Spectroscopy) provides a handful method in characterizing the chemical structure of materials. The rationale behind FTIR is that the chemical bonds in materials exhibit typical absorption behavior when exposed to infrared light rays at different frequencies/wavelengths. The IR spectrum presents a fingerprint of a material in terms of its chemical components. IR spectroscopy is also helpful when investigating the chemical structure change that occurs during certain processes such as polymerization or cross-linking procedures (Sandeep et al. 2012; Ebara et al. 2014).

12 Applications of Smart Hydrogels

Environment-responsive (smart) hydrogels have been the focus of intense attention based on their response ability to minute changes in a number of different aspects of the environment ranging from temperature and pressure to pH and glucose concentration (Lim et al. 2014). Building on this capability, smart hydrogels have found use in various applications that fall inside the biomedical arena including drug delivery, bioseparation, tissue engineering, biosensors, artificial muscles, chemical valves, enzyme and cell immobilization, blood-compatible applications and wound healing (Peppas 2004; Lee et al. 2013; Qiu and Park 2001).

The first synthetic hydrogel was developed by researchers at DuPont in 1936 (Strain et al. 1939), which was then investigated for its use in contact lens application by Wichterle and Lim (1960), Ebara et al. (2014). Thus, contact lenses provide one of the earliest applications of hydrogels. Certain features of hydrogels including appropriate mechanical stability, suitable refractive index, and high oxygen permeability rendered these materials an alternative material for contact lens applications (Peppas 2004). The following subsections investigate hydrogels in terms of their applications.

12.1 “On–Off” Drug Delivery Systems

Even though substantial advancement has been realized in controlled drug delivery systems, more progress is yet to be achieved in the treatment of a number of clinical disorders including diabetes and heart diseases. In the mentioned cases, the active drug ingredient should be released at the proper time at the proper site in response to the concentration of specific biomolecules or fluctuating metabolic requirements. Environment-responsive hydrogels have emerged as promising for use in self-regulatory drug delivery systems for treating such disorders. Via use of

environment-responsive hydrogels, it is theoretically possible to sense a signal brought on by a disease, measure the signal magnitude, and respond to release the corresponding amount of drug (Qiu and Park 2012).

As mentioned above, self-regulatory insulin delivery forms one of the holy grails of controlled drug delivery. The uniqueness of insulin delivery comes from the fact that long-term release is not desired. Insulin should start to be released at the right time, should be released in the right amount and the release should be ceased at the exact time to avoid hypoglycemia as mentioned before (Lee et al. 2013).

Another shortcoming of conventional drug delivery is in the area of controlled release of peptide and protein drugs (Qiu and Park 2001). Hydrogels may present benefits in this area, too, as they interact less strongly with the protein and peptide drugs (Ebara et al. 2014).

Based on their structures, hydrogels may exhibit some advantages in comparison to conventional dosage formulations such as that are used in sustained drug release, and in turn decreased administration dose, less side-effects; targeted drug release, prevention of irritation based on drug contact (Sandeep et al. 2012).

By using hydrogels as drug carriers, the active drug ingredient can be protected by hostile environments within the organisms such as enzymes that can degrade them as well as high acidity as in the stomach (Qiu and Park 2012). On the other hand, hydrogels can protect the tissues from the unwanted side-effects of the drug material by releasing them not in their way to the specific site but only at the specific site where necessary (Khodamoradi and Khodamoradi 2014). As an example, pH-responsive hydrogels may allow the release of drug materials in a predetermined site of the gastrointestinal tract based on the local pH level (Maziad et al. 2015).

The rate of the drug release can be modulated by the change the hydrogels undergo, such as volume or sol–gel phase transitions, triggered by certain stimuli (Qiu and Park 2001). Different routes may be implemented to control the rate of drug release such as arranging the cross-linking density (Khodamoradi and Khodamoradi 2014), choosing monomers with different levels of hydrophilicity, and controlling hydrophilic and hydrophobic monomer contents (Ebara et al. 2014). Additionally, modification of the shape and size of hydrogels hydrogel may be other methods of modifying the drug release rate (Khodamoradi and Khodamoradi 2014).

12.2 Injectable Hydrogels

One of the means to provide sustained drug release is placing the medication in a carrier and then injecting/implanting the carrier into the organism. Accordingly, injecting gel-forming biopolymers receives attention in the preparation of therapeutic implants and drug delivery systems (Ebara et al. 2014). Hydrogels offer some advantages to be injected into the body tissue as they lead to minimal invasive effects and adjusts the shape to the host tissue (Smart Hydrogels for Biomedical

Applications 2015). Injection of hydrogels has been successfully implemented in delivering biologically active growth factors as well as live cells for tissue engineering applications (Ebara et al. 2014).

12.3 Tissue Engineering

Tissue engineering is a novel technology aiming to design and develop substitutes to native tissues. In the design of tissue engineering systems, scaffolds, which are 3D structures, take a special place. The duties of scaffolds include supporting cell adhesion, migration, proliferation, and differentiation. Among various scaffold materials, hydrogels hold a special position as they mimic the natural tissues (Ebara et al. 2014). Moreover, bioactive molecules and pharmaceutical materials can be included in the structure of the hydrogel, which may show interactions with proteins, induce growth of cells and manipulate cell migration. Another merit of hydrogels is their versatility, as it is possible to fine-tune their properties by appropriate selection of molecular building blocks, production method and other parameters (Smart Hydrogels for Biomedical Applications 2015) including polymer chain network density (Khodamoradi and Khodamoradi 2014).

Natural and synthetic hydrogels have been investigated in terms of use as scaffolds in cartilage, tendon, ligament, skin, vocal cord, kidney tissue, blood vessel and heart valve tissue engineering (Ebara et al. 2014; Peppas 2004). The natural/natural derivative hydrogels used in tissue engineering applications include alginate, chitosan, agarose, collagen, gelatin, fibrin, and hyaluronic acid (HA), while their synthetic counterparts can be given as polyurethanes, PEO, PNIPAAm, poly(vinyl alcohol), poly(acrylic acid) and poly(propylene fumarate-co-ethylene glycol). Injectable hydrogels have also received attention for tissue engineering applications. In a relevant example, hydrogels encapsulating growth factors or live cells can be injected into the wound site, where they undergo sol-gel transition in response to various stimuli (Ebara et al. 2014).

Costa-Almeida et al. (2016) developed a hybrid hydrogel-fiber system for tissue engineering applications. Cell-laden hydrogel fibers were reinforced with a strong biodegradable fiber that was assembled via textile braiding technology to replace the tendon structure. The hydrogel consisted methacryloyl gelatin (GelMA) and alginate, where the first one was cross-linked in calcium chloride bath and the latter via exposure to UV light. Encapsulated mesenchymal stem cells (MSCs) and MC-3T3 fibroblasts, which were homogeneously distributed throughout the hydrogel layer showed viability up to 14 days in culture. The attained mechanical properties were comparable to those of tendons (Costa-Almeida et al. 2016).

In a different thermo-responsive hydrogel tissue engineering application, Stile et al. (1999) synthesized loosely cross-linked PNIPAAm and P(NIPAAm-co-AAc) hydrogels by using *N,N'*-methylenebis(acrylamide) cross-linking agent. The hydrogels possessed transparent appearances and extreme pliability at room

temperature, while they became opaque and rigid at body temperature (37 °C) (Ebara et al. 2014; Stile et al. 1999).

Environmental-responsive hydrogels may also find use in cell encapsulation applications which are used in diabetes, hemophilia, cancer, and renal failure treatments. Some properties of hydrogels including biocompatibility, microporosity, and reduced surface irritation of host tissues render them promising for cell encapsulation technology. Hydrogels can be obtained with tailored pore size distribution which allows nutrient and waste transfer but blocks immune system elements. Among different types, hydrogels based on genetically modified alginates and PEO have been investigated in terms of use in cell encapsulation systems. The major challenge pertaining to the use of hydrogels is related to the toxicity of the reagents and byproducts of cross-linking (Williams et al. 2005). In a study, cell death was reported to increase with increment in exposed unreacted side chains (Salinas et al. 2007; Ebara et al. 2014).

In a study, temperature-responsive cross-linked nanofibers were developed which captured, encapsulated, and released cells by dynamically wrapping, swelling, and shrinking, and the transformation between fibrous structure and the hydrogel-like structure was induced by a change in the medium temperature. Via this method, not only cells, but also bioactive compounds can be captured, encapsulated and released including peptides and antibodies that can be utilized for separating, purifying, preserving, and delivering target cells and molecules (Kim et al. 2012; Ebara et al. 2014).

Hydrogel systems which mimic extra cellular material (ECM) have also been developed. Lutolf and Hubbell (2005) designed an ECM-mimicking enzyme-responsive PEG-based hydrogels via the use of oligopeptides as cross-linkers. The hydrogel acted as a scaffold. The peptide sequences can be cleaved by matrix metalloproteinases (MMPs) and a gel that allows cell infiltration is formed. MMPs constitute an enzyme family that can lead to the breakdown of ECM molecules for tissue remodeling and in times of disease. This introduction of sites that can be cleaved by MMPs suitable for ECM-mimicking systems. The possibility of utilization of this system in bone tissue engineering was examined by filling bone morphogenetic protein-2 (BMP-2), that plays role in bone formation, into the hydrogel. In another study, an ECM-mimicking system was prepared by producing NIPAAm-AAc-based hydrogel cross-linked with Arg-Gly-Asp-modified poly(acrylic acid) and MMP-13/collagenase-3-degradable peptide sequence by Kim et al. (2005). The system, which showed degradation in the presence of collagenase showed increased migration of rat calvarial osteoblast cells compared to their undegradable counterpart (Ebara et al. 2014; Kim et al. 2005).

Vrana et al. (2009) produced polyvinyl alcohol (PVA)-gelatin hydrogels via freeze-thawing (cryogelation) process to encapsulate bovine arterial smooth muscle cells at different serum, DMSO, and cell culture medium concentrations. Increased DMSO and serum concentrations improved cell viability. The researchers reported that cell-laden hydrogels with tailored mechanical properties can be prepared and stored by applying freeze-thawing process (Vrana et al. 2009).

12.4 Biomimetic Actuators

Living organisms convert chemical energy into mechanical energy isothermally for body movements including muscular contraction, and flagellar and ciliary movement (Qiu and Park 2012). In an attempt to mimic the conversion of chemical energy to mechanical energy in biological organisms, electro-responsive hydrogels are used (Kumar, n.d.). These systems can be utilized as actuators or artificial muscles in various applications. Mechanical movement of hydrogels can be obtained in response to alternating voltages in the presence of electrodes. Repeated bending and stretching can be formed as the motion is dependent on the electric field direction (Ebara et al. 2014; Qiu and Park 2012).

Poly(vinyl alcohol)-poly (acrylic acid) acid chains show rapid bending deformation behavior upon application of electrical field. A gel rod with 1 mm diameter bent to a semi circle shape within 1 s due to an electrical field. Sinusoidally varying electrical field can form dynamic mechanical movement. The gels contain positively charged surfactant molecules bonded on polyanionic polymers like poly (2 acrylamido-2 methyl-1-propane sulfonic acid). Gels incorporating *N*-isopropyl acryl amide and acrylic acid copolymers have been found effective in forming bio-chemo-mechanical systems. Contrary to biological systems, biomimetic actuators can endure very unpleasing conditions (Kumar, n.d.).

In a related study, weakly cross-linked poly(2-acrylamido-2-methyl propanesulfonic acid) hydrogels were produced. When the polyanionic hydrogel is introduced to a medium incorporating positively charged surfactant molecules, the hydrogel's surface that faces the cathode becomes covered with surfactant molecules which in turn reduces the overall negative charge. This leads to local shrinkage of the hydrogel causing hydrogel bending. If an oscillating electrode polarity is applied, the hydrogel repeats its oscillatory motion, forming a worm-like motion (Qiu and Park 2001; Osada et al. 1992).

Conducting polymers including polypyrrole (PPy), polythiophene, and polyaniline have received research interest due to the possibility of motion forming induced by electrical stimuli. In an interesting study, contraction of PPy films was reported to be triggered by an electric field. Water vapor absorption leads to the movement of the film. The reversible water vapor absorption drives the film motion (Ebara et al. 2014; Okuzaki et al. 2010).

Not only electric-, but also temperature-responsive hydrogels have found use in actuators. In a related study, PNIPAAm is used in the production of an actuator that bends upon a change in temperature. Hu et al. (1995) developed semi-IPN PNIPAAm - poly(acrylamide) (PAAm)-based hydrogels that bend into circles with an increase in temperature. These hydrogels were designed to grasp or release an object in response to change in water temperature (Ebara et al. 2014).

In another study, a bilayer film was produced from PNIPAAm and poly (ϵ -caprolactone) (PCL). Whereas the first polymer exhibits solubility transition at

33 °C, the latter one is hydrophobic and insoluble in water. Swelling and shrinking of PNIPAAm leads to the reversible rolling motion of the film (Ebara et al. 2014; Stoychev et al. 2011).

In a different thermo-responsive hydrogel system, actuators were fabricated based on PNIPAAm possessing two different nanostructured gradients. Bending motion occurs due to the difference in the physical structure of the two sides (Ebara et al. 2014; Asoh et al. 2008).

In an optical-responsive example, Zhang et al. (2011) developed composite hydrogels from single-walled carbon nanotube and PNIPAAm. The hydrogel responds to near-IR laser excitation very fast (Ebara et al. 2014).

There are hydrogels that produce mechanical motion triggered by chemical stimuli other than physical stimuli. Among, different chemical stimuli-responsive hydrogels, pH-responsive hydrogels possess a unique place in biomedicine as different parts of the human body present different pH values, such as pH variations throughout the gastrointestinal tract, in specific tissues such as infected or tumoral areas. pH-responsive hydrogels which present folding motion are prepared by incorporation of weak polyelectrolytes as active polymers. The ions of the ionic groups are balanced with ions of the opposite charge which diffuse in and out of the network structure. This situation results in instantaneous variations in their characteristics with temporal activation, as seen in living organisms, including muscle and ciliary motion, pulsatile hormone secretion, as well as brain waves (Ebara et al. 2014).

Luchnikov et al. developed bilayered (Luchnikov et al. 2005) polystyrene-poly(4-vinyl pyridine) and trilayered polystyrene-poly(4-vinyl pyridine) -PDMS hydrogels which can roll at low pH as protonation and swelling of poly(4-vinyl pyridine) takes place. In another work, Bassik et al. (2010) prepared bilayer PEG/P(NIPAAm-co-AAc) hydrogels which can show snapping response triggered by pH change (Ebara et al. 2014).

Physical stimuli-responsive hydrogels present an advantage compared to their chemical stimuli-responsive counterparts: physical stimuli (light, heat, magnetic field, ...), have the ability to penetrate through materials, whereas it is a challenge to form changes in chemical stimuli quickly and precisely at the desired location especially within hydrogels. This situation has accelerated research efforts on developing actuators from physical stimuli-responsive hydrogel systems (Ebara et al. 2014).

Ebara et al. (Techawanitchai et al. 2012a) investigated the light-induced proton-releasing reaction of photoacid generators. The pKa of photoacid generators in the excited state differs substantially from its value in the ground state. Photoacid generators were integrated into pH-responsive P(NIPAAm-co-CIPAAm) hydrogels and UV irradiation triggered rapid proton release which led to decrease of intragel pH to below the pKa of P(NIPAAm-co-CIPAAm). The researchers reported reversible bending of PAG-integrated pH-responsive polyacid P(NIPAAm-co-CIPAAm) and poly base P(NIPAAm-co-N,N'-dimethylaminopropylacrylamide: DMAPAAm)-based bilayer hydrogels induced by light (Asoh and Kikuchi 2010). The mentioned two layers were bonded by the formation of a semi-IPN

incorporating linear poly(acrylic acid) and branched poly(ethyleneimine) polymer chains, that produce polyion complexes at the interface of the two hydrogels through electrophoresis (Techawanitchai et al. 2012b). The reversible bending behavior was induced by “on–off” UV irradiation. The system can find use in different applications such as mechanical actuators, robotics, microfluidic technologies, and controlled drug release (Ebara et al. 2014).

Stimulus-responsive hydrogels can be also used in microfluidic devices in order to decrease system complexity (Dong and Jiang 2007). Microfluidics is related to control and manipulation of small fluid volumes (Whitesides 2006). Even though recent advancement in microfabrication techniques including multilayer soft lithography allows the design of complex microchips possessing numerous independent valves, most of the microfluidic materials do not possess stand-alone capabilities. On the other hand, stimuli-responsive hydrogels which have the ability to respond to external stimuli can be incorporated into microfluidic devices to cater for various applications such as chemical synthesis, bio/chemical analysis, cell manipulation, and biomedical monitoring. In a related study, Beebe et al. (2000) developed a pH-responsive hydrogel-based valve that responds to the pH of the flowing solution with an opening closing motion. By using hydrogels that are responsive to pH and temperature together with electroplated nickel (Ni) impellers, and magnetic stirrers, autonomous micromixers, and micropumps were fabricated (Agarwal et al. 2005). In that study, the Ni impeller was coupled with a rotating magnetic stirrer under it, which was constantly on. At low pH, the hydrogel ring shrinks, and the Ni impeller rotates freely, whereas at high pH the hydrogel swells and restrict the motion (Ebara et al. 2014).

Besides stimulus-responsive hydrogel systems which form motions induced by an external signal, interest in self-actuating materials has seen increased recently. In a related study, Feinberg et al. (2007) developed an engineered tissue- and synthetic polymer thin film-based biohybrid self-walking bioactuator. They used cardiomyocyte culture on PDMS thin films micropatterned with ECM proteins. Yoshida and Okano (2010) developed another self-walking actuator which shows worm-like motion without any external stimuli. The oscillating motion is generated with chemical energy of an oscillating reaction: the BZ reaction (Vanag et al. 2000) which takes place inside the hydrogel. They produced a copolymer hydrogel of NPAAm in which ruthenium(II) tris-(2,2'-bipyridine) ($\text{Ru}(\text{bpy})_3^{2+}$), is covalently linked to the polymer chain. $\text{Ru}(\text{bpy})_3^{2+}$ acts as a catalyst of the BZ reaction. The P(NIPAAm-*co*- $\text{Ru}(\text{bpy})_3$) gel shows swelling and deswelling forms at the oxidized and reduced states of $\text{Ru}(\text{bpy})_3$, in consecutive order. Such self-walking actuators can be utilized in biomimetic robots (Ebara et al. 2014).

12.4.1 Sensors

Biomolecule-responsive hydrogels can be utilized in sensors which sense the concentration of specific biomolecules. In related examples, intensely studied

glucose-responsive hydrogels can sense the blood glucose levels and release insulin according to the glucose levels. Among them, NIPAAm copolymer microgels have been studied successfully in glucose-sensing systems (Ebara et al. 2014; Matsumoto et al. 2012; Gerlach and Arndt 2009).

In another study, Miyata and coworkers developed a specific antigen-responsive semi-IPN hydrogel system (Miyata et al. 1999, 2002). The hydrogel was produced via polymerization of the vinyl-conjugated goat anti-rabbit (GAR) IgG and a subsequent copolymerization of GAR IgG with vinyl-modified rabbit IgG, by using MBAAm as a cross-linking agent. The noncovalent cross-links between the grafted antigens and the antibodies lead the hydrogel network to shrink if no antigens are present. On the other hand, swelling of the hydrogel occurs if there are free antigens in the system due to cleavage of the antigen-antibody cross-links (Ebara et al. 2014).

Molecular imprinting can be applied for preparation of macromolecular matrices or hosts which can exhibit selective molecular recognition. This is made possible via allowing the matrices to “memorize” the outfits of targeted guests. In an early study Oya et al. (1999) developed stimuli-responsive hydrogels that can recognize and capture target molecules. The hydrogels contain polymer networks of two or more monomer moieties. Whereas one monomer is responsible for complex forming with the template (such as functional monomers that can interact with a target molecule via ionic bonds), the other monomer lets the network show reversible swelling and shrinking behavior induced by changes in the medium (such as a smart component like NIPAAm). An accurate chemical architecture of macromolecules allows recognition of target molecules among closely related molecules. Such hydrogels can find use in bioseparation systems, immunoassays, and biosensor recognition elements (Ebara et al. 2014; Oya et al. 1999).

Researchers also developed hydrogels that are responsive to glycoprotein (α -fetoprotein, AFP) which is a tumor marker. The hydrogel presented a change in volume induced by the presence of the tumor marker. The hydrogel which is glycoprotein imprinted shrinks when the target gel is present in the medium and allows diagnosis of tumor-specific marker glycoproteins and may find use in molecular diagnostics and smart systems (Ebara et al. 2014; Miyata et al. 2006).

Hydrogels can be developed to detect different levels of various analytes via selection of suitable competing ligand-receptor systems and tailoring a polymer membrane's permeability. In a relevant study, a membrane system of a hydrogel that is responsive to a metabolite, nicotinamide adenine dinucleotide, was studied in terms of controlled diffusion of model proteins. The hydrogels contained immobilized ligands and receptors. In the mentioned study, the ligand (cibacron blue) and the receptor (lysozyme) were bonded to dextran via covalent links. As a competing ligand, nicotinamide adenine dinucleotide competed with cibacron blue in terms of interacting with lysozyme. The model protein (cytochrome C and hemoglobin) permeability of the hydrogel was investigated at nicotinamide adenine dinucleotide concentrations (Ebara et al. 2014; Tang et al. 2004).

12.5 *Bioseparation*

Environmental-responsive hydrogels have found use in bioseparation systems can be classified as valves that control permeability through membranes, and affinity separation systems that function by recognition of monomeric strands (Kopeček 2007). These bioseparation systems have been explained in the sections above.

12.6 *Self-Healing*

Materials that are capable of self-healing have been developed from linear polymers, metal ion-polymer systems, dendrimer-clay systems, supramolecular networks, and multicomponent systems (Thakur and Kessler 2015). The multicomponent thermosetting systems utilize embedded chemical agents in crack reparation, whereas supramolecular networks and noncovalent hydrogels use secondary interactions like hydrogen bonds, ionic, hydrophobic interactions (Phadke et al. 2012), π - π stacking, and charge transfer for self-healing (Ebara et al. 2014). On the other hand, self-healing of covalent hydrogels, which may find use in various biomedical applications, is still difficult due to water presence and irreversible chemical cross-links (Phadke et al. 2012).

Phadke et al. (2012) proposed a self-healing mechanism for covalent hydrogels that functions by the introduction of dangling hydrocarbon side chains to the polymer network. The side chains include polar functional moieties in order to form hydrogen bonds between two sections of the hydrogel in the case of rupture. To allow for efficient healing, the network should be flexible, the functional groups should be accessible, and the side chains should be long enough. At the same time, the length of the side chains should not prevent functional group interaction and cause the hydrophobic collapse of the side chains. The hydrophobic and the hydrophilic groups of the side chains should be in balance.

Although stimuli-responsive hydrogels generally possess passive structures, there is a growing interest in self-healing hydrogels. Self-healing hydrogels can initiate autonomic healing in order to repair damage and, consequently, allow for safer and longer lasting products by minimizing the risks and complications in biomedical applications. An early developed self-healing mechanism is based on microencapsulation of a healing agent, which is a reactive species that polymerizes or goes into reaction with the matrix when the encapsulating hydrogel ruptures. As the reaction is irreversible and the reactive species is consumed, the healing process cannot be repeatable. Hydrogels, among other materials, that can undergo repetitive self-healing attracts recent scientific and commercial interest (Ebara et al. 2014; Syrett et al. 2010; White et al. 2001).

Varghese et al. (2001) reported that hydrogels prepared from acryloyl-6-aminocaproic acid precursors exhibit ideal hydrophobic and hydrophilic interaction balance that lets its side chains bond to exogenous metal ions (Varghese et al. 2001)

and to extracellular proteins (Ayala et al. 2011). Thus, the researchers claim that with their flexible side chains, the elastomeric acryloyl-6-aminocaproic acid-based hydrogels might mediate formation of hydrogen bonds across two hydrogel interfaces via amide and carboxylic groups (Phadke et al. 2012).

Metal-ligand interactions are also promising for self-healing of hydrogels as they are thermodynamically stable and kinetically labile. Furthermore, the reversibility can be tailored via the use of different metal ions. Sato et al. (2013) developed hydrogels that show fast self-healing via selective formation of metal-ligand complexes between determined metal ions and phosphate end groups of PEG. Rapid hydrogel formation was observed with the use of tri-valent metal ions with small radii such as Fe^{3+} , Al^{3+} , Ti^{3+} , and Ga^{3+} . The biomimetic phosphate-metal-ion-based self-healable hydrogels may find use in various biomedical applications (Ebara et al. 2014; Sato et al. 2013).

13 Future Trends

As mentioned in the preceding sections, environment-responsive or so-called 'smart' hydrogels have the unique capability to respond to changes that take place in different properties of the medium. This remarkable feature makes these interesting materials suitable to be used in various biomedical applications in terms of differing pH, temperature, ion concentrations, antigens, etc., found in the human body, or light, electrical, etc., stimuli that can be directed from a source outside. To give an example, an intensively studied area is controlled drug delivery system that utilizes the pH differences throughout the digestive tract.

The greatest drawback of hydrogels is their slow response. Hence, hydrogels presenting faster response should be developed. By preparing hydrogels thinner and smaller, the faster response may be achieved, but at the expense of mechanical strength. Another approach may be taken by preparing heterogeneous hydrogels such one possessing microporous structure to increase the contacting interface area between the polymer and water. Different polymer network architectures may also be investigated (Ebara et al. 2014). However, when trying to achieve faster responses, the mechanical performance should not be compromised (Kopeček 2007). Other future research studies may relate to designing hydrogels with enhanced biocompatibility and biodegradability via use of novel polymers and cross-linking agents (Ebara et al. 2014; Lee et al. 2013).

The biocompatibility that is the safety of any material to be used in the biomedical area is a major concern to be addressed. Similar to other biomedical materials, before clinical use, the safety of hydrogels should be proven. This cannot be realized without being in use for extended periods of time with showing no serious side effect. Thus, materials used in FDA-approved products can be preferred for hydrogel preparation (Lee et al. 2013).

Biodegradability is a feature that is required for materials to be used in vivo. To give an example, biodegradable implants do not necessitate additional surgical

operation for removal (Lee et al. 2013). In deed, the biodegradation should take place without releasing unwanted materials into the human organism (Yilmaz 2015b).

Besides experimental studies, theatrical research also greatly increases our knowledge of these environment-responsive materials. During the design of novel hydrogels, the investigation of structure-property relationships should not be omitted. The principles of supramolecular chemistry may be utilized when designing hydrogels with tailored properties. Protein engineering might also allow precision control over micro-structure of hydrogels (Ebara et al. 2014). Biomimetic/bioinspired approaches may be taken for hydrogel preparation (such as genetically engineering) or for its functioning (e.g., mimicking pancreas for diabetes treatment) (Lee et al. 2013).

Currently, there are a limited number of FDA-approved hydrogel-based clinical products. Thus, the clinical research lags behind hydrogel development studies. As most of the novel hydrogel design studies take place without considering the final application, an inevitable mismatch takes places between the properties of the designed material and the needs of the final application. This situation also contributes to the lag between the novel hydrogel development and clinical research (Lee et al. 2013).

To address the problem related to the incoordination between the hydrogel material design and application studies Lee et al. (2013) propose a research approach. According to the approach, the first step is the identification of the target application, and the second step is hydrogel material development. To be able to take this approach, the research team should have sound knowledge on the physiological requirements as well as an understanding of the structure-property relations and the preparation methodology of hydrogels (Lee et al. 2013).

14 Conclusion

Multicomponent, semi-IPN, or IPN hydrogels are interesting materials which are composed of at least of two different components and are able to respond to various stimuli, that is the change in certain properties of the medium such as temperature, pH, ion concentration, and so on. Based on this unique feature, these environmental-responsive materials may find use in biomedical applications in terms of changes in the properties of the medium in the human organism which occur naturally or induced by an outside source.

Environmental-responsive hydrogels respond to changes in the physical, chemical, biological properties of the medium by showing a change in their size, shape, color, solubility and so on. They can be fabricated from natural or synthetic components by a number of production methods including physical cross-linking and chemical cross-linking techniques as well as other novel fabrication methods such as cross-linking with genetically engineered protein domains.

Environmental-responsive hydrogels have found use in various subfields of the biomedical research area including drug delivery, biosensors, tissue engineering, and actuators. Whereas hydrogels are promising materials, they also entail some drawbacks which should be overcome, before these materials can be used clinically. To address the major concerns, the response rates should be increased while maintaining the necessary mechanical performance. Biodegradability and biocompatibility are other development fields. Environmentally responsive hydrogels with the desired properties can be prepared by use of the right components, production methods and forming the right polymer architecture.

References

- Agarwal AK, Sridharamurthy SS, Beebe DJ, Jiang H (2005) Programmable autonomous micromixers and micropumps. *J Microelectromech Syst* 14:1409–1421
- Akala Emmanuel O, Kopeckova Pavla, Kopecek Jindrich (1998) Novel pH-sensitive hydrogels with adjustable swelling kinetics. *Biomaterials* 19(11–12):1037–1047. doi:[10.1016/S0142-9612\(98\)00023-4](https://doi.org/10.1016/S0142-9612(98)00023-4)
- Al-Assaf S, Dickson P, Phillips GO, Thompson C, Torres JC (2009) Compositions comprising polysaccharide gums, vol WO2009/016362 A2. Phillips Hydrocolloid Research Limited (UK), Reckitt Benckiser (UK)
- Aoki H, Al-Assaf S, Katayama T, Phillips GO (2007a) Characterization and properties of *Acacia senegal* (L.) Willd. Var. Senegal with enhanced properties (Acacia (Sen) SUPER GUM(TM)): part 2—mechanism of the maturation process. *Food Hydrocolloids* 21:329–337
- Aoki H, Katayama T, Ogasawara T, Sasaki Y, Al-Assaf S, Phillips GO (2007b) Characterization and properties of *Acacia senegal* (L.) Willd. Var. Senegal with enhanced properties (Acacia (Sen) SUPER GUM(TM)): Part 5. Factors affecting the emulsification of *Acacia senegal* and Acacia (Sen) SUPER GUM(TM). *Food Hydrocoll* 21:353–358
- Asoh T-A, Kikuchi A (2010) Electrophoretic adhesion of stimuli-responsive hydrogels. *Chem Commun* 46:7793–7795
- Asoh T-A, Matsusaki M, Kaneko T, Akashi M (2008) Fabrication of temperature-responsive bending hydrogels with a nanostructured gradient. *Adv Mater* 20:2080–2083
- Ayala R, Zhang C, Yang D, Hwang Y, Aung A, Shroff SS, Arce FT, Lal R, Arya G, Varghese S (2011) Engineering the cell-material interface for controlling stem cell adhesion, migration, and differentiation. *Biomaterials* 32(15):3700–3711
- Bajpai AK, Shrivastava J (2005) In vitro enzymatic degradation kinetics of polymeric blends of crosslinked starch and carboxymethyl cellulose. *Polym Int* 54:1524–1536
- Banta S, Wheeldon IR, Blenner M (2010) Protein engineering in the development of functional hydrogels. *Annu Rev Biomed Eng* 12(1):167–186. doi:[10.1146/annurev-bioeng-070909-105334](https://doi.org/10.1146/annurev-bioeng-070909-105334)
- Bassik N, Abebe BT, Lafiin KE, Gracias DH (2010) Photolithographically patterned smart hydrogel based bilayer actuators. *Polymer* 50:6093–6098
- Beebe DJ, Moore JS, Bauer JM, Yu Q, Liu RH, Devadoss C, Jo B-H (2000) Functional hydrogel structures for autonomous flow control inside microfluidic channels. *Nature* 404:588–590
- Chang C, Zhang L (2011) Cellulosebased hydrogels: present status and application prospects. *Carbohydr Polym* 84:40–53
- Chang C, Zhang L, Zhou J, Zhang L, Kennedy JF (2010) Structure and properties of hydrogels prepared from cellulose in NaOH/urea aqueous solutions. *Carbohydr Polym* 82:122–127

- Chenite A, Chaput C, Wang D, Combes C, Buschmann MD, Hoemann CD, Leroux JC, Selmani A, Atkinson BL, Binette F (2000) Novel injectable neutral solutions of chitosan form biodegradable gels in situ. *Biomaterials* 21:2155–2161
- Costa-Almeida R, Tamayol A, Yazdi IK, Avci H, Fallahi A, Annabi N, Reis RL, Gomes ME, Khademhosseini A (2016) Mechanically reinforced hydrogel fibers for tendon tissue engineering. In: 5th Portuguese young chemists meeting (5th PYCheM) and 1st European young chemists meeting (1st EYCheM). Guimarães, Portugal
- Dai WS, Barbari TA (1999) Hydrogel membranes with mesh size asymmetry based on the gradient crosslinking of poly(vinyl alcohol). *J Membr Sci* 156:67–79
- de Jong SJ, De Smedt SC, Wahls MWC, Demeester J, Kettenes-van den Bosch JJ, Hennink WE (2000) Novel self-assembled hydrogels by stereocomplex formation in aqueous solution of enantiomeric lactic acid oligomers grafted to dextran. *Macromolecules* 33:3680–3686
- De La Rosa VR, Woisel P, Hoogenboom R (2016) Supramolecular control over thermoresponsive polymers. *Mater Today* 19(1):44–55. doi:10.1016/j.matod.2015.06.013
- de Nooy AEJ, Capitani D, Masci G, Crescenzi V (2000) Ionic polysaccharide hydrogels via the Passerini and Ugi multicomponent condensations: synthesis, behavior and solid-state NMR characterization. *Biomacromolecules* 1:259–267
- Dong L, Jiang H (2007) Autonomous microfluidics with stimuli-responsive hydrogels. *Soft Matter* 3:1223–1230
- Dusek K, Patterson D (1968) Transition in swollen polymer networks induced by intramolecular condensation. *J Polym Sci A* 6:1209–1216
- Ebara M, Kotsuchibashi Y, Narain R, Idota N, Kim Y-J, Hoffman JM, Uto K, Aoyagi T (2014) *Smart biomaterials*. Springer, Japan
- Ehrick JD, Deo SK, Browning TW, Bachas LG, Madou MJ, Daunert S (2005) Genetically engineered protein in hydrogels tailors stimuli-responsive characteristic. *Nat Mater* 4(4):298–302
- Eiselt P, Lee KY, Mooney DJ (1999) Rigidity of two-component hydrogels prepared from alginate and poly(ethylene glycol)-diamines. *Macromolecules* 32:5561–5566
- El-Sherbiny I, Yacoub N (2013) Hydrogel scaffolds for tissue engineering: progress and challenges. *Global Cardiol Sci Pract* 3:316–342. doi:10.5339/gcsp.2013.38
- Elvin CM, Carr AG, Huson MG, Maxwell JM, Pearson RD, Vuocolo T, Liyou NE, Wong DCC, Merritt DJ, Dixon NE (2005) Synthesis and properties of crosslinked recombinant pro-resilin. *Nature* 437:999–1002
- Esteban C, Severian D (2000) Polyionic hydrogels based on xanthan and chitosan for stabilising and controlled release of vitamins. WO0004086, issued 2000
- Feinberg AW, Feigel A, Shevkoplyas SS, Sheehy S, Whitesides GM, Parker KK (2007) Muscular thin films for building actuators and powering devices. *Science* 317:1366–1370
- Fernandez-Tarrio M, Yañez F, Immesoete K, Alvarez-Lorenzo C, Concheiro A (2008) Pluronic and tetronic copolymers with polyglycolized oils as self-emulsifying drug delivery systems. *AAPS PharmSciTech* 9(2):471–479
- Flory PJ (1942) Thermodynamics of high polymer solutions. *J Chem Phys* 10:51–61
- Gerlach G, Arndt K-F (2009) *Hydrogel sensors and actuators: engineering and technology*. Springer, New York
- Gong JP, Katsuyama Y, Kurokawa T, Osada Y (2003) Double-network hydrogels with extremely high mechanical strength. *Adv Mater* 15(14):1155–1158
- Gupta M, Gupta AK (2004) In-vitro cytotoxicity studies of hydrogels pullulan nanoparticles prepared by AOT/n-hexane micellar system. *J Pharm Pharm Sci* 7(1):38–46
- Gupta AK, Siddiqui AW (2012) Environmental responsive hydrogels: a novel approach in drug delivery system. *J Drug Deliv Therap* 2(1):1–8. http://www.academia.edu/1389831/ENVIRONMENTAL_RESPONSIVE_HYDROGELS_A_NOVEL_APPROACH_IN_DRUG_DELIVERY_SYSTEM
- Haraguchi K, Takehisa T (2002) Nanocomposite hydrogels: a unique organic ± inorganic network structure with extraordinary mechanical, optical, and swelling/de-swelling properties. *Adv Mater* 14(16):1120–1124

- Hassan CM, Doyle FJI, Peppas NA (1997) Dynamic behavior of glucose-responsive poly (methacrylic acid-g-ethylene glycol) hydrogels. *Macromolecules* 30:6166–6173
- Hennink WE, Nostrum CF (2002) Novel crosslinking methods to design hydrogels. *Adv Drug Deliv Rev* 54:13–36
- Hoffman AS (1997) Intelligent polymers. In: Park K (ed) *Controlled drug delivery: challenge and strategies*. American Chemical Society, Washington, DC, pp 485–497
- Hoffman AS (2002) Hydrogels for biomedical applications. *Adv Drug Deliv Rev* 54:3–12
- Hovgaard L, Brondsted H (1995) Dextran hydrogels for colon-specific drug delivery. *J Control Release* 36(1–2):159–166. doi:[10.1016/0168-3659\(95\)00049-E](https://doi.org/10.1016/0168-3659(95)00049-E)
- Hrouz J, Ilavský M, Ulbrich K, Kopeček J (1981) The photoelastic behaviour of dry and swollen networks of poly(N,N-diethylacrylamide) and of its copolymers with N-Tert. butylacrylamide. *Eur Polym J* 17:361–366
- Hu Z, Zhang X, Li Y (1995) Synthesis and application of modulated polymer gels. *Science* 269:525–527
- Hua L (2009) *Smart hydrogel modelling*. Springer, New York
- Huang CC, Ravindran S, Yin Z, George A (2014) 3-D self-assembling leucine zipper hydrogel with tunable properties for tissue engineering. *Biomaterials* 35(20):5316–5326
- Huggins ML (1942) Some properties of solutions of long-chain compounds. *J Phys Chem* 46:151–158
- Jafari B, Rafie F, Davaran S (2011) Preparation and characterization of a novel smart polymeric hydrogel for drug delivery of insulin. *BioImpacts* 1:135–143
- Jameela SR, Jayakrishnan A (1995) Glutaraldehyde cross-linked chitosan microspheres as a long acting biodegradable drug delivery vehicle: studies on the in vitro release of mitoxantrone and in vivo degradation of microspheres in rat muscle. *Biomaterials* 16:769–775
- Jin Y, Yamanaka J, Sato S, Miyata I, Yomota C, Yonese M (2001) Recyclable characteristics of hyaluronate-polyhydroxyethyl acrylate blend hydrogel for controlled releases. *J Control Release* 73:173–181
- Jin R, Moreira Teixeira LS, Dijkstra PJ, Karperien M, van Blitterswijk ZY, Zhong CA, Feijena J (2009) Injectable chitosan-based hydrogels for cartilage tissue engineering. *Biomaterials* 30 (13):2544–2551
- Kang SI, Bae YH (2003) A sulfonamide based glucose-responsive hydrogel with covalently immobilized glucose oxidase and catalase. *J Control Release* 86(1):115–121
- Khan GMA, Yilmaz ND, Yilmaz K (2016) Recent developments in design and manufacturing of biocomposites of bombyx mori silk fibroin. In: *Handbook of composites from renewable materials*. Wiley Scrivener, USA
- Khodamoradi N, Khodamoradi P (2014) A brief review on application of smart hydrogels in drug delivery. In: *International conference on chemistry, biomedical and environment engineering*, Antalya, pp 28–33. doi:[10.17758/IAAST.A1014025](https://doi.org/10.17758/IAAST.A1014025)
- Kim W (2013) Recombinant protein polymers in biomaterials. *Front Biosci* 18:289–304
- Kim JJ, Park K (2001) Modulated insulin delivery from glucose-sensitive hydrogel dosage forms. *J Control Release* 77(1–2):39–47
- Kim MS, Park K (2012) Injectable hydrogels. In: B Bhusnan (ed). Springer, Berlin
- Kim SJ, Yoon SG, Lee SM, Lee JH, Kim SI (2003) Characteristics of electrical responsive alginate/poly(diallyldimethylammonium chloride) IPN hydrogel in HCl solutions. *Sens Actuators B Chem* 96(1–2):1–5
- Kim S, Chung EH, Gilbert M, Healy KE (2005) Synthetic MMP-13 degradable ECMs based on poly(N-isopropylacrylamide-Co-acrylic acid) semi-interpenetrating polymer networks. I. Degradation and cell migration. *J Biomed Mater Res Part A* 75A:73–88
- Kim Y-J, Ebara M, Aoyagi T (2012) A smart nanofiber web that captures and releases cells. *Angew Chem Int* 51:10537–10541
- Kopeček J (2007) Hydrogel biomaterials: a smart future? *Biomaterials* 28(34):5185–5192
- Kopeček J, Yang J (2009) Peptide-directed self-assembly of hydrogels. *Acta Biomater* 5(3):805–816. doi:[10.1126/scisignal.2001449.Engineering](https://doi.org/10.1126/scisignal.2001449.Engineering)
- Kuijpers AJ, van Wachem PB, van Luyn MJA, Engbers GHM, Krijgsveld J, Zaat SAJ, Dankert J, Feijen J (2000) In vivo and in vitro release of lysozyme from cross-linked gelatin hydrogels: a

- model system for the delivery of antibacterial proteins from prosthetic heart valves. *J Control Release* 67:323–336
- Kumar A, Srivastava A (2010) Cell separation using cryogel-based affinity chromatography. *Nat Protoc* 5:1737–1747. doi:[10.1038/nprot.2010.135](https://doi.org/10.1038/nprot.2010.135)
- Langer R, Vacanti J (1993) Tissue engineering. *Science* 260:920–926
- Lee KK, Cussler EL, Marchetti M, McHugh MA (1990) Pressure-dependent phase transitions in hydrogels. *Chem Eng Sci* 45:766–767
- Lee ES, Gao Z, Bae YH (2008) Recent progress in tumor pH targeting nanotechnology. *J Control Release* 132:164–170
- Lee SC, Kwon IK, Park K (2013) Hydrogels for delivery of bioactive agents: a historical perspective. *Adv Drug Deliv Rev* 65(1):17–20. doi:[10.1016/j.addr.2012.07.015](https://doi.org/10.1016/j.addr.2012.07.015)
- Li Y, Liu C, Tan Y, Xu K, Lu C, Wang P (2014) In situ hydrogel constructed by starch-based nanoparticles via a Schiff base reaction. *Carbohydr Polym* 110:87–94
- Lim DW, Park TG (2000) Stereocomplex formation between enantiomeric PLA–PEG–PLA triblock copolymers: characterization and use as protein-delivery microparticulate carriers. *J Appl Polym Sci* 75:1615–1623
- Lim HL, Hwang Y, Kar M, Varghese S (2014) Smart hydrogels as functional biomimetic systems. *Biomater Sci* 2(5):603–618. doi:[10.1039/c3bm60288e](https://doi.org/10.1039/c3bm60288e)
- Luchini A, Geho DH, Bishops B, Tran D, Xia C, Dufour RL, Jones CD et al (2008) Smart hydrogel particles: biomarker harvesting: one-step affinity purification, size exclusion, and protection against degradation. *Nano Lett* 8(1):350–361. doi:[10.1021/nl072174l](https://doi.org/10.1021/nl072174l)
- Luchnikov V, Sydorenko O, Stamm M (2005) Self-rolled polymer and composite polymer/metal micro- and nanotubes with patterned inner walls. *Adv Mater* 17:1177–1182
- Luo Y, Kirker KR, Prestwich GD (2000) Cross-linked hyaluronic acid hydrogel films: new biomaterials for drug delivery. *J Control Release* 69:169–184
- Lutolf MP, Hubbell JA (2005) Synthetic biomaterials as instructive extracellular microenvironments for morphogenesis in tissue engineering. *Nat Biotech* 23:47–55
- Maeda S, Hara Y, Sakai T, Yoshida R, Hashimoto S (2007) Self-walking gel. *Adv Mater* 19:3480–3484
- Magnin D, Lefebvre J, Chornet E, Dumitriu S (2004) Physicochemical and structural characterization of a polyionic matrix of interest in biotechnology, in the pharmaceutical and biomedical fields. *Carbohydr Polym* 55(4):437–453
- Martens P, Anseth KS (2000) Characterization of hydrogels formed from acrylate modified poly (vinyl alcohol) macromers. *Polymer* 41:7715–7722
- Mateescu A, Wang Y, Dostalek J, Jonas U (2012) Thin hydrogel films for optical biosensor applications. *Membranes* 2(1):49–69. doi:[10.3390/membranes2010040](https://doi.org/10.3390/membranes2010040)
- Matsumoto A, Ishii T, Nishida J, Matsumoto H, Kataoka K, Miyahara Y (2012) A synthetic approach toward a self-regulated insulin delivery system. *Angew Chem Int Ed* 51:2124–2128
- Maziad NA, El-hamouly S, Zied E, El-Kelani TA, Nasef NR (2015) Radiation preparation of smart hydrogel has antimicrobial properties for controlled release of ciprofloxacin in drug delivery systems. *Asian J Pharm Clin Res* 8(3):193–200
- Megeed Z, Cappello J, Ghandehari H (2002) Genetically engineered silk-elastinlike protein polymers for controlled drug delivery. *Adv Drug Deliv Rev* 54:1075–1091
- Millon LE, Wan WK (2006) The polyvinyl alcohol-bacterial cellulose system as a new nanocomposite for biomedical applications. *J Biomed Mater Res B Appl Biomater* 79(2):245–253
- Millon LE, Guhadós G, Wan W (2008) Anisotropic polyvinyl alcohol-bacterial cellulose nanocomposite for biomedical applications. *J Biomed Mater Res Part B Appl Biomater* 86(2):444–452. doi:[10.1002/jbm.b.31040](https://doi.org/10.1002/jbm.b.31040)
- Miyata T, Asami N, Urugami T (1999) A reversibly antigen-responsive hydrogel. *Nature* 399:766–769
- Miyata T, Urugami T, Nakamae K (2002) Biomolecule-sensitive hydrogels. *Adv Drug Deliv Rev* 54(1):79–98. doi:[10.1016/S0169-409X\(01\)00241-1](https://doi.org/10.1016/S0169-409X(01)00241-1)
- Miyata T, Jige M, Nakaminami T, Urugami T (2006) Tumor marker-responsive behavior of gels prepared by biomolecular imprinting. *Proc Natl Acad Sci U S A* 103:1190–1193

- Molinaro G, Leroux J-C, Damas J, Adam A (2002) Biocompatibility of thermosensitive chitosan-based hydrogels: an in vivo experimental approach to injectable biomaterials. *Biomacromolecules* 23:2717–2722
- Morimoto N, Hirano S, Takahashi H, Loethen S, Thompson DH, Akiyoshi K (2013) Self-assembled pH-sensitive cholesteryl pullulan nanogel as a protein delivery vehicle. *Biomacromolecules* 14(1):56–63
- Moschou EA, Bachas LG, Daunert S (2008) Smart hydrogel materials. Handbook of biosensors and biochips. Part three. Wiley, New York
- Murakami Y, Maeda M (2005) DNA-responsive hydrogels that can shrink or swell. *Biomacromolecules* 6(6):2927–2929
- Murdan S (2003) Electro-responsive drug delivery from hydrogels. *J Control Release* 92(1–2):1–17. doi:10.1016/S0168-3659(03)00303-1
- Na K, Bae YH (2004) Self assembled hydrogel nanoparticles responsive to tumor extracellular pH from pullulan derivative/sulfonamide conjugate: characterization, aggregation and adriamycin release in-vitro. *Pharm Res* 19(5):681–688
- Naderi-Meshkin H, Andreas K, Matin MM, Sittinger M, Bidkhorri HR, Ahmadiankia N, Bahrami AR, Ringe J (2014) Chitosan-based injectable hydrogel as a promising in situ forming scaffold for cartilage tissue engineering. *Cell Biol Int* 38(1):72–84
- Nagarkar S, Nicolai T, Chassenieux C, Lele A (2010) Structure and gelation mechanism of silk hydrogels. *Phys Chem Chem Phys* 12(15):3834–3844. doi:10.1039/b916319k
- Ogihara NL, Ghirlanda G, Bryson JW, Gingery M, DeGrado WF, Eisenberg D (2001) Design of three-dimensional domain-swapped dimers and fibrous oligomers. *Proc Natl Acad Sci* 98:1404–1408
- Okumura Y, Ito K (2001) The polyrotaxane gels: a topological gel by figure-of-eight cross-links. *Adv Mater* 13:485–487
- Okuzaki H, Hosaka K, Suzuki H, Ito T (2010) Effect of temperature on humido-sensitive conducting polymer actuators. *Sens Actuators A Phys* 157:96–99
- Osada Y, Okuzaki H, Hori H (1992) A polymer gel with electrically driven motility. *Nature* 355:242–244
- Oya T, Enoki T, Grosberg AY, Masamune S, Sakiyama T, Takeoka Y, Tanaka K et al (1999) Reversible molecular adsorption based on multiple-point interaction by shrinkable gels. *Science* 286:1543–1545
- Paleos GA (2012) What are hydrogels? <http://pittsburghplastics.com/assets/files/WhatAreHydrogels.pdf>
- Peppas NA (2004) Hydrogels. In: Ratner BD (ed) *Biomaterials science: an introduction to materials in medicine*. Academic Press, California, pp 100–107
- Peppas NA, Klier J (1991) Controlled release by using poly(methacrylic acid-g-ethylene glycol) hydrogels. *J Control Release* 16:203–214
- Petka WA, Harden JL, McGrath KP, Wirtz D, Tirrell DA (1998) Reversible hydrogels from self-assembling artificial proteins. *Science* 281:389–392
- Phadke A, Zhang C, Arman B, Hsu C-C, Mashelkar RA, Lele AK, Tauber MJ, Arya G, Varghese S (2012) From the cover: rapid self-healing hydrogels. *Proc Natl Acad Sci* 109(12):4383–4388. doi:10.1073/pnas.1201122109
- Pickup JC, Hussain F, Evans ND, Rolinski OJ, Birch DJS (2005) Fluorescence-based glucose sensors. *Biosens Bioelectron* 20(12):2555–2565. doi:10.1016/j.bios.2004.10.002
- Pourjavadi A, Zohuriaan-Mehr MJ (2002) Modification of carbohydrate polymers via grafting in air. 2. Ceric-Initiated graft copolymerization of acrylonitrile onto natural and modified polysaccharides. *Starch-Starke* 54:482–488
- Pourjavadi A, Barzegar S, Zeidabadi F (2007) Synthesis and properties of biodegradable hydrogels of κ -carrageenan grafted acrylic acid-Co-2-acrylamido-2-methylpropanesulfonic acid as candidates for drug delivery systems. *React Funct Polym* 67(7):644–654
- Priya James H, John R, Alex A (2014) Smart polymers for the controlled delivery of drugs—a concise overview. *Acta Pharm Sin B* 4(2):120–127. doi:10.1016/j.apsb.2014.02.005

- Qiu Y, Park K (2001) Environment-sensitive hydrogels for drug delivery. *Adv Drug Deliv Rev* 53(3):321–339
- Qiu Y, Park K (2012) Environment-sensitive hydrogels for drug delivery. *Adv Drug Deliv Rev* 64:49–60. doi:10.1016/j.addr.2012.09.024
- Rolinski OJ, Birch DJS, McCartney LJ, Pickup JC (2001) Sensing metabolites using donor–acceptor nanodistributions in fluorescence resonance energy transfer. *Appl Phys Lett* 78:2796–2798
- Sadeghi M (2011) Synthesis of starch-g-poly(acrylic acid-co-2-hydroxy ethyl methacrylate) as a potential pH-sensitive hydrogel-based drug delivery system. *Turk J Chem* 35:723–733
- Said HM, Alla SGA, El-Naggar AWM (2004) Synthesis and characterization of novel gels based on carboxymethyl cellulose/acrylic acid prepared by electron beam irradiation. *React Funct Polym* 61:397–404
- Salinas CN, Cole BB, Kasko AM, Anseth KS (2007) Chondrogenic differentiation potential of human mesenchymal stem cells photoencapsulated within poly(ethylene glycol)-arginine-glycine-aspartic acid-serine thiol-methacrylate mixed-mode networks. *Tissue Eng* 13:1025–1034
- Sandeep C, Harikumar SL, Kanupriya (2012) Hydrogels: a smart drug delivery system. *Int J Res Pharm Chem* 2(3):603–614
- Sato T, Ebara M, Tanaka S, Asoh T-A, Kikuchi A, Aoyagi T (2013) Rapid self-healable poly(ethylene glycol) hydrogels formed by selective metal-phosphate interactions. *PCCP* 15:10628–10635
- Shi J, Guobao W, Chen H, Zhong W, Qiu X, Xing MMQ (2014) Schiff based injectable hydrogel for in situ pH-triggered delivery of doxorubicin for breast tumor treatment. *Polym Chem* 5:6180–6189
- Smart Hydrogels for Biomedical Applications (2015) Aachen
- Stile RA, Burghardt WR, Healy KE (1999) Synthesis and characterization of injectable poly(N-Isopropylacrylamide)-based hydrogels that support tissue formation in vitro. *Macromolecules* 32:7370–7379
- Stoychev G, Puretskiy N, Ionov L (2011) Self-folding all-polymer thermoresponsive microcapsules. *Soft Matter* 7:3277–3279
- Strain DE, Kennelly RG, Dittmar HR (1939) Methacrylate resins. *Ind Eng Chem* 31:382–387
- Sumaru K, Ohi K, Takagi T, Kanamori T, Shinbo T (2006) Photoresponsive properties of poly(N-isopropylacrylamide) hydrogel partly modified with spirobenzopyran. *Langmuir* 22:4353–4356
- Syrett JA, Becer CR, Haddleton DM (2010) Self-healing and self-mendable polymers. *Polym Chem UK* 1:978–987
- Ta HT, Dass CR, Dunstan DE (2008) Injectable chitosan hydrogels for localised cancer therapy. *J Control Release* 126(3):205–216
- Tae G, Kornfeld JA, Hubbell JA (2005) Sustained release of human growth hormone from in situ forming hydrogels using self-assembly of fluoroalkyl-ended poly(ethylene glycol). *Biomaterials* 26(25):5259–5266
- Takashima Y, Hatanaka S, Otsubo M, Nakahata M, Kakuta T, Hashidzume A, Yamaguchi H, Harada A (2012) Expansion–contraction of photoresponsive artificial muscle regulated by host–guest interactions. *Nat Commun* 3:1270
- Takigami M, Amada H, Nagasawa N, Yagi T, Kasahara T, Takigami S, Tamada M (2007) Preparation and properties of CMC gel. *Trans Mater Res Soc Jpn* 32(3):713–716
- Tan H, Chub CR, Payneb KA, Marra KG (2009) Injectable in situ forming biodegradable chitosan–hyaluronic acid based hydrogels for cartilage tissue engineering injectable in situ forming biodegradable chitosan–hyaluronic acid based hydrogels for cartilage tissue engineering. *Biomaterials* 30(13):2499–2506
- Tanaka T (1978) Collapse of gels and the critical endpoint. *Phys Rev Lett* 40:820–823
- Tang M, Zhang R, Bowyer A, Eisenthal R, Hubble J (2004) NAD-sensitive hydrogel for the release of macromolecules. *Biotechnol Bioeng* 87:791–796
- Tanigo T, Takaoka R, Tabata Y (2010) Sustained release of water-insoluble simvastatin from biodegradable hydrogel augments bone regeneration. *J Control Release* 143:201–206

- Techawanitchai P, Ebara M, Idota N, Aoyagi T (2012a) Light-induced spatial control of pH jump reaction at smart gel interface. *Colloids Surf B Biointerfaces* 99:53–59
- Techawanitchai P, Ebara M, Idota N, Asoh T-A, Kikuchi A, Aoyagi T (2012b) Photoswitchable control of pH-responsive actuators via pH jump reaction. *Soft Matter* 8:2844–2851
- Thakur VK, Kessler MR (2014a) Free radical induced graft copolymerization of ethyl acrylate onto SOY for multifunctional materials. *Mater Today Commun* 1(1–2):34–41
- Thakur VK, Kessler MR (2014b) Synthesis and characterization of AN-g-SOY for sustainable polymer composites. *ACS Sustain Chem Eng* 2(10):2454–2460
- Thakur VK, Kessler MR (2015) Self-healing polymer nanocomposite materials: a review. *Polymer* 69:369–383
- Thakur VK, Thakur MK (2014a) Recent advances in graft copolymerization and applications of chitosan: a review. *ACS Sustain Chem Eng* 2(12):2637–2652
- Thakur VK, Thakur MK (2014b) Recent trends in hydrogels based on psyllium polysaccharide: a review. *J Clean Prod* 82:1–15
- Thakur VK, Thakur MK (2015) Recent advances in green hydrogels from lignin: a review. *Int J Biol Macromol* 72:834–847
- Thakur VK, Voicu SI (2016) Recent advances in cellulose and chitosan based membranes for water purification: a concise review. *Carbohydr Polym* 146:148–165
- Thakur VK, Thakur MK, Gupta RK (2013a) Graft copolymers from cellulose: synthesis, characterization and evaluation. *Carbohydr Polym* 97:18–25
- Thakur VK, Thakur MK, Gupta RK (2013b) Rapid synthesis of graft copolymers from natural cellulose fibers. *Carbohydr Polym* 98:820–828
- Thakur VK, Singha AS, Thakur MK (2013c) Synthesis of natural cellulose-based graft copolymers using methyl methacrylate as an efficient monomer. *Adv Polym Technol* 32(S1):E741–E748
- Thakur VK, Thakur MK, Gupta RK (2013d) Graft copolymers from natural polymers using free radical polymerization. *Int J Polym Anal Charact* 18(7):495–503
- Thakur MK, Thakur VK, Gupta RK, Pappu A (2016) Synthesis and applications of biodegradable soy based graft copolymers: a review. *ACS Sustain Chem Eng* 4(1):1–17
- Tsuji H, Horii F, Nakagawa M, Ikada Y, Odani H, Kitamaru R (1992) Stereocomplex formation between enantiomeric poly(lactic Acid)s. 7. Phase structure of the stereocomplex crystallized from a dilute acetonitrile solution as studied by high-resolution solid-state Carbon-13 NMR spectroscopy. *Macromolecules* 25:4114–4118
- Vakkalanka SK, Brazel CS, Peppas NA (1996) Temperature- and pH-sensitive terpolymers for modulated delivery of streptokinase. *J Biomater Sci Poly Ed* 8:119–129
- Valuev IL, Vanchugova LV, Valuev LI (2011) Glucose-sensitive hydrogel systems. *Polym Sci Ser A* 53(5):385–389. doi:10.1134/S0965545X11050099
- Vanag VK, Yang L, Dolnik M, Zhabotinsky AM, Epstein IR (2000) Oscillatory cluster patterns in a homogeneous chemical system with global feedback. *Nature* 406:389–391
- Varghese S, Lele AK, Srinivas D, Sastry M, Mashelkar RA (2001) Novel macroscopic self-organization in polymer gels. *Adv Mater* 13:1544–1548
- Vrana NE, O’Grady A, Kay E, Cahill PA, McGuinness GB (2009) Cell encapsulation within PVA-based hydrogels via freeze-thawing: a one-step scaffold formation and cell storage technique. *J Tissue Eng Regen Med* 3(7):567–572
- Wan W-K, Millon L (2006) Poly(vinyl alcohol)-bacterial cellulose nanocomposite. EP1660147 A1, issued 2006
- Wang C, Stewart RJ, Kopecek J (1999) Hybrid hydrogels assembled from synthetic polymers and coiled-coil protein domains. *Nature* 397(6718):417–420
- White SR, Sottos NR, Geubelle PH, Moore JS, Kessler MR, Sriram SR, Brown EN, Viswanathan S (2001) Autonomic healing of polymer composites. *Nature* 409:794–797
- Whitesides GM (2006) The origins and the future of microfluidics. *Nature* 442:368–373
- Wichterle O, Lim D (1960) Hydrophilic gels for biological use. *Nature* 185:117–118
- Williams CG, Malik AN, Kim TK, Manson PN, Elisseeff JH (2005) Variable cytocompatibility of six cell lines with photoinitiators used for polymerizing hydrogels and cell encapsulation. *Biomaterials* 26:1211–1218

- Xu C, Kopeček J (2008) Genetically engineered block copolymers: influence of the length and structure of the coiled-coil blocks on hydrogel self-assembly. *Pharm Res* 25(3):674–682
- Xu C, Breedveld V, Kopeček J (2005) Reversible hydrogels from self-assembling genetically engineered protein block copolymers. *Biomacromolecules* 6(3):1739–1749
- Kumar A (n.d.) Smart polymeric biomaterials: where chemistry and biology can merge
- Yanga J-A, Yeoma J, Hwanga BW, Hoffman AS, Hahn SK (2014) In situ-forming injectable hydrogels for regenerative medicine. *Prog Polym Sci* 39(12):1973–1986
- Yilmaz ND (2009) Acoustic properties of biodegradable nonwovens. NC State University, Raleigh
- Yilmaz ND (2015a) Agro-residual fibers as potential reinforcement elements for biocomposites. In: Thakur VK (ed) *Lignocellulosic polymer composites: processing, characterization and properties*. Wiley Scrivener, Hoboken, pp 233–270
- Yilmaz ND (2015b) Biomedical applications of microbial cellulose nanocomposites. In: *Biodegradable polymeric nanocomposites: advances in biomedical applications*. Wiley Scrivener, Hoboken, pp 231–249
- Yilmaz ND, Powell NB (2015) Biocomposite structures as noise control elements. In: Thakur VK, Kessler M (eds) *Green biorenewable biocomposites: from knowledge to industrial applications*, vol 405. Apple Academic Press/CRC Press, Boca Raton
- Yilmaz ND, Cilgi GK, Yilmaz K (2015) Natural polysaccharides as pharmaceutical excipients. In: Thakur VK, Thakur MK (eds) *Handbook of polymers for pharmaceutical technologies*, Volume 3, biodegradable polymers. Wiley Scrivener, Hoboken, pp 483–516
- Yilmaz ND, Khan GMA, Yilmaz K (2016) Biofiber reinforced acrylated epoxidized soybean oil (AESO) Composites. In: Thakur VK, Thakur MK (eds) *Handbook of composites from renewable materials*. Wiley Scrivener, Hoboken
- Yoshida R, Okano T (2010) Stimuli-responsive hydrogels and their application to functional materials. In: Ottenbrite RM, Park K, Okano T (eds) *Biomedical applications of hydrogels handbook*. Springer, New York, pp 19–43
- Zhang X, Pint CL, Lee MH, Schubert BE, Jamshidi A, Takei K, Ko H et al (2011) Optically- and thermally-responsive programmable materials based on carbon nanotube-hydrogel polymer composites. *Nano Lett* 11:3239–3244
- Zhang C, Losego MD, Braun PV (2013) Hydrogel-based glucose sensors: effects of phenylboronic acid chemical structure on response. *Chem Mater* 25(15):3239–3250
- Zhao QS, Ji QX, Xing K, Li XY, Liu CS, Chen XG (2009) Preparation and characteristics of novel porous hydrogel films based on chitosan and glycerophosphate. *Carbohydr Polym* 76:410–416

Chapter 11

Emulgels: Application Potential in Drug Delivery

Amit Verma, Ankit Jain, Ankita Tiwari and Sanjay K. Jain

Abstract Emulgels have been extensively employed as emerging drug delivery systems for the administration of lipophilic or hydrophobic drugs, particularly as a boon for dermal health and cosmetic science. Emulgels are considered as emulsions of either oil-in-water (O/W) or water-in-oil (W/O) type in which the gels are incorporated. The emulgels are not only increasing the stability of entrapped bioactive, but are also controlling its release. Permeation enhancers such as isopropyl alcohol (IPA) and polyethylene glycol (PEG) facilitate the percutaneous absorption of drug. The comprehensive investigation of rheological behaviour and release characteristics of emulgels are significant aspects for successful design and development of the emulgels. In this chapter, the key parameters related to preparation, characterization and evaluation of emulgels are discussed. Moreover, their applications in drug delivery are also elaborated.

Keywords Emulgel · Drug delivery · Emulsions · Topical drug delivery
Cosmetics

1 Introduction

Since many decades, human beings have been facing several illness/infections/diseases which can affect their health and well-being. Various attempts are made in the discovery of several drugs, medicine and drug delivery systems administered through different routes to manage or cure such type of diseases and to achieve

A. Verma · A. Tiwari · S.K. Jain (✉)
Pharmaceutics Research Projects Laboratory, Department of Pharmaceutical Sciences,
Dr. Hari Singh Gour Central University, Sagar 470 003, Madhya Pradesh, India
e-mail: drskjainin@yahoo.com

A. Jain
Institute of Pharmaceutical Research, GLA University, NH-2, Mathura-Delhi Road,
Mathura 281406, Uttar Pradesh, India

© Springer International Publishing AG 2018
V.K. Thakur and M.K. Thakur (eds.), *Functional Biopolymers*,
Springer Series on Polymer and Composite Materials,
https://doi.org/10.1007/978-3-319-66417-0_11

better therapeutic benefits. Topical route is the most preferable route for the skin disorders (Kumari et al. 2016).

Drug delivery systems applied topically have several benefits over other formulations such as capability to deliver drug specifically to the site of action as well as overcome the problems associated with oral administration of drug such as GIT incompatibility and first pass effect which in turn improves bioavailability of entrapped drug (Subudhi et al. 2015; Jain and Jain 2015a). The percutaneous absorption of the topically applied drug may be enhanced by addition of permeation enhancers and improving drug release from the topical formulation (Kikwai et al. 2005; Moshfeghi and Peyman 2005; Rosen and Abribat 2005; Jain and Jain 2016a).

After the 1980s, the emulsion-based gels have been widely accepted for the dermatological application due to their oily nature and good retention and penetration power. Emulgels are most widely used in the cosmetics and pharmacy for the local and systemic effects of the entrapped drug. It is also a good carrier for the hydrophilic drugs as it facilitates drug penetration into the skin. The O/W type of emulgel systems can be easily removed with water when it is required. Hence, it is also called as water-washable emulgel system (Khunt et al. 2012; Singla et al. 2012). Emulgel is a drug delivery system with gel-like consistency and three-D cross-linked polymeric network which entraps the aqueous or hydro-alcoholic material in huge amount (Kumar and Verma 2010). There are two types of emulgels, i.e. oil-in-water and water-in-oil which are used for drug delivery (Mohamed 2004). The drug is entangled in the cross-linked network of emulgel that favours controlled drug release for a long period (Fig. 1).

The bioadhesive nature of emulgel provides prolonged duration of contact with the skin (Alexander et al. 2011). The emulsion and gel properties of emulgel provide better control of drug release on topical application (Jain et al. 2011). Due to washable nature of oil-in-water emulgels, they are widely used in general cosmetic preparations, while water-in-oil emulgels which are emollient in nature, are used more frequently for the skin diseases and (Mohamed 2004; Elbayoumi and Torchilin 2008; Torchilin 2008; Alexander et al. 2012). Emulsions with a thixotropic character possess an enhanced penetrability in the skin, so, when such emulsions are formulated into gel-based preparations, they provide an improved stability and enhanced penetrability. These types of gel-based systems have several

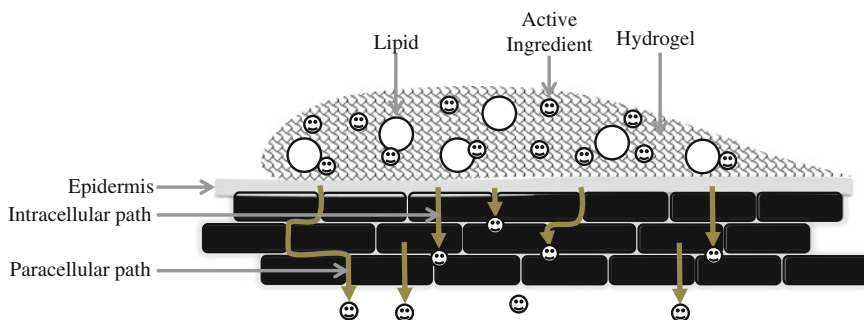


Fig. 1 Schematic representation of Emulgel diffusion via skin layers

properties such as thixotropy, greaselessness, quick spreadability, ease of removability, emollience, non-stainability, competency with several excipients and miscibility with various therapeutics make them a suitable candidate for topical applications (Panwar et al. 2011; Sarisozen et al. 2012). The better stability and optimum release characteristics depend on the type and amount of polymer employed to form the gel matrix (Kale and Torchilin 2007a, b, Jain and Jain 2016b). But, emulgel also has few limitations like poor penetration of macroparticulate system through skin and sometimes causes bubble entrapment during the formulation (Joshi et al. 2011). However, emulgels exhibit various benefits of both emulsions and gels and have better acceptability for patients. It can be easily employed onto the skin surface due its non-greasy behaviour as compared to other conventional systems such as creams, ointments which are too much thick and greasy in nature and expect extra rubbing (Weissig et al. 2000).

Emulsion based (oil-in-water) systems entrap hydrophobic drugs in the oil compartment and release the drug in a slow manner onto the skin via external compartment of emulgel. Hence, recently emulgel systems have been employed as a potential topical drug delivery system for the delivery of lipophilic drugs, i.e. ketoconazole, acyclovir, diclofenac and calcipotriol (Badilli et al. 2011, 2013, 2014; Dixit et al. 2011; Caddeo et al. 2013).

Nowadays, several diseases and infections caused by bacterial, viral and fungal species, i.e. eczema, *Herpes simplex*, acne have been treated by the use of emulgel-based preparations (Raut et al. 2012). Scientists have worked on emulgel preparations containing antifungal drugs which have been used in the treatment of various fungal diseases such as candidiasis and also evaluated the efficacy of such formulations. (Ghorab et al. 2011; Mundada and Avari 2011). Emulgel preparations have been explored for benefits in combating infections caused by fungi. Researchers are trying to develop emulgels of different drugs which may be helpful in treating several dermatological disorders (Utreja et al. 2011; Caddeo et al. 2013; Rahmani-Neishaboor et al. 2013).

1.1 Benefits of Emulgel Drug Delivery System

Emulgels are usually used as topical drug delivery system, but they can be administered through other routes of administration (i.e. buccal, rectal, etc.). It has numerous advantages in the field of cosmetics and dermatology. It could serve as a potential drug delivery system in context of better stability, longer retention time and incorporation ability of various drugs. Benefits of emulgel are summarized in Fig. 2.

1.1.1 Incorporation of Lipophilic Drugs

In the gel formulation, the hydrophobic drug does not get easily incorporated in system due to its limited solubility which in turn affects its release profile. Emulgel

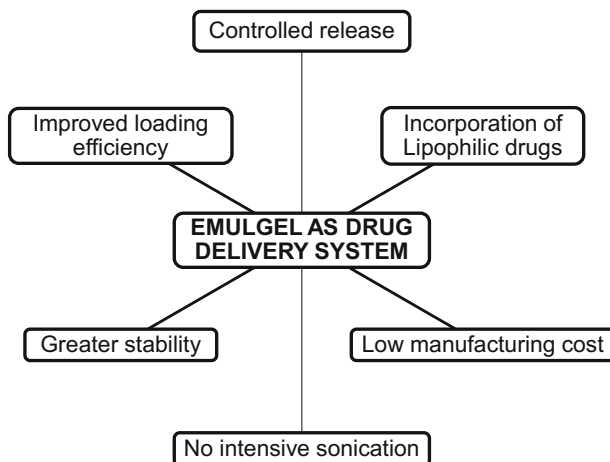


Fig. 2 Advantages of emulgel as drug delivery system

is a promising carrier system for lipophilic drugs. Since, emulgel formulation contains an emulsion system, lipophilic drug can be easily incorporated in the oil phase of preparation. This feature of emulgel provides improved stability and better release of therapeutics from the formulation.

1.1.2 Improved Loading Efficiency

Several nano-sized particulate and vesicular carrier systems show dose dumping or drug leakage due to their structure resulting in poor entrapment efficacy. However, gel-based system has a network of polymer with emulsion environment that can easily entangle the drug, which results in a greater loading of drug than others.

1.1.3 Greater Stability

Emulgels depict better stability as compared to other topical formulations such as creams and ointments. Creams exhibit problem of phase inversion or cracking whereas, rancidity is the most common problem associated with ointment preparations employing oil. Usually, emulgel-based preparations do not show such problems.

1.1.4 Feasibility of Manufacturing with Low Cost

Ingredients like oil, polymer, etc. which are used in the manufacturing of emulgels have low cost and an ease of availability which in turn decreases the cost of

emulgel. Preparation methods for the emulgel are less complicated and tedious which do not require any specialized instruments.

1.1.5 Controlled Release

The drug molecules are entrapped in the network-like structures of emulgel, which results in a slow and controlled release of entrapped drug.

1.1.6 No Intensive Sonication

The ultrasonication is required in most of the vesicular preparations which may cause degradation of the entrapped drug due to heat generation or high sonication energy but, formulation methods for emulgel do not require any sonication step (Panwar et al. 2011; Djordjevic et al. 2003).

2 Formulation Considerations for Emulgel

In recent years, several novel polymers have been discovered which provide enhanced gelling ability to the emulgel. Efficient emulsifiers are employed to decrease surface and interfacial tension and viscosity builders to increase the viscosity of the aqueous phase, resulting in a successful emulgel formulation (Gupta et al. 2010). By using the appropriate type and amount of gelling agent and oil phase, the rheological behaviour of emulgel could be effectively controlled.

2.1 Oil Phase Selection Criteria

Emulgel is the composite of simple emulsion with a gel and is gelled with the help of an appropriate gelling agent. On the basis of applications and compositions, the emulgels are of two types O/W (oil-in-water) and W/O (water-in-oil). The basic criteria for the selection of oil phase and relative quantity primarily depends on the final use of emulgel formulation. Various lipids of natural or synthetic origin are used as oil phase in different pharmaceutical- and cosmetic-based emulgel formulations. Numerous types of oil used in the formulation and development of emulgel have different characteristics and applications (Khan et al. 2013). The types and concentration of oil phase must be optimized during the development of emulgel formulation. The effect of oil phase can be assessed with the help of evaluation parameters like viscosity, permeability and stability. Geranium is one of them which is significantly employed for the formulation and development of emulgel due to its insecticidal and antibacterial activity. Geranium emulgel formulations are

applied in staunch bleeding, healing of wounds, ulcers, skin diseases and treatment of diarrhoea, dysentery and colic diseases. (Koshkaryev et al. 2011; Bowey et al. 2012). Emulgel containing garlic may be effectively used in burning wound healing (Ibrahim and Shehata 2012).

An investigation of ethanolic extracts of some plants like *Armelianobilis*, *Garcianaindica*, *Boehaviadiffusa*, *Solanum albicaule*, *Vitexnigundu*, *Buniunpersicum*, *Acacia concinna* and *Albizialebeck* demonstrated their antimicrobial potential against the bacterial and fungal species due to the presence of several essential oils as chemical constituents. (Sawant and Torchilin 2010). Molecule quercetin serves as an antioxidant and is available in different types of formulations, i.e. creams or gels but its high penetrability was explored when formulated in emulsion-based preparations. Hence, several oils which are obtained from various biological sources showed their ability in the development of emulgel preparation and also potentiated the effect of drug due to their own therapeutic value. Several oil phases employed for the manufacturing of emulgel are being discussed in Table 1.

Shahin et al. (2011a, b) utilized the jojoba oil as oil phase and formulated the clotrimazole containing antifungal emulgel. The combination of both jojoba oil and clotrimazole produces the synergistic effect and effectively reduced the inflammation (Shahin et al. 2011a). Different animal models have been used to describe this anti-inflammatory effect to combat inflammation (Habashy et al. 2005). Perioli et al. (2008) developed a buccal emulgel formulation by using neutral lipid glycerol behenate as oil phase (Compritrol[®]888ATO). This emulsion system was effectively prepared using low to medium oil phase content (oil to water ratio is from 0.3 to 0.4). The viscosity of the formulation was acceptable for syringeability and injectability in case of parenteral administration with the help of pre-filled syringes (Perioli et al. 2008). Liquid paraffin and mineral oils can also be used as oil components for many emulgel preparations (Deveda et al. 2010; Khullar et al. 2012). The type of gelling agent and amount of both emulsifier and oil phase affect the drug release pattern from the emulgel system. This was analysed by the use of 2³ factorial designs. Different evaluation parameters like physical appearance, rheological behaviour, drug release, antifungal property and stability were used to investigate this emulgel system. The liquid paraffin in low amount with high concentration of emulsifier satisfied the criteria of material of choice for the HMPc-based emulgel formulation. Cetostearyl alcohol was employed as oil phase for the formulation of a vaginal emulgel. This vaginal emulgel containing benzydamine (0.5% w/w) was evaluated for mucoadhesion force, rheological behaviour and release characteristic and compared with marketed vaginal cream of Tantum Rosa. It was observed that cetostearyl alcohol containing emulgel explored highest adhesion force about 0.57 N. The oil phase present between the chains of polymeric network produced an open and stretched structure having an ability to attach the various groups onto the mucosal surface. At that time, cetostearyl alcohol due to its emulsification characteristics participated in the emulsion stability. Several oil phases employed in the emulgel formulations which affect drug release feature and other properties are described in Table 2.

Table 1 Several oil phases employed for the manufacturing of emulgel

Category	Oils with their Source	Inherent property	Reported formulations	Benefits as Emulgel formulations	Drug incorporated	References
Vegetable oil	Castor oil/ <i>Ricinus communis</i>	Anti-inflammatory and antioxidant	Ointment, microemulsions, nanoemulsions, creams	Efficient anti-inflammatory drug formulated with castor oil based Emulgel preparations which can be applied effectively for the treatment of arthritis and other inflammation conditions	Topical NSAIDs and antioxidants	Maissa et al. (2010), Zhu et al. (2006) and Lawrence and Rees (2012)
	Olive oil/ <i>Olea europaea</i>	Moisturizer, antioxidant and anti-cancer	Emulsions, microemulsions	Olive oil has antioxidant and moisturizing effect and can be used in the formulation of emulgel based cosmetic preparations	Antioxidants and antimicrobials	Di Mattia et al. (2009), Lupi et al. (2012) and Hartman et al. (2009)
	Wheat germ oil/ <i>Triticum aestivum</i>	Anti-inflammatory and antioxidant	Microemulsions, lotions, Cream	Emulgel based cosmetic preparation formulated with wheat germ oil potentially treats skin disorder like eczema, psoriasis, sun burn	Topical steroids, topical NSAIDs and drugs for psoriasis	Karabacak et al. (2011), Malecka (2002) and Jing et al. (2003)
	Thyme oil/ <i>Thymus vulgaris</i> L.	Antispasmodic, anti-rheumatic and Bactericidal	Biodegradable film, nanoemulsions, cream	Emulgel formulated with thyme oil which shows synergistic effect with antibacterial drug and is utilized for the treatment of bacterial infections like B-Colitis, infections in urethra, genitals as well as on wound	Topical antibiotics, topical NSAIDs	Pires et al. (2011), Ziani et al. (2011), Lee et al. (2005) and Lu et al. (2011)
	Balsam oil/ <i>Myroxylon balsamum</i> Linn.	Antibacterial, anti-parasitic, antiseptic and antifungal	Gel, emulsion, ointment	Balsam oil based emulgel preparation can be employed in parasitic infections such as ringworm, itch mite, eggs and scabies	Antifungals and topical antibiotics	Beitz (2005)
	Myrrh oil/ <i>Commiphora myrrha</i>	Antimicrobial, antiviral and antifungal	Emulsion, gel	Emulgel preparations containing myrrh oil are effectively used in the treatment of viral infections like measles, pox, mumps and fungal diseases	Antifungal and antiviral	Tipton et al. (2003)

(continued)

Table 1 (continued)

Category	Oils with their Source	Inherent property	Reported formulations	Benefits as Emulgel formulations	Drug incorporated	References
	Birch oil/ <i>Betula alba</i>	Analgescic, antiseptic	Cream, ointment, gel	Formulation of emulgel with birch oil may become suitable analgesic for effective treatment of sore muscles, sprains and painful joints due to its anti-inflammatory and antispasmodic properties	Topical NSAIDs, corticosteroids and antimicrobials	Jager et al. (2008)
	Rose hip oil/wild rose bush (<i>Rosa moschata</i> or <i>Rosa rubiginosa</i>)	Antibacterial	Lotion, gel	Emulgel preparations with rose hip oil are used for treatment of acne, scars, eczema because of its anti-inflammatory action	Topical steroids and topical NSAIDs drugs	Machmudah et al. (2007) and Kirkeskov et al. (2011)
Synthetic	Isopropyl myristate	Emollient, moisturizer	Micro emulsion, emulsions and gel	Emulgel developed with Isopropyl myristate can be used suitably for treatment the of skin disorders like acne	Drugs for acne, topical steroids	Podlogar et al. (2004), Tomsic et al. (2006) and Nandi et al. (2003)
	Wool wax/Lanolin; Sebaceous glands of wool bearing animals	Lubricant, moisturizer It has semi-solid consistency	Emulsion, microemulsion and cream	Moisturizing effect with longer lasting action may be obtained	Antimicrobials and antifungal	Bashura et al. (1969)

Table 2 Improved results of drug employed with different oil system incorporated in Emulgel

Oil phase with their property	Concentration to be used (% w/w)	Drug of interest	Outcomes	References
Liquid paraffin; Moisturizer, emollient	5	Chlorphenesin, itraconazole, ketoconazole, miconazole and mefenamic acid	An inverse correlation was observed between the oil phase concentration and rate and extent of drug release	Deveda et al. (2010), Mohamed (2004), Jain et al. (2010) and Khullar et al. (2012)
Jojoba oil; Antifungal, antioxidant.	30	Clotrimazole	Formulation of emulgel with a combination of two gelling agents (i.e. carbopol and HPMC) presented greater drug release	Shahin et al. (2011a)
Compritol 888 ATO; High melting point lipid, provides controlled or delayed release	1–3	Flurbiprofen	Formulation with low to medium oil phase content (oil to water weight ratio of 0.3–0.4% w/w) was considered as an effective carrier	Perioli et al. (2008)
Isopropyl myristate; Emollient, penetration enhancer	5–10	Ketorolac	There was no significant change in release rate of drug	El-Setouhy and El-Ashmony (2010) and Ibrahim and Shehata (2012)
White Vaseline; Moisturizer, hypoallergenic	7.2%	Benzydamine	This emulgel formulation exhibited excellent mucoadhesivity with efficient drug release as compared to marketed preparation	Perioli et al. (2009)
White Vaseline; Moisturizer, hypoallergenic	26.64	Kanamycin	White Vaseline based emulgel had better stability and rheological properties and significant antimicrobial efficacy against <i>A. madurae</i>	Lopez-Cervantes et al. (2009)

Other types of oils or lipids like paraffin wax, cetostearyl alcohol and oleic acid may also be utilized in the emulgel as oil phase. Paraffin wax has shown crystalline property as oil content. Paraffin wax when employed as phase change material (PCM) has several benefits over others due to its comparatively high latent heat, chemical inertness and low vapour pressure. When paraffin is distributed in aqueous phase, the paraffin/water emulsion is produced. This emulsion is more efficient due to its higher accelerated exchange of heat and insignificant thermal resistance (Golemanov et al. 2006). The topical preparation of emulgel having 2.5% Transcutol as penetration enhancer produced 1.7 times more enhanced flux and permeation coefficient as compared to marketed formulations such as cream and ointment. Fatty acid such oleic acid may be used as an oil phase of emulsion component of emulgel. Oleic acid is a mono-unsaturated omega-9 fatty acid present in various vegetable and animal fats (Villarreal-Lozoya et al. 2007).

2.2 Selection Criteria for Emulsifier

Emulgels are usually formulated by the mixing of oil and water and gelled by the addition of suitable gelling agent but they are thermodynamically unstable. For stability enhancement a suitable emulsifying agent should be employed in appropriate amount, which leads to lowering of interfacial tension between oil and water phase and subsequently results in the development of a thermodynamically stable emulgel. Improved stabilization of dispersed globules with emulsifying agents is demonstrated in Fig. 3.

An ideal emulsifier has a proper HLB (hydrophilic lipophilic balance) value and ability to develop stable emulsion system (Sklenar et al. 2012). Trial and error method is employed to determine the type and amount of emulsifier (Singh et al. 2011; Zhang et al. 2012). Non-ionic surfactants tweens which have HLB values more than 9 can be used to formulate the O/W emulsion-based emulgel system while lipophilic surfactant of HLB value less than 9 can be employed for the formulation of W/O emulgel system.

Generally a combination of emulsifiers should be used during preparation of an emulgel. Tween 20 is oriented in the aqueous phase while span 20 is arranged in oil phase (Jain et al. 2010; Khunt et al. 2012). Chemically both are sorbitan lauric acid esters and contain same cyclic structure. However, additional polyoxyethylene units are present in the structure of Tween (Kerwin 2008; Shen et al. 2011). Span 20/Tween 20 blend produces more stable emulsion as compared when Tween or Span system is used alone (Vilasau et al. 2011). Pemulen is a polymeric emulsifying agent which was employed in the emulgel meant for buccal administration. Pemulens is tailored with hydrophobic copolymer acrylic acid (Acrylates/C10–C30 alkyl acrylates) and could serve as primary emulsifying agent of o/w emulsion as well as viscosity modifier. It has a small lipophilic portion which gets introduced into oil droplets while larger hydrophilic portion produces a microgel around the droplet leading to a stable o/w emulsion system (Szűcs et al. 2008). Usually,

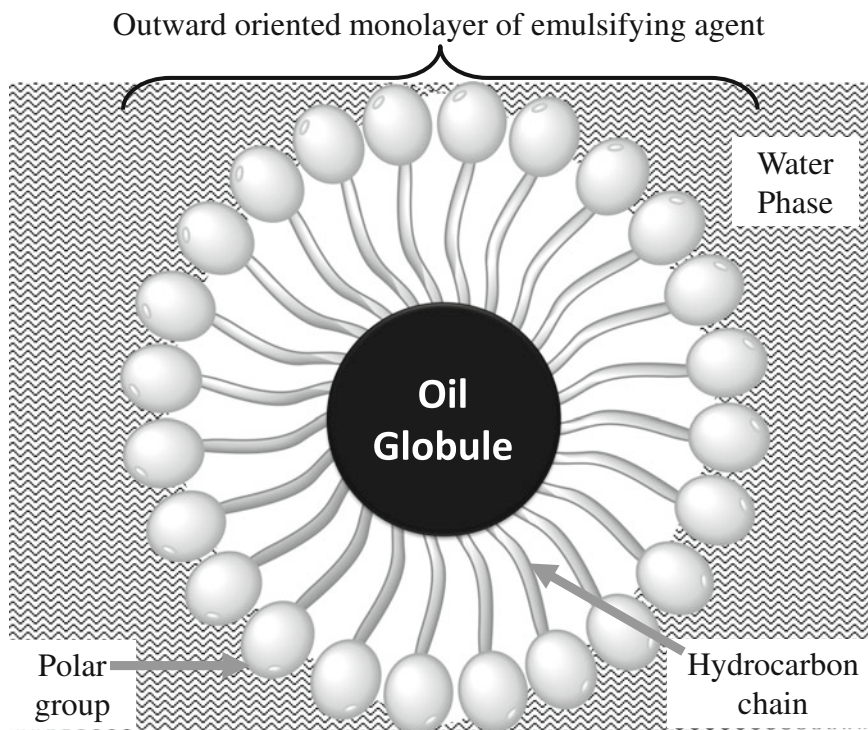


Fig. 3 Improved stabilization of dispersed globules with emulsifying agents

surfactants employed in the emulgel formulation have toxic properties and may create some health-related issues. To minimize this problem, surfactant of natural origin may serve as an alternative. These bio-surfactants are obtained from several microbial species. Bio-surfactants are highly sticky in nature and show both hydrophilic and hydrophobic characteristics due to the presence of short-chain fatty acid tail and large polar head groups. Bio-surfactants effectively reduce the surface tension as well as interfacial tension same as chemical surfactant. They have lower toxicity, higher biodegradability, greater compatibility with environment, potential foaming ability and highest stability and activity at extreme temperature and pH. These characteristics make them a better commercial alternative of chemical emulsifying agents.

2.3 Gelling Agent Selection Criteria

Emulgel requires gelling properties which can be fulfilled by using a gelling agent which provides a gelled structure. Gelling agents are of two types either natural or

synthetic. Addition of gelling agent into emulgel system gives thixotropic properties (Singla et al. 2012). According to the Swedish National Encyclopedia (1989–1996) (Lee et al. 2009), thixotropy is “characteristic feature of viscous or gel-like structures”. These structures are converted into liquid state when stress is applied and when the pressure is lowered, they regain the previous viscous consistency. In thixotrophy process, a reversible transition is shown between the gel and sol (gel–sol–gel transition). This phenomenon occurs due to the time-dependent changes in the viscosity under the influence of pH, temperature or change in the component without any alteration in the system volume. The schematic representation of thixotropic behaviour of emulgel is shown in Fig. 4 (Mewis and Wagner 2009).

Gel–sols–gel behaviour provides improved stability and higher bioavailability to the system (Jain et al. 2013a, b). However, stability of emulgel system can be influenced by several factors such as temperature, pH, amount and combination of polymers, modification in polymer, introduction of ions (cations or anions) into the system. Hydroxy propyl methyl cellulose (HPMC) is a semi-synthetic polymer used in the emulgel preparation. It has polymeric chains with network structure interconnected via cross-linking (Barreiro-Iglesias et al. 2003).

Gelling agent affects the release characteristic of drug from the emulgel (Jain and Jain 2015b). It has been observed that the rate of drug release and concentration of gelling agent shows a reciprocal relation. The emulgel formulation demonstrated the non-Newtonian shear thinning behaviour with small or without thixotropy. The viscosity of system can also be affected by the concentration or type of gelling agent. Stability studies in several stress conditions like centrifugation, higher temperature or longer storage expressed greater stability of emulgel formulations containing low concentration of Carbopol or a combination of two gelling agents as compared to other preparations (Shahin et al. 2011a). Emulgel of HPMC showed better drug release property than Carbopol emulgel (Mohamed 2004). Polymer chains get expanded by the neutralization of aqueous dispersion of polymer with the help of NaOH, which formed a clear stable gel. For complete hydration of polymer, the gel should be stored at 4 °C for 24 h followed by addition of oil phase. Pemulen is a polymeric emulsifier which also has a mucoadhesive property. Pemulen as a gelling component is best suited for oral administration of emulgel.

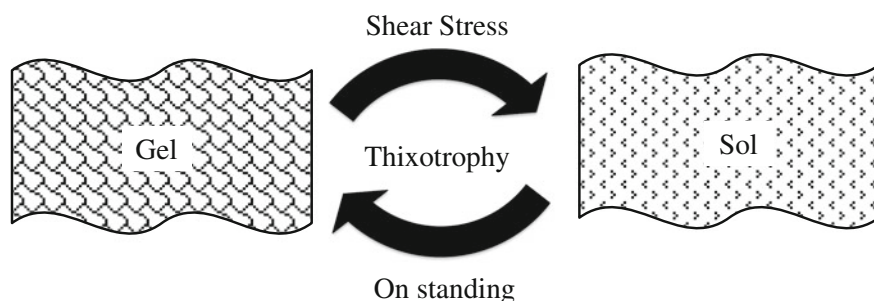


Fig. 4 Thixotropic behaviour of gel (gel–sol–gel property)

On the basis of rheological analysis, it was concluded that mucoadhesive polymer pemulen based emulgel formulation showed better retention time than marketed formulation in oral cavity for the treatment of local inflammation. The polymeric acrylic emulsifier used in the emulgel preparations is providing better consistent stability as well as mucoadhesivity which results in longer retention time and reduced number of dose (Perioli et al. 2008).

The concentration and characteristics of gelling agent used in the emulgel preparation are described in Table 3.

Various types of natural, synthetic and semi-synthetic gelling substances are employed for the formulation of emulgel. Natural gelling agents have many limitations because they are sensitive for the microbial contamination. So, instead of natural gelling compound, several synthetic or semi-synthetic gelling agents may be employed. Usually cellulose-based synthetic or semi-synthetic derivatives are employed as gelling agent. Sodium carboxymethyl cellulose is the most commonly used cellulose derivative. Sodium CMC shows higher stability in an autoclave during sterilization so suitably used in the formulation of sterile jellies. Sodium CMC as gelling agent in 5% concentration was employed in the colocynth topical gel, having anti-inflammatory property. This colocynth gel decreased the 64.95% oedema more significantly than volteran emulgel.

2.4 Penetration Enhancers Selection Criteria

From the absorption point of view, skin is the most potent barrier for several molecules or drugs. Skin has several barrier layers to hinder the drug absorption from the topical preparations. Several compounds referred as penetration enhancers have been employed to promote the drug absorption from the skin into the blood. These substances enhance the penetration ability of drug moieties via skin. Penetration enhancers may follow different mechanisms for the improved absorption. They may disrupt the highly arranged lipid structure of stratum corneum or interact with protein present between the cells, fluidize the lipid channels which are present between corneocytes or increase the partitioning of the drug as co enhancer/solvent into the stratum corneum. Some enhancers act both on non-polar and polar pathways by changing the multi-laminate route for penetration (Benson 2005). Penetration enhancers which are used in the topical emulgel formulations for improved absorption are listed in Table 4.

3 Formulation Methods

Different methods are employed for the manufacturing of emulgel by using several types of formulation additives. Mohamed (2004) described one method of preparation in his research. This emulsion system (o/w or w/o) was formed followed by

Table 3 Various gelling agents used for the formulation of Emulgel

Gelling agent	Usual concentration (% w/w)	Incorporated Drug	Result	Benefits	References
Pluronic F127	1–3	Piroxicam	Capable in producing desired gelling characteristics and appearance as compared to HPMC and Carbopol	It shows better solubility in cold water with good clarity	Shokri et al. (2012)
HPMC®	2.5	Clorphenesin	Exhibited enhanced drug release rate as compared with emulgel of Carbopol 934	Develops neutral gels of good stability and better viscosity, microbial resistance. Film of HPMC shows appreciable strength	Mohamed (2004) and Perfoli et al. (2009)
	5	Benzylamine	It may express good release profiles, rheological properties but less mucoadhesivity		
	1	Chlorphenesin	It can demonstrate significant drug release with better stability and antifungal activity	Emulgel was prepared with very less concentrations and delivered the incorporated drug in a controlled manner	Deveda et al. (2010), Mohamed (2004) and Lopez-Cervantes et al. (2009)
Carbopol 934	1	Itraconazole	Produces a higher viscous preparation and exhibits poor drug release		
	1.78	Kanamycin	Shows appreciable drug release rate		
Carbopol 940	1	Mefenamic acid	Higher amount of penetration enhancer (clove oil) can enhance release rate of drug	Gel shows high viscous consistency and provides a controlled release of drug	Khullar et al. (2012)

(continued)

Table 3 (continued)

Gelling agent	Usual concentration (% w/w)	Incorporated Drug	Result	Benefits	References
Combination of HPMC and Carbopol	1.2	Ketorolac and clotrimazole	Higher stability with excellent drug release and improved antimicrobial activity	Combination of both develops a more stable emulgel as compared with individual gelling agents	El-Setouhy and El-Ashmony (2010) and Shahin et al. (2011a)
Pemulen	0.1–0.4	Flurbiprofen	Prepared formulation has good stability, proper consistency and mucoadhesivity	It exhibits better stability, minimum irritancy and produces a rapid release of drug from oil phase	Perioli et al. (2008)
NaCMC	3–4	Benzylamine	It has been observed as excellent in terms of manageability and higher adhesion power to vaginal mucosa	Effective for sterile gels as it can withstand high temperatures during autoclaving without serious deterioration	Perioli et al. (2009)

Table 4 List of Penetration enhancers

Dosage form	Penetration or permeation enhancer	Usual concentration (% w/w)
Gel	Oleic acid	1
	Lecithine	5
	Urea	10
	Isopropyl myristate	5
	Linoleic acid	5
Emulgel	Clove oil	8
	Menthol	5
	Cinnamon	8

incorporating the gelling agent to form an emulgel. For the emulgel formulation, initially aqueous phase should be developed by dissolving Tween into the purified water. Preservatives like methyl and propyl paraben are dissolved in the propylene glycol solvent resulting in formation of another solution and both the solutions are then mixed together. Finally, aqueous phase is formed and kept aside. Second phase of emulsion is oil phase which is formed by dissolving Span 20 in light liquid paraffin.

Both oil phase and aqueous phases are heated up to 70–80 °C separately, then both phases are blended with each other with constant stirring up to the room temperature. HPMC or Carbopol as gelling agent is dispersed in the water to form gel phase. Then both emulsion phases and gel are mixed together in ratio of 1:1 with gentle stirring. Perioli et al. (2008) also described another method for the development of emulgel (Perioli et al. 2008). They reported design and characterization of emulgel for buccal purpose. Three steps are required for the preparation of emulgel (1) dispersion of polymer in water resulting in formation of polymeric solution, (2) neutralization of the aqueous dispersion of polymer with base and (3) emulsification of oil phase with aqueous phase. Pemulen 1621 (TR-1) in three different percentages 0.3, 0.4 and 0.5%, w/v is needed for the manufacturing of polymeric aqueous phase. Polymeric dispersion is prepared by the addition of deionized water with uninterrupted stirring at 900 rpm, at room temperature for 20 min time period utilizing a mechanical stirrer, which is equipped with impellers of three helical blades. Then, sodium hydroxide solution (18% w/v) is introduced into the prepared polymeric dispersion to form neutralized polymeric slurry with ultimate pH value of 5.5, 6.0 and 6.5. In this neutralization process, the elongation of polymeric chain occurs resulting in the formation of a stable gel. Before introducing the oil phase, the polymeric gel should be stored at 4 °C for 24 h for complete hydration of polymeric gel. When hydration is over, oil phase in different ratios 0.5, 1.0 and 1.5 is added into polymeric dispersion at 80 °C and 800 rpm with continuous stirring. The temperature of entire system is allowed to cool down with a controlled pH. Shahin et al. (2011a, b) reported a different protocol for the development of clotrimazole emulgel as a drug delivery system. In this method, drug is dissolved in oily phase (jojoba oil) of emulsion which contains Span 60 (Shahin et al. 2011b). This surfactant dispersion is carried out by

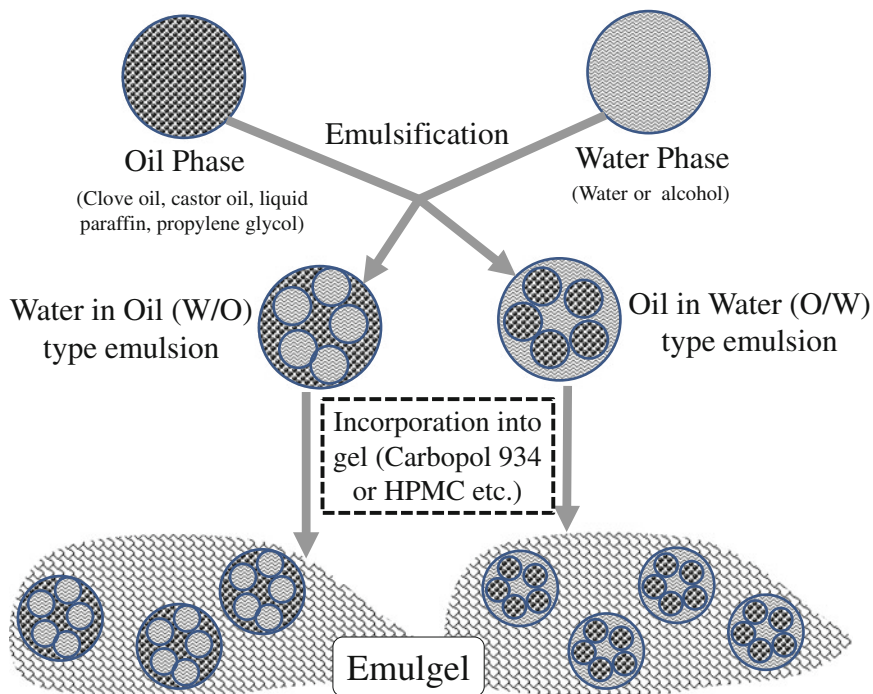


Fig. 5 Schematic representation of method of preparation of emulgel

continuous stirring at 75 °C with subsequent cooling up to room temperature followed by the incorporation of Carbopol into the oil phase. In second step, Brij-35 is added into the propylene glycol followed by incorporation of this solution into water to form aqueous phase. And finally, oil phase is incorporated into the aqueous phase and is mixed with overhead mixer at 10,000 rpm for about 10 min to prepare an emulsion system. This emulsion system is subjected for homogenization at 10,000 rpm for less time as stated above (about 5 min) Suitable gelling agents such as triethanolamine (formulation having Carbopol either alone or in combination) and/or HPMC is introduced into the previously prepared emulsion and is continuously stirred with overhead mixer for 45 min at 200 rpm to get stable emulgel formulation. Figure 5 represents the general method for the formulation of emulgel.

4 Routes of Administration for Emulgel Formulation

Generally emulgel is applied topically because it prolongs the retention of drug so that the drug can easily act either locally as well as systemically. Due to its emulsion nature, it can improve the drug penetration into the skin and easily gain access in the blood and provide an appropriate pharmacological response.

Oral route shows first pass metabolism, topical application of formulation overcomes this problem. But as compared to the other routes, topical formulation shows limited bioavailability due to the presence of several barriers in the skin (i.e. epidermis, dermis and hypodermis, etc.). However, topical route is the most preferred route for the application of emulgel drug delivery system. Rectal, buccal, vaginal and nasal routes have also been investigated for the application of emulgel formulation. It can be directly employed on to the mucus membrane providing an increased rate and extent of absorption (bioavailability) thereby improving the efficacy of emulgel. Various routes for the emulgel drug delivery administration are summarized with several aspects in Table 5.

5 Characterization of Emulgel

Emulgel is formulated using any of the optimized method employing suitable materials like oil, gelling agent and sometimes penetration enhancer. The prepared emulgel should follow the ideal and combined characteristics of emulsion and gel. These emulgel formulations successfully exhibited their effect either on site of application or action site. Emulgel drug delivery systems were evaluated for several characterization parameters (Ellaithy and El-Shaboury 2002; Mohamed 2004; Kasliwal et al. 2008; Singla et al. 2012).

5.1 *Physical Evaluation*

Colour, homogeneity, phase separation and consistency are the various parameters measured for the physical characterization of emulgel formulations.

5.2 *Rheological Behaviour*

Since emulgel is a viscous preparation, determination of rheological behaviour is a mandatory requirement. For this, different types of viscometers are employed. The cone and plate viscometer with spindle 52 is used to measure the viscosity of several emulgel formulations at 25 °C. (Perioli et al. 2008; Shen et al. 2015).

5.3 *Spreading Coefficient*

Mutimer et al. (1956) proposed the apparatus used for the determination of emulgel formulation. This instrument consists of a wooden block, which is attached with a

Table 5 Recent advancements of Emulgels with different categories of drugs and their routes of administration

Route of administration	Class	Drug	Outcome	Uses	References
Buccal	NSAIDS	Flurbiprofen	Emulgel formulation exhibited excellent retention period as compared to marketed formulation for treatment of oral cavity inflammations	Analgesic and anti-inflammatory	Perioli et al. (2008)
Vaginal	NSAIDS	Benzylamine	Emulgel of Benzylamine having NaCMC 3% and cetosteryllic alcohol possessed better mucoadhesion in vaginal mucosa	Analgesic, anti-inflammatory, local anaesthetic	Perioli et al. (2009)
Topical	Aminoglycoside antibiotic	Kanamycin	Exhibited enough technological properties for being employed as auxiliary in mycetoma treatment	Treatment of mycetoma	Lopez-Cervantes et al. (2009)
	NSAID	Ketorolac trometamol	Significantly effective for dermal and transdermal delivery of ketorolac trometamol	Highly analgesic	El-Setouhy and El-Ashmony (2010)
		Diclofenac sodium	Emulgel with methyl paraben in 0.2% has been observed as an efficient formulation to prevent microbial attack	Anti-inflammatory and analgesic	Ajazuddin et al. (2013)
	NSAID	Mefenamic acid	Emulgel with anti-inflammatory analgesic agents has served as a potential topical drug delivery system	Anti-inflammatory and analgesic	Khullar et al. (2012)
	Corticosteroid	Clobetasol	It is observed that emulgel showed excellent drug release than from PGLA microspheres	Treatment of psoriasis	Badili et al. (2011)
	Alkaloid	Tetra hydropalmitine	Emulgel formulation with Carbopol 971 and penetration enhancer NMP showed excellent permeation	Liver damage and muscle relaxant	Li et al. (2011)

(continued)

Table 5 (continued)

Route of administration	Class	Drug	Outcome	Uses	References
	Antifungal	Chlorphenesin	Maximum drug release and better antifungal activity has been observed when emulgel containing HPMC with little amount of liquid paraffin and suitable emulsifying agent in high percentage is added to it	Mycosis, candidiasis and fungal infection	Mohamed (2004)
		Itraconazole	Emulgel showed effective, safe and sustained delivery of antifungal agent	Blastomycosis, histoplasmosis	Deveda et al. (2010)
		Ketoconazole	Drug delivery occurred in controlled manner as compared to cream	Athlete foot, ring worm, candidiasis	Jain et al. (2010)
		Miconazole nitrate	Exhibited controlled delivery of miconazole nitrate effectively	Athlete foot, ring worm	Jain et al. (2011)

pulley at one terminal. This technique is employed to determine the spreadability on the basis of “Slip” and “Drag” properties of emulgel formulations. A ground glass slide is set on this wooden block. An emulgel under study with an excess quantity (about 2 g) is put on this ground slide. Another glass slide of dimension same as ground slide is put onto the emulgel and connected with hook. A weight of 1 kg is put on the top of both the slides for definite time (about 5 min) which helps in air expulsion and makes a uniform emulgel film between the slides. If emulgel is present in excess, it can be scrapped off from the edges of instrument. To pull the top plate, a definite weight (about 80 g) is placed in the pan. With the aid of the string connected to the hook, the time (in seconds) taken by the top slide to cover the 7.5 cm distance is recorded (Mutimer et al. 1956).

5.4 Swelling Index

Swelling index is an important characteristic of the emulgel formulation. For the measurement of swelling index, 1 g of emulgel preparation was put on a porous aluminium foil which was kept in a 50 ml beaker containing 10 ml of 0.1 N sodium hydroxide. This emulgel sample was removed at a definite time interval. Swelling index can be determined by the following formula:

$$\text{Swelling index (SW)\%} = \frac{w_t - w_0}{w_0} \times 100,$$

where

- (SW) % Equilibrium percentage swelling,
 W_t Weight of emulgel after swelling at time t ,
 W_0 Initial weight of emulgel at zero time.

5.5 Extrudability Study of Topical Emulgel (Tube Test)

Extrudability Study is a fundamental test used to calculate the force needed to extrude the topical preparation like emulgel from tube. This technique is employed for the measurement of applied shear in the area of rheogram which corresponds to the rate of shear, exceeding the yield value and showing the consequent plug flow. This evaluation technique is used for the determination of emulgel extrudability based on the percentage quantity of emulgel and extrusion of emulgel from lacquered collapsible tube of aluminium with the use of weight in grams which necessitated extruding at least 0.5 cm emulgel ribbon in time of 10 s. If more amount was applied then it showed greater extrudability. This operation was performed three times (triplicate) and average value was measured for this study. The following formula can be used to calculate the extrudability:

$$\text{Extrudability} = \frac{\text{Applied weight to extrude emulgel from tube (in g)}}{\text{Area (in cm}^2\text{)}}.$$

5.6 Drug Content Determination

Emulgel is a potential carrier for the drugs applied topically, so drug content determination is the most critical evaluation parameter. For this, 1 g sample of emulgel was dissolved in a suitable solvent to prepare a solution proceeded by filtration to obtain a clear solution. This clear solution was analysed for drug content using suitable analytical instrument

5.7 Ex Vivo Bioadhesive Strength

Bioadhesive strength can be measured by modified analytical two pan balance method.

5.8 In Vitro/Permeation Studies

Franz diffusion cell is employed for the in vitro release or permeation studies.

5.9 Skin Irritation Test (Patch Test)

Skin irritation test is performed on the rat's shaven skin and a total set of eight rats can be used. After the application of emulgel, various effects like colour change, change in appearance of rat's skin were observed up to 24 h. If any symptoms of irritation were explored in more than two rats, the analysis ought to be repeated. In the case of the absence of any irritation, test can be ascertained as pass.

5.10 Stability Studies

Various oils and ingredients from natural origin are used for the manufacturing of emulgel formulation. Proper storage conditions like temperature, humidity and container, etc. should be employed. Hence, stability studies are performed for emulgel formulation. The prepared emulgel formulations are kept in five collapsible

tubes of aluminium and proceeded for stability studies under 5, 25 °C/60% RH, 30 °C/65% RH and 40 °C/75% RH conditions for 3 months' time duration. In every 15-day time interval, samples are withdrawn from these formulations and analysed for several evaluation parameters such as physical appearance, pH, rheological behaviour, drug content and drug release profiles (Niazi 2009).

6 Marketed Preparations

Some emulgel formulations are commercially very popular for the treatment of several diseases and ill conditions. Voltaren Emulgel is a white gel having pleasant fragrance with non-greasy property. This Voltaren Emulgel contains drug diclofenac sodium (as diclofenac diethylamine) in 1% w/w concentration which acts as a non-steroidal anti-inflammatory molecule. It shows potential benefits in the case of inflamed tendons, ligaments, muscles and joints suffering from trauma as well as in soft-tissue rheumatism and localized rheumatic conditions. Similar types of formulations are manufactured by Torrent Pharma with trade name Diclomax. They are employed significantly in various conditions like in localized forms of soft-tissue rheumatism, e.g. tendovaginitis, shoulder-hand syndrome, bursitis, rheumatic diseases, osteoarthritis of the spine and peripheral joints, periarthropathy, inflammation of the ligaments, tendons, muscles, and joints due to trauma, sprains, strains and bruises. Another type of emulgel is Kleraderm Gaia Emulgel which is used for vaginal antiseptic purpose (Arnstein 2012). Its pH should be same as the physiological pH of vagina in order to avoid any irritation and inflammation. Gaja Emulgel is used for the treatment of vaginal dryness, dehydration and redness. Pantho Eva is a marketed formulation of emulgel which produces softening or moisturizing effect on the skin. It is usually prescribed for anal fissures, nipple fissures, wounds, burns, ulcers and skin dryness resulting from exposure to sun rays. These formulations are enlisted in Table 6.

7 Future Perspectives

Most of the drugs which are generally used in formulation of dosage form are either weakly acidic or basic, hence they show poor solubility which is the significant problem while developing any formulation. Some drugs having hydrophilic characteristic, create problems during development of any new drug delivery system. Hydrophobic nature of drug leads to poor water solubility and less bioavailability. The delivery of such type of drugs has several challenges for biological system. The hydrophobic drugs can be easily formulated as oil-based preparations. Numerous drug delivery systems, i.e. cream, ointment, lotion and paste are used for topical applications. Generally, these topical preparations contain different oleaginous bases like petrolatum, bees wax or vegetable oils. These bases due to their suitable

Table 6 Different marketed preparations

Brand name of product	Incorporated drug	Manufacturing company
Voltaren emulgel	Diclofenac diethyl ammonium	Novartis Pharma
Miconaz H emulgel	Miconazole nitrate, Hydrocortisone	Medical union Pharmaceuticals
Excec gel	Clindamycin, Adapalene	Zee laboratories
Pernox gel	Benzoyl peroxide	Cosme Remedies Ltd
Lupigyl gel	Metronidazole	Lupin Pharma
Clinagel	Clindamycin phosphate	Allantoin Stiefel Pharma
Topinate gel	Clobetasol propionate	Systopic Pharma
Kojivit gel	Kojic acid, Dipalmitate Arbutin, Octinoxate	Micro Gratia Pharma
Acent gel	Aceclofenac, Methyl salisylate, Capsaicin	Intra labs India Pvt Ltd
Avindo gel	Azithromycin	Cosme Pharma laboratories
Cloben gel	Clotrimazole, Beclomethasone, Dipropionate, Neomycin	Indoco Remedies
Nadicin cream	Nadifloxacin	Psychoremedies
Zorotene gel	Tezarotene	Elder Pharmaceuticals

hydrophobic property do not produce any interaction with water resulting in an excellent emollient action. But, these oleaginous bases decrease the drug release from the dosage forms and produce thick and greasy consistency. However, gel-based formulations create an aqueous atmosphere for the drug moiety which provides better dissolution and faster drug release as compared to other topical preparations. Emulgel is a suitable topical drug delivery system for lipophilic drugs where oily phase contains the drug molecule. According to future prospects, emulgel drug delivery system will be potentially useful for the delivery of several hydrophobic drugs as well as hydrophilic drugs. These advantages prove that emulgel is an efficient and productive drug delivery system than the other topical dosage forms.

8 Conclusion

Emulgel is a non-sticky, non-greasy formulation and incorporates both types of drugs, i.e. lipophilic and hydrophilic. Emulgel provides better drug entrapment; drug release and no irritation at the application site make it a better and an efficient drug delivery system as compared to other topical formulations. It has dual characteristics of formulation, i.e. emulsion and gel hence, provides effective sustained and controlled release and minimizes some problems such as dose dumping which are common in many sustained and controlled release formulations. Conventional

emulsion formulations have several problems such as cracking, creaming, phase separation, coalescence and phase inversion but, when they will be formulated with gel all such problems could be overcome and an emulgel with improved stability can be developed. Various dermatological problems and diseases can be easily managed or cured by the application of emulgel, because it can be formulated with a vast variety of drugs and developed as an emerging and potential drug delivery system.

Acknowledgements Author A.J. acknowledges Council of Industrial and Scientific Research (New Delhi, India) for Senior Research Fellowship.

References

- Ajazuddin A, Alexander A, Khichariya A, Gupta S, Patel RJ, Giri TK, Tripathi DK (2013) Recent expansions in an emergent novel drug delivery technology: Emulgel. *J Control Release* 171:122–132
- Alexander A, Ajazuddin D, Verma T, Swarna MJ, Patel S (2011) Mechanism responsible for mucoadhesion of mucoadhesive drug delivery system: a review. *Int J Appl Biol Pharm Technol* 2:434–442
- Alexander A, Dwivedi S, Giri TK, Saraf S, Saraf S, Tripathi DK (2012) Approaches for breaking the barriers of drug permeation through transdermal drug delivery. *J Control Release* 164: 26–40
- Arnstein PM (2012) Evolution of topical NSAIDs in the guidelines for treatment of osteoarthritis in elderly patients. *Drugs Aging* 29:523–531
- Badilli U, Amasya G, Özkan S, Tarimci N (2013) Simultaneous determination of clobetasol propionate and calcipotriol in a novel fixed dose emulgel formulation by LC-UV. *Chromatographia* 76:133–140
- Badilli U, Amasya G, Şen T, Tarimci N (2014) Topical emulgel formulation containing inclusion complex of calcipotriol with cyclodextrin. *J Incl Phenom Macrocycl Chem* 78:249–255
- Badilli U, Şen T, Tarimci N (2011) Microparticulate based topical delivery system of clobetasol propionate. *AAPS Pharm Sci Tech* 12:949–957
- Barreiro-Iglesias R, Alvarez-Lorenzo C, Concheiro A (2003) Controlled release of estradiol solubilized in carbopol/surfactant aggregates. *J Control Release* 93:319–330
- Bashura GS, Gluzman M, Labuns’Kii EV, Trunova MA, Levitskaia IB (1969) Study of surface-active and emulsifying properties of oxyethylated alcohols of wool wax in the preparation of ointments and emulsions. I. *Farm Zh* 24:53–57
- Beitz JM (2005) Heparin-induced thrombocytopenia syndrome bullous lesions treated with trypsin-balsam of peru-castor oil ointment: a case study. *Ostomy Wound Manag* 51(52–4): 56–58
- Benson HA (2005) Transdermal drug delivery: penetration enhancement techniques. *Curr Drug Deliv* 2:23–33
- Bowey K, Tanguay J-F, Tabrizian M (2012) Liposome technology for cardiovascular disease treatment and diagnosis. *Expert Opin Drug Deliv* 9:249–265
- Caddeo C, Sales OD, Valenti D, Sauri AR, Fadda AM, Manconi M (2013) Inhibition of skin inflammation in mice by diclofenac in vesicular carriers: liposomes, ethosomes and PEVs. *Int J Pharm* 443:128–136
- Deveda P, Jain A, Vyas N, Khambete H, Jain S (2010) Gellified emulsion for sustain delivery of itraconazole for topical fungal diseases. *Int J Pharm Pharm Sci* 2:104–112
- di Mattia C, Sacchetti G, Mastrocola D, Pittia P (2009) Effect of phenolic antioxidants on the dispersion state and chemical stability of olive oil O/W emulsions. *Food Res Int* 42:1163–1170

- Dixit AS, Charyulu N, Nayari H (2011) Design and evaluation of novel emulgel containing Acyclovir for herpes simplex keratitis. *Lat Am J Pharm* 30:844
- Djordjevic J, Michniak B, Uhrich KE (2003) Amphiphilic star-like macromolecules as novel carriers for topical delivery of nonsteroidal anti-inflammatory drugs. *AAPs Pharmsci* 5:1–12
- El-Setouhy DA, El-Ashmony SM (2010) Ketorolac trometamol topical formulations: release behaviour, physical characterization, skin permeation, efficacy and gastric safety. *J Pharm Pharmacol* 62:25–34
- Elbayoumi TA, Torchilin VP (2008) Liposomes for targeted delivery of antithrombotic drugs. *Expert Opin Drug Deliv* 5:1185–1198
- Ellaithy H, El-Shaboury K (2002) The development of Cutina lipogels and gel microemulsion for topical administration of fluconazole. *AAPS Pharm Sci Tech* 3:77–85
- Ghorab DM, Amin MM, Khowessah OM, Tadros MI (2011) Colon-targeted celecoxib-loaded Eudragit(R) S100-coated poly-epsilon-caprolactone microparticles: preparation, characterization and in vivo evaluation in rats. *Drug Deliv* 18:523–535
- Golemanov K, Tcholakova S, Denkov ND, Gurov T (2006) Selection of surfactants for stable paraffin-in-water dispersions, undergoing solid-liquid transition of the dispersed particles. *Langmuir* 22:3560–3569
- Gupta A, Mishra A, Singh A, Gupta V, Bansal P (2010) Formulation and evaluation of topical gel of diclofenac sodium using different polymers. *Drug Invention Today* 2:250–253
- Habashy RR, Abdel-Naim AB, Khalifa AE, Al-Azizi MM (2005) Anti-inflammatory effects of jojoba liquid wax in experimental models. *Pharmacol Res* 51:95–105
- Hartman C, Ben-Artzi E, Berkowitz D, Elhasid R, Lajterer N, Postovski S, Hadad S, Shamir R (2009) Olive oil-based intravenous lipid emulsion in pediatric patients undergoing bone marrow transplantation: a short-term prospective controlled trial. *Clin Nutr* 28:631–635
- Ibrahim MM, Shehata TM (2012) The enhancement of transdermal permeability of water soluble drug by niosome-emulgel combination. *J Drug Deliv Sci Technol* 22:353–359
- Jager S, Laszczyk MN, Scheffler A (2008) A preliminary pharmacokinetic study of betulin, the main pentacyclic triterpene from extract of outer bark of birch (*Betulae alba* cortex). *Molecules* 13:3224–3235
- Jain A, Deveda P, Vyas N, Chauhan J, Khambete H, Jain S (2011) Development of antifungal emulsion based gel for topical fungal infection (s). *IJPRD* 2:18–22
- Jain A, Gautam SP, Gupta Y, Khambete H, Jain S (2010) Development and characterization of ketoconazole emulgel for topical drug delivery. *Der pharmacia sinica* 1:221–231
- Jain A, Gulbake A, Jain A, Shilpi S, Hurkat P, Jain SK (2013a) Dual drug delivery using “smart” liposomes for triggered release of anticancer agents. *J Nanopart Res* 15:1–12
- Jain A, Gulbake A, Shilpi S, Jain A, Hurkat P, Jain SK (2013b) A new horizon in modifications of chitosan: syntheses and applications. *Crit Rev Ther Drug Carrier Syst* 30:91–181
- Jain A, Jain SK (2015a) Colon targeted liposomal systems (CTLS): theranostic potential. *Curr Mol Med* 15:621–633
- Jain A, Jain SK (2015b) Environmentally responsive chitosan-based nanocarriers (CBNs). *Handb Polym Pharm Technol Biodegrad Polym* 3:105
- Jain A, Jain SK (2016a) In vitro release kinetics model fitting of liposomes: an insight. *Chem Phys Lipid* 201:28–40
- Jain A, Jain SK (2016b) Stimuli-responsive smart liposomes in cancer targeting. *Curr Drug Targets* 17. doi:10.2174/1389450117666160208144143, <http://www.eurekaselect.com/139308/article>
- Jing F, An X, Shen W (2003) The characteristics of hydrolysis of triolein catalyzed by wheat germ lipase in water-in-oil microemulsions. *J Mol Catal B Enzym* 24–25:53–60
- Joshi B, Singh G, Rana A, Saini S, Singla V (2011) Emulgel: a comprehensive review on the recent advances in topical drug delivery. *Int Res J Pharm* 2:66–70
- Kale AA, Torchilin VP (2007a) Enhanced transfection of tumor cells in vivo using “Smart” pH-sensitive TAT-modified pegylated liposomes. *J Drug Target* 15:538–545
- Kale AA, Torchilin VP (2007b) “Smart” drug carriers: PEGylated TATp-modified pH-sensitive liposomes. *J Liposome Res* 17:197–203

- Karabacak M, Kanbur M, Eraslan G, Soyer Sarica Z (2011) The antioxidant effect of wheat germ oil on subchronic coumaphos exposure in mice. *Ecotoxicol Environ Saf* 74:2119–2125
- Kasliwal N, Derle D, Negi J, Gohil J (2008) Effect of permeation enhancers on the release and permeation kinetics of meloxicam gel formulations through rat skin. *Asian J Pharm Sci* 3: 193–199
- Kerwin BA (2008) Polysorbates 20 and 80 used in the formulation of protein biotherapeutics: structure and degradation pathways. *J Pharm Sci* 97:2924–2935
- Khan J, Alexander A, Saraf S, Saraf S (2013) Recent advances and future prospects of phyto-phospholipid complexation technique for improving pharmacokinetic profile of plant actives. *J Control Release* 168:50–60
- Khullar R, Kumar D, Seth N, Saini S (2012) Formulation and evaluation of mefenamic acid emulgel for topical delivery. *Saudi Pharm J* 20:63–67
- Khunt DM, Mishra AD, Shah DR (2012) Formulation design and development of piroxicam emulgel. *Int J PharmTech Res* 4:1332–1344
- Kikwai L, Babu RJ, Prado R, Kolot A, Armstrong CA, Ansel JC, Singh M (2005) In vitro and in vivo evaluation of topical formulations of spantide II. *AAPS Pharm Sci Tech* 6:E565–E572
- Kirkeskov B, Christensen R, Bugel S, Bliddal H, Danneskiold-Samsøe B, Christensen LP, Andersen JR (2011) The effects of rose hip (*Rosa canina*) on plasma antioxidative activity and C-reactive protein in patients with rheumatoid arthritis and normal controls: a prospective cohort study. *Phytomedicine* 18:953–958
- Koshkaryev A, Thekkedath R, Pagano C, Meerovich I, Torchilin VP (2011) Targeting of lysosomes by liposomes modified with octadecyl-rhodamine B. *J Drug Target* 19:606–614
- Kumar L, Verma R (2010) In vitro evaluation of topical gel prepared using natural polymer. *Int J Drug Deliv* 2:58–63
- Kumari A, Jain A, Hurkat P, Verma A, Jain SK (2016) Microsponges: a pioneering tool for biomedical applications. *Crit Rev Ther Drug Carrier Syst* 33:77–105
- Lawrence MJ, Rees GD (2012) Microemulsion-based media as novel drug delivery systems. *Adv Drug Deliv Rev* 64:175–193
- Lee CH, Moturi V, Lee Y (2009) Thixotropic property in pharmaceutical formulations. *J Controlled Release* 136:88–98
- Lee S-J, Umano K, Shibamoto T, Lee K-G (2005) Identification of volatile components in basil (*Ocimum basilicum* L.) and thyme leaves (*Thymus vulgaris* L.) and their antioxidant properties. *Food Chem* 91:131–137
- Li C, Liu C, Liu J, Fang L (2011) Correlation between rheological properties, in vitro release, and percutaneous permeation of tetrahydropalmatine. *AAPS Pharm Sci Tech* 12:1002–1010
- Lopez-Cervantes M, Escobar-Chavez JJ, Casas-Alancaster N, Quintanar-Guerrero D, Ganem-Quintanar A (2009) Development and characterization of a transdermal patch and an emulgel containing kanamycin intended to be used in the treatment of mycetoma caused by *Actinomyces madurae*. *Drug Dev Ind Pharm* 35:1511–1521
- Lu F, Ding Y-C, Ye X-Q, Ding Y-T (2011) Antibacterial effect of cinnamon oil combined with thyme or clove oil. *Agric Sci China* 10:1482–1487
- Lupi F, Gabriele D, Facciolo D, Baldino N, Seta L, de Cindio B (2012) Effect of organogelator and fat source on rheological properties of olive oil-based organogels. *Food Res Int* 46:177–184
- Machmudah S, Kawahito Y, Sasaki M, Goto M (2007) Supercritical CO₂ extraction of rosehip seed oil: Fatty acids composition and process optimization. *J Supercrit Fluids* 41:421–428
- Maïssa C, Guillon M, Simmons P, Vehige J (2010) Effect of castor oil emulsion eyedrops on tear film composition and stability. *Contact Lens Anterior Eye* 33:76–82
- Malecka M (2002) Antioxidant properties of the unsaponifiable matter isolated from tomato seeds, oat grains and wheat germ oil. *Food Chem* 79:327–330
- Mewis J, Wagner NJ (2009) Thixotropy. *Adv Coll Interface Sci* 147:214–227
- Mohamed MI (2004) Optimization of chlorphenesin emulgel formulation. *AAPS J* 6:e26
- Moshfeghi AA, Peyman GA (2005) Micro- and nanoparticulates. *Adv Drug Deliv Rev* 57 :2047–2052

- Mundada A, Avari J (2011) Novel biomaterial for transdermal application: in vitro and in vivo characterization. *Drug Deliv* 18:424–431
- Mutimer MN, Riffkin C, Hill JA, Glickman ME, Cyr GN (1956) Modern ointment base technology. II. Comparative evaluation of bases. *J Am Pharm Assoc Am Pharm Assoc* 45:212–218
- Nandi I, Bari M, Joshi H (2003) Study of isopropyl myristate microemulsion systems containing cyclodextrins to improve the solubility of 2 model hydrophobic drugs. *AAPS Pharm Sci Tech* 4:E10
- Niazi SK (2009) Handbook of pharmaceutical manufacturing formulations: sterile products. CRC Press, Boca Raton
- Panwar A, Upadhyay N, Bairagi M, Gujar S, Darwhekar G, Jain D (2011) Emulgel: a review. *Asian J Pharm Life Sci* 2231:4423
- Perioli L, Ambrogi V, Venezia L, Giovagnoli S, Pagano C, Rossi C (2009) Formulation studies of benzydamine mucoadhesive formulations for vaginal administration. *Drug Dev Ind Pharm* 35:769–779
- Perioli L, Pagano C, Mazzitelli S, Rossi C, Nastruzzi C (2008) Rheological and functional characterization of new antiinflammatory delivery systems designed for buccal administration. *Int J Pharm* 356:19–28
- Pires C, Ramos C, Teixeira G, Batista I, Mendes R, Nunes L, Marques A (2011) Characterization of biodegradable films prepared with hake proteins and thyme oil. *J Food Eng* 105:422–428
- Podlogar F, Gašperlin M, Tomšič M, Jamnik A, Rogáč MB (2004) Structural characterisation of water–Tween 40®/Imwitor 308®–isopropyl myristate microemulsions using different experimental methods. *Int J Pharm* 276:115–128
- Rahmani-Neishaboor E, Jallili R, Hartwell R, Leung V, Carr N, Ghahary A (2013) Topical application of a film-forming emulgel dressing that controls the release of stratifin and acetylsalicylic acid and improves/prevents hypertrophic scarring. *Wound Repair Regen* 21: 55–65
- Raut S, Uplanchiwar V, Bhadoria S, Gahane A, Jain SK, Patil S (2012) Comparative evaluation of Zidovudine loaded hydrogels and emulgels. *Res J Pharm Technol* 5:41–45
- Rosen H, Aribat T (2005) The rise and rise of drug delivery. *Nat Rev Drug Discov* 4:381–385
- Sarisozen C, Vural I, Levchenko T, Hincal AA, Torchilin VP (2012) PEG-PE-based micelles co-loaded with paclitaxel and cyclosporine A or loaded with paclitaxel and targeted by anticancer antibody overcome drug resistance in cancer cells. *Drug Deliv* 19:169–176
- Sawant RR, Torchilin VP (2010) Multifunctionality of lipid-core micelles for drug delivery and tumour targeting. *Mol Membr Biol* 27:232–246
- Shahin M, Hady SA, Hammad M, Mortada N (2011a) Novel jojoba oil-based emulsion gel formulations for clotrimazole delivery. *AAPS Pharm Sci Tech* 12:239–247
- Shahin M, Hady SA, Hammad M, Mortada N (2011b) Optimized formulation for topical administration of clotrimazole using Pemulen polymeric emulsifier. *Drug Dev Ind Pharm* 37:559–568
- Shen L, Guo A, Zhu X (2011) Tween surfactants: adsorption, self-organization, and protein resistance. *Surf Sci* 605:494–499
- Shen Y, Ling X, Jiang W, Du S, Lu Y, Tu J (2015) Formulation and evaluation of Cyclosporin A emulgel for ocular delivery. *Drug Deliv* 22:911–917
- Shokri J, Azarmi S, Fasihi Z, Hallaj-Nezhadi S, Nokhodchi A, Javadzadeh Y (2012) Effects of various penetration enhancers on percutaneous absorption of piroxicam from emulgels. *Res Pharm Sci* 7:225–234
- Singh B, Khurana L, Bandyopadhyay S, Kapil R, Katare OO (2011) Development of optimized self-nano-emulsifying drug delivery systems (SNEDDS) of carvedilol with enhanced bioavailability potential. *Drug Deliv* 18:599–612
- Singla V, Saini S, Joshi B, Rana A (2012) Emulgel: a new platform for topical drug delivery. *Int J Pharma Bio Sci* 3:485–498
- Sklenar Z, Horackova K, Bakhouché H, Slanar O (2012) Magistral prepared lidocaine-gel for topical application on skin. *Ceska Slov Farm* 61:163–168

- Subudhi M, Jain A, Jain A, Hurkat P, Shilpi S, Gulbake A, Jain S (2015) Eudragit S100 coated citrus pectin nanoparticles for colon targeting of 5-fluorouracil. *Materials* 8:832–849
- Szűcs M, Sandri G, Bonferoni MC, Caramella CM, Vaghi P, Szabó-Révész P, Erős I (2008) Mucoadhesive behaviour of emulsions containing polymeric emulsifier. *Eur J Pharm Sci* 34:226–235
- Tipton DA, Lyle B, Babich H, Dabbous M (2003) In vitro cytotoxic and anti-inflammatory effects of myrrh oil on human gingival fibroblasts and epithelial cells. *Toxicol In Vitro* 17:301–310
- Tomsic M, Podlogar F, Gasperlin M, Bester-Rogac M, Jamnik A (2006) Water-Tween 40/Imwitor 308-isopropyl myristate microemulsions as delivery systems for ketoprofen: small-angle X-ray scattering study. *Int J Pharm* 327:170–177
- Torchilin V (2008) Antibody-modified liposomes for cancer chemotherapy. *Expert Opin Drug Deliv* 5:1003–1025
- Utreja P, Jain S, Tiwary A (2011) Localized delivery of paclitaxel using elastic liposomes: formulation development and evaluation. *Drug Deliv* 18:367–376
- Vilasau J, Solans C, Gómez M, Dabrio J, Mújika-Garai R, Esquena J (2011) Phase behaviour of a mixed ionic/nonionic surfactant system used to prepare stable oil-in-water paraffin emulsions. *Colloids Surf A* 384:473–481
- Villarreal-Lozoya JE, Lombardini L, Cisneros-Zevallos L (2007) Phytochemical constituents and antioxidant capacity of different pecan [*Carya illinoensis* (Wangenh.) K. Koch] cultivars. *Food Chem* 102:1241–1249
- Weissig V, Lizano C, Torchilin VP (2000) Selective DNA release from DQAsome/DNA complexes at mitochondria-like membranes. *Drug Deliv* 7:1–5
- Zhang J, Wang C, Wang J, Qu Y, Liu G (2012) In vivo drug release and antibacterial properties of vancomycin loaded hydroxyapatite/chitosan composite. *Drug Deliv* 19:264–269
- Zhu K, Zhou H, Qian H (2006) Antioxidant and free radical-scavenging activities of wheat germ protein hydrolysates (WGPH) prepared with alcalase. *Process Biochem* 41:1296–1302
- Ziani K, Chang Y, McLandsborough L, McClements DJ (2011) Influence of surfactant charge on antimicrobial efficacy of surfactant-stabilized thyme oil nanoemulsions. *J Agric Food Chem* 59:6247–6255